BIOMARKER EXPLORATION IN NEUROPSYCHIATRY: UNDERSTANDING OF THE PATHOPHYSIOLOGY AND THERAPEUTIC IMPLICATIONS

EDITED BY: HuaLin Cai, Pei Jiang and Xiang Yang Zhang

PUBLISHED IN: Frontiers in Pharmacology, Frontiers in Neuroscience, Frontiers in Psychiatry, Frontiers in Neurology and Frontiers in Genetics

frontiers Research Topics

frontiers

ISSN 1664-8714
ISBN 978-2-88971-690-6
DOI 10.3389/978-2-88971-690-6

About Frontiers

Frontiers is more than just an open-access publisher of scholarly articles: it is a pioneering approach to the world of academia, radically improving the way scholarly research is managed. The grand vision of Frontiers is a world where all people have an equal opportunity to seek, share and generate knowledge. Frontiers provides immediate and permanent online open access to all its publications, but this alone is not enough to realize our grand goals.

Frontiers Journal Series

The Frontiers Journal Series is a multi-tier and interdisciplinary set of open-access, online journals, promising a paradigm shift from the current review, selection and dissemination processes in academic publishing. All Frontiers journals are driven by researchers for researchers; therefore, they constitute a service to the scholarly community. At the same time, the Frontiers Journal Series operates on a revolutionary invention, the tiered publishing system, initially addressing specific communities of scholars, and gradually climbing up to broader public understanding, thus serving the interests of the lay society, too.

Dedication to Quality

Each Frontiers article is a landmark of the highest quality, thanks to genuinely collaborative interactions between authors and review editors, who include some of the world's best academicians. Research must be certified by peers before entering a stream of knowledge that may eventually reach the public - and shape society; therefore, Frontiers only applies the most rigorous and unbiased reviews.
Frontiers revolutionizes research publishing by freely delivering the most outstanding research, evaluated with no bias from both the academic and social point of view. By applying the most advanced information technologies, Frontiers is catapulting scholarly publishing into a new generation.

What are Frontiers Research Topics?

Frontiers Research Topics are very popular trademarks of the Frontiers Journals Series: they are collections of at least ten articles, all centered on a particular subject. With their unique mix of varied contributions from Original Research to Review Articles, Frontiers Research Topics unify the most influential researchers, the latest key findings and historical advances in a hot research area! Find out more on how to host your own Frontiers Research Topic or contribute to one as an author by contacting the Frontiers Editorial Office: frontiersin.org/about/contact

BIOMARKER EXPLORATION IN NEUROPSYCHIATRY: UNDERSTANDING OF THE PATHOPHYSIOLOGY AND THERAPEUTIC IMPLICATIONS

Topic Editors:
HuaLin Cai, Central South University, China
Pei Jiang, Jining First People's Hospital, China
Xiang Yang Zhang, University of Texas Health Science Center at Houston, United States

Citation: Cai, H., Jiang, P., Zhang, X. Y., eds. (2021). Biomarker Exploration in Neuropsychiatry: Understanding of the Pathophysiology and Therapeutic Implications. Lausanne: Frontiers Media SA. doi: 10.3389/978-2-88971-690-6

Table of Contents

frontiers in Neuroscience

EDITORIAL
published: 29 September 2021
doi: 10.3389/fnins.2021.743276

Editorial: Biomarker Exploration in Neuropsychiatry: Understanding of the Pathophysiology and Therapeutic Implications

Hualin Cai[1,2]*, *Pei Jiang*[3] *and Xiangyang Zhang*[4,5]

[1] Department of Pharmacy, Second Xiangya Hospital of Central South University, Changsha, China, [2] The Institute of Clinical Pharmacy, Central South University, Changsha, China, [3] Institute of Clinical Pharmacology, Jining First People's Hospital, Jining Medical University, Jining, China, [4] CAS Key Laboratory of Mental Health, Institute of Psychology, Chinese Academy of Sciences, Bejing, China, [5] Department of Psychology, University of Chinese Academy of Sciences, Bejing, China

Keywords: genomics, proteomics, metabolomics, neuroimaging, biomarkers, psychiatry

Editorial on the Research Topic

Biomarker Exploration in Neuropsychiatry: Understanding of the Pathophysiology and Therapeutic Implications

This Research Topic, consisting of fifteen research and review articles, aimed to expand our knowledge and understanding of inspiring advances in various technologies which have provided us with new avenues to investigate biomarkers in neuropsychiatric disorders. Among these technologies, rapid developments in bioinformatics allow us to use computation to extract key information from biological databases. It includes the collection, manipulation and modeling of data for analysis, visualization, or prediction through the development of algorithms and software. It gives the researchers the new skills of finding the needle in a haystack. Here, Huang et al. searched the Gene Expression Omnibus (GEO) database for microarray studies of fibroblasts, lymphoblasts, and post-mortem brains of schizophrenia patients. They demonstrated that high FOS expression in non-neural peripheral samples and low FOS expression in brain tissues exist in schizophrenia patients. Since FOS is thought to play an important role in the pathophysiology of schizophrenia (Monfil et al., 2018), they further carried out Kyoto Encyclopedia of Genes and Genomes (KEGG) enrichment analysis and revealed that "amphetamine addiction" was among the top 10 significantly enriched KEGG pathways. Likewise, the protein-protein interaction network analysis indicated that proteins closely interacting with FOS-encoded protein were also involved in the amphetamine addiction pathway. To the end, the authors propose that FOS and amphetamine-related genes may be involved in schizophrenia pathogenesis and represent novel biomarkers for its diagnosis in clinical practice.

In addition to bioinformatics, the analysis of structural covariance networks (SCNs) has been successfully applied to obtain the abnormality in brain connectivity of neuropsychiatric disorders. This technology based on voxel-based morphometry, can generate a map of correlation between the gray matter volume of a targeted brain region and the other regions (Zielinski et al., 2010). As such, SCNs analysis is regarded as a potential tool to reflect developmental coordination or synchronized maturation between different regions of the brain. Here, Wang et al. investigated abnormalities in SCNs between hippocampal subfields and the whole cerebral cortex in amnestic mild cognitive impairment (aMCI) and in subcortical vascular mild cognitive impairment (svMCI) patients, and then made comparisons of these abnormalities between the two subtypes. They found: (1) significant correlations between hippocampal subfields,

Edited and reviewed by:
Nicholas M. Barnes, University of Birmingham, United Kingdom

***Correspondence:**
Hualin Cai
hualincai@csu.edu.cn

Specialty section:
This article was submitted to Neuropharmacology, a section of the journal Frontiers in Neuroscience

Received: *18 July 2021*
Accepted: *03 September 2021*
Published: *29 September 2021*

Citation:
Cai H, Jiang P and Zhang X (2021) Editorial: Biomarker Exploration in Neuropsychiatry: Understanding of the Pathophysiology and Therapeutic Implications. Front. Neurosci. 15:743276. doi: 10.3389/fnins.2021.743276

fusiform gyrus, and entorhinal cortex in gray matter volume in each group; (2) as compared to normal controls, an increased association between the left CA1/CA4/DG/subiculum and the left temporal pole in aMCI group, and covariations between the hippocampal subfields (bilateral CA1, left CA2/3) and the orbitofrontal cortex in svMCI group; (3) an decreased association between hippocampal subfields and the right fusiform gyrus, as well as increased association between the bilateral subiculum/presubiculum and bilateral entorhinal cortex, when aMCI group was compared to svMCI group. These findings demonstrate that there is altered whole-brain structural covariance of the hippocampal subfields in svMCI and aMCI patients and provide insights to the imaging biomarkers of different mild cognitive impairment subtypes.

Omics-technologies, including genomics, transcriptomics, proteomics, and metabolomics, have revolutionized biomedical research over the past two decades, and are now poised to play a transformative role in the explorations of biomarkers for neuropsychiatric disorders. In the study by Brandão-Teles et al. using human oligodendrocyte cell line as the model, the authors performed a mass spectrometry-based, bottom-up shotgun proteomic analysis to identify different effects triggered by typical (chlorpromazine and haloperidol) and atypical (quetiapine and risperidone) antipsychotic drugs. The results showed that the two types of antipsychotic drugs shared common effects on spliceosome machinery, eukaryotic initiation factor-2 signaling, rapamycin (mTOR) signaling pathway, ubiquitination pathway, energy metabolism, and 14-3-3 family proteins. Drug-specific differences triggered by antipsychotics were also observed, suggesting that (1) risperidone has more pathways in common with the two typical antipsychotics than with quetiapine; (2) chlorpromazine appears to increase protein levels, whereas haloperidol has the opposite action; (3) quetiapine alters fewer proteins than the other three drugs. Although *in vitro* studies may have discrepancies with the *in vivo* scenario, these detailed findings shed light on the biochemical pathways underlying the mechanisms these antipsychotics, which may guide the identification of novel treatment biomarkers and the development of new therapeutic strategies. To decipher the complexity and heterogeneity of neuropsychiatric disorders, integration of proteomics, bioinformatics and systems biology can be even more powerful (Guingab-Cagmat et al., 2013). Hypothalamus has important modulatory functions in the brain and controls the activity of hypothalamic-pituitary-adrenal (HPA) axis responding to stress (Myers et al., 2014). Herein, Zhang et al. established a chronic corticosterone-induced mouse model of depression to assess the antidepressant-like effects and mechanisms of baicalin, using a combined method of proteomics and systems biology. Using proteomics, they found 370 differentially expressed proteins in the depression rat model after baicalin treatment, including 114 up-regulation and 256 down-regulation in hypothalamus. Then systems biology analysis was performed to narrow down the information, and indicates that differentially expressed proteins are focused on phosphoserine binding and phosphorylation, especially participate in glucocorticoid receptor (GR) signaling pathway. Finally, the findings demonstrate that baicalin can reduce hypothalamic GR phosphorylation to remodel and normalize the negative feedback of HPA axis.

Metabolomics is a global approach to understanding regulation of metabolic pathways and networks of a biological system, and emerges as another powerful tool for identification of biomarkers in central nervous system research. Here, for the first time, Papadopoulou et al. conducted a targeted metabolomics study based on mass spectrometry platform, to compare the serum metabolomes including up to 300 metabolites of a characterized group of mothers suffering from post-partum depression (PPD) and a control group of mothers. They demonstrated increased levels of glutathione-disulfide, adenylosuccinate, and adenosine triphosphate (ATP) in the PPD group, which are involved in oxidative stress, nucleotide biosynthesis and energy production pathways. Moreover, the metabolomic findings are further validated in a separate cohort of PPD mothers and controls. Importantly, the data indicate that PPD-induced molecular alterations are detectable in the periphery and may open up new perspectives for more studies aiming at early detection and diagnosis for PPD. Although studies in peripheral samples are essential for developing safe, non-invasive diagnostic and screening approaches for neuropsychiatric disorders, the specificity of disease-related molecular correlates in peripheral material has always been one of the biggest challenges we are facing (Filiou and Turck, 2011). Herein, Zhou et al. compared plasma free fatty acid (FFA) levels and profiles among healthy controls (HCs), affective psychosis (AP) patients with bipolar disorder/major depression as disease-controls, and first-episode antipsychotic-naïve schizophrenia (FEANS) patients, using a more focused quantitative metabolomic strategy performed with capillary gas chromatography. The FFAs are involved in many important biochemical reactions such as membrane regeneration, oxidation, and prostaglandin production, which have important implications in schizophrenia pathology (Yao and Reddy, 2002). Interestingly, as compared with HCs, a significant reduction of total FFAs levels and disrupted metabolism of fatty acids especially in saturated and n-6 fatty acid families were observed in FEANS patients. In the meantime, the reduction of 16:0, 18:2n6c, and 20:4n6 levels were merely detected in FEANS patients rather than in AP patients, which have extensive symptomatic and genetic overlap with schizophrenia. Collectively, these findings could help us better understand the lipid metabolism with regard to schizophrenia pathophysiology and provide insights into searching for disease-specific biomarkers.

Despite the abovementioned "omics" technologies, discovery of biomarkers is sometimes based on an underlying assumption regarding the pathogenesis and pathophysiology of the disease, a traditional strategy which can be termed as "hypothesis-driven." Several hypothesis-driven biomarker verification studies have been collected in this Research Topic. As it is well-known that altered HPA axis function has played an important role in the neurodegenerative process in schizophrenia (Walker and Diforio, 1997), here Liu et al. performed a quantitative analysis of the peripheral blood mRNA expression of GR, GR transcripts containing exons 1B (GR-1B), and neuron specific

enolase (NSE) genes and serum cortisol and NSE (a specific serum marker for neuronal damage). In this study, they found abnormal serum levels of cortisol in chronic schizophrenia patients and NSE protein levels in first-episode schizophrenia patients, respectively. Additionally, further evidence of altered NSE mRNA in chronic schizophrenia, GR mRNA in both first-episode and chronic schizophrenia and decreased GR-1B mRNA in chronic vs. first-episode schizophrenia were identified. These abnormalities particularly implicate the disrupted HPA axis and the dysregulation of GR mRNA and protein expression can be manifested at different stages of schizophrenia. Based on the assumption that abnormal immune system and immunological responses may be related with the etiology of schizophrenia (Monji et al., 2013), here another investigation implemented by Zhu et al. recruited 69 FEANS patients, 87 chronic schizophrenia patients and 61 HCs. They demonstrated that serum TNF-α and IL-1β levels in chronic schizophrenia were significantly higher than HCs, whereas their concentrations in FEANS patients were significantly lower as compared with both chronic schizophrenia patients and HCs. A moderate correlation between serum TNF-α/IL-1β levels and PANSS negative subscale was also found in chronic schizophrenia patients instead of FEANS. They concluded that altered immune response in chronic patients may be associated with the progression, psychotropic drugs, or other factors occur during chronic stage. The ATP-binding cassette subfamily B member 1 (ABCB1) gene is a multidrug resistance protein 1 (MDR1) gene encodes p-glycoprotein (P-gp). This protein expressed in the blood-brain barrier protects the brain from drugs or neurotoxic substances, and thus may play an important role in the bioavailability and response to central nervous system drugs (de Klerk et al., 2013). Here, Shan et al. explored the potential correlations of therapeutic responses with selective serotonin reuptake inhibitors (SSRIs) and serotonin-norepinephrine reuptake inhibitors (SNRIs) in a local Chinese Han population consisting of 292 patients with major depression. Interestingly, they found that the ABCB1 gene polymorphisms (the TT genotype of rs2032583) could be a predictive factor of better treatment responses to SNRIs in the Chinese population, which however, ought to be replicated in future studies with a larger cohort. Timely updates of underlying mechanisms and pathophysiology can help to generate new hypotheses, and thus may greatly accelerate new drug development and biomarker discovery. Here, Gong et al., for the first time, provided new evidence highlighting the involvement of biomarkers of renin-angiotensin system (RAS) in inflammation-impeded brain insulin pathway, which results in compromised neurobehavioral changes. The data suggests that inhibition of RAS seems to be a promising strategy to block or even cut-off the cross-talk and vicious cycle between RAS and immune system, which could serve as a potential therapeutic target for the inflammation-associated neuropsychiatric disorders such as depression.

Second-generation antipsychotics, also named atypical antipsychotic drugs (AAPDs), are first-line antipsychotics with greater improvement of negative symptoms and fewer extrapyramidal symptoms than first-generation antipsychotic drugs. However, metabolic side effects, especially well-documented dyslipidemia, type II diabetes, and weight gain induced by prolonged usage of AAPDs raise the risk of cardiovascular diseases, resulting in patient non-compliance, relapse, and increased mortality (Mitchell et al., 2013). Since related side effects could vary from patient to patient, potential biomarkers screening to predict the risk of metabolic side effects of antipsychotic drug is becoming a hot area in pharmacogenomic research. Here, Li N. et al. systematically reviewed recently updated findings on the pharmacogenomics and gene polymorphisms related to lipid disturbances of AAPDs, with the aim to find the possible relations between central and peripheral pathways. In the review, evidence indicated that in central nervous system, HTR2C, DRD2, LEP, NPY, MC4R, BDNF, CNR1 polymorphisms play an important role in regulating food intake, and they can be affected by AAPDs. Meanwhile, the lipid metabolism in peripheral tissues may be altered by the SNPs of LEP, NPY, MC4R, CNR1, INSIG2, and ADRA2A. Among these genes, complex pathways are involved in the modulation of energy intake and energy expenditure, representing orexigenic and anorexigenic mechanisms. The disturbance in glucose metabolism is another aspect of AAPD-induced adverse effects. Recently, accumulating evidence suggests that Wnt signaling pathway has a pivotal role in the pathogenesis of schizophrenia and molecular cascades of antipsychotic actions. TCF7L2, the key effector of Wnt signaling pathway, is strongly associated with glucose homeostasis (Singh, 2013). Here, a mechanism study performed by Li R. et al. explore the characteristics of metabolic disturbance induced by olanzapine and their associations to TCF7L2. Significantly increased body weight, fasting insulin, homeostasis model assessment-insulin resistance index, and TCF7L2 protein expression in liver, skeletal muscle, and adipose tissues were found, which could be reversed by metformin co-treatment. The results illustrate that TCF7L2 overexpression in liver, skeletal muscle, and adipose tissues may serve as a potential mechanism/biomarker indicative of olanzapine induced metabolic changes. Anti-N-methyl-D-aspartate receptor (anti-NMDAR) encephalitis is an autoimmune encephalitis and is often combined with psychiatric symptoms, such as severe hallucination, delusion, and aggressive behaviors (Warren et al., 2018). Some scholars hypothesized that NMDAR dysfunction was the "final common pathway" underlying the pathogenesis of schizophrenia (Wang et al., 2017). Therefore, it is believed that schizophrenia and anti-NMDAR encephalitis may have certain shared underpinnings and could be on the same spectrum (Maneta and Garcia, 2014). Here, Yang et al. reported a series of three cases of anti-NMDAR encephalitis with psychiatric symptoms. Using the anti-NMDAR antibodies in cerebrospinal fluid and serum as the treatment biomarker, they found that the AAPD clozapine may be effective, if the psychiatric symptoms could not be controlled after intravenous immunoglobulin and hormone therapy. It is noteworthy that quetiapine and aripiprazole were ineffective and olanzapine even worsened the psychiatric symptoms of these cases. It is speculated that the distinct affinity of receptor subtypes may play a role but the exact mechanism warrants further investigations.

Previously, metabolomes illustrating what happened in the organism, were generally considered as end products of

genomes and thus most of their fate was to be excreted as waste. However, new advances have modified the theory and demonstrated that downstream metabolite concentrations can regulate upstream gene expression, which can in turn exert certain therapeutic effects by regulating cascades of biological process and metabolic activity (Bradley et al., 2009). Hydrogen sulfide (H_2S) is regarded as the one of the most important endogenous gasotransmitter, and plays a number of roles in the central nervous system under pathological and physiological conditions such as anti-inflammation, cytoprotection, anti-apoptosis, and antioxidation (Kimura, 2013). Endogenous H_2S is mainly produced from L-cysteine, cystathionine, and β-mercaptopyruvic acid in mitochondria. Here, Wen et al. carried out a study showing the multifaceted vasoprotection of H_2S on cerebral ischemia/reperfusion injury. They demonstrated that both endogenous and exogenous H_2S had prominent protection on vasomotor dysfunction and neuronal injury induced by transient middle cerebral artery occlusion in rats. Specifically, K_{Ca} channel might be involved in the cerebrovascular relaxation to H_2S, which is endothelium-dependent. Increasing evidence suggests that many neurosteroids have neuroprotective properties on the central nervous system. Although the mechanisms are far from fully elucidated, progesterone (PROG) and its active metabolite allopregnanolone (ALLO) have eminent neuroprotective effects against some nervous system diseases, including traumatic brain injury and spinal cord injury and schizophrenia-related cognitive impairment (Cai et al., 2018). Herein, Cao et al. investigated the capability of different dose of PROG/ALLO ($8.16\,mg\ kg^{-1}$) on ameliorating ketamine-induced cognitive deficits, and related mechanisms via the progesterone receptor membrane component 1 (PGRMC1) pathway in hippocampus and prefrontal cortex were elaborated simultaneously. The results showed that PROG or ALLO could reverse the impaired spatial learning and memory abilities induced by ketamine, which was accompanied with the upregulation of PGRMC1/EGFR/GLP-1R/PI3K/Akt pathway in the two brain regions. Additionally, the coadministration of PGRMC1 specific inhibitor AG205 abolished their neuroprotective effects, suggesting the crucial role of PGRMC1 underlying the neuroprotection mechanisms of PROG/ALLO. The study may shed light on future clinical practice utilizing neurosteroid adjunctive therapy to enhance cognitive function in neuropsychiatric diseases by targeting on PGRMC1 signaling.

In summary, this collection highlights the wide range of technological strategies for discovery and validation of biomarkers in neuropsychiatric disorders. And new understanding of the mechanisms underlying the therapeutic effects of some metabolic biomarkers are also discussed. These studies enrich the pool of potential biomarkers for future clinical application, which not only facilitate objective diagnosis of neuropsychiatric diseases but also help develop promising avenues to improve treatment responses.

AUTHOR CONTRIBUTIONS

HC wrote the draft. PJ and XZ provided comments for revisions. All authors approved the publication of this editorial.

FUNDING

This work was supported in part by the grants from Hunan Provincial Natural Science Foundation of China [2021JJ30922], Hunan Provincial Health Commission Research Project [202113010595], Wu Jieping Medical Foundation Funded Special Clinical Research Project [320.6750.2020-04-2], Changsha Municipal Natural Science Foundation [kq2007045] and the Fundamental Research Funds for the Central Universities of Central South University [2019zzts1049, 2020zzts884, 2021zzts1073].

REFERENCES

Bradley, P. H., Brauer, M. J., Rabinowitz, J. D., and Troyanskaya, O. G. (2009). Coordinated concentration changes of transcripts and metabolites in Saccharomyces cerevisiae. *PLoS. Comput. Biol.* 5:e1000270. doi: 10.1371/journal.pcbi.1000270

Cai, H. L., Zhou, X., Dougherty, G. G., Reddy, R. D, Haas, G. L, Montrose, D. M., Keshavan, M., Yao, J. K. (2018). Pregnenolone-progesterone-allopregnanolone pathway as a potential therapeutic target in first-episode antipsychotic-naïve patients with schizophrenia. *Psychoneuroendocrinology*. 90, 43–51. doi: 10.1016/j.psyneuen.2018.02.004

de Klerk, O. L., Nolte, I. M., Bet, P. M., Bosker, F. J., Snieder, H., Den Boer, J. A., et al. (2013). ABCB1 gene variants influence tolerance to selective serotonin reuptake inhibitors in a large sample of Dutch cases with major depressive disorder. *Pharmacogenomics. J.* 13, 349–353. doi: 10.1038/tpj.2012.16

Filiou, M. D., and Turck, C. W. (2011). General overview: biomarkers in neuroscience research. *Int. Rev. Neurobiol.* 101, 1–17. doi: 10.1016/B978-0-12-387718-5.00001-8

Guingab-Cagmat, J. D., Cagmat, E. B., Hayes, R. L., and Anagli, J. (2013). Integration of proteomics, bioinformatics, and systems biology in traumatic brain injury biomarker discovery. *Front. Neurol.* 4:61. doi: 10.3389/fneur.2013.00061

Kimura, H. (2013). Physiological role of hydrogen sulfide and polysulfide in the central nervous system. *Neurochem. Int.* 63, 492–497. doi: 10.1016/j.neuint.2013.09.003

Maneta, E., and Garcia, G. (2014). Psychiatric manifestations of anti-NMDA receptor encephalitis: neurobiological underpinnings and differential diagnostic implications. *Psychosomatics* 55, 37–44. doi: 10.1016/j.psym.2013.06.002

Mitchell, A. J., Vancampfort, D., Sweers, K., van Winkel, R., Yu, W., and De Hert, M. (2013). Prevalence of metabolic syndrome and metabolic abnormalities in schizophrenia and related disorders–a systematic review and meta-analysis. *Schizophr. Bull.* 39, 306–318. doi: 10.1093/schbul/sbr148

Monfil, T., Vazquez Roque, R. A., Camacho-Abrego, I., Tendilla-Beltran, H., Iannitti, T., Meneses-Morales, I., et al. (2018). Hyper-response to novelty increases c-Fos expression in the hippocampus and prefrontal cortex in a rat model of Schizophrenia. *Neurochem. Res.* 43, 441–448. doi: 10.1007/s11064-017-2439-x

Monji, A., Kato, T. A., Mizoguchi, Y., Horikawa, H., Seki, Y., Kasai, M., et al. (2013). Neuroinflammation in schizophrenia especially focused on the role of microglia. *Prog. Neuropsychopharmacol. Biol. Psychiatry*. 42, 115–121. doi: 10.1016/j.pnpbp.2011.12.002

Myers, B., McKlveen, J. M., and Herman, J. P. (2014). Glucocorticoid actions on synapses, circuits, and behavior: implications for the energetics of stress. *Front. Neuroendocrinol.* 35, 180–196. doi: 10.1016/j.yfrne.2013.12.003

Singh, K. K. (2013). An emerging role for Wnt and GSK3 signaling pathways in schizophrenia. *Clin. Genet.* 83, 511–517. doi: 10.1111/cge.12111

Walker, E. F., and Diforio, D. (1997). Schizophrenia: a neural diathesis-stress model. *Psychol. Rev.* 104, 667–685. doi: 10.1037/0033-295X.104.4.667

Wang, J., Zhang, B., Zhang, M., Chen, J., Deng, H., Wang, Q., et al. (2017). Comparisons between psychiatric symptoms of patients with anti-NMDAR encephalitis and new-onset psychiatric patients. *Neuropsychobiology* 75, 72–80. doi: 10.1159/000480514

Warren, N., Siskind, D., and O'Gorman, C. (2018). Refining the psychiatric syndrome of anti-N-methyl-d-aspartate receptor encephalitis. *Acta. Psychiatr. Scand.* 138, 401–408. doi: 10.1111/acps.12941

Yao, J. K., and Reddy, R. D. (2002). Membrane pathology in schizophrenia: implication for arachidonic acid signaling. *Sci. World J.* 2, 1922–1936. doi: 10.1100/tsw.2002.870

Zielinski, B. A., Gennatas, E. D., Zhou, J., and Seeley, W. W. (2010). Network-level structural covariance in the developing brain. *Proc. Natl. Acad. Sci. U.S.A.* 107, 18191–18196. doi: 10.1073/pnas.1003109107

Conflict of Interest: The authors declare that the research was conducted in the absence of any commercial or financial relationships that could be construed as a potential conflict of interest.

Publisher's Note: All claims expressed in this article are solely those of the authors and do not necessarily represent those of their affiliated organizations, or those of the publisher, the editors and the reviewers. Any product that may be evaluated in this article, or claim that may be made by its manufacturer, is not guaranteed or endorsed by the publisher.

frontiers in Pharmacology

ORIGINAL RESEARCH
published: 16 April 2018
doi: 10.3389/fphar.2018.00379

The Wnt Signaling Pathway Effector TCF7L2 Mediates Olanzapine-Induced Weight Gain and Insulin Resistance

*Ranran Li[1], Jianjun Ou[1], Li Li[1], Ye Yang[1], Jingping Zhao[1] and Renrong Wu[1,2]**

[1] Department of Psychiatry, The Second Xiangya Hospital of Central South University, Changsha, China, [2] Shanghai Institute for Biological Science, Chinese Academy of Sciences, Shanghai, China

Olanzapine is a widely used atypical antipsychotic medication for treatment of schizophrenia and is often associated with serious metabolic abnormalities including weight gain and impaired glucose tolerance. These metabolic side effects are severe clinical problems but the underpinning mechanism remains poorly understood. Recently, growing evidence suggests that Wnt signaling pathway has a critical role in the pathogenesis of schizophrenia and molecular cascades of antipsychotics action, of which Wnt signaling pathway key effector TCF7L2 is strongly associated with glucose homeostasis. In this study, we aim to explore the characteristics of metabolic disturbance induced by olanzapine and to elucidate the role of TCF7L2 in this process. C57BL/6 mice were subject to olanzapine (4 mg/kg/day), or olanzapine plus metformin (150 mg/kg/day), or saline, respectively, for 8 weeks. Metabolic indices and TCF7L2 expression levels in liver, skeletal muscle, adipose, and pancreatic tissues were closely monitored. Olanzapine challenge induced remarkably increased body weight, fasting insulin, homeostasis model assessment-insulin resistance index, and TCF7L2 protein expression in liver, skeletal muscle, and adipose tissues. Notably, these effects could be effectively ameliorated by metformin. In addition, we found that olanzapine-induced body weight gain and insulin resistance actively influence the expression of TCF7L2 in liver and skeletal muscle, and elevated level of insulin determines the increased expression of TCF7L2 in adipose tissue. Our results demonstrate that TCF7L2 participates in olanzapine-induced metabolic disturbance, which presents a novel mechanism for olanzapine-induced metabolic disturbance and a potential therapeutic target to prevent the associated metabolic side effects.

Keywords: olanzapine, Wnt signaling pathway, atypical antipsychotics, TCF7L2, weight gain, insulin resistance

OPEN ACCESS

Edited by:
Pei Jiang,
Jining Medical University, China

Reviewed by:
Luigia Trabace,
University of Foggia, Italy
Sulev Kõks,
University of Tartu, Estonia

****Correspondence:***
Renrong Wu
wurenrong@csu.edu.cn

Specialty section:
This article was submitted to Neuropharmacology, a section of the journal Frontiers in Pharmacology

Received: *28 January 2018*
Accepted: *03 April 2018*
Published: *16 April 2018*

Citation:
Li R, Ou J, Li L, Yang Y, Zhao J and Wu R (2018) The Wnt Signaling Pathway Effector TCF7L2 Mediates Olanzapine-Induced Weight Gain and Insulin Resistance. Front. Pharmacol. 9:379. doi: 10.3389/fphar.2018.00379

INTRODUCTION

Schizophrenic patients possess an approximately 20% shortened lifespan compared with the general population. One of the main causes of premature mortality is metabolic syndrome (MetS) (Hennekens et al., 2005; Raedler, 2010), which is twice higher in schizophrenia patients, featuring insulin resistance, glucose intolerance, dyslipidemia, hypertension, type 2 diabetes mellitus (T2DM), cardiovascular disease, and obesity (Rethelyi and Sawalhe, 2011). Largely due

to MetS (Ryan et al., 2003; Mathieu et al., 2009; Rheaume et al., 2009), the first-episode, drug-naïve patients present impaired glucose tolerance, insulin resistant, higher levels of plasma glucose (Ryan et al., 2003; Spelman et al., 2007), and increased visceral fat distribution (Thakore et al., 2002; Ryan et al., 2004). In a recent systematic review and meta-analysis (Mitchell et al., 2013b), the overall incidence rate of MetS is 32.5% in schizophrenia patients and related disorders. In clozapine-prescribed patients, the proportion could be as high as 51.9% than that in unmedicated patients (20.2%) (Mitchell et al., 2013a). Furthermore, MetS is also associated with increased risk of cardiovascular diseases and all-cause mortality (Lakka et al., 2002).

Increasing evidence shows that atypical antipsychotics (APPs) are associated with metabolic adverse effects, such as weight gain, obesity, glucose intolerance, dyslipidemia, and MetS (Newcomer, 2007; De Hert et al., 2011; Mitchell et al., 2013b). Compared to the first-episode and unmedicated schizophrenia patients, the prevalence of metabolic disturbance is significantly higher in patients on established antipsychotic drugs (9.8% for unmedicated, 9.9% for first episode, and 35.3% for medicated patients) (Chadda et al., 2013; Mitchell et al., 2013a). Numerous studies have demonstrated that APPs are crucial in the high prevalence of MetS in patients with schizophrenia (Alvarez-Jimenez et al., 2008; Malhotra et al., 2013). Among APPs, olanzapine is widely used for management of patients with schizophrenia and other psychiatric disorders and produces the most serious abnormalities in glucose and lipid metabolism (Alvarez-Jimenez et al., 2008; Komossa et al., 2010). The molecular mechanism underlying olanzapine-induced metabolic disturbance remains largely unknown, although H(1)-histamine receptor has been involved in the APPs-induced weight gain (Kroeze et al., 2003). Interestingly, molecular genetics data show that genes regulating glucose metabolism predispose human population to schizophrenia susceptibility (Hansen et al., 2011; Alkelai et al., 2012). Of these genes, *TCF7L2* is found to be associated with schizophrenia, which is the best replicated risk factor for T2DM, and exhibits the strongest association to diabetes susceptibility (Grant, 2012). Previous study suggested that TCF7L2 may stimulate the pancreatic β-cells proliferation and affect the production of glucagon-like peptide-1 in intestinal endocrine cells (Jin and Liu, 2008). As a transcriptional regulator of the canonical Wnt signaling pathway, it also regulates cell fate specification during development and cell proliferation (Peifer and Polakis, 2000; Clevers, 2006; MacDonald et al., 2009). Previous study suggests that Wnt signaling pathway may be associated with schizophrenia, and expression of Wnt-related proteins is altered following APPs treatment, for example, the expression of β-catenin and glycogen synthase kinase-3 (GSK-3) protein are increased in rat medial prefrontal cortex and striatum after APPs administration (Alimohamad et al., 2005a).

Indeed, converging evidence has recently showed that the protein kinase B (Akt)/GSK-3 and Wnt signaling pathways could play a key role in the pathogenesis of schizophrenia and the molecular mechanisms of APPs (Alimohamad et al., 2005a; Freyberg et al., 2010; Singh, 2013). It has been reported that AKT1 gene polymorphisms are associated with schizophrenia (Xu et al., 2007), and antipsychotic drugs modulate the Akt/GSK-3 and Wnt signaling pathways in order to correct the deficits induced by the gene mutation (Alimohamad et al., 2005b). Furthermore, the downstream molecule of the diabetes risk genes, *TCF7L2*, is associated with schizophrenia (Hansen et al., 2011). These findings prompt us to investigate the possible involvement of the TCF7L2 in olanzapine-induced metabolic disturbances.

Metformin, a widely used biguanide antihyperglycemic drug for T2DM, has been effectively used to prevent antipsychotic-induced weight gain and other metabolic adverse events (Jarskog et al., 2013; Boyda et al., 2014). Metformin normalizes blood glucose levels by suppressing hepatic gluconeogenesis and increases peripheral tissue insulin sensitivity (Kirpichnikov et al., 2002).

In our current study, our goal was to explore the molecular mechanisms and the protective effects of metformin against olanzapine-induced metabolic disturbance. Male mice were included in order to exclude sex differences (Cooper et al., 2007; Wu et al., 2007; Li et al., 2016). Mice were subject to olanzapine, olanzapine plus metformin, or saline for 8 weeks, respectively, and the variables including weight, fasting blood glucose, and insulin and oral glucose tolerance test (OGTT) were determined prior to and after drug administration. Blood lipid profile and the expression of TCF7L2 were also monitored in individual tissues at the end of each treatment paradigm.

MATERIALS AND METHODS

Animals

Male C57BL/6 mice (18.9–22.6 g, 26–30 days old) were obtained from Hunan Slack King Laboratory Animal Co., Ltd. They were housed at 22 ± 2°C, 55 ± 15% humidity on a 12 h light/dark cycle (lights on at 7:00 am). Food and water were allowed *ad libitum* throughout the study. The mice were fasted for about 12 h before the start of experiments (when the mice were 8-week-old). This study was carried out in accordance with the recommendations of Guide for the Care and Use of Laboratory Animal (NRCU, 1996), Animal Ethics Committee of the Second Xiangya Hospital of the Central South University. The protocol was approved by the Ethics Committee of the Second Xiangya Hospital of Central South University. After 1 week of acclimatization, the 8-week-old mice were randomly divided into three groups (10 per group) as follows: group 1 (sham mice) received a standard chow diet plus saline, group 2 received a standard diet plus olanzapine, and group 3 received a standard diet plus olanzapine and metformin.

Drug Treatment

Olanzapine (brand name: Zyprexa) was purchased from Eli Lilly, United States. Metformin hydrochloride was obtained from Hunan Xiangya Pharmaceutical Co., Ltd., Changsha, China. Olanzapine was dissolved in 0.9% saline solution and maintained in one gavage administration (4 mg/kg/day) every day for 8 weeks. Olanzapine (4 mg/kg/day, oral) and metformin hydrochloride (150 mg/kg/day, oral) were prepared as previously (Matsui et al., 2010; Savoy et al., 2010). The vehicle solution for metformin was 0.9% saline solution. All the drugs were prepared

freshly prior to usage and administered orally (gastric gavage) between 9:00 and 14:00 h every day.

Study Design

Mice (n = 10 per group) were randomly assigned into three groups. Group 1 was subject to daily gavage of 0.9% saline solution, while group 2 received daily gavage of olanzapine and group 3 was given olanzapine and metformin. After 1 week of acclimatization and fasting for 12 h, the baseline measurement of body weight, whole-blood glucose level, serum insulin level, and OGTT were determined prior to the administration of olanzapine. The body weight of the mice was monitored weekly. After 8 weeks of treatment, 10 mice in each group were fasted 12 h and gavaged with glucose (2 g/kg body weight), blood glucose was measured at baseline and at 0, 30, 60, 90, and 120 min after glucose load. On the next day, at least 8 h after being fasted, the mice were killed by decapitation. Blood samples were collected, serum insulin level, blood lipid level [including total cholesterol, low-density lipoprotein cholesterol (LDL-C), triglycerides and, high-density lipoprotein cholesterol (HDL-C)], and OGTT were determined. The liver, adipose, skeletal muscle, and pancreatic tissues were collected, immediately frozen in liquid nitrogen, and stored at −80°C until further analysis. A part of the pancreatic tissue was fixed with 4% paraformaldehyde in PBS and stored at 4°C for immunofluorescence staining.

Metabolic Measures

Blood glucose was determined by clipping tails and using the glucometer (EKF Diagnostics, Germany). For fasting insulin measurement, blood samples were collected and centrifuged (3500 rpm, 20 min, 4°C) to separate the serum and stored at −80°C until assay. Serum insulin level was measured quantitatively using a Mouse Ultrasensitive Insulin ELISA kit (ALPCO Diagnostics, United States). The mice fasted for 12 h were given with glucose (2 g/kg, p.o.). Blood samples were collected from tail tip incision at 0, 30, 60, 90, and 120 min after glucose administration. Blood glucose concentration was plotted against time, and area under the curve (AUCg) was calculated following trapezoidal rules (Dora et al., 2008). Serum concentrations of triglycerides, total cholesterol, HDL, and LDL were measured with an autobiochemical analyzer (C8000, Abbott, United States).

Insulin resistance index was calculated based on the homeostatic model assessment of insulin resistance (HOMA-IR): [fasting insulin (mIU/L) × fasting glucose (mmol/L)]/22.5 (Mather, 2009).

RNA Extraction and Real-Time Quantitative PCR

Total RNA was extracted from pancreatic tissues by using the SYBR Green PCR kit (F-415XL, Thermo, United States). RNA was reverse-transcribed using the protocol provided in the kit (K1622, Thermo, United States). The primer sequences are listed in **Table 1**. The gene was amplified through RT-PCR method using the SYBRGreen PCR kit (Thermo, United States). GAPDH was used as the reference gene. Amplification was run for 40 cycles. Samples were denatured at 95°C, followed by annealing at 60°C. The mRNA expression of the *TCF7L2* gene was quantitatively analyzed using Applied Biosystems 7300 Real-Time PCR System (Applied Biosystems, Thermo, United States). Data were analyzed with $2^{-\Delta\Delta CT}$ (Schmittgen and Livak, 2008).

Immunofluorescence Staining and Imaging

Pancreatic tissues were fixed for 4 h in 4% paraformaldehyde in PBS and embedded for paraffin sectioning (5 μm). The sections were deparaffinised, rehydrated, and incubated overnight at 4°C with goat antisera against insulin, TCF7L2 antibody (1:60–70, D-4, sc-166699, Santa Cruz, CA, United States), and DAPI (AR1176, Wuhan Boster Company). The sections were subsequently probed with secondary antibodies for 20 min at 37°C (Yang et al., 2012). Images of the pancreatic tissues were acquired using a fluorescent inverted microscope (Olympus IX71, Japan). For morphometric analysis, the fluorescence intensity of pancreatic sections was quantified using the Image J 1.37c[1].

Western Blot Analysis

TCF7L2 proteins in the pancreas were extracted for Western blot analysis (Yang et al., 2012). Frozen tissues were homogenized in RIPA lysis buffer (Solarbio, Beijing, China) and centrifuged at 12,000 rpm for 10 min at 4°C to collect the supernatant. Protein concentrations of the tissue lysates were determined by bicinchoninic acid method. Tissue lysates were separated by SDS–PAGE and transferred to PVDF membranes. Proteins were probed with rabbit anti-TCF7L2 (1:2500, Abcam Inc., United Kingdom) or mouse anti-actin (1:1000, TA-09, ZSGB-Bio Co., Ltd., Beijing, China) antibodies and incubated with peroxidase-conjugated affiniPure Goat Anti-Mouse IgG (H+L) secondary antibody (1:3000, ZB-2305, ZSGB-Bio Co., Ltd., Beijing, China). The proteins were visualized using a Western Lightning Plus Enhanced Chemiluminescence reagent (ECL, Amersham, United States). Density of the bands was analyzed with a GDS-8000 system (UVP CA, United States).

Statistical Analysis

Statistics was performed using SPSS 19.0 (Chicago, IL, United States). Statistical differences in measures of the different groups were analyzed by one-way ANOVA followed by Tukey's multiple-comparison *post hoc* test. The weight levels at different time points were compared across groups using repeated measures ANOVA. Statistical power of the main results

[1]http://rsb.info.nih.gov/ij/

TABLE 1 | PCR primer sequences used to quantify mRNA levels of *TCF7L2* gene by real-time PCR.

Primer	Sequence	Pos	Size (bps)
TCF7L2 F	5′-GTCCTCGCTGGTCAATGAATC-3′		
TCF7L2 R	5′-CCGCTTCTTCCAAACTTTCCC-3′	667–791 C	125
GAPDH F	5′-ATCACTGCCACCCAGAAG-3′		
GAPDH R	5′-TCCACGACGGACACATTG-3′	585–775	191

was calculated with G*Power 3.1. Correlations were identified using Pearson's correlation. Multivariate linear regression was performed to examine the relationship between TCF7L2 expression and the change of weight, fasting blood glucose, fasting insulin, AUCg, and HOMA-IR during the 8-week study period. A second analysis was conducted with the metabolic indexes as independent variables and TCF7L2 expression as the dependent variable, with the probability of entry set at 0.10 and removal at 0.15, reporting the coefficient of determination values that were significant at p-level of 0.05. All data were presented as mean ± SEM. Statistical significance was defined as $p \leq 0.05$.

RESULTS

Effect of Olanzapine on Body Weight

No significant difference was found in the body weight of the three groups (one-way ANOVA, $F_{2,27} = 1.029$, $p = 0.371$) prior to any treatment. However, olanzapine treatment induced a significantly higher body weight than control group and metformin group during (**Figure 1A**) and also after (**Figure 1B**, one-way ANOVA, $F_{2,27} = 0.521$, $p = 0.012$) the 8 weeks of treatment, although all three groups displayed significantly increased mean body weight after drug administration. The alteration of body weight from baseline to week 1 and week 8 was summarized in **Figures 1C,D**. As indicated in the figure, the increase of mean body weight in mice was significantly higher in olanzapine group than control group at week 1 and week 8 (one-way ANOVA, $F_{2,27} = 7.217$, $p = 0.003$; $F_{2,27} = 5.28$, $p = 0.012$), moreover, treatment with metformin plus olanzapine significantly ameliorated the mean body weight increase induced by olanzapine at week 1 and week 8 ($p = 0.032$ and $p = 0.018$, respectively). The statistic power of body weight gain at week 1 and week 8 was 0.77 and 0.67, respectively.

Effect of Olanzapine on Fasting Glucose, Fasting Insulin, HOMA-IR, OGTT, and AUCg

As shown in **Figures 2A–C**, after 8 weeks of drug treatment, olanzapine-treated mice significantly increased fasting insulin level and HOMA-IR compared with control group mice (one-way ANOVA, $F_{2,27} = 29.724$, $p < 0.001$; $F_{2,27} = 29.724$, $p < 0.001$), whereas no significant difference was found in the fasting glucose between groups (one-way ANOVA, $F_{2,27} = 0.37$, $p = 0.694$). Moreover, we assessed the effect of metformin on the metabolic disturbances induced by olanzapine and found that metformin remarkably reversed olanzapine-induced fasting insulin elevation and insulin resistance (both $p < 0.001$), which was consistent with previous studies (Wang et al., 2012).

To investigate insulin resistance and pancreatic beta-cell function, we conducted the OGTT at week 8. Compared with olanzapine group, metformin plus olanzapine treated mice significantly reduced the blood glucose level at OGTT 30, 90, and 120 min (**Figures 2D,E**), and the glucose level was also lower compared with placebo group mice at OGTT 90 and 120 min. Oral glucose tolerance test following 8 weeks of treatment in the mice revealed that AUCg values were significantly lower in the metformin group compared with olanzapine group (one-way ANOVA, $F_{2,27} = 7.787$, $p = 0.001$). The AUCg value did not differ between the olanzapine treatment and control group ($p = 0.209$). The statistic power of fasting insulin level, HOMA-IR, and AUCg at the end of 8 weeks was 0.98, 0.96, and 0.79, respectively.

Effect of Olanzapine on Blood Lipid

In order to evaluate whether olanzapine could induce any significant difference in blood lipid between control and olanzapine treatment animals, we measured the serum total cholesterol, HDL-C, LDL-C, and triglyceride levels in the three groups after treatment completion. Olanzapine group displayed a significantly higher serum LDL-C level than control group ($p = 0.034$), which could be massively improved by metformin (**Figure 3A**, $p = 0.02$), while no significant difference was found in the level of total cholesterol and HDL-C between the treatments (one-way ANOVA, $F_{2,27} = 0.536$, $p = 0.591$; $F_{2,27} = 0.765$, $p = 0.475$). In addition, the triglyceride levels in metformin treatment group was significantly lower than the olanzapine treatment group and control group (**Figure 3**). The statistic power of LDL-C and TG at the end of 8 weeks was 0.79 and 0.97.

Effect of Olanzapine on TCF7L2 Expression in Liver, Skeletal Muscle, Adipose, and Pancreas

TCF7L2 expressing level in liver, skeletal muscle, and adipose tissues is associated with glucose metabolism and insulin resistance (Boj et al., 2012; Kaminska et al., 2012; Singh et al., 2013). As shown in **Figures 4A–C**, we detected significant difference of TCF7L2 protein expression in liver, skeletal muscle, and adipose tissues between treatment groups (one-way ANOVA, $F_{2,27} = 20.842$, $F_{2,27} = 13.345$, and $F_{2,27} = 20.149$, respectively, all $p < 0.001$). Compared with the control, olanzapine treatment obviously increased TCF7L2 protein expression in liver, skeletal muscle, and adipose tissues ($p < 0.001$), which can be effectively reduced by metformin ($p < 0.001$). There was no significant difference in the level of TCF7L2 expression in these tissues between metformin treatment group and control group ($p > 0.05$). The statistic power of TCF7L2 protein in liver, skeletal muscle, and adipose tissues was 0.94, 0.88, and 0.95, respectively. To further explore the mechanisms of olanzapine in MetS, we determined the expression of *TCF7L2* mRNA and TCF7L2 protein in pancreas. However, there was no significant difference of *TCF7L2* mRNA or TCF7L2 protein expression among the three groups ($p > 0.05$) as shown in (**Figure 5**).

Relationship Between TCF7L2 Protein Expression and Metabolic Measures

To investigate the relationship between the TCF7L2 protein expression and metabolic variables changes, we performed multiple linear regression analysis to evaluate the association of TCF7L2 protein expression and altered body weight, blood glucose, fasting insulin, HOMA-IR, and AUCg after olanzapine challenge. TCF7L2 protein expression was significantly correlated

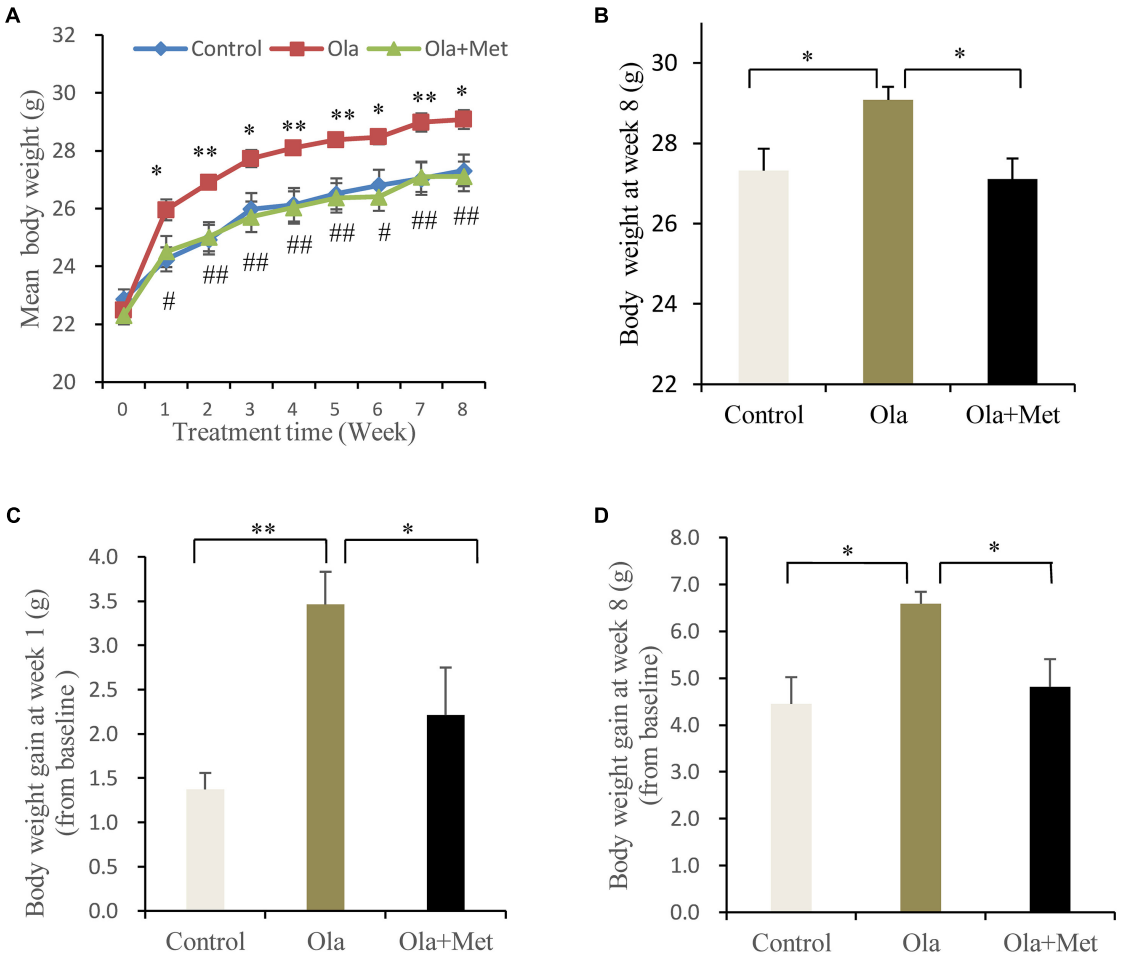

FIGURE 1 | Comparison of the body weight between different treatment groups in C57BL/6 mice. C57BL/6 mice were treated with olanzapine (4 mg/kg/day, Ola), olanzapine (4 mg/kg/day, Ola) + metformin (150 mg/kg/day, Met), or saline for 8 weeks. **(A)** Body weight of mice from olanzapine group (Ola), olanzapine + metformin group (Ola +Met), and control group (Control) during 8-week of treatment. $^{*}p < 0.05$, $^{**}p < 0.01$, Ola vs. Control group; $^{\#}p < 0.05$,$^{\#\#}p < 0.01$, Ola +Met vs. Ola group. **(B)** Body weight measured at the end of 8-week treatment. **(C)** Body weight gain after the first week of treatment. **(D)** Body weight gain after 8 weeks treatment. All the results ($n = 10$ for each group) were expressed as mean ± SEM. $^{*}p < 0.05$, $^{**}p < 0.01$.

with changes in body weight, fasting insulin, HOMA-IR, and AUCg from baseline to week 8 (**Table 2**). The results demonstrated that the extent of increases in body weight, HOMA-IR, and AUCg exerted a greater influence on TCF7L2 protein expression elevation in liver, with coefficient of determination (R^2) value of 0.461 ($p < 0.001$). Similarly, we used the same multivariate linear regression model to investigate the changes of these variables in skeletal muscle and adipose tissues, and found that the extent of increases in HOMA-IR and body weight had a greater impact on TCF7L2 protein expression elevation in skeletal muscle, with R^2 value of 0.352 ($p = 0.003$), and the increase of insulin level contributed to major impact on TCF7L2 protein expression elevation in adipose tissues, with R^2 value of 0.408 ($p < 0.001$).

TABLE 2 | The correlation analysis between TCF7L2 protein expression and changes of metabolic measures.

TCF7L2 expression	Person correlation coefficient			
	Weight change	Fasting insulin change	HOMA-IR change	AUCg change
Liver	0.457**	0.592***	0.636***	0.460**
Skeletal muscle	0.459**	0.499**	0.503**	0.399*
Adipose	0.377*	0.639***	0.584***	0.364*

Test statistic: multivariate linear regression analysis. $^{*}p < 0.05$, $^{**}p < 0.01$, $^{***}p < 0.001$.

DISCUSSION

The exact mechanism of olanzapine-induced metabolic disturbance remains unclear and numerous animal and post-mortem studies have demonstrated that Wnt signaling pathways are associated with schizophrenia and the intracellular

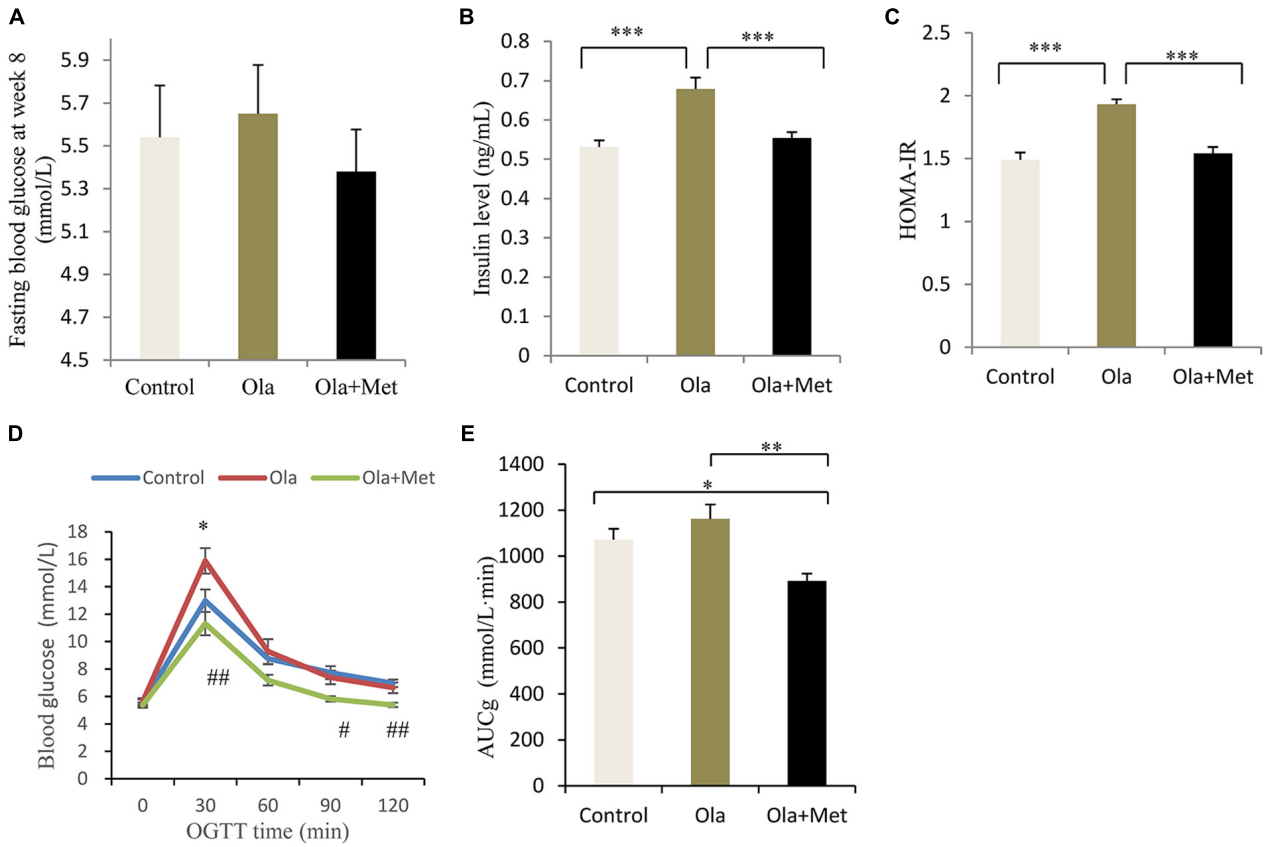

FIGURE 2 | Comparison of the fasting glucose, insulin level, insulin resistance, and glucose tolerance between different treatment groups in C57BL/6 mice. C57BL/6 mice were treated with olanzapine (4 mg/kg/day, Ola), olanzapine (4 mg/kg/day, Ola) + metformin (150 mg/kg/day, Met), or saline for 8 weeks. Effect of different treatment groups on fasting glucose **(A)**, insulin level **(B)**, and HOMA-IR **(C)** at the end of 8-week treatment. **(D)** Oral glucose tolerance test (OGTT) on overnight fasted mice from olanzapine group, olanzapine + metformin group, and control group after 8 weeks of treatment. Blood glucose level was measured before and 30, 60, 90, and 120 min after glucose administration (2 g/kg body weight). $^{*}p < 0.05$, Ola vs. Control group; $^{\#}p < 0.05$, $^{\#\#}p < 0.01$, Ola +Met vs. Ola group. **(E)** Area under curve of glucose (AUCg) of three treatment groups determined by OGTT. AUCg was calculated following trapezoidal rule from 0 to 120 min. Values (n = 10 for each group) were reported as mean ± SEM. $^{*}p < 0.05$, $^{**}p < 0.01$, and $^{***}p < 0.001$.

mechanism of antipsychotic medications (Koros and Dorner-Ciossek, 2007; Sutton et al., 2007; Freyberg et al., 2010; Sutton and Rushlow, 2011). TCF7L2, a key effector of Wnt signaling pathway, performs important metabolic functions in several tissues, including the pancreas, liver, fats, and gut. In the present study, we explored the possible relationship between olanzapine-induced metabolic disturbance and TCF7L2 expression. We found that olanzapine could significantly increase TCF7L2 protein expression in the liver, skeletal muscle, and adipose tissues after 8 weeks of treatment, whereas metformin could remarkably reduce the TCF7L2 protein expression after olanzapine challenge. We further explored the relationship between TCF7L2 protein expression in these tissues and changes in metabolic variables. Our results demonstrated that the extent of increases in some metabolic variables (body weight, insulin resistance, AUCg, and insulin) actively influences the TCF7L2 expression in the liver, skeletal muscle, and adipose tissues.

Consistent with previous clinical and animal studies (Alvarez-Jimenez et al., 2008; Coccurello et al., 2009; Komossa et al., 2010; Kim et al., 2014), the present study confirms that olanzapine could significantly induce weight gain, insulin resistance, and impaired glucose tolerance. Although we did not observe any significant change of fasting glucose in mice with olanzapine treatment, the insulin resistance index was significantly higher after olanzapine challenge. Similarly, Girault et al. (2014) reported that chronic olanzapine treatment (5 weeks) could cause increase in insulin without blood glucose elevation. The observed olanzapine-induced insulin resistance in this study is parallel with a previous study which demonstrated the existence of hyperinsulinemia and insulin resistance independently from body weight gain and psychiatric disease through the use of olanzapine for 9 days in healthy subjects (Teff et al., 2013). These results suggest that olanzapine exerts direct effects on some insulin-sensitive tissues independent of mechanisms underpinning the metabolic abnormalities. Although no significant difference in AUCg was observed between the olanzapine and control groups, an increasing trend in blood glucose was evident in the olanzapine group at OGTT 30 min (p = 0.063). The greatest weight gain was observed in the first week of drug administration, which is consistent with

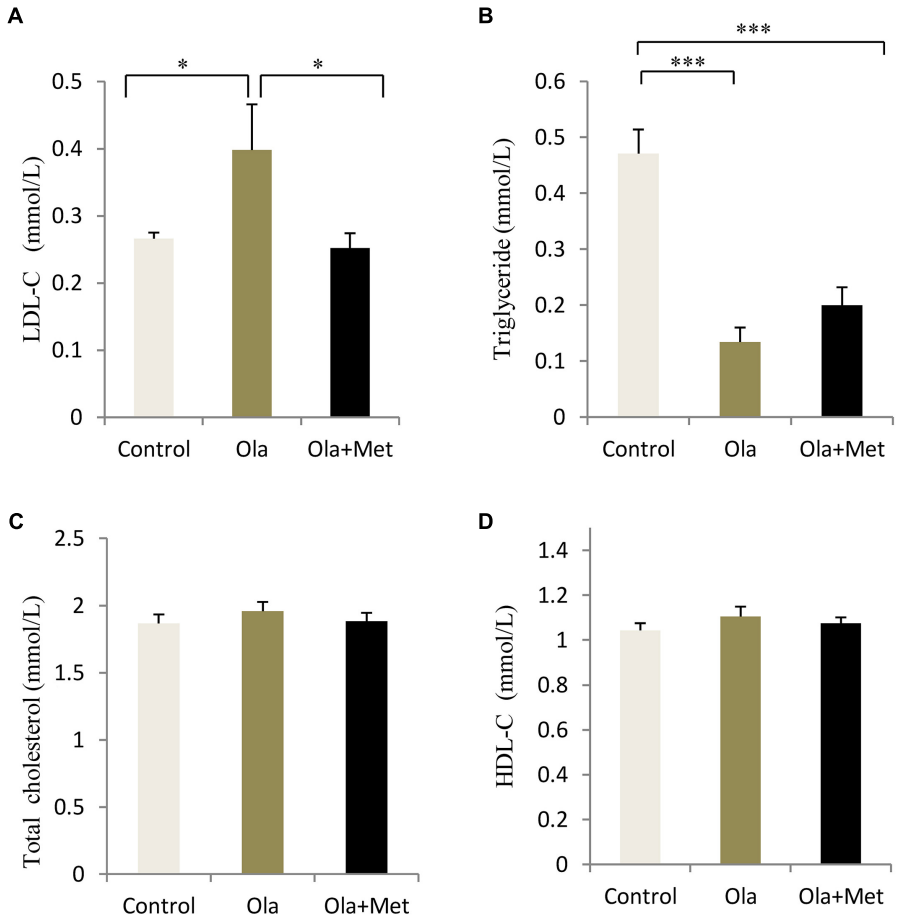

FIGURE 3 | Comparison of the blood lipid between different treatment groups in C57BL/6 mice. C57BL/6 mice were treated with olanzapine (4 mg/kg/day, Ola), olanzapine (4 mg/kg/day, Ola) + metformin (150 mg/kg/day, Met), or saline for 8 weeks. Effect of different treatment groups on LDL-C **(A)**, triglyceride **(B)**, total cholesterol **(C)**, and **(D)**, HDL-C at the end of 8-week treatment. All of the results are expressed as the mean ± SEM. $^{*}p < 0.05$, $^{***}p < 0.001$.

clinical observation that the first year is critical for development of weight gain and metabolic abnormalities in the first treated episode of psychosis (Perez-Iglesias et al., 2013; Tek et al., 2015). In the present study, we failed to observe significant alterations in blood total cholesterol and HDL-C levels after treatment with olanzapine or olanzapine plus metformin. Consistently, clinical data also demonstrate that atypical APPs are associated with increased blood lipid levels in patients with schizophrenia (Pramyothin and Khaodhiar, 2010; Kaushal et al., 2012; Schreiner et al., 2012). Moreover, Koro et al. (2002) reported that olanzapine treatment is associated with a nearly fivefold increase in the prevalence of hyperlipidemia in contrast to the general population using a large database (which contains over 18,000 patients with schizophrenia). The effect of APPs on blood lipid profile in rodent models seems controversial, which showed no alteration (Albaugh et al., 2006), or significant increase in triglyceride level after chronic olanzapine administration (Skrede et al., 2012; Zugno et al., 2012). Yet, a recent animal study (Horska et al., 2016) demonstrated that olanzapine is associated with hypertriglyceridemia and lowered LDL-C levels at the 8th day of olanzapine treatment, but these alterations could not persist after 8 weeks of olanzapine administration, and no significant alteration in blood lipid profiles was detected in later phase of olanzapine treatment. In the present study, we have observed a massively decreased triglyceride after olanzapine treatment. This seems contradictive with MetS-related insulin resistance but features an impaired lipid oxidation caused by olanzapine. In line with our findings, Albaugh et al. (2012) also reported a significantly reduced triglycerides and free fatty acids after olanzapine challenge *in vivo*. They further demonstrated that this is largely due to the rapid and inappropriate utilization of lipids triggered by olanzapine. Although data from previous literature remain controversial, in our study, 4 mg/kg dose of olanzapine did not significantly elevate triglyceride levels, possibly because of the short duration of treatment or the improper dosage of olanzapine. However, our data showed that olanzapine could significantly increase LDL-C levels, which is consistent with previous reports (Kaushal et al., 2012; Shao P. et al., 2013).

Recently, metformin was shown to effectively attenuate antipsychotic-induced weight gain, insulin resistance, and glucose dysregulation (Hasnain et al., 2010; Praharaj et al., 2011; Wang et al., 2012; Chen et al., 2013; Jarskog et al.,

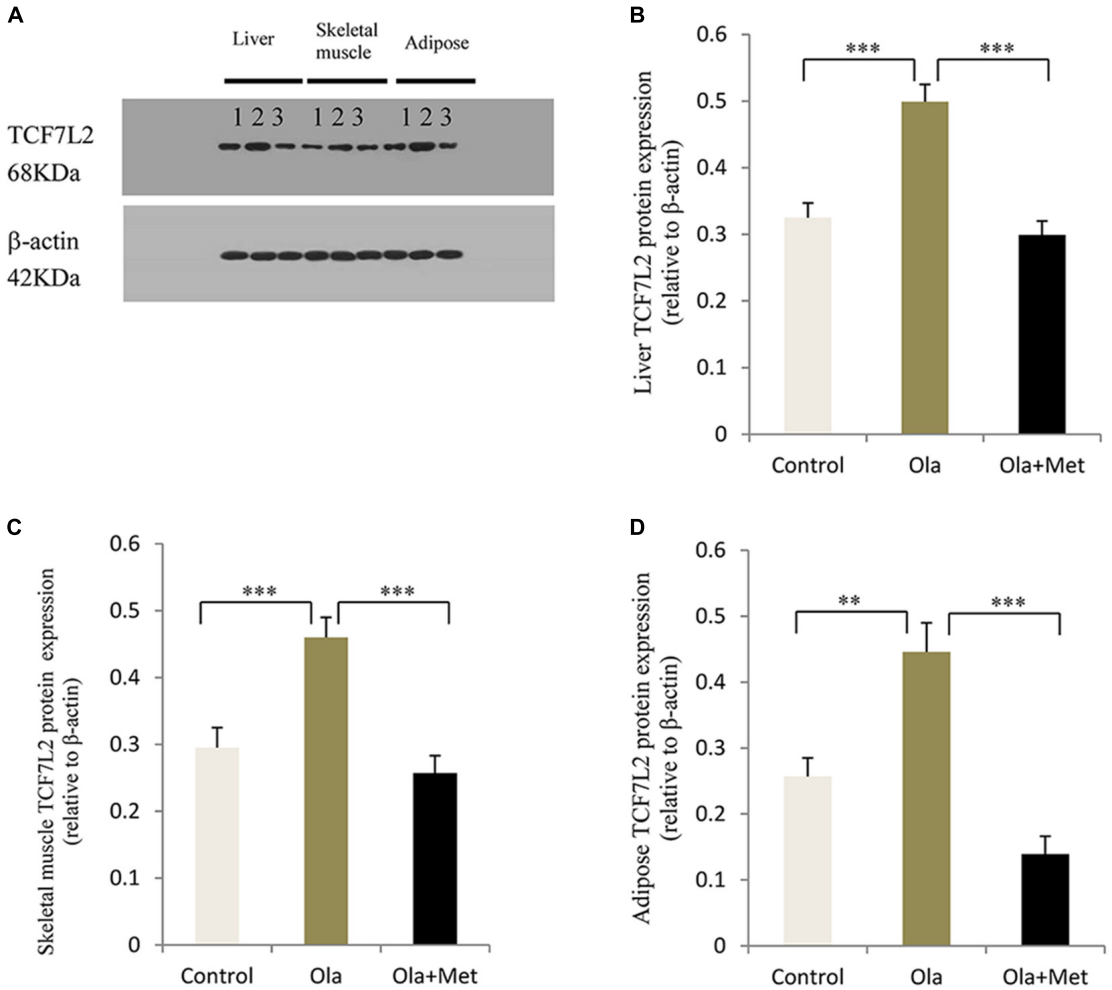

FIGURE 4 | Effect of olanzapine on TCF7L2 protein expression in liver, skeletal muscle, and adipose tissue in C57BL/6 mice. C57BL/6 mice were treated with olanzapine (4 mg/kg/day, Ola), olanzapine (4 mg/kg/day, Ola) + metformin (150 mg/kg/day, Met), or saline for 8 weeks. **(A)** Protein expression level of TCF7L2 in liver, skeletal muscle, and adipose tissue of mice was measured via western blotting. Representative immunoblot images of TCF7L2 are shown. 1, 2, and 3 represents Control, Ola, and Ola + Met group, respectively. **(B)** Quantitative analysis was used to qualify the TCF7L2 protein expression level in liver. **(C)** Quantitative analysis was used to qualify the TCF7L2 protein expression level in skeletal muscle. **(D)** Quantitative analysis was used to qualify the TCF7L2 protein expression level in adipose tissue. $n = 10$ for each group. All of the results are expressed as the mean ± SEM. $^{**}p < 0.01$, $^{***}p < 0.001$.

2013; Boyda et al., 2014). Therefore, we examined the effects of metformin against olanzapine-induced metabolic abnormalities. Our findings are consistent with previous studies, that metformin could ameliorate olanzapine-induced metabolic abnormalities, such as weight gain, glucose intolerance, and insulin resistance. Meanwhile, metformin reduced TCF7L2 protein expression in liver, skeletal muscle, and adipose tissues, which is much higher in olanzapine treatment group, suggesting a close association between olanzapine-induced metabolic disturbance and TCF7L2 expression. The results were further supported by the fact that obesity surgery-induced weight loss could regulate the alternative splicing of TCF7L2 in subcutaneous fat. Moreover, the TCF7L2 variant is associated with fasting glucose as well as impaired insulin action in adipose tissue (Kaminska et al., 2012).

TCF7L2 is one of the strongest susceptibility genes for T2DM across different ethnicities (Grant et al., 2006). Among the *TCF7L2* polymorphisms-associated metabolic disturbance, the T-allele of rs7903146 in *TCF7L2* is the most consistent loci which is linked to schizophrenia and schizoaffective disorders (Hansen et al., 2011). As a component of the β-catenin/TCF transcription factor, TCF7L2 plays an important role in conveying Wnt signaling pathway in regulating gene expression. It has been suggested that Wnt signaling pathway and β-catenin/transcription factor could suppress hepatic gluconeogenesis through a liver-specific TCF7L2 dominant-negative transgenic mouse model (Ip et al., 2015). Animal studies also reported a strong association between liver-specific TCF7L2 overexpression and increased hepatic glucose production, and as an example, liver-specific TCF7L2 overexpression could increase hepatic glucose production (Boj et al., 2012). The role of TCF7L2 extends to non-pancreatic tissues, a recent study that revealed that *TCF7L2* overexpression in non-pancreatic tissues leads to

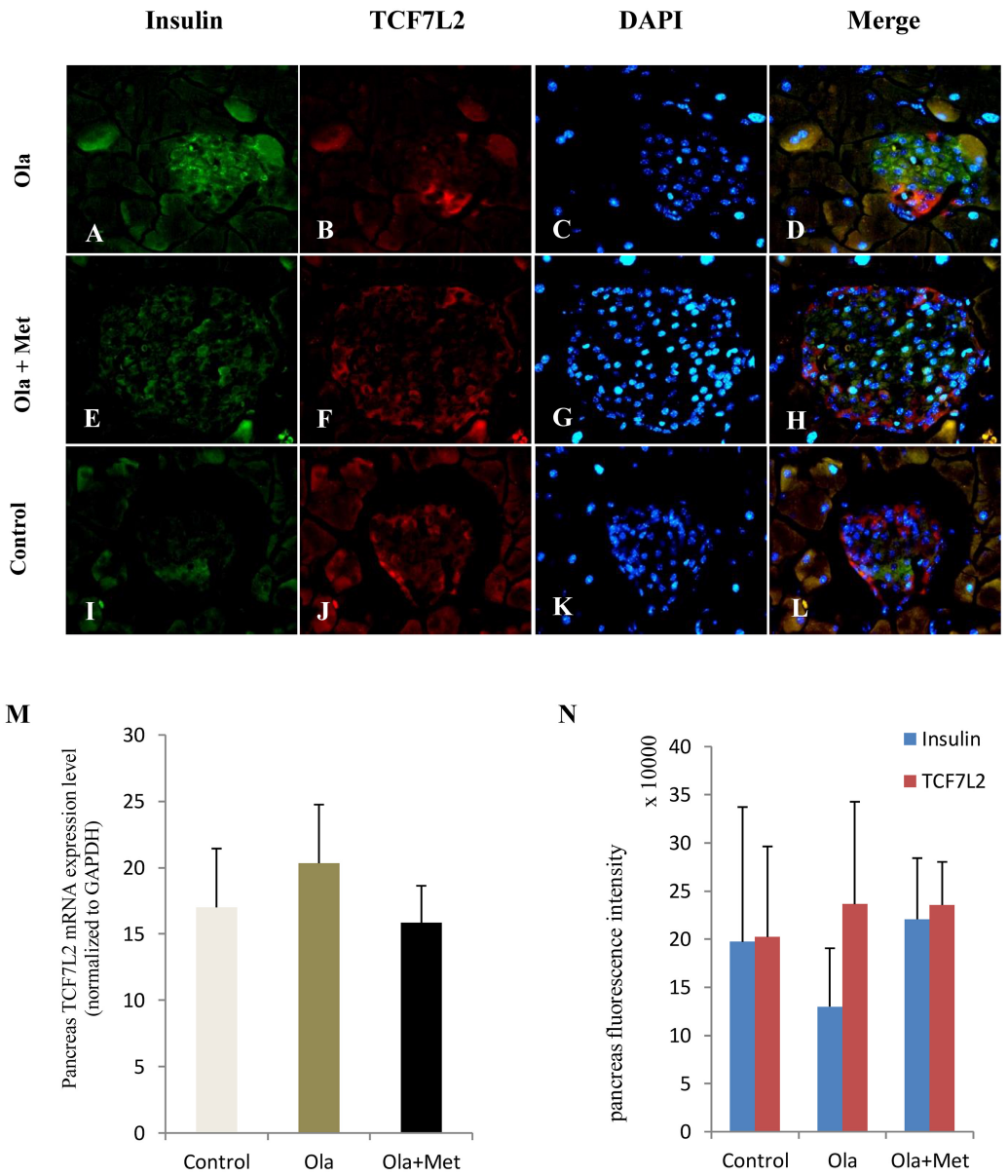

FIGURE 5 | Effect of olanzapine on expressions of TCF7L2 in pancreas islets in C57BL/6 mice. C57BL/6 mice were treated with olanzapine (4 mg/kg/day, Ola), olanzapine (4 mg/kg/day, Ola) + metformin (150 mg/kg/day, Met), or saline for 8 weeks. **(A–L)** Representative images of immunofluorescence images of islets stained with antibodies to insulin (green), TCF7L2 (red), and DAPI (blue). Microscopic magnification 400×. **(M)** Quantitative analysis of *TCF7L2* mRNA expression in pancreas islets. $n = 4$ for each group. **(N)** Quantitative analysis of TCF7L2 protein expression in pancreas islets. Values are expressed as the mean ± SEM. Total pancreatic fluorescence intensity was quantified using the Image J 1.37c. $n = 4$ for each group.

worsened glucose intolerance, and that the function of TCF7L2 in maintaining glucose metabolic balance in peripheral tissues may be more robust (Bailey et al., 2015). Previous studies have shown that antipsychotic medications may exert their actions by modulating the activity and expression of Akt/GSK-3β and Wnt-related intracellular signaling factors (Freyberg et al., 2010; Sutton and Rushlow, 2011). For example, administration of haloperidol or clozapine could alter GSK-3 and β-catenin protein levels in the rat prefrontal cortex while both GSK-3 and TCF7L2 transcription factors are key downstream regulators in the canonical Wnt/β-catenin pathway (Struewing et al., 2010). Our data imply that the altered TCF7L2 expression may be related to the effect of olanzapine on metabolic tissues.

In the present study, TCF7L2 protein levels were significantly higher in the liver, skeletal muscle, and adipose tissues of the olanzapine-treated mice than that in the control, and significantly lower in metformin-plus-olanzapine-treated mice. Interestingly, TCF7L2 protein expression in the liver, skeletal muscle, and adipose tissues was positively correlated with changes in body weight, fasting insulin, HOMA-IR, and AUCg.

To our knowledge, this is the first animal study to examine the association between TCF7L2 expression and olanzapine-induced metabolic abnormalities. The function of TCF7L2 in pancreas is well-studied using TCF7L2-overexpressing transgenic mice, Savic et al. (2011) have demonstrated robust glucose intolerance in multiple non-pancreatic tissues, including brain, stomach, intestine, and pancreas, and *TCF7L2*-null mice displayed improved glucose tolerance and lower insulin levels. Similarly, liver-specific knockout mice exhibit improved glucose homeostasis, and that liver-specific overexpression of *TCF7L2* mRNA leads to hepatic glucose production (Boj et al., 2012). Similarly, feeding can influence the overexpression of *TCF7L2* mRNA in epididymal fat tissue of C57BL/6J mice; moreover, high concentrations of insulin could inhibit the TCF7L2 level in adipocytes (Chen et al., 2015). Our data demonstrated that TCF7L2 expression in the liver and adipose tissue may play a critical role in regulating glucose metabolism. An explanation for the altered TCF7L2 expression in liver and adipose tissues may be related to weight gain, insulin resistance, and insulin level elevation induced by APPs. Interestingly, hyperinsulinemia could increase TCF7L2 mRNA expression, and subjects with low insulin sensitivity had higher TCF7L2 mRNA expression in skeletal muscle tissue (Karczewska-Kupczewska et al., 2016). In line with these data, we hypothesize that increased TCF7L2 expression in skeletal muscle might promote glucose uptake during insulin resistance conditions. Despite of the observed changes in TCF7L2 expression in liver, skeletal muscle, and adipose tissue, we did not use inhibitors to antagonize or suppress TCF7L2 specifically, and thus it remains uncertain whether the olanzapine-induced metabolic dysfunction is mediated by TCF7L2. Intriguingly, a study of African-American patients with schizophrenia reported an interaction between APPs treatment and TCF7L2 under a multiplicative scale (Irvin et al., 2009). Indeed, as APPs may alleviate symptoms of schizophrenia through Wnt signaling pathway mediated by D_2 dopamine receptor (Sutton et al., 2007), our results emphasize the potential pharmacogenetical and clinical relevance of TCF7L2 for antipsychotic-induced metabolic dysfunction in schizophrenia and provide a novel mechanism of TCF7L2 in antipsychotic-induced metabolic disturbance. However, further studies are needed to determine the role of TCF7L2 and other components of Wnt signaling pathway in antipsychotic-induced metabolic disturbance.

Notably, the mRNA and protein expression levels of TCF7L2 in pancreas did not differ in different groups in our study. By contrast, previous studies reported that TCF7L2 expression in human islets increased by fivefolds in T2DM compared with nondiabetic individuals (Lyssenko et al., 2007). *In vitro*, elevated glucose concentration can reduce beta-cell proliferation and induce beta-cell apoptosis in cultured human islets, and these effects are reversible by TCF7L2 overexpression. By contrast, a previous study reported an opposite direction of regulating the level of TCF7L2 mRNA (upregulated) and protein (downregulated) in islets in diabetes (Le Bacquer et al., 2011). We observed no alterations in TCF7L2 expression in the pancreatic tissue, although the TCF7L2 is frequently considered to have physiological effects on β cells. The precise nature of the TCF7L2 expression in pancreatic and its etiological basis in APPs-induced metabolic disturbance remains the subject of future study.

Interestingly, oxidative stress also plays a key role in the higher incidence of metabolic dysfunction of schizophrenia. For example, Schiavone et al. (2017) found that redox imbalance plays a crucial role in the visceral fat elevation in an animal model of psychosis. Also, abnormal oxidative stress has been reported in first episode patients with schizophrenia, with increased level of thiobarbituric acid reactive substances and malondialdehyde, which are important end-point products of lipid peroxidation (Flatow et al., 2013). Indeed, in addition to a role in the pathophysiology of schizophrenia, oxidative stress has also been implicated in antipsychotic-induced metabolic dysfunction (Baig et al., 2010; Gilca et al., 2014). It has been reported that lipid peroxidation was altered in rat liver and brain following antipsychotic administration in rats, moreover, APPs can also elevate lipid peroxidation in human plasma (Dietrich-Muszalska et al., 2013). However, how antipsychotic work on antioxidant enzymes appears controversial and inconsistent (Parikh et al., 2003; Martins et al., 2008; Andreazza et al., 2015) in rat brain tissue after antipsychotic administration. A recent meta-analysis (Flatow et al., 2013) also revealed that there is no replicable and significant correlation between oxidative stress indexes and clinical features. Given previous studies of altered lipid peroxidation in antipsychotic-treated rats, and oxidative stress is closely related to insulin resistance (Ando and Fujita, 2009), the potential role of oxidative stress in antipsychotic-induced metabolic dysfunction should be further elucidated.

This study has several limitations. Firstly, we utilized healthy adult mice to analyze the mechanism of olanzapine-induced metabolic disturbance. The use of a mouse model for schizophrenia would be more reasonable given that schizophrenia itself may predispose individuals to T2DM. Secondly, the limited serum volume did not allow us to measure the *TCF7L2* mRNA levels in the liver, skeletal muscle, and adipose tissues, which can be a mediator of the observed outcomes. Thirdly, although significant differences in TCF7L2 protein expression were detected in the mentioned tissues, detecting the differences of TCF7L2 expression in mice brain and gut tissues is also a sensible approach, since proglucagon gene expression in brain and gut may be controlled by TCF7L2 and Wnt signaling pathway (Shao W. et al., 2013). Finally, we only observed the effects of single antipsychotic, single dose of olanzapine, and one antidiabetic drug. Because of many atypical APPs could induce metabolic dysregulation and multiple type of antidiabetic drug could treat diabetes, it is necessary to determine whether such findings with olanzapine apply to other APPs. Further studies are required to detect the difference in metabolic measures between antipsychotic-treated normal and specific-tissue knockout mice.

CONCLUSION

Our study illustrates that olanzapine induces weight gain, fasting insulin elevation, glucose intolerance, and increase of TCF7L2 protein expression in liver, skeletal muscle, and adipose tissues of mice. These metabolic abnormalities and the increased TCF7L2

expression in those tissues could be effectively ameliorated by metformin. TCF7L2 overexpression in liver, skeletal muscle, and adipose tissues may represent a potential mechanism through which metabolic changes occurred following olanzapine treatment.

AUTHOR CONTRIBUTIONS

RL, JO, LL, and YY conducted all the experiments and collected all data. RL analyzed the data and wrote the first draft of the manuscript. JO organized the database. RW and JZ supervised the whole work. All authors contributed to manuscript revision and approved the submitted version.

FUNDING

The research was supported by grant 2016YFC1306900 from the National Key Research and Development Program of China and the National Natural Science Foundation of China (Grant Nos. 81371481 and 81622018).

REFERENCES

Albaugh, V. L., Henry, C. R., Bello, N. T., Hajnal, A., Lynch, S. L., and Halle, B. et al. (2006). Hormonal and metabolic effects of olanzapine and clozapine related to body weight in rodents. *Obesity* 14, 36–51. doi: 10.1038/oby.2006.6

Albaugh, V. L., Vary, T. C., Ilkayeva, O., Wenner, B. R., Maresca, K. P., and Joyal, J. L. et al. (2012). Atypical antipsychotics rapidly and inappropriately switch peripheral fuel utilization to lipids, impairing metabolic flexibility in rodents. *Schizophr. Bull.* 38, 153–166. doi: 10.1093/schbul/sbq053

Alimohamad, H., Rajakumar, N., Seah, Y. H., and Rushlow, W. (2005a). Antipsychotics alter the protein expression levels of beta-catenin and GSK-3 in the rat medial prefrontal cortex and striatum. *Biol. Psychiatry* 57, 533–542. doi: 10.1016/j.biopsych.2004.11.036

Alimohamad, H., Sutton, L., Mouyal, J., Rajakumar, N., and Rushlow, W. J. (2005b). The effects of antipsychotics on beta-catenin, glycogen synthase kinase-3 and dishevelled in the ventral midbrain of rats. *J. Neurochem.* 95, 513–525. doi: 10.1111/j.1471-4159.2005.03388.x

Alkelai, A., Greenbaum, L., Lupoli, S., Kohn, Y., Sarner-Kanyas, K., and Ben-Asher, E. et al. (2012). Association of the type 2 diabetes mellitus susceptibility gene, TCF7L2, with schizophrenia in an Arab-Israeli family sample. *PLoS One* 7:e29228. doi: 10.1371/journal.pone.0029228

Alvarez-Jimenez, M., Gonzalez-Blanch, C., Crespo-Facorro, B., Hetrick, S., Rodriguez-Sanchez, J. M., and Perez-Iglesias, R. et al. (2008). Antipsychotic-induced weight gain in chronic and first-episode psychotic disorders: a systematic critical reappraisal. *CNS Drugs* 22, 547–562. doi: 10.2165/00023210-200822070-00002

Ando, K., and Fujita, T. (2009). Metabolic syndrome and oxidative stress. *Free Radic. Biol. Med.* 47, 213–218. doi: 10.1016/j.freeradbiomed.2009.04.030

Andreazza, A. C., Barakauskas, V. E., Fazeli, S., Feresten, A., Shao, L., and Wei, V. et al. (2015). Effects of haloperidol and clozapine administration on oxidative stress in rat brain, liver and serum. *Neurosci. Lett.* 591, 36–40. doi: 10.1016/j.neulet.2015.02.028

Baig, M. R., Navaira, E., Escamilla, M. A., Raventos, H., and Walss-Bass, C. (2010). Clozapine treatment causes oxidation of proteins involved in energy metabolism in lymphoblastoid cells: a possible mechanism for antipsychotic-induced metabolic alterations. *J. Psychiatr. Pract.* 16, 325–333. doi: 10.1097/01.pra.0000388627.36781.6a

Bailey, K. A., Savic, D., Zielinski, M., Park, S. Y., Wang, L. J., and Witkowski, P. et al. (2015). Evidence of non-pancreatic beta cell-dependent roles of Tcf7l2 in the regulation of glucose metabolism in mice. *Hum. Mol. Genet.* 24, 1646–1654. doi: 10.1093/hmg/ddu577

Boj, S. F., van Es, J. H., Huch, M., Li, V. S., Jose, A., and Hatzis, P. et al. (2012). Diabetes risk gene and Wnt effector Tcf7l2/TCF4 controls hepatic response to perinatal and adult metabolic demand. *Cell* 151, 1595–1607. doi: 10.1016/j.cell.2012.10.053

Boyda, H. N., Procyshyn, R. M., Asiri, Y., Wu, C., Wang, C. K., and Lo, R. et al. (2014). Antidiabetic-drug combination treatment for glucose intolerance in adult female rats treated acutely with olanzapine. *Prog. Neuropsychopharmacol. Biol. Psychiatry* 48, 170–176. doi: 10.1016/j.pnpbp.2013.10.006

Chadda, R. K., Ramshankar, P., Deb, K. S., and Sood, M. (2013). Metabolic syndrome in schizophrenia: differences between antipsychotic-naive and treated patients. *J. Pharmacol. Pharmacother.* 4, 176–186. doi: 10.4103/0976-500X.114596

Chen, C. H., Huang, M. C., Kao, C. F., Lin, S. K., Kuo, P. H., and Chiu, C. C. et al. (2013). Effects of adjunctive metformin on metabolic traits in nondiabetic clozapine-treated patients with schizophrenia and the effect of metformin discontinuation on body weight: a 24-week, randomized, double-blind, placebo-controlled study. *J. Clin. Psychiatry* 74, e424–e430. doi: 10.4088/JCP.12m08186

Chen, Z. L., Shao, W. J., Xu, F., Liu, L., Lin, B. S., and Wei, X. H. et al. (2015). Acute Wnt pathway activation positively regulates leptin gene expression in mature adipocytes. *Cell. Signal.* 27, 587–597. doi: 10.1016/j.cellsig.2014.12.012

Clevers, H. (2006). Wnt/beta-catenin signaling in development and disease. *Cell* 127, 469–480. doi: 10.1016/j.cell.2006.10.018

Coccurello, R., Brina, D., Caprioli, A., Conti, R., Ghirardi, O., and Schepis, F. et al. (2009). 30 days of continuous olanzapine infusion determines energy imbalance, glucose intolerance, insulin resistance, and dyslipidemia in mice. *J. Clin. Psychopharmacol.* 29, 576–583. doi: 10.1097/JCP.0b013e3181bfe13e

Cooper, G. D., Pickavance, L. C., Wilding, J. P., Harrold, J. A., Halford, J. C., and Goudie, A. J. (2007). Effects of olanzapine in male rats: enhanced adiposity in the absence of hyperphagia, weight gain or metabolic abnormalities. *J. Psychopharmacol.* 21, 405–413. doi: 10.1177/0269881106069637

De Hert, M., Dobbelaere, M., Sheridan, E. M., Cohen, D., and Correll, C. U. (2011). Metabolic and endocrine adverse effects of second-generation antipsychotics in children and adolescents: a systematic review of randomized, placebo controlled trials and guidelines for clinical practice. *Eur. Psychiatry* 26, 144–158. doi: 10.1016/j.eurpsy.2010.09.011

Dietrich-Muszalska, A., Kopka, J., and Kwiatkowska, A. (2013). The effects of ziprasidone, clozapine and haloperidol on lipid peroxidation in human plasma (in vitro): comparison. *Neurochem. Res.* 38, 1490–1495. doi: 10.1007/s11064-013-1050-z

Dora, J. M., Kramer, C. K., and Canani, L. H. (2008). Standards of medical care in diabetes–2008: response to Hirsch, Inzucchi, and Kirkman. *Diabetes Care* 31:e44.. doi: 10.2337/dc08-0109

Flatow, J., Buckley, P., and Miller, B. J. (2013). Meta-analysis of oxidative stress in schizophrenia. *Biol. Psychiatry* 74, 400–409. doi: 10.1016/j.biopsych.2013.03.018

Freyberg, Z., Ferrando, S. J., and Javitch, J. A. (2010). Roles of the Akt/GSK-3 and Wnt signaling pathways in schizophrenia and antipsychotic drug action. *Am. J. Psychiatry* 167, 388–396. doi: 10.1176/appi.ajp.2009.08121873

Gilca, M., Piriu, G., Gaman, L., Delia, C., Iosif, L., and Atanasiu, V. et al. (2014). A study of antioxidant activity in patients with schizophrenia taking atypical antipsychotics. *Psychopharmacology* 231, 4703–4710. doi: 10.1007/s00213-014-3624-0

Girault, E. M., Guigas, B., Alkemade, A., Foppen, E., Ackermans, M. T., and la Fleur, S. E. et al. (2014). Chronic treatment with olanzapine increases adiposity by changing fuel substrate and causes desensitization of the acute metabolic side effects. *Naunyn Schmiedebergs Arch. Pharmacol.* 387, 185–195. doi: 10.1007/s00210-013-0933-5

Grant, S. F. (2012). Understanding the elusive mechanism of action of TCF7L2 in metabolism. *Diabetes Metab. Res. Rev.* 61, 2657–2658. doi: 10.2337/db12-0891

Grant, S. F., Thorleifsson, G., Reynisdottir, I., Benediktsson, R., Manolescu, A., and Sainz, J. et al. (2006). Variant of transcription factor 7-like 2 (TCF7L2) gene confers risk of type 2 diabetes. *Nat. Genet.* 38, 320–323. doi: 10.1038/ng1732

Hansen, T., Ingason, A., Djurovic, S., Melle, I., Fenger, M., and Gustafsson, O. et al. (2011). At-risk variant in TCF7L2 for type II diabetes increases risk of schizophrenia. *Biol. Psychiatry* 70, 59–63. doi: 10.1016/j.biopsych.2011.01.031

Hasnain, M., Vieweg, W. V., and Fredrickson, S. K. (2010). Metformin for atypical antipsychotic-induced weight gain and glucose metabolism dysregulation: review of the literature and clinical suggestions. *CNS Drugs* 24, 193–206. doi: 10.2165/11530130-000000000-00000

Hennekens, C. H., Hennekens, A. R., Hollar, D., and Casey, D. E. (2005). Schizophrenia and increased risks of cardiovascular disease. *Am. Heart J.* 150, 1115–1121. doi: 10.1016/j.ahj.2005.02.007

Horska, K., Ruda-Kucerova, J., Babinska, Z., Karpisek, M., Demlova, R., and Opatrilova, R. et al. (2016). Olanzapine-depot administration induces time-dependent changes in adipose tissue endocrine function in rats. *Psychoneuroendocrinology* 73, 177–185. doi: 10.1016/j.psyneuen.2016.07.218

Ip, W., Shao, W., Song, Z., Chen, Z., Wheeler, M. B., and Jin, T. (2015). Liver-specific expression of dominant-negative transcription factor 7-like 2 causes progressive impairment in glucose homeostasis. *Diabetes Metab. Res. Rev.* 64, 1923–1932. doi: 10.2337/db14-1329

Irvin, M. R., Wiener, H. W., Perry, R. P., Savage, R. M., and Go, R. C. (2009). Genetic risk factors for type 2 diabetes with pharmacologic intervention in African-American patients with schizophrenia or schizoaffective disorder. *Schizophr. Res.* 114, 50–56. doi: 10.1016/j.schres.2009.07.008

Jarskog, L. F., Hamer, R. M., Catellier, D. J., Stewart, D. D., Lavange, L., and Ray, N. et al. (2013). Metformin for weight loss and metabolic control in overweight outpatients with schizophrenia and schizoaffective disorder. *Am. J. Psychiatry* 170, 1032–1040. doi: 10.1176/appi.ajp.2013.12010127

Jin, T., and Liu, L. (2008). The Wnt signaling pathway effector TCF7L2 and type 2 diabetes mellitus. *Mol. Endocrinol.* 22, 2383–2392. doi: 10.1210/me.2008-0135

Kaminska, D., Kuulasmaa, T., Venesmaa, S., Kakela, P., Vaittinen, M., and Pulkkinen, L. et al. (2012). Adipose tissue TCF7L2 splicing is regulated by weight loss and associates with glucose and fatty acid metabolism. *Diabetes Metab. Res. Rev.* 61, 2807–2813. doi: 10.2337/db12-0239

Karczewska-Kupczewska, M., Stefanowicz, M., Matulewicz, N., Nikolajuk, A., and Straczkowski, M. (2016). Wnt signaling genes in adipose tissue and skeletal muscle of humans with different degrees of insulin sensitivity. *J. Clin. Endocrinol. Metab.* 101, 3079–3087. doi: 10.1210/jc.2016-1594

Kaushal, J., Bhutani, G., and Gupta, R. (2012). Comparison of fasting blood sugar and serum lipid profile changes after treatment with atypical antipsychotics olanzapine and risperidone. *Singapore Med. J.* 53, 488–492.

Kim, H., Park, M., Lee, S. K., Jeong, J., Namkoong, K., and Cho, H. S. et al. (2014). Phosphorylation of hypothalamic AMPK on serine(485/491) related to sustained weight loss by alpha-lipoic acid in mice treated with olanzapine. *Psychopharmacology* 231, 4059–4069. doi: 10.1007/s00213-014-3540-3

Kirpichnikov, D., McFarlane, S. I., and Sowers, J. R. (2002). Metformin: an update. *Ann. Intern. Med.* 137, 25–33. doi: 10.7326/0003-4819-137-1-200207020-00009

Komossa, K., Rummel-Kluge, C., Hunger, H., Schmid, F., Schwarz, S., and Duggan, L. et al. (2010). Olanzapine versus other atypical antipsychotics for schizophrenia. *Cochrane Database Syst. Rev.* 3:CD006654. doi: 10.1002/14651858.CD006654.pub2

Koro, C. E., Fedder, D. O., L'Italien, G. J., Weiss, S., Magder, L. S., and Kreyenbuhl, J. et al. (2002). An assessment of the independent effects of olanzapine and risperidone exposure on the risk of hyperlipidemia in schizophrenic patients. *Arch. Gen. Psychiatry* 59, 1021–1026. doi: 10.1001/archpsyc.59.11.1021

Koros, E., and Dorner-Ciossek, C. (2007). The role of glycogen synthase kinase-3beta in schizophrenia. *Drug News Perspect.* 20, 437–445. doi: 10.1358/dnp.2007.20.7.1149632

Kroeze, W. K., Hufeisen, S. J., Popadak, B. A., Renock, S. M., Steinberg, S., and Ernsberger, P. et al. (2003). H1-histamine receptor affinity predicts short-term weight gain for typical and atypical antipsychotic drugs. *Neuropsychopharmacology* 28, 519–526. doi: 10.1038/sj.npp.1300027

Lakka, H. M., Laaksonen, D. E., Lakka, T. A., Niskanen, L. K., Kumpusalo, E., and Tuomilehto, J. et al. (2002). The metabolic syndrome and total and cardiovascular disease mortality in middle-aged men. *JAMA* 288, 2709–2716. doi: 10.1001/jama.288.21.2709

Le Bacquer, O., Shu, L., Marchand, M., Neve, B., Paroni, F., and Kerr, C. J. et al. (2011). TCF7L2 splice variants have distinct effects on beta-cell turnover and function. *Hum. Mol. Genet.* 20, 1906–1915. doi: 10.1093/hmg/ddr072

Li, Q., Chen, D., Liu, T., Walss-Bass, C., de Quevedo, J. L., and Soares, J. C. et al. (2016). Sex differences in body mass index and obesity in chinese patients with chronic schizophrenia. *J. Clin. Psychopharmacol.* 36, 643–648. doi: 10.1097/JCP.0000000000000594

Lyssenko, V., Lupi, R., Marchetti, P., Del, G. S., Orho-Melander, M., and Almgren, P. et al. (2007). Mechanisms by which common variants in the TCF7L2 gene increase risk of type 2 diabetes. *J. Clin. Invest.* 117, 2155–2163. doi: 10.1172/JCI30706

MacDonald, B. T., Tamai, K., and He, X. (2009). Wnt/beta-catenin signaling: components, mechanisms, and diseases. *Dev. Cell* 17, 9–26. doi: 10.1016/j.devcel.2009.06.016

Malhotra, N., Grover, S., Chakrabarti, S., and Kulhara, P. (2013). Metabolic syndrome in schizophrenia. *Indian J. Psychol. Med.* 35, 227–240. doi: 10.4103/0253-7176.119471

Martins, M. R., Petronilho, F. C., Gomes, K. M., Dal-Pizzol, F., Streck, E. L., and Quevedo, J. (2008). Antipsychotic-induced oxidative stress in rat brain. *Neurotox. Res.* 13, 63–69. doi: 10.1007/BF03033368

Mather, K. (2009). Surrogate measures of insulin resistance: of rats, mice, and men. *Am. J. Physiol. Endocrinol. Metab.* 296, E398–E399. doi: 10.1152/ajpendo.90889.2008

Mathieu, P., Poirier, P., Pibarot, P., Lemieux, I., and Despres, J. (2009). Visceral obesity the link among inflammation, hypertension, and cardiovascular disease. *Hypertension* 53, 577–584. doi: 10.1161/HYPERTENSIONAHA.108.110320

Matsui, Y., Hirasawa, Y., Sugiura, T., Toyoshi, T., Kyuki, K., and Ito, M. (2010). Metformin reduces body weight gain and improves glucose intolerance in high-fat diet-fed C57BL/6J mice. *Biol. Pharm. Bull.* 33, 963–970. doi: 10.1248/bpb.33.963

Mitchell, A. J., Vancampfort, D., De Herdt, A., Yu, W., and De Hert, M. (2013a). Is the prevalence of metabolic syndrome and metabolic abnormalities increased in early schizophrenia? A comparative meta-analysis of first episode, untreated and treated patients. *Schizophr. Bull.* 39, 295–305. doi: 10.1093/schbul/sbs082

Mitchell, A. J., Vancampfort, D., Sweers, K., van Winkel, R., Yu, W., and De Hert, M. (2013b). Prevalence of metabolic syndrome and metabolic abnormalities in schizophrenia and related disorders–a systematic review and meta-analysis. *Schizophr. Bull.* 39, 306–318. doi: 10.1093/schbul/sbr148

Newcomer, J. W. (2007). Antipsychotic medications: metabolic and cardiovascular risk. *J. Clin. Psychiatry* 68(Suppl 4), 8–13.

NRCU Research (1996). *Guide for the Care and Use of Laboratory Animals*. Washington, DC: National Academies Press.

Parikh, V., Khan, M. M., and Mahadik, S. P. (2003). Differential effects of antipsychotics on expression of antioxidant enzymes and membrane lipid peroxidation in rat brain. *J. Psychiatr. Res.* 37, 43–51. doi: 10.1016/S0022-3956(02)00048-1

Peifer, M., and Polakis, P. (2000). Wnt signaling in oncogenesis and embryogenesis–a look outside the nucleus. *Science* 287, 1606–1609. doi: 10.1126/science.287.5458.1606

Perez-Iglesias, R., Martinez-Garcia, O., Pardo-Garcia, G., Amado, J. A., Garcia-Unzueta, M. T., and Tabares-Seisdedos, R. et al. (2013). Course of weight gain and metabolic abnormalities in first treated episode of psychosis: the first year is a critical period for development of cardiovascular risk factors. *Int. J. Neuropsychopharmacol.* 17, 41–51. doi: 10.1017/S1461145713001053

Praharaj, S. K., Jana, A. K., Goyal, N., and Sinha, V. K. (2011). Metformin for olanzapine-induced weight gain: a systematic review and meta-analysis. *Br. J. Clin. Pharmacol.* 71, 377–382. doi: 10.1111/j.1365-2125.2010.03783.x

Pramyothin, P., and Khaodhiar, L. (2010). Metabolic syndrome with the atypical antipsychotics. *Curr. Opin. Endocrinol. Diabetes Obes.* 17, 460–466. doi: 10.1097/MED.0b013e32833de61c

Raedler, T. J. (2010). Cardiovascular aspects of antipsychotics. *Curr. Opin. Psychiatry* 23, 574–581. doi: 10.1097/YCO.0b013e32833f46c9

Rethelyi, J., and Sawalhe, A. D. (2011). [Comorbidity of metabolic syndrome, diabetes and schizophrenia: theoretical and practical considerations]. *Orv. Hetil.* 152, 505–511. doi: 10.1556/OH.2011.29079

Rheaume, C., Arsenault, B. J., Belanger, S., Perusse, L., Tremblay, A., and Bouchard, C. et al. (2009). Visceral obesity, cardiorespiratory fitness, and blood pressure in healthy middle-aged men and women. *Circulation* 119, E275–E275. doi: 10.1161/HYPERTENSIONAHA.111.180349

Ryan, M. C., Collins, P., and Thakore, J. H. (2003). Impaired fasting glucose tolerance in first-episode, drug-naive patients with schizophrenia. *Am. J. Psychiatry* 160, 284–289. doi: 10.1176/appi.ajp.160.2.284

Ryan, M. C., Flanagan, S., Kinsella, U., Keeling, F., and Thakore, J. H. (2004). The effects of atypical antipsychotics on visceral fat distribution in first episode, drug-naive patients with schizophrenia. *Life Sci.* 74, 1999–2008. doi: 10.1016/j.lfs.2003.08.044

Savic, D., Ye, H., Aneas, I., Park, S. Y., Bell, G. I., and Nobrega, M. A. (2011). Alterations in TCF7L2 expression define its role as a key regulator of glucose metabolism. *Genome Res.* 21, 1417–1425. doi: 10.1101/gr.123745.111

Savoy, Y. E., Ashton, M. A., Miller, M. W., Nedza, F. M., Spracklin, D. K., and Hawthorn, M. H. et al. (2010). Differential effects of various typical and atypical antipsychotics on plasma glucose and insulin levels in the mouse: evidence for the involvement of sympathetic regulation. *Schizophr. Bull.* 36, 410–418. doi: 10.1093/schbul/sbn104

Schiavone, S., Camerino, G. M., Mhillaj, E., Zotti, M., Colaianna, M., and De Giorgi, A. et al. (2017). Visceral fat dysfunctions in the rat social isolation model of psychosis. *Front. Pharmacol.* 8:787. doi: 10.3389/fphar.2017.00787

Schmittgen, T. D., and Livak, K. J. (2008). Analyzing real-time PCR data by the comparative C(T) method. *Nat. Protoc.* 3, 1101–1108. doi: 10.1038/nprot.2008.73

Schreiner, A., Niehaus, D., Shuriquie, N. A., Aadamsoo, K., Korcsog, P., and Salinas, R. et al. (2012). Metabolic effects of paliperidone extended release versus oral olanzapine in patients with schizophrenia: a prospective, randomized, controlled trial. *J. Clin. Psychopharmacol.* 32, 449–457. doi: 10.1097/JCP.0b013e31825cccad

Shao, P., Ou, J., Wu, R., Fang, M., Chen, H., and Xu, Y. et al. (2013). [Effects of ziprasidone and olanzapine on glucose and lipid metabolism in first-episode schizophrenia]. *Zhong Nan Da Xue Xue Bao Yi Xue Ban* 38, 365–369. doi: 10.3969/j.issn.1672-7347.2013.04.005

Shao, W., Wang, D., Chiang, Y. T., Ip, W., Zhu, L., and Xu, F. et al. (2013). The Wnt signaling pathway effector TCF7L2 controls gut and brain proglucagon gene expression and glucose homeostasis. *Diabetes Metab. Res. Rev.* 62, 789–800. doi: 10.2337/db12-0365

Singh, K. K. (2013). An emerging role for Wnt and GSK3 signaling pathways in schizophrenia. *Clin. Genet.* 83, 511–517. doi: 10.1111/cge.12111

Singh, R., De Aguiar, R. B., Naik, S., Mani, S., Ostadsharif, K., and Wencker, D. et al. (2013). LRP6 enhances glucose metabolism by promoting TCF7L2-dependent insulin receptor expression and IGF receptor stabilization in humans. *Cell Metab.* 17, 197–209. doi: 10.1016/j.cmet.2013.01.009

Skrede, S., Ferno, J., Vazquez, M. J., Fjaer, S., Pavlin, T., and Lunder, N. et al. (2012). Olanzapine, but not aripiprazole, weight-independently elevates serum triglycerides and activates lipogenic gene expression in female rats. *Int. J. Neuropsychopharmacol.* 15, 163–179. doi: 10.1017/S1461145711001271

Spelman, L. M., Walsh, P. I., Sharifi, N., Collins, P., and Thakore, J. H. (2007). Impaired glucose tolerance in first-episode drug-naive patients with schizophrenia. *Diabet. Med.* 24, 481–485. doi: 10.1111/j.1464-5491.2007.02092.x

Struewing, I., Boyechko, T., Barnett, C., Beildeck, M., Byers, S. W., and Mao, C. D. (2010). The balance of TCF7L2 variants with differential activities in Wnt-signaling is regulated by lithium in a GSK3beta-independent manner. *Biochem. Biophys. Res. Commun.* 399, 245–250. doi: 10.1016/j.bbrc.2010.07.062

Sutton, L. P., Honardoust, D., Mouyal, J., Rajakumar, N., and Rushlow, W. J. (2007). Activation of the canonical Wnt pathway by the antipsychotics haloperidol and clozapine involves dishevelled-3. *J. Neurochem.* 102, 153–169. doi: 10.1111/j.1471-4159.2007.04527.x

Sutton, L. P., and Rushlow, W. J. (2011). The effects of neuropsychiatric drugs on glycogen synthase kinase-3 signaling. *Neuroscience* 199, 116–124. doi: 10.1016/j.neuroscience.2011.09.056

Teff, K. L., Rickels, M. R., Grudziak, J., Fuller, C., Nguyen, H. L., and Rickels, K. (2013). Antipsychotic-induced insulin resistance and postprandial hormonal dysregulation independent of weight gain or psychiatric disease. *Diabetes Metab. Res. Rev.* 62, 3232–3240. doi: 10.2337/db13-0430

Tek, C., Kucukgoncu, S., Guloksuz, S., Woods, S. W., Srihari, V. H., and Annamalai, A. (2015). Antipsychotic-induced weight gain in first-episode psychosis patients: a meta-analysis of differential effects of antipsychotic medications. *Early Interv. Psychiatry* 10, 193–202. doi: 10.1111/eip.12251

Thakore, J. H., Mann, J. N., Vlahos, I., Martin, A., and Reznek, R. (2002). Increased visceral fat distribution in drug-naive and drug-free patients with schizophrenia. *Int. J. Obes. Relat. Metab. Disord.* 26, 137–141. doi: 10.1038/sj.ijo.0801840

Wang, M., Tong, J. H., Zhu, G., Liang, G. M., Yan, H. F., and Wang, X. Z. (2012). Metformin for treatment of antipsychotic-induced weight gain: a randomized, placebo-controlled study. *Schizophr. Res.* 138, 54–57. doi: 10.1016/j.schres.2012.02.021

Wu, R. R., Zhao, J. P., Zhai, J. G., Guo, X. F., and Guo, W. B. (2007). Sex difference in effects of typical and atypical antipsychotics on glucose-insulin homeostasis and lipid metabolism in first-episode schizophrenia. *J. Clin. Psychopharmacol.* 27, 374–379. doi: 10.1097/JCP.0b013e3180cac8db

Xu, M. Q., Xing, Q. H., Zheng, Y. L., Li, S., Gao, J. J., and He, G. et al. (2007). Association of AKT1 gene polymorphisms with risk of schizophrenia and with response to antipsychotics in the Chinese population. *J. Clin. Psychiatry* 68, 1358–1367. doi: 10.4088/JCP.v68n0906

Yang, H., Li, Q., Lee, J. H., and Shu, Y. (2012). Reduction in Tcf7l2 expression decreases diabetic susceptibility in mice. *Int. J. Biol. Sci.* 8, 791–801. doi: 10.7150/ijbs.4568

Zugno, A. I., Barcelos, M., Oliveira, L., Canever, L., Luca, R. D., and Fraga, D. B. et al. (2012). Energy metabolism, leptin, and biochemical parameters are altered in rats subjected to the chronic administration of olanzapine. *Rev. Bras. Psiquiatr.* 34, 168–175. doi: 10.1590/S1516-44462012000200009

Conflict of Interest Statement: The authors declare that the research was conducted in the absence of any commercial or financial relationships that could be construed as a potential conflict of interest.

frontiers in Neuroscience

ORIGINAL RESEARCH
published: 11 May 2018
doi: 10.3389/fnins.2018.00296

Altered Serum Tumor Necrosis Factor and Interleukin-1β in First-Episode Drug-Naive and Chronic Schizophrenia

*Furong Zhu[1], Lulu Zhang[2], Fang Liu[3], Renrong Wu[1], Wenbin Guo[1], Jianjun Ou[1], Xiangyang Zhang[4] and Jingping Zhao[1,5]**

[1] Mental Health Institute of the Second Xiangya Hospital, Central South University, Chinese National Clinical Research Center on Mental Health Disorders, Chinese National Technology Institute on Mental Disorders, Hunan Key Laboratory of Psychiatry and Mental Health, Changsha, China, [2] Department of Psychiatry, Guangzhou First People's Hospital, the Second Affiliated Hospital of South China University of Technology, Guangzhou, China, [3] First Affiliated Hospital of Kunming Medical University, Kunming, China, [4] Department of Psychiatry and Behavioral Sciences, UT Houston Medical School, The University of Texas Health Science Center, Houston, TX, United States, [5] Guangzhou Hui Ai Hospital, Affliated Brain Hospital of Guangzhou Medical University, Guangzhou, China

OPEN ACCESS

Edited by:
Pei Jiang,
Jining Medical University, China

Reviewed by:
Luigia Trabace,
University of Foggia, Italy
Luc Ver Donck,
Janssen Research & Development, Belgium

***Correspondence:**
Jingping Zhao
zhaojingping@csu.edu.cn

Specialty section:
This article was submitted to Neuropharmacology, a section of the journal Frontiers in Neuroscience

Received: *11 December 2017*
Accepted: *16 April 2018*
Published: *11 May 2018*

Citation:
Zhu F, Zhang L, Liu F, Wu R, Guo W, Ou J, Zhang X and Zhao J (2018) Altered Serum Tumor Necrosis Factor and Interleukin-1β in First-Episode Drug-Naive and Chronic Schizophrenia. Front. Neurosci. 12:296. doi: 10.3389/fnins.2018.00296

Objective: Abnormality of the immune system might play a significant role in the pathogenesis of schizophrenia. We want to identity whether the serum TNF-α and IL-1β levels were changed in FEDN patients and CP and to investigate the relationship between both cytokines and psychopathological symptoms.

Methods: We recruited 69 FEDN patients, 87 CP and 61 healthy controls. Schizophrenia symptomatology was evaluated with the Positive and Negative Syndrome Scale (PANSS), the Scale for the Assessment of Negative Symptoms (SANS) and Clinical Global Impression Scale (CGI). Serum TNF-α and IL-1β levels were examined using sandwich enzyme-linked immunosorbent assay (ELISA).

Results: TNF-α and IL-1β levels in CP were significantly higher compared to healthy controls, but TNF-α and IL-1β levels in FEDN patients were significantly lower than in both CP and healthy controls. A moderate correlation between serum TNF-α or IL-1β levels and PANSS negative subscore was found in CP. But there was no correlation between altered cytokines and clinical symptoms in FEDN patients.

Conclusions: Increased TNF-α and IL-1β levels in chronic patients may be associated with the progression, psychotropic drugs or other factors occur during chronic stage. Immune modulating treatments may become a new strategy of therapy for this subgroup of patients.

Keywords: schizophrenia, cytokines, TNF-α, IL-1β, negative symptoms

INTRODUCTION

Schizophrenia is a chronic and severe mental disorder with significant impairment in psychosocial functioning. The mechanisms of schizophrenia are essentially unclear. More and more evidence suggest that abnormal immune system and immunological responses may be related with the etiology of schizophrenia'; (DeLegge and Smoke, 2008; Miller et al., 2011; Monji et al., 2013). Treatment of anti-inflammatory medications for schizophrenia has further supported that neuroinflammation may contribute to the etiology of this disorder (Sommer et al., 2014; Goldsmith et al., 2016).

Cytokines are the important messengers between the central nervous system (CNS) and immune cells. They play an important role not only in the cell-cell communication but also in the function of the immune system in the central nervous system (CNS) (Müller et al., 2015). A number of cytokines such as tumor necrosis factor (TNF)-α, interleukin (IL)-2, IL-1, and IL-6 have been found to involve in neuro-immune-endocrine communication and regulate neuronal activities in the mature CNS (Behrens et al., 2008; Fan et al., 2015; Schiavone and Trabace, 2017; Schiavone et al., 2017). Previous data have found altered levels of cytokines in the cerebrospinal fluid and the peripheral blood of patients with schizophrenia (Garver et al., 2003; Potvin et al., 2008; Rodrigues-Amorim et al., 2017), suggesting that cytokines may play an essential role in the etiology of schizophrenia (Fan et al., 2007; Song et al., 2009).

TNF-α and IL-1β are the proinflammatory cytokines. Both TNF-α and IL-1β play essential roles in the immune response because they promote dopaminergic neuronal differentiation of neural stem cells and regulate the development of dopamine neurons (Rodriguez-Pallares et al., 2005). They are also participated in the selective vulnerability of the nigrostriatal pathway related with dopaminergic neurotoxicity (Ferrari et al., 2006; Sriram et al., 2006). Both TNF-α and IL-1β were among the mostly reported cytokines in schizophrenia. For example, Liu et. al reported that schizophrenia patients had significantly overexpressed TNF-α and IL-1β in blood mononuclear cells (Liu et al., 2010). Recently, one study found that TNF-α and IL-1β were increased in the blood of first onset and acute relapse patients with schizophrenia (Wang et al., 2014). We found significantly increased TNF-α and IL-1β levels in an immune-related animal model that imitated negative symptoms in schizophrenia in our recent study (Zhu et al., 2014a). It has been hypothesized that increased levels of TNF-α and IL-1β may elevate the immune responses of other cytokines, resulting in an imbalance of Th1/Th2 cytokines in schizophrenia (Müller et al., 2000).

But until now, no study has simultaneously reported TNF-α and IL-1β in both first-episode drug-naïve (FEDN) and chronic patients (CP) with schizophrenia. In this study we wanted to know whether the serum TNF-α and IL-1β levels were changed in FEDN patients and CP, and we also aimed to investigate the relationship between the both cytokines and psychopathological symptoms.

METHODS

Subjects

Sixty-nine (male/female = 46/23) FEDN patients and 87 (male/female = 44/43) CP who met DSM-IV criteria for schizophrenia were recruited from the First Affiliated Hospital of Kunming Medical University and Guangzhou Baiyun Psychiatric Hospital. They included both inpatients and outpatients. The inclusion criteria for FEDN patients were: (1) between 18 and 45 years; (2) course of illness $\leq$ 2 years; (3) naïve to all psychotropic medications; (4) a stable living arrangement. The inclusion criteria for CP were: (1) aged 18–45 years; (2) course of illness $\geq$ 5 years; (3) on psychotropic medications; (4) able to understand the process of the study. The exclusion criteria were: (1) a psychiatric diagnosis other than schizophrenia (determined by SCID); (2) serious or unstable medical conditions including heart disease, epilepsy, hepatic or renal diseases, diabetes, aplastic anemia, systemic lupus erythematous or asthma; (3) planning to become pregnant, or were pregnant or breastfeeding. (4) Subjects with ongoing infections, allergies or past history of autoimmune disorders. (5) subjects suffered from substance abuse/dependence other than tobacco (which was based on subject and family report), received immunosuppressive drugs, or took medications for physical diseases.

Sixty-one healthy subjects (male/female = 31/30) were recruited from the local community in Kunming and Guangzhou. A clinical psychiatrist assessed the mental status and family history of any psychiatric disorder of the healthy controls. All of the healthy controls had no history of psychiatric diseases and a family history of psychiatric disorder. The other details of the exclusion criteria of healthy controls are the same as the patients' exclusion criteria except number one.

We obtained a complete medical history, physical examination and laboratorial tests from patients and control subjects.. All subjects were Han Chinese and gave signed informed consent to participate in the study. The study protocol was approved by the ethics committee of the First Affiliated Hospital of Kunming Medical University and Guangzhou Baiyun Psychiatric Hospital. Then we gained the complete medical history, physical examination and laboratorial examination.

Clinical Measures

Two experienced psychiatrists evaluated patients' symptoms by PANSS and the Scale for the Assessment of Negative Symptoms (SANS). Also, the Clinical Global Impressions Severity Scale (CGI-S) was used for severity of psychotic symptoms. All the researchers were trained to use the scales and passed the conformance tests.

Serum TNF-α and IL-1β Measurements

Venous blood was collected between 7 and 8 a.m. following an overnight fast. All the blood samples were detected within 1 year after they were collected. The serum was separated and stored at −80°C until assayed. Serum TNF-α and IL-1β levels

TABLE 1 | Demographics of FEDN, chronic patients with schizophrenia and healthy controls.

	FEDN($n = 69$)	Chronic patients ($n = 87$)	Healthy controls ($n = 61$)	χ^2 orF	df	*P*-value
Sex(M/F)	46/23	44/43	31/30	0.087	2	0.087
Age(years)	25.8 ± 5.9	32.9 ± 7.1	29.5 ± 6.7	22.0	2	< 0.001**
Education(years)	10.5 ± 2.9	11.0 ± 3.1	12.1 ± 2.6	5.2	2	0.006**
Course of disease(years)	0.8 ± 0.2	6.8 ± 1.4		55.0	154	< 0.001**
PANSS total score	84.9 ± 11.2	78.5 ± 7.1		18.9	154	< 0.001**
P subscore	18.2 ± 4.3	14.9 ± 2.6		37.4	154	< 0.001**
N subscore	25.6 ± 3.8	26.2 ± 3.0		5.0	154	0.241
G subscore	41.7 ± 7.6	37.4 ± 3.8		31.1	154	< 0.001**
SANS score	58.7 ± 13.5	64.7 ± 9.8		9.7	154	< 0.001**
CGI	5.5 ± 1.2	4.3 ± 0.8		15.9	154	< 0.001**
IL-1β(pg/ml)	1.7 ± 0.2	19.3 ± 11.3	8.3 ± 7.5	91.6[a]	2	< 0.001**[a]
TNF-α(pg/ml)	8.2 ± 2.0	28.1 ± 13.3	15.4 ± 7.0	90.5	2	< 0.001**

*FEDN, first-episode drug-naïve; PANSS, Positive and Negative Syndrome Scale; P subscore, positive subscore; N subscore, negative subscore; G subscore, general psychopathology subscore; SANS, Scale for the Assessment of Negative Symptoms; CGI, Clinical Global Impression Scale; IL-1β, Interleukin-1β; TNF-α, tumor necrosis factor-α. [a]Refer to the results after natural logarithmic transformation was performed for IL-1β. Age of onset, education, IL-1 β and TNF-α among the three groups were compared by ANOVA. **P < 0.001.*

were examined by enzyme-linked immunosorbent assay (ELISA) using an available kit (Bender Med Systems GmbH Campus Vienna Biocenter 2A-1030 Vienna, Austria, Europe).

The standard and sample testing were performed using duplicate assays by the same investigator who knowed nothing about the study. The sensitivities for TNF-α and IL-1β were 0.3 and 5.0 pg/ml, respectively. The inter-assay coefficients were 8.6 and 8.1%, respectively. The intra-assay variation coefficients were 5.1 and 7.7%, respectively.

Statistical Analysis

The Kolmogorov–Smirnov tests were performed to test the normal distribution of data. Continuous variables were presented as mean ± standard deviation ($\bar{x} \pm$ SD). Categorical variables were recorded using frequencies and percentages. We used the one-way ANOVA for continuous variables and the χ^2-test for categorical variables to test the between-group comparisons.

Since IL-1β was not normally distributed in the three groups, natural logarithmic transformation was performed for IL-1β. We used a univariate analysis of covariance (ANCOVA) controlling for age and gender to analyze TNF-α and IL-1β levels in the three groups. We used Bonferroni test to make *Post-hoc* comparisons between groups. Psychopathology on the PANSS, SANS, and CGI-S were compared between the two patient groups by one-way ANOVA and correlated with cytokine levels by calculating the partial correlation coefficients controlling for age, gender and course of illness. Differences at $p<0.05$ level were considered to be significant. Statistical analysis were performed using SPSS 20.0 (SPSS Inc., Chicago, IL).

RESULTS

Demographic Data

Table 1 shows significant differences in age ($p < 0.001$), and education ($p < 0.01$) among three groups. There was also a statistically significant difference in course of illness ($p < 0.001$) between FEDN patients and CP. Gender among the three groups showed no difference ($p > 0.05$).

TNF-α, IL-1β and Symptoms

All the blood samples were assayed within 1 year. There was no significant correlation between IL-1β or TNF-α levels and storage days (all $p > 0.05$). The PANSS total score, positive (P) and general psychopathology (G) subscores as well as CGI score showed significant differences between two patient groups (all $p < 0.001$) as exhibited in **Table 1**, with higher scores in FEDN patients than CP. However, the SANS score was significantly higher in chronic than FEDN patients ($p < 0.001$).

As shown in **Table 1** ANCOVA analysis revealed a significant difference in IL-1β ($F = 87.5$, $df = 2$, $p < 0.0001$)and TNF-α ($F = 90.5$, $df = 2$, $p < 0.0001$) levels among the three groups. *Post-hoc* analysis showed that TNF-α ($p < 0.0001$, **Figure 1**) and IL-1β ($p < 0.0001$, **Figure 1**) were significantly decreased in FEDN patients than both CP and healthy controls. Further, TNF-α ($p < 0.0001$, **Figure 1**) and IL-1β ($p < 0.0001$, **Figure 1**) were significantly higher in CP than in both FEDN patients and healthy controls.

Correlation Among TNF-α, IL-1β and Symptoms

By using partial correlation analysis, we found a moderately positive correlation between IL-1β and the PANSS negative subscore ($r = 0.525$, $p < 0.01$, **Figure 2**), or between TNF-α and the PANSS negative subscore in CP ($r = 0.523$, $p < 0.01$, **Figure 2**), but no significant correlation between cytokine serum levels and PANSS positive subscore or general subscore ($p > 0.05$) was found in these patients. But we found no correlation between IL-1β or TNF-α and any clinical symptoms in FEDN patients (all $p > 0.05$). In addition, a significantly positive correlation between TNF-α and IL-1β was found in CP ($r = 0.964$, $p < 0.001$) but not in FEDN patients ($p > 0.05$).

DISCUSSION

This study had two important findings. Firstly, TNF-α and IL-1β serum levels were significantly higher in CP than both healthy controls and FEDN patients, while TNF-α and IL-1β serum levels were significantly decreased in the FEDN patients than both healthy controls and CP. Secondly, both TNF-α and IL-1β showed moderately positive correlations with the PANSS negative subscore in the CP but not in FEDN patients with schizophrenia.

For reason of the disease state, illness duration, medication, the timing of the assays and so on, the reports on levels of TNF-α and IL-1β in schizophrenia have been inconsistent. But our results are in accord with previous reports that TNF-α and IL-1β were increased in chronic schizophrenia patients (Söderlund et al., 2009; Miller et al., 2011; Monji et al., 2013; Song et al., 2014; Zhu et al., 2015). The increased TNF-α and IL-1β in chronic patients maybe related with the long-term antipsychotic treatments. Whether antipsychotic treatment may affect serum cytokine levels has been controversial (Potvin et al., 2008; Miller et al., 2011; Tourjman et al., 2013). Some review papers point out that antipsychotic medications have anti-inflammatory effects in schizophrenia.. But no studies have reported the direct relationship between TNF-α or IL-1β and antipsychotics. The increased TNF-α and IL-1β in chronic patients may be related with older age, smoking or higher body mass indices (BMI). Interestingly, a positive correlation between TNF-α and IL-1β was found in CP but not in FEDN patients. Few studies has explored the interaction between TNF-α and IL-1β in patients with schizophrenia. Only one previous study reported a significant positive correlation between levels of TNF-α and IL-1β in schizophrenia patients (Liu et al., 2010). This supports that pro-inflammatory cytokines don't work independently but affect on the neuroimmunological network by means of mutual interactions. How the interaction between TNF-α and IL-1β is participated in the pathogenesis of schizophrenia warrants the further investigation.

Further, compared with healthy controls, a significant decrease in TNF-α and IL-1β levels were found in FEDN patients. These changes may be related with age, illness duration (Fawzi et al., 2011), cigarette smoking, disease state (Miller et al., 2011), the heterogeneity of schizophrenia, antipsychotic treatment (Davey et al., 2012), and comorbid obesity (Song et al., 2014), etc. This finding was inconsistent with the previous studies (Song et al., 2009; Müller et al., 2015). Interestingly, our results are in accordance with a recent study finding significantly higher IL-3 levels in CP but significantly fewer IL-3 levels in FEDN patients (Fu et al., 2016). They speculated that the reduced IL-3 levels in FEDN patients might be associated with neuronal apoptosis and abnormal early development of the CNS. In some situations, pro-inflammatory effects may have relation to important side effects, such as their responses to stress (Hinze-Selch et al., 2000; Zhang et al., 2005) and weight gain (Drzyzga et al., 2006). Some studies have proved that heightened stress is immunosuppressive (Adamo, 2012), and thus, the decreased TNF-α and IL-1β in our current study may be caused by stress in first episode schizophrenia, since the experience of acute psychosis in schizophrenia patients is stressful itself. The underlying mechanisms for the decreased TNF-α and IL-1β levels in FEDN patients with schizophrenia should be further investigated. In addition, we also found that both TNF-α and IL-1β showed moderately positive associations with the PANSS negative subscore in the CP. A recent study found a significant correlation between IL-3 levels and the PANSS G subscore only in CP(Fu et al., 2016). Another study also found that a significant decrease in IL-10 levels was reported in the FEDN patients and serum IL-10 was inversely correlated with the PANSS cognitive factor subscores, as well as with the PANSS negative symptom (Xiu et al., 2014). Taken together, these results point out that different cytokines may be related with clinical symptoms of schizophrenia.

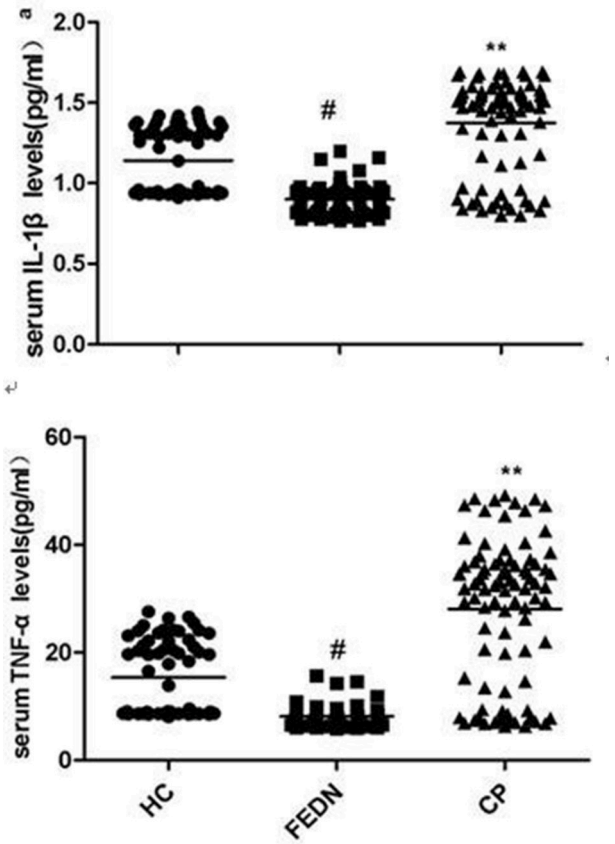

FIGURE 1 | Serum TNF-α or IL-1β levels in FEDN ($n = 69$), CP ($n = 87$) and HC ($n = 61$).

Microglia are the resident macrophage in the brain and they are also the primary reservoirs of pro-inflammatory cytokines in the CNS (Monji et al., 2009). It is highly likely that the activated microglia may produce cytokines which probably cause toxicity to neurons and decrease in neurogenesis, which may be participated in the pathogenesis of negative symptoms in schizophrenia (Monji et al., 2013). In our current study, both TNF-α and IL-1β showed moderately positive associations with the PANSS negative subscore in the CP. As discussed above, TNF-α and IL-1β were participated in the processes of neurogenesis or white matter abnormalities, suggesting that altered TNF-α and IL-1β may be associated with negative

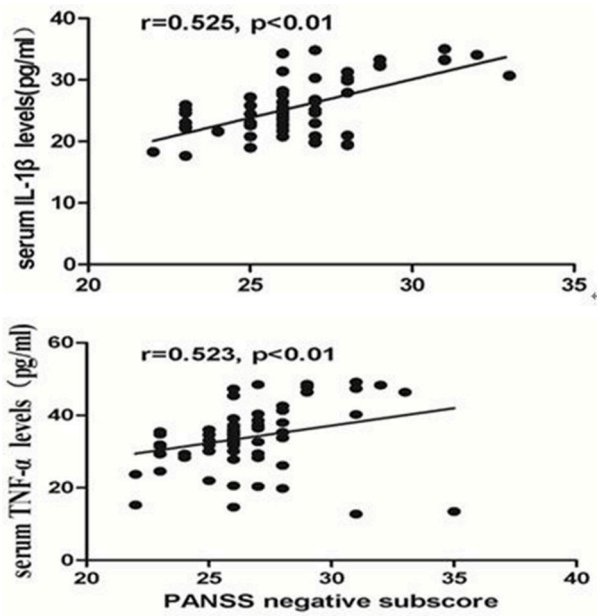

FIGURE 2 | Moderate Significant positive correlation between the serum TNF-α or IL-1β levels and the PANSS negative subscore in chronic patients.

symptoms of schizophrenia. A previous study found that the VNTR polymorphism in the IL-1RN gene may predict the improvement of negative symptom in schizophrenic patients which are treated with antipsychotic drugs (Mata et al., 2006). In our previous study, we found significant and persistent increases in the number of activated microglial cells and cytokines in an immune-related animal model that imitated negative symptoms in schizophrenia (Zhu et al., 2014a,b). We also found that minocycline, an inhibitor of microglial activation had significant efficacy for negative symptoms of schizophrenia (Liu et al., 2014). Taken all together, these findings suggest that the increased TNF-α and IL-1β, which may be caused by the activated microglia are related with negative symptoms of schizophrenia and anti-inflammatory may have therapeutic effects on clinical symptoms, especially on negative symptoms in schizophrenia.

The study has some limitations. Firstly, the sample size is relatively smaller. Secondly, we just measured only two cytokines. Previous studies have demonstrated that many cytokines are involved in immune dysfunction in schizophrenia. Therefore, further investigation will be needed to evaluate the role of other cytokines in psychopathologic mechanisms of schizophrenia. Thirdly, we did not collect some important clinical information, such as smoking, BMI and other data, which may affect the TNF-α and IL-1β levels in schizophrenia patients. For example, the popularity of smoking is much greater in schizophrenia patients than in the healthy population. One study reported that cigarette smoke played the harmful effects on human health by reason of its suppressive effects on the immune system (Zhang et al., 2008). Moreover, a previous study showed that smokers had lower IL-2 and IL-6 levels than non-smokers in chronic schizophrenia patients (Zhang et al., 2008). Unluckily, we did not gather smoking data in our current study, which should be added in future investigation. The role of smoking in altered cytokine levels in schizophrenia warrants further investigation.

CONCLUSION

In summary, our data showed that TNF-α and IL-1β levels were decreased in FEDN patients, but elevated in CP. The increase of TNF-α and IL-1β levels may be related with the psychotropic drugs as well as the progression of the disease. The increased TNF-α and IL-1β were just moderately related with the negative symptoms in CP, but it is a helpful hint that there is a greater contribution of immune abnormality to the progression in this subgroup of patients and that immune modulating treatments may become a new strategy of therapy for this subgroup of patients.

AUTHOR CONTRIBUTIONS

JZ: designed the study; FZ: wrote the protocol and the first draft of the manuscript; LZ and FL: collected the original data; RW, WG, and JO: undertook the statistical analysis; XZ: revised the draft of the manuscript. All authors contributed to and have approved the final manuscript.

FUNDING

This work was funded by the Natural Science Foundation of China (81361120396, 81471363, 81630033, 81501161), National Key Research and Development Program (2016YFC1306900), National Clinical Research Center on Mental Disorders (2015BAI13B02), the Medical Science Research Foundation of Guangdong Province (Grant No. A2015071), and the Natural Science Foundation of Guangdong Province (Grant No. 2017A030313809).

REFERENCES

Adamo, S. A. (2012). The effects of the stress response on immune function in invertebrates: an evolutionary perspective on an ancient connection. *Horm. Behav.* 62, 324–330. doi: 10.1016/j.yhbeh.2012.02.012

Behrens, M. M., Ali, S. S., and Dugan, L. L. (2008). Interleukin-6 mediates the increase in NADPH-oxidase in the ketamine model of schizophrenia. *J. Neurosci.* 28, 13957–13966. doi: 10.1523/JNEUROSCI.4457-08.2008

Davey, K. J., O'Mahony, S. M., Schellekens, H., O'Sullivan, O., Bienenstock, J., Cotter, P. D., et al. (2012). Gender-dependent consequences of chronic olanzapine in the rat: effects on body weight, inflammatory, metabolic and microbiota parameters. *Psychopharmacology* 221, 155–169. doi: 10.1007/s00213-011-2555-2

DeLegge, M. H., and Smoke, A. (2008). Neurodegeneration and inflammation. *Nutr. Clin. Pract.* 23, 35–41. doi: 10.1177/011542650802300135

Drzyzga, L., Obuchowicz, E., Marcinowska, A., and Herman, Z. S. (2006). Cytokines in schizophrenia and the effects of antipsychotic drugs. *Brain Behav. Immun.* 20, 532–545. doi: 10.1016/j.bbi.2006.02.002

Fan, N., Luo, Y., Xu, K., Zhang, M., Ke, X., Huang, X., et al. (2015). Relationship of serum levels of TNF-α, IL-6 and IL-18 and schizophrenia-like symptoms in chronic ketamine abusers. *Schizophr. Res.* 169, 10–15. doi: 10.1016/j.schres.2015.11.006

Fan, X., Goff, D. C., and Henderson, D. C. (2007). Inflammation and schizophrenia. *Expert Rev. Neurother.* 7, 789–796. doi: 10.1586/14737175.7.7.789

Fawzi, M. H., Fawzi, M. M., Fawzi, M. M., and Said, N. S. (2011). C-reactive protein serum level in drug-free male Egyptian patients with schizophrenia. *Psychiatry Res.* 190, 91–97. doi: 10.1016/j.psychres.2011.05.010

Ferrari, C. C., Pott Godoy, M. C., Tarelli, R., Chertoff, M., Depino, A. M., and Pitossi, F. J. (2006). Progressive neurodegeneration and motor disabilities induced by chronic expression of IL-1β in the substantia nigra. *Neurobiol. Dis.* 24, 183–193. doi: 10.1016/j.nbd.2006.06.013

Fu, Y. Y., Zhang, T., Xiu, M. H., Tang, W., Han, M., Yun, L. T., et al. (2016). Altered serum levels of interleukin-3 in first-episode drug-naive and chronic medicated schizophrenia. *Schizophr. Res.* 176, 196–200. doi: 10.1016/j.schres.2016.05.010

Garver, D. L., Tamas, R. L., and Holcomb, J. A. (2003). Elevated interleukin-6 in the cerebrospinal fluid of a previously delineated schizophrenia subtype. *Neuropsychopharmacology* 28, 1515–1520. doi: 10.1038/sj.npp.1300217

Goldsmith, D. R., Rapaport, M. H., and Miller, B. J. (2016). A meta-analysis of blood cytokine network alterations in psychiatric patients: comparisons between schizophrenia, bipolar disorder and depression. *Mol. Psychiatry* 21, 1696–1709. doi: 10.1038/mp.2016.3

Hinze-Selch, D., Deuschle, M., Weber, B., Heuser, I., and Pollmächer, T. (2000). Effect of coadministration of clozapine and fluvoxamine versus clozapine monotherapy on blood cell counts, plasma levels of cytokines and body weight. *Psychopharmacology* 149, 163–169. doi: 10.1007/s002139900351

Liu, F., Guo, X., Wu, R., Ou, J., Zheng, Y., Zhang, B., et al. (2014). Minocycline supplementation for treatment of negative symptoms in early-phase schizophrenia: a double blind, randomized, controlled trial. *Schizophr. Res.* 153, 169–176. doi: 10.1016/j.schres.2014.01.011

Liu, L., Jia, F., Yuan, G., Chen, Z., Yao, J., Li, H., et al. (2010). Tyrosine hydroxylase, interleukin-1β and tumor necrosis factor-α are overexpressed in peripheral blood mononuclear cells from schizophrenia patients as determined by semi-quantitative analysis. *Psychiatry Res.* 176, 1–7. doi: 10.1016/j.psychres.2008.10.024

Mata, I., Crespo-Facorro, B., Pérez-Iglesias, R., Carrasco-Marín, E., Arranz, M. J., Pelayo-Teran, J. M., et al. (2006). Association between the interleukin-1 receptor antagonist gene and negative symptom improvement during antipsychotic treatment. *Am. J. Med. Genet. B Neuropsychiatr. Genet.* 141B, 939–943. doi: 10.1002/ajmg.b.30405

Miller, B. J., Buckley, P., Seabolt, W., Mellor, A., and Kirkpatrick, B. (2011). Meta-analysis of cytokine alterations in schizophrenia: clinical status and antipsychotic effects. *Biol. Psychiatry* 70, 663–671. doi: 10.1016/j.biopsych.2011.04.013

Monji, A., Kato, T. A., Mizoguchi, Y., Horikawa, H., Seki, Y., Kasai, M., et al. (2013). Neuroinflammation in schizophrenia especially focused on the role of microglia. *Prog. Neuropsychopharmacol. Biol. Psychiatry* 42, 115–121. doi: 10.1016/j.pnpbp.2011.12.002

Monji, A., Kato, T., and Kanba, S. (2009). Cytokines and schizophrenia: microglia hypothesis of schizophrenia. *Psychiatry Clin. Neurosci.* 63, 257–265. doi: 10.1111/j.1440-1819.2009.01945.x

Müller, N., Riedel, M., Gruber, R., Ackenheil, M., and Schwarz, M. J. (2000). The immune system and schizophrenia. An integrative view. *Ann. N. Y. Acad. Sci.* 917, 456–467. doi: 10.1111/j.1749-6632.2000.tb05410.x

Müller, N., Weidinger, E., Leitner, B., and Schwarz, M. J. (2015). The role of inflammation in schizophrenia. *Front. Neurosci.* 9:372. doi: 10.3389/fnins.2015.00372

Potvin, S., Stip, E., Sepehry, A. A., Gendron, A., Bah, R., and Kouassi, E. (2008). Inflammatory cytokine alterations in schizophrenia: a systematic quantitative review. *Biol. Psychiatry* 63, 801–808. doi: 10.1016/j.biopsych.2007.09.024

Rodrigues-Amorim, D., Rivera-Baltanas, T., Spuch, C., Caruncho, H. J., González-Fernandez, Á., Olivares, J. M., et al. (2017). Cytokines dysregulation in schizophrenia: a systematic review of psychoneuroimmune relationship. *Schizophr. Res.* doi: 10.1016/j.schres.2017.11.023. [Epub ahead of print].

Rodriguez-Pallares, J., Guerra, M. J., and Labandeira-Garcia, J. L. (2005). Angiotensin, I. I., and interleukin-1 interact to increase generation of dopaminergic neurons from neurospheres of mesencephalic precursors. *Brain Res. Dev. Brain Res.* 158, 120–122. doi: 10.1016/j.devbrainres.2005.06.009

Schiavone, S., Mhillaj, E., Neri, M., Morgese, M. G., Tucci, P., Bove, M., et al. (2017). Early loss of blood-brain barrier integrity precedes NOX2 elevation in the prefrontal cortex of an animal model of psychosis. *Mol. Neurobiol.* 54, 2031–2044. doi: 10.1007/s12035-016-9791-8

Schiavone, S., and Trabace, L. (2017). Inflammation, stress response, and redox dysregulation biomarkers: clinical outcomes and pharmacological implications for psychosis. *Front. Psychiatry* 8:203. doi: 10.3389/fpsyt.2017.00203

Söderlund, J., Schröder, J., Nordin, C., Samuelsson, M., Walther-Jallow, L., Karlsson, H., et al. (2009). Activation of brain interleukin-1β in schizophrenia. *Mol. Psychiatry* 14, 1069–1071. doi: 10.1038/mp.2009.52

Sommer, I. E., van Westrhenen, R., Begemann, M. J., de Witte, L. D., Leucht, S., and Kahn, R. S. (2014). Efficacy of anti-inflammatory agents to improve symptoms in patients with schizophrenia: an update. *Schizophr. Bull.* 40, 181–191. doi: 10.1093/schbul/sbt139

Song, X., Fan, X., Li, X., Zhang, W., Gao, J., Zhao, J., et al. (2014). Changes in pro-inflammatory cytokines and body weight during 6-month risperidone treatment in drug naive, first-episode schizophrenia. *Psychopharmacology* 231, 319–325. doi: 10.1007/s00213-013-3382-4

Song, X. Q., Lv, L. X., Li, W. Q., Hao, Y. H., and Zhao, J. P. (2009). The interaction of nuclear factor-kappa B and cytokines is associated with schizophrenia. *Biol. Psychiatry* 65, 481–488. doi: 10.1016/j.biopsych.2008.10.018

Sriram, K., Miller, D. B., and O'Callaghan, J. P. (2006). Minocycline attenuates microglial activation but fails to mitigate striatal dopaminergic neurotoxicity: role of tumor necrosis factor-alpha. *J. Neurochem.* 96, 706–718. doi: 10.1111/j.1471-4159.2005.03566.x

Tourjman, V., Kouassi, É., Koué, MÈ., Rocchetti, M., Fortin-Fournier, S., Fusar-Poli, P., et al. (2013). Antipsychotics' effects on blood levels of cytokines in schizophrenia: a meta-analysis. *Schizophr. Res.* 151, 43–47. doi: 10.1016/j.schres.2013.10.011

Wang, Q., Liu, J., Liu, Y. P., Li, X. Y., Ma, Y. Y., Wu, T. F., et al. (2014). Methylenetetrahydrofolate reductase deficiency-induced schizophrenia in a school-age boy. *Zhongguo Dang Dai Er Ke Za Zhi* 16, 62–66. doi: 10.7499/j.issn.1008-8830.2014.01.014

Xiu, M. H., Yang, G. G., Tan, Y. L., Chen, D. C., Tan, S. P., Wang, Z. R., et al. (2014). Decreased interleukin-10 serum levels in first-episode drug-naive schizophrenia: relationship to psychopathology. *Schizophr. Res.* 156, 9–14. doi: 10.1016/j.schres.2014.03.024

Zhang, X. Y., Cao, L. Y., Song, C., Wu, G. Y., Chen, D. C., Qi, L. Y., et al. (2008). Lower serum cytokine levels in smokers than nonsmokers with chronic schizophrenia on long-term treatment with antipsychotics. *Psychopharmacology* 201, 383–389. doi: 10.1007/s00213-008-1295-4

Zhang, X. Y., Zhou, D. F., Cao, L. Y., Wu, G. Y., and Shen, Y. C. (2005). Cortisol and cytokines in chronic and treatment-resistant patients with schizophrenia: association with psychopathology and response to antipsychotics. *Neuropsychopharmacology* 30, 1532–1538. doi: 10.1038/sj.npp.1300756

Zhu, F., Zhang, L., Ding, Y. Q., Zhao, J., and Zheng, Y. (2014a). Neonatal intrahippocampal injection of lipopolysaccharide induces deficits in social behavior and prepulse inhibition and microglial activation in rats: Implication for a new schizophrenia animal model. *Brain Behav. Immun.* 38, 166–174. doi: 10.1016/j.bbi.2014.01.017

Zhu, F., Zheng, Y., Ding, Y. Q., Liu, Y., Zhang, X., Wu, R., et al. (2014b). Minocycline and risperidone prevent microglia activation and rescue behavioral deficits induced by neonatal intrahippocampal injection of lipopolysaccharide in rats. *PLoS ONE* 9:e93966. doi: 10.1371/journal.pone.0093966

Zhu, Q., Li, X., Hie, G., Yuan, X., Lü, L., and Song, X. (2015). Analysis of the changes of serum high mobility group protein B1 and cytokines in first-episode schizophrenia patients. *Zhonghua Yi Xue Za Zhi* 95, 3818–3822. doi: 10.3760/cma.j.issn.0376-2491.2015.47.005

Conflict of Interest Statement: The authors declare that the research was conducted in the absence of any commercial or financial relationships that could be construed as a potential conflict of interest.

frontiers in Neurology

ORIGINAL RESEARCH
published: 22 May 2018
doi: 10.3389/fneur.2018.00342

Altered Whole-Brain Structural Covariance of the Hippocampal Subfields in Subcortical Vascular Mild Cognitive Impairment and Amnestic Mild Cognitive Impairment Patients

Xuetong Wang[1,2†], Yang Yu[3,4†], Weina Zhao[3,4,5†], Qiongling Li[1,2], Xinwei Li[1,2], Shuyu Li[1,2], Changhao Yin[5*] and Ying Han[3,4*]*

[1] School of Biological Science and Medical Engineering, Beihang University, Beijing, China, [2] Beijing Advanced Innovation Centre for Biomedical Engineering, Beihang University, Beijing, China, [3] Center of Alzheimer's Disease, Beijing Institute for Brain Disorders, Beijing, China, [4] Department of Neurology, XuanWu Hospital, Capital Medical University, Beijing, China, [5] Department of Neurology, Hongqi Hospital, Mudanjiang Medical University, Mudanjiang, China

OPEN ACCESS

Edited by:
HuaLin Cai,
Central South University,
China

Reviewed by:
Ricardo Insausti,
Universidad de Castilla-La Mancha, Spain
Julie A. Dumas,
University of Vermont,
United States

***Correspondence:**
Shuyu Li
shuyuli@buaa.edu.cn;
Changhao Yin
yinchanghao7916@sina.com;
Ying Han
hanying@xwh.ccmu.edu.cn

[†]These authors have contributed equally to this work.

Specialty section:
This article was submitted to Neuropharmacology, a section of the journal Frontiers in Neurology

Received: 11 December 2017
Accepted: 30 April 2018
Published: 22 May 2018

Citation:
Wang X, Yu Y, Zhao W, Li Q, Li X, Li S, Yin C and Han Y (2018) Altered Whole-Brain Structural Covariance of the Hippocampal Subfields in Subcortical Vascular Mild Cognitive Impairment and Amnestic Mild Cognitive Impairment Patients. Front. Neurol. 9:342. doi: 10.3389/fneur.2018.00342

The hippocampus plays important roles in memory processing. However, the hippocampus is not a homogeneous structure, which consists of several subfields. The hippocampal subfields are differently affected by many neurodegenerative diseases, especially mild cognitive impairment (MCI). Amnestic mild cognitive impairment (aMCI) and subcortical vascular mild cognitive impairment (svMCI) are the two subtypes of MCI. aMCI is characterized by episodic memory loss, and svMCI is characterized by extensive white matter hyperintensities and multiple lacunar infarctions on magnetic resonance imaging. The primary cognitive impairment in svMCI is executive function, attention, and semantic memory. Some variations or disconnections within specific large-scale brain networks have been observed in aMCI and svMCI patients. The aim of this study was to investigate abnormalities in structural covariance networks (SCNs) between hippocampal subfields and the whole cerebral cortex in aMCI and svMCI patients, and whether these abnormalities are different between the two groups. Automated segmentation of hippocampal subfields was performed with FreeSurfer 5.3, and we selected five hippocampal subfields as the seeds of SCN analysis: CA1, CA2/3, CA4/dentate gyrus (DG), subiculum, and presubiculum. SCNs were constructed based on these hippocampal subfield seeds for each group. Significant correlations between hippocampal subfields, fusiform gyrus (FFG), and entorhinal cortex (ERC) in gray matter volume were found in each group. We also compared the differences in the strength of structural covariance between any two groups. In the aMCI group, compared to the normal controls (NC) group, we observed an increased association between the left CA1/CA4/DG/subiculum and the left temporal pole. Additionally, the hippocampal subfields (bilateral CA1, left CA2/3) significantly covaried with the orbitofrontal cortex in the svMCI group compared to the NC group. In the aMCI group compared to the svMCI group, we observed decreased association between hippocampal subfields and the right FFG, while we also

observed an increased association between the bilateral subiculum/presubiculum and bilateral ERC. These findings provide new evidence that there is altered whole-brain structural covariance of the hippocampal subfields in svMCI and aMCI patients and provide insights to the pathological mechanisms of different MCI subtypes.

Keywords: hippocampal subfields, amnestic mild cognitive impairment, subcortical vascular mild cognitive impairment, structural covariance networks, MRI

INTRODUCTION

The hippocampus is part of the limbic system. It plays important roles in memory processing, especially spatial memory (1). Studies have shown that the hippocampus can be affected by a variety of neurological diseases such as epilepsy and schizophrenia (2, 3). Importantly, hippocampal disruption is an early sign of Alzheimer's disease (AD) and other forms of dementia (4).

However, the hippocampus is not a homogeneous structure, which consists of several subfields, specifically the cornu ammonis (CA) areas 1–4, the dentate gyrus (DG), the subiculum, and the presubiculum (5). The hippocampus subfields have distinct anatomy and functions (6). Notably, evidence supports the distinct connectivity between hippocampal subfields and other brain regions. The major input to the hippocampus is the performant path, coming from the entorhinal cortex (ERC) that connects with the DG and CA3 pyramidal neurons. In addition, the efferent fibers, which may originate from CA or subiculum, terminate in many brain regions (e.g., entorhinal area, posterior cingulate, medial frontal cortex, and gyrus rectus) (7). Previous studies reported that the hippocampal subfields were differently affected by many neurodegenerative diseases, especially mild cognitive impairment (MCI) (8, 9).

Mild cognitive impairment is a diagnosis given to older adults who have cognitive impairments but that does not interfere significantly with their daily activities (10). It is regarded as the transitional stage between normal aging and dementia. Amnestic mild cognitive impairment (aMCI) and subcortical vascular mild cognitive impairment (svMCI) are two subtypes of MCI, both associated with deficits in multiple cognitive domains, with the same chief complaints in memory deficits, but the pathogenesis of aMCI and svMCI are different (11, 12). The aMCI is characterized by episodic memory loss (13) and represents the prodromal stage of AD (14, 15). The svMCI is regarded as a prodromal stage of subcortical vascular dementia, showing extensive white matter hyperintensities and multiple lacunar infarctions on magnetic resonance imaging (16). The cognitive impairment of svMCI is mainly manifested in executive function, attention, and semantic memory (17–19). Importantly, some variations or disconnections within specific large-scale brain networks were observed in aMCI and svMCI patients (20–24). For example, patients with aMCI showed a pattern of brain disconnection between the posterior cingulate cortex (PCC), the medial prefrontal cortex (PFC), and the rest of the brain (21). A few studies have reported that aMCI patients were characterized by aberrance in resting-state functional connectivity of specific hippocampal subregions (such as DG and subiculum) (25, 26). Additionally, svMCI patients presented extensive decreased functional connectivity density and functional amplitude of spontaneous low-frequency oscillations in the medial PFC (22). However, it is unknown whether aMCI and svMCI patients have abnormalities in structural connections between hippocampal subfields and the cerebral cortex and whether these abnormalities are different between aMCI and svMCI.

Structural covariance networks (SCNs), based on voxel-based morphometry (VBM), generate a map of correlation between the gray matter (GM) volume of a region of interest and the other regions (27, 28). SCNs are regarded as the potential tool to reflect developmental coordination or synchronized maturation between regions of the brain (29). In addition, SCN analysis has been successfully applied to obtain the abnormality in brain connectivity in some neuropsychiatric disorders (30–32). In this study, SCNs were employed to characterize the structural connections between hippocampal subfields and the cerebral cortex. We selected five hippocampal subfields using an automated segmentation method as seeds to build the SCNs in aMCI patients, svMCI patients, and normal controls (NC). Finally, we compared the differences in strength of structural covariance between groups.

MATERIALS AND METHODS

Participants

Patients with svMCI and aMCI were recruited through the memory clinic of the neurology department of Xuanwu Hospital, Capital Medical University, Beijing, China. Two experienced neurologists diagnosed all patients using the Petersen criteria (33). Healthy controls were recruited from the local community through advertisements. Subjects were excluded if they had the following clinical characteristics: (i) depressive symptoms with a Hamilton Depression Rating Scale score > 24; (ii) non-MCI disease that cause cognitive impairments, such as psychiatric disease, systemic disease, or alcohol or drug abuse; (iii) factors that would make neuropsychological testing infeasible, such as visual abnormalities, severe aphasia, or motor disorders. Written informed consent was obtained from all participants. According to the diagnostic criteria and exclusion criteria, there were 29 svMCI patients, 33 aMCI patients, and 36 NC subjects included in this study. All participants received a standardized clinical evaluation protocol including a global cognitive functioning test [i.e., Mini Mental Status Examination (MMSE)] and other cognitive assessments (i.e., AVLT). **Table 1** shows the detailed demographic characteristics of the participants. This study was

TABLE 1 | Demographics of participants [mean ± SD (range)].

	NC (n = 36)	svMCI (n = 29)	aMCI (n = 33)
Gender (M/F)	16/20	11/18	13/20
Age (years)	62.5 ± 6.6 (46–76)	63 ± 8.7 (46–77)	66 ± 8.4 (51–80)
Years of education	9.9 ± 4.6 (0–17)	8.6 ± 3.7 (0–17)	10.8 ± 4.1 (0–18)
AVLT-immediate recall	8.8 ± 1.9 (5.3–13.7)	6.9 ± 1.9 (3.3–10.3)*	6.0 ± 1.5 (3.3–9)*
AVLT-delayed recall	9.39 ± 3.26 (0–15)	6.2 ± 3.0 (0–13)*	3.5 ± 3.0 (0–12)*
AVLT-recognition	11.17 ± 2.68 (3–15)	10.07 ± 2.4 (3–14)	7.1 ± 4.2 (3–14)
MMSE	27.3 ± 2.3 (21–30)	25.6 ± 3.4 (16–30)	24.9 ± 3.1 (17–30)*
MoCa	26.0 ± 3.5 (15–30)	19.9 ± 3.9 (13–26)*	19.7 ± 4.1 (11–26)*

ANOVA was performed, followed by Bonferroni post hoc analysis.
**P < 0.05 between NC and svMCI or aMCI.*
NC, normal controls; svMCI, vascular mild cognitive impairment; aMCI, amnestic mild cognitive impairment; AVLT, auditory verbal learning test; MMSE, Mini Mental Status Examination; MoCa, Montreal Cognitive Assessment.

approved by the medical research ethics committee and the institutional review board of Xuanwu Hospital, Capital Medical University, Beijing, China.

Image Acquisition

Structural MR images were acquired using sagittal magnetization-prepared rapid gradient echo (MP-RAGE) three-dimensional T1-weighted imaging sequence on a 3.0 T Siemens scanner at Xuanwu Hospital, Capital Medical University. The image parameters included repetition time (TR) = 1,900 ms; echo time (TE) = 2.2 ms; inversion time = 900 ms; flip angle = 9°; field of view = 224 mm × 256 mm; matrix size = 448 × 512; 176 slices; and slice thickness = 1.0 mm.

Segmentation of Hippocampal Subfields

Automated segmentation of the hippocampal subfields was performed with the hippo-subfields module in FreeSurfer version 5.3,[1] which uses the Bayesian statistical model built from manual segmentation of the right hippocampus in 0.38 mm × 0.38 mm × 0.8 mm *in vivo* MRI scans in 10 subjects (34). The results consisted of a collection of images that indicated each voxel's posterior probability of belonging to different subregions in native space. By maximizing the posterior probability of the different subregions, the hippocampus of each subject was segmented to seven subfields: CA1, CA2/3, CA4/DG, presubiculum, subiculum, fimbria, and the hippocampal fissure. Previous research has reported that the fimbria and the hippocampal fissure showed relatively lower segmentation accuracies than other subfields (35, 36). Importantly, because the fimbria (white matter) and hippocampal fissure (cerebrospinal fluid) did not belong to GM, they were discarded in the subsequent SCN analysis. There is an illustration for the right hippocampal subfield segmentations for one NC subject in **Figure 1**.

Image Processing

First, non-uniformity intensity correction of the structural magnetic resonance imaging data was performed with FreeSurfer.

[1]http://freesurfer.net.

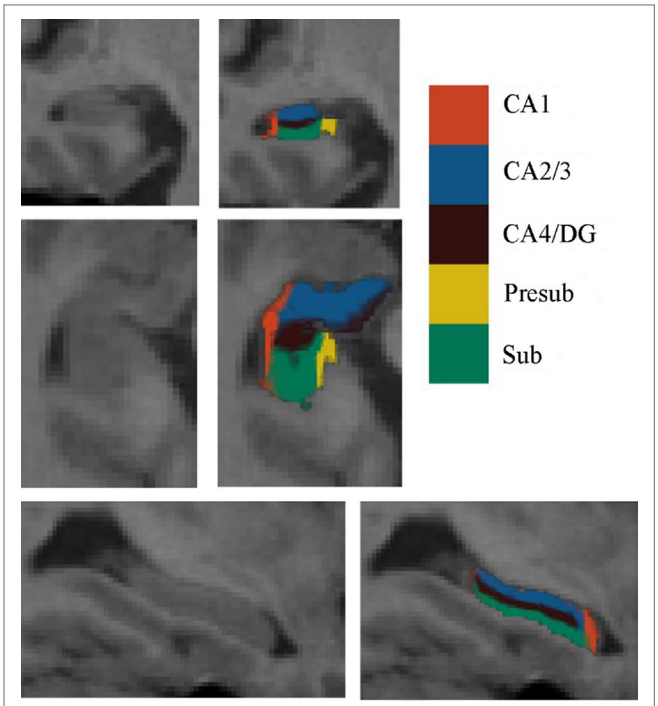

FIGURE 1 | Right hippocampal subfield segmentation for one normal control subject. From left to right: cross-sectional slice of an MRI scan and corresponding automated segmentation of five subfields. Abbreviations: CA, cornu ammonis; DG, dentate gyrus; Presub, presubiculum; Sub, subiculum.

Then, the results after NU intensity correction were analyzed using Statistical Parametric Mapping software package in MATLAB (SPM12[2]). Following the inspection of image quality, we used VBM (VBM8 toolbox[3]) to extract the GM volume map of each subject (37). Additionally, we employed a spatially adaptive non-local denoising filter (38) and a hidden Markov random field model (39) to reduce the impact of noise in the GM volume map. Then, the images were transformed into the DARTEL template (40) from the Montreal Neurological Institute (MNI) space through the high-dimensional diffeomorphic anatomical registration using the exponentiated lie algebra (DARTEL) approach, which is a non-linear spatial normalization method. Subsequently, the voxel values were modulated to preserve regional volume information using the Jacobian determinants (41). Finally, we smoothed the modulated images using Gaussian Kernel specified in 12 mm full width at half maximum.

Definition of Seed Regions

For each subject, the deformation field derived from the NU intensity corrected image to normalized image was applied to the hippocampal subfields' label image in native space. To reduce the possible impact of segmentation inaccuracy on subsequent analysis, the transformed hippocampal subfield labels were combined for all subjects and the 100% overlapped regions were

[2]http://www.fil.ion.ucl.ac.uk/spm.
[3]http://www.neuro.uni-jena.de/vbm/.

selected. Then, these regions on each side were masked using the hippocampal label from the Harvard-Oxford subcortical structural atlas. Additionally, if there existed overlap for any two hippocampal subfields, the overlapped regions were removed. After that, the seed region for each hippocampal subfield was defined in MNI space. All the seed regions (in black color) were overlaid to the probabilistic atlas (in Heat color) of hippocampal subfields (34), as shown in **Figure 2**. The seeds almost located within the atlas.

Construction of Structural Covariance Networks

For each group, the strength of structural covariance between each subfield seed and all other regions across the whole brain were obtained by applying multiple regression models in SPM12 to perform a voxel-based statistical analysis on the smoothed and modulated GM image. We imported the extracted mean GM volume from each seed as a covariate. As the age and gender would influence the GM volumes, we removed the effects of gender and age on the structural covariance networks by entering them as confounding covariates. The resulting covariance patterns were employed with thresholds at $P < 0.05$ with the false discovery rate (FDR) correction and reserved positive covariance. Finally, the results were displayed on the MNI template in the BrainNet Viewer software[4] (42).

Between-Group Differences in the Structural Association

Many studies have indicated that the different slopes for any pair of voxels may represent the difference in their structural association (43, 44). To evaluate the difference in strength of structural covariance between groups, we performed a between-group

[4]http://www.nitrc.org/projects/bnv/.

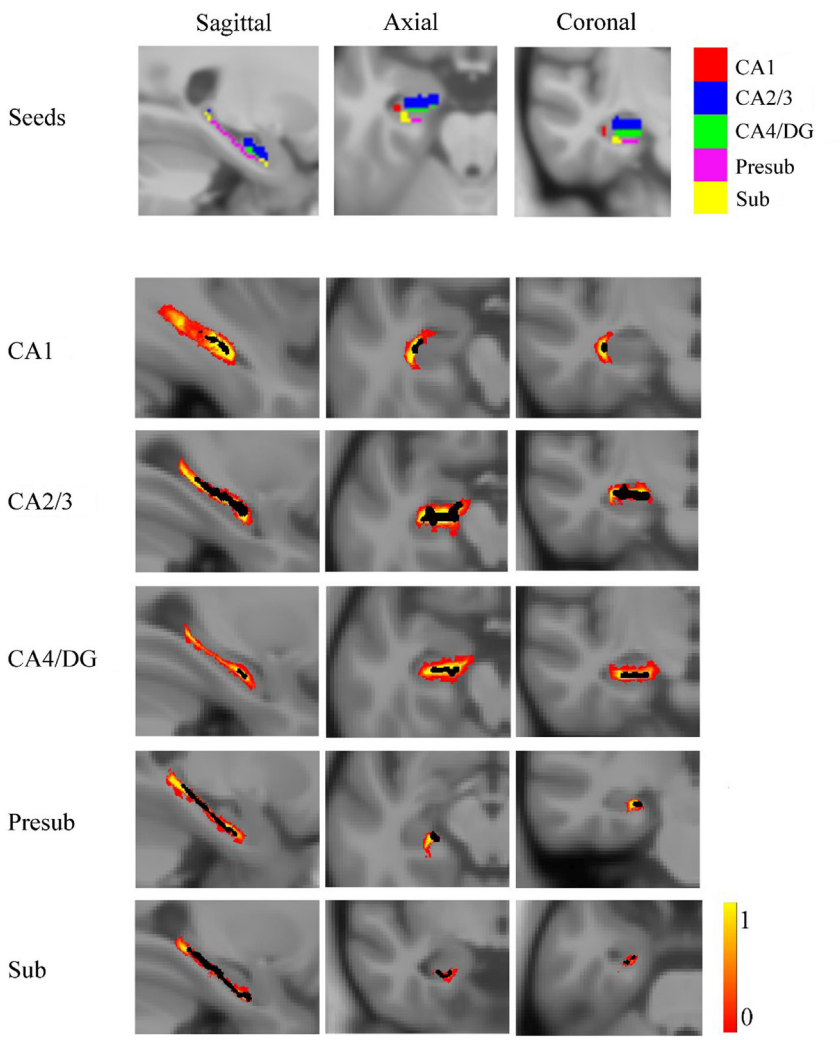

FIGURE 2 | The seed regions compared to probabilistic atlases. At the top of the figure, the seeds are shown in Montreal Neurological Institute space. In the lower part of the figure, the probabilistic atlases are viewed in heat color maps, and the volumes of seeds are overlaid with black color. Abbreviations: CA, cornu ammonis; DG, dentate gyrus; Presub, presubiculum; Sub, subiculum.

analysis of slopes. The analysis used a multiple classic interaction linear model:

$$y = \beta_0 + \beta_1 X + \beta_2 G + \beta_3 (G \times X) + \beta_4 \text{Age} + \beta_5 \text{Gender} + \varepsilon$$

G was used as a grouping variable, and two groups were put into the same model, where $G = 1$ for the one group, and $G = 0$ for another group. The gender and age may affect the association of two voxels, so they were considered as independent variables in a linear model, where X represented the averaged GM volume in each seed, and y represented the GM volumes of each voxel in whole brain. Then, the linear regression model between y and X was adjusted by adding a gender term *Gender*, an age term *Age*, a group term G, and an interaction term $G \times X$. Specific t-value contrasts were established to map the significant different voxels in slopes between any two groups. The significant differences between groups were obtained based on the two-tailed Gaussian random field (GRF) correction, with a voxel level of $P < 0.01$ and a cluster level of $P < 0.05$.

RESULTS

Demographics

Table 1 shows demographics of the healthy controls, svMCI patients, and aMCI patients. There were no significant differences in sex, age, and years of education between groups. However, significant differences between groups were found in the AVLT-immediate recall ($F = 12.059$, $P < 0.001$), AVLT-delayed recall ($F = 11.501$, $P < 0.001$), AVLT-recognition recall ($F = 2.804$, $P = 0.066$), MMSE ($F = 3.3765$, $P = 0.27$), and Montreal Cognitive Assessment ($F = 27.276$, $P < 0.001$) through one-way analysis of variance. The following *post hoc* test revealed that AVLT-immediate recall, AVLT-delayed recall, and MoCa in patients of aMCI and svMCI were significantly lower than scores in controls. In addition, the score of MMSE was significantly lower in the aMCI group than in the control group, but there was no significant difference in score of MMSE between the svMCI and NC groups.

Structural Covariance Networks Within Groups

The SCN patterns of the left and right hippocampal subfields in the three groups are shown in **Figures 3** and **4**, respectively. Each of the hippocampal subfield seed regions covaried with the ERC and fusiform gyrus (FFG) among the three groups. The regions showing significant correlations with hippocampal subfields were relatively larger in the aMCI group than the svMCI group and NC group.

Structural Covariance Networks in the aMCI Group

Left

In the aMCI group, in addition to the ERC and FFG, the left CA1 covaried with the left temporal pole (TP), right angular gyrus, subcallosal cortex, and thalamus. For the left CA2/3 network, the structural maps involved the ERC and FFG, subcallosal cortex, thalamus, and angular gyrus. The left CA4/DG correlated regions were similar to the regions in the left CA2/3 network in the aMCI group, but it additionally included the right superior frontal gyrus. For the aMCI group, the left subiculum and left presubiculum covariance maps involved the left TP, subcallosal cortex, thalamus, superior and middle frontal gyrus, right middle occipital gyrus, and bilateral angular gyrus.

Right

In the aMCI group, the right CA1 covaried with the ERC and FFG, right TP, PCC, and angular gyrus. CA2/3 showed significant correlation with entorhinal areas, thalamus, bilateral TP, middle frontal gyrus, PCC, and angular gyrus. The CA4/DG correlated regions were similar to the regions covaried with the right CA2/3 subfield in the aMCI group. For the right presubiculum networks, the covariance maps of the right presubiculum involved entorhinal areas, thalamus, bilateral TP, PCC, and angular gyrus. The subiculum showed significant covariance with the ERC, FFG, and right angular gyrus.

Structural Covariance Networks in the svMCI Group

Left

The left CA1 showed significant correlations with the ERC, FFG, superior occipital gyrus, orbitofrontal cortex (OFC), and right TP in the svMCI group. The covariance maps of the left CA2/3 involved the FFG, right TP, OFC, occipital pole, and entorhinal areas in the svMCI group. The left CA4/DG covariance maps were similar to the covariance maps of the left CA2/3 in the svMCI group. In the svMCI group, the maps of the left presubiculum and left subiculum were virtually identical, and the covaried regions included the FFG, ERC, fusiform, and right TP.

Right

The right CA1 covaried with the ERC, FFG, superior occipital gyrus, right TP, and OFC in the svMCI group. The right CA2/3 covaried with entorhinal areas, right TP, and superior occipital gyrus. The right CA4/DG covaried with entorhinal areas, fusiform, right TP, superior occipital gyrus, and subcallosal cortex. The regions covaried with the right presubiculum were similar to those regions connected with the right CA4/DG subfield in the svMCI group. In addition, the covariance maps of the right subiculum hippocampal subfields involved entorhinal areas, fusiform, right TP, and superior occipital gyrus.

Structural Covariance Networks in the NC Group

Left

The left CA1 covaried with the bilateral ERC and FFG in the NC group. In addition to the ERC and FFG, the covariance regions with the left CA2/3 also included the left precuneus cortex. The left CA4/DG covariance maps were extremely similar to the maps of the left CA1 subfield in the NC group. For the left subiculum and left presubiculum networks, both covariance maps involved the left precentral gyrus, FFG, and ERC in NC subjects.

Right

The right CA1 covaried with the ERC and FFG in the NC group. In addition to the ERC and FFG, the covariance regions with the right CA2/3 also involved the right OFC. The right CA4/DG

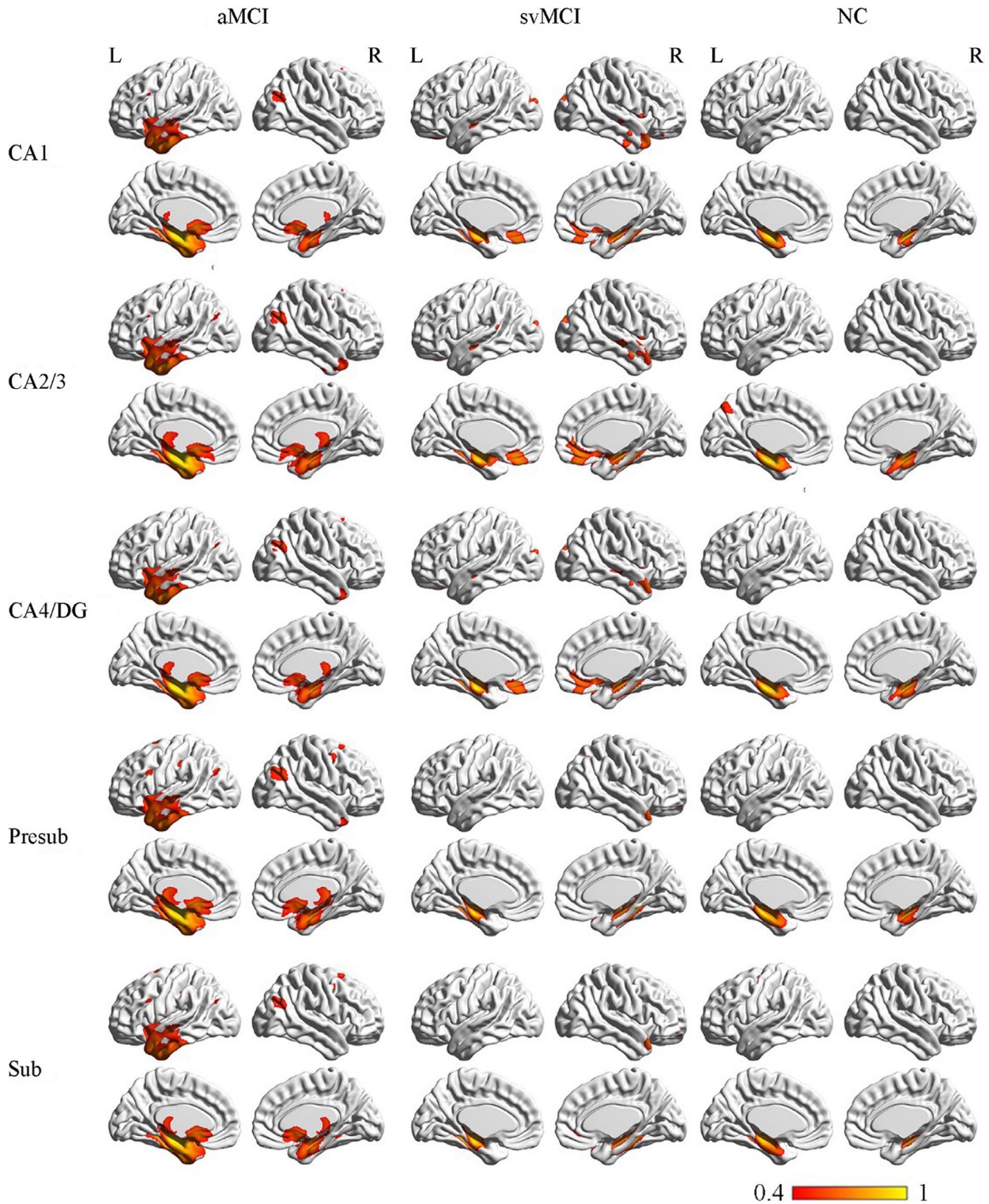

FIGURE 3 | Structural covariance networks of left hippocampal subfields in the three groups. Statistical maps of regions significantly correlated with the seed region in each group. The results are presented as CC values ($P < 0.05$, false discovery rate corrected). Abbreviations: L, left; R, right; CC, correlation coefficient; NC, normal controls; svMCI, vascular mild cognitive impairment; aMCI, amnestic mild cognitive impairment; CA, cornu ammonis; DG, dentate gyrus; Presub, presubiculum; Sub, subiculum.

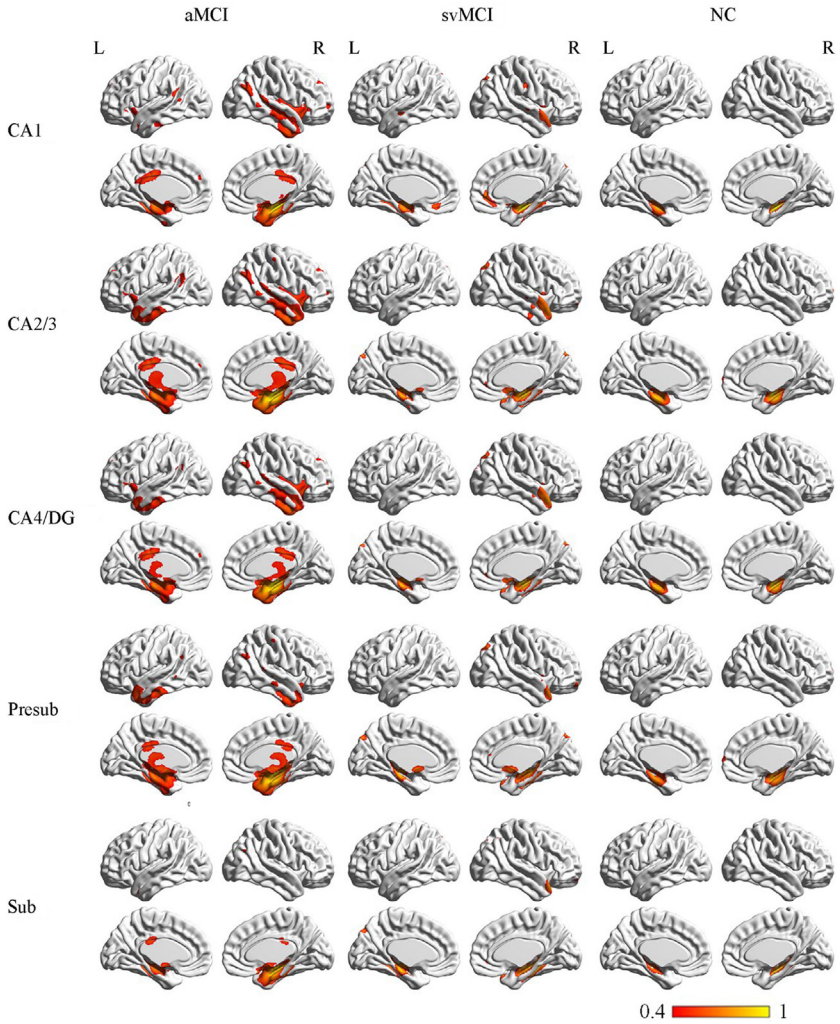

FIGURE 4 | Structural covariance networks of right hippocampal subfields in the three groups. Statistical maps of regions significantly correlated with the seed region in each group. The results are presented as CC values ($P < 0.05$, false discovery rate corrected). Abbreviations: L, left; R, right; CC, correlation coefficient; NC, normal controls; svMCI, subcortical vascular mild cognitive impairment; aMCI, amnestic mild cognitive impairment; CA, cornu ammonis; DG, dentate gyrus; Presub, presubiculum; Sub, subiculum.

correlated regions included the ERC and FFG in the NC group. The right presubiculum showed significant correlations with the right OFC, FFG, and ERC in NC subjects. The right subiculum covaried with the ERC and FFG.

Significant Difference in the Structural Associations Between Groups

aMCI Group vs. NC Group

There were some significant differences observed between the aMCI group and NC group when the strength of the structural correlations was considered (**Table 2**; **Figure 5**). There was a significant increased association between the hippocampal subfields and other brain regions that was found in the aMCI group compared to the NC group. The left CA1, left CA4/DG, left presubiculum, and left subiculum showed increased covariance with the left pole in the aMCI group compared to NC. In addition, increased significant covariance was found between the left CA1/left subiculum and left postcentral gyrus (POG), right CA2/3 and right middle/inferior temporal gyrus (ITG), and right CA1 and left angular gyrus in the aMCI group compared to the NC group.

svMCI Group vs. NC Group

The significant differences of the association slope between the svMCI group and the NC group are shown in **Table 2** and **Figure 6**. There were significant increased associations between the bilateral CA1/left CA2/3 and OFC in the svMCI group compared to the NC group. Then, the left presubiculum showed increased covariance with the right FFG in the aMCI group relative to the svMCI group. The right CA1 showed increased covariance with the right prefrontal gyrus in the svMCI group compared to the NC group.

TABLE 2 | Significant between-group differences in structural association between selected regions of interest and other cortical areas.

Contrast	Seed	BA	Region	MNI coordinates			Peak intensity	Cluster size (voxels)
				X	*Y*	*Z*		
aMCI vs. NC								
aMCI > NC	L_CA1	21/20	L TP	−60	6	−23	3.58	3,132
	L_CA1	3/4/6	L POG/PRG	−47	−23	63	3.75	1,472
	L_CA4/DG	21/20	L TP	−59	6	−23	3.49	2,047
	L_presubiculum	21/20	L TP	−57	9	−26	3.44	5,562
	L subiculum	3/4/6	L POG/PRG	−50	−23	60	3.93	1,796
	L subiculum	21/20	L TP	−57	8	−23	3.63	3,135
	R_CA1	40/39	L ANG/SMG	−51	−51	15	3.76	1,594
	R_CA2/3	21/20	R MTG/ITG	53	−33	−17	3.71	1,386
svMCI vs. NC								
svMCI > NC	L_CA1	11/10	OFC	−8	39	−23	4.23	2,359
	R_CA1	11/10	OFC	−8	39	−17	3.91	2,432
	R_CA1	10	R PFC	36	62	11	3.99	1,657
	L_CA2/3	11	OFC	−5	41	−24	3.91	1,564
	L_presubiculum	36/37	R FFG	35	−33	−14	4.05	2,261
aMCI vs. svMCI								
aMCI > svMCI	L_presubiculum	34/28/35	L ERC/PRC	−11	−6	−21	4.58	1,653
	L_subiculum	34/28/35	L ERC/PRC	−11	−5	−21	4.17	1,811
	R_prsubiculum	34/28/35	R ERC/PRC	15	−9	−21	4.37	1,188
	R_subiculum	34/28/35	R ERC/PRC	15	−9	−26	3.79	1,214
svMCI > aMCI	L_CA4/DG	36/37	R FFG	35	−33	−17	4.36	1,403
	L_presubiculum	36/37	R FFG	27	−33	−14	4.32	1,987
	L_subiculum	36/37	R FFG	38	−38	−11	4.59	2,208

The regions listed showed significant between-group differences (Gaussian random field-corrected at voxel level: $P < 0.01$ and cluster level: $P < 0.05$), and peak coordinates are reported in standard MNI space.

BA, Brodmann area; L, left; R, right; NC, normal controls; svMCI, vascular mild cognitive impairment; aMCI, amnestic mild cognitive impairment; CA, cornu ammonis; DG, dentate gyrus; ERC, entorhinal cortex; FFG, fusiform gyrus; TP, temporal pole; MTG, middle temporal gyrus; ITG, inferior temporal gyrus; POG, postcentral gyrus; PRG, precentral gyrus; PRC, perirhinal cortex; OFC, orbitofrontal cortex; PFC, prefrontal cortex; SMG, supramarginal gyrus; ANG, angular gyrus.

aMCI Group vs. svMCI Group

As shown in **Table 2** and **Figure 7**, there were significant increased associations between several hippocampal subfields (bilateral presubiculum, bilateral subiculum) and the bilateral ERC in the aMCI group compared to the svMCI group. Then, left hippocampal subfields mostly showed decreased covariance with the right FFG in the aMCI group relative to the svMCI group.

DISCUSSION

In this study, we selected hippocampal subfields as seeds to build SCNs among three groups. Specifically, hippocampal subfields correlated with the TP, thalamus, subcallosal cortex, and posterior cingula cortex in the aMCI group, while hippocampal subfields significantly covaried with the OFC in the svMCI group. Finally, we compared the differences in strength of structural covariance between groups. The results demonstrated that there were abnormal structural associations between hippocampal subfields and the cerebral cortex in aMCI and svMCI patients, and these abnormalities were different between them.

Structural Covariance Networks Within Groups

In our study, positive correlations between hippocampal subfields and FFG, and ERC in GM volume were found in each group. To some extent, these positive correlations suggested synchronous GM changes in these regions (29, 32). The ERC and FFG are anatomically adjacent to the hippocampus. Importantly, there were many intrinsic connections between the hippocampus, ERC, and FFG (7).

All the hippocampal subfields showed significantly positive structural covariance with the thalamus in the aMCI group. A previous study reported atrophy of the thalamus in aMCI patients (45). The positive structural covariance could be explained by the synchronous atrophy between the thalamus and hippocampus in the aMCI group. The subiculum and entorhinal cortices were found to project to the thalamus (1). There were many disruptions in the thalamus functional connectivity in aMCI including thalamo-hippocampus, thalamo-temporal, thalamo-visual, and thalamo-default network (46). Some cognitive impairments in aMCI, such as visual–spatial perception syndrome and visual hallucinations, may be due to thalamus atrophy and abnormalities in thalamus-related networks.

We also observed positive structural associations between the left hippocampal subfields and subcallosal cortex in the aMCI group. This suggested right subcallosal cortex atrophy in aMCI patients (47). In addition, significant correlations between cognitive scores on the episodic memory task and increased functional connectivity between the subcallosal cortex and hippocampus were found in aMCI patients (48). This indicated

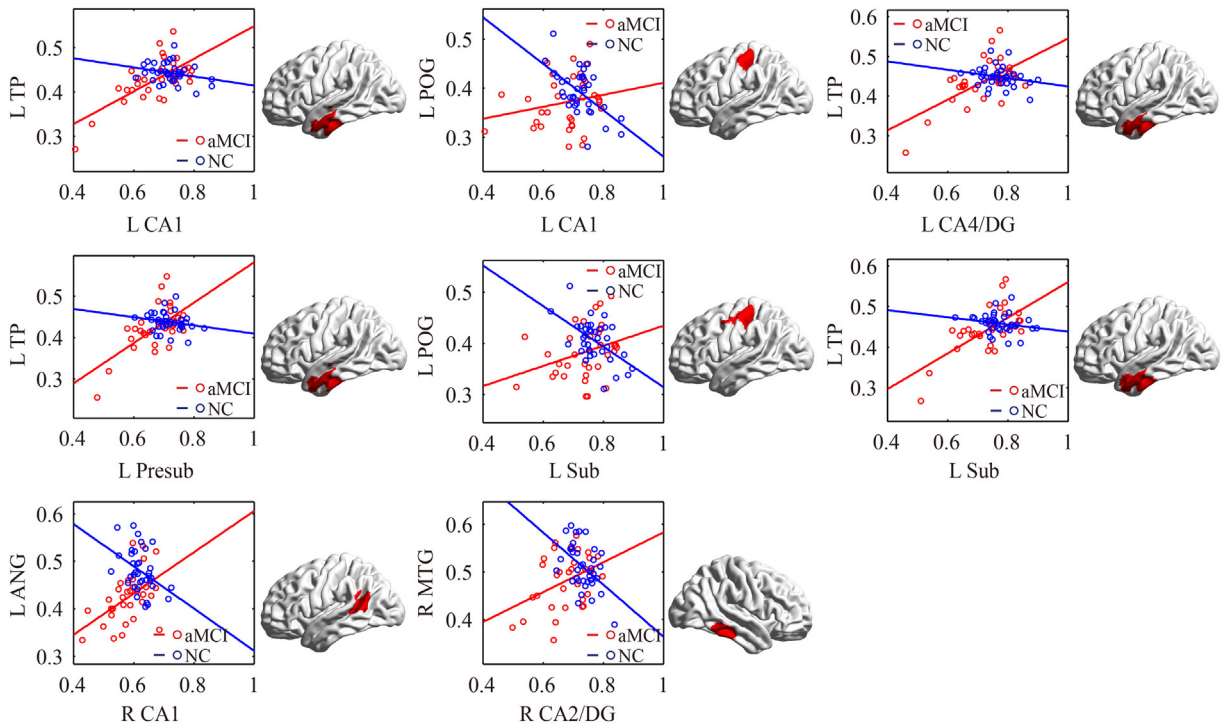

FIGURE 5 | Significant between-group differences in structural association for aMCI and NC. A cluster showing significant structural difference (Gaussian random field-corrected at voxel level: $P < 0.01$ and cluster level: $P < 0.05$) between aMCI and NC is presented on the right, and a plot of slope differences between the seed region and cluster region is presented on the left. Abbreviations: L, left; R, right; NC, normal controls; aMCI, amnestic mild cognitive impairment; CA, cornu ammonis; DG, dentate gyrus; Presub, presubiculum; Sub, subiculum; TP, temporal pole; POG, postcentral gyrus; ANG, angular gyrus.

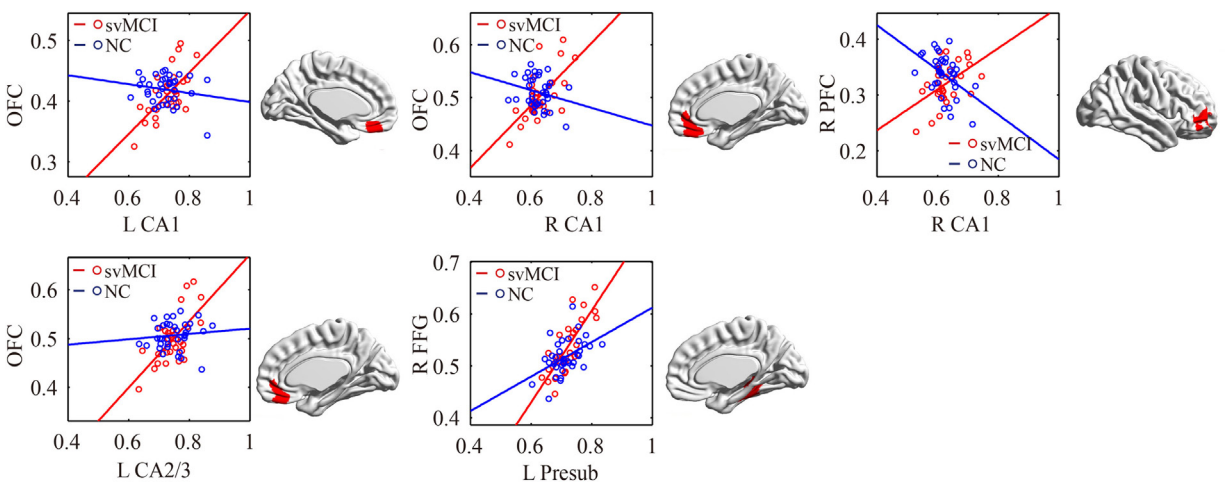

FIGURE 6 | Significant between-group differences in structural association for svMCI and NC. A cluster showing significant structural difference (Gaussian random field-corrected at voxel level: $P < 0.01$ and cluster level: $P < 0.05$) between svMCI and NC is presented on the right, and a plot of slope differences between the seed region and cluster region is presented on the left. Abbreviations: L, left; R, right; NC, normal controls; svMCI, subcortical vascular mild cognitive impairment; CA, cornu ammonis; DG, dentate gyrus; Presub, presubiculum; Sub, subiculum; OFC, orbitofrontal cortex; PFC, prefrontal cortex; FFG, fusiform gyrus.

that the abnormal structural correlations in the subcallosal cortex could be related to the observed memory deficits in aMCI patients.

We found significantly positive structural associations between the right hippocampal subfields and PCC in the aMCI group. Many histopathological (49), structural (50), and functional imaging (51, 52) studies consistently reported that the PCC was an important structure in the pathophysiology of AD and aMCI. Importantly, the functional disconnection of hippocampal subregions and PCC may be a main factor of impaired episodic

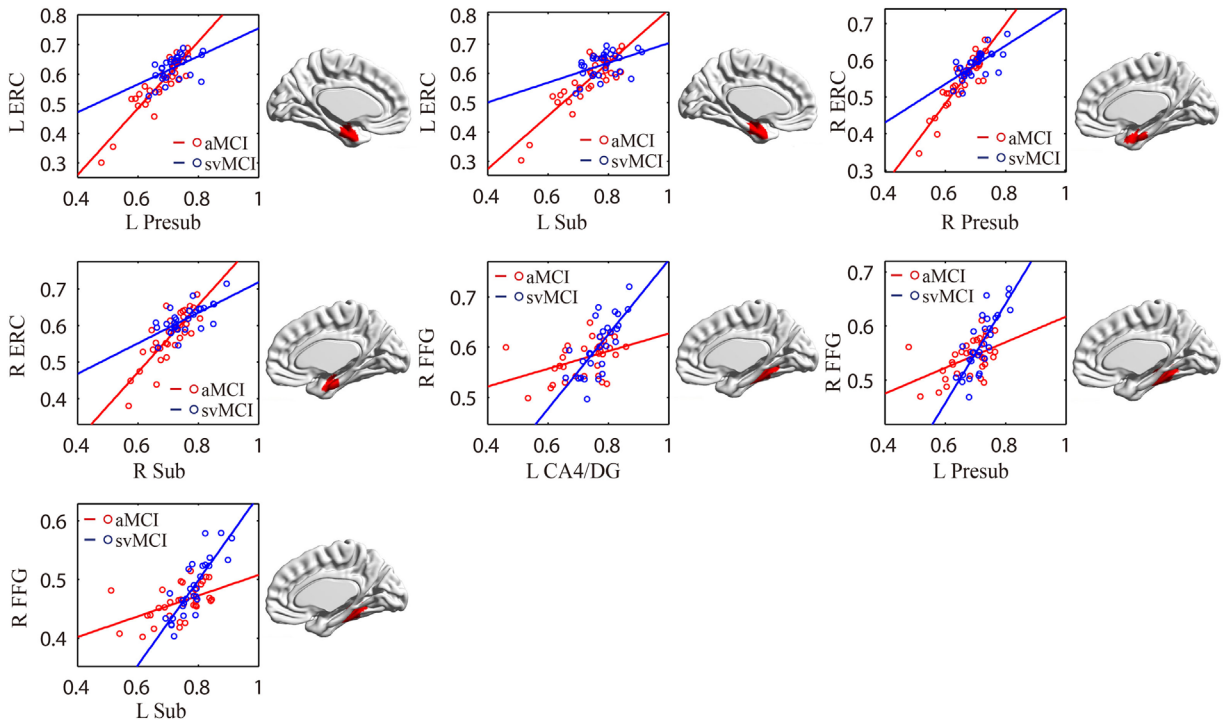

FIGURE 7 | Significant between-group differences in structural association for aMCI and svMCI. A cluster showing significant structural difference (Gaussian random field-corrected at voxel level: $P < 0.01$ and cluster level: $P < 0.05$) is presented on the right, and a plot of slope differences between the seed region and cluster region is presented on the left. Abbreviations: L, left; R, right; aMCI, amnestic mild cognitive impairment; svMCI, subcortical vascular mild cognitive impairment; CA, cornu ammonis; DG, dentate gyrus; Presub, presubiculum; Sub, subiculum; ERC, entorhinal cortex; FFG, fusiform gyrus.

memory in aMCI (20). Because the developmental trajectory of the structural network may associate with its functional specialization (53), the abnormality between PCC and hippocampal subfields may underpin the episodic memory deficits observed in aMCI.

Significant Differences in SCNs Between Groups

We observed that the increased connections between the right FFG and left presubiculum were stronger in svMCI than in the aMCI and NC groups. Previous studies have shown FFG atrophy in svMCI patients (24, 54). The FFG is related to semantic processing (55). Thus, the abnormal structural correlations between hippocampal subfields and the FFG could have an effect on the reduced capacity for semantic memory. Our results indicated that abnormality between the hippocampal subfields and FFG was distinct in svMCI, which was characterized by the main deficit of semantic memory compared to aMCI.

In the aMCI group, compared to the svMCI group, we observed an increased association between the bilateral presubiculum/subiculum and the ERC. The pathway from CA1 to the subiculum and projections to the ERC form the principal output from the hippocampus. The connections between CA1, subiculum, and ERC were associated with episodic memory processing (26). Therefore, the synchronous atrophy in the ERC and hippocampal subregions may suggest the disruption of episodic memory distinctly in aMCI patients.

The left CA1/CA4/DG/subiculum showed significantly increased structural association with the left TP in aMCI patients compared to NC. The stronger structural covariance potentially indicates synchronous GM changes in these regions affected by the disease (29). Thus, we speculate that the increased structural covariance between hippocampal subfields and the temporal gyrus suggests synchronous atrophy in the aMCI group. Several studies have shown atrophy in the temporal gyrus, especially in the medial and ITG, which supports our results (8, 56). The TP is associated with both social and emotional processes, which mainly involves face recognition and theory of mind (57). Chen et al. also indicated decreased connectivity between the middle hippocampus and middle temporal gyrus (MTG) in functional connectivity (26). We assumed that the synchronous atrophy between the hippocampus and MTG could explain the disrupted functional connectivity between them.

We also observed increased structural associations between the left CA1/subiculum and left POG in aMCI compared to NC. Left POG atrophy was reported in aMCI patients (58). Additionally, NC subjects had greater activations than aMCI patients during "Binds," which probe object memory in the left POG, and our findings on the abnormal structural correlation with the left POG could be related to early signs of object memory deficits in aMCI patients (53).

In addition, bilateral CA1 and left CA2/3 showed significantly positive associations with the OFC in the svMCI group compared

to the NC group. In addition, we found increased covariance between the right CA1 and right PFC in svMCI compared to NC. For PET imaging, the patients with svMCI showed hypometabolism in the inferior and medial frontal cortices adjacent to the cingulate gyrus (59). Importantly, the prefrontal gyrus is associated with executive function, which has a deficit in svMCI patients (60). Additionally, frontal-subcortical circuits, including hippocampus and OFC, mediate many aspects of human behavior, especially executive function (61). We assume that abnormal structural covariance between hippocampal subfields and the OFC indicates deficit of executive function in svMCI patients.

This study still has several limitations. First, we did not study the structural connectivity based on diffusion-weighted imaging (DWI) of the white matter pathway between hippocampal subfields and the whole brain cortex. There was a lack of systematic comparisons of structural covariance networks and DWI-based networks. Our findings of SCNs among the three groups should be cautiously extended to other structural networks. Second, in this study, due to the limited segmentation accuracies of hippocampal subfields in regular T1 images, we focused on the SCN analysis of each subfield instead of volumetric analysis of subfields. In the future, the volumetric analysis of hippocampal subfields would be helpful to understand the hippocampal abnormalities in the two MCI subtypes with the improvement of segmentation accuracies of hippocampal subfields in regular T1 images.

ETHICS STATEMENT

This study was approved by the medical research ethics committee and the institutional review board of Xuanwu Hospital, Capital Medical University, Beijing, China.

AUTHOR CONTRIBUTIONS

Conceived and designed the experiments: SL and XL. Analyzed the data: XW. Contributed reagents/materials/analysis tools: YY, YH, CY, and WZ. Wrote the paper: XW, SL, XL, QL, and YY.

FUNDING

This work was supported by National Natural Science Foundation of China (Grant No. 81622025, 81471731, 31371007, 81430037, 81771795 and 61633018), the Fundamental Research Funds for the Central Universities (No. YWF-17-BJ-J-11), and National Key Research and Development Program of China (No. 2016YFC1306300).

REFERENCES

1. Amaral D, Lavenex P. Hippocampal neuroanatomy. In: Andersen P, Morris R, Amaral D, Bliss T, O'Keefe J, editors. *The Hippocampus Book*. New York: Oxford University Press (2007). p. 37–144.
2. Harrison PJ. The hippocampus in schizophrenia: a review of the neuropathological evidence and its pathophysiological implications. *Psychopharmacology* (2004) 174(1):151–62. doi:10.1007/s00213-003-1761-y
3. Kuruba R, Hattiangady B, Shetty AK. Hippocampal neurogenesis and neural stem cells in temporal lobe epilepsy. *Epilepsy Behav* (2009) 14(1):65–73. doi:10.1016/j.yebeh.2008.08.020
4. Hampel H, Bürger K, Teipel SJ, Bokde AL, Zetterberg H, Blennow K. Core candidate neurochemical and imaging biomarkers of Alzheimer's disease. *Alzheimer Dement* (2008) 4(1):38–48. doi:10.1016/j.jalz.2007.08.006
5. Duvernoy HM. *The Human Hippocampus: Functional Anatomy, Vascularization and Serial Sections with MRI*. Springer Science & Business Media (2005).
6. Fanselow MS, Dong H-W. Are the dorsal and ventral hippocampus functionally distinct structures? *Neuron* (2010) 65(1):7–19. doi:10.1016/j.neuron.2009.11.031
7. Rajmohan V, Mohandas E. The limbic system. *Indian J Psychiatry* (2007) 49(2):132. doi:10.4103/0019-5545.33264
8. Whitwell JL, Shiung MM, Przybelski S, Weigand SD, Knopman DS, Boeve BF, et al. MRI patterns of atrophy associated with progression to AD in amnestic mild cognitive impairment. *Neurology* (2008) 70(7):512–20. doi:10.1212/01.wnl.0000280575.77437.a2
9. Li X, Li D, Li Q, Li Y, Li K, Li S, et al. Hippocampal subfield volumetry in patients with subcortical vascular mild cognitive impairment. *Sci Rep* (2016) 6. doi:10.1038/srep20873
10. Petersen RC, Smith GE, Waring SC, Ivnik RJ, Tangalos EG, Kokmen E. Mild cognitive impairment: clinical characterization and outcome. *Arch Neurol* (1999) 56(3):303–8. doi:10.1001/archneur.56.3.303
11. Petersen RC, Aisen P, Boeve BF, Geda YE, Ivnik RJ, Knopman DS, et al. Mild cognitive impairment due to Alzheimer disease in the community. *Ann Neurol* (2013) 74(2):199–208. doi:10.1002/ana.23931
12. Sachdev P, Kalaria R, O'Brien J, Skoog I, Alladi S, Black SE, et al. Diagnostic criteria for vascular cognitive disorders: a VASCOG statement. *Alzheimer Dis Assoc Disord* (2014) 28(3):206. doi:10.1097/WAD.0000000000000034
13. Murphy KJ, Troyer AK, Levine B, Moscovitch M. Episodic, but not semantic, autobiographical memory is reduced in amnestic mild cognitive impairment. *Neuropsychologia* (2008) 46(13):3116–23. doi:10.1016/j.neuropsychologia.2008.07.004
14. Petersen RC. Mild cognitive impairment clinical trials. *Nat Rev Drug Discov* (2003) 2(8):646. doi:10.1038/nrd1155
15. Visser PJ, Kester A, Jolles J, Verhey F. Ten-year risk of dementia in subjects with mild cognitive impairment. *Neurology* (2006) 67(7):1201–7. doi:10.1212/01.wnl.0000238517.59286.c5
16. Mendonca A, Ribeiro F, Guerreiro M, Palma T, Garcia C. Clinical significance of subcortical vascular disease in patients with mild cognitive impairment. *Eur J Neurol* (2005) 12(2):125–30. doi:10.1111/j.1468-1331.2004.00892.x
17. Erkinjuntti T. Subcortical ischemic vascular disease and dementia. *Int Psychogeriatr* (2003) 15(S1):23–6. doi:10.1017/S1041610203008925
18. Kim SH, Kang HS, Kim HJ, Moon Y, Ryu HJ, Kim MY, et al. The effect of ischemic cholinergic damage on cognition in patients with subcortical vascular cognitive impairment. *J Geriatr Psychiatry Neurol* (2012) 25(2):122–7. doi:10.1177/0891988712445089
19. Kwon OD. Cognitive features of vascular dementia. In: Heinbockel T, editor. *Neuroscience*. Rijeka, Croatia: InTech (2012). p 127–38.
20. Bai F, Liao W, Watson DR, Shi Y, Wang Y, Yue C, et al. Abnormal whole-brain functional connection in amnestic mild cognitive impairment patients. *Behav Brain Res* (2011) 216(2):666–72. doi:10.1016/j.bbr.2010.09.010
21. Gili T, Cercignani M, Serra L, Perri R, Giove F, Maraviglia B, et al. Regional brain atrophy and functional disconnection across Alzheimer's disease evolution. *J Neurol Neurosurg Psychiatry* (2011) 82(1):58–66. doi:10.1136/jnnp.2009.199935
22. Yi L, Wang J, Jia L, Zhao Z, Lu J, Li K, et al. Structural and functional changes in subcortical vascular mild cognitive impairment: a combined voxel-based morphometry and resting-state fMRI study. *PLoS One* (2012) 7(9):e44758. doi:10.1371/journal.pone.0044758
23. Nowrangi MA, Lyketsos CG, Leoutsakos J-MS, Oishi K, Albert M, Mori S, et al. Longitudinal, region-specific course of diffusion tensor imaging measures in mild cognitive impairment and Alzheimer's disease. *Alzheimer Dement* (2013) 9(5):519–28. doi:10.1016/j.jalz.2012.05.2186
24. Zhou X, Hu X, Zhang C, Wang H, Zhu X, Xu L, et al. Aberrant functional connectivity and structural atrophy in subcortical vascular cognitive

impairment: relationship with cognitive impairments. *Front Aging Neurosci* (2016) 8:14. doi:10.3389/fnagi.2016.00014
25. Bai F, Xie C, Watson DR, Shi Y, Yuan Y, Wang Y, et al. Aberrant hippocampal subregion networks associated with the classifications of aMCI subjects: a longitudinal resting-state study. *PLoS One* (2011) 6(12):e29288. doi:10.1371/journal.pone.0029288
26. Chen J, Duan X, Shu H, Wang Z, Long Z, Liu D, et al. Differential contributions of subregions of medial temporal lobe to memory system in amnestic mild cognitive impairment: insights from fMRI study. *Sci Rep* (2016) 6:sre26148. doi:10.1038/srep26148
27. Mechelli A, Friston KJ, Frackowiak RS, Price CJ. Structural covariance in the human cortex. *J Neurosci* (2005) 25(36):8303–10. doi:10.1523/JNEUROSCI.0357-05.2005
28. Zielinski BA, Gennatas ED, Zhou J, Seeley WW. Network-level structural covariance in the developing brain. *Proc Natl Acad Sci U S A* (2010) 107(42):18191–6. doi:10.1073/pnas.1003109107
29. Alexanderbloch A, Giedd JN, Bullmore E. Imaging structural co-variance between human brain regions. *Nat Rev Neurosci* (2013) 14(5):322–36. doi:10.1038/nrn3465
30. McAlonan GM, Cheung V, Cheung C, Suckling J, Lam GY, Tai K, et al. Mapping the brain in autism. A voxel-based MRI study of volumetric differences and intercorrelations in autism. *Brain* (2004) 128(2):268–76. doi:10.1093/brain/awh332
31. Cardoner N, Soriano-Mas C, Pujol J, Alonso P, Harrison BJ, Deus J, et al. Brain structural correlates of depressive comorbidity in obsessive–compulsive disorder. *Neuroimage* (2007) 38(3):413–21. doi:10.1016/j.neuroimage.2007.07.039
32. Li X, Cao Q, Pu F, Li D, Fan Y, An L, et al. Abnormalities of structural covariance networks in drug-naïve boys with attention deficit hyperactivity disorder. *Psychiatry Res* (2015) 231(3):273–8. doi:10.1016/j.pscychresns.2015.01.006
33. Petersen RC. Mild cognitive impairment as a diagnostic entity. *J Intern Med* (2004) 256(3):183–94. doi:10.1111/j.1365-2796.2004.01388.x
34. Van Leemput K, Bakkour A, Benner T, Wiggins G, Wald LL, Augustinack J, et al. Automated segmentation of hippocampal subfields from ultra-high resolution in vivo MRI. *Hippocampus* (2009) 19(6):549–57. doi:10.1002/hipo.20615
35. Kühn S, Musso F, Mobascher A, Warbrick T, Winterer G, Gallinat J. Hippocampal subfields predict positive symptoms in schizophrenia: first evidence from brain morphometry. *Transl Psychiatry* (2012) 2(6):e127. doi:10.1038/tp.2012.51
36. Koch K, Reess TJ, Rus OG, Zimmer C. Extensive learning is associated with gray matter changes in the right hippocampus. *Neuroimage* (2016) 125:627–32. doi:10.1016/j.neuroimage.2015.10.056
37. Tohka J, Zijdenbos A, Evans A. Fast and robust parameter estimation for statistical partial volume models in brain MRI. *Neuroimage* (2004) 23(1):84–97. doi:10.1016/j.neuroimage.2004.05.007
38. Manjón JV, Coupé P, Martí-Bonmatí L, Collins DL, Robles M. Adaptive non-local means denoising of MR images with spatially varying noise levels. *J Magn Reson Imaging* (2010) 31(1):192–203. doi:10.1002/jmri.22003
39. Rajapakse JC, Giedd JN, Rapoport JL. Statistical approach to segmentation of single-channel cerebral MR images. *IEEE Trans Med Imaging* (1997) 16(2):176–86. doi:10.1109/42.563663
40. Ashburner J. A fast diffeomorphic image registration algorithm. *Neuroimage* (2007) 38(1):95–113. doi:10.1016/j.neuroimage.2007.07.007
41. Good CD, Johnsrude IS, Ashburner J, Henson RNA, Friston KJ, Frackowiak RSJ. A voxel-based morphometric study of ageing in 465 normal adult human brains. *Neuroimage* (2001) 14(1):21–36. doi:10.1006/nimg.2001.0786
42. Xia M, Wang J, He Y. BrainNet Viewer: a network visualization tool for human brain connectomics. *PLoS One* (2013) 8(7):e68910. doi:10.1371/journal.pone.0068910
43. Lerch JP, Worsley K, Shaw WP, Greenstein DK, Lenroot RK, Giedd J, et al. Mapping anatomical correlations across cerebral cortex (MACACC) using cortical thickness from MRI. *Neuroimage* (2006) 31(3):993–1003. doi:10.1016/j.neuroimage.2006.01.042
44. Li X, Pu F, Fan Y, Niu H, Li S, Li D. Age-related changes in brain structural covariance networks. *Front Hum Neurosci* (2013) 7(1):265–9. doi:10.3389/fnhum.2013.00098
45. Balthazar M, Yasuda C, Pereira F, Pedro T, Damasceno B, Cendes F. Differences in grey and white matter atrophy in amnestic mild cognitive impairment and mild Alzheimer's disease. *Eur J Neurol* (2009) 16(4):468–74. doi:10.1111/j.1468-1331.2008.02408.x
46. Cai S, Huang L, Zou J, Jing L, Zhai B, Ji G, et al. Changes in thalamic connectivity in the early and late stages of amnestic mild cognitive impairment: a resting-state functional magnetic resonance study from ADNI. *PLoS One* (2015) 10(2):e0115573. doi:10.1371/journal.pone.0115573
47. Shiino A, Watanabe T, Maeda K, Kotani E, Akiguchi I, Matsuda M. Four subgroups of Alzheimer's disease based on patterns of atrophy using VBM and a unique pattern for early onset disease. *Neuroimage* (2006) 33(1):17–26. doi:10.1016/j.neuroimage.2006.06.010
48. Bai F, Zhang Z, Watson DR, Yu H, Shi Y, Yuan Y, et al. Abnormal functional connectivity of hippocampus during episodic memory retrieval processing network in amnestic mild cognitive impairment. *Biol Psychiatry* (2009) 65(11):951–8. doi:10.1016/j.biopsych.2008.10.017
49. Rowe CC, Ng S, Ackermann U, Gong SJ, Pike K, Savage G, et al. Imaging-amyloid burden in aging and dementia. *Neurology* (2007) 68(20):1718. doi:10.1212/01.wnl.0000261919.22630.ea
50. Pengas G, Hodges JR, Watson P, Nestor PJ. Focal posterior cingulate atrophy in incipient Alzheimer's disease. *Neurobiol Aging* (2010) 31(1):25. doi:10.1016/j.neurobiolaging.2008.03.014
51. Liang WS, Reiman EM, Valla J, Dunckley T, Beach TG, Grover A, et al. Alzheimer's disease is associated with reduced expression of energy metabolism genes in posterior cingulate neurons. *Proc Natl Acad Sci U S A* (2008) 105(11):4441. doi:10.1073/pnas.0709259105
52. Sole AD, Clerici F, Chiti A, Lecchi M, Mariani C, Maggiore L, et al. Individual cerebral metabolic deficits in Alzheimer's disease and amnestic mild cognitive impairment: an FDG PET study. *Eur J Nucl Med Mol Imaging* (2008) 35(7):1357–66. doi:10.1007/s00259-008-0773-6
53. Chiang HS, Mudar R, Rackley A, Venza E, Pudhiyidath A, Van JJ, et al. An early fMRI marker of semantic memory deficits in people with amnestic mild cognitive impairment. *Alzheimers Dement* (2013) 9(4):580–580. doi:10.1016/j.jalz.2013.05.1151
54. Li M, Meng Y, Wang M, Yang S, Wu H, Zhao B, et al. Cerebral gray matter volume reduction in subcortical vascular mild cognitive impairment patients and subcortical vascular dementia patients, and its relation with cognitive deficits. *Brain Behav* (2017) 7(8):e00745. doi:10.1002/brb3.745
55. Wagner AD, Schacter DL, Rotte M, Koutstaal W, Maril A, Dale AM, et al. Building memories: remembering and forgetting of verbal experiences as predicted by brain activity. *Science* (1998) 281(5380):1188–91. doi:10.1126/science.281.5380.1188
56. Duara R, Loewenstein D, Potter E, Appel J, Greig M, Urs R, et al. Medial temporal lobe atrophy on MRI scans and the diagnosis of Alzheimer disease. *Neurology* (2008) 71(24):1986–92. doi:10.1212/01.wnl.0000336925.79704.9f
57. Olson IR, Plotzker A, Ezzyat Y. The enigmatic temporal pole: a review of findings on social and emotional processing. *Brain* (2007) 130(7):1718–31. doi:10.1093/brain/awm052
58. Zhang H, Sachdev PS, Wen W, Kochan NA, Crawford JD, Brodaty H, et al. Gray matter atrophy patterns of mild cognitive impairment subtypes. *J Neurol Sci* (2012) 315(1–2):26–32. doi:10.1016/j.jns.2011.12.011
59. Seo SW, Cho SS, Park A, Chin J, Na DL. Subcortical vascular versus amnestic mild cognitive impairment: comparison of cerebral glucose metabolism. *J Neuroimaging* (2009) 19(3):213–9. doi:10.1111/j.1552-6569.2008.00292.x
60. Koechlin E, Summerfield C. An information theoretical approach to prefrontal executive function. *Trends Cogn Sci* (2007) 11(6):229–35. doi:10.1016/j.tics.2007.04.005
61. Bonelli RM, Cummings JL. Frontal-subcortical circuitry and behavior. *Dialogues Clin Neurosci* (2007) 9(2):141–51.

Conflict of Interest Statement: The authors declare that the research was conducted in the absence of any commercial or financial relationships that could be construed as a potential conflict of interest.

frontiers in Neurology

ORIGINAL RESEARCH
published: 19 October 2018
doi: 10.3389/fneur.2018.00779

Vascular Protection of Hydrogen Sulfide on Cerebral Ischemia/Reperfusion Injury in Rats

Ji-Yue Wen[1†], *Mei Wang*[2†], *Ya-Nan Li*[1†], *Hui-Hui Jiang*[1], *Xuan-Jun Sun*[1] *and Zhi-Wu Chen*[1*]

[1] *Department of Pharmacology, Anhui Medical University, Hefei, China,* [2] *Department of Pharmacy, Children's Hospital of Soochow University, Suzhou, China*

This study was undertaken to demonstrate the vascular protection of exogenous and endogenous hydrogen sulfide (H_2S) on cerebral ischemia/reperfusion (I/R) injury. The effect of H_2S on cerebrovascular dysfunction in middle cerebral artery (MCA) and neuronal damage were measured after cerebral I/R induced by transient middle cerebral artery occlusion (MCAO) in cystathionine c-lyase (CSE) knockdown and wild-type rats. The effect of sodium hydrosulfide (NaHS, donor of exogenous H_2S), L-cysteine (L-Cys, substrate of endogenous H_2S), and endothelium cells on the responses of isolated MCA derived from non-ischemic rats was also evaluated to assess the underlying mechanism of H_2S-mediate cerebral vasodilation. The results revealed that the contraction and dilation of MCA profoundly decreased after cerebral I/R. The vascular dysfunction became more grievous in CSE knockdown rats than in wild-type rats. Interestingly, this vascular dysfunction was significantly alleviated by NaHS supplementation. Moreover, both NaHS and L-cysteine could induce remarkable relaxation in the isolated MCA, which was eliminated by co-application of potassium channel blockers ChTx and Apamin, or endothelial removal. By contrast, adding endothelium cells cultured *in vitro* together with ACh into the luminal perfusate could mimic non-NO and non-PGI_2 relaxation in endothelium-denuded MCA, once CSE was knocked down from endothelium cells, and its effect on vasorelaxation was abolished. Furthermore, the indexes of neuronal injury were measured after cerebral I/R to confirm the neuroprotection of H_2S, and we found that the neurological scores, cerebral infarction volume, brain water content, malondialdehyde content, and serum lactate dehydrogenase activity (a marker of cellular membrane integrity) were significantly higher in CSE knockdown rats than in normal control rats. It is not surprising that NaHS could alleviate the cerebral injury. These findings revealed that H_2S has a protective effect on cerebral I/R injury via its upregulation of the endothelium-dependent contraction and dilation function of cerebral vessels, which may be related to activating potassium channel.

Keywords: hydrogen sulfide, ischemia/reperfusion, vascular function, neuronal injury, K_{ca} channel

OPEN ACCESS

Edited by:
Pei Jiang,
Jining Medical University, China

Reviewed by:
Kevin Donald Broad,
University College London,
United Kingdom
Sulev Kõks,
University of Tartu, Estonia

***Correspondence:**
Zhi-Wu Chen
chpharmzw@163.com

[†] *These authors have contributed equally to this work*

Specialty section:
This article was submitted to Neuropharmacology, a section of the journal Frontiers in Neurology

Received: *28 June 2018*
Accepted: *29 August 2018*
Published: *19 October 2018*

Citation:
Wen J-Y, Wang M, Li Y-N, Jiang H-H, Sun X-J and Chen Z-W (2018) Vascular Protection of Hydrogen Sulfide on Cerebral Ischemia/Reperfusion Injury in Rats. Front. Neurol. 9:779. doi: 10.3389/fneur.2018.00779

INTRODUCTION

Ischemic stroke is one of the most common cerebrovascular diseases with high mortality and disability rate. Previous studies have shown that ischemia could reduce the cerebral vascular response and change the tension of the vessels, which is the leading cause of disruption of the cerebral blood flow around the ischemic area, and the following hypotension and hypercapnia induced by ischemia could induce vascular dysfunction and finally neuronal injury (1, 2). Autoregulation of cerebral blood vessels is of great importance to protect the neuron against ischemia injury during the hypercapnia and hypotension condition (3, 4). Therefore, the effective treatment for ischemic stroke depends on a functional and patent vasculature, and hence vascular protection is regarded as an important therapeutic approach to reduce stroke damage (5).

Hydrogen sulfide (H_2S) is regarded as the third endogenous gasotransmitter (6), following carbon monoxide (CO) and nitric oxide (NO). Accumulated evidence indicates that H_2S plays a much more active and important role against ischemia/reperfusion (I/R) injury, such as kidney I/R injury (7), myocardial I/R injury (8), and cerebral I/R injury (9). Endogenous H_2S is mainly produced from L-cysteine (L-Cys) in intracytoplasm by cystathionine r-lyase (CSE), cystathionine β-synthase (CBS), and β-mercaptopyruvic acid in mitochondria by 3-mercaptopyruvate sulfurtransferase (3-MST) (10). In the vasculature, the endogenous H_2S is mainly produced from L-cysteine by CSE in endothelium (11).

H_2S plays a number of roles in the central nervous system (CNS) under pathological and physiological states such as anti-inflammation, cytoprotection, antiapoptosis, and antioxidation (12–14). In our previous studies, we found that H_2S mediated the hyperpolarization and dilation of rat cerebral arteries including the MCA and the basilar artery (BA) (15, 16). However, the effect of H_2S on the cerebrovascular dysfunction after cerebral I/R is still unclear. In addition, we previously also found that intravenous injection with CSE-siRNA and atelocollagen in rats could remarkably knock down the CSE mRNA and protein expression *in vivo* in cerebral vessels and reduce the production of H_2S. Moreover, we have revealed that NaHS could augment the K_{Ca} current in CBA vascular smooth muscle cells (17). Therefore, we tested the hypothesis in this study, whether H_2S could attenuate the cerebrovascular dysfunction and the neuronal damage that follows cerebral I/R. Likewise, we followed the same CSE-siRNA- transfection approach to knockdown the CSE expression and reduce the H_2S production for investigating the effect of endogenous H_2S on cerebrovascular dysfunction and neuronal damage. In addition, we also sought to explore the role of exogenous H_2S on cerebral I/R injury and further investigate the underlying mechanism of vascular protection of H_2S.

MATERIALS AND METHODS

Reagents

CSE-siRNA and negative siRNA were purchased from GenePharma (Shanghai, China), and atelocollagen was purchased from KOKEN (Tokyo, Japan); CSE antibody was purchased from Santa Cruz (Delaware Ave, USA); NaHS, Acetylcholine(ACh), bradykinin, 9, 11-dideoxy-11α, 9α-epoxy-methanoprostaglandin $F_{2\alpha}$ (U46619), and Vinpocetine were purchased from Sigma Chemicals (St. Louis, USA); lactate dehydrogenase (LDH) and malondialdehyde (MDA) assay kits were purchased from Nanjing Jiancheng Biological Co (Nanjing, China). ChTx, Apamin, L-Cys, L-NG-nitroarginine methyl ester (L-NAME), and indomethacin (Indo) were purchased from sigma Chemicals (St. Louis, USA); Krebs solution (comprising the following (mM): NaCl 118, KCl 3.4, $CaCl_2$ 2.5, KH_2PO_4 1.2, $MgSO_4$ 1.2, $NaHCO_3$ 25, and glucose 11.1) was aerated with a mixture of 95% O_2 and 5% CO_2 and oxygenated during the incubation period.

Experimental Animals

Adult male Sprague-Dawley (SD) rats, weighing between 250 and 300 g, were obtained from the Experimental Animal Center of Anhui Medical University. The animals were allowed free access to water and rodent chow. All experimental procedures were approved by the Ethics Review Committee of Anhui Medical University, which comply with the Guide for the Care and Use of laboratory Animals published by the US National Institutes of Health (NIH publication no. 85-23, revised 2011).

Cell Cultures

Human umbilical vein endothelial cells, EAhy926, were purchased from the Cell Bank, Shanghai Institutes for Biological Sciences, Chinese Academy of Sciences, and were cultured with high glucose Dulbecco's Modified Eagle Medium containing 10% heat-inactivated fetal bovine serum (Gibco), and were transfected by siRNA to knock down the expression of CSE according to the previous research (18).

CSE-siRNA Transfection and Cerebral I/R Injury Model in Rats

As described in our previous study (17), the CSE was knocked down with siRNA-transfection technique. The decrease of CSE and its mRNA expression in MCA was used as the indicator of CSE knockdown, measured by western blot and real-time PCR analysis. At 48 h after siRNA-transfection, the cerebral I/R injury of rats was induced by MCAO under chloral hydrate anesthesia (350 mg/kg, ip) (19). Briefly, a 4-0 nylon monofilament suture (total length: 30 mm; diameter: 0.23 mm) was dipped in melted hard wax at the head end, slightly inserted into the right common carotid artery, and pushed ∼18–22 mm from the carotid bifurcation to the internal carotid; blood flow of MCA was then blocked at the origin. After 2 h of ischemia, the suture was carefully withdrawn for reperfusion for 24 h. Rats of the non-CSE-siRNA transfected experiment were grouped as: (1) Sham ($n = 10$); (2) MCAO ($n = 10$); (3) MCAO+1×10^{-5} mol/kg NaHS ($n = 10$); (4) MCAO+1×10^{-6} mol/kg NaHS ($n = 10$); (5) MCAO+1×10^{-7} mol/kg NaHS ($n = 10$). Sham group animals were also subjected to the above procedures, except for suture insertion. Rats of CSE-siRNA transfected experiment were grouped as: (1) Sham ($n = 10$); (2) Control ($n = 10$); (3) CSE-siRNA ($n = 10$); (4) CSE-siRNA+NaHS ($n = 10$). Sham group animals were also subjected to the above procedures, except for

suture insertion. NaHS was injected into the tail vein of rats after ischemia, while the sham and control rats were injected with saline.

Cerebral Vessel Experiment

As described previously (17), the brains of MCAO or non-ischemic rats were rapidly removed after sacrifice under anesthesia and placed in precooled Krebs solution. MCA was carefully isolated immediately and cut into serial segments of 3 mm in length. Subsequently, both ends of the vessel segment were cannulated with glass micropipettes, secured with a nylon monofilament suture and then placed in a perfusion chamber. Thereafter, the segments were equilibrated with 37°C Krebs solutions and continuously aerated with a gas mixture of 95% O_2 and 5% CO_2 and then pressurized to 85 mmHg. The luminal flow was then adjusted to 150 μl/min. After 60 min of equilibrium, 1×10^{-7} mol/l U46619 or 30 mmol/L KCl was added to the luminal perfusate until a stable contraction was obtained. The diameter of the artery of non-ischemic rats was continually measured utilizing E-rule software, and MCA tension of MCAO rats was measured by myograph (17). The percentage of maximum diameter (% Dmax) was calculated and used to evaluate the vascular dilation of non-ischemic rats using the following formula: Dilation (%) = $(D_x - D_{min})/(D_{max} - D_{min}) \times 100\%$, where D_x is the diameter after administration of NaHS, L-Cys, or endothelial cells, D_{min} is the stable diameter of artery precontracted with U46619 or KCl, and D_{max} is the initial diameter. The maximum rate of vascular dilation of MCAO rats was calculated using the following formula: Dilation (%) = $(T_{min}\text{-}T_x)/(T_{min} - T_{max}) \times 100\%$, where T_{min} is the stably tension of artery precontracted with U46619, T_x is the vascular tension after administration of ACh or vinpocetine, and T_{max} is the initially vascular tension.

Evaluation of Neurological Score

Neurological score (20) of rats was evaluated at 24 h after reperfusion. It was scored on a five-point scale: (1) score 0: no neurologic deficit; (2) score 1: a mild focal neurologic deficit (failure to extend left forepaw fully); (3) score 2: a moderate focal neurologic deficit (circling to the left); (4) score 3: a severe focal deficit (falling to the left); (5) score 4: rat could not walk spontaneously and had a depressed level of consciousness.

Determination of Infarction Volume and Brain Water Content

At the end of the neurological score test, the rats were sacrificed with anesthesia. The brains were rapidly removed and sliced coronally at a 2 mm interval. The brain slices were then incubated in the dark in 2% TTC in phosphate-buffered solution (PBS) at 37°C for 30 min for staining. Subsequently, the stained slices were placed in 4% paraformaldehyde for 10 min. All the stained brain slices were photographed subsequently to delineate the area of infarct size using Image J, version 1.6 (National Institutes of Health, Bethesda, MD, USA). As described previously (9), the percentage of infarction volume was determined by normalizing the whole brain.

The dry-wet approach was used to measure the brain water content (21). In short, the fresh slices of each brain were weighed to attain the wet weight. The fresh tissues were then dried in an oven at 105°C for 48 h and weighed again to obtain the dry weight. Brain water content was calculated using the following formula:

Brain water content (%) = (wet weight – dry weight)/wet weight × 100%.

Measurement of Serum LDH Activity and MDA Level

Briefly, serum and supernatant of brain tissue homogenate of rats were collected and transferred to 96 well plates for LDH activity and MDA level analysis, using the biochemistry assay kit (Jiancheng Bioengineering Ltd, Nanjing, China) and abiding by the manufacturer's manual.

Statistical Analysis

Statistical analysis was performed by one-way analysis of variance (ANOVA) followed by the Duncan test to determine the difference between groups. Blood vessel data is presented as mean ± SD, and the other data are expressed as mean ± SEM. The $p < 0.05$ are considered significant.

RESULTS

Effect of H_2S on Cerebrovascular Function of Rats

Exogenous H_2S Attenuated Cerebrovascular Dysfunction Induced by Cerebral I/R

Changes of vascular tension in MCA from MCAO rats were examined after cerebral I/R. As shown in **Figure 1**, in the sham group, 1×10^{-7} mmol/L U46619 evoked significant constriction in MCA with maximum response (E_{max}) of 1.88 ± 0.19 mN. The contraction in MCA from MCAO rats to U46619 was profoundly decreased and the E_{max} was reduced to 0.39 ± 0.12 mN, but the reduction was significantly ameliorated by $1 \times 10^{-5} \sim 1 \times 10^{-7}$ mol/kg NaHS supplement. Furthermore, the ACh-mediated relaxations in MCA were also remarkably inhibited by MCAO, with the E_{max} being reduced from 68.27 ± 3.71% of the sham group rats to 8.91 ± 3.66% of the model group rats, and the dilation dysfunction in MCA was also attenuated by $1 \times 10^{-5} \sim 1 \times 10^{-7}$ mol/kg NaHS supplement. In addition, vinpocetine-mediated non-endothelium-dependent relaxation in MCA was also significantly attenuated in the model group (E_{max}: 68.44 ± 12.21% in the model group and 151.48 ± 25.32% in the sham group). Interestingly, the decrease of vascular relaxation to vinpocetine injured by cerebral I/R was similarly ameliorated by $1 \times 10^{-6} \sim 1 \times 10^{-7}$ mol/kg NaHS supplement. These results indicated that exogenous H_2S has a protective effect on the cerebrovascular dysfunction injured by cerebral I/R.

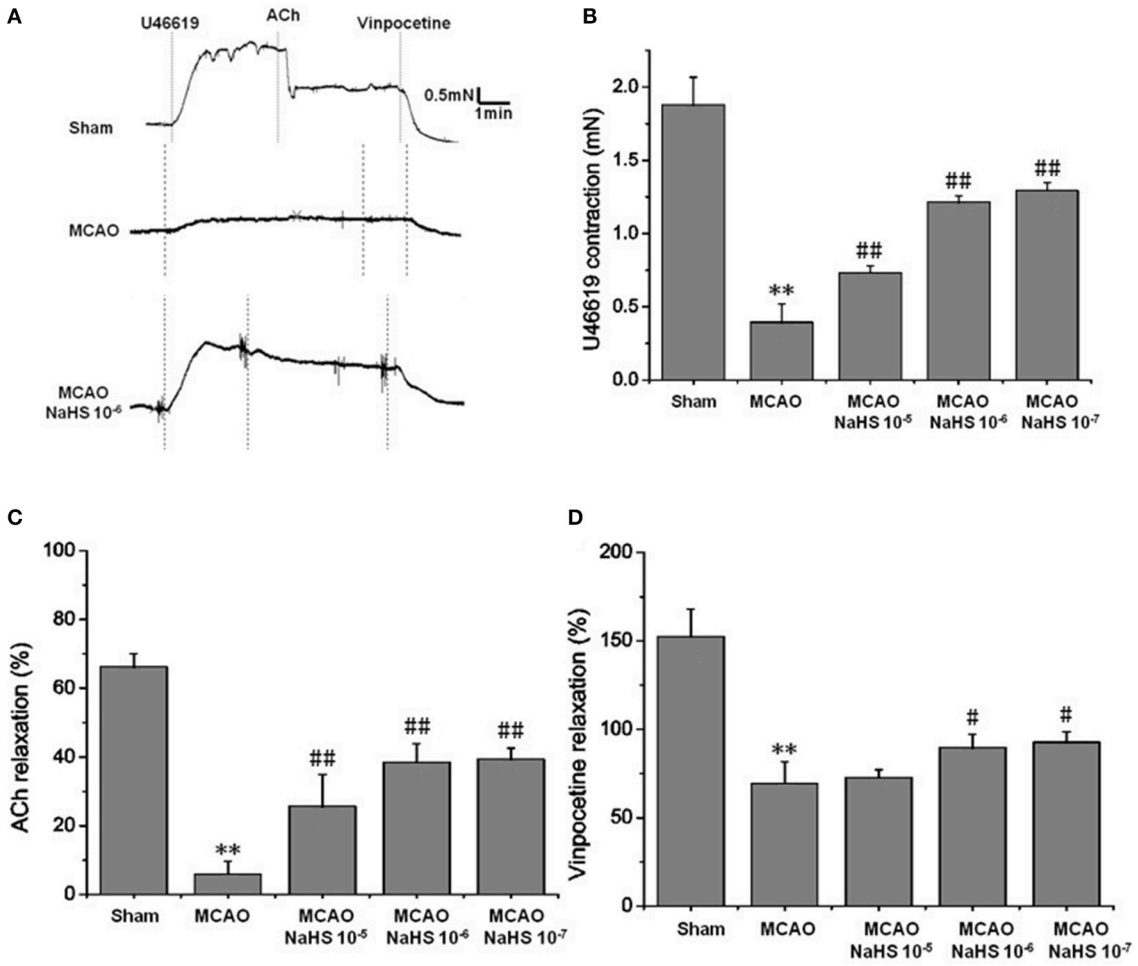

FIGURE 1 | Exogenous H_2S attenuated cerebrovascular dysfunction induced by cerebral I/R in rats (mean ± SD, $n = 8$). **(A)** Original tracings of U46619-, ACh-, vinpocetine- and NaHS-induced responses of MCA derived from MCAO rats. **(B)** The effect of NaHS on U46619 meditated MCA contraction. **(C)** The effect of NaHS on ACh-meditated relaxation in MCA preconstricted with U46619. **(D)** The effect of NaHS on vinpocetine-meditated relaxation in MCA preconstricted with U46619. $^{**}P < 0.01$ vs. sham, $^{\#\#}P < 0.01$ vs. MCAO, $^{\#}P < 0.05$ vs. MCAO.

Effect of Endogenous H_2S on Cerebrovascular Dysfunction Injured by Cerebral I/R

In order to clarify the effect of endogenous H_2S on cerebrovascular dysfunction injured by cerebral I/R, we examined the changes of vascular tension in MCA from CSE knocked down rats after cerebral I/R. As shown in **Figure 2**, MCA almost had no contractile response to U-46619 (E_{max}: 0.11 ± 0.01 mN) in CSE knock down rats after cerebral I/R, which could be significantly elevated by 1×10^{-6} mol/kg NaHS supplement (E_{max}: 0.59 ± 0.03 mN). Similarly, CSE knockdown attenuated both ACh- and vinpocetine-mediated relaxation of MCA from MCAO rats. E_{max} of ACh-mediated relaxation was reduced from 8.91 ± 3.66% in the MCAO group of wild-type rats to 2.48 ± 2.65% in the CSE-siRNA group; E_{max} of vinpocetine-mediated relaxation was reduced from 68.44 ± 12.21% in the MCAO group of wild-type rats to 8.42 ± 3.47% in the CSE-siRNA group. Interestingly, supplementing with NaHS could also further elevate the ACh- and vinpocetine-mediated vascular relaxation of MCAO rats. These results indicate that the CSE knockdown could induce significant vascular dysfunction, which can be ameliorated by exogenous H_2S.

Effect of Ca^{2+}-Activated K^+ (K_{Ca}) Channel Blockers on H_2S-Mediated Relaxation of MCA

We next sought to demonstrate further the effect of H_2S on MCA and explore the underlying mechanism using K_{Ca} channel blockers CTX and Apa. The results of changes of vascular diameter as shown in **Figure 3A** and **Table 1**, the NaHS could induce concentration-dependent dilation in MCA precontracted with U46619 from non-ischemic rats, which was obviously abolished by co-application of CTX and Apa, E_{max} of vascular relaxation being reduced from 76.23 ± 7.4 to

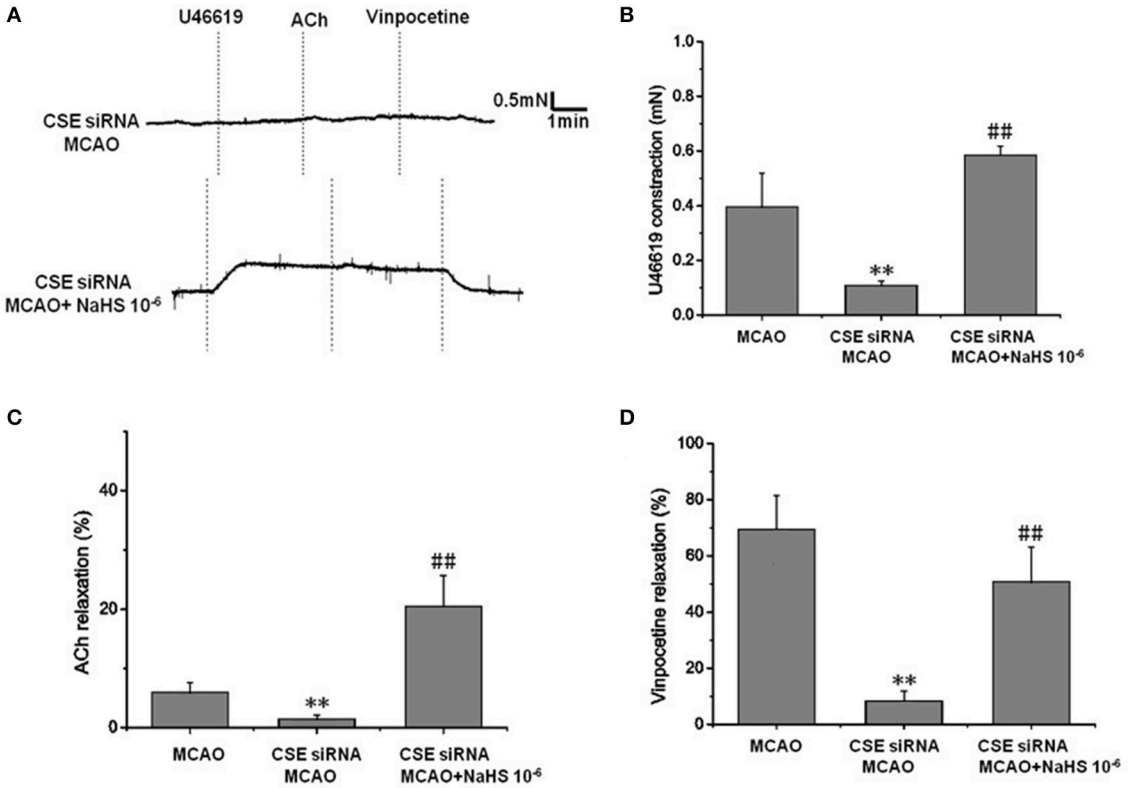

FIGURE 2 | Effect of endogenous H_2S on cerebrovascular dysfunction injured by cerebral I/R (mean ± SD, $n = 8$). **(A)** Original tracings of U46619-, ACh-, vinpocetine-, and NaHS-induced responses of MCA derived from CSE knocked down rats after MCAO. **(B)** The effect of CSE knockdown and NaHS on U46619-meditated contraction. **(C)** The effect of CSE knockdown on and NaHS- or ACh-meditated relaxation. **(D)** The effect of CSE knockdown and NaHS on vinpocetine-meditated relaxation. $^{**}P < 0.01$ vs. sham, $^{\#\#}P < 0.01$ vs. MCAO.

8.75 ± 1.7% after co-application of CTX and Apa. Moreover, L-Cys, the substrate of endogenous H_2S-producing enzyme similarly induced a concentration-dependent dilation in MCA precontracted with U46619 (**Figure 3B**, E_{max}: 79.28 ± 5.4%, $p < 0.01$ vs. the vehicle group). However, the relaxation in MCA to L-Cys was also obviously abolished by co-application of CTX and Apa, E_{max} being reduced from 79.3 ± 5.4 to 9.7 ± 2.0% (**Figure 3D**). These data suggested that K_{Ca} channel might be involved in the H_2S-induced cerebrovascular relaxation.

Effect of Vascular Endothelium on H_2S-Mediated Relaxation of MCA

As shown in **Figures 3B,C** and **Table 1**, the removal of vascular endothelium significantly reduced the relaxation of MCA to L-Cys, with E_{max} being reduced to 8.8 ± 3.8%. Co-adding of ACh and endothelium cells (EAhy926 cells) cultured *in vitro* into luminal perfusate could induce a non-NO and non-PGI_2 relaxation in endothelium-denuded rat MCA precontracted with KCl (**Figure 4**, E_{max}: 66.1 ± 1.6%). However, co-application of ACh and EAhy926 cells of CSE knockdown cannot induce the relaxation in the endothelium-denuded MCA. These results further suggest that vascular endothelium participated in the relaxation in rat MCA, and that endothelial H_2S might mediate vasodilation in the blood vessel.

Effects of H_2S on Neuronal Injury Induced by MCAO in Rats

The rats were transfected with siRNA to knock down the expression of CSE and used to investigate the role of endogenous H_2S on neuronal injury induced by MCAO.

Effect of H_2S on Neurological Score

The neurologic deficit scores of rats are presented in **Figure 5A**. No neurologic deficits were observed in the sham group. Moderate neurologic deficits (average score: 3) were observed at 24 h after reperfusion in control group rats, while in the CSE-siRNA group, the rats had significant neurologic deficits (average score: 3.5), and interestingly, the neurologic deficits were remarkably inhibited by 1×10^{-6} mol/kg NaHS supplementation within 30 min after ischemia.

Effect of H_2S on the Infarction Volume

As shown in **Figures 5B,C**, I/R remarkably induced cerebral infarction in rats. However, the increase of the infarction volume in the CSE knockdown rats was more significant than that in the control group rats. NaHS (1×10^{-6} mol/kg) supplementation

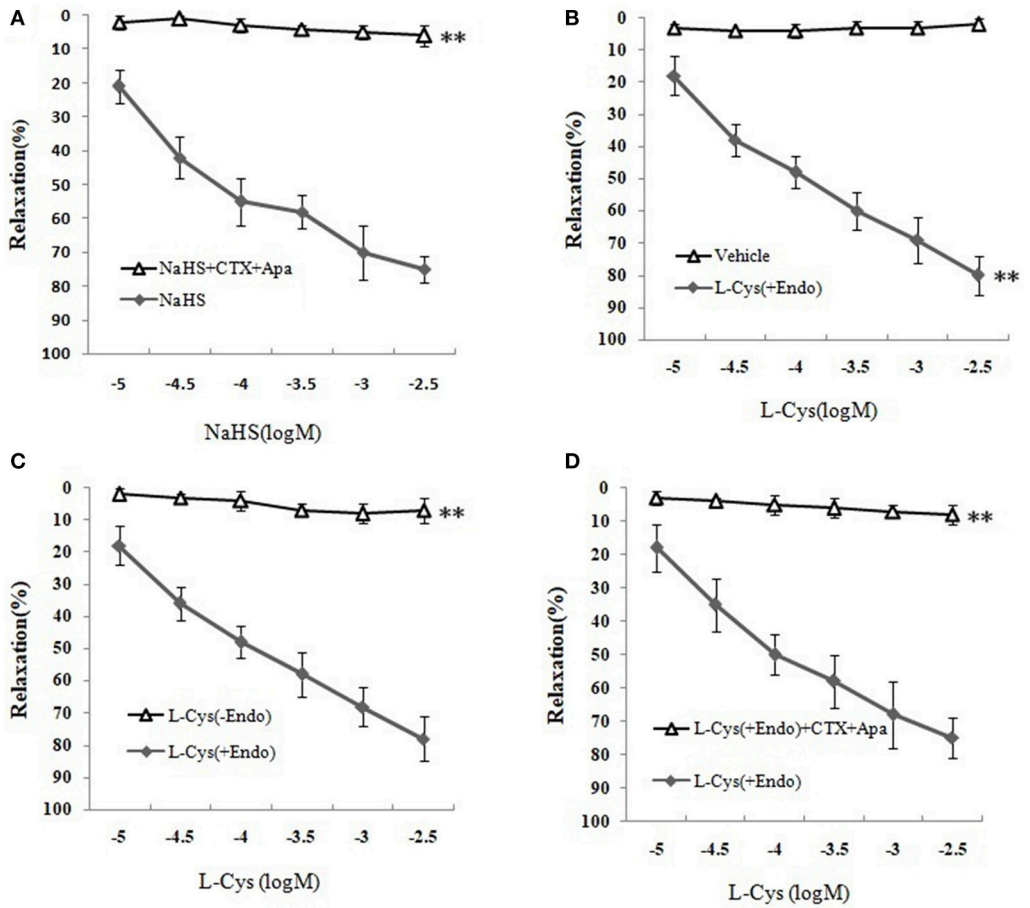

FIGURE 3 | Effects of K_{Ca} channel blockers CTX and Apa on H_2S-mediated relaxation in MCA of normal rats (mean ± SD, $n = 8$). **(A)** Effects of CTX and Apa on NaHS-induced relaxation. **(B)** Effect of L-Cys on relaxation in U46619-preconstricted rat MCA. **(C)** Effects of the endothelium removal on the L-Cys- induced relaxation. $^{**}P < 0.01$ vs. L-Cys (+Endo). **(D)** Effect of CTX and Apa on L-Cys-induced relaxation in MCA. $^{**}P < 0.01$ vs. NaHS or vehicle or L-Cys (+Endo).

TABLE 1 | Effects of CTX plus Apa on relaxation of MCA to NaHS or L-Cys, and role of vascular endothelium in L-Cys-induced relaxation in the MCA (Mean ± SD, $n = 8$).

Group	Maximum possible effect (%)
Vehicle	8.03 ± 1.1
NaHS	76.23 ± 7.4**
NaHS+ CTX+Apa	8.75 ± 1.7*
L-Cys(+Endo)	79.28 ± 5.4**
L-Cys(-Endo)	8.85 ± 3.8##
L-Cys +Apa +CTX	9.7 ± 2.0##

$^{**}P < 0.01$ vs. vehicle; $^{*}P < 0.01$ vs. NaHS; $^{\#\#}P < 0.01$ vs. L-Cys (+Endo).

significantly reduced the infarction volume in CSE knockdown rats alike.

Effect of H_2S on Brain Water Content in Rats

Brain water content among the other factors is regarded as being responsible for the neuronal dysfunction after brain ischemia (22) and can be used as an indicator of brain edema (21). The results (**Figure 5D**) showed that MCAO markedly increased the brain water content in CSE knockdown rats when compared to untreated rats of the control group, which could be significantly inhibited by NaHS (1×10^{-6} mol/kg) supplementation.

Serum LDH Activity and MDA Level in Brain Tissue

LDH leakage from cells to serum and MDA, a product of lipid peroxidation, are major indexes of ischemia injury. In the control group (**Figure 6**) there was a significant increase of LDH activity in serum and MDA content in cerebral tissue induced by cerebral I/R, and the results indicated that I/R could induce significant cerebral injury. However, the injury was more remarkable in CSE knockdown rats than in the control group ($p < 0.01$) and was significantly inhibited by NaHS (1×10^{-6} mol/kg) supplementation.

These results confirmed that H_2S has a remarkable protective effect on MCAO-induced neuronal injury.

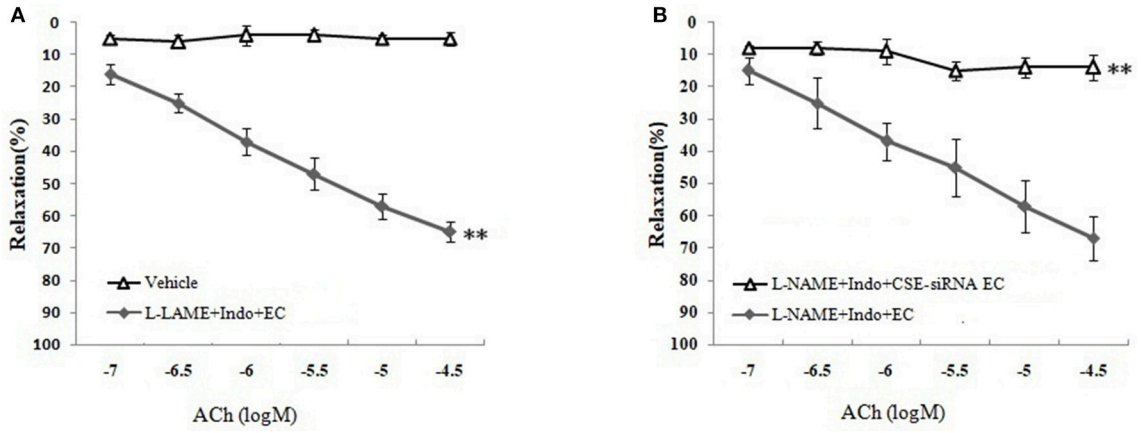

FIGURE 4 | Role of endothelial CSE in ACh-induced non-NO- non-PGI_2 relaxation in endothelium-denuded rat MCA (mean ± SD, $n = 8$). **(A)** Effect of EAhy926 cells (endothelial cell, EC) on ACh-induced non-NO- non-PGI_2 relaxation in KCl-preconstricted endothelium-denuded rat MCA. **(B)** Effect of EAhy926 cells with CSE knockdown (CSE-siRNA EC) on ACh-induced non-NO- non-PGI_2 relaxation in KCl-preconstricted endothelium-denuded rat MCA. $^{**}P < 0.01$ vs. vehicle or L-NAME+Indo+EC.

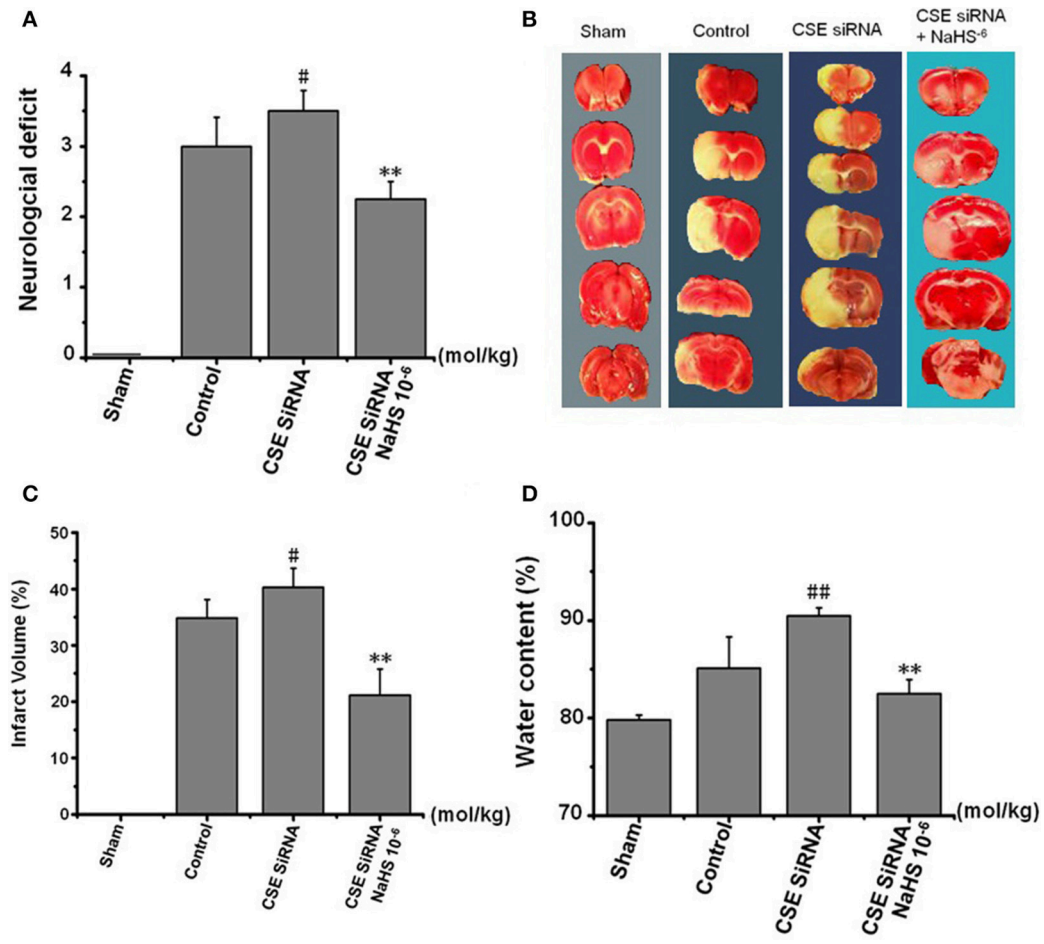

FIGURE 5 | Effect of CSE knockdown (CSE siRNA) on neuronal injury induced by MCAO in rats (Mean ± SEM, $n = 8$). **(A)** Neurological deficits. **(B)** Infarct volume. **(C)** Quantitative analysis of brain infarct volume. **(D)** Brain water content. $^{\#}P < 0.05$ vs. control, $^{\#\#}P < 0.01$ vs. control, $^{**}P < 0.01$ vs. CSE siRNA.

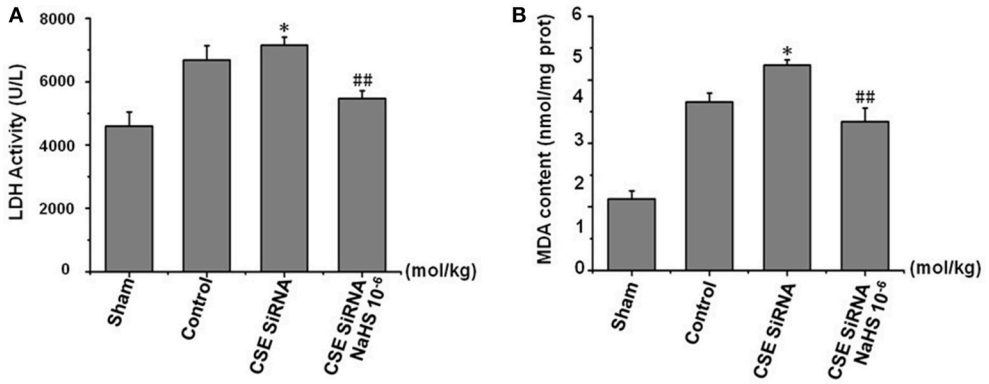

FIGURE 6 | Effect of CSE knockdown (CSE siRNA) on MCAO rat serum LDH activity and MDA content in brain tissue (mean ± SEM, $n = 8$). **(A)** Serum LDH activity. **(B)** MDA content in brain tissue. $^{*}P < 0.05$ vs. control; $^{\#\#}P < 0.01$ vs. CSE isRNA.

DISCUSSION

Cerebral I/R injury is a serious and common clinical disease. The tissue plasminogen activator (t-PA) is the only FDA-approved treatment for acute brain ischemia. However, only a small proportion of brain ischemia patients are eligible to receive tPA treatment because it carries a high risk of secondary impairments, such as bleeding/hemorrhagic transformation and severe neurodegeneration (23, 24). Thus, the main priority is to explore the neuroprotective strategies and find new drugs for possible clinical use.

Previous studies have reported that cerebral I/R decreases endothelial vasoreactivity, impairs blood flow restoration, and also causes further brain injury (5). H_2S is a novel vasoactivator, and research has pointed out that H_2S is helpful for cerebral ischemic injury. Although the role of H_2S on cerebral I/R injury has attracted the interest of many researchers, the mechanism involved in the effect of H_2S on cerebral I/R injury is still not completely clear (9). The aim of this study was designed to clarify the vascular protection of H_2S on neurovascular dysfunction after cerebral I/R. The results showed that the contraction and dilation of MCA profoundly decrease after cerebral I/R. The reduction in the contraction and dilation was significantly ameliorated by $1\times10^{-5} \sim 1\times10^{-7}$ mol/kg NaHS supplement. Not surprisingly, in CSE knockdown rats, MCA almost loses its dilation to ACh or vinpocetion, and constriction to U46619 after cerebral I/R, which could also be significantly ameliorated by 1×10^{-6} mol/kg NaHS supplement. These data indicated that H_2S had a significant protection on cerebrovascular dysfunction induced by cerebral I/R.

We next sought to investigate the mechanism of MCA relaxation on to H_2S using K_{Ca} channel blockers and endothelial removal. As has previously been established, H_2S has been classified as a novel gasotransmitter signaling molecule in CNS, which is involved in various signal transmissions such as the regulation of ion channels (14). Furthermore, the cerebral endothelium has a key role in the regulation of vascular tone because the endothelium could release H_2S and other relaxing factors such as NO and PGI_2 to relax vascular smooth muscle cells (VSMC) (17). In the present study, we found that the relaxation of isolated MCA to H_2S donor NaHS and L-Cys (substrate of endogenous H_2S-producing enzyme) was abolished by the co-application of the intermediate-conductance K_{Ca} channel blocker CTX and small-conductance K_{Ca} channel blocker Apa. In parallel, similar dilation of MCA elicited by L-Cys was blocked by endothelial removal. However, adding endothelium cells (EAhy926) cultured *in vitro* to luminal perfusate could mediate non-NO and non-PGI_2 vasorelaxation to ACh in endothelium-denuded MCA, but the relaxation was abolished by CSE knockdown in EAhy926 cells. These results provided solid evidence that the vasodilation of cerebral vessels to H_2S is endothelium-dependent and might relate to activate the K_{Ca} channel.

To further confirm the protective effects of H_2S on neuronal injury after cerebral I/R, the MCAO was still used as a model of focal cerebral I/R and associated with an increase of infarction volume, brain water content, and neurological scoring (25). Our data revealed that cerebral I/R injury led to a significant increase of cerebral infarction, brain edema, and neurological deficits, thereby suggesting an eminently neuronal injury. In addition, it is widely accepted that oxygen-free radicals in neurocytes induced by cerebral I/R injury and subsequent lipid peroxidation play a key role in the pathophysiology of I/R injury. Hence, like MDA, a product of lipid peroxidation, LDH leakage has also been applied to assess cerebral I/R injury (9, 26). In agreement with the previous result, we found that cerebral I/R injury led to a significant increase of serum LDH activity and MDA content in MCAO rats. However, all the above injury indicators occurred more grievously in CSE knockdown rats than in the normal control group, and could be remarkably inhibited by 1×10^{-6} mol/kg NaHS supplementation. Together with treatment, the effect of H_2S donor NaHS on the injury suggests that H_2S could inhibit cerebral I/R-induced increases of cerebral infarction, brain edema and neurological deficits, LDH leakage, and lipid peroxidation.

These findings provide more details and demonstrate that H_2S has a protective effect on neuronal injury induced by MCAO.

In conclusion, our study is the first to show the multifaceted vasoprotection of H_2S on cerebral I/R injury. We found that (1) both endogenous and exogenous H_2S had eminent protection on vasomotor dysfunction induced by MCAO in rats; (2) K_{Ca} channel might be involved in the cerebrovascular relaxation to H_2S; (3) the cerebrovascular relaxation to H_2S is endothelium-dependent; (4) both endogenous and exogenous H_2S had a protective effect on neuronal injury after cerebral I/R in rats.

AUTHOR CONTRIBUTIONS

Z-WC, J-YW, and MW participated in research design and experiments. H-HJ and X-JS contributed new reagents and analytical tools. H-HJ and X-JS performed data analysis. Z-WC, J-YW, and Y-NL contributed to writing of the manuscript.

FUNDING

This work was supported by grant from the National Natural Science Foundation of China (Nos. 81173596 and 81374002).

REFERENCES

1. Suh JY, Shim WH, Cho G, Fan X, Kwon SJ, Kim JK, et al. Reduced microvascular volume and hemispherically deficient vasoreactivity to hypercapnia in acute ischemia: MRI study using permanent middle cerebral artery occlusion rat model. *J Cereb Blood Flow Metab.* (2015) 35:1033–43. doi: 10.1038/jcbfm.2015.22
2. Schroder HC, Steffen R, Wenger R, Ugarkovic D, Muller WE. Age-dependent increase of DNA topoisomerase II activity in quail oviduct; modulation of the nuclear matrix-associated enzyme activity by protein phosphorylation and poly(ADP-ribosyl)ation. *Mutat Res.* (1989) 219:283–94. doi: 10.1016/0921-8734(89)90030-1
3. Levine AB, Punihaole D, Levine TB. Characterization of the role of nitric oxide and its clinical applications. *Cardiology* (2012) 122:55–68. doi: 10.1159/000338150
4. Jujo K, Ii M, Sekiguchi H, Klyachko E, Misener S, Tanaka T, Tongers J, et al. CXC-chemokine receptor 4 antagonist AMD3100 promotes cardiac functional recovery after ischemia/reperfusion injury via endothelial nitric oxide synthase-dependent mechanism. *Circulation* (2013) 127:63–73. doi: 10.1161/CIRCULATIONAHA.112.099242
5. Palomares SM, Cipolla MJ. Vascular protection following cerebral ischemia and reperfusion. *J Neurol Neurophysiol.* (2011). p S1–004. doi: 10.4172/2155-9562.S1-004
6. Chen J, Gao J, Sun W, Li L, Wang Y, Bai S, et al. Involvement of exogenous H2S in recovery of cardioprotection from ischemic post-conditioning via increase of autophagy in the aged hearts. *Int J Cardiol.* (2016) 220:681–92. doi: 10.1016/j.ijcard.2016.06.200
7. Lobb I, Jiang J, Lian D, Liu W, Haig A, Saha MN, et al. Hydrogen sulfide protects renal grafts against prolonged cold ischemia-reperfusion injury via specific mitochondrial actions. *Am J Transplant.* (2017) 17:341–352. doi: 10.1111/ajt.14080
8. Donnarumma E, Ali MJ, Rushing AM, Scarborough AL, Bradley JM, Organ CL, et al. Zofenopril protects against myocardial ischemia-reperfusion injury by increasing nitric oxide and hydrogen sulfide bioavailability. *J Am Heart Assoc.* (2016) 5:e003531. doi: 10.1161/JAHA.116.003531
9. Jiang WW, Huang BS, Han Y, Deng LH, Wu LX. Sodium hydrosulfide attenuates cerebral ischemia/reperfusion injury by suppressing overactivated autophagy in rats. *FEBS Open Bio.* (2017) 7:1686–1695. doi: 10.1002/2211-5463.12301
10. Guo W, Cheng ZY, Zhu YZ. Hydrogen sulfide and translational medicine. *Acta Pharmacol Sin.* (2013) 34:1284–91. doi: 10.1038/aps.2013.127
11. Yang G, Wu L, Jiang B, Yang W, Qi J, Cao K, et al. H2S as a physiologic vasorelaxant: hypertension in mice with deletion of cystathionine gamma-lyase. *Science* (2008) 322:587–90. doi: 10.1126/science.1162667
12. Hu LF, Wong PT, Moore PK, Bian JS. Hydrogen sulfide attenuates lipopolysaccharide-induced inflammation by inhibition of p38 mitogen-activated protein kinase in microglia. *J Neurochem.* (2007) 100:1121–8. doi: 10.1111/j.1471-4159.2006.04283.x
13. Kimura H. Physiological role of hydrogen sulfide and polysulfide in the central nervous system. *Neurochem Int.* (2013) 63:492–7. doi: 10.1016/j.neuint.2013.09.003
14. Wang R. Physiological implications of hydrogen sulfide: a whiff exploration that blossomed. *Physiol Rev.* (2012) 92:791–896. doi: 10.1152/physrev.00017.2011
15. Cai SN FY, Chen ZW. The hyperpolorization produced by H2S in VSMC from middle cerebral artery of rat. *Chin J Clin Pharmacol Ther.* (2011) 16:5.
16. Fan YF, Chen ZW, Guo Y, Wang QH, Song B. Cellular mechanisms underlying Hyperin-induced relaxation of rat basilar artery. *Fitoterapia* (2011) 82:626–31. doi: 10.1016/j.fitote.2011.01.023
17. Wang M, Hu Y, Fan Y, Guo Y, Chen F, Chen S, et al. Involvement of hydrogen sulfide in endothelium-derived relaxing factor-mediated responses in rat cerebral arteries. *J Vasc Res* (2016) 53:172–185. doi: 10.1159/000448712
18. Xuanjun S, Youyang H, Zhiwu C. The effects of CSEsiRNA on the expression of CSE and H2 S in EAhy926 cells. *Acta Universitatis Medicinalis Anhui* (2012) 47:904–907.
19. Wen JY, Chen ZW. Protective effect of pharmacological preconditioning of total flavones of abelmoschl manihot on cerebral ischemic reperfusion injury in rats. *Am J Chin Med.* (2007) 35:653–61. doi: 10.1142/S0192415X07005144
20. Longa EZ, Weinstein PR, Carlson S, Cummins R. Reversible middle cerebral artery occlusion without craniectomy in rats. *Stroke* (1989) 20:84–91. doi: 10.1161/01.STR.20.1.84
21. Yu T, Chen QE, Chen ZW, Xiong Z, Ye M. Protective effects of total flavones of rhododendra against global cerebral ischemia reperfusion injury. *Am J Chin Med.* (2009) 37:877–87. doi: 10.1142/S0192415X09007284
22. Brouns R, De Deyn PP. The complexity of neurobiological processes in acute ischemic stroke. *Clin Neurol Neurosurg.* (2009) 111:483–95. doi: 10.1016/j.clineuro.2009.04.001
23. Kaur J, Zhao Z, Klein GM, Lo EH, Buchan AM. The neurotoxicity of tissue plasminogen activator? *J Cereb Blood Flow Metab.* (2004) 24:945–63. doi: 10.1097/01.WCB.0000137868.50767.E8
24. Wang T, Duan S, Wang H, Sun S, Han B, Fu F. Neurological function following cerebral ischemia/reperfusion is improved by the Ruyi Zhenbao pill in a rats. *Biomed Rep.* (2016) 4:161–166. doi: 10.3892/br.2016.568
25. Huang JL, Liu WW, Sun XJ. Hydrogen inhalation improves mouse neurological outcomes after cerebral ischemia/reperfusion independent of anti-necroptosis. *Med Gas Res.* (2018) 8:1–5. doi: 10.4103/2045-9912.229596
26. Kamat PK, Kalani A, Givvimani S, Sathnur PB, Tyagi SC, Tyagi N. Hydrogen sulfide attenuates neurodegeneration and neurovascular dysfunction induced by intracerebral-administered homocysteine in mice. *Neuroscience* (2013) 252:302–19. doi: 10.1016/j.neuroscience.2013.07.051

Conflict of Interest Statement: The authors declare that the research was conducted in the absence of any commercial or financial relationships that could be construed as a potential conflict of interest.

frontiers in Pharmacology

ORIGINAL RESEARCH
published: 05 March 2019
doi: 10.3389/fphar.2019.00186

Biochemical Pathways Triggered by Antipsychotics in Human Oligodendrocytes: Potential of Discovering New Treatment Targets

*Caroline Brandão-Teles[1], Valéria de Almeida[1], Juliana S. Cassoli[1,2] and Daniel Martins-de-Souza[1,3,4]**

[1] Laboratory of Neuroproteomics, Department of Biochemistry and Tissue Biology, Institute of Biology, University of Campinas, Campinas, Brazil, [2] Faculdade de Palmas, Palmas, Brazil, [3] UNICAMP's Neurobiology Center, Campinas, Brazil, [4] Instituto Nacional de Biomarcadores em Neuropsiquiatria, Conselho Nacional de Desenvolvimento Científico e Tecnológico, São Paulo, Brazil

Schizophrenia is a psychiatric disorder that affects more than 21 million people worldwide. It is an incurable disorder and the primary means of managing symptoms is through administration of pharmacological treatments, which consist heavily of antipsychotics. First-generation antipsychotics have the properties of D_2 receptor antagonists. Second-generation antipsychotics are antagonists of both D_2 and $5HT_2$ receptors. Recently, there has been increasing interest in the effects of antipsychotics beyond their neuronal targets and oligodendrocytes are one of the main candidates. Thus, our aim was to evaluate the molecular effects of typical and atypical drugs across the proteome of the human oligodendrocyte cell line, MO3.13. For this, we performed a mass spectrometry-based, bottom-up shotgun proteomic analysis to identify differences triggered by typical (chlorpromazine and haloperidol) and atypical (quetiapine and risperidone) antipsychotics. Proteins which showed changes in their expression levels were analyzed *in silico* using Ingenuity® Pathway Analysis, which implicated dysregulation of canonical pathways for each treatment. Our results shed light on the biochemical pathways involved in the mechanisms of action of these drugs, which may guide the identification of novel biomarkers and the development of new and improved treatments.

Keywords: schizophrenia, mechanism of action, proteomics, biomarkers, chlorpromazine, haloperidol, quetiapine, risperidone

OPEN ACCESS

Edited by:
HuaLin Cai,
Second Xiangya Hospital of Central South University, China

Reviewed by:
William Davies,
Cardiff University, United Kingdom
Marián Castro,
University of Santiago de Compostela, Spain

***Correspondence:**
Daniel Martins-de-Souza
dmsouza@unicamp.br;
danms90@gmail.com

Specialty section:
This article was submitted to Neuropharmacology, a section of the journal Frontiers in Pharmacology

Received: *15 January 2018*
Accepted: *14 February 2019*
Published: *05 March 2019*

Citation:
Brandão-Teles C, de Almeida V, Cassoli JS and Martins-de-Souza D (2019) Biochemical Pathways Triggered by Antipsychotics in Human Oligodendrocytes: Potential of Discovering New Treatment Targets. Front. Pharmacol. 10:186. doi: 10.3389/fphar.2019.00186

INTRODUCTION

Schizophrenia is a chronic and debilitating psychiatric disorder characterized by positive (e.g., hallucinations and delusions), negative (e.g., anhedonia, alogia, apathy, and poor self-care), and cognitive (e.g., deficits in executive function, working memory, and recognition memory) symptoms. The risk for schizophrenia is 0.7% in the broad population but increases with the degree of genetic relationship (Hayashi-Takagi, 2016). Treatment is based on administration of antipsychotics to reduce the recurrence and severity of psychosis and improve general symptoms, thereby providing some degree of improvement in quality of life for patients. Antipsychotics can be divided into two categories known as typical (first-generation) and atypical (second-generation) drugs. A common pharmacological property presented by these classes is the blockage of the dopamine D_2 receptor (Shen, 1999; Leucht et al., 2009; Kantoff et al., 2010).

First-generation antipsychotics such as chlorpromazine and haloperidol are effective in reducing positive symptoms, but they can cause severe side effects such as extrapyramidal symptoms and tardive dyskinesia. Additionally, these drugs do not treat negative and cognitive symptoms, which contribute to most of the deficiency associated with schizophrenia (Lieberman et al., 2005). Second-generation antipsychotics like quetiapine and risperidone are also effective to attenuate positive symptoms and are more effective in reducing negative symptoms compared to first-generation drugs. However, severe side effects such as weight gain, metabolic syndrome, and sedation may occur (Leucht et al., 2009).

The pathophysiology of schizophrenia has been associated with disturbances in several neurotransmitter systems. One of the most well-established theories is the dopamine hypothesis, which agrees with current antipsychotics targeting dopaminergic systems. This and other hypotheses have normally implicated neurons, although other molecular mechanisms involving different cell types in the brain may be associated with the pathophysiology of schizophrenia (Coyle, 1996; Ju and Cui, 2015). Oligodendrocytes are the cells responsible for myelination in the central nervous system (CNS) through expression of genes that encode myelin structural proteins in a specific and regulated manner, and myelination of axon fibers by oligodendrocytes is essential for the rapid conduction of action potentials (Buntinx et al., 2003).

Scientific evidence suggests that one of the reasons for neuronal disconnection is due to disruptions in myelination. This could be due to poor functioning of oligodendrocytes. Such a disruption may lead to dysfunctions of perception, behavior and cognition as seen in schizophrenia as reviewed by Takahashi (Takahashi et al., 2011). It has already been shown that there is a prominent reduction in the density of oligodendrocytes in the prefrontal cortex of these patients (Hof et al., 2003; Uranova et al., 2004). In addition, it has already been seen in the dorsolateral prefrontal cortex alteration in expression levels in genes related to myelination of patients with schizophrenia compared to control (Hakak et al., 2001). Evidence for myelin-related changes in schizophrenia is also provided through studies with animal models. Animals treated with NMDA receptor antagonists (NMDAr), a pharmacological model of schizophrenia (Paulson et al., 2003; Neill et al., 2010) showed a decrease in the total volume of white matter and corpus callosum compared to control animals. Furthermore, levels of myelin basic protein (MBP) in these animals were found to be decreased (Xiu et al., 2014). In addition, transcriptomic studies using post mortem brain tissue have implicated that genetic variation in OLIG2, CNP, MAG, and MOG can be associated to myelination and oligodendrocyte function in schizophrenia (Hakak et al., 2001; Georgieva et al., 2006). It is important to mention that myelination continues throughout development of the young adult brain, coinciding with the average age of onset of the pathology. We have demonstrated recently an increase in the levels of many proteins in cultured oligodendrocytes treated with MK-801, an antagonist of the NMDA receptor, suggesting that these cells may be targets for antipsychotics (Cassoli et al., 2016).

Here we performed a quantitative proteomic analysis to investigate changes in protein expression triggered by antipsychotics in a cell line of human oligodendrocytes (MO3.13). The effects of two first-generation (chlorpromazine and haloperidol) and two second-generation (quetiapine and risperidone) antipsychotics were investigated. Our aim was to better understand the biochemical pathways involved in the mechanisms of action of these drugs in attempt to find new biomarkers and targets which may increase our understanding of the disease and therapeutic response and assist in the development of more specific and improved treatments for patients with schizophrenia.

EXPERIMENTAL PROCEDURES

Cell Culture, Treatments, and Proteome Extraction

Human hybrid MO3.13 cells are classified as an immature oligodendrocyte cell line (Buntinx et al., 2003; Cassoli et al., 2017). Our group using a 2D liquid chromatographic strategy combined with UDMS^E acquisitions have established a complete dataset of proteins expressed by the MO3.13 cells. More than 10,000 proteins expressed in this cell line have been identified, and it is possible to find the receptors mentioned in this study, such as the dopamine D_2 receptor, target of antipsychotics (Cassoli et al., 2017).

MO3.13 cells were grown in DMEM medium supplemented with 0.5% penicillin/streptomycin (Sigma-Aldrich, St. Louis, MO, United States) and 10% heat-inactivated fetal bovine serum (Life Technologies, Darmstadt, Germany) at 37°C in a humidified atmosphere containing 5% CO_2 as described previously (Brandão-Teles et al., 2017). The cells were treated with each antipsychotic once and collected after 8h as follows with respect to dosage and drug: Group 1–10 μM chlorpromazine; Group 2–50 μM haloperidol; Group 3–50 μM quetiapine; Group 4–50 μM risperidone; Group 5–chlorpromazine and haloperidol vehicle solution (0.01 M HCl); Group 6 – quetiapine and risperidone vehicle solution (DMSO). Each treatment was done in biological triplicate. The antipsychotic doses were chosen as described previously (Martins-de-Souza et al., 2011). MO3.13 cells were centrifuged at 1,200 *g* for 5 min and the pellets homogenized in a lysis buffer consisting of 6 M urea, 2 M thiourea, 10 mM DTT, with protease and phosphatase inhibitors, 0.1 mM sodium pervanadate (lysis buffer). Protein lysates were centrifuged at 14,000 *g* for 45 min at 4°C in order to remove pelleted lipids and other vestiges. The supernatants were collected, desalted and concentrated as described in Brandão-Teles et al. (2017). Protein concentrations were determined by Qubit® Protein Assay Kit.

NanoLC-ESI MS/MS

Proteomic analyses were performed in a bidimensional microUPLC tandem nanoESI-UDMS^E platform by multiplexed data-independent acquisitions experiments, using a 2D-RP/RP Acquity UPLC M-Class System (Waters Corporation, Milford, MA, United States) coupled to a Synapt G2-Si mass spectrometer

(Waters Corporation, Milford, MA, United States). The samples were fractionated using a one-dimension reversed-phase approach. Peptide samples (0.5 μg) were loaded into a M-Class HSS T3 column (100 Å, 1.8 μm, 75 μm × 150 mm, Waters Corporation, Milford, MA, United States). The fractionation was achieved using an acetonitrile gradient from 7 to 40% (v/v) over 95 min at a flow rate of 0.4 μL/min directly into Synapt G2-Si mass spectrometer. For every measurement, MS and MS/MS data were acquired in positive resolution mode with a resolving power around 25,000 FWHM. Ion mobility separation of precursor ions method (Geromanos et al., 2012) was used over a range of 50–2000 m/z and a cross-section resolving power of at least 40 Ω/ΔΩ. Precursor ion information was collected in low-energy MS mode by applying a constant collision energy of 4 eV in the range of 50–2000 m/z. Fragment ion information was obtained in the elevated energy scan using drift-time specific collision energies as detailed previously (Cassoli et al., 2017). The spectral acquisition time in each mode was 0.6 s with a 0.05 s-interscan delay, resulting in an overall cycle time of 1.3 s for the acquisition of one cycle of low and high energy data. The lock mass channel was sampled every 30 s. The mass spectrometer was calibrated using a human [Glu1]-Fibrinopeptide B (785.8426 m/z) solution delivered through the reference sprayer of the NanoLock Spray source. All proteomics analyses were run in technical duplicate.

Data Processing and Database Searches

Proteins were identified and quantified using dedicated algorithms and searching against the UniProt Human Proteomic Database of *Homo sapiens*, version 2018/02 (Li et al., 2009; Cassoli and Martins-de-Souza, 2017). The databases used were reversed "on the fly" during the database queries by the software to assess the false-positive identification rate. For correct spectral processing and database searching conditions, we used the Progenesis QI for Proteomics software package with Apex3D, Peptide 3D, and Ion Accounting informatics (Waters Corporation). This software starts with loading of the LC-MS data, followed by alignment and peak detection, which creates a list of interesting peptide ions that are explored within Peptide Ion Stats by multivariate statistical methods. The processing parameters used were 150 counts for the low-energy threshold, 50.0 counts for the elevated energy threshold, and 750 counts for the intensity threshold. Automatic alignment of the runs (all runs in the experiment was assessed for suitability) was used for the processing. In peak picking, it was used 5 as maximum ion charge and the sensitivity value was selected as 4. Moreover, the following parameters were considered in identification of peptides/proteins: (1) digestion by trypsin with at most one missed cleavage; (2) variable modification by oxidation (M) and fixed modification by carbamidomethyl (C); and (3) a false discovery rate (FDR) less than 1%. Two or more ion fragments per peptide, five or more fragments per protein and one or more peptides per protein were required for ion matching. Data were analyzed by on-way analysis of variance (ANOVA) with treatment factor p-value <0.05 compared to vehicle group. Identifications that did not satisfy these criteria were rejected. The experiment design was defined (Group 1–6) and label free protein quantitation was done using Hi-N ($N = 3$) method.

Analysis *in silico*

For interpreting the functional significance of differentially expressed proteins, their UniProt accession IDs were uploaded into the Ingenuity Pathways Knowledgebase (IPKB) through the algorithm Ingenuity Pathway Analysis (IPA, Ingenuity Systems, Qiagen, Redwood, CA, United States[1]) to determine potential interactions between these proteins, between these proteins and other proteins, to canonical pathways and to disease lists contained in the IPKB. The parameters used were the software default and p-value less than 0.05. Additional information can be found on Ingenuity Systems' website[1].

Immunohistochemistry

MO3.13 cells for immunohistochemistry (adapted from Taraboletti et al., 2017) were grown in circular glass microscope slides in a six-well plate at a density of $3{,}5 \times 10^4$ and treated as described previously. After the treatments, the cells were initially fixed with 4% paraformaldehyde for 20 min, washed three times and conserved in PBS. The microscope slides were washed in PBS three times and were then incubated with glycine 0.1 M for 30 min. After three additional washes, the cells were blocked for 5 min in PBS containing 10% fetal bovine serum. The cells were then incubated at 4°C overnight with primary antibodies in blocking solution (Taraboletti et al., 2017). We used the following primary antibodies: Anti-Cytochrome C antibody (1:400; Abcam; ab13575); and mTOR (1:400; Cell Signaling; 2983S). The cells were then washed with PBS and incubated with secondary antibodies and DAPI (1:100) for 1h at 37°C. The secondary antibodies were Alexa Fluor 594 goat anti-mouse or anti-rabbit used at a dilution of 1:400. The cells were fixed using mounting medium (Dako Faramount Aqueous Mounting Medium, Ref S3025) and imaged using an Cytation 5, BioTek and quantified using Fiji: an open-source platform for biological-image analysis. GraphPad Prism software version 8.0 was used to perform the statistical analyses.

Oxidative Stress Indicator

MO3.13 cells were seeded on 12-well plate at a density of $4{,}5 \times 10^4$ per well. After 48 h the cells were treated with Haloperidol for 4 h as described previously. After the treatment we added CM-H2DCFDA, according to the manual description (1:1000; Thermo; C6827), for 10 min in the dark to analyze the reactive oxygen species. The wells were, then, washed three times with PBS and 0.5 ml of DMEM supplemented with 0.5% penicillin/streptomycin and 10% heat-inactivated fetal bovine serum was added to each well. Fluorescence was measured using a Cytation 5 (BioTek).

RESULTS

All antipsychotics affected the expression levels of some proteins (**Figure 1**) and consequently triggered changes in several biological processes, according to the *in silico* IPA profiling. Some

[1] www.ingenuity.com

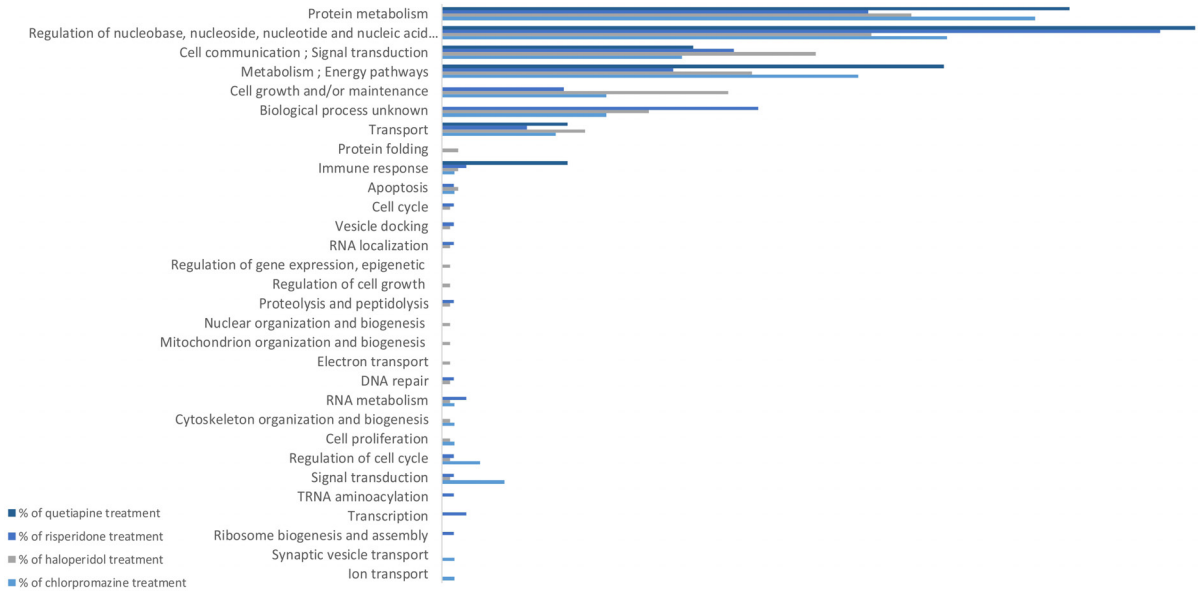

FIGURE 1 | GO biological processes affected by antipsychotic treatment in MO3.13 cell cultures.

of these differences were common among treatments and others were specific to each antipsychotic analyzed.

We identified in chlorpromazine treatment a total of 1138 proteins, of these 195 proteins presented changes in the abundance. In the case of haloperidol, we identified 1252 proteins with 316 presented different levels, compared to the levels of these proteins in untreated control cells (**Supplementary Tables S1**, **S2**, respectively). Proteins with different abundances affected 77 and 105 canonical pathways in cells treated with chlorpromazine and haloperidol, respectively (**Supplementary Table S3**). For atypical antipsychotics, in the quetiapine treatment we identified a total of 2201 proteins in which 19 proteins have their expression altered, while risperidone we identified 1705 proteins, of these 197 proteins presented changes in the abundance (**Supplementary Tables S4**, **S5**, respectively). These proteome changes were implicated in 17 and 32 conical pathways, respectively (**Supplementary Table S6**).

Figure 1 shows the biological processes which were affected both uniquely and in common by the tested antipsychotics. All antipsychotics caused changes in protein metabolism. The quetiapine treatment affected fewer biological processes compared to other antipsychotics, reflected by the lowest number of proteins expressed at different levels in the MO3.13 cells. Most of the differentially expressed proteins in quetiapine treatment are associated with the regulation of nucleobase, nucleoside, nucleotide and nucleic acid metabolism. Some processes were affected by only one treatment, which are: ion transport and synaptic vesicle transport, by chlorpromazine; electron transport, mitochondrial organization and biogenesis, nuclear organization and biogenesis, regulation of cell growth, and regulation of gene expression (epigenetic), by haloperidol; and ribosome biogenesis and assembly, and transcription pathways by risperidone albeit at a lower scale.

Proteins identified with different abundances were analyzed at IPA according to their canonical pathways. We only considered pathways with p-value less than 0.05. For typical antipsychotics, haloperidol modulated more canonical pathways (105) than chlorpromazine treatment (77) (**Supplementary Table S3**). In addition, 23,8% of the pathways were altered by both drugs, suggesting similarities in their mechanisms of action.

For atypical antipsychotics, no overlaps in the canonical pathways affected were observed. Quetiapine only enriched 17 canonical pathways, while the risperidone treatment led to an enrichment of 32 canonical pathways. Compared to typical antipsychotics, 2.3 and 5.2% of the pathways enriched by chlorpromazine and haloperidol, respectively, overlapped with those triggered by risperidone, but no overlap was observed between risperidone and quetiapine. Although presenting specific pathway differences, this does not rule out the possibility that risperidone may eventually use routes similar to typical antipsychotics while modulating the MO3.13 cell response. Depending on the dosage, risperidone may be considered clinically as a typical antipsychotic and this could be due to the high specificity of the effects induced by the risperidone treatment.

In order to validate some of the proteins we found differentially expressed in the treatments we performed immunocytochemistry for mTOR and cytochrome C. Our results showed that although chlorpromazine, haloperidol, and risperidone altered proteins belonging to mTOR pathways, only chlorpromazine affected mTOR protein directly (**Figure 2**). We found an increase in cytochrome C expression promoted by quetiapine treatment (**Supplementary Figure S1**). Additionally, to detect reactive oxygen species (ROS) in MO3.13 after the treatment with haloperidol we added CM-H2DCFDA, a cell permeable, non-fluorescent precursor of DCF, and read in the

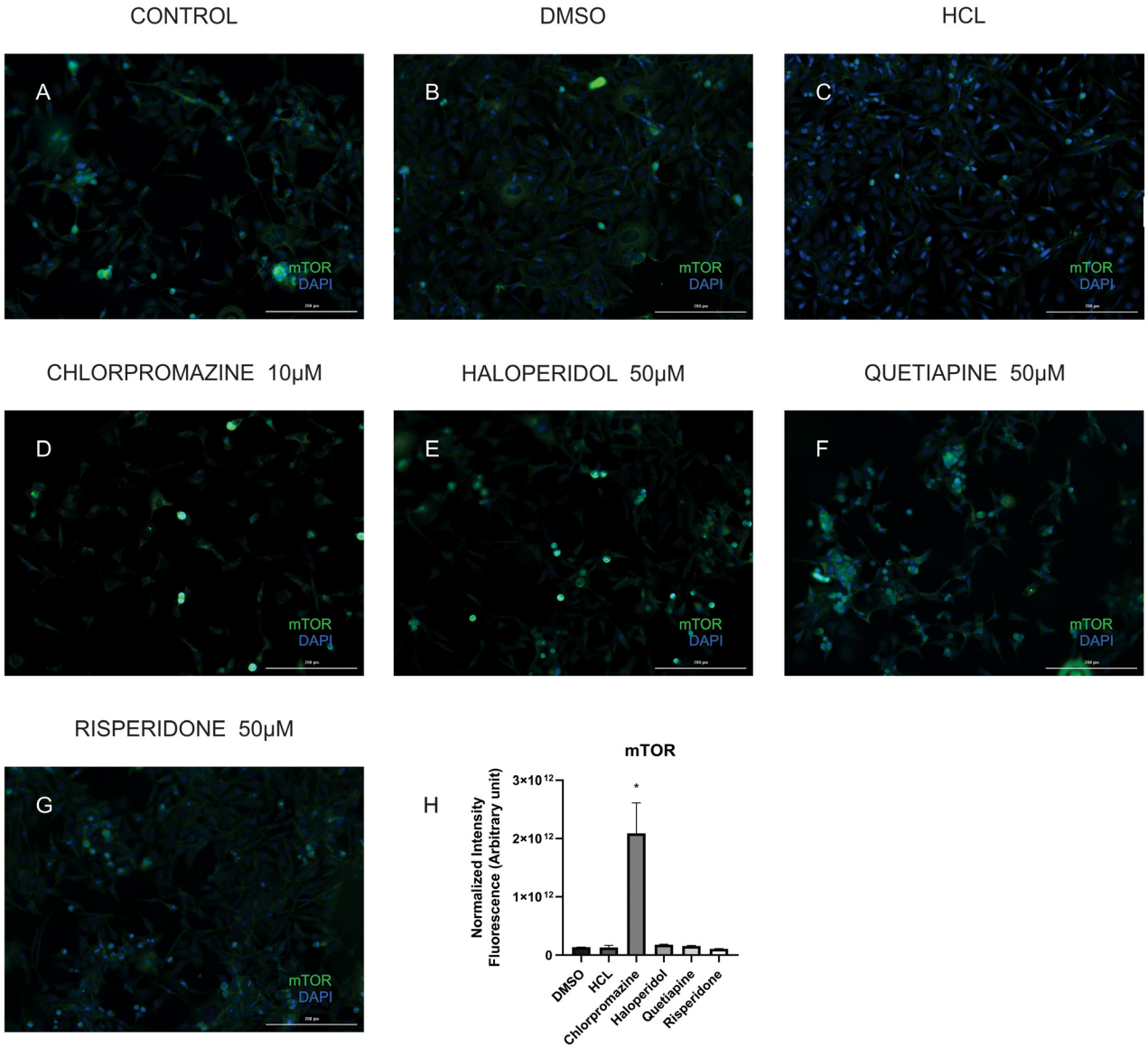

FIGURE 2 | Representative images of MO3.13 cells treated for 8 h **(A)**, vehicles (DMSO, HCl; **B,C**), chlorpromazine 10 μM **(D)**, haloperidol 50 μM **(E)**, quetiapine 50 μM **(F)**, and risperidone 50 μM **(G)** stained for mTOR (green)/Dapi (blue). **(H)** Statistic chart showing normalized intensity fluorescence for mTOR for each treatment (*$P < 0.05$). Scale bars = 200 μm.

fluorescence microplate reader (Eruslanov and Kusmartsev, 2010). We observed that, compared to vehicle, haloperidol increased ROS production in the cells (**Figure 3**).

DISCUSSION

Most of what we know about antipsychotic mechanisms of action was discovered originally through effects on receptors in neuronal studies. However, fewer studies have been carried out investigating the effects of these drugs on glial cells. Considering the growing interest in the role of oligodendrocytes in neurotransmission, it makes sense to characterize the modulatory effects of antipsychotics on the biological processes of these cells. Thus, we investigated the acute response of healthy oligodendrocytes to both first- and second-generation antipsychotics through identification of proteins that were changed subsequently in their abundance. Here we demonstrated that antipsychotics affected in a different manner the proteome of oligodendrocyte. This information can be observed in IPA analyses through the canonical pathways' ratio, that means the ratio of the number of proteins affected by treatments divided by the total number of proteins that belong to the same pathway. The canonical pathway coverage ratios for each of the treatment types ranged from 0.02–1 for haloperidol, 0.02–0.5 for chlorpromazine and risperidone, and

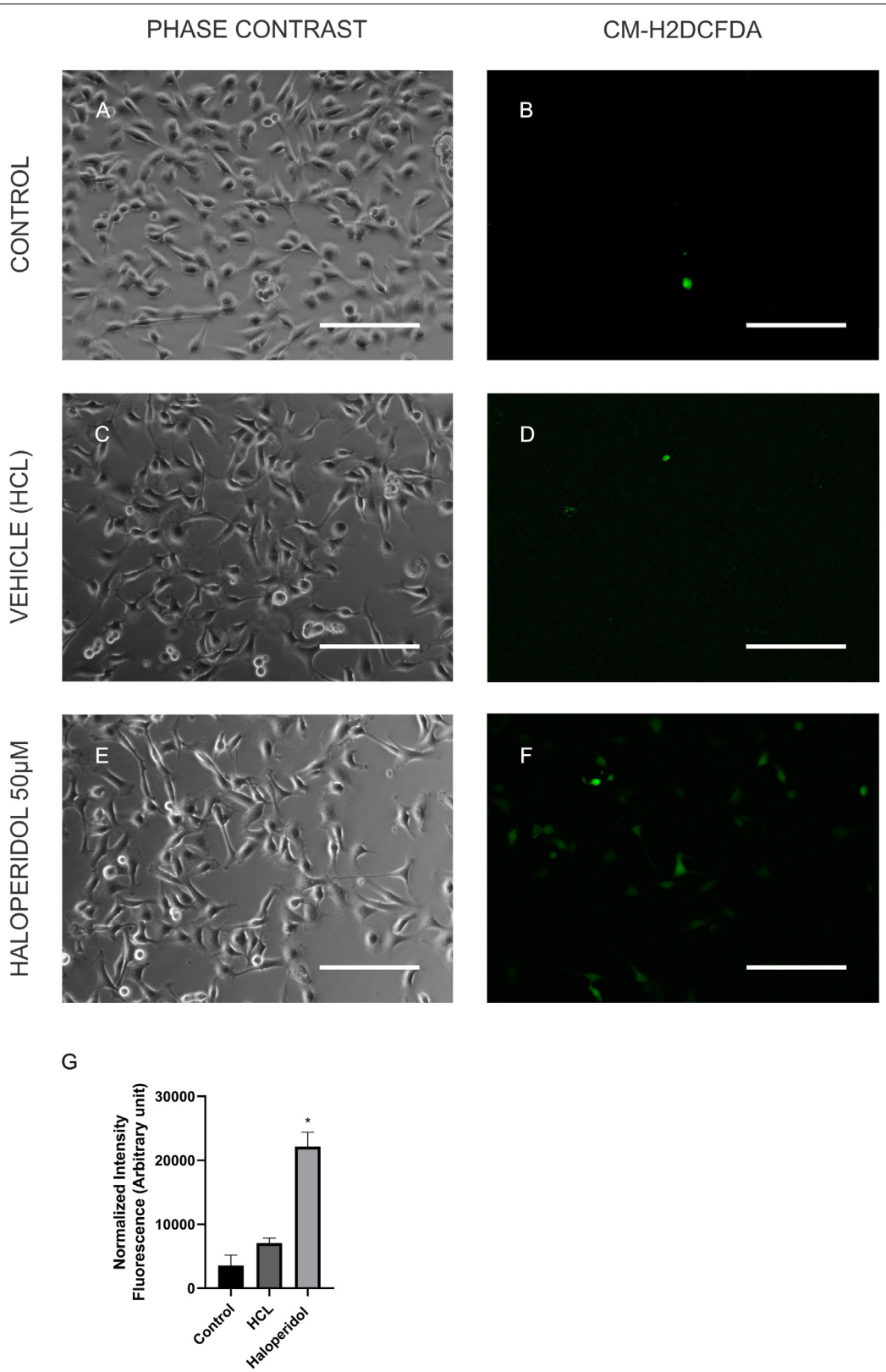

FIGURE 3 | MO3.13 after treatment with control **(A,B)**, vehicle (HCL; **C,D**), and haloperidol 50 μM **(E,F)** for 4 h, and incubation with CM-H2DCFDA. Fluorescence is shown here in false colors and green for CM-H2DCFDA. **(G)** Statistic chart showing normalized intensity fluorescence for CM-H2DCFDA for each treatment (*$P < 0.05$). Scale bars = 200 μm.

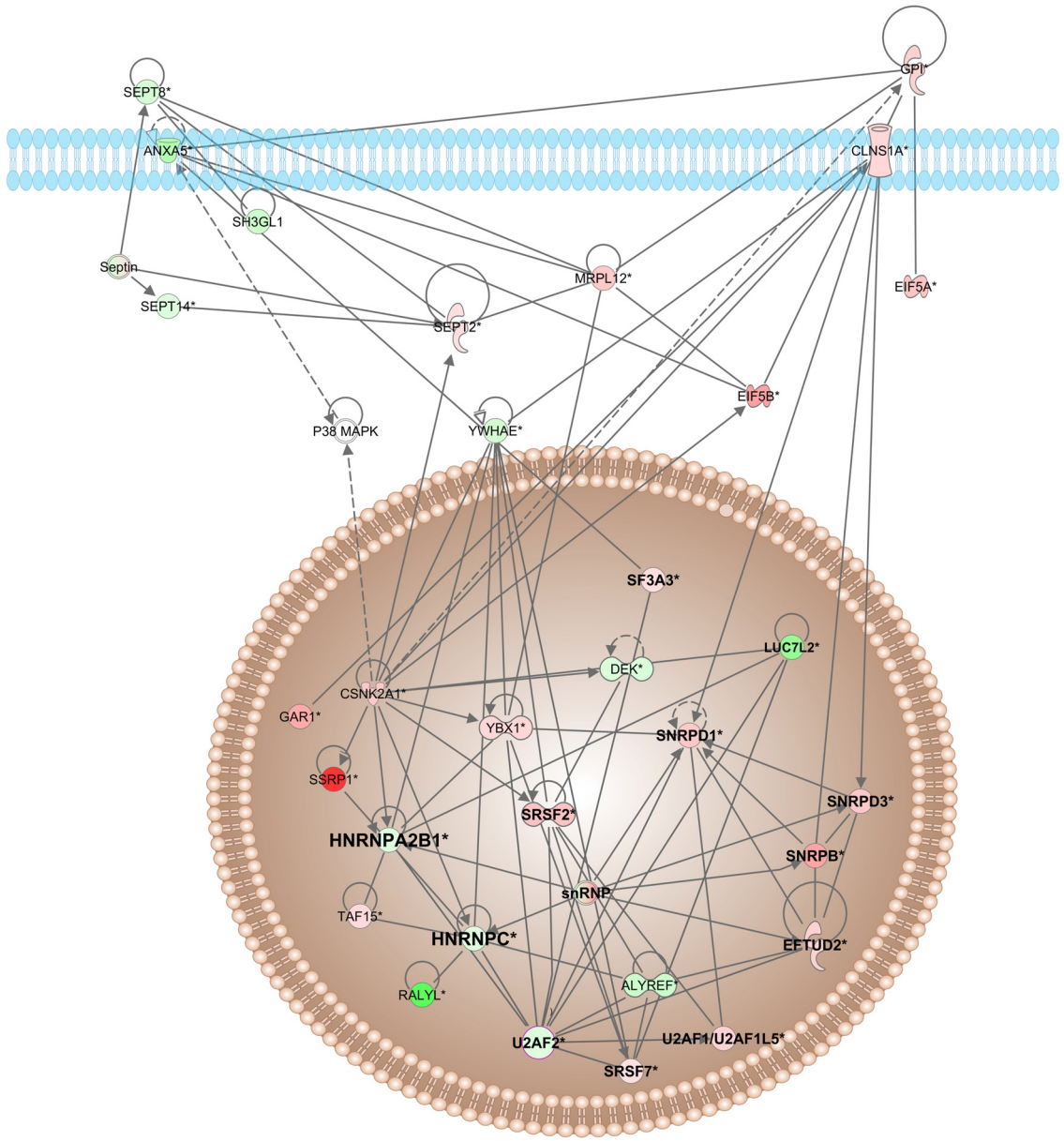

FIGURE 4 | Network interactions, and their interactors, of differentially expressed proteins of haloperidol-treated oligodendrocytes. The network was generated from differentially expressed proteins by IPA. Colored interactors represent proteins previous found in the proteome. Highlighted proteins were belonging to splicing machinery. Full and dashed lines depict direct and indirect connections, respectively.

0.008–0.06 for quetiapine with ratios closer to 1 indicating higher coverage.

Common Effects

Spliceosome

The spliceosome machinery is composed of five different ribonucleoprotein (RNP) subunits and numerous protein cofactors that together will participate in the splicing process, i.e., removal of the introns in the pre-mRNA (Matera and Wang, 2014). In this study, proteins belonging to spliceosome machinery were affected by all treatments. Among the proteins identified, chlorpromazine increased levels of proteins belonging to nuclear heterogeneous ribonucleoprotein family (hnRNP), such as hnRNPC, nhRNPK, hnRNPA1L2, and hnRNPC, and decreased levels of hnRNPA3. The haloperidol treatment also increased the levels of hnRNPF, hnRNPA3, and decreased hnRNPH2 (**Figure 4**). Most of the proteins affected by risperidone treatment were decreased, such as hnRNPH2, hnRNPH, hnRNPD, hnRNPA1, hnRNPU, hnRNPM, and hnRNPA0. Quetiapine

treatment only altered the levels of two proteins, the Pre-mRNA-processing-splicing factor (PRPF8) and U6 snRNA-associated Sm-like protein (LSM2). Recently, we observed changes in eight proteins belonging to the hnRNP family in oligodendrocytes treated with clozapine (Cassoli et al., 2016). We also found altered levels of hnRNPC, hnRNPK and hnRNPU in *post mortem* samples of the anterior temporal lobe (ATL) from patients with schizophrenia (Saia-cereda and Santana, 2017). Additionally, we found changes in hnRNPC levels in the temporo-posterior gyrus of patients with schizophrenia (Martins-de-Souza et al., 2009). Finally, Iwata et al. (2011) reported that overexpression of the hnRNP C2 variant leads to a decrease in MBP expression. There are few studies linking spliceosome machinery mutations and psychiatric diseases, probably due to the critical role for survival (Glatt et al., 2011).

EIF2

Another effect of antipsychotics is related to the translation initiation factors, an important group of proteins required for protein synthesis on ribosomes. EIF2 (eukaryotic initiation factor-2) mediates the binding of Met-tRNA to the ribosome in a GTP-dependent manner (Carter, 2007). While chlorpromazine and haloperidol increased the expression most of proteins associated with EIF2 signaling, risperidone treatment decreased this protein. Although quetiapine treatment did not affect EIF2 signaling, this data suggests that first and second antipsychotics may have differential effects on protein synthesis.

mTOR

The mammalian target of rapamycin (mTOR) signaling pathway plays an important role in regulation of protein synthesis, mainly in neurodevelopment and synaptic plasticity (Yoon et al., 2008). One study observed that acute treatment with the NMDA receptor antagonist MK-801 resulted in increased phosphorylation of proteins in the mTOR-p70S6K pathway in rat frontal cortex (Yoon et al., 2008). Another investigation showed that haloperidol treatment appears to activate the AKT-mTORC1 pathway leading to changes in protein synthesis (Bowling et al., 2014). We observed that chlorpromazine, haloperidol and risperidone affected proteins belonging to mTOR pathway. Most proteins affected by chlorpromazine are increased, while treatment with risperidone decreased protein levels. In contrast, treatment with haloperidol similarly affected the proteins, both raising and decreasing their expression. Additionally, we could observed that only chlorpromazine affected directly the levels of mTOR (**Figure 3**). These differential effects could be due to variations in brain regions and cell types as we have specifically investigated an oligodendrocyte cell line in this study and because the treatments have many different mechanisms of action.

Ubiquitination Pathway

We also observed that the treatment with chlorpromazine and haloperidol resulted in alterations in the levels of proteins associated with the ubiquitination pathway. The treatment with chlorpromazine increased levels of heat shock family proteins (HSP90AA1, HSP90B1, HSPA6, and HSPE1) and proteins belonging to the proteasome (HSPE1, PSMC5, PSMD3, and PSMD13). The treatment with haloperidol also increased levels of proteins belonging to heat shock family (HSPA4, HSPA9, HSPA1A/HSPA1B, and HSPA4L) and proteasome proteins (PSMA6, PSMB6, PSMC2, PSMD4, PSMD7, and PSMD12). The main role of ubiquitination pathway is protein degradation through the conjugation of various portions of ubiquitin to the target protein followed by degradation of the protein bound to the polyubiquitin chain by the 26S proteasome complex (Ryan et al., 2006). Studies have shown decreased expression of genes related to this pathway in the dentate granule neurons and prefrontal cortex of schizophrenia patients (Middleton et al., 2002; Altar et al., 2005). Another study which carried out a blood-based microarray analysis found changes in the ubiquitin proteasome pathway of schizophrenia patients (Bousman et al., 2010). We suggest that chlorpromazine and haloperidol may restore the levels of the proteins involved in the ubiquitin pathway in schizophrenia, possibly aiding cellular processes regulated by this pathway such as signal transduction, synaptic plasticity, intracellular trafficking, endocytosis, DNA repair, and neural activity.

Energy Metabolism

Multiple studies have demonstrated a dysregulation in energy metabolism in schizophrenia. Proteomics analysis of *post mortem* brains of patients with schizophrenia showed alterations in the levels of energy metabolism-associated proteins, such as aldolase C (ALDOC), enolase 2 (ENO2), and glyceraldehyde-3-phosphate dehydrogenase (GAPDH) (Saia et al., 2015). Another investigation using samples of *post mortem* hippocampus of patients with schizophrenia found that glycolysis- and gluconeogenesis-associated proteins were altered, as seen by decreased levels of ALDOC and increased ENO1 (Schubert et al., 2015). Changes in energy metabolism have also been implicated in the effects of antipsychotics in oligodendrocytes. A study showed that haloperidol increased the amount of glucose and decreased the lactate levels present in the extracellular medium of cultured oligodendrocytes, suggesting that haloperidol affected glucose uptake in these cells (Steiner et al., 2014). In the present study, all the proteins related to glycolysis and gluconeogenesis were increased by haloperidol and decreased by chlorpromazine, whereas none of the atypical antipsychotics used in this study altered the levels of proteins belonging this pathway.

14-3-3 Family

Another set of proteins found at altered levels following chlorpromazine and haloperidol treatments, was proteins from the 14-3-3 family. There are seven known mammalian 14-3-3 isoforms, and 14-3-3 proteins are abundant in the brain, accounting for approximately 1% of the total soluble proteins (Fu et al., 2000). 14-3-3 proteins play fundamental roles in many processes, including the cell cycle, apoptosis, synaptic plasticity, and neuronal differentiation and migration (Fu et al., 2000). In this study, the haloperidol treatment led to decreased levels of 14-3-3 epsilon (YWHAE), and the chlorpromazine treatments induced increased levels of 14-3-3 beta/alpha (YWHAB), 14-3-3 zeta/delta (YWHAZ) and 14-3-3 gamma (YWHAG). Several studies found changes in proteins of the 14-3-3 family in brain

tissues from schizophrenia patients (Middleton et al., 2005; Schubert et al., 2015; Qing et al., 2016). Our group found disruption of 14-3-3 signaling in the corpus callosum of patients with schizophrenia (Saia et al., 2015). We also observed that clozapine treatment resulted in increased levels of 14-3-3 protein eta (YWHAH) (Cassoli et al., 2016). However, we did not observe these effects of the atypical antipsychotics used in this study.

Drug-Specific Differences Triggered by Antipsychotics in the Oligodendrocytes Proteome

Chlorpromazine

Neuregulins are member proteins of the epidermal growth factor (EGF) family and are ligands for tyrosine kinases receptors (ErbB family), which play a key role in the development, maintenance, and repair of the nervous system. Recent genetic studies have demonstrated a possible role of neuregulin 1 and its receptor erbB in the pathophysiology of schizophrenia (Hashimoto et al., 2004; Hahn et al., 2006; Avramopoulos, 2017). Moreover, neuregulins play roles in some processes implicated in schizophrenia, such as neuronal migration, neurotransmitter function such as NMDA, GABA, α-7, as well as dopamine and oligodendrocyte biology (Law et al., 2006). Although one study using mRNA expression profiling found no changes in neuregulins (type I, type II, and type III) in the dorsolateral prefrontal cortex of patients with schizophrenia (Hashimoto et al., 2004), another study analyzed mRNA abundance of Neuregulin I (types I-IV) in the hippocampus of patients with schizophrenia and found a variation in the expression of these isoforms (Law et al., 2006). Although neuregulin expression was not affected by chlorpromazine, according to the IPA analysis, some neuregulin-associated proteins, such as HSP90AA1, HSP90B1, MAP2K1, and RPS6 were altered.

Haloperidol

A regular side effect of haloperidol treatment and its limitation in the clinic is the extrapyramidal symptoms and tardive dyskinesia. However, the exact pathophysiology of how this drug induces these side effects is not totally clear (Perera et al., 2011). Oxidative stress constitutes a potential pathogenic mechanism that may contribute to movement disturbances, especially to tardive dyskinesia (Perera et al., 2011; Wu et al., 2014; Samad and Haleem, 2017). Recent studies have shown that the repeated administration of haloperidol is able to induce tardive dyskinesia in rats (Samad and Haleem, 2017). Another study using plasma and the enzyme manganese superoxide dismutase (MnSOD) as a biomarker of patients with schizophrenia analyzed the relationship of oxidative stress and tardive dyskinesia. This study suggested that tardive dyskinesia is more severe in patients suffering from oxidative stress (Wu et al., 2014). Furthermore, haloperidol was able to induce oxidative stress, potentially by decreasing the levels of mnSOD and glutathione peroxidase (GPx) in rats (Perera et al., 2011). Here, we do not observed alterations in levels of mnSOD or GPx, but the levels of other glutathione proteins were altered in oligodendrocytes treated with haloperidol, indicating a possible increase of oxidative stress in these cells (**Figure 3**). However, further investigations are needed to understand possible outcomes for white matter in the schizophrenia.

Quetiapine

Quetiapine has higher affinity for serotonin 5HT2 receptors than D2 dopamine receptors (Leucht et al., 1999). Here, compared to the other drugs, quetiapine altered fewer proteins (19). Interestingly, we also observed this profile in the proteome and lipidome from plasma samples of schizophrenia patients (unpublished data). Leucht et al. (2015) recently presented a study using an approach for dose equivalence of second-generation antipsychotic drugs for olanzapine 1 mg/day. The dose equivalent to 1 mg/d olanzapine were quetiapine 32.3 mg/day. In our study we used the same dose for all drugs. In this regard, we hypothesized that a higher concentration of quetiapine would be needed to have a significant response. Although IPA analysis showed associations with 17 canonical pathways, we did not have a ratio higher than 0.06. In this way, there is still little information in our data about these pathways for supporting any relation of these to schizophrenia. However, these results may be relevant to a more specific mechanism of action of quetiapine, although is not clear whether these are side effect or efficacy-related.

Risperidone

Purine and pyrimidine nucleotides are essential for nucleic acid synthesis, providing energy and contributing for many other fundamental processes in the cells (Handford et al., 2006). The purinergic system is not only present in neurons in CNS, but studies have been shown that some purines have specialized roles in glial cells (Handford et al., 2006). Purinergic signaling in glial cells regulates proliferation, motility, survival, differentiation, myelination and participate in the communication between neurons and glial cells (Chadwick and Goode, 2008). The purinergic hypothesis of schizophrenia is based on that a dysfunction of purinergic signaling can be associated with many aspects of the pathology (Inoue et al., 1996; Lara and Souza, 2000). A meta-analysis showed improvement in the positive symptoms and slightly important progressing in the negative symptoms of patients with purinergic modulators (Hirota and Kishi, 2013). Here, the treatment with risperidone altered some proteins belonging to the pathway purine nucleotides *de novo* biosynthesis II. Thus, these data indicate that one of the mechanisms of action of risperidone may be to modulate the purinergic system, which would explain its effectiveness in the treatment of schizophrenia.

CONCLUSION

Considering the results discussed above, this study has led to identification of some pathways and proteins that can be modulated by antipsychotics in oligodendrocytes. It was possible to observe that risperidone had more pathways in common

with chlorpromazine and haloperidol than with quetiapine. It is known that different doses of this drug can lead to different responses in patients, with the capability of behaving as a typical antipsychotic rather than an atypical one. Thus, we suggest that the dose used in the present study resulted in a closer response to typical antipsychotics. In addition, chlorpromazine appears to act by increasing protein levels, whereas haloperidol has the opposite effect. Although both are first-generation antipsychotics, they appear to have different mechanisms of action in oligodendrocytes. Finally, quetiapine altered fewer proteins compared to the other three drugs. Although *in vitro* studies have numerous limitations and may be distant from the *in vivo* scenario, our results provide detailed information on proteins and pathways modulated by the antipsychotics studied here and show the importance of studying cell types other than neurons to fully comprehend the molecular changes involved in both the disease and treatment response. Furthermore, antipsychotics can modulate important functions of oligodendrocytes and this deserves further investigation, since in schizophrenia was found dysregulations in the white matter and alterations in the functions of these cells.

DATA AVAILABILITY

The datasets generated for this study can be found in the ProteomeXchange http://www.proteomexchange.org/Project accession: PXD008892.

AUTHOR CONTRIBUTIONS

CB-T conceived and designed the study and wrote the first draft and final version of the manuscript. JC helped in experimental design and performed the mass spectrometry experiments. VdA helped in data interpretation and manuscript revision. DM-d-S conceived, supervised, and finalized the manuscript.

FUNDING

CB-T, VdA, JC, and DM-d-S were supported by FAPESP (São Paulo Research Foundation), grants 2015/23049-0, 2017/18242-1, 2014/14881-1, 2014/10068-4, 2017/25588-1, and 2018/03673-1. DM-d-S was also supported by The Brazilian National Council for Scientific and Technological Development (CNPq), grant 460289/2014-4 and Serrapilheira Institute, grant number Serra-1709-16349.

SUPPLEMENTARY MATERIAL

The Supplementary Material for this article can be found online at: https://www.frontiersin.org/articles/10.3389/fphar.2019.00186/full#supplementary-material

FIGURE S1 | Representative images of MO3.13 cells treated for 8 h with vehicle solution (DMSO; **A**) and quetiapine 50 μM **(B)** stained for cytochrome C (green)/Dapi (blue). **(C)** Statistic chart showing normalized intensity fluorescence for cytochrome C for each treatment (*$P < 0.05$). Scale bars = 200 μm.

TABLE S1 | Proteins affected by chlorpromazine treatment.

TABLE S2 | Proteins affected by haloperidol treatment.

TABLE S3 | Ingenuity canonical pathway analysis for oligodendrocyte treated with first generation antipsychotics.

TABLE S4 | Proteins affected by quetiapine treatment.

TABLE S5 | Proteins affected by risperidone treatment.

TABLE S6 | Ingenuity canonical pathway analysis for oligodendrocyte treated with second generation antipsychotics.

REFERENCES

Altar, C. A., Jurata, L. W., Charles, V., Lemire, A., Liu, P., Bukhman, Y., et al. (2005). Deficient hippocampal neuron expression of proteasome, ubiquitin, and mitochondrial genes in multiple schizophrenia cohorts. *Biol. Psychiatry* 58, 85–96. doi: 10.1016/j.biopsych.2005.03.031

Avramopoulos, D. (2017). Neuregulin 3 and its roles in schizophrenia risk and presentation. *Am. J. Med. Genet. B Neuropsychiatr. Genet.* 177, 257–266. doi: 10.1002/ajmg.b.32552

Bousman, C. A., Chana, G., Glatt, S. J., Chandler, S. D., May, T., Lohr, J., et al. (2010). Positive symptoms of psychosis correlate with expression of ubiquitin proteasome genes in peripheral blood. *Am. J. Med. Genet. B Neuropsychiatr. Genet.* 153, 1336–1341. doi: 10.1002/ajmg.b.31106

Bowling, H., Zhang, G., Bhattacharya, A., Pérez-Cuesta, L. M., Deinhardt, K., Hoeffer, C. A., et al. (2014). Antipsychotics activate mTORC1-dependent translation to enhance neuronal morphological complexity. *Sci. Signal.* 7:ra4. doi: 10.1126/scisignal.2004331

Brandão-Teles, C., Martins-de-Souza, D., Guest, P. C., and Cassoli, J. S. (2017). MK-801-treated oligodendrocytes as a cellular model to study schizophrenia. *Adv. Exp. Med. Biol.* 974, 269–277. doi: 10.1007/978-3-319-52479-5_25

Buntinx, M., Vanderlocht, J., Hellings, N., Vandenabeele, F., Lambrichts, I., Raus, J., et al. (2003). Characterization of three human oligodendroglial cell lines as a model to study oligodendrocyte injury: morphology and oligodendrocyte-specific gene expression. *J. Neurocytol.* 32, 25–38. doi: 10.1023/A:1027324230923

Carter, C. J. (2007). EIF2B and oligodendrocyte survival: where nature and nurture meet in bipolar disorder and schizophrenia? *Schizophr. Bull.* 33, 1343–1353. doi: 10.1093/schbul/sbm007

Cassoli, J. S., Brandão-Teles, C., Santana, A. G., Souza, G. H. M. F., and Martins-de-Souza, D. (2017). Ion mobility-enhanced data-independent acquisitions enable a deep proteomic landscape of oligodendrocytes. *Proteomics* 17:1700209. doi: 10.1002/pmic.201700209

Cassoli, J. S., Iwata, K., Steiner, J., Guest, P. C., Turck, C. W., Nascimento, J. M., et al. (2016). Effect of MK-801 and clozapine on the proteome of cultured human oligodendrocytes. *Front. Cell Neurosci.* 10:52. doi: 10.3389/fncel.2016.00052

Cassoli, J. S., and Martins-de-Souza, D. (2017). "Comprehensive shotgun proteomic analyses of oligodendrocytes using ion mobility and data-independent acquisition," in *Current Proteomic Approaches Applied to Brain Function*, eds J. Fernández-Irigoyen and E. Santamaría (New York, NY: Humana Press), 65–74. doi: 10.1007/978-1-4939-7119-0_5

Chadwick, D. J., and Goode, J. (2008). Purinergic signalling in neuron-glia interactions. *Purinergic Signal. Neuron Glia Interact.* 7, 1–291. doi: 10.1002/9780470032244

Coyle, J. T. (1996). The glutamatergic dysfunction hypothesis for schizophrenia. *Harv. Rev. Psychiatry* 3, 241–253. doi: 10.3109/10673229609017192

Eruslanov, E., and Kusmartsev, S. (2010). Indentification of ROS using oxidized DCFDA and flow-cytometry. *Methods Mol. Biol.* 594, 57–72. doi: 10.1007/978-1-60761-411-1

Fu, H., Subramanian, R. R., and Masters, S. C. (2000). 14-3-3 P ROTEINS: structure, function, and regulation. *Annu. Rev. Pharmacol. Toxicol.* 40, 617–647. doi: 10.1146/annurev.pharmtox.40.1.617

Georgieva, L., Moskvina, V., Peirce, T., Norton, N., Bray, N. J., Jones, L., et al. (2006). Convergent evidence that oligodendrocyte lineage transcription factor 2 (OLIG2) and interacting genes influence susceptibility to schizophrenia. *Proc. Natl. Acad. Sci. U.S.A.* 103, 12469–12474. doi: 10.1073/pnas.0603029103

Geromanos, S. J., Hughes, C., Ciavarini, S., Vissers, J. P. C., and Langridge, J. I. (2012). Using ion purity scores for enhancing quantitative accuracy and precision in complex proteomics samples. *Anal. Bioanal. Chem.* 404, 1127–1139. doi: 10.1007/s00216-012-6197-y

Glatt, S. J., Cohen, O. S., Faraone, S. V., and Tsuang, M. T. (2011). Dysfunctional gene splicing as a potential contributor to neuropsychiatric disorders. *Am. J. Med. Genet. B Neuropsychiatr. Genet.* 156, 382–392. doi: 10.1002/ajmg.b.31181

Hahn, C.-G., Wang, H.-Y., Cho, D.-S., Talbot, K., Gur, R. E., Berrettini, W. H., et al. (2006). Altered neuregulin 1-erbB4 signaling contributes to NMDA> receptor hypofunction in schizophrenia. *Nat. Med.* 12, 824–828. doi: 10.1038/nm1418

Hakak, Y., Walker, J. R., Li, C., Wong, W. H., Davis, K. L., Buxbaum, J. D., et al. (2001). Genome-wide expression analysis reveals dysregulation of myelination-related genes in chronic schizophrenia. *Proc. Natl. Acad. Sci. U.S.A.* 98, 4746–4751. doi: 10.1073/pnas.081071198

Handford, M., Rodriguez-Furlán, C., and Orellana, A. (2006). Nucleotide-sugar transporters: structure, function and roles in vivo. *Braz. J. Med. Biol. Res.* 39, 1149–1158. doi: 10.1590/S0100-879X2006000900002

Hashimoto, R., Straub, R. E., Weickert, C. S., Hyde, T. M., Kleinman, J. E., and Weinberger, D. R. (2004). Expression analysis of neuregulin-1 in the dorsolateral prefrontal cortex in schizophrenia. *Mol. Psychiatry* 9, 299–307. doi: 10.1038/sj.mp.4001434

Hayashi-Takagi, A. (2016). Synapse pathology and translational applications for schizophrenia. *Neurosci. Res.* 114, 3–8. doi: 10.1016/j.neures.2016.09.001

Hirota, T., and Kishi, T. (2013). Adenosine hypothesis in schizophrenia and bipolar disorder: a systematic review and meta-analysis of randomized controlled trial of adjuvant purinergic modulators. *Schizophr. Res.* 149, 88–95. doi: 10.1016/j.schres.2013.06.038

Hof, P. R., Haroutunian, V., Friedrich, V. L., Byne, W., Buitron, C., Perl, D. P., et al. (2003). Loss and altered spatial distribution of oligodendrocytes in the superior frontal gyrus in schizophrenia. *Biol. Psychiatry* 53, 1075–1085. doi: 10.1016/S0006-3223(03)00237-3

Inoue, K., Koizumi, S., and Ueno, S. (1996). Implication of ATP receptors in brain functions. *Prog. Neurobiol.* 50, 483–492. doi: 10.1016/S0301-0082(96)00037-8

Iwata, K., Matsuzaki, H., Manabe, T., and Mori, N. (2011). Altering the expression balance of hnRNP C1 and C2 changes the expression of myelination-related genes. *Psychiatry Res.* 190, 364–366. doi: 10.1016/j.psychres.2011.05.043

Ju, P., and Cui, D. (2015). The involvement of N-methyl-d-aspartate receptor (NMDAR) subunit NR1 in the pathophysiology of schizophrenia. *Acta Biochim. Biophys. Sin.* 48, 209–219. doi: 10.1093/abbs/gmv135

Kantoff, P. W., Higano, C. S., Shore, N. D., Berger, E. R., Small, E. J., Penson, D. F., et al. (2010). Effectiveness of antipsychotic drugs in patients with chronic schizophrenia. *Clin. Trials* 363, 411–422. doi: 10.1056/NEJMoa1402121

Lara, D. R., and Souza, D. O. (2000). Schizophrenia: a purinergic hypothesis. *Med. Hypotheses* 54, 157–166. doi: 10.1054/mehy.1999.0003

Law, A. J., Lipska, B. K., Weickert, C. S., Hyde, T. M., Straub, R. E., Hashimoto, R., et al. (2006). Neuregulin 1 transcripts are differentially expressed in schizophrenia and regulated by 5' SNPs associated with the disease. *Proc. Natl. Acad. Sci.* 103, 6747–6752. doi: 10.1073/pnas.0602002103

Leucht, S., Corves, C., Arbter, D., Engel, R. R., Li, C., and Davis, J. M. (2009). Second-generation versus first-generation antipsychotic drugs for schizophrenia: a meta-analysis. *Lancet* 373, 31–41. doi: 10.1016/S0140-6736(08)61764-X

Leucht, S., Pitschel-Walz, G., Abraham, D., and Kissling, W. (1999). Efficacy and extrapyramidal side-effects of the new antipsychotics olanzapine, quetiapine, risperidone, and sertindole compared to conventional antipsychotics and placebo. A meta-analysis of randomized controlled trials. *Schizophr. Res.* 35, 51–68. doi: 10.1016/S0920-9964(98)00105-4

Leucht, S., Samara, M., Heres, S., Patel, M. X., Furukawa, T., Cipriani, A., et al. (2015). Dose equivalents for second-generation antipsychotic drugs: the classical mean dose method. *Schizophr. Bull.* 41, 1397–1402. doi: 10.1093/schbul/sbv037

Li, G.-Z., Vissers, J. P. C., Silva, J. C., Golick, D., Gorenstein, M. V., and Geromanos, S. J. (2009). Database searching and accounting of multiplexed precursor and product ion spectra from the data independent analysis of simple and complex peptide mixtures. *Proteomics* 9, 1696–1719. doi: 10.1002/pmic.200800564

Lieberman, J. A., Stroup, T. S., Mcevoy, J. P., Swartz, M. S., Rosenheck, R. A., Perkins, D. O., et al. (2005). Effectiveness of antipsychotic drugs in patients with chronic schizophrenia. *N. Engl. J. Med.* 353, 1209–1223. doi: 10.1056/NEJMoa051688

Martins-de-Souza, D., Gattaz, W. F., Schmitt, A., Novello, J. C., Marangoni, S., Turck, C. W., et al. (2009). Proteome analysis of schizophrenia patients Wernicke's area reveals an energy metabolism dysregulation. *BMC Psychiatry* 9:17. doi: 10.1186/1471-244X-9-17

Martins-de-Souza, D., Lebar, M., and Turck, C. W. (2011). Proteome analyses of cultured astrocytes treated with MK-801 and clozapine: similarities with schizophrenia. *Eur. Arch. Psychiatry Clin. Neurosci.* 261, 217–228. doi: 10.1007/s00406-010-0166-2

Matera, A. G., and Wang, Z. (2014). A day in the life of the spliceosome. *Nat. Rev. Mol. Cell Biol.* 15, 108–121. doi: 10.1038/nrm3742

Middleton, F. A., Mirnics, K., Pierri, J. N., Lewis, D. A., and Levitt, P. (2002). Gene expression profiling reveals alterations of specific metabolic pathways in schizophrenia. *J. Neurosci.* 22, 2718–2729. doi: 10.1523/JNEUROSCI.22-07-02718.2002

Middleton, F. A., Peng, L., Lewis, D. A., Levitt, P., and Mirnics, K. (2005). Altered expression of 14-3-3 genes in the prefrontal cortex of subjects with schizophrenia. *Neuropsychopharmacology* 30, 974–983. doi: 10.1038/sj.npp.1300674

Neill, J. C., Barnes, S., Cook, S., Grayson, B., Idris, N. F., McLean, S. L., et al. (2010). Animal models of cognitive dysfunction and negative symptoms of schizophrenia: focus on NMDA receptor antagonism. *Pharmacol. Ther.* 128, 419–432. doi: 10.1016/j.pharmthera.2010.07.004

Paulson, L., Martin, P., Persson, A., Nilsson, C. L., Ljung, E., Westman-Brinkmalm, A., et al. (2003). Comparative genome- and proteome analysis of cerebral cortex from MK-801-treated rats. *J. Neurosci. Res.* 71, 526–533. doi: 10.1002/jnr.10509

Perera, J., Tan, J. H., Jeevathayaparan, S., Chakravarthi, S., and Haleagrahara, N. (2011). Neuroprotective effects of alpha lipoic Acid on haloperidol-induced oxidative stress in the rat brain. *Cell Biosci.* 1:12. doi: 10.1186/2045-3701-1-12

Qing, Y., Sun, L., Yang, C., Jiang, J., Yang, X., Hu, X., et al. (2016). Dysregulated 14-3-3 family in peripheral blood leukocytes of patients with schizophrenia. *Sci. Rep.* 6:23791. doi: 10.1038/srep23791

Ryan, M. M., Lockstone, H. E., Huffaker, S. J., Wayland, M. T., Webster, M. J., and Bahn, S. (2006). Gene expression analysis of bipolar disorder reveals downregulation of the ubiquitin cycle and alterations in synaptic genes. *Mol. Psychiatry* 11, 965–978. doi: 10.1038/sj.mp.4001875

Saia, V. M., Juliana, C., Andrea, S. C., Falkai, P., Nascimento, J. M., and Martins-de-Souza, D. (2015). Proteomics of the corpus callosum unravel pivotal players in the dysfunction of cell signaling, structure, and myelination in schizophrenia brains. *Eur. Arch. Psychiatry Clin. Neurosci.* 265, 601–612. doi: 10.1007/s00406-015-0621-1

Saia-cereda, V. M., and Santana, A. G. (2017). The nuclear proteome of white and gray matter from schizophrenia postmortem brains. *Mol. Neuropsychiatry* 3, 37–52. doi: 10.1159/000477299

Samad, N., and Haleem, D. J. (2017). Antioxidant effects of rice bran oil mitigate repeated haloperidol-induced tardive dyskinesia in male rats. *Metab. Brain Dis.* 32, 1099–1107. doi: 10.1007/s11011-017-0002-8

Schubert, K. O., Föcking, M., and Cotter, D. R. (2015). Proteomic pathway analysis of the hippocampus in schizophrenia and bipolar affective disorder implicates 14-3-3 signaling, aryl hydrocarbon receptor signaling, and glucose metabolism: potential roles in GABAergic interneuron pathology. *Schizophr. Res.* 167, 64–72. doi: 10.1016/j.schres.2015.02.002

Shen, W. W. (1999). A history of antipsychotic drug development. *Compr. Psychiatry* 40, 407–414. doi: 10.1016/S0010-440X(99)90082-2

Steiner, J., Martins-de-Souza, D., Schiltz, K., Sarnyai, Z., Westphal, S., Isermann, B., et al. (2014). Clozapine promotes glycolysis and myelin lipid synthesis in

cultured oligodendrocytes. *Front. Cell. Neurosci.* 8:384. doi: 10.3389/fncel.2014.00384

Takahashi, N., Sakurai, T., Davis, K. L., and Buxbaum, J. D. (2011). Linking oligodendrocyte and myelin dysfunction to neurocircuitry abnormalities in schizophrenia. *Prog. Neurobiol.* 93, 13–24. doi: 10.1016/j.pneurobio.2010.09.004

Taraboletti, A., Walker, T., Avila, R., Huang, H., Caporoso, J., Manandhar, E., et al. (2017). Cuprizone intoxication induces cell intrinsic alterations in oligodendrocyte metabolism independent of copper chelation. *Biochemistry* 56, 1518–1528. doi: 10.1021/acs.biochem.6b01072

Uranova, N. A., Vostrikov, V. M., Orlovskaya, D. D., and Rachmanova, V. I. (2004). Oligodendroglial density in the prefrontal cortex in schizophrenia and mood disorders: a study from the stanley neuropathology consortium. *Schizophr. Res.* 67, 269–275. doi: 10.1016/S0920-9964(03)00181-6

Wu, J. Q., Chen, D. C., Tan, Y. L., Tan, S. P., Wang, Z. R., Xiu, M. H., et al. (2014). Cognition impairment in schizophrenia patients with tardive dyskinesia: association with plasma superoxide dismutase activity. *Schizophr. Res.* 152, 210–216. doi: 10.1016/j.schres.2013.11.010

Xiu, Y., Kong, X.-R., Zhang, L., Qiu, X., Chao, F.-L., Peng, C., et al. (2014). White matter injuries induced by mk-801 in a mouse model of schizophrenia based on NMDA Antagonism. *Anat. Rec.* 297, 1498–1507. doi: 10.1002/ar.22942

Yoon, S. C., Seo, M. S., Kim, S. H., Jeon, W. J., Ahn, Y. M., Kang, U. G., et al. (2008). The effect of MK-801 on mTOR/p70S6K and translation-related proteins in rat frontal cortex. *Neurosci. Lett.* 434, 23–28. doi: 10.1016/j.neulet.2008.01.020

Conflict of Interest Statement: The authors declare that the research was conducted in the absence of any commercial or financial relationships that could be construed as a potential conflict of interest.

frontiers in Pharmacology

CORRECTION
published: 09 April 2019
doi: 10.3389/fphar.2019.00344

Corrigendum: Biochemical Pathways Triggered by Antipsychotics in Human Oligodendrocytes: Potential of Discovering New Treatment Targets

Caroline Brandão-Teles[1], *Valéria de Almeida*[1], *Juliana S. Cassoli*[1,2] *and Daniel Martins-de-Souza*[1,3,4]*

[1] Laboratory of Neuroproteomics, Department of Biochemistry and Tissue Biology, Institute of Biology, University of Campinas, Campinas, Brazil, [2] Faculdade de Palmas, Palmas, Brazil, [3] UNICAMP's Neurobiology Center, Campinas, Brazil, [4] Instituto Nacional de Biomarcadores em Neuropsiquiatria, Conselho Nacional de Desenvolvimento Científico e Tecnológico, São Paulo, Brazil

Keywords: schizophrenia, mechanism of action, proteomics, biomarkers, chlorpromazine, haloperidol, quetiapine, risperidone

OPEN ACCESS

Approved by:
Frontiers in Pharmacology Editorial Office,
Frontiers Media SA, Switzerland

***Correspondence:**
Daniel Martins-de-Souza
dmsouza@unicamp.br;
danms90@gmail.com

Specialty section:
This article was submitted to Neuropharmacology, a section of the journal Frontiers in Pharmacology

Received: *18 March 2019*
Accepted: *19 March 2019*
Published: *09 April 2019*

Citation:
Brandão-Teles C, de Almeida V, Cassoli JS and Martins-de-Souza D (2019) Corrigendum: Biochemical Pathways Triggered by Antipsychotics in Human Oligodendrocytes: Potential of Discovering New Treatment Targets. Front. Pharmacol. 10:344. doi: 10.3389/fphar.2019.00344

A Corrigendum on

Biochemical Pathways Triggered by Antipsychotics in Human Oligodendrocytes: Potential of Discovering New Treatment Targets
by Brandão-Teles, C., de Almeida, V., Cassoli, J. S., and Martins-de-Souza, D. (2019). Front. Pharmacol. 10:186. doi: 10.3389/fphar.2019.00186

The title of the article has been changed from "Oligodendrocytes: Potential of Discovering New Treatment Targets" to "Biochemical Pathways Triggered by Antipsychotics in Human Oligodendrocytes: Potential of Discovering New Treatment Targets."

The authors apologize for this error and state that this does not change the scientific conclusions of the article in any way. The original article has been updated.

frontiers in Genetics

ORIGINAL RESEARCH
published: 22 March 2019
doi: 10.3389/fgene.2019.00232

Central and Peripheral Changes in FOS Expression in Schizophrenia Based on Genome-Wide Gene Expression

Jing Huang[1,2†], Fangkun Liu[3†], Bolun Wang[4], Hui Tang[1,2], Ziwei Teng[1,2], Lehua Li[1,2], Yan Qiu[1,2], Haishan Wu[1,2] and Jindong Chen[1,2*]*

[1] Department of Psychiatry, The Second Xiangya Hospital, Central South University, Changsha, China, [2] Mental Health Institute of the Second Xiangya Hospital, Central South University, Chinese National Clinical Research Center for Mental Disorders (Xiangya), Chinese National Technology Institute on Mental Disorders, Hunan Key Laboratory of Psychiatry and Mental Health, Changsha, China, [3] Department of Neurosurgery, Xiangya Hospital, Central South University, Changsha, China, [4] Department of Orthopedics, The Second Xiangya Hospital, Central South University, Changsha, China

OPEN ACCESS

Edited by:
Pei Jiang,
Jining Medical University, China

Reviewed by:
Paul Tooney,
University of Newcastle, Australia
Kazim Yalcin Arga,
Marmara University, Turkey

***Correspondence:**
Haishan Wu
wuhaishan@csu.edu.cn
Jindong Chen
chenjindong@csu.edu.cn

† These authors have contributed equally to this work

Specialty section:
This article was submitted to Behavioral and Psychiatric Genetics, a section of the journal Frontiers in Genetics

Received: *24 October 2018*
Accepted: *04 March 2019*
Published: *22 March 2019*

Citation:
Huang J, Liu F, Wang B, Tang H, Teng Z, Li L, Qiu Y, Wu H and Chen J (2019) Central and Peripheral Changes in FOS Expression in Schizophrenia Based on Genome-Wide Gene Expression. Front. Genet. 10:232. doi: 10.3389/fgene.2019.00232

Schizophrenia is a chronic, debilitating neuropsychiatric disorder. Multiple transcriptomic gene expression profiling analysis has been used to identify schizophrenia-associated genes, unravel disease-associated biomarkers, and predict clinical outcomes. We aimed to identify gene expression regulation, underlying pathways, and their roles in schizophrenia pathogenesis. We searched the Gene Expression Omnibus (GEO) database for microarray studies of fibroblasts, lymphoblasts, and post-mortem brains of schizophrenia patients. Our analysis demonstrated high FOS expression in non-neural peripheral samples and low FOS expression in brain tissues of schizophrenia patients compared with healthy controls. FOS exhibited predictive value for schizophrenia patients in these datasets. Kyoto Encyclopedia of Genes and Genomes (KEGG) enrichment analysis revealed that "amphetamine addiction" was among the top 10 significantly enriched KEGG pathways. FOS and FOSB, which are implicated in the amphetamine addiction pathway, were up-regulated in schizophrenia fibroblast samples. Protein–protein interaction (PPI) network analysis revealed that proteins closely interacting with FOS-encoded protein were also involved in the amphetamine addiction pathway. Pearson correlation test indicated that FOS showed positive correlation with genes in the amphetamine pathway. The results revealed that FOS was acceptable as a biomarker for schizophrenia and may be involved in schizophrenia pathogenesis.

Keywords: schizophrenia, GEO, re-analysis, FOS, amphetamine addiction pathway

INTRODUCTION

Schizophrenia is a chronic and debilitating neuropsychiatric disorder affecting 1% of the population, posing a severe social and economic burden on societies worldwide (McGrath et al., 2008; Howes and Murray, 2014). Common symptoms include positive and negative symptoms and cognitive deficits (Lewis et al., 2012). Besides its complex symptomatology, schizophrenia is considered a neurodevelopmental disorder with heterogeneous, polygenic, and highly heritable

etiology (Quadrato et al., 2016). Schizophrenia affects gross architectural structures, specific cell types, and ion channels across different brain regions, including the prefrontal cortex, thalamus, thalamic reticular nucleus, and basal ganglia (Heyes et al., 2015; Mouchlianitis et al., 2016; Goff et al., 2017). However, there is heterogeneity in the molecular and genetic phenotypes of patients. The precise etiology and pathogenesis underlying schizophrenia are not fully known. Identifications of gene changes as biomarkers for schizophrenia may be helpful for diagnostic assessment of patients.

Strong evidence suggests that dysfunction of multiple neurotransmitter systems may contribute to the pathophysiology of schizophrenia, including dopamine (DA), glutamate, and serotonin neurotransmission (de Bartolomeis et al., 2014). For example, *N*-methyl-D-aspartate (NMDA) receptor antagonists such as phencyclidine (PCP), ketamine, and MK-801 have psychotomimetic effects and have been used to generate pharmacological animal models of schizophrenia (Zuo et al., 2009). Another well-established pre-clinical schizophrenia rodent model is based on amphetamine (AMPH)-induced dopaminergic dysregulation (Renard et al., 2016). AMPH-induced schizophrenia-like sensorimotor cognitive deficits are severely disrupted in schizophrenia (Pedrazzi et al., 2015; Renard et al., 2016). Genes involved in these pathways have been examined to better understand the pathogenesis of schizophrenia and points to new targets for therapeutic investigation (Karam et al., 2010; Hall et al., 2015; Network et al., 2015). Environmental risk factors and their interactions with gene expression also play important roles in schizophrenia pathophysiology (Van Winkel et al., 2010). Understanding the affected pathways and specific gene expression profiles in the pathogenesis of schizophrenia may help to uncover disease-associated biomarkers for risk assessment, regulatory mechanisms, and personalization of treatment.

The recently developed technique of gene expression profiling analysis of the whole transcriptome has been widely used to identify schizophrenia-associated genes, unravel disease-associated biomarkers, and predict clinical outcomes. Several whole-genome expression studies have utilized gene expression data from human fibroblasts, blood, and post-mortem brain samples to identify gene alterations in schizophrenia patients compared with healthy controls (Rollins et al., 2010; Cattane et al., 2015). Expression studies on post-mortem brains and peripheral cells demonstrated overlapping gene expression results; however, contrasting results have also been observed in different studies. The heterogeneity between gene expression profiles in peripheral cells and in post-mortem brains can be attributed to intrinsic differences in expression levels between the central nervous system (CNS) and peripheral tissues; and confounding factors in patients themselves, including the course of disease, age, living habits, environmental events, and clinical medications. These problems can be partly solved by integrated analysis of gene expression data from multiple studies and multiple tissues.

On this basis, the aim of our study was to elucidate gene expression changes in the pathogenesis of schizophrenia and to acquire new potential biomarkers for diagnostic prediction. We searched for microarray data for schizophrenia from the Gene Expression Omnibus (GEO) database. Different gene expression microarray studies with schizophrenia samples were selected and compared to perform a reliable genome-wide gene expression profiling analysis. First, we analyzed different microarray gene expression studies with a sample of fibroblasts from schizophrenia patients and controls to identify differentially expressed genes. Second, we compared the gene alteration results observed in different schizophrenia post-mortem brain expression studies. Third, we compared the results by analyzing gene expression changes in samples from schizophrenia mice models. Our analysis enables identification of gene expression regulation in different body areas of schizophrenia patients, disease progression, and confirmation of pre-clinical studies. This study may help us identify risk genes for schizophrenia and the underlying pathways. Our study may be applicable in elucidating the pathogenesis of other neuropsychiatric disorders.

MATERIALS AND METHODS

Inclusion Criteria

To identify specific gene expression changes in schizophrenia, we performed a systematic search in the GEO database for schizophrenia studies. The keywords used for the GEO database search were: "schizophrenia" AND "expression profiling by array" for "study type" AND "tissue" for "attribute name" AND "homo sapiens" for "organism." Details of the search strategy and analysis process are outlined in **Supplementary Figure S1**. The final studies were selected based on the criteria that (1) transcriptomic profiles were analyzed in skin fibroblasts of schizophrenia patients; (2) original data in CEL format could be downloaded; and (3) matched samples of healthy controls were used.

After screening 26 studies in GEO, the GEO dataset GSE62333[1] was selected, which studied 20 schizophrenia patients matched with 20 healthy controls with human skin fibroblast samples based on the GPL11532 [HuGene-1_1-st] Affymetrix Human Gene 1.1 ST Array (Cattane et al., 2015). Array GPL11532 has 33,297 probes. All schizophrenia patients fulfilled the DSM-IV criteria for schizophrenia. The control samples consisted of healthy volunteers without drug or alcohol abuse and without family history of psychiatric diseases. Other diseases such as hypothyroidism or hyperthyroidism, metabolic disorders, and serious illnesses were also excluded in both groups.

To maintain consistency, we also selected GEO datasets with lymphoblast samples from schizophrenia patients. Finally, dataset GSE73129[2], which is based on platform GPL570 [HG-U133_Plus_2] Affymetrix Human Genome U133 Plus 2.0 Array was selected for validation. Array GPL570 contained 54,675 probes. Human lymphoblast samples from 36 schizophrenia patients and 41 healthy controls were included. We compared gene expression levels in human prefrontal cortex samples

[1]https://www.ncbi.nlm.nih.gov/geo/query/acc.cgi?acc=GSE62333
[2]https://www.ncbi.nlm.nih.gov/geo/query/acc.cgi?acc=GSE73129

in GSE92538[3], comprising 45 schizophrenia patients and 46 healthy controls. We also validated the results with a genome-wide transcriptomics analysis of mouse prefrontal cortex and hippocampus samples. GSE10784[4] was selected, which contained 10 Df(16)A/+ mice and 10 control mice.

Data Analysis

Gene Expression Omnibus[5] provides raw data (CEL file) and normalized data downloads of the: (1) citation information, (2) geo-annotation, and (3) statistical matrix. Four GEO datasets were included in the analysis, GSE62333, GSE73129, GSE92538, and GSE10784. All of the original data came from publicly available datasets.

R language was mainly used for statistical analysis. The original CEL data was subjected to background correction, normalization, and expression calculation before further analysis. We completed the data preprocessing by RMA (R package "affy") (Gautier et al., 2004). Probes that did not match any known genes were removed. Only probes with the highest interquartile range were included for further analysis, if more than one probe matched with a gene. The selected probes were subjected to annotation using the R annotation the package "annotate." The gene expression profiling data was transformed by $\log_2$ and extracted for DEG identification and analysis. The DEGs were identified using the R package "limma." Spearman correlation analysis was performed using the "circlize" package (Gu et al., 2014), ROC curves were derived using the "pROC" package (Robin et al., 2011). Principal component analysis (PCA) was performed using the prcomp function of R "stats" package, and visualization was done using the ggplot2 package. The heatmap of DEGs was generated by clustering (using the R package "pheatmap") with p-value <0.05 between schizophrenia and control samples. Associated KEGG (Kyoto Encyclopedia of Genes and Genomes) enrichment analysis of the 250 DEGs was generated by Omics Bean and illustrates the results of KEGG pathway analysis. STRING database (version 9.1) was used to analyze protein–protein interaction (PPI) networks of the candidate genes. Dot plots of expression levels of identified genes were drawn by GraphPad Prism. All statistical tests were two-sided. A p-value less than 0.05 is considered to be statistically significant.

RESULTS

Identification and Functional Analysis of Differentially Expressed Genes (DEGs) in Schizophrenia and Healthy Control

The GEO dataset GSE62333 was selected to identify DEGs in human skin fibroblast samples from schizophrenia patients and matched healthy controls. After the samples were normalized by the robust multichip averaging (RMA) process, the expression levels (transformed by $\log_2$) of all included samples were extracted. The DEGs between two groups were calculated by the Classical Bayesian algorithm with 33,297 probes included. After screening using the criteria of $|FC| > 1.2$ and p-value < 0.05, 1,022 probes with significantly different expression levels between the two groups (517 up-regulated probes and 505 down-regulated probes) were identified. Probes that did not match any known genes were removed in further analysis. We selected the 250 probes with the highest inter-quartile range (125 up-regulated probes and 125 down-regulated probes, respectively). A heatmap that shows the 250 top-regulated genes matched with 250 probes between schizophrenia and control groups is presented in **Figure 1A**. The hierarchical clustering of these 250 genes demonstrated significant differences between schizophrenia and control groups.

We performed KEGG enrichment analysis of the 250 DEGs for functional analysis to identify the biological processes, pathways, and networks shared by these genes. The top 10 significantly enriched KEGG pathways (p-value < 0.05) were "AMPH addiction," "oxytocin signaling," "pathways in cancer," "estrogen signaling," "vascular smooth muscle contraction," "Ras signaling," "AGE-RAGE signaling pathway in diabetic complications," "choline metabolism in cancer," "Chagas disease," and "Rap1 signaling." The network model generated by Omics Bean illustrates the results of KEGG pathway enrichment analysis (**Figure 1B**). A histogram was plotted based on the functional analysis to display the percentage of genes affected in these pathways (**Figure 1C**).

FOS Up-Regulation in Schizophrenia Peripheral Samples

After confirming the pathways of 250 DEGs by KEGG enrichment analysis, we ranked the top 10 DEGs between the schizophrenia and control samples to determine which pathways these genes were involved in. The top five up-regulated genes (*FOSB, MMP1, FOS, RANBP3L*, and *SNORA38B*) and top five down-regulated genes (*SNORA68, SNORA23, SNORA20, ACTG2*, and *SNORA3A*) were arranged by degree of change. Detailed information on these genes is listed in **Table 1**. Dot plots illustrated that all 10 DEGs were differentially expressed between the two groups (p-value < 0.05), suggesting that these genes may be useful as biomarkers of schizophrenia (**Figure 2**). We also performed PCA and while there was a separation of some samples into diagnostic groups, overall there was no clear separation between control and SCZ samples (**Supplementary Figure S2**).

Among the top 10 DEGs, five of them (*SNORA38B, SNORA68, SNORA23, SNORA20*, and *SNORA3A*) were non-coding genes. Five of the top 10 DEGs were protein-coding genes (*RANBP3L, ACTG2, MMP1, FOSB*, and *FOS*). Two genes in the *FOS* family (*FOS* and *FOSB*) were up-regulated in schizophrenia samples. Among the top 10 DEGs, *FOS* was most closely related to schizophrenia pathogenesis. Previous research has shown that NMDA receptor antagonist-induced and AMPH-induced pharmacological animal models of schizophrenia can up-regulate *FOS* gene expression (Zuo et al., 2009; Renard et al., 2016). And we have observed that "AMPH addiction" was one of the most significantly enriched KEGG pathways in schizophrenia samples.

[3]https://www.ncbi.nlm.nih.gov/geo/query/acc.cgi?acc=GSE92538

[4]https://www.ncbi.nlm.nih.gov/geo/query/acc.cgi?acc=GSE10784

[5]https://www.ncbi.nlm.nih.gov/geo/

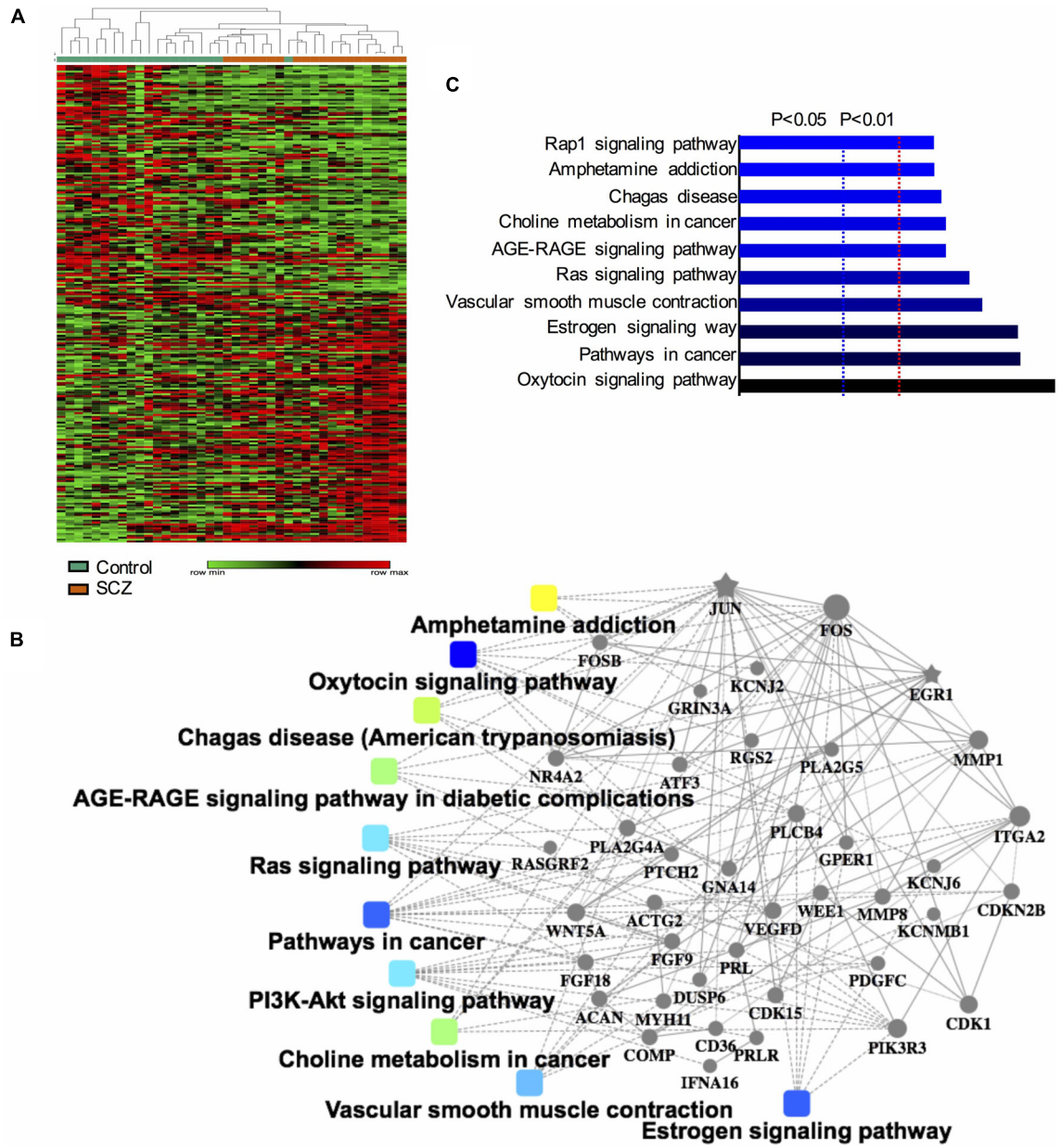

FIGURE 1 | Identification and functional analysis of 250 differentially expressed genes (DEGs) between schizophrenia and healthy control samples in GEO dataset GSE62333. **(A)** Heatmap showing 250 DEGs (| FC| $>$ 1.3, p-value $<$ 0.05) between schizophrenia and control samples. Each column represents the expression level of a gene, and each row represents a sample. The color scale below the heatmap represents the raw Z-score ranging from green to red (low to high expression level). Dendrograms above correspond to the Pearson correlation-based hierarchical clustering of the 250 genes. **(B)** Associated KEGG signaling pathways of the 250 DEGs. The network model generated by Omics Bean illustrates the results of KEGG pathway and biological process enrichment analysis. **(C)** A histogram according to the KEGG functional analysis displaying the percentage of genes affected in these pathways.

This suggested that *FOS* may have some connection with AMPH addiction pathway in schizophrenia samples.

Based on these findings, we constructed PPI networks of FOS to explore the known and predicted proteins interacted with FOS, as well as the underlying pathways using STRING. The STRING database is a biological database and web resource which can be used for exploring the known and predicted interaction networks of a particular protein. Ten gene-encoded proteins (JUN, CREB1, ATF2, JUNB, JUND, MAPK1, MAPK3, MAPK8, MAPK9, and IL2) were in the interaction network of FOS (**Figure 3A**). The edges between FOS and its 10 predicted functional partners represent protein–protein associations. The edges between the proteins do not necessarily imply binding interactions; edges in different colors point to different methods of identifying interactions. Already-known interactions can be found from curated databases or experimental results. Predicted

TABLE 1 | Top 10 differentially expressed genes, either up-regulated or down-regulated.

Gene symbol	Gene	Category	logFC	Fold-change	*P*-value
FOSB	FosB proto-oncogene, AP-1 transcription factor subunit	Protein coding	2.28	4.8567795	0.0005
MMP1	Matrix metallopeptidase 1	Protein coding	1.99	3.97237	<0.0001
FOS	Fos proto-oncogene, AP-1 transcription factor subunit	Protein coding	1.96	3.8906198	0.0007
SNORA38B	Small nucleolar RNA, H/ACA box 38B	RNA	1.37	2.5847057	0.0073
RANBP3L	RAN binding protein 3 like	Protein coding	1.27	2.4116157	0.0092
SNORA68	Small nucleolar RNA, H/ACA box 68	RNA	−1.64	−3.11665832	<0.0001
SNORA23	Small nucleolar RNA, H/ACA box 23	RNA	−1.63	−3.09512999	<0.0001
SNORA20	Small nucleolar RNA, H/ACA box 20	RNA	−1.62	−3.07375036	0.0002
ACTG2	Actin, gamma 2, smooth muscle, enteric	Protein coding	−1.59	−3.01049349	0.0143
SNORA3A	Small nucleolar RNA, H/ACA box 3A	Protein coding	−1.58	−2.9896985	< 0.0001

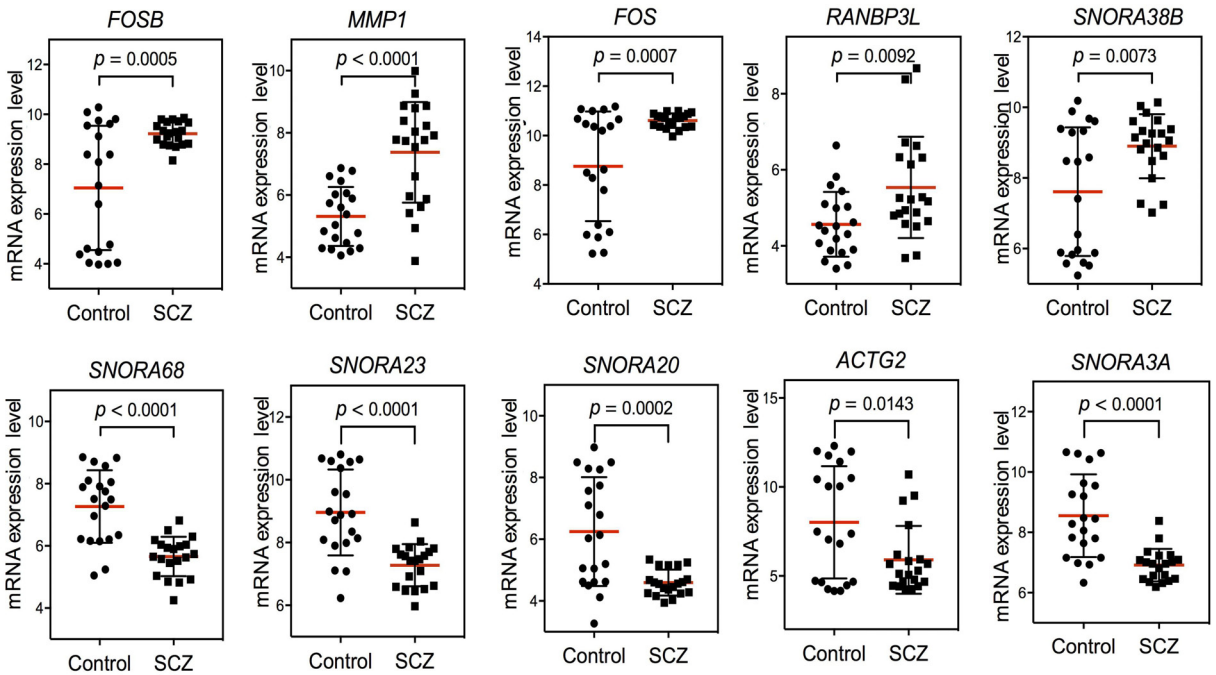

FIGURE 2 | Scatter plot of expression levels of the identified top 10 differentially expressed genes (DEGs) in GEO dataset GSE62333. The top five up-regulated genes (*FOSB*, *MMP1*, *FOS*, *RANBP3L*, and *SNORA38B*) and top five down-regulated genes (*SNORA68*, *SNORA23*, *SNORA20*, *ACTG2*, and *SNORA3A*) were arranged by degree of change. Detailed information on these genes is listed in **Table 1**.

interactions arise from text mining, co-expression, and protein homology. All proteins interacting with FOS were generated from known results from curated databases and experiments. Several interactions were predicted by text mining or co-expression. Further functional enrichment analysis of the protein network in KEGG pathways revealed that FOS protein is involved in the AMPH pathway. Three proteins that interact with FOS protein (JUN, CREB1, and ATF2) were also implicated in the AMPH pathway (**Figure 3B**). Proteins closely interacting with FOS protein were also found to participate in other psychoactive drug pathways, such as cocaine addiction and alcoholism. KEGG functional enrichment analysis of all genes in the network is shown in **Figure 3C**.

Our finding from PPI networks of FOS suggested FOS is tightly related to genes involved in FOS. Therefore, we further explicate the roles of the *FOS* gene and the AMPH pathway in the pathogenesis of schizophrenia. We calculated genes involved in the AMPH pathway from the 1,022 probes with significantly different gene expression levels (using the R package "pheatmap"). Seven genes in the AMPH pathway are shown in the heatmap (**Figure 4A**). To examine the relationship between *FOS* and other genes in the AMPH pathway, we calculated a Spearman correlation of gene expression levels of fold changes using the GSE62333 dataset. The results indicated that *FOS* was positively correlated with other genes in the AMPH pathway, especially *FOSB, JUN, and GRIA3* (**Figure 4B**). Corrgram is a visual display technique to represent the pattern of correlations. To get further understanding the relationship between *FOS* gene and the AMPH pathway, Corrgram was derived according to *r*-value between *FOS* and six genes in the AMPH pathway

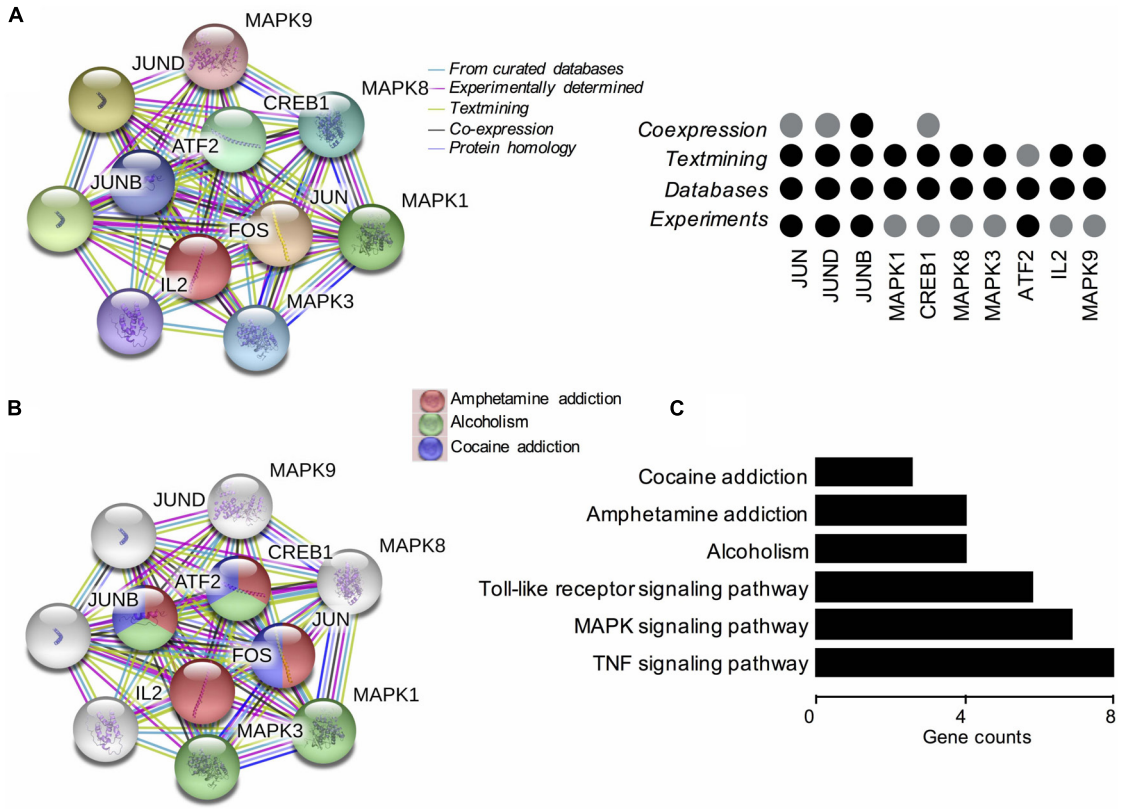

FIGURE 3 | Functional protein–protein network analysis of *FOS* gene using STRING database. **(A)** The protein–protein interaction network of FOS and 10 other proteins. Proteins are presented by network nodes of different colors. The edges between FOS and its predicted functional partners represent protein–protein associations. Categorized identification of protein–protein interactions using different methods are labeled by circles. Already known interactions can be found from curated databases or experimental results. Predicted interactions can come from text mining, co-expression, and protein homology. **(B)** Further functional enrichment analysis of the protein network in KEGG pathways. FOS, JUN, CREB1, and ATF2 are involved in the amphetamine pathway. Proteins closely interacting with FOS protein also participate in other psychoactive drug pathways, such as cocaine addiction and alcoholism. **(C)** KEGG functional enrichment analysis of all genes in the protein–protein interaction network.

(**Figure 4C**). There was a positive correlation between *FOS* and the following genes: *FOSB* (r = 0.73, p = 1.02E-07), *JUN* (r = 0.66, p = 0.000003) *GRIA3* (r = 0.38, p = 0.014374). There was a negative correlation between *FOS* and *CALM3* (r = −0.49, p = 0.001441). There was no correlation between FOS and the following genes: *PRKCA* (r = 0.28, p = 0.076489), *GRIN3A* (r = −0.006, p = 0.966528).

To overcome the limitations of individual studies, we validated our findings in dataset GSE73129. The results showed a significant difference of *FOS* expression between schizophrenia and control lymphoblast samples. No differences were found in other genes involved in the AMPH pathway (**Figure 5A**). The results from two GEO datasets GSE62333 and GSE73129 demonstrated up-regulated expression of *FOS* in fibroblast and lymphoblast samples from schizophrenia patients, which were involved in the AMPH pathway. These non-neural peripheral cells may be useful for studying molecular signatures in psychiatric disorders (Cattane et al., 2015; Horiuchi et al., 2016). Post-mortem brains are also valuable tools to identify molecular alterations in these diseases. To further address the role of *FOS* in schizophrenia pathogenesis, we analyzed human postmortem dorsolateral prefrontal cortex samples and brain tissues of a schizophrenia 22q11-deletion mouse model (Stark et al., 2008; Hagenauer et al., 2016). *FOS* gene expression was significantly down-regulated in CNS tissues, regardless of the source of postmortem tissue (UCDavis or UMichigan) or the region of mouse brain (prefrontal cortex or hippocampus) (**Figures 5B,C**). To measure the predictive value of *FOS* in the datasets we used, ROC curves for FOS expression in schizophrenia samples and control samples were performed. The area under the curve (AUC) is 78.6% and 71.8% in GSE62333 and GSE73129 dataset, respectively. The AUC in GSE92538 is 77.6% (UCDavis) and 79.4% (UMichigan), respectively. The AUC in GSE10784 is 86.0% (prefrontal cortex) and 71.0% (hippocampus), respectively. The highest AUC was observed in the prefrontal cortex samples of GSE10784 dataset. These results suggested that *FOS* is acceptable as a biomarker of schizophrenia. Details were presented in **Figure 6**.

Collectively, our findings revealed that *FOS,* which is involved in the AMPH pathway, is significantly up-regulated in human fibroblast samples and can be validated in peripheral lymphoblast samples. Further analysis showed contrasting expression of *FOS*

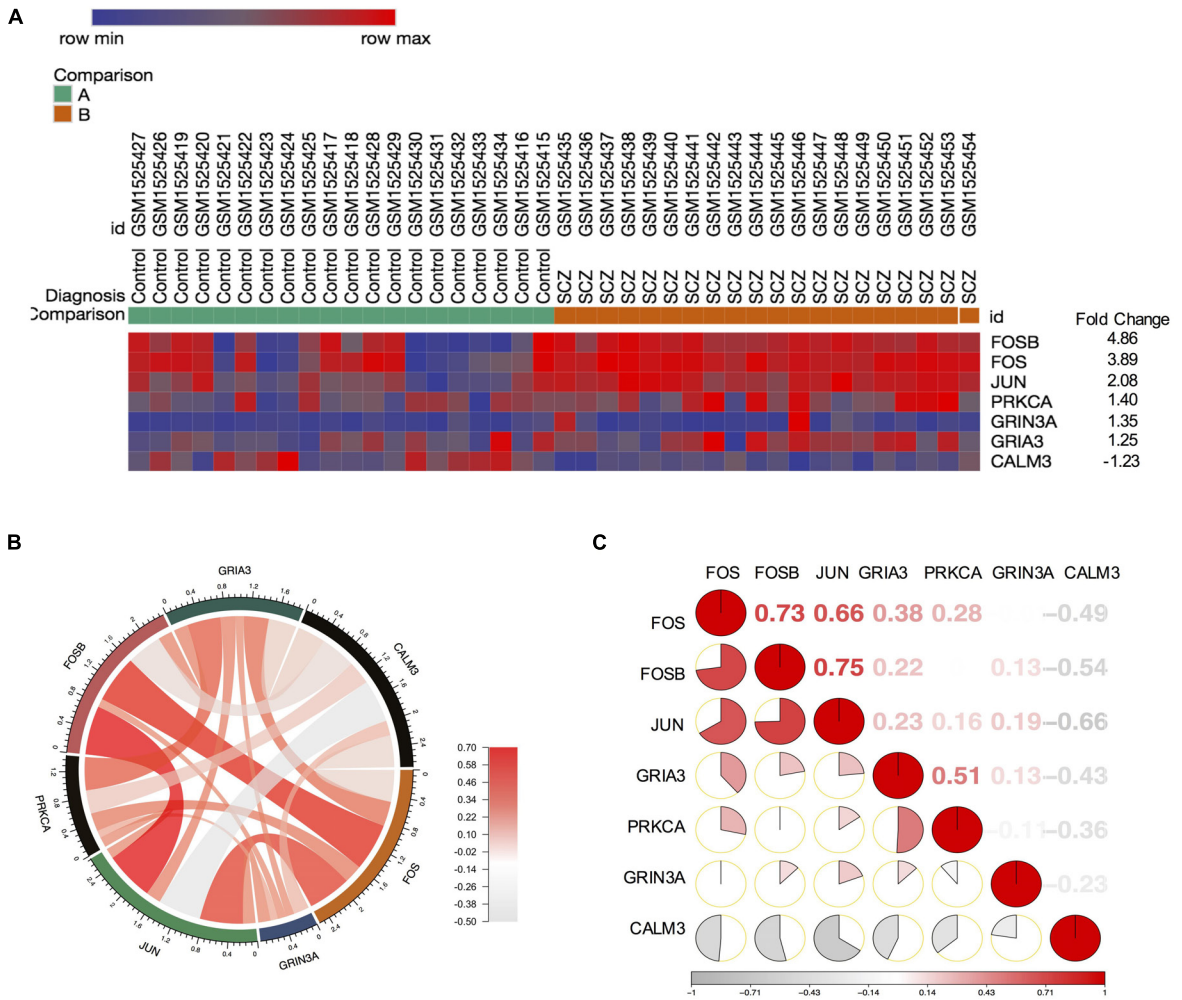

FIGURE 4 | *FOS* was positively correlated with *FOSB*, *JUN*, and *GRIA3* in the amphetamine pathway in GEO dataset GSE62333. Spearman correlation of related gene expression levels of fold changes were calculated for further analysis. **(A)** Heatmap showing genes involved in the amphetamine pathway from 1,022 probes with significantly different gene expression levels (using the R package "pheatmap"). **(B)** Correlation between *FOS* and other genes in the amphetamine pathway (*FOSB*, *JUN*, *PRKCA*, *GRIA3*, *GRIN3A* and *CALM3*). **(C)** Corrgram shows the correlation of *FOS* with other six genes in the amphetamine pathway. The cells of the matrix were shaded to show the correlation value. The correlation *r*-value between FOS and six genes in the amphetamine pathway were *FOSB* (r = 0.73, p = 1.02E-07), *JUN* (r = 0.66, p = 0.000003) *GRIA3* (r = 0.38, p = 0.014374), *PRKCA* (r = 0.28, p = 0.001441), *GRIN3A* (r = –0.006, p = 0.966528), *CALM3* (r = –0.49, p = 0.001441), respectively.

in CNS tissues. *FOS* was down-regulated in human postmortem dorsolateral prefrontal cortex samples and brain tissues of a schizophrenia 22q11-deletion mouse model.

DISCUSSION

In this study, we performed a systematic search on the GEO database for microarray studies of schizophrenia with samples from patients' fibroblasts, lymphoblasts, post-mortem human brains, and brains from a mouse model of schizophrenia. Unlike previous studies, which analyzed peripheral or CNS samples only from schizophrenia patients, we identified *FOS* expression changes in different tissues. Skin fibroblasts, lymphocytes, and lymphoblasts are frequently used in schizophrenia gene expression analysis because of the difficulty in obtaining CNS tissues or cells from schizophrenia patients. Postmortem brains are another good source that help to address this problem. Our study, which analyzed *FOS* gene expression in peripheral and CNS tissues, provides a new window into the molecular changes underlying schizophrenia pathogenesis.

In our analysis, we re-analyzed publicly available microarray gene expression data and obtained different conclusions. A previous study of GEO datasets GSE62333 also reported the up-regulation of *FOSB* and *FOS* in the fibroblasts of schizophrenia patients and mainly focused on *EGR1* and other genes as biomarkers for disease diagnosis (Cattane et al., 2015). Our analysis focused on gene expression changes and related pathways contributing to the pathogenesis of schizophrenia. The analysis of the top 10 DEGs in schizophrenia and healthy

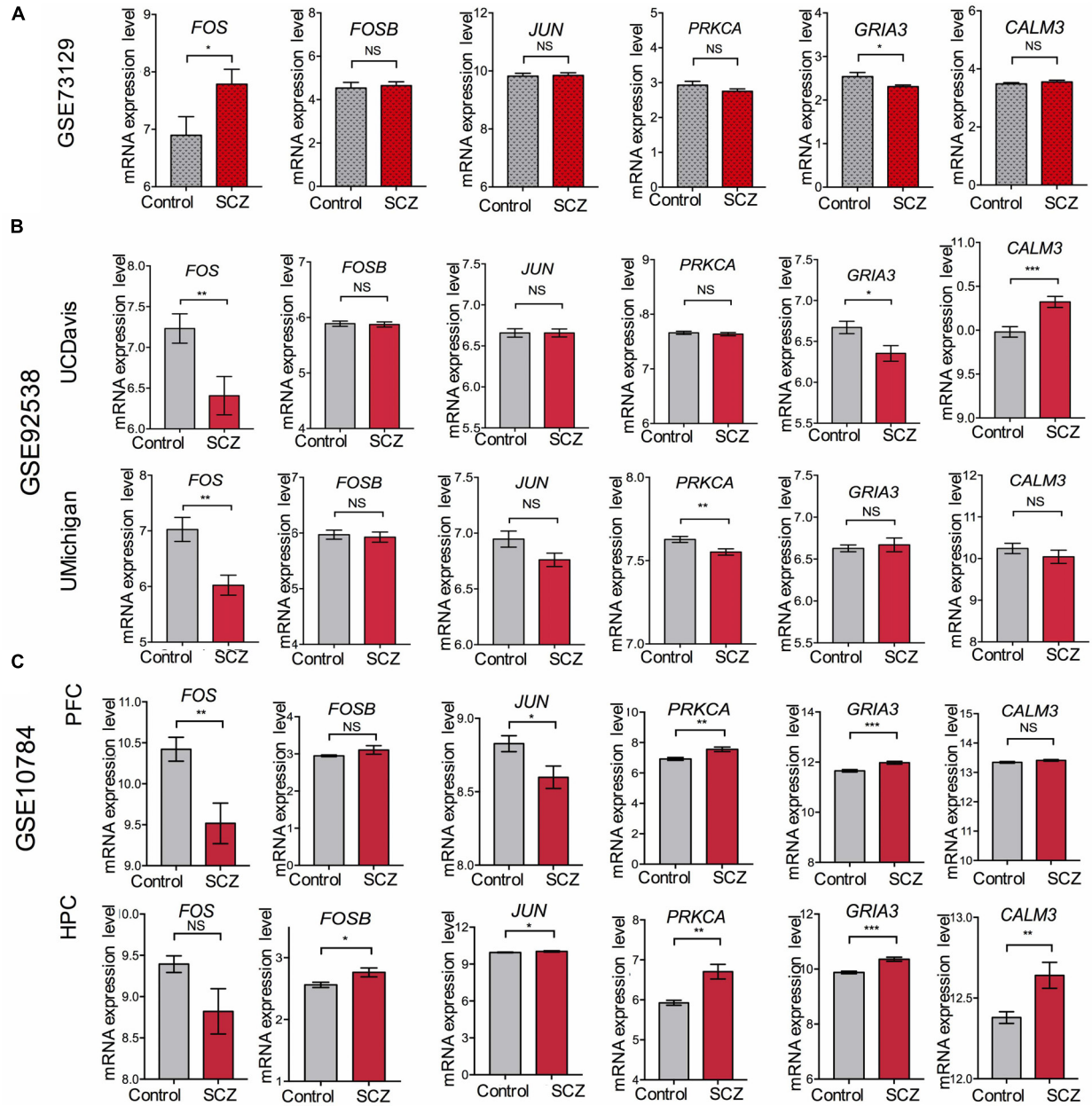

FIGURE 5 | Validation of expression levels of *FOS* and other genes involved in the amphetamine pathway in GEO datasets GSE73129, GSE92538, and GSE10784. The expression of *FOS*, *FOSB*, *JUN*, *PRKCA*, *GRIA3*, and *CALM3* between schizophrenia and control lymphoblast samples have been presented in the histograms. MRNA expression level means the intensity of the detected fluorescence intensity transformed by $\log_2$. NS indicates not significant, * indicates p-value < 0.05, ** indicates p-value < 0.01, ***indicates p-value < 0.001. **(A)** Expression levels of *FOS* and other genes involved in the amphetamine pathway between schizophrenia and control lymphoblast samples in GEO dataset GSE73129. **(B)** Expression levels of *FOS* and other genes involved in the amphetamine pathway in human post-mortem dorsolateral prefrontal cortex samples from UCDavis or UMichigan. Samples were collected from schizophrenia patients and healthy controls. **(C)** *FOS* and other genes involved in the amphetamine pathway expression changes in the prefrontal cortex (PFC) and hippocampus (HPC) of the Df(16)A+/– schizophrenia mouse model.

samples revealed that *FOS* and *FOSB* (which are involved in the AMPH addiction pathway), were significantly up-regulated in schizophrenia fibroblast samples. Protein functional network analysis revealed proteins closely interacting with FOS that were also involved in the AMPH addiction pathway. These findings were consistent with our KEGG enrichment analysis results, which listed "AMPH addiction" as one of the top 10 significantly enriched KEGG pathways. Additionally, Spearman correlation analyzing samples in dataset GSE62333 indicated that *FOS* was positively correlated with *FOSB, JUN, and GRIA3* in the AMPH pathway, and negatively correlated with *CALM3* in the AMPH pathway. Thus, our results support previous findings and reveal

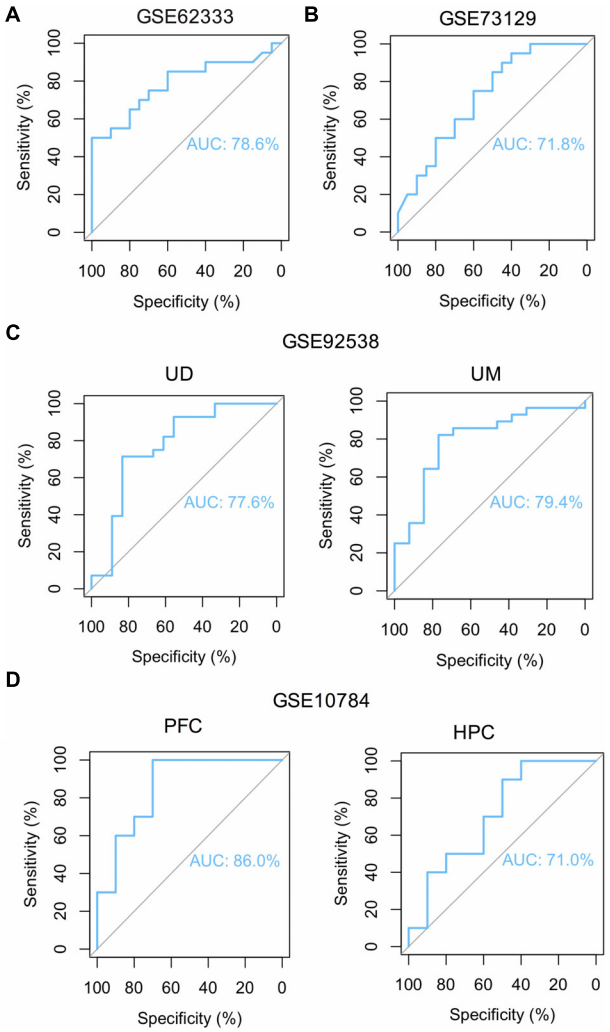

FIGURE 6 | ROC curve analysis reveals the predictive value of *FOS* for schizophrenia patients in different GEO datasets. Area under the curve (AUC) is measured in order to determine the predictive value of the used datasets. **(A)** ROC curve of *FOS* in GEO dataset GSE62333 which analyzed lymphoblast samples from schizophrenia patients and controls ($P < 0.05$). **(B)** ROC curve of *FOS* in GEO dataset GSE73129 which analyzed lymphoblast samples from schizophrenia patients and controls ($P < 0.05$). **(C)** ROC curve of *FOS* in GEO dataset GSE92538 which analyzed human post-mortem dorsolateral prefrontal cortex samples from UCDavis (UD) or UMichigan (UM). Samples were collected from schizophrenia patients and healthy controls ($P < 0.05$). **(D)** ROC curve of *FOS* in GEO dataset GSE10784 which analyzed the prefrontal cortex (PFC) and hippocampus (HPC) samples from the Df(16)A+/– schizophrenia mouse model ($P < 0.05$).

a previously unrecognized pathway connected with *FOS* in the pathogenesis of schizophrenia.

As one of the most studied immediate early genes in the brain, *FOS* is highly expressed in addiction to psychoactive drugs such as AMPH, alcohol, and cocaine (Gallo et al., 2018). It also has been reported to be differentially expressed in schizophrenia samples, either through experimental or expression profiling studies (Zuo et al., 2009; Cattane et al., 2015; Renard et al., 2016; Monfil et al., 2018). Besides, *FOS* is thought to play an important role in the pathophysiology of schizophrenia (Zuo et al., 2009; Renard et al., 2016; Monfil et al., 2018). We observed that *FOS* expression was highly up-regulated in schizophrenia group of dataset GSE62333 which was then validated in another dataset GSE73129. ROC curves indicated fair predictive values of the datasets we analyzed. These combined results suggested FOS is acceptable as a biomarker of schizophrenia. Detection of FOS in blood samples may be helpful for schizophrenia diagnosis. Further exploration using postmortem human brains and 22q11-deletion mouse brain samples suggested that FOS is up-regulated in non-neural peripheral samples and down-regulated in brain tissues of schizophrenia patients compared with those of healthy controls. The alteration of *FOS* expression in peripheral and CNS tissues of schizophrenia indicates that this gene is sensitive for schizophrenia.

Among the top 10 DEGs we detected, five of them (*SNORA38B, SNORA68, SNORA23, SNORA20*, and *SNORA3A*) were non-coding genes. The ratio of non-coding to protein-coding genes is considered a function of developmental complexity. Prokaryotes have less than 25% non-coding DNA, while humans have approximately 98.5% non-coding DNA. RNA-based regulation is devoted to the majority of advances in human genomic programming (Mattick, 2004). Increasing evidence suggests that non-coding RNAs play an important role in neural development and function, and neurological disease progression (Mehler and Mattick, 2006). Although non-coding RNAs such as small nucleolar RNAs (snoRNAs), microRNAs and long non-coding RNAs (LncRNAs), have been studied in disease etiology (Barry, 2014; Lai et al., 2016), the involvement of *SNORA38B*, *SNORA68, SNORA23, SNORA20*, and *SNORA3A* in the pathogenesis of schizophrenia has yet to be reported. However, snoRNAs may play important roles in brain development and neurological disease progression (Pang et al., 2006). Recent studies have indicated that snoRNAs are highly expressed in tumor cells and are involved in cell behavior and oncogenesis (Williams and Farzaneh, 2012; Gong et al., 2017; Zhou et al., 2017).

Five of the top 10 DEGs were protein-coding genes (*RANBP3L, ACTG2, MMP1, FOSB*, and *FOS*). *RANBP3L* is a gene involved in detoxification which mediates bone morphogenetic protein (BMP)-specific nuclear export of SMAD to terminate BMP signaling (Chen et al., 2015). The involvement of *RANBP3L* in schizophrenia has yet to be reported, but exon microarray analysis of human dorsolateral prefrontal cortex revealed up-regulation of this gene in alcoholism (Manzardo et al., 2014). *ACTG2* encodes gamma 2 enteric actin, which is a smooth muscle actin found in enteric tissues and is crucial for enteric muscle contraction (Thorson et al., 2014; Wangler et al., 2014; Matera et al., 2016). *ACTG2* has yet to be associated with schizophrenia. Another actin-coding gene, *ACTG1*, is associated with brain development and hearing loss (Perrin et al., 2010; Park et al., 2013). Matrix metalloproteases (MMPs) are involved in the degradation of basement membrane and extracellular matrix (ECM) components in physiological and pathological processes, such as tissue development, wound healing, and tumor invasiveness (Poola et al., 2005). As a member of the MMP

family, *MMP1* encodes an enzyme that breaks down the ECM, and promotes tumor cell division and metastasis. Studies have shown that activator protein-1 (AP-1) genes *FOS* and *JUN* can regulate *MMP1* gene expression in invasive tumors (Poola et al., 2005; Uhlirova and Bohmann, 2006; Baker et al., 2018). MMP-mediated ECM disruption is also involved in the pathogenesis of schizophrenia. MMP modulators may therefore be a potential therapeutic target for the treatment of schizophrenia (Chopra et al., 2015). Besides, FOS proteins can dimerize with JUN proteins to form the transcription factor complex AP-1, which regulates cell proliferation, differentiation, and transformation (Milde-Langosch, 2005). Few studies have reported functions of *FOSB* in the CNS. However, a truncated splice variant of *FOSB* named *Delta-FOSB* is involved in behavior and addiction to drugs (Nestler, 2008; Ruffle, 2014). *FOS* was up-regulated in schizophrenia samples and is a recognized marker of neural activation (Gallo et al., 2018).

There are several limitations in our study. First, the gene expression profiles could be affected by many factors, such as differences in methodology and/or sample preparation, patient characteristics, platform, and data analysis (Sullivan et al., 2006; Mistry and Pavlidis, 2010; Kumarasinghe et al., 2012; Mistry et al., 2013). Studies on schizophrenia are often associated with small sample sizes which may result in low statistical power. Second, several studies reported that peripheral cells may not reflect the gene expression profile of the human brain. Furthermore, using postmortem brains to understand dynamic changes in disease progression and development of complications is challenging (Rollins et al., 2010; Tylee et al., 2013; Cattane et al., 2015; Horiuchi et al., 2016). Finally, confirmatory experiments and comparison of results with microarray gene expression modifications from re-analysis will enable validation of our results.

CONCLUSION

To conclude, our results indicate that *FOS* was significantly up-regulated in schizophrenia fibroblast and lymphoblast samples. Exploration of *FOS* gene expression in CNS tissues revealed that this gene was largely down-regulated in datasets GSE92538 and GSE10784. The signatures we identified are consistent with current hypotheses of molecular dysfunction in schizophrenia, including alteration of the *FOS* gene and involvement of the AMPH addiction pathway. *FOS* and AMPH-related genes may thus represent novel biomarkers for diagnosis of schizophrenia in clinical practice.

AUTHOR CONTRIBUTIONS

JH and FL performed data extraction and prepared the manuscript. BW, HT, and ZT reviewed the literature and performed the quality assessment. YQ and LL reviewed the revised manuscript and checked the grammars. HW and JC supervised all the work.

FUNDING

This work was supported by the National Natural Science Foundation of China (81270019) and National Science Foundation for Young Scientists of China (81501163). The funders had no involvement in any aspect of this study or manuscript preparation.

ACKNOWLEDGMENTS

The authors would like to thank the reviewers for their valuable comments and suggestions to improve the quality of the paper.

SUPPLEMENTARY MATERIAL

The Supplementary Material for this article can be found online at: https://www.frontiersin.org/articles/10.3389/fgene.2019.00232/full#supplementary-material

FIGURE S1 | Flowchart showing the identification and selection of microarray studies from Gene Expression Omnibus (GEO) and the data analysis procedure.

FIGURE S2 | Transcriptomic analysis via principle component analysis including control and SCZ samples in GEO dataset GSE62333 using top 10 differentially expressed genes.

REFERENCES

Baker, J., Falconer, A. M. D., Wilkinson, D. J., Europe-Finner, G. N., Litherland, G. J., and Rowan, A. D. (2018). Protein kinase D3 modulates MMP1 and MMP13 expression in human chondrocytes. *PLoS One* 13:e0195864. doi: 10.1371/journal.pone.0195864

Barry, G. (2014). Integrating the roles of long and small non-coding RNA in brain function and disease. *Mol. Psychiatry* 19, 410–416. doi: 10.1038/mp.2013.196

Cattane, N., Minelli, A., Milanesi, E., Maj, C., Bignotti, S., Bortolomasi, M., et al. (2015). Altered gene expression in schizophrenia: findings from transcriptional signatures in fibroblasts and blood. *PLoS One* 10:e0116686. doi: 10.1371/journal.pone.0116686

Chen, F., Lin, X., Xu, P., Zhang, Z., Chen, Y., Wang, C., et al. (2015). Nuclear export of smads by RanBP3L regulates bone morphogenetic protein signaling and mesenchymal stem cell differentiation. *Mol. Cell Biol.* 35, 1700–1711. doi: 10.1128/MCB.00121-15

Chopra, K., Baveja, A., and Kuhad, A. (2015). MMPs: a novel drug target for schizophrenia. *Expert. Opin. Ther. Targets* 19, 77–85. doi: 10.1517/14728222.2014.957672

de Bartolomeis, A., Latte, G., Tomasetti, C., and Iasevoli, F. (2014). Glutamatergic postsynaptic density protein dysfunctions in synaptic plasticity and dendritic spines morphology: relevance to schizophrenia and other behavioral disorders pathophysiology, and implications for novel therapeutic approaches. *Mol. Neurobiol.* 49, 484–511. doi: 10.1007/s12035-013-8534-3

Gallo, F. T., Katche, C., Morici, J. F., Medina, J. H., and Weisstaub, N. V. (2018). Immediate early genes, memory and psychiatric disorders: focus on c-Fos, Egr1 and Arc. *Front. Behav. Neurosci.* 12:79. doi: 10.3389/fnbeh.2018.00079

Gautier, L., Cope, L., Bolstad, B. M., and Irizarry, R. A. (2004). Affy analysis of Affymetrix GeneChip data at the probe level. *Bioinformatics* 20, 307–315. doi: 10.1093/bioinformatics/btg405

Goff, D. C., Falkai, P., Fleischhacker, W. W., Girgis, R. R., Kahn, R. M., Uchida, H., et al. (2017). The long-term effects of antipsychotic medication on clinical course in schizophrenia. *Am. J. Psychiatry* 174, 840–849. doi: 10.1176/appi.ajp.2017.16091016

Gong, J., Li, Y., Liu, C. J., Xiang, Y., Li, C., Ye, Y., et al. (2017). A pan-cancer analysis of the expression and clinical relevance of small nucleolar RNAs in human cancer. *Cell Rep.* 21, 1968–1981. doi: 10.1016/j.celrep.2017.10.070

Gu, Z., Gu, L., Eils, R., Schlesner, M., and Brors, B. (2014). circlize implements and enhances circular visualization in R. *Bioinformatics* 30, 2811–2812. doi: 10.1093/bioinformatics/btu393

Hagenauer, M. H., Schulmann, A., Li, J. Z., Vawter, M. P., Walsh, D. M., Thompson, R. C., et al. (2018). Inference of cell type content from human brain transcriptomic datasets illuminates the effects of age, manner of death, dissection, and psychiatric diagnosis. *PLoS ONE* 13:e0200003. doi: 10.1371/journal.pone.0200003

Hall, J., Trent, S., Thomas, K. L., O'Donovan, M. C., and Owen, M. J. (2015). Genetic risk for schizophrenia: convergence on synaptic pathways involved in plasticity. *Biol. Psychiatry* 77, 52–58. doi: 10.1016/j.biopsych.2014.07.011

Heyes, S., Pratt, W. S., Rees, E., Dahimene, S., Ferron, L., Owen, M. J., et al. (2015). Genetic disruption of voltage-gated calcium channels in psychiatric and neurological disorders. *Prog. Neurobiol.* 134, 36–54. doi: 10.1016/j.pneurobio.2015.09.002

Horiuchi, Y., Kondo, M. A., Okada, K., Takayanagi, Y., Tanaka, T., Ho, T., et al. (2016). Molecular signatures associated with cognitive deficits in schizophrenia: a study of biopsied olfactory neural epithelium. *Transl. Psychiatry* 6:e915. doi: 10.1038/tp.2016.154

Howes, O. D., and Murray, R. M. (2014). Schizophrenia: an integrated sociodevelopmental-cognitive model. *Lancet* 383, 1677–1687. doi: 10.1016/S0140-6736(13)62036-X

Karam, C. S., Ballon, J. S., Bivens, N. M., Freyberg, Z., Girgis, R. R., Lizardi-Ortiz, J. E., et al. (2010). Signaling pathways in schizophrenia: emerging targets and therapeutic strategies. *Trends Pharmacol. Sci.* 31, 381–390. doi: 10.1016/j.tips.2010.05.004

Kumarasinghe, N., Tooney, P. A., and Schall, U. (2012). Finding the needle in the haystack: a review of microarray gene expression research into schizophrenia. *Aust. N. Z. J. Psychiatry* 46, 598–610. doi: 10.1177/0004867412442405

Lai, C. Y., Lee, S. Y., Scarr, E., Yu, Y. H., Lin, Y. T., Liu, C. M., et al. (2016). Aberrant expression of microRNAs as biomarker for schizophrenia: from acute state to partial remission, and from peripheral blood to cortical tissue. *Transl. Psychiatry* 6:e717. doi: 10.1038/tp.2015.213

Lewis, D. A., Curley, A. A., Glausier, J. R., and Volk, D. W. (2012). Cortical parvalbumin interneurons and cognitive dysfunction in schizophrenia. *Trends Neurosci.* 35, 57–67. doi: 10.1016/j.tins.2011.10.004

Manzardo, A. M., Gunewardena, S., Wang, K., and Butler, M. G. (2014). Exon microarray analysis of human dorsolateral prefrontal cortex in alcoholism. *Alcohol. Clin. Exp. Res.* 38, 1594–1601. doi: 10.1111/acer.12429

Matera, I., Rusmini, M., Guo, Y., Lerone, M., Li, J., Zhang, J., et al. (2016). Variants of the ACTG2 gene correlate with degree of severity and presence of megacystis in chronic intestinal pseudo-obstruction. *Eur. J. Hum. Genet.* 24, 1211–1215. doi: 10.1038/ejhg.2015.275

Mattick, J. S. (2004). RNA regulation: a new genetics? *Nat. Rev. Genet.* 5, 316–323. doi: 10.1038/nrg1321

McGrath, J., Saha, S., Chant, D., and Welham, J. (2008). Schizophrenia: a concise overview of incidence, prevalence, and mortality. *Epidemiol. Rev.* 30, 67–76. doi: 10.1093/epirev/mxn001

Mehler, M. F., and Mattick, J. S. (2006). Non-coding RNAs in the nervous system. *J. Physiol.* 575, 333–341. doi: 10.1113/jphysiol.2006.113191

Milde-Langosch, K. (2005). The Fos family of transcription factors and their role in tumourigenesis. *Eur. J. Cancer* 41, 2449–2461. doi: 10.1016/j.ejca.2005.08.008

Mistry, M., Gillis, J., and Pavlidis, P. (2013). Genome-wide expression profiling of schizophrenia using a large combined cohort. *Mol. Psychiatry* 18, 215–225. doi: 10.1038/mp.2011.172

Mistry, M., and Pavlidis, P. (2010). A cross-laboratory comparison of expression profiling data from normal human postmortem brain. *Neuroscience* 167, 384–395. doi: 10.1016/j.neuroscience.2010.01.016

Monfil, T., Vazquez Roque, R. A., Camacho-Abrego, I., Tendilla-Beltran, H., Iannitti, T., Meneses-Morales, I., et al. (2018). Hyper-response to novelty increases c-Fos expression in the hippocampus and prefrontal cortex in a rat model of Schizophrenia. *Neurochem. Res.* 43, 441–448. doi: 10.1007/s11064-017-2439-x

Mouchlianitis, E., McCutcheon, R., and Howes, O. D. (2016). Brain-imaging studies of treatment-resistant schizophrenia: a systematic review. *Lancet Psychiatry* 3, 451–463. doi: 10.1016/S2215-0366(15)00540-4

Nestler, E. J. (2008). Review. Transcriptional mechanisms of addiction: role of DeltaFosB. *Philos. Trans. R. Soc. Lond. B Biol. Sci.* 363, 3245–3255. doi: 10.1098/rstb.2008.0067

Network, T., O'Dushlaine, C., Rossin, L., Lee, P. H., Duncan, L., Parikshak, N. N., et al. (2015). Psychiatric genome-wide association study analyses implicate neuronal, immune and histone pathways. *Nat. Neurosci.* 18:199. doi: 10.1038/nn.3922

Pang, K. C., Frith, M. C., and Mattick, J. S. (2006). Rapid evolution of noncoding RNAs: lack of conservation does not mean lack of function. *Trends Genet.* 22, 1–5. doi: 10.1016/j.tig.2005.10.003

Park, G., Gim, J., Kim, A. R., Han, K. H., Kim, H. S., Oh, S. H., et al. (2013). Multiphasic analysis of whole exome sequencing data identifies a novel mutation of ACTG1 in a nonsyndromic hearing loss family. *BMC Genomics* 14:191. doi: 10.1186/1471-2164-14-191

Pedrazzi, J. F., Issy, A. C., Gomes, F. V., Guimaraes, F. S., and Del-Bel, E. A. (2015). Cannabidiol effects in the prepulse inhibition disruption induced by amphetamine. *Psychopharmacology* 232, 3057–3065. doi: 10.1007/s00213-015-3945-7

Perrin, B. J., Sonnemann, K. J., and Ervasti, J. M. (2010). beta-actin and gamma-actin are each dispensable for auditory hair cell development but required for Stereocilia maintenance. *PLoS Genet.* 6:e1001158. doi: 10.1371/journal.pgen.1001158

Poola, I., DeWitty, R. L., Marshalleck, J. J., Bhatnagar, R., Abraham, J., and Leffall, L. D. (2005). Identification of MMP-1 as a putative breast cancer predictive marker by global gene expression analysis. *Nat. Med.* 11, 481–483. doi: 10.1038/nm1243

Quadrato, G., Brown, J., and Arlotta, P. (2016). The promises and challenges of human brain organoids as models of neuropsychiatric disease. *Nat. Med.* 22, 1220–1228. doi: 10.1038/nm.4214

Renard, J., Loureiro, M., Rosen, L. G., Zunder, J., de Oliveira, C., Schmid, S., et al. (2016). Cannabidiol counteracts amphetamine-induced neuronal and behavioral sensitization of the mesolimbic dopamine pathway through a Novel mTOR/p70S6 kinase signaling pathway. *J. Neurosci.* 36, 5160–5169. doi: 10.1523/JNEUROSCI.3387-15.2016

Robin, X., Turck, N., Hainard, A., Tiberti, N., Lisacek, F., Sanchez, J.-C., et al. (2011). pROC: an open-source package for R and S+ to analyze and compare ROC curves. *BMC Bioinformatics* 12:77. doi: 10.1186/1471-2105-12-77

Rollins, B., Martin, M. V., Morgan, L., and Vawter, M. P. (2010). Analysis of whole genome biomarker expression in blood and brain. *Am. J. Med. Genet. B. Neuropsychiatr. Genet.* 153B, 919–936. doi: 10.1002/ajmg.b.31062

Ruffle, J. K. (2014). Molecular neurobiology of addiction: what's all the (Delta)FosB about? *Am. J. Drug Alcohol. Abuse* 40, 428–437. doi: 10.3109/00952990.2014.933840

Stark, K. L., Xu, B., Bagchi, A., Lai, W. S., Liu, H., Hsu, R., et al. (2008). Altered brain microRNA biogenesis contributes to phenotypic deficits in a 22q11-deletion mouse model. *Nat. Genet.* 40, 751–760. doi: 10.1038/ng.138

Sullivan, P. F., Fan, C., and Perou, C. M. (2006). Evaluating the comparability of gene expression in blood and brain. *Am. J. Med. Genet. B Neuropsychiatr. Genet.* 141B, 261–268. doi: 10.1002/ajmg.b.30272

Thorson, W., Diaz-Horta, O., Foster, J. II, Spiliopoulos, M., Quintero, R., Farooq, A., et al. (2014). De novo ACTG2 mutations cause congenital distended bladder, microcolon, and intestinal hypoperistalsis. *Hum. Genet.* 133, 737–742. doi: 10.1007/s00439-013-1406-0

Tylee, D. S., Kawaguchi, D. M., and Glatt, S. J. (2013). On the outside, looking in: a review and evaluation of the comparability of blood and brain "-omes". *Am. J. Med. Genet. B Neuropsychiatr. Genet.* 162B, 595–603. doi: 10.1002/ajmg.b.32150

Uhlirova, M., and Bohmann, D. (2006). JNK- and Fos-regulated Mmp1 expression cooperates with Ras to induce invasive tumors in Drosophila. *EMBO J.* 25, 5294–5304. doi: 10.1038/sj.emboj.7601401

Van Winkel, R., Esquivel, G., Kenis, G., Wichers, M., Collip, D., Peerbooms, O., et al. (2010). REVIEW: Genome-wide findings in schizophrenia and the role of gene-environment interplay. *CNS Neurosci. Ther.* 16, e185–e192. doi: 10.1111/j.1755-5949.2010.00155.x

Wangler, M. F., Gonzaga-Jauregui, C., Gambin, T., Penney, S., Moss, T., Chopra, A., et al. (2014). Heterozygous de novo and inherited mutations in the smooth muscle actin (ACTG2) gene underlie megacystis-microcolon-intestinal hypoperistalsis syndrome. *PLoS Genet.* 10:e1004258. doi: 10.1371/journal.pgen.1004258

Williams, G. T., and Farzaneh, F. (2012). Are snoRNAs and snoRNA host genes new players in cancer? *Nat. Rev. Cancer* 12, 84–88. doi: 10.1038/nrc3195

Zhou, F., Liu, Y., Rohde, C., Pauli, C., Gerloff, D., Kohn, M., et al. (2017). AML1-ETO requires enhanced C/D box snoRNA/RNP formation to induce self-renewal and leukaemia. *Nat. Cell Biol.* 19, 844–855. doi: 10.1038/ncb3563

Zuo, D. Y., Cao, Y., Zhang, L., Wang, H. F., and Wu, Y. L. (2009). Effects of acute and chronic administration of MK-801 on c-Fos protein expression in mice brain regions implicated in schizophrenia with or without clozapine. *Prog. Neuropsychopharmacol. Biol. Psychiatry* 33, 290–295. doi: 10.1016/j.pnpbp.2008.12.002

Conflict of Interest Statement: The authors declare that the research was conducted in the absence of any commercial or financial relationships that could be construed as a potential conflict of interest.

frontiers in Pharmacology

ORIGINAL RESEARCH
published: 02 April 2019
doi: 10.3389/fphar.2019.00318

The Involvement of Renin-Angiotensin System in Lipopolysaccharide-Induced Behavioral Changes, Neuroinflammation, and Disturbed Insulin Signaling

Xiaoxue Gong[1†], Hui Hu[2†], Yi Qiao[3], Pengfei Xu[1], Mengqi Yang[1], Ruili Dang[1], Wenxiu Han[1], Yujin Guo[1], Dan Chen[1] and Pei Jiang[1]*

[1] Institute of Clinical Pharmacy and Pharmacology, Jining First People's Hospital, Jining Medical University, Jining, China, [2] Department of Cardiology, Jining First People's Hospital, Jining Medical University, Jining, China, [3] Department of Public Health, Jining Medical University, Jining, China

OPEN ACCESS

Edited by:
Rodrigo Pacheco,
Fundación Ciencia and Vida, Chile

Reviewed by:
Cristián A. Amador,
Universidad Autónoma de Chile, Chile
Andres Herrada,
Universidad Autónoma de Chile, Chile

***Correspondence:**
Pei Jiang
jiangpeicsu@sina.com

[†] These authors have contributed equally to this work

Specialty section:
This article was submitted to Neuropharmacology, a section of the journal Frontiers in Pharmacology

Received: 28 November 2018
Accepted: 15 March 2019
Published: 02 April 2019

Citation:
Gong X, Hu H, Qiao Y, Xu P, Yang M, Dang R, Han W, Guo Y, Chen D and Jiang P (2019) The Involvement of Renin-Angiotensin System in Lipopolysaccharide-Induced Behavioral Changes, Neuroinflammation, and Disturbed Insulin Signaling. Front. Pharmacol. 10:318. doi: 10.3389/fphar.2019.00318

Brain insulin signaling is accounted for the development of a variety of neuropsychiatric disorders, such as anxiety and depression, whereas both inflammation and the activated renin-angiotensin system (RAS) are two major contributors to insulin resistance. Intriguingly, inflammation and RAS can activate each other, forming a positive feedback loop that would result in exacerbated unwanted tissue damage. To further examine the interrelationship among insulin signaling, neuroinflammation and RAS in the brain, the effect of repeated lipopolysaccharide (LPS) exposure and co-treatment with the angiotensin II (Ang II) receptor type 1 (AT1) blocker, candesartan (Cand), on anxiety and depression-like behaviors, RAS, neuroinflammation and insulin signaling was explored. Our results demonstrated that prolonged LPS challenge successfully induced the rats into anxiety and depression-like state, accompanied with significant neural apoptosis and neuroinflammation. LPS also activated RAS as evidenced by the enhanced angiotensin converting enzyme (ACE) expression, Ang II generation and AT1 expression. However, blocking the activated RAS with Cand co-treatment conferred neurobehavioral protective properties. The AT1 blocker markedly ameliorated the microglial activation, the enhanced gene expression of the proinflammatory cytokines and the overactivated NF-κB signaling. In addition, Cand also mitigated the LPS-induced disturbance of insulin signaling with the normalized phosphorylation of serine 307 and tyrosine 896 of insulin receptor substrate-1 (IRS-1). Collectively, the present study, for the first time, provided the direct evidence indicating that the inflammatory condition may interact with RAS to impede brain insulin pathway, resulting in neurobehavioral damage, and inhibiting RAS seems to be a promising strategy to block the cross-talk and cut off the vicious cycle between RAS and immune system.

Keywords: lipopolysaccharide, depression, renin-angiotensin system, inflammation, insulin pathway

INTRODUCTION

Renin-angiotensin system (RAS) is originally acknowledged for its role in the regulation of blood pressure, but now it is generally accepted that brain has its intrinsic RAS with the major components, including angiotensin converting enzyme (ACE) and angiotensin II (Ang II) receptor type 1 (AT1), widely distributed in the central nervous system (Haspula and Clark, 2018; Uijl et al., 2018). The brain RAS actively participates in various neurological functions, including cognition, memory, emotion and stress response, and RAS over-activation has been identified in several neuropsychiatric disorders, including Alzheimer's disease, epilepsy and depression (Yagi et al., 2013; Gebre et al., 2018). Intriguingly, these disorders are also frequently characterized with neurodegeneration, inflammation and brain insulin resistance. In this context, the interrelationship between RAS and these neuropathological progresses is attracting increasing attention, since Ang II is recognized as a pleiotropic factor locally metabolized in the brain (Saavedra, 2017).

It has been demonstrated that RAS stimulation mediates oxidative and inflammatory damage in the liver, the pancreas, the kidney and the brain (Capettini et al., 2012; Gaddam et al., 2014; Biancardi et al., 2017). By binding to AT1, Ang II also induces disturbed glucose metabolism and insulin resistance in the liver, adipocyte and pancreas (Favre et al., 2015). On the other hand, interference with RAS using either ACE inhibitors (ACEIs) or AT1 blockers confers protective effects against excessive inflammatory activation and improves insulin sensitivity (Luther and Brown, 2011; Favre et al., 2015). Despite the consensus that neuroinflammation and insulin resistance are two hallmarks of neuropathy, in both of which RAS plays an essential role, the evidence concerning intricate interrelationship among RAS, immune system and insulin signaling is limited and controversial, especially in the brain.

Therefore, in this study, we used repeated treatment of the endotoxin, lipopolysaccharide (LPS), to provoke sustained neuroinflammation, and explored the potential beneficial effects of AT1 receptor blocker, candesartan (Cand), treatment on LPS-induced abnormalities in behavioral changes, neuroimmune activation, and insulin signaling.

MATERIALS AND METHODS

Animals

Male, Sprague-Dawley rats (200–230 g) were housed under standard conditions of temperature (23 ± 2°) and light (12:12 h light/dark cycle), with free access to standard rodent chow and water. Each rat was housed in a separate cage and recorded with body weight daily. All animal use procedures were carried out in accordance with the Regulations of Experimental Animal Administration issued by the State Committee of Science and Technology of the People's Republic of China, with the approval of the Animal Ethics Committee of the Jining Medical University (NO. 20170037).

Drug Treatment

Rats were randomly divided into three groups: Control, LPS and LPS+Cand. Rats received LPS or normal saline via intraperitoneal injection at a dose of 500 μg/kg every 2 days for a total of 7 injections. The dose of LPS was chosen to effectively provoke depressive-like behaviors and neuroinflammation based on our previous research (Jiang et al., 2017; Yang et al., 2018). Animals in LPS+Cand group received daily Cand (1 mg/kg, dissolved in 1% DMSO) by oral gavage over 2 weeks covering the whole LPS treatment process, while the other two groups were treated with the vehicle (1% DMSO in saline). The timeline of the experimental protocol is depicted in **Figure 1A**. The dose of Cand was selected based the previous finding that at this dose, Cand effectively blocks central AT1 receptors (Benicky et al., 2011; de Souza Gomes et al., 2015). Body weight of these rats was monitored throughout the experiment, and the drug doses were adjusted accordingly.

Behavioral Tests

Elevated Plus Maze (EPM) Test

EPM test was performed to evaluate the LPS-induced anxiety-like behavior in rats. In brief, the maze apparatus was a cross-shaped Plexiglas platform with two opposite open arms (OA, 50 × 10 cm) and two opposite closed arms (CA, 50 × 10 cm) with 40 cm walls, connected by a central platform (CP, 10 × 10 cm) and elevated 50 cm from the floor in a dimly lit room. The animals were placed at the center of the apparatus with its head facing toward an open arm. The total number of entries into the open and closed arms, and the time spent in each arm during the 5 min period were recorded with a video camera mounted vertically above the apparatus.

Forced Swim Test (FST)

The paradigm is based upon the evaluation of immobility, as a measure of behavioral despair in stressful and inescapable situations (Liao et al., 2018). In brief, each rat was placed in a Plexiglas cylinder (45 cm height, 25 cm diameter) containing approximately 35 cm of water (24 ± 1°) for 15 min. The rats were then dried and removed to their home cage. They were placed again in the cylinders 24 h later, and a 5 min swim test was conducted. Each test session was videotaped and the duration of immobility, which is defined as floating passively and only making slight movements to keep the head above water, was scored by an experienced observer blind to the experimental design.

Novelty-Suppressed Feeding Test (NSFT)

Before testing, rats were food deprived for 24 h in their home cages. The rats were placed in an open field (75 × 75 × 40 cm) with a small amount of food placed on a piece of white paper (10 × 10 cm) in the center. Animals were allowed to explore the open field for 8 min. The latency to feed, specifically the time it took for the rat to approach and take the first bite of the food, was recorded by a stopwatch.

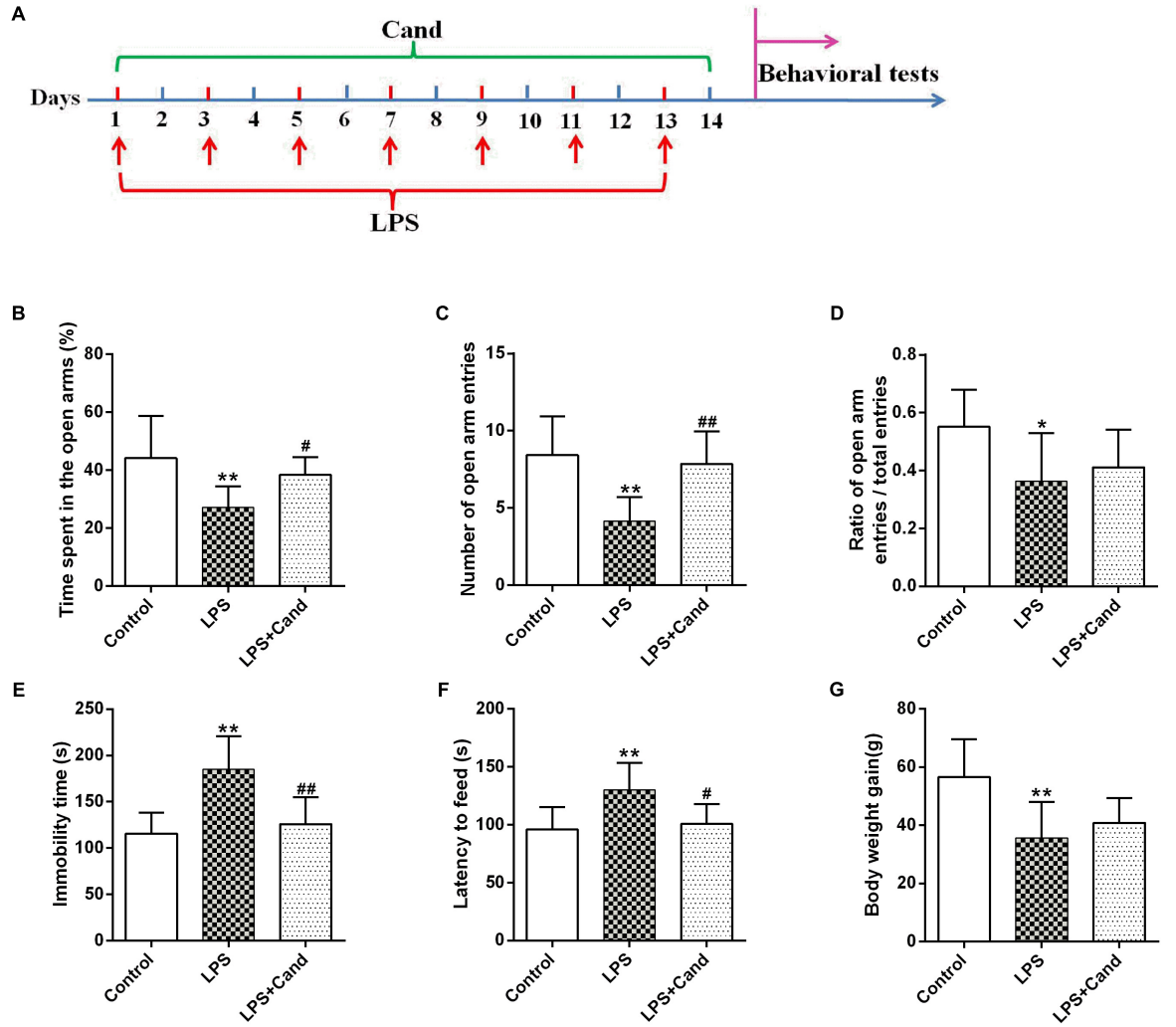

FIGURE 1 | Timeline of experimental procedures **(A)** and effect of Candesartan (Cand) treatment on LPS-induced behavioral deficits in elevated plus maze (EPM) test **(B–D)**, forced swim test (FST) **(E)** and novelty-suppressed feeding test (NSFT) **(F)**, and body weight gain **(G)**. Data are means ± SD (n = 7–9). $^{*}p < 0.05$, $^{**}p < 0.01$ compared to Control group. $^{\#}p < 0.05$, $^{\#\#}p < 0.01$ compared to LPS group.

Histopathological Staining

Brains were collected and the hippocampus was rapidly dissected from representative animals in each group. The hippocampus was fixed in 10% phosphate-buffered paraformaldehyde and then embedded in paraffin, prepared for histopathological examination and immunohistochemical staining. The paraffin tissue blocks were prepared for sectioning at 5μm thickness by sledge microtome. The obtained tissue sections were stained by hematoxylin and eosin (H&E). The number of damaged cells characterized by contraction of the nucleus, cellular edema, vacuolization, and darkened nucleus, were counted. The presence of apoptosis was assessed by the terminal deoxynucleotidyl transferase-mediated FITC-dUTP nick end labeling (Tunel) method, which detects fragmentation of DNA in the nucleus during apoptotic cell death *in situ* (Zhou et al., 2018), following the manufacturer's protocol (Keygen Biotech, Nanjing, China). The average ratio of total TUNEL-positive neurocyte number was calculated. This ratio represented the apoptotic index of the sample and was compared between groups.

Immunofluorescent Staining

For the immunofluorescent histochemistry analysis, paraffin-embedded coronal sections of the hippocampus (6 μm thickness) were dewaxed in xylol, rehydrated, and rinsed in phosphate-buffered saline (PBS). Antigen retrieval was performed by boiling the sections on an electric stove in a citric acid buffer (0.01 mol/L, pH 6.0), followed by incubation with blocking 5% goat serum for 1 h at room temperature. The sections were then incubated with the primary antibody anti-IBA-1 (Abcam, 1:200). The sections were washed with PBS three times and stained with DAPI (Beyotime Biotechnology, China) to stain the cell nuclei. Immunofluorescent images were taken with an inverted fluorescence microscope (Olympus, Japan).

Ang II Analysis

The hippocampus was homogenized and centrifuged at 9500 rpm for 20 min at 4°C. The supernatant was used for the measurement of Ang II by using a commercially available Enzyme-Linked Immunosorbent Assay (ELISA) kit (Cusabio, China).

Real-Time PCR Analysis

Total RNA was extracted by using Trizol reagent (invitrogen, United States) following the manufacturer's instructions. Quantitative PCR was performed on Bio-rad Cx96 Detection System (Bio-rad, United States) using SYBR green PCR kit (Applied Bio-systems, United States) and gene-specific primers (**Table 1**). Each cDNA was tested in triplicate. Thermo profile conditions were: 50°C for 2 min, 95°C for 10 min, 40 cycles of amplification at 95°C for 15 s and 60°C for 1 min. Relative quantitation for PCR product was normalized to β-actin as an internal standard.

Western Blot Analysis

For western blotting analysis, total protein was prepared from the right hippocampus, and the protein concentrations were analyzed using Bradford method. Samples were loaded on precast 12% SDS-PAGE gels with approximately 50 μg protein in each lane. The following antibodies and concentrations were used over night at 4°C; p-IKKβ (Ser177) (Cell signaling, 1:1000), IKKβ (Cell signaling, 1:1000), IκB (Cell signaling, 1:1000), P65 (Cell signaling, 1:1000), IRβ (Abcam, 1:1000), p-IRS (Ser307) (Sigma-Aldrich, 1:1000), p-IRS (Tyr896) (Abcam, 1:1000), IRS (Abcam, 1:500), and β-actin (Proteintech, 66009-1-Ig; 1:4000). It was then probed with HRP-conjugated secondary antibody for 40 min. The film signals were digitally scanned and then quantified using Image J software. The signals were normalized to β-actin as an internal standard. Original images of Western blot are supplied in **Supplementary Material**.

TABLE 1 | Primer sequences used for the qPCR analysis.

Gene	Sense primer (5′–3′)	Antisense primer (5′–3′)	Amplicon length (bp)
ACE	CAGAGGCCAACTG GCATTAT	CTGGAAGTTGCTCAC GTCAA	137
AT1	CACCCGATCACCGA TCAC	CAGCCATTTTATACCAATCT CTCA	110
IL-1β	AGGTCGTCATCATCC CACGAG	GCTGTGGCAGCTAC CTATGTCTTG	119
IL-6	CACAAGTCCGGA GAGGAGAC	ACAGTGCATCATCGCT GTTC	167
IL-10	GTTTTACCTGGTA GAAGTGATGCC	CCACTGCCTTGCTTTTA TTCTC	155
iNOS	AGTGGCAACAT CAGGTCGG	CGATGCACAACTGGG TGAAC	166
Cox2	GCATTCTTTGCC CAGCACTT	GTCTTTGACTGTGG GAGGAT	210
CD68	CCACAGGCAGCAC AGTGGACA	TCCACAGCAGAAGC TTTGGCCC	135
Arg-1	GGGAAAAGCCAAT GAACAGC	CCAAATGACGCATA GGTCAGG	148
CD206	AGTTGGGTTCT CCTGTAGCCCAA	ACTACTACCTGAGCCCA CACCTGCT	161
β-Actin	CATCCTGCGTCT GGACCTGG	TAATGTCACGCA CGATTTCC	116

Data Analysis

Results from the experiment were expressed as means ± SD and analyzed using SPSS version 17.0 software. Normality of distribution was assessed by the Lilliefors test, and homogeneity of variance was tested with the Levene's test. Differences between groups were determined by one-way analysis of variance (ANOVA) test, followed by LSD test for *post hoc* comparisons when equal variances were assumed. The prior level of significance was established at $p < 0.05$.

RESULTS

Neuroprotective Effects of Cand Against LPS-Induced Behavioral Deficits and Neural Death

As previously reported Guo et al. (2016) and Dang et al. (2017), repeated administration of LPS successfully induced an anxiogenic effect as evidenced by the decreased time spent in the open arms and reduced number and ratio of open arm entries (**Figures 1B–D**). LPS also induced the animals to a depression-like state with increased immobility time in FST (**Figure 1E**) and longer latency to feed in NSFT (**Figure 1F**). However, daily treatment of Cand partly restored the LPS-induced behavioral changes, increasing open arm spent time and open arm entries in the EPM test, and decreasing the immobility time and latency to feed in FST and NSFT, respectively, indicating both anxiolytic and antidepressive effects. While repeated LPS treatment suppressed the body weight growth, co-treatment with Cand didn't significantly affect the body weight gain (**Figure 1G**). Additionally, we found Cand treatment ameliorated nuclear condensation and acidophilic degeneration in H&E histopathological examination. In consistence, by using Tunel method, the LPS-induced neural apoptosis was also mitigated by Cand treatment (**Figure 2**).

Brain RAS Activation in LPS-Exposed Rats

As revealed in **Figure 3**, our results showed that sustained LPS exposure enhanced ACE expression, increased hippocampal status of Ang II and induced AT1 expression, suggesting that the continuous inflammatory process leads to brain RAS activation. Cand treatment had no effect on ACE and Ang II levels, but decreased AT1 expression compared with LPS-treated group.

Anti-inflammatory Effect of Cand in LPS-Exposed Rats

In line with our previous findings (Jiang et al., 2017), LPS induced microglial activation as revealed by the IBA-1 immunofluorescent results, which was pronouncedly alleviated by Cand co-administration (**Figure 4A**). In accordance with the microglial activation, the hippocampal mRNA expression

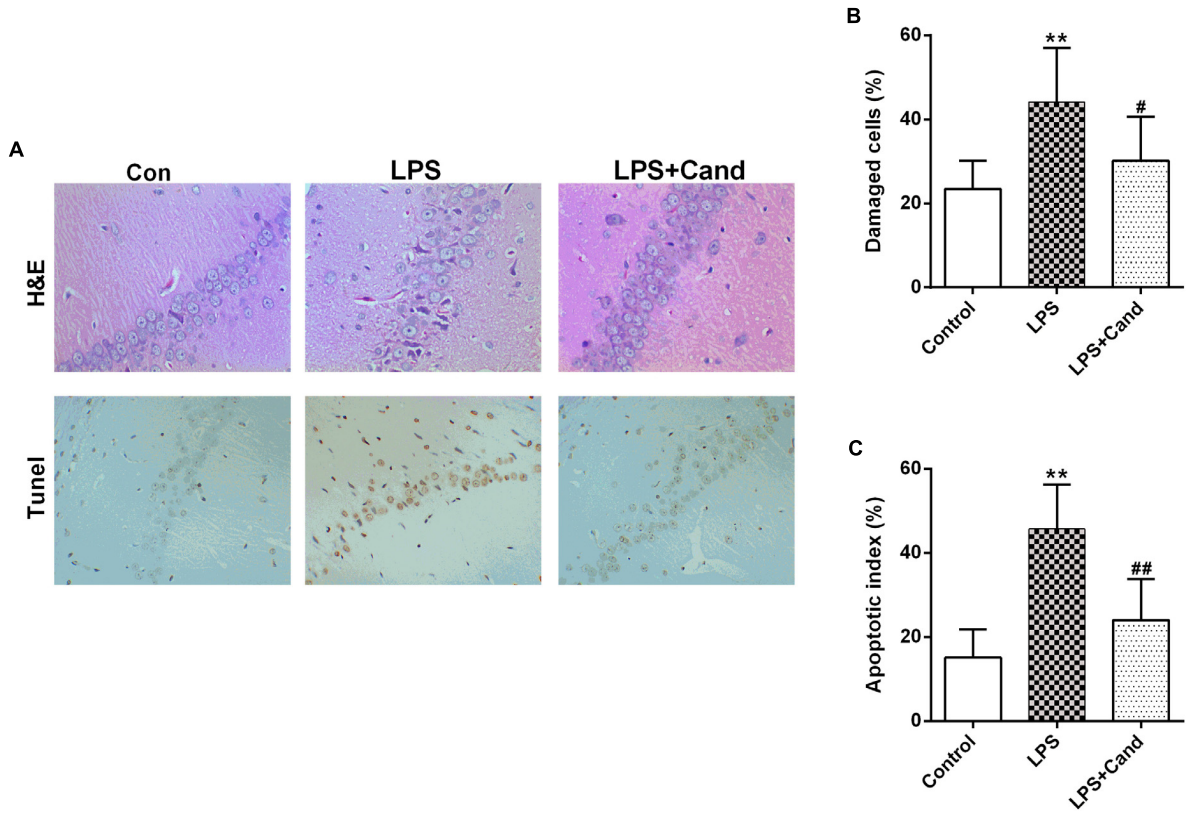

FIGURE 2 | Effect of Candesartan (Cand) treatment on LPS-induced histopathological changes in H&E staining and apoptosis in Tunel test **(A)**. Damaged cells in H&E staining **(B)** and apoptotic cells in Tunel test were counted, respectively. Data are means ± SD ($n = 7$). $^{**}p < 0.01$ compared to Control group. $^{\#}p < 0.05$, $^{\#\#}p < 0.01$ compared to LPS group.

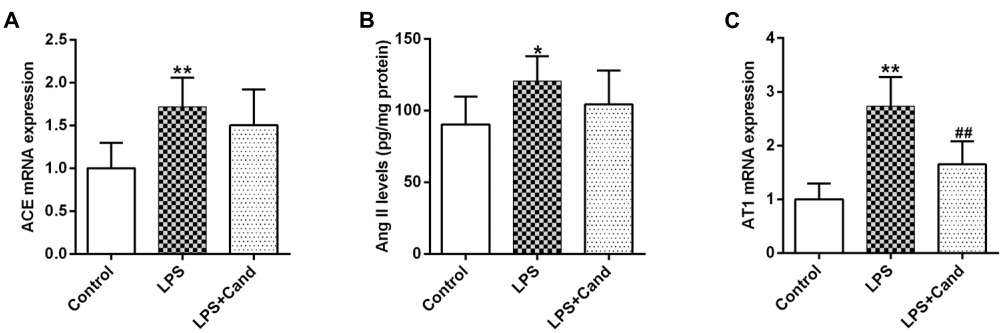

FIGURE 3 | Effect of lipopolysaccharide (LPS) and Candesartan (Cand) treatment on ACE mRNA expression **(A)**, Ang II levels **(B),** and AT1 expression **(C)**. Data are means ± SD ($n = 7$). $^{*}p < 0.05$, $^{**}p < 0.01$ compared to Control group. $^{\#\#}p < 0.01$ compared to LPS group.

of pro-inflammatory cytokines, including IL-1β and IL-6, the anti-inflammatory cytokine, IL-10, and the inflammation mediating enzymes, including the nitric oxide (NO)-producing isoenzyme inducible NO synthase (iNOS) and cyclooxygenase 2 (COX-2) were synchronously increased, which were prevented by Cand administration except for IL-10 that Cand slightly but significantly further amplified the LPS-induced IL-10 expression (**Figures 4B–F**). Upon inflammatory stimulation, the microglia is prone to polarize into proinflammatory M1 phenotype and the proinflammatory cytokines are mediators or biomarkers of M1 cells (Zhang B. et al., 2018). Likewise, CD68, another biomarker of M1 phenotype was induced in LPS exposed group (**Figure 4G**), further supporting the notion that LPS stimuli would lead to M1 polarization. Interestingly, similar as IL-10, repeated LPS exposure also enhanced the expression of M2 markers, arginase-1 (Arg-1) and CD206, indicating a potential compensatory response (**Figures 4H–J**). Meanwhile, Cand treatment not only mitigated the LPS-induced M1 polarization, but also

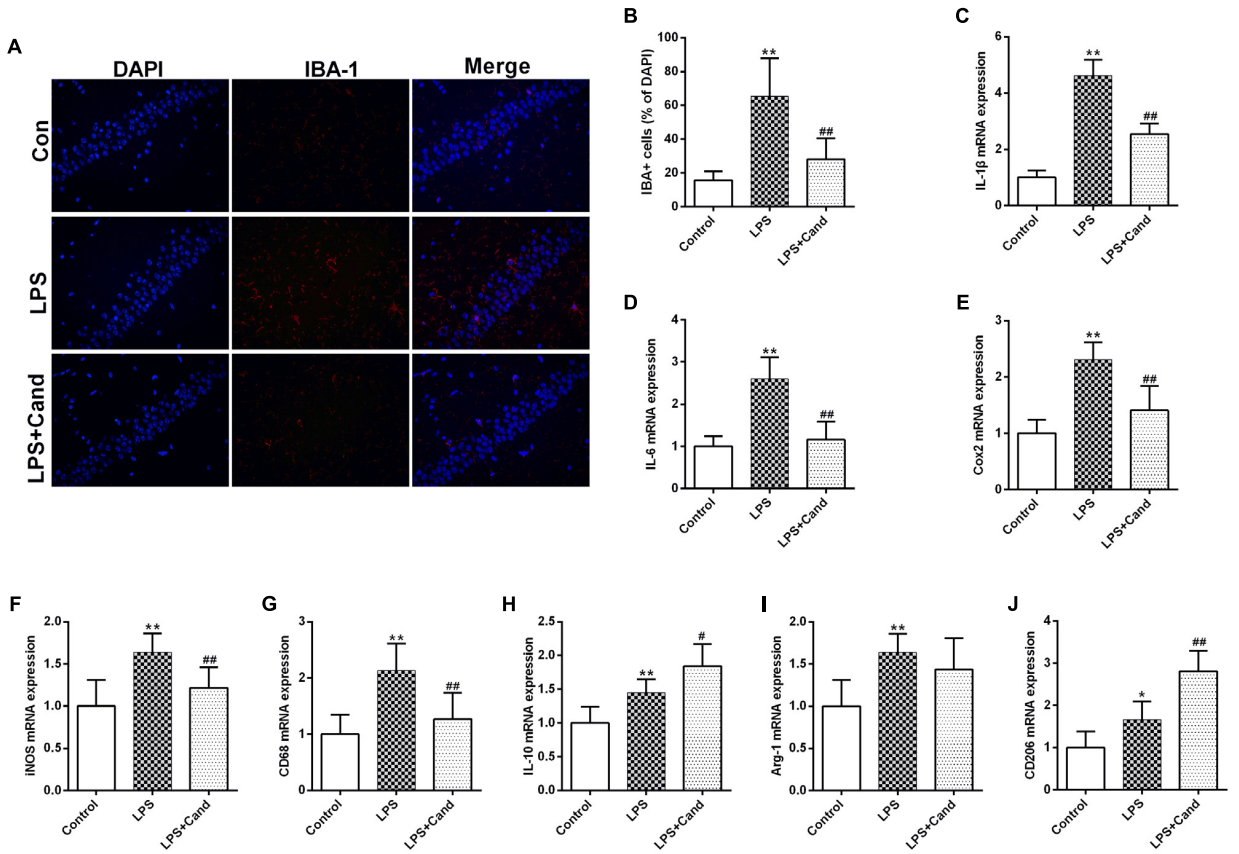

FIGURE 4 | Anti-inflammatory effect candesartan (Cand) following repeated lipopolysaccharide (LPS) exposure. Microglial activation (Iba-1 immunofluorescence) **(A,B)** and mRNA expression of IL-1β **(C)**, IL-6 **(D)**, Cox2 **(E)**, iNOS **(F)**, CD68 **(G)**, IL-10 **(H)**, Arg-1 **(I)**, and CD206 **(J)**. Data are means ± SD ($n = 7$). $^{*}p < 0.05$, $^{**}p < 0.01$ compared to Control group. $^{\#}p < 0.05$, $^{\#\#}p < 0.01$ compared to LPS group.

further shifted the microglia into M2 phenotype with increased expression of Arg-1 and CD206 compared with LPS group.

The Effect of Cand on LPS-Induced NF-κB Signaling

NF-κB signaling plays a fundamental role in response to inflammatory activator such as LPS (Lee et al., 2018). To further explore the mechanisms, we then analyzed the essential members of NF-κB family (**Figure 5A**). As expected, LPS stimuli activated IκBs kinase (IKK) with increased phosphorylation of IKK at serine 177 residue (**Figure 5B**), which resulted in IκB degradation (**Figure 5C**) and P65 activation (**Figure 5D**) compared with the control group. Cand treatment inhibited the LPS-induced IKK phosphorylation and P65 overactivation while preserved IκB stability. These data indicated that Cand may exert an anti-inflammatory effect by modulating the NF-κB signal pathway.

The Effect of Cand and LPS on Hippocampal Insulin Pathway

Both inflammation and activated RAS are two major contributors to insulin resistance (Sarlus et al., 2013; Ramalingam et al., 2017). To examine their interactions in the brain, we evaluated the insulin signaling in the hippocampus following LPS and Cand treatment (**Figure 6A**). Although LPS and Cand both had no significant effects on IRβ expression (**Figure 6B**), repeated LPS treatment enhanced the inhibitory phosphorylation of IRS at serine 307 (**Figure 6C**) and suppressed IRS tyrosine 896 phosphorylation (**Figure 6D**) that is required for signal transduction (Akiyama et al., 2013), whereas blocking AT1 by Cand treatment reversed these effects and improved insulin signaling, partly normalizing p-IRS (Ser307) and p-IRS (Tyr896) status.

DISCUSSION

The progression of a series of neuropsychiatric disorders, such as depression, is associated with continuous subclinical inflammatory process. However, most of the studies examined the acute effect of LPS, and the evidence concerning the neuropathological changes following sustained inflammatory stimuli is limited. In line with our previous research, repeated administration of LPS induced anxiety and depression-like behaviors, as well as neuroinflammation, in rats, which resembles the clinical profile of depression that depressive patients are

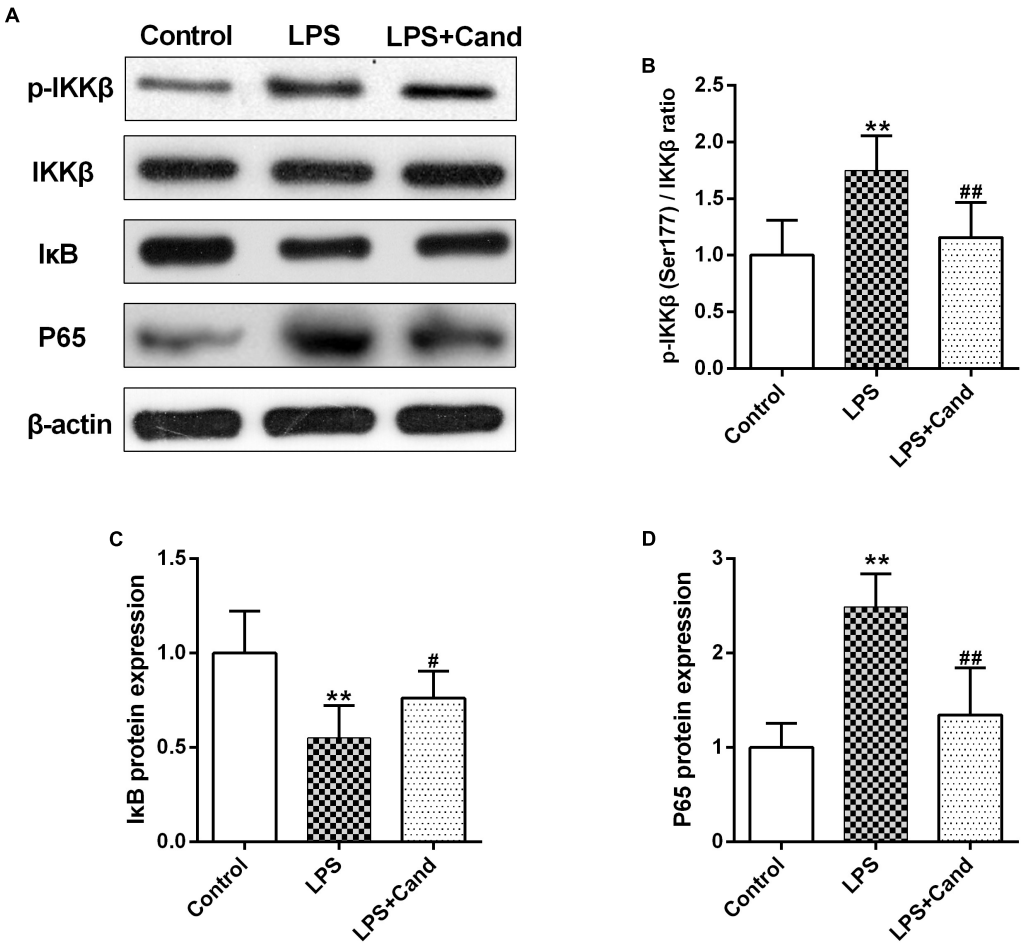

FIGURE 5 | Effect of lipopolysaccharide (LPS) and Candesartan (Cand) treatment on NF-κB signaling. Representative blots **(A)** and statistical graphs of relative p-IKKβ (Ser177)/IKKβ ratio **(B)**, IκB protein expression **(C)** and P65 protein expression **(D)** ($n = 7$). Data are means ± SD. $^{**}p < 0.01$ compared to Control group. $^{\#}p < 0.05$, $^{\#\#}p < 0.01$ compared to LPS group.

prone to under chronic subclinical inflammatory state (Dang et al., 2017). The neuroinflammatory process was reflected by the LPS-induced microglial activation, the enhanced expression of proinflammatory cytokines, IL-1β and IL-6, and the upregulated iNOS and Cox2 expression. Unexpectedly, the anti-inflammatory cytokine, IL-10, was also induced by prolonged exposure to LPS, which is in contrast with previous findings that acute LPS treatment inhibited IL-10 expression (Kavanagh et al., 2004), indicating a potential compensatory mechanism that may mediate endotoxin tolerance following sustained LPS treatment.

RAS functions as a hormone system that is capable of acting directly in many tissues in an autocrine and paracrine way. RAS is originally recognized as a blood pressure controller, and now is implicated in multifactorial brain function. All the components of the classic RAS have been identified in both neuronal and glial cells (Jackson et al., 2018). Microglia is considered as the resident macrophage in the brain, responsible for the neural immune responses under stressful conditions (Liu et al., 2019). The localized brain RAS activation is associated with neuroinflammation and neuropathy as demonstrated by the facts that central administration of Ang II, the major prohypertensive ligand of AT1 receptor, induces neuroinflammation and oxidative stress *in vivo* and *in vitro* (Bild et al., 2013; Bali and Jaggi, 2016; Abdul-Muneer et al., 2018), and AT1 receptor blockade ameliorates inflammation and improves brain function in animal models of epilepsy, brain ischemia and neurodegeneration (Saavedra et al., 2011; Tchekalarova et al., 2015; Valenzuela et al., 2016). Microglia, similar with macrophages, can develop into proinflammatory M1 phenotype and immunoregulatory M2 phenotype (Liu et al., 2019). In the context of immune stimuli, the localized RAS system in microglial cells would be activated, which plays an essential role in microglial polarization, promoting the transformation of microglia into M1 phenotype (Labandeira-Garcia et al., 2017). Consistent with this, our data showed the activated RAS in the brain with enhanced ACE and AT1 mRNA expression, and elevated Ang II status in the context of repeated LPS stimuli. In addition, our phenotypic analysis of microglia in the hippocampal CA1 region showed that the M1 markers iNOS and CD68 were increased. These findings are in line with acute LPS treatment (Benicky et al., 2011),

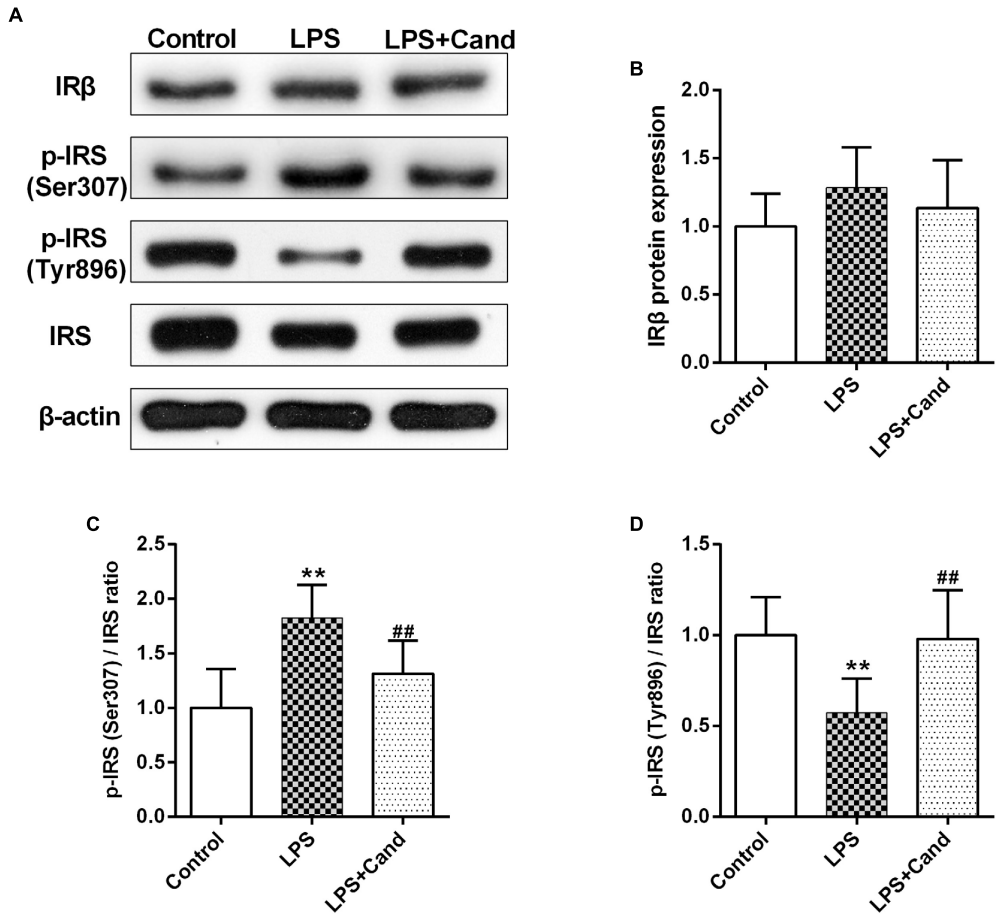

FIGURE 6 | Effect of lipopolysaccharide (LPS) and Candesartan (Cand) treatment on insulin signaling. Representative blots **(A)** and statistical graphs of relative IRβ protein expression **(B)** and the ratios of p-IRS (Ser307)/IRS **(C)** and p-IRS (Tyr896)/IRS **(D)**. Data are means ± SD ($n = 7$). $^{**}p < 0.01$ compared to Control group. $^{\#\#}p < 0.01$ compared to LPS group.

indicating that the brain RAS can be ignited by both short and longtime neuroimmune activation, which may further worsen the inflammatory situation and trigger the positive feedback between RAS and immune system (Bhat et al., 2016), resulting in uncontrolled neuroinflammatory progression. Intriguingly, it should be noted that the M2 markers, IL-10, Arg-1, and CD206, were also synchronously increased following sustained LPS exposure, suggesting an adaptive compensatory response, which might be associated with the mechanism of LPS tolerance (Zhang Z. et al., 2018).

However, blocking AT1 receptor by Cand, as shown in our study and previous findings, contains anti-inflammatory properties (Bhat et al., 2016). While Cand can efficiently cross the blood brain barrier and effectively block brain AT1 receptor (Benicky et al., 2011), the treatment protocol didn't significantly normalize the LPS-activated RAS except for the partly restored AT1 expression. Nevertheless, daily Cand administration during LPS challenge process attenuated the inflammatory response, suppressing microglial activation and the expression of inflammatory mediators. Additionally, Cand treatment shifted microglia from M1 to M2 phenotype with decreased expression of M1 markers (iNOS and CD68) and increased expression of M2 marker (CD206) compared with LPS group, further confirming the involvement of RAS system in the LPS-induced disturbance in microglial polarization. Aside from neuroimmune modulating actions, Cand treatment also prevented the brain from LPS-induced neural apoptosis and exerted anti-anxiety and anti-depression effects. The AT1 antagonism may cut off the deteriorating feedback loop between RAS and immune system, thereby resulting in neuroprotective activities and improving neurobehavioral functions. Although multiple lines of evidence suggest that blocking AT1 receptor contains anti-inflammatory, anti-oxidative and anti-apoptotic properties, it should be noted that Cand may interact with other targets independent of AT1 receptor. One previous interesting research showed that Cand effectively suppresses TNF-induced inflammatory process and reinstates redox homeostasis in renal tubular epithelial cells lacking AT1, and Cand may possess intrinsic antioxidant activity (Chen et al., 2008). To this end, further studies using AT1 knockdown animals or other AT1 inhibitors with more selectivity, such as azilsartan (Kajiya et al., 2011; Ojima et al., 2011), are

warranted given that the pharmacological action of Cand seems to be complex.

Insulin resistance is a major consequence of inflammation, contributing to a variety of brain dysfunctions as glucose is the brain's main energy source for neurotransmission, synaptic plasticity and neurogenesis (Clark et al., 2012; Kleinridders et al., 2014). Inflammatory stimuli may evoke insulin resistance via the activation of NF-κB signaling. Under normal condition, NF-κB exists in an inactive state in the cellular cytoplasm, where it is bound to the inhibitor of NF-κB (IκB). Once activated, the IκB kinase (IKK) phosphorylates IκB, which would lead to IκB degradation and P65 translocation to the nucleus, promoting the expression of proinflammatory mediators (Li et al., 2012). The activated IKK can also phosphorylate IRS-1 at serine residue, impeding tyrosine phosphorylation and insulin signal transduction (Copps and White, 2012). Although the cross-talk between insulin signaling and inflammation is well-studied in the periphery, the evidence concerning the relationship in the brain is limited. A recent study showed that single intraperitoneal LPS injection activates insulin signaling with enhanced IRS-1 tyrosine phosphorylation (Tyr1222) in the hypothalamus (Rorato et al., 2017). In contrast, Iloun et al. (2018) found that hippocampal insulin pathway is inhibited with increased IRS-1 (Ser307) expression 6 days after one dose of intracerebroventricular LPS injection. These discrepancies might be attributed to the treatment protocols and various brain areas used in the different study. The present study observed increased phosphorylated serine residue (Ser307) but decreased phosphorylated tyrosine residue (Tyr896), strongly indicating that continuous inflammatory state may impede insulin pathway, confirming the theory that inflammation interferes with insulin signaling to promote neurological and behavioral deficits, and IKK may mediate not only LPS-induced neuroinflammation, but also disturbance of insulin signaling in the brain.

Aside from inflammation, RAS may also hamper insulin signaling by directly inhibiting phosphatidylinositol 3-kinase (PI3K) cascade or indirectly through provoking inflammation and oxidative stress (Favre et al., 2015). Indeed, RAS is intrinsic to pancreatic islets and insulin-targeted tissues including adipose, skeletal muscle and liver, whereas both clinical and basic studies demonstrated that RAS blockade improves glucose homeostasis and prevents diabetes (Luther and Brown, 2011; Bangalore et al., 2016). In this context, we further explored whether angiotensin receptor blockers (ARBs) are also effective in brain insulin pathway. Our data showed that Cand alleviated LPS-induced IRS-1 phosphorylation on serine 307 and restored IRS-1 phosphorylation on tyrosine 896 in the hippocampus, implying that ARBs might be beneficial on brain insulin signaling as well. By blocking the AT1 receptor, Cand may restrain the reciprocal influence of RAS and inflammatory pathway on each other to limit the deleterious impacts of these two risk factors on insulin signaling.

In summary, the present study showed that LPS-induced anxiety and depression-like behaviors might be associated with brain RAS activation, neuroinflammation and disturbed brain insulin signaling, which were partly restored by Cand treatment, highlighting the involvement of RAS in inflammation-impeded insulin pathway in the brain and providing a potential drug target for the inflammation-associated neurological disorders such as depression. While the present research mainly focused on the neuroprotective mechanisms of Cand, it is important to note that we fails to evaluate the baseline effect of Cand, which is a major limitation of the study.

DATA AVAILABILITY

The datasets generated for this study are available on request to the corresponding author.

AUTHOR CONTRIBUTIONS

XG, PJ, and YQ designed the study and wrote the protocol. XG, HH, PX, RD, MY, and WH performed the experiments and analyzed the data. XG, HH, and DC drafted the manuscript. PJ, MY, and YG revised the manuscript content. All authors read and approved the final manuscript.

FUNDING

The study was supported by the National Natural Science Foundation of China (PJ, 81602846 and YQ, 31600947) and Taishan Scholar Project of Shandong Province (PJ, tsqn201812159).

SUPPLEMENTARY MATERIAL

The Supplementary Material for this article can be found online at: https://www.frontiersin.org/articles/10.3389/fphar.2019.00318/full#supplementary-material

REFERENCES

Abdul-Muneer, P. M., Bhowmick, S., and Briski, N. (2018). Angiotensin II causes neuronal damage in stretch-injured neurons: protective effects of losartan, an angiotensin T1 receptor blocker. *Mol. Neurobiol.* 55, 5901–5912. doi: 10.1007/s12035-017-0812-z

Akiyama, M., Liew, C. W., Lu, S., Hu, J., Martinez, R., Hambro, B., et al. (2013). X-box binding protein 1 is essential for insulin regulation of pancreatic alpha-cell function. *Diabetes* 62, 2439–2449. doi: 10.2337/db12-1747

Bali, A., and Jaggi, A. S. (2016). Angiotensin II-triggered kinase signaling cascade in the central nervous system. *Rev. Neurosci.* 27, 301–315. doi: 10.1515/revneuro-2015-0041

Bangalore, S., Fakheri, R., Toklu, B., and Messerli, F. H. (2016). Diabetes mellitus as a compelling indication for use of renin angiotensin system blockers: systematic review and meta-analysis of randomized trials. *BMJ* 352:i438. doi: 10.1136/bmj.i438

Benicky, J., Sanchez-Lemus, E., Honda, M., Pang, T., Orecna, M., Wang, J., et al. (2011). Angiotensin II AT1 receptor blockade ameliorates brain

inflammation. *Neuropsychopharmacology* 36, 857–870. doi: 10.1038/npp.2010.225

Bhat, S. A., Goel, R., Shukla, R., and Hanif, K. (2016). Angiotensin receptor blockade modulates NFkappaB and STAT3 signaling and inhibits glial activation and neuroinflammation better than angiotensin-converting enzyme inhibition. *Mol. Neurobiol.* 53, 6950–6967. doi: 10.1007/s12035-015-9584-5

Biancardi, V. C., Bomfim, G. F., Reis, W. L., Al-Gassimi, S., and Nunes, K. P. (2017). The interplay between Angiotensin II, TLR4 and hypertension. *Pharmacol. Res.* 120, 88–96. doi: 10.1016/j.phrs.2017.03.017

Bild, W., Hritcu, L., Stefanescu, C., and Ciobica, A. (2013). Inhibition of central angiotensin II enhances memory function and reduces oxidative stress status in rat hippocampus. *Prog. Neuropsychopharmacol. Biol. Psychiatry* 43, 79–88. doi: 10.1016/j.pnpbp.2012.12.009

Capettini, L. S., Montecucco, F., Mach, F., Stergiopulos, N., Santos, R. A., and da Silva, R. F. (2012). Role of renin-angiotensin system in inflammation, immunity and aging. *Curr. Pharm. Des.* 18, 963–970. doi: 10.2174/138161212799436593

Chen, S., Ge, Y., Si, J., Rifai, A., Dworkin, L. D., and Gong, R. (2008). Candesartan suppresses chronic renal inflammation by a novel antioxidant action independent of AT1R blockade. *Kidney Int.* 74, 1128–1138. doi: 10.1038/ki.2008.380

Clark, I., Atwood, C., Bowen, R., Paz-Filho, G., and Vissel, B. (2012). Tumor necrosis factor-induced cerebral insulin resistance in Alzheimer's disease links numerous treatment rationales. *Pharmacol. Rev.* 64, 1004–1026. doi: 10.1124/pr.112.005850

Copps, K. D., and White, M. F. (2012). Regulation of insulin sensitivity by serine/threonine phosphorylation of insulin receptor substrate proteins IRS1 and IRS2. *Diabetologia* 55, 2565–2582. doi: 10.1007/s00125-012-2644-8

Dang, R., Zhou, X., Xu, P., Guo, Y., Gong, X., Wang, S., et al. (2017). ω-3 polyunsaturated fatty acid supplementation ameliorates lipopolysaccharide-induced behavioral deficits and modulates neurotrophic factors in rats: focus on tPA/PAI-1 system and BDNF-TrkB signaling. *J. Funct. Foods* 30, 74–80. doi: 10.1016/j.jff.2017.01.010

de Souza Gomes, J. A., de Souza, G. C., Berk, M., Cavalcante, L. M., de Sousa, F. C., Budni, J., et al. (2015). Antimanic-like activity of candesartan in mice: possible involvement of antioxidant, anti-inflammatory and neurotrophic mechanisms. *Eur. Neuropsychopharmacol.* 25, 2086–2097. doi: 10.1016/j.euroneuro.2015.08.005

Favre, G. A., Esnault, V. L., and Van Obberghen, E. (2015). Modulation of glucose metabolism by the renin-angiotensin-aldosterone system. *Am. J. Physiol. Endocrinol. Metab.* 308, E435–E449. doi: 10.1152/ajpendo.00391.2014

Gaddam, R. R., Chambers, S., and Bhatia, M. (2014). ACE and ACE2 in inflammation: a tale of two enzymes. *Inflamm. Allergy Drug Targets* 13, 224–234. doi: 10.2174/1871528113666140713164506

Gebre, A. K., Altaye, B. M., Atey, T. M., Tuem, K. B., and Berhe, D. F. (2018). Targeting renin-angiotensin system against Alzheimer's disease. *Front. Pharmacol.* 9:440. doi: 10.3389/fphar.2018.00440

Guo, Y., Cai, H., Chen, L., Liang, D., Yang, R., Dang, R., et al. (2016). Quantitative profiling of neurotransmitter abnormalities in the hippocampus of rats treated with lipopolysaccharide: focusing on kynurenine pathway and implications for depression. *J. Neuroimmunol.* 295-296, 41–46. doi: 10.1016/j.jneuroim.2016.04.006

Haspula, D., and Clark, M. A. (2018). Molecular basis of the brain renin angiotensin system in cardiovascular and neurologic disorders: uncovering a key role for the astroglial angiotensin type 1 receptor AT1R. *J. Pharmacol. Exp. Ther.* 366, 251–264. doi: 10.1124/jpet.118.248831

Iloun, P., Abbasnejad, Z., Janahmadi, M., Ahmadiani, A., and Ghasemi, R. (2018). Investigating the role of P38, JNK and ERK in LPS induced hippocampal insulin resistance and spatial memory impairment: effects of insulin treatment. *EXCLI J.* 17, 825–839. doi: 10.17179/excli2018-1387

Jackson, L., Eldahshan, W., Fagan, S. C., and Ergul, A. (2018). Within the brain: the renin angiotensin system. *Int. J. Mol. Sci.* 19:E876. doi: 10.3390/ijms19030876

Jiang, P., Guo, Y., Dang, R., Yang, M., Liao, D., Li, H., et al. (2017). Salvianolic acid B protects against lipopolysaccharide-induced behavioral deficits and neuroinflammatory response: involvement of autophagy and NLRP3 inflammasome. *J. Neuroinflamm.* 14:239. doi: 10.1186/s12974-017-1013-4

Kajiya, T., Ho, C., Wang, J., Vilardi, R., and Kurtz, T. W. (2011). Molecular and cellular effects of azilsartan: a new generation angiotensin II receptor blocker. *J. Hypertens.* 29, 2476–2483. doi: 10.1097/HJH.0b013e32834c46fd

Kavanagh, T., Lonergan, P. E., and Lynch, M. A. (2004). Eicosapentaenoic acid and gamma-linolenic acid increase hippocampal concentrations of IL-4 and IL-10 and abrogate lipopolysaccharide-induced inhibition of long-term potentiation. *Prostaglandins Leukot. Essent. Fatty Acids* 70, 391–397. doi: 10.1016/j.plefa.2003.12.014

Kleinridders, A., Ferris, H. A., Cai, W., and Kahn, C. R. (2014). Insulin action in brain regulates systemic metabolism and brain function. *Diabetes* 63, 2232–2243. doi: 10.2337/db14-0568

Labandeira-Garcia, J. L., Rodriguez-Perez, A. I., Garrido-Gil, P., Rodriguez-Pallares, J., Lanciego, J. L., and Guerra, M. J. (2017). Brain renin-angiotensin system and microglial polarization: implications for aging and neurodegeneration. *Front. Aging Neurosci.* 9:129. doi: 10.3389/fnagi.2017.00129

Lee, J. Y., Joo, B., Nam, J. H., Nam, H. Y., Lee, W., Nam, Y., et al. (2018). An aqueous extract of herbal medicine ALWPs enhances cognitive performance and inhibits LPS-induced neuroinflammation via FAK/NF-kappaB signaling pathways. *Front. Aging Neurosci.* 10:269. doi: 10.3389/fnagi.2018.00269

Li, J., Tang, Y., and Cai, D. (2012). IKKbeta/NF-kappaB disrupts adult hypothalamic neural stem cells to mediate a neurodegenerative mechanism of dietary obesity and pre-diabetes. *Nat. Cell Biol.* 14, 999–1012. doi: 10.1038/ncb2562

Liao, D., Guo, Y., Xiang, D., Dang, R., Xu, P., Cai, H., et al. (2018). Dysregulation of Neuregulin-1/ErbB signaling in the hippocampus of rats after administration of doxorubicin. *Drug Des. Devel. Ther.* 12, 231–239. doi: 10.2147/DDDT.S151511

Liu, Q., Zhang, Y., Liu, S., Liu, Y., Yang, X., Liu, G., et al. (2019). Cathepsin C promotes microglia M1 polarization and aggravates neuroinflammation via activation of Ca(2+)-dependent PKC/p38MAPK/NF-kappaB pathway. *J. Neuroinflamm.* 16:10. doi: 10.1186/s12974-019-1398-3

Luther, J. M., and Brown, N. J. (2011). The renin-angiotensin-aldosterone system and glucose homeostasis. *Trends Pharmacol. Sci.* 32, 734–739. doi: 10.1016/j.tips.2011.07.006

Ojima, M., Igata, H., Tanaka, M., Sakamoto, H., Kuroita, T., Kohara, Y., et al. (2011). In vitro antagonistic properties of a new angiotensin type 1 receptor blocker, azilsartan, in receptor binding and function studies. *J. Pharmacol. Exp. Ther.* 336, 801–808. doi: 10.1124/jpet.110.176636

Ramalingam, L., Menikdiwela, K., LeMieux, M., Dufour, J. M., Kaur, G., Kalupahana, N., et al. (2017). The renin angiotensin system, oxidative stress and mitochondrial function in obesity and insulin resistance. *Biochim. Biophys. Acta Mol. Basis Dis.* 1863, 1106–1114. doi: 10.1016/j.bbadis.2016.07.019

Rorato, R., Borges, B. C., Uchoa, E. T., Antunes-Rodrigues, J., Elias, C. F., and Elias, L. L. K. (2017). LPS-induced low-grade inflammation increases hypothalamic JNK expression and causes central insulin resistance irrespective of body weight changes. *Int. J. Mol. Sci.* 18:E1431. doi: 10.3390/ijms18071431

Saavedra, J. M. (2017). Beneficial effects of angiotensin II receptor blockers in brain disorders. *Pharmacol. Res.* 125(Pt A), 91–103. doi: 10.1016/j.phrs.2017.06.017

Saavedra, J. M., Sanchez-Lemus, E., and Benicky, J. (2011). Blockade of brain angiotensin II AT1 receptors ameliorates stress, anxiety, brain inflammation and ischemia: therapeutic implications. *Psychoneuroendocrinology* 36, 1–18. doi: 10.1016/j.psyneuen.2010.10.001

Sarlus, H., Wang, X., Cedazo-Minguez, A., Schultzberg, M., and Oprica, M. (2013). Chronic airway-induced allergy in mice modifies gene expression in the brain toward insulin resistance and inflammatory responses. *J. Neuroinflamm.* 10:99. doi: 10.1186/1742-2094-10-99

Tchekalarova, J., Loyens, E., and Smolders, I. (2015). Effects of AT1 receptor antagonism on kainate-induced seizures and concomitant changes in hippocampal extracellular noradrenaline, serotonin, and dopamine levels in Wistar-Kyoto and spontaneously hypertensive rats. *Epilepsy Behav.* 46, 66–71. doi: 10.1016/j.yebeh.2015.03.021

Uijl, E., Ren, L., and Danser, A. H. J. (2018). Angiotensin generation in the brain: a re-evaluation. *Clin. Sci.* 132, 839–850. doi: 10.1042/CS20180236

Valenzuela, R., Costa-Besada, M. A., Iglesias-Gonzalez, J., Perez-Costas, E., Villar-Cheda, B., Garrido-Gil, P., et al. (2016). Mitochondrial angiotensin receptors in dopaminergic neurons. Role in cell protection and aging-related vulnerability to neurodegeneration. *Cell Death Dis.* 7:e2427. doi: 10.1038/cddis.2016.327

Yagi, S., Akaike, M., Ise, T., Ueda, Y., Iwase, T., and Sata, M. (2013). Renin-angiotensin-aldosterone system has a pivotal role in cognitive impairment. *Hypertens. Res.* 36, 753–758. doi: 10.1038/hr.2013.51

Yang, M., Dang, R., Xu, P., Guo, Y., Han, W., Liao, D., et al. (2018). Dl-3-n-Butylphthalide improves lipopolysaccharide-induced depressive-like behavior in rats: involvement of Nrf2 and NF-kappaB pathways. *Psychopharmacology* 235, 2573–2585. doi: 10.1007/s00213-018-4949-x

Zhang, B., Wei, Y. Z., Wang, G. Q., Li, D. D., Shi, J. S., and Zhang, F. (2018). Targeting MAPK pathways by naringenin modulates microglia M1/M2 polarization in lipopolysaccharide-stimulated cultures. *Front. Cell Neurosci.* 12:531. doi: 10.3389/fncel.2018.00531

Zhang, Z., Ji, M., Liao, Y., Yang, J., and Gao, J. (2018). Endotoxin tolerance induced by lipopolysaccharide preconditioning protects against surgeryinduced cognitive impairment in aging mice. *Mol. Med. Rep.* 17, 3845–3852. doi: 10.3892/mmr.2018.8370

Zhou, X., Xu, P., Dang, R., Guo, Y., Li, G., Qiao, Y., et al. (2018). The involvement of autophagic flux in the development and recovery of doxorubicin-induced neurotoxicity. *Free Radic. Biol. Med.* 129, 440–445. doi: 10.1016/j.freeradbiomed.2018.10.418

Conflict of Interest Statement: The authors declare that the research was conducted in the absence of any commercial or financial relationships that could be construed as a potential conflict of interest.

frontiers in Neuroscience

CASE REPORT
published: 09 April 2019
doi: 10.3389/fnins.2019.00315

Effect of Clozapine on Anti-N-Methyl-D-Aspartate Receptor Encephalitis With Psychiatric Symptoms: A Series of Three Cases

Ping Yang[1†], Liang Li[2†], Shuaishuai Xia[2], Bin Zhou[1], Yong Zhu[1], Gaoya Zhou[1], Erwen Tu[1], Tianhao Huang[3], Huiyong Huang[2‡] and Feng Li[2,4*‡]*

[1] Department of Psychiatry, Hunan Brain Hospital, Clinical Medical School, Hunan University of Chinese Medicine, Changsha, China, [2] Provincial Key Laboratory of TCM Diagnostics, Hunan University of Chinese Medicine, Changsha, China, [3] Shanghai Institute of Measurement and Testing Technology, Shanghai, China, [4] School of Dentistry, University of California, Los Angeles, Los Angeles, CA, United States

OPEN ACCESS

Edited by:
Pei Jiang,
Jining Medical University, China

Reviewed by:
Chen Zhang,
Shanghai Mental Health Center (SMHC), China
Outi Mantere,
McGill University, Canada

***Correspondence:**
Huiyong Huang
huanghy68@126.com
Feng Li
fengli787@qq.com

[†]These authors have contributed equally to this work

[‡]These authors have contributed equally to this work and share senior authorship

Specialty section:
This article was submitted to Neuropharmacology, a section of the journal Frontiers in Neuroscience

Received: *30 November 2018*
Accepted: *19 March 2019*
Published: *09 April 2019*

Citation:
Yang P, Li L, Xia S, Zhou B, Zhu Y, Zhou G, Tu E, Huang T, Huang H and Li F (2019) Effect of Clozapine on Anti-N-Methyl-D-Aspartate Receptor Encephalitis With Psychiatric Symptoms: A Series of Three Cases. Front. Neurosci. 13:315. doi: 10.3389/fnins.2019.00315

The main clinical manifestations of anti-N-methyl-D-aspartate receptor (anti-NMDAR) encephalitis are acute or subacute seizures, cognition impairment, and psychiatric symptoms. Nowadays, the scheme of antipsychotic therapy for this disease has not been established. This study reports three cases of anti-NMDAR encephalitis with psychiatric symptoms. The anti-NMDAR antibodies in cerebrospinal fluid (CSF) and serum were positive. The psychiatric symptoms still existed after intravenous immunoglobulin (IVIG) treatment; thus, clozapine was used for antipsychotic therapy. Case 1 was a 37-year-old man who suffered from bad mood and suicide behaviors for 1 month. Hallucination and delusion still existed after IVIG treatment and hormone therapy, and the symptoms were relieved when given clozapine for 12 months. Case 2 was a 28-year-old man who was admitted to our hospital due to injuring other people and destructive behaviors for 2 days. He showed irritability, bad temper, declined cognition, and severe delusion of persecution after IVIG treatment and hormone therapy, but the psychiatric symptoms disappeared when given clozapine for 3 months. Case 3 was a 23-year-old man who suffered from headache and babbing for 7 days. Symptoms such as irritability, bad temper, babbing, and injuring other people still existed after IVIG treatment and hormone therapy, but they disappeared when given clozapine for 2 months. Therefore, we suggest that during the treatment of anti-NMDAR encephalitis with psychiatric symptoms, if the anti-NMDAR antibodies in CSF and serum were positive, and psychiatric symptoms could not be controlled after IVIG and hormone therapy, clozapine may work.

Keywords: clozapine, anti-NMDA receptor encephalitis, psychiatric symptoms, antipsychotic therapy, intravenous immunoglobulin, hormone

INTRODUCTION

Anti-N-methyl-D-aspartate receptor (anti-NMDAR) encephalitis is an autoimmune encephalitis induced by anti-NMDAR (Jiang et al., 2018). Dalmau et al. (2007) reported anti-NMDAR as the pathogenic antibody and diagnostic marker of this disease in 2007. Since then, the number of newly diagnosed cases has increased year by year (Beecher et al., 2018). At present, anti-NMDAR

encephalitis has become a representative in the disease spectrum of autoimmune encephalitis. The number of newly diagnosed cases of anti-NMDAR encephalitis has exceeded that of enterovirus encephalitis and herpes simplex encephalitis (Gable et al., 2012). It often combined with psychiatric symptoms, such as severe hallucination, delusion, and aggressive behaviors (Warren et al., 2018). However, there is no standard treatment for encephalitis with psychiatric symptoms, which brings serious risks and burdens to society and families. This study reported three cases of anti-NMDAR encephalitis with psychiatric symptoms. The anti-NMDAR antibodies were positive in their cerebrospinal fluid (CSF) and blood. All of them were treated with clozapine in our hospital.

CASE REPORT

Case 1

A 37-year-old male peasant presented with a 4-week history of low spirit, bad mood, suicide behaviors, and suspicion prior to hospitalization. He was diagnosed with severe depression and received sertraline (50–100 mg) and olanzapine (10 mg), but the situation became worse with declined cognition function and epileptic seizures after 7 days of treatment. The CSF pressure was 240 cmH_2O and leukocyte count was 10×10^6/L. The anti-NMDAR antibodies in CSF and serum were 1:32 (**Figures 1A,B**). Initial electroencephalography (EEG) showed epileptic activity with sharp-slow waves in the right anterior frontotemporal region (**Figure 2**). The chest and abdomen were detected with B-ultrasound and CT to exclude tumor. He received intravenous immunoglobulin (IVIG; 25 g/day, 5 days), methylprednisolone (1,000 mg, 3 days + 500 mg, 3 days), and prednisolone (0–60 mg, 12 weeks) for two courses; levetiracetam (1,500 mg, bid) and valproic acid (500 mg, bid) were used to control epilepsy. The patient showed severe heart failure and respiratory failure, with persistent psychiatric symptoms, such as visual hallucination, auditory hallucination, and delusion. When given olanzapine (10–20 mg/day, 3 days) and aripiprazole (2.5–10 mg/day, 7 days), these psychiatric symptoms could not be alleviated. Aggressive behaviors occurred when given olanzapine; muscle stiffness and slurred speech occurred when given aripiprazole. After cessation of olanzapine and aripiprazole, the use of clonazepam (2 mg, bid) led to clinical improvement. Thus, he was sedated with midazolam (2–4 mg/h, 45 days) during the period he was in the intensive care unit (ICU). The patient received quetiapine (50 mg/day to 0.4 g/day, 30 days) and clonazepam (2–6 mg/day, 35 days) from the ICU, but he still had severe visual hallucination and auditory hallucination after 6 months of treatment. Positive and Negative Syndrome Scale (PANSS) total score (Kay et al., 1987) was 112. The anti-NMDAR antibodies in CSF and serum were 1:10 and 1:320, respectively (**Figures 1C,D**), and the antibodies against AMPA1, AMPA2, LGI1, CASPR2, and GABAb were negative (Suh-Lailam et al., 2013). Head-enhanced magnetic resonance imaging (MRI) showed encephalatrophy (**Figures 3A,B**), and no epileptic waves were found in EEG. Then, he was given clozapine (50–300 mg/day), with 218.8 ng/ml plasma concentration

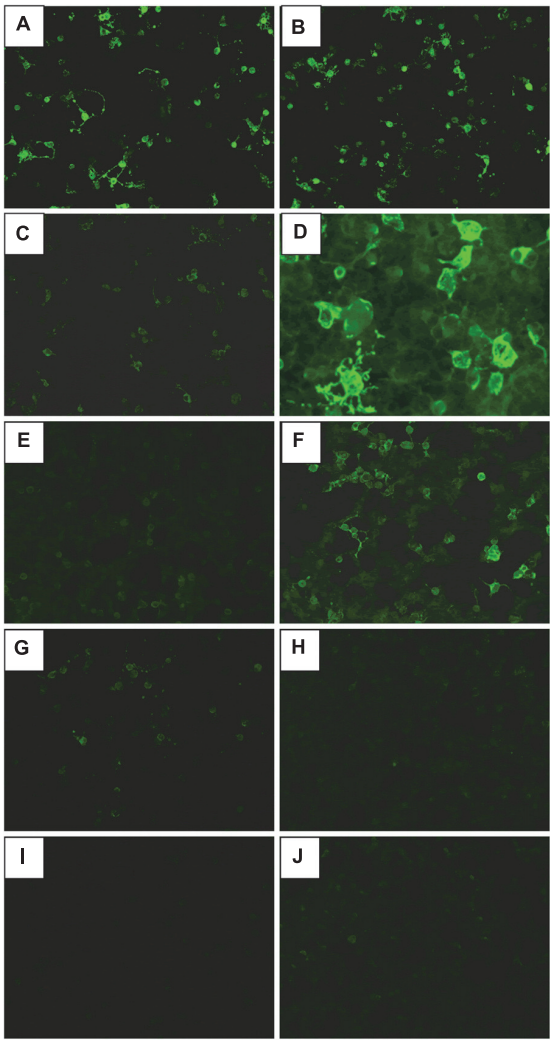

FIGURE 1 | The anti-NMDA receptor (anti-NMDAR) antibodies in CSF **(A,C,E,G,I)** and serum **(B,D,F,H,J)**. **(A,B)** Initial day in case 1. **(C,D)** Before treatment of clozapine in case 1. **(E,F)** After 18-month treatment of clozapine in case 1. **(G,H)** Before treatment of clozapine in case 2. **(I,J)** Before treatment of clozapine in case 3.

(**Figure 4A**; Zhou et al., 2004). Meanwhile, he was still treated with valproic acid (500 mg, bid) for epilepsy control. Eighteen months later, the anti-NMDAR antibodies in CSF and serum were 1:10 and 1:32 (**Figures 1E,F**), respectively. Up to now, the patient was able to live and work normally, with stable situation and no psychiatric symptoms. PANSS total score was 26.

Case 2

A 28-year-old male painter suffered from behavioral changes for 1 week after flu prior to hospitalization to the ICU of the local hospital. Head MRI showed long T1 and long T2 signal intensities in the left temporal lobe, and enhanced MRI showed irregular light enhancement (**Figures 3C,D**). The anti-NMDAR antibodies in CSF and serum were negative. With the diagnosis of viral encephalitis, the patient received antiviral therapy for

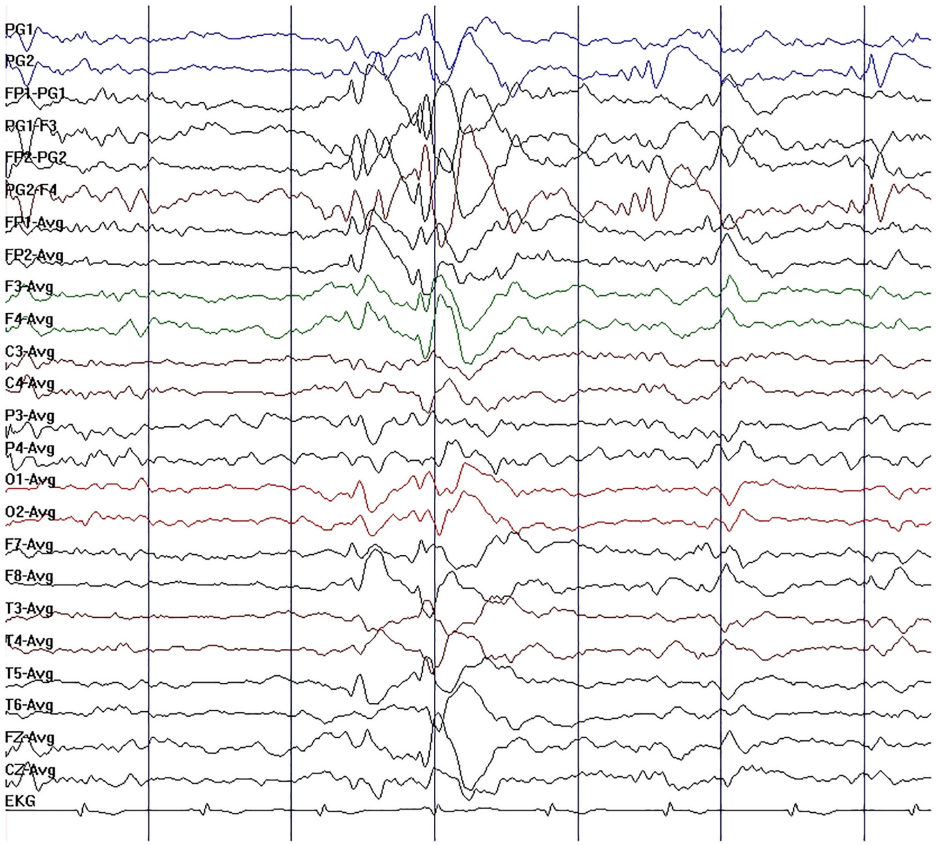

FIGURE 2 | Initial electroencephalography (EEG) in case 1. EEG showed moderate slow-wave discharge, with medium-wave amplitude, appearing as a single emission or continuous occurrence in right sphenoidal electrode, frontal pole, frontal, and pretemporal regions.

35 days, together with methylprednisolone (1,000 mg, 3 days + 500 mg, 3 days) and prednisolone (35–60 mg, 30 days). Then, he left the hospital. Unfortunately, he was admitted to our hospital 2 days after his discharge due to aggressive behaviors, injuring other people, irritability, and severe delusion of persecution. He was given acyclovir and olanzapine (10–20 mg/day), but the symptoms deteriorated with severe violent behavior and declined cognition function after 7 days of treatment. The CSF pressure was 200 cmH_2O. Total cell count was 58×10^6/L, and leukocyte count was 38×10^6/L. The anti-NMDAR antibodies in CSF and serum were both 1:10 (**Figures 1G,H**), and the antibodies against AMPA1, AMPA2, LGI1, CASPR2, and GABAb were negative (Suh-Lailam et al., 2013). The chest and abdomen were detected with B-ultrasound and CT to exclude tumor. After treatment with IVIG (30 g/day, 5 days), methylprednisolone (1,000 mg, 3 days + 500 mg, 3 days), and prednisolone (0–60 mg, 12 weeks), the psychiatric symptoms became worse; even olanzapine (10–20 mg/day, 15 days), quetiapine (25–400 mg/day, 15 days), diazepam (5–10 mg/day, 15 days), and clonazepam (2–6 mg/day, 15 days) did not work. PANSS total score (Kay et al., 1987) was 103. Finally, the patient was given clozapine (25–300 mg/day), with 90.6 ng/ml plasma concentration (**Figure 4B**; Zhou et al., 2004), and all the psychiatric symptoms disappeared completely 3 months later. The patient was discharged. Followed up for 6 months, all the clinical symptoms disappeared. The anti-NMDAR antibodies in CSF and serum were negative, but no obvious changes could be observed in enhanced head MRI. PANSS total score was 21.

Case 3

A 23-year-old male student was admitted to the local hospital due to headache, babbing, and aggressive behaviors for 1 week. After 7 days of treatment with penicillin and acyclovir, the symptoms were not relieved and then he was transferred to our hospital. No abnormality was found in enhanced head MRI. The CSF pressure was 100 cmH_2O. Total cell count and leukocyte count were normal. The protein concentration was 0.46 g/L. The anti-NMDAR antibodies in CSF and serum were 1:1 and 1:10, respectively (**Figures 1I,J**), and the antibodies against AMPA1, AMPA2, LGI1, CASPR2, and GABAb were negative (Suh-Lailam et al., 2013). The chest and abdomen were detected with B-ultrasound and CT to exclude tumor. PANSS total score (Kay et al., 1987) was 97. After treatment with IVIG (25 g/day, 5 days), methylprednisolone (1,000 mg, 3 days + 500 mg, 3 days), and prednisolone (0–60 mg, 12 weeks), followed by antipsychotic therapy with olanzapine (10–20 mg/day, 15 days), quetiapine (25–400 mg/day, 15 days), and clonazepam

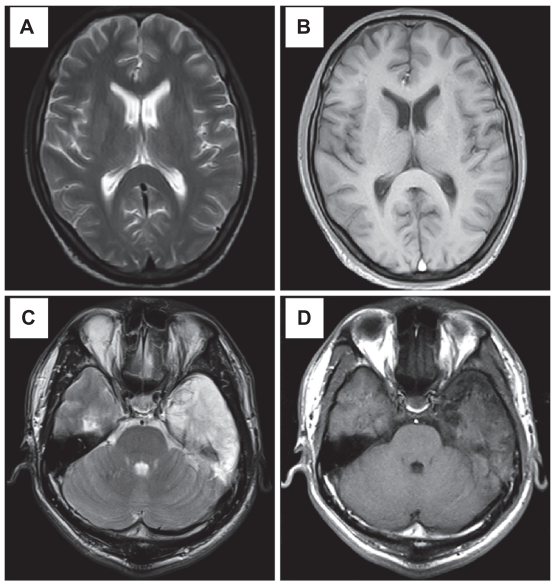

FIGURE 3 | Results of head MRI. **(A,B)** Head MRI showed encephalatrophy in case 1. **(C,D)** Head MRI showed long T1 and long T2 signal intensities in the left temporal lobe, and enhanced MRI stated irregular light enhancement in case 2. **(A,C)** T2WI; **(B,D)** T1-weighted sequence after gadolinium enhancement.

(2–4 mg/day, 30 days), the patient still showed visual hallucination and aggressive behaviors. Then, he was given clozapine (50–100 mg/day), with 65.3 ng/ml plasma concentration (**Figure 4C**; Zhou et al., 2004). The psychiatric symptoms disappeared after 2 months of treatment. Followed up for 6 months, he was able to live and work normally. The anti-NMDAR antibodies in CSF and serum were negative. PANSS total score was 18.

DISCUSSION

The incidence of anti-NMDAR encephalitis is second only to acute disseminated encephalomyelitis in autoimmune encephalitis (Granerod et al., 2010). Anti-NMDAR encephalitis may initially present with multiple psychiatric symptoms, which results in being misdiagnosed as primary psychiatric disease (Dalmau et al., 2008).

A study showed that among 111 anti-NMDAR encephalitis patients, 65 (58.6%) presented various psychiatric features, 43 (38.7%) were admitted initially to a psychiatric unit, and 2 (1.8%) were transferred from other inpatient units to a psychiatric unit before being finally correctly diagnosed (Lejuste et al., 2016). It was reported that catatonia was highly suggestive of NMDAR encephalitis, helping to diagnose anti-NMDAR encephalitis (Mythri and Mathew, 2016). The three patients in this study presented depression and aggressive behaviors, without catatonic syndrome. They were diagnosed with viral encephalitis and primary psychiatric disorder in the early stage, which delayed treatment. Gurrera believed that without appropriate treatment, patients are likely to suffer a protracted course with significant residual disability or death (Gurrera, 2018). At present, there is no formal antipsychotic treatment program for anti-NMDAR encephalitis with psychiatric symptoms. There are only few case reports about this; thus, treatment of such patients becomes more difficult. No specific medicine was found to improve the patient's psychiatric symptoms. For example, in the two cases reported by Kuppuswamy, olanzapine only worked in one patient, while aggravating the other patient's mental symptoms (Kuppuswamy et al., 2014). The side effects of some drugs, such as aripiprazole and haloperidol, even worsen the difficulties experienced during treatment (Chapman and Vause, 2011). In case 1, before the use of clozapine, the severe side effects caused by antipsychotics resulted in many extrapyramidal symptoms and serious aggressive behaviors. The dose of the medicine could not be increased gradually as usual, and the treatment had to be interrupted.

It was reported that NMDAR hypofunction was a potential mechanism resulting in schizophrenia, which complemented the most widespread explanatory mechanism of "dopamine hypothesis" for schizophrenia (Ramanathan et al., 2014). Some scholars declared that NMDAR dysfunction was the "final common pathway" underlying the pathogenesis of schizophrenia, and it was associated with both positive and negative symptoms (Wang et al., 2017). Anti-NMDAR antibodies were also found in schizophrenia patients (Koshiyama et al., 2018; Xie and Huang, 2018). Thus, some researchers believed that schizophrenia and anti-NMDAR encephalitis may have the same underlying mechanism and could be on the same spectrum (Maneta and Garcia, 2014). However, there is not enough proof to date to verify whether they are diseases on the same spectrum or under two different conditions.

The NMDAR, an ionotropic glutamate receptor, is related to synaptic plasticity, neuronal maturation, study, and memory (Hanson et al., 2015). NMDARs are heteromers of NMDAR1 and NMDAR2 subunits, which bind with glycine and glutamate, respectively (Tachibana et al., 2013). NMDAR hyperfunction is proposed to result in psychosis (Liu et al., 2015). Anti-NMDAR encephalitis represents a state of NMDAR hypofunction caused by autoantibodies against NMDAR (Warikoo et al., 2018). Thus, antipsychotic drugs affecting glutamate should be chosen during the treatment. Studies have shown that clozapine was the first atypical antipsychotic drug created successfully in the late 1960's. It is a diphenyldiazepine antipsychotic drug, with strong sedative and hypnotic effects, which can directly inhibit the ascending reticular activating system in the brainstem. It can selectively act on the mesencephalic limbic dopamine and the 5-serotonin (5-HT) systems, as well as the muscarinic and α1-noradrenergic receptor systems. Clozapine blocks the dopamine receptors reversibly and increases dopamine retroconversion. It has strong anticholinergic, antisympathetic, and antihistamine effects (Shi et al., 2007). At present, the pharmacological research based on the glutamatergic hypothesis of schizophrenia can go further among all the most promising mechanisms. It was reported that clozapine can affect 5-HT2A and D4 receptors, increase the release of dopamine, and selectively increase the concentration of Glu in the prefrontal cortex (Lopez-Munoz and Alamo, 2011).

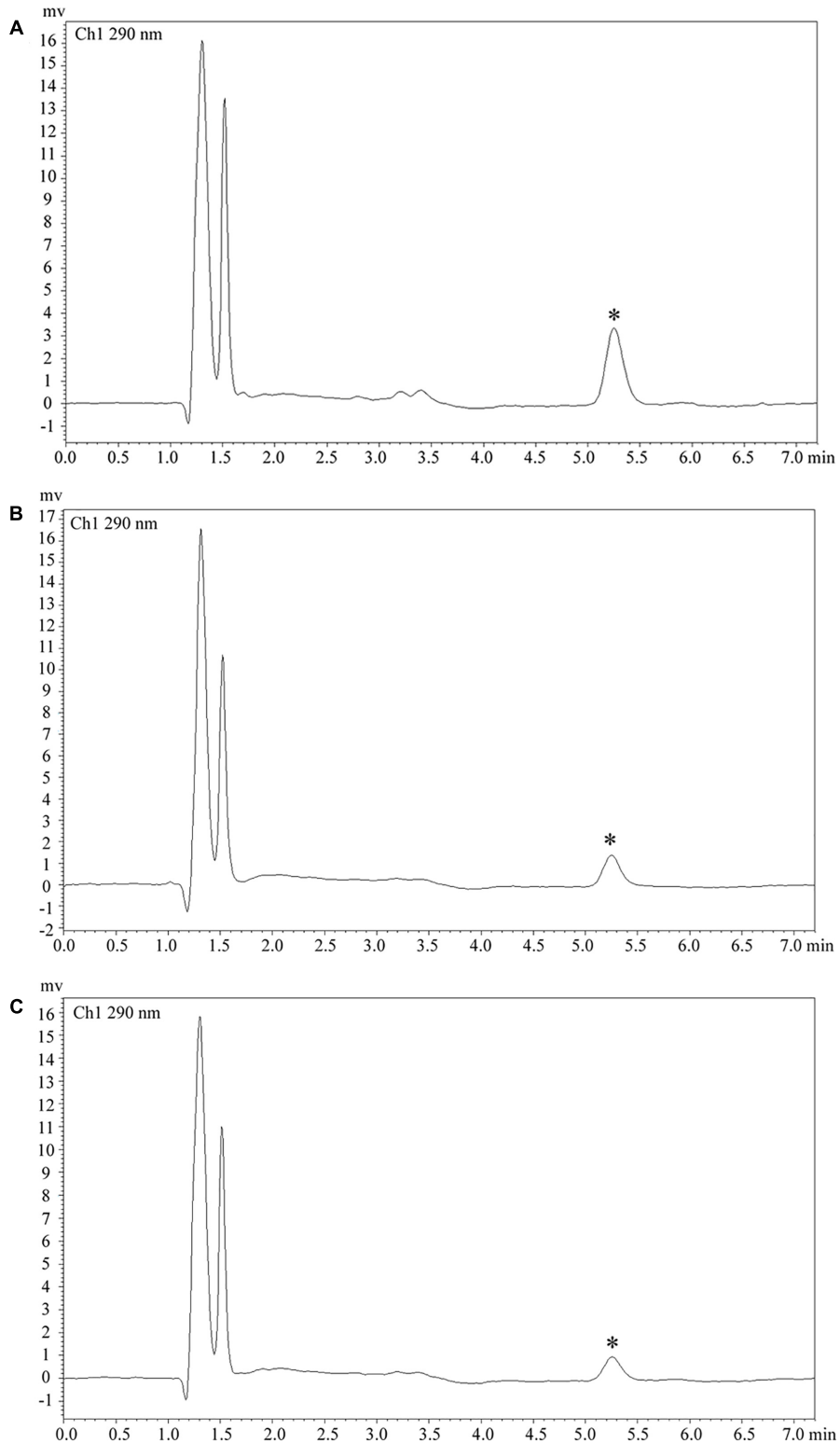

FIGURE 4 | Clozapine plasma concentration. **(A)** Plasma concentration was 218.8 ng/ml in case 1. **(B)** Plasma concentration was 90.6 ng/ml in case 2. **(C)** Plasma concentration was 65.3 ng/ml in case 3. Asterisks (*) represent the chromatogram peak of clozapine.

Incrocci et al. (2018) stated that the atypical antipsychotic clozapine potently blocked the disruption of the sensorimotor gating induced by NMDA antagonists. Rebollo et al. (2018) found that decreasing hypersynchronization in the local circuit may be one of the mechanisms of clozapine in preventing schizophrenia symptoms derived from NMDA hypofunction.

In this study, three patients of anti-NMDAR encephalitis with psychiatric symptoms were included. They had aggressive behaviors, even injured other people and destroyed objects. After IVIG treatment and hormone therapy, the use of various antipsychotics, such as midazolam, olanzapine, quetiapine, and aripiprazole, could not alleviate psychiatric symptoms. Olanzapine even aggravated their aggressive behaviors. Some researchers suggested that modern electroconvulsive therapy (MECT) should be used appropriately (Mann et al., 2012; Jones et al., 2015). However, anti-NMDAR encephalitis mainly showed epileptic seizures, status epilepticus, ventilation and air exchange dysfunction, autonomic nervous dysfunction, and multisystem complications. The situation was so serious that the patients had to be treated with intubation and auxiliary ventilation in the ICU. Therefore, MECT was not suitable for them. Furthermore, severe psychiatric symptoms prevented the patients from completing intensive care. In case 1 of this study, intensive care was interrupted due to severe visual and auditory hallucinations. With the improvement of seizure control, ventilation, and air exchange dysfunction, clozapine (300 mg) was used, and the psychiatric symptoms completely disappeared after 1 year of treatment. The patients in cases 2 and 3 showed violence and serious injuring tendency. The aggressive behaviors occurred after treatment of olanzapine, and other antipsychotics such as quetiapine and aripiprazole could not control psychiatric symptoms. In the end, they were given clozapine 300 and 100 mg, respectively, which controlled the symptoms well.

To sum up, clozapine can be used in the treatment of anti-NMDAR encephalitis with psychiatric symptoms. The disease should be under the control of epilepsy and good ventilation function; otherwise, clozapine may induce epilepsy (Bolu et al., 2017). It may be the reason why many doctors are reluctant to select clozapine. Therefore, when clozapine is used, it is important to monitor the EEG regularly to assess the risk of epilepsy. These three patients received EEG monitoring every month after taking clozapine, and the results were normal. Furthermore, antiepileptics, such as sodium valproate and levetiracetam, should not be ignored if necessary. Clozapine must be used on the basis of the ineffectiveness of three antipsychotics to anti-NMDAR encephalitis, just like the treatment of refractory schizophrenia. In this study, quetiapine and aripiprazole were ineffective to all the patients, and the psychiatric symptoms worsened after olanzapine. It is speculated that the affinity of receptor subtypes is different, and the exact mechanism needs further study.

CONCLUSION

We report three cases of anti-NMDAR encephalitis with psychiatric symptoms. During the treatment of the disease, if the psychiatric symptoms could not be controlled after IVIG and hormone therapy, clozapine may work.

ETHICS STATEMENT

This study was approved by the Ethics Committee of the Hunan Brain Hospital. A written informed consent was obtained from the patients for the publication of this case report.

AUTHOR CONTRIBUTIONS

PY and LL conceived the idea, revised all the literature, and wrote the manuscript. SX, YZ, and GZ collected the clinical data. BZ and TH analyzed and interpreted the head MRI. ET performed and analyzed the EEG. HH and FL contributed to the revision of the manuscript and read and approved the submitted version.

FUNDING

This work was supported by grants from the National Natural Science Foundation of China (Grant Nos. 81603512 and 81874429), the Hunan Chinese Medicine Science and Research Project (Grant No. 201818), and the Science and Technology Innovation Project of Hunan Province (Grant Nos. 2017SK50317 and 2017SK50313).

ACKNOWLEDGMENTS

The authors would like to thank the patients and their family members for their cooperation.

REFERENCES

Beecher, G., Wagner, A. N., Abele, J., and Smyth, P. (2018). Teaching neuroimages: prosopagnosia heralding anti-NMDA receptor encephalitis. *Neurology* 90, e2012–e2013. doi: 10.1212/WNL.0000000000005611

Bolu, A., Akarsu, S., Pan, E., Aydemir, E., and Oznur, T. (2017). Low-dose clozapine-induced seizure: a case report. *Clin. Psychopharmacol. Neurosci.* 15, 190–193. doi: 10.9758/cpn.2017.15.2.190

Chapman, M. R., and Vause, H. E. (2011). Anti-NMDA receptor encephalitis: diagnosis, psychiatric presentation, and treatment. *Am. J. Psychiatry* 168, 245–251. doi: 10.1176/appi.ajp.2010.10020181

Dalmau, J., Gleichman, A. J., Hughes, E. G., Rossi, J. E., Peng, X., Lai, M., et al. (2008). Anti-NMDA-receptor encephalitis: case series and analysis of the effects of antibodies. *Lancet Neurol.* 7, 1091–1098. doi: 10.1016/S1474-4422(08)70224-2

Dalmau, J., Tuzun, E., Wu, H. Y., Masjuan, J., Rossi, J. E., Voloschin, A., et al. (2007). Paraneoplastic anti-N-methyl-D-aspartate receptor encephalitis associated with ovarian teratoma. *Ann. Neurol.* 61, 25–36. doi: 10.1002/ana.21050

Gable, M. S., Sheriff, H., Dalmau, J., Tilley, D. H., and Glaser, C. A. (2012). The frequency of autoimmune N-methyl-D-aspartate receptor encephalitis surpasses that of individual viral etiologies in young individuals enrolled in the

California encephalitis project. *Clin. Infect. Dis.* 54, 899–904. doi: 10.1093/cid/cir1038

Granerod, J., Ambrose, H. E., Davies, N. W., Clewley, J. P., Walsh, A. L., Morgan, D., et al. (2010). Causes of encephalitis and differences in their clinical presentations in England: a multicentre, population-based prospective study. *Lancet Infect. Dis.* 10, 835–844. doi: 10.1016/S1473-3099(10)70222-X

Gurrera, R. J. (2018). Frequency and temporal sequence of clinical features in adults with anti-NMDA receptor encephalitis presenting with psychiatric symptoms. *Psychol. Med.* doi: 10.1017/S0033291718003665 [Epub ahead of print].

Hanson, E., Armbruster, M., Cantu, D., Andresen, L., Taylor, A., Danbolt, N. C., et al. (2015). Astrocytic glutamate uptake is slow and does not limit neuronal NMDA receptor activation in the neonatal neocortex. *Glia* 63, 1784–1796. doi: 10.1002/glia.22844

Incrocci, R. M., Paliarin, F., and Nobre, M. J. (2018). Prelimbic NMDA receptors stimulation mimics the attenuating effects of clozapine on the auditory electrophysiological rebound induced by ketamine withdrawal. *Neurotoxicology* 69, 1–10. doi: 10.1016/j.neuro.2018.08.013

Jiang, N., Guan, H., Lu, Q., Ren, H., and Peng, B. (2018). Features and prognostic value of quantitative electroencephalogram changes in critically ill and non-critically ill anti-NMDAR encephalitis patients: a pilot study. *Front. Neurol.* 9:833. doi: 10.3389/fneur.2018.00833

Jones, K. C., Schwartz, A. C., and Hermida, A. P. (2015). Kahn DA. A case of anti-NMDA receptor encephalitis treated with ECT. *J. Psychiatr. Pract.* 21, 374–380. doi: 10.1097/PRA.0000000000000100

Kay, S. R., Fiszbein, A., and Opler, L. A. (1987). The positive and negative syndrome scale (PANSS) for schizophrenia. *Schizophr. Bull.* 13, 261–276. doi: 10.1093/schbul/13.2.261

Koshiyama, D., Kirihara, K., Tada, M., Nagai, T., Fujioka, M., Ichikawa, E., et al. (2018). Electrophysiological evidence for abnormal glutamate-GABA association following psychosis onset. *Transl. Psychiatry* 8:211. doi: 10.1038/s41398-018-0261-0

Kuppuswamy, P. S., Takala, C. R., and Sola, C. L. (2014). Management of psychiatric symptoms in anti-NMDAR encephalitis: a case series, literature review and future directions. *Gen. Hosp. Psychiatry* 36, 388–391. doi: 10.1016/j.genhosppsych.2014.02.010

Lejuste, F., Thomas, L., Picard, G., Desestret, V., Ducray, F., Rogemond, V., et al. (2016). Neuroleptic intolerance in patients with anti-NMDAR encephalitis. *Neurol. Neuroimmunol. Neuroinflamm.* 3:e280. doi: 10.1212/NXI.0000000000000280

Liu, H., Jian, M., Liang, F., Yue, H., and Han, R. (2015). Anti-N-methyl-D-aspartate receptor encephalitis associated with an ovarian teratoma: two cases report and anesthesia considerations. *BMC Anesthesiol.* 15:150. doi: 10.1186/s12871-015-0134-5

Lopez-Munoz, F., and Alamo, C. (2011). Neurobiological background for the development of new drugs in schizophrenia. *Clin. Neuropharmacol.* 34, 111–126. doi: 10.1097/WNF.0b013e318215c2f7

Maneta, E., and Garcia, G. (2014). Psychiatric manifestations of anti-NMDA receptor encephalitis: neurobiological underpinnings and differential diagnostic implications. *Psychosomatics* 55, 37–44. doi: 10.1016/j.psym.2013.06.002

Mann, A., Machado, N. M., Liu, N., Mazin, A. H., Silver, K., and Afzal, K. I. (2012). A multidisciplinary approach to the treatment of anti-NMDA-receptor antibody encephalitis: a case and review of the literature. *J. Neuropsychiatry Clin. Neurosci.* 24, 247–254. doi: 10.1176/appi.neuropsych.11070151

Mythri, S. V., and Mathew, V. (2016). Catatonic syndrome in anti-NMDA receptor encephalitis. *Indian J. Psychol. Med.* 38, 152–154. doi: 10.4103/0253-7176.178812

Ramanathan, S., Mohammad, S. S., Brilot, F., and Dale, R. C. (2014). Autoimmune encephalitis: recent updates and emerging challenges. *J. Clin. Neurosci.* 21, 722–730. doi: 10.1016/j.jocn.2013.07.017

Rebollo, B., Perez-Zabalza, M., Ruiz-Mejias, M., Perez-Mendez, L., and Sanchez-Vives, M. V. (2018). Beta and gamma oscillations in prefrontal cortex during NMDA hypofunction: an *in vitro* model of schizophrenia features. *Neuroscience* 383, 138–149. doi: 10.1016/j.neuroscience.2018.04.035

Shi, W. X., Zhang, X. Y., Pun, C. L., and Bunney, B. S. (2007). Clozapine blocks D-amphetamine-induced excitation of dopamine neurons in the ventral tegmental area. *Neuropsychopharmacology* 32, 1922–1928. doi: 10.1038/sj.npp.1301334

Suh-Lailam, B. B., Haven, T. R., Copple, S. S., Knapp, D., Jaskowski, T. D., and Tebo, A. E. (2013). Anti-NMDA-receptor antibody encephalitis: performance evaluation and laboratory experience with the anti-NMDA-receptor IgG assay. *Clin. Chim. Acta* 421, 1–6. doi: 10.1016/j.cca.2013.02.010

Tachibana, N., Kinoshita, M., Saito, Y., and Ikeda, S. (2013). Identification of the N-methyl-D-aspartate receptor (NMDAR)-related epitope, NR2B, in the normal human ovary: implication for the pathogenesis of anti-NMDAR encephalitis. *Tohoku J. Exp. Med.* 230, 13–16. doi: 10.1620/tjem/230.13

Wang, J., Zhang, B., Zhang, M., Chen, J., Deng, H., Wang, Q., et al. (2017). Comparisons between psychiatric symptoms of patients with anti-NMDAR encephalitis and new-onset psychiatric patients. *Neuropsychobiology* 75, 72–80. doi: 10.1159/000480514

Warikoo, N., Brunwasser, S. J., Benz, A., Shu, H. J., Paul, S. M., Lewis, M., et al. (2018). Positive allosteric modulation as a potential therapeutic strategy in anti-NMDA receptor encephalitis. *J. Neurosci.* 38, 3218–3229. doi: 10.1523/JNEUROSCI.3377-17.2018

Warren, N., Siskind, D., and O'Gorman, C. (2018). Refining the psychiatric syndrome of anti-N-methyl-d-aspartate receptor encephalitis. *Acta Psychiatr. Scand.* 138, 401–408. doi: 10.1111/acps.12941

Xie, Y., and Huang, X. F. (2018). Commentary: GLYX-13 ameliorates schizophrenia-like phenotype induced by MK-801 in mice: role of hippocampal NR2B and DISC1. *Front. Mol. Neurosci.* 11:315. doi: 10.3389/fnmol.2018.00315

Zhou, Z., Li, X., Li, K., Xie, Z., Cheng, Z., Peng, W., et al. (2004). Simultaneous determination of clozapine, olanzapine, risperidone and quetiapine in plasma by high-performance liquid chromatography-electrospray ionization mass spectrometry. *J. Chromatogr. B Analyt. Technol. Biomed. Life Sci.* 802, 257–262. doi: 10.1016/j.jchromb.2003.11.037

Conflict of Interest Statement: The authors declare that the research was conducted in the absence of any commercial or financial relationships that could be construed as a potential conflict of interest.

frontiers in Pharmacology

ORIGINAL RESEARCH
published: 04 July 2019
doi: 10.3389/fphar.2019.00761

ABCB1 Gene Is Associated With Clinical Response to SNRIs in a Local Chinese Han Population

Xiao-Xiao Shan[1,2†], Yan Qiu[1,2†], Wei-Wei Xie[3], Ren-Rong Wu[1,2], Yan Yu[4], Hai-Shan Wu[1,2] and Le-Hua Li[1,2*]*

[1] Department of Psychiatry, the Second Xiangya Hospital, Central South University, Changsha, China, [2] Mental Health Institute of the Second Xiangya Hospital, Central South University, Chinese National Clinical Research Center on Mental Disorders, Chinese National Technology Institute on Mental Disorders, Human Key Laboratory of Psychiatry and Mental Health, Changsha, China, [3] Department of Psychiatry, Ningbo Kangning Hospital, Ningbo, China, [4] The People's Hospital of Hunan Province, Changsha, China

OPEN ACCESS

Edited by:
Pei Jiang,
Jining Medical University, China

Reviewed by:
Zunnan Huang,
Guangdong Medical College, China
Sarah Allegra,
University of Turin, Italy

***Correspondence:**
Hai-Shan Wu
wuhaishan@csu.edu.cn
Le-Hua Li
lilehua@csu.edu.cn

†These authors have contributed equally to this work.

Specialty section:
This article was submitted to Neuropharmacology, a section of the journal Frontiers in Pharmacology

Received: *17 August 2018*
Accepted: *12 June 2019*
Published: *04 July 2019*

Citation:
Shan X-X, Qiu Y, Xie W-W, Wu R-R, Yu Y, Wu H-S and Li L-H (2019) ABCB1 Gene Is Associated With Clinical Response to SNRIs in a Local Chinese Han Population. Front. Pharmacol. 10:761. doi: 10.3389/fphar.2019.00761

Background: The relation between the *ATP-binding cassette subfamily B member 1* (*ABCB1*) gene and major depressive disorder (MDD) has been studied in a local Chinese Han population. MDD is associated with the rs2032582 (*G2677T*) and rs1128503 (*C1236T*) single-nucleotide polymorphisms (SNPs) of *ABCB1* but not with rs1045642, rs2032583, rs2235040, and rs2235015. This study aims to explore the potential correlations of therapeutic responses with selective serotonin reuptake inhibitors (SSRIs) and serotonin-norepinephrine reuptake inhibitors (SNRIs) in a local Chinese Han population.

Methods: The study population included 292 patients with MDD. All patients were assessed at baseline and at first, second, fourth, and sixth weeks according to the 17-item Hamilton Rating Scale for Depression (HAM-D17) to determine their therapeutic responses to SSRIs and SNRIs.

Results: In the SSRI therapy group, the genotype or allele distribution of six SNPs was not significantly different between responders and nonresponders. In the SNRI therapy group, only rs2032583 was associated with a therapeutic response to SNRIs. The C allele of the *ABCB1* rs2032583 polymorphism was negatively correlated with therapeutic responses according to logistic regression analysis.

Conclusion: The *ABCB1 gene polymorphisms may* not be associated with therapeutic responses to SSRIs but not with SNRIs. The TT genotype of rs2032583 could be a predictive factor of improved treatment responses to SNRIs in the Chinese population. These findings should be replicated in future studies with larger patient groups.

Keywords: *ABCB1* gene, clinical response, SNRIs, major depressive disorder, local Chinese Han population

INTRODUCTION

The *ATP-binding cassette subfamily B member 1* (*ABCB1*) gene, a *multidrug resistance protein 1* (*MDR1*) gene, is located on the chromosomal region 7q21.1 and encodes p-glycoprotein (P-gp), which plays an important role in drug bioavailability and response to drugs. P-gp is a 1280-amino acid transporter and serves as a genetically polymorphic efflux transporter that removes foreign

substances from cells. This protein is expressed in the blood–brain barrier and protects the brain from drugs or neurotoxic substances, such as glucocorticoids and amyloid beta (de Klerk et al., 2013).

After treatment with regular doses of antidepressants, several patients with major depressive disorder (MDD) fail to obtain satisfactory therapeutic effects, and some patients even incur serious side effects. Among patients with MDD treated with a single antidepressant medication, only 50% of patients received adequate clinical response, and 30% of patients achieved recovery. There was a delayed response to symptom relief, ranging from 4 to 8 weeks. During this period, the risk of suicide increased significantly, whereas another 10% of the patients were ineffective for any kind of antidepressant medication (Weizman et al., 2012). *ABCB1* gene polymorphisms affect the ability of drugs to pass through the blood–brain barrier into the central nervous system, leading to inadequate drug concentrations in the brain (Uhr et al., 2008). *ABCB1* gene polymorphisms can predict the effect of antidepressant drugs that are *MDR1* substrates (Mihaljevic Peles et al., 2008; Sarginson et al., 2010).

Some drugs have been identified as substrates of P-gp. These drugs include nortriptyline, imipramine, escitalopram, amitriptyline, paroxetine, venlafaxine, and citalopram; and those with non-*ABCB1* substrates include bupropion, mirtazapine, and fluoxetine (Mihaljevic Peles et al., 2008). The *ABCB1* gene has single-nucleotide polymorphisms (SNPs) in the encoding regions. Variants such as C3435T (rs1045642), G2677T/A (rs2032582), and rs2032583 are the most commonly studied. Ameyaw et al. (2001) reported that *ABCB1* gene knockout mice possessed insufficient P-gp, leading to high drug concentrations in the blood and weak ability to eliminate drugs. The plasma concentrations of drugs in mice without the *ABCB1* gene were fivefold higher and seven- to 36-fold higher in the cerebrospinal fluid (Ameyaw et al., 2001).The concentrations of citalopram, venlafaxine, and d-venlafaxine in the brain of mutant mice were 3.0, 1.7, and 4.1 times higher than those in their wild-type littermates (Uhr et al., 2008). *In vivo* studies indicated that mdr1 ab (−/−) mutant mice possessed higher cerebral concentrations of paroxetine compared with those of mdr1ab (+/+) control mice. This finding suggests that P-gp could prevent paroxetine from entering into the brain (Uhr et al., 2003). Patients with the CC genotype of SNP rs2232583 in the *ABCB1* gene exhibited a higher response rate than that of patients with the TT genotype after 4 weeks of antidepressant treatment. However, in the non-P-gp substrate mirtazapine group, no difference in genotype was observed between remission and nonremission groups (Uhr et al., 2007). A similar result was also found by Sarginson et al. (2010). Moreover, Dong et al. reported that *ABCB1* gene polymorphisms rs4728697, rs2032583, and rs58898486 were associated with depression therapeutic response, and rs17064 was related to the curative effect of desipramine (Dong et al., 2009). *ABCB1* haplotypes and SNPs rs1045642, rs2032582, and rs2032583 affect responses to antidepressant treatment (Menu et al., 2010; Rosenhagen and Uhr, 2011; Lin et al., 2011; Singh et al., 2012; de Klerk et al., 2013).

A total of 292 Chinese patients with MDD and 208 unrelated control individuals from a local Chinese Han population were studied. There are few studies on the relationship between gene polymorphism of *ABCB1* and depression in the Chinese Han population; only a team of Taiwan scholars studied the relationship between the efficacy of escitalopram and gene polymorphism of *ABCB1* in patients with depression (Lin et al., 2011). The purpose of this study was to further understand the relationship between the two in the Chinese Han population and to provide a theoretical basis for individualized treatment.

MATERIALS AND METHODS

Subjects

A total of 292 patients with MDD and 208 healthy controls were included in this study. All participants were biologically unrelated and of Chinese Han ethnicity. The patients were diagnosed as having MDD as defined in the Axis I of the *Diagnostic and Statistical Manual of Mental Disorders, Fourth Edition, Text Revision* (DSM-IV-TR) and obtained scores ≥18 by the 17-item Hamilton Depression (HAM-D17) Rating Scale. A consensus diagnosis by at least two psychiatrists was made for each patient according to the DSM-IV criteria. Patients were not eligible to participate in the study if they have any other mental disorder according to DSM-IV-TR Axis I criteria, had major physical and neurological illnesses and sequelae of serious illness, or serious suicide attempts and behavior. Patients were also excluded if they had used electroconvulsive therapy or antipsychotic drugs with long-lasting effects within the last 6 months or any antipsychotic drugs within the last 4 weeks. The mean ages ± standard deviations of the patients and controls were 30.89 ± 10.92 years and 31.71 ± 8.25 years, respectively. Among the 292 patients with MDD, 71.6% had a single episode and 28.4% had recurrent episodes. The study protocol was approved by the Medical Ethics Committee of Second Xiangya Hospital, Central South University. Written informed consent was obtained from each patient after the study was explained.

Study Design

Eligible patients were treated with one of the five antidepressants (escitalopram, paroxetine, sertraline, duloxetine, and venlafaxine) for 6 weeks. All patients affirmed a regular dose intake of antidepressant drug per day during the study. The primary efficacy measurement was the change in the HAM-D17 total score from baseline until the end of the study period. Patients were evaluated at screening, baseline, and on the first, second, fourth, and sixth weeks of treatment. Response was defined as changes in the HAM-D17 total score of ≥50%.

Sample Collection and DNA Extraction

Peripheral blood samples were collected from ethylene diamine tetraacetic acid (EDTA)-containing tubes following the standard venipuncture technique. Genomic DNA was extracted from whole blood according to standard procedures. In this study,

we selected SNPs by the following three methods: literature reviewing, searching for Tag-SNP, and searching for functional variant sites by FAST SNP. Finally, we investigated the following six SNPs of the *ABCB1* gene: SNP1 (rs1045642) in exon 27, SNP2 (rs2032583) in intron 22, SNP3 (rs2032582) in exon 22, SNP4 (rs2235040) in intron boundary exon 21, SNP5 (rs1128503) in exon 13, and SNP6 (rs2235015) in intron 5 of the *ABCB1* gene. All genotyping experiments were carried out by Shanghai BioWing Applied Biotechnology Company (http://www.biowing.com.cn). The AxyPrep Blood Genomic DNA Kit was used for extraction, and the ligase detection reaction (LDR) was used to detect the six SNPs. The LDR was performed in 30 cycles at 95°C for 2 min, 94°C for 15 s, and 50°C for 25 s. Target DNA sequences were amplified using a multiplex polymerase chain reaction method. The fluorescent products of the LDR were differentiated using a 3730 ABI sequencer.

Haplotype and Statistical Analysis

Two independent sample *t*-test and χ^2 test were used to examine the clinical and demographic variables between responders and nonresponders. Genotype and allele frequency distributions were compared between the patients and controls and between the responders and nonresponders using the χ^2 test for independence. The observed genotype frequencies were compared with the predicted frequencies to investigate the concordance with the Hardy–Weinberg (H-W) equilibrium. Logistic regression analysis was used to estimate the therapeutic effect associated with each genotype; odds ratios with 95% confidence intervals were obtained. A $p < 0.05$ was considered to be statistically significant. The SHEsis online analysis software was used for linkage disequilibrium and haplotype analysis. Logistic regression analyses were performed using Statistical Package for the Social Sciences version 17.0 for Windows software (SPSS Inc., Chicago, IL). Adjustment for multiple comparisons was performed by Bonferroni correction.

RESULTS

Comparison of General Data Between Control and Case Groups

A total of 208 cases in the control group, 101 males and 107 females, the average age was 31.71 ± 8.25 years. There were 292 patients in the study group, 143 males and 149 females; the average age was 30.89 ± 10.92 years. There was no significant difference in gender and age composition between the control group and the case group ($\chi^2 = 0.008$, $p = 0.927$; $t = 0.954$, $p = 0.341$), which was comparable.

Hardy–Weinberg Balance Analysis of *ABCB1* Gene Polymorphisms in the Control and Case Groups

Among the 208 control subjects, the theoretical number of genotypes was 81, the number of genotypes of CT was 98, and the number of genotypes of TT was 29. H-W analysis showed that there was no significant difference in the actual genotype distribution of rsl045642 SNP and the theoretical gene type distribution under H-W equilibrium, $\chi^2 = 1.231$, $p = 0.267$. According to this method, the H-W balance test was performed on the polymorphic loci rsl045642, rs2032583, rs2032582, rs2235040, rsl128503, and rs2235015 between the control group and the case group. As shown in **Table 1**, the six SNPs loci in the control and case groups all met the H-W balance. The population selected in this study is representative of the Han population and suitable for genetic analysis.

Comparison of Clinical Features Among the Responders and Nonresponders

Among the 292 patients included in this study, 39 patients dropped out because of adverse effects ($n = 12$), withdrawal of consent ($n = 9$), contrary to the scheme ($n = 2$), and lost to

TABLE 1 | Equilibrium test of six single-nucleotide polymorphisms (SNPs) between the control group and the case group.

SNP	Genotype	Controls (n = 208)				Cases (n = 292)			
		Actual number	Theoretical number	χ^2	p	Actual number	Theoretical number	χ^2	p
rs1045642	CC	85	81	1.23	0.267	103	109	2.27	0.132
	CT	90	98			151	139		
	TT	33	29			38	44		
rs2032583	CT	22	21	0.65	0.42	38	37	1.41	0.234
	TT	186	187			254	255		
rs2032582	GG	78	72	3.39	0.065	86	78	3.44	0.06
	GT	88	101			130	146		
	TT	42	36			76	68		
rs2235040	AG	22	21	0.65	0.42	40	38	1.58	0.21
	GG	186	187			252	254		
rs1128503	CC	39	34	1.8	0.18	40	35	1.97	0.161
	CT	91	100			121	132		
	TT	78	73			131	126		
rs2235015	GG	187	188	0.59	0.44	254	255	1.414	0.23
	GT	21	20			38	37		

follow-up (n = 16); lastly, 253 patients completed the study. Clinical characteristics, use of drugs, and average drug doses between responders and nonresponders are shown in **Table 2**. No significant differences were found between the two groups according to the above indicators.

Genotype and Allele Frequencies in the Responders and Nonresponders

Genotype and allele distributions for the examined *ABCB1* gene SNPs in nonresponders and responders are shown in **Table 3**. The genotype and allelic distributions of rs1045642, rs2032582, rs2235040, rs1128503, and rs2235015 SNPs were not significantly different between nonresponders and responders. For rs2032583, genotype and allelic distributions significantly differed between the nonresponders and responders. The distribution of TT genotype and T allele frequency was higher in the responders than that in the nonresponders ($p = 0.027$, $p = 0.033$, respectively).

ABCB1 Gene Polymorphism Loci and Clinical Response to Selective Serotonin Reuptake Inhibitors

For SSRIs (sertraline, paroxetine, and escitalopram), no significant difference in genotype and allele frequency distribution was observed between the responders and nonresponders ($p > 0.05$) (**Table 4**).

The efficacy of SSRIs was examined for genotypes in the SSRI treatment group according to the HAM-D17 scores, decreased scores, and reducing score rate during the first, second, fourth, and sixth weeks. The HAM-D17 scores, decreased scores, and reducing score rate at the first, second, fourth, and sixth weeks were not significantly different among rs1045642, rs2032583, rs2032582, rs1128503, and rs2235015 ($p > 0.05$). HAM-D17 decreased scores and reducing score rate did not reveal any significant difference with rs2235040 (**Table 5**); however, a significant difference was observed for the genotype of rs2235040 in the HAM-D17 scores (F = 4.349, $p = 0.039$) (**Figure 1**).

ABCB1 Gene Polymorphism Loci and Clinical Response to Serotonin–Norepinephrine Reuptake Inhibitors

For SNRIs (venlafaxine and duloxetine), no significant difference was observed in the distribution of genotype and allele frequency of the rs1045642, rs2032582, rs2235040, rs1128503, and rs2235015 SNPs between the responders and nonresponders ($p > 0.05$). For rs2032583, the T allele frequency and TT genotype were significantly increased in the responders compared with those in the nonresponders ($p = 0.025$ and $p = 0.018$, respectively) (**Table 6**).

For SNRIs (venlafaxine and duloxetine), no significant difference was observed for the rs1045642, rs2032582, and rs1128503 SNPs in any of the HAM-D17 scores, decreased scores, and reducing score rate during the first, second, fourth, and sixth weeks ($p > 0.05$). For rs2032583, the HAM-D17 scores of TT genotype are lower than those of the CT genotype, whereas the decreased scores and reducing score rate are higher than those of the CT genotype (**Table 7** and **Figure 2**). The GG genotypes of rs2235040 have lower HAM-D17 scores than AG genotypes and higher decreased score and reducing score rate than AG genotypes (**Table 8** and **Figure 3**). For rs2235015, the GG genotypes have lower HAM-D17 scores than those of the GT genotypes and higher in decreased score and reducing score rate than those of the GT genotypes (**Table 9** and **Figure 4**).

DISCUSSION

We investigated the association among the six SNPs of the *ABCB1* gene and therapeutic response in the local Chinese Han population. Among the five SNPs, only one SNP (rs2032583)

TABLE 2 | Clinical features, dosage, and drug among the responders and the nonresponders.

		Nonresponders (n = 54)	Responders (n = 199)	F	p
Age (years)		31.19 ± 10.124	30.78 ± 11.484	1.089	0.298
Weight		60.778 ± 9.162	57.31 ± 9.3811	0.033	0.856
Education		12.17 ± 3.994	11.93 ± 3.968	0.274	0.601
Sex	Male *n* (%)	27(50)	98(49.2)	0.012	0.912
	Female *n* (%)	27(50)	101(50.8)		
Marriage	Spinsterhood *n* (%)	29(53.7)	105(52.8)	2.441	0.119
	Married *n* (%)	21(38.9)	86(43.2)		
	Divorced *n* (%)	3(5.6)	8(4.0)		
	Remarriage *n* (%)	1(1.9)	0(0.0)		
Drug	Escitalopram *n* (%)	19(35.2)	67(33.7)	5.713	
	Paroxetine *n* (%)	6(11.1)	44(22.1)		
	Venlafaxine *n* (%)	19(35.2)	46(23.1)		0.222
	Duloxetine *n* (%)	7(13.0)	34(17.1)		
	Sertraline *n* (%)	3(5.6)	8(4.0)		
Doses	Escitalopram	10.79 ± 2.507	10.67 ± 2.446	3.723	
	Paroxetine	21.67 ± 4.082	20.91 ± 2.908		
	Venlafaxine	157.89 ± 23.648	158.15 ± 23.602		0.055
	Duloxetine	60.0 ± 0.00	60.0 ± 0.00		
	Sertraline	58.33 ± 14.434	105.63 ± 52.470		

TABLE 3 | Genotype and allele frequencies of six SNPs of the ABCB1 gene in the nonresponders and the responders.

Genotype/ allele	Responders (n = 199)(%)	Nonresponders (n = 54)(%)	χ^2	*p*	OR (95% CI)		Adjust OR (95% CI)	
rs1045642								
CC	73 (36.7)	21 (38.9)			1		1	
CT	97 (48.7)	26 (48.1)	0.136	0.934	1.073	0.560–2.056	1.159	0.575–2.336
TT	29 (14.6)	7 (13.0)			1.192	0.457–3.105	0.826	0.301–2.270
C allele	243 (61.1)	68 (63.0)			1		1	
T allele	155 (38.9)	40 (37.0)	0.131	0.718	1.084	0.699–1.683	0.762	0.299–1.945
rs2032583								
TT	175 (87.9)	41 (75.9)			1		1	
CT	24 (12.1)	13 (24.1)	4.91	0.027*	0.433*	0.203–0.921	0.4*	0.179–0.896
T allele	374 (94.0)	95 (88.0)			1		1	
C allele	24 (6.0)	13 (12.0)	4.52	0.033*	0.469*	0.23–0.955	0.4*	0.179–0.8966
rs2032582								
GG	63 (31.7)	16 (29.6)			1		1	
GT	81 (40.7)	25 (46.3)	0.574	0.751	0.823	0.405–1.671	0.878	0.41–1.877
TT	55 (27.6)	13 (24.1)			1.074	0.475–2.431	0.917	0.386–2.178
G allele	207 (52.0)	57 (52.8)			1		1	
T allele	191 (48.0)	51 (47.2)	0.02	0.887	1.031	0.674–1.579	0.989	0.473–2.07
rs2235040								
AG	27 (13.6)	12 (22.2)			1		1	
GG	172 (86.4)	42 (77.8)	2.44	0.118	1.82	0.852–3.888	2.031	0.905–4.558
A allele	27 (6.8)	12 (11.1)			1		1	
G allele	371 (93.2)	96 (88.9)	2.236	0.135	1.718	0.839–3.515	2.047	0.919–4.56
rs1128503								
CC	26 (13.1)	8 (14.8)			1		1	
CT	79 (39.7)	27 (50.0)	2.554	0.279	0.9	0.364–2.225	0.905	0.348–2.352
C allele	131 (32.9)	43 (39.8)			1		1	
T allele	267 (67.1)	65 (60.2)	1.793	0.181	1.348	0.87–2.09	1.41	0.727–2.734
rs2235015								
GG	174 (87.4)	42 (77.8)			1		1	
GT	25 (12.6)	12 (22.2)	3.174	0.075	0.503	0.234–1.082	0.416	0.204–1.04
G allele	373 (93.7)	96 (88.9)			1		1	
T allele	25 (6.3)	12 (11.1)	2.924	0.087	0.536	0.26–1.108	0.530	0.21–1.01

**Statistically significant difference between the groups ($p < 0.05$).*
CI, confidence interval; OR, odds ratio.

differed in genotype and allele frequencies between the responders and nonresponders. In particular, the TT genotype of this SNP was significantly more common in the responders than that in the nonresponders. This finding suggests that the C allele of rs2032583 may be a risk factor for MDD. In the SSRI therapy group, no correlation was found between the six SNPs of the *ABCB1*gene and therapeutic response to SSRIs ($p > 0.05$). However, for the SNRI therapy group, only rs2032583 is associated with a therapeutic response to SNRIs in patients with MDD. The C allele of the *ABCB 1* gene SNP rs2032583 was negatively correlated with therapeutic response according to the logistic regression analyses. The genotype of *ABCB1* gene SNPs rs2235015 and rs2235040 were associated with decreased score and reducing score rate in the SNRIs therapy group, but because of the small sample size, there was no significant difference in the final effective and ineffective grouping. This finding indicated that *ABCB1* gene polymorphisms may not be associated with the treatment response to SSRIs, but with SNRIs. The TT genotype of the *ABCB1* gene SNP rs2032583 could be a predictive factor of improved treatment response to SNRIs. To our knowledge, this study is the first to report the genetic association of *ABCB1* gene polymorphism with therapeutic responses in a case-control design in Chinese Han people in Mainland China.

P-gp can restrict the entry of various substrates, such as antidepressants, from the bloodstream into the brain. Studies on *ABCB1* knockout animals have shown that *ABCB1*−/− mice possess higher intracerebral concentrations of escitalopram, trimipramine, amitriptyline, doxepin, venlafaxine, and paroxetine compared with those in wild-type mice (Uhr et al., 2000; Uhr et al., 2002; Uhr et al., 2003). Kato et al. (2008) reported a significant association of the nonsynonymous SNP *G2677T/A* (rs2032582) with treatment response to paroxetine in depressed patients. Moreover, the wild variant haplotype *3435C–2677G–1236T* is associated with poor response (Kato et al., 2008). In contrast, Nikisch et al. (2008) found that depressed patients harboring the *2677 GG/GT* genotype responded to escitalopram treatment significantly better than patients with the *2677TT* genotype and suggested that this polymorphism could be used as genetic markers for predicting treatment response to escitalopram treatment in MDD ($n = 15$). Uhr et al. (2008) showed that polymorphisms in the *ABCB1* gene predict the response to antidepressant treatment in depressed patients ($n = 133$) receiving

TABLE 4 | Genotype, allelic distribution of all genotyped single nucleotide polymorphisms among the treatment responders and nonresponders for selective serotonin reuptake inhibitor (SSRI) drugs group.

	Responders (*n* = 119) (%)	Nonresponders (*n* = 28) (%)	χ^2	*p*	OR (95% CI)	Adjust OR (95% CI)
rs1045642						
CC	42 (35.3)	9 (32.1)			1	1
CT	60 (50.4)	14 (50.0)	0.259	0.879	0.918 (0.364–2.317)	0.717 (0.255–2.02)
TT	17 (14.3)	5 (17.9)			0.729 (0.213–2.492)	0.389 (0.098–1.551)
C allele	144 (60.5)	32 (57.1)			1	1
T allele	94 (39.5)	24 (42.9)	0.213	0.644	0.87 (0.483–1.57)	0.479 (0.143–1.601)
rs2032583						
TT	106 (89.1)	24 (85.7)			1	1
CT	13 (10.9)	4 (14.3)	0.25	0.617	0.736 (0.221–2.455)	0.751 (0.205–2.747)
T allele	225 (94.5)	52 (92.9)			1	1
C allele	13 (5.5)	4 (7.1)	0.235	0.628	0.751 (0.235–2.397)	0.751 (0.205–2.747)
rs2032582						
GG	38 (31.9)	5 (17.9)			1	1
GT	53 (44.5)	14 (50.0)	2.352	0.309	0.498 (0.165–1.501)	0.336 (0.09–1.256)
TT	28 (23.5)	9 (32.1)			0.409 (0.124–1.355)	0.237 (0.057–0.984)
G allele	129 (54.2)	24 (42.9)			1	1
T allele	109 (45.8)	32 (57.1)	2.338	0.126	0.634 (0.352–1.14)	0.509 (0.189–1.37)
rs2235040						
AG	15 (12.6)	4 (14.3)			1	1
GG	104 (87.4)	24 (85.7)	0.056	0.813	1.156 (0.352–3.794)	1.129 (0.316–4.032)
A allele	15 (6.3)	4 (7.1)			1	1
G allele	223 (93.7)	52 (92.9)	0.052	0.82	1.144 (0.364–3.588)	1.129 (0.316–4.032)
rs1128503						
CC	16 (13.4)	2 (7.1)			1	1
CT	39 (32.8)	14 (50.0)	3.124	0.21	0.348 (0.071–1.711)	0.303 (0.057–1.627)
TT	64 (53.8)	12 (42.9)			0.667 (0.135–3.282)	0.483 (0.091–2.57)
C allele	71 (29.8)	18 (32.1)			1	1
T allele	167 (70.2)	38 (67.9)	0.115	0.735	1.114 (0.596–2.083)	1.224 (0.494–3.033)
rs2235015						
GG	106 (89.1)	24 (85.7)			1	1
GT	13 (10.9)	4 (14.3)	0.25	0.617	0.736 (0.221–2.455)	0.696 (0.191–2.543)
G allele	225 (94.6)	52 (92.9)			1	1
T allele	13 (5.5)	4 (7.1)	0.235	0.628	0.751 (0.235–2.397)	0.751 (0.235–2.397)

TABLE 5 | Rs2235040 and response to antidepressants.

		1 week	2 weeks	4 weeks	6 weeks	F	p
Decreased score	AG (*n* = 19)	1.42 ± 1.71	5.47 ± 5.28	12.47 ± 5.78	17.42 ± 5.27	0.147	0.702
	GG (*n* = 128)	1.93 ± 2.49	5.74 ± 4.57	11.75 ± 5.99	15.82 ± 6.37		
Reducing score rate (%)	AG (*n* = 19)	5.31 ± 6.43	20.74 ± 18.96	47.36 ± 19.63	67.3 ± 17.42	0.323	0.571
	GG (*n* = 128)	8.38 ± 11.31	24.50 ± 19.09	49.64 ± 22.97	67.04 ± 23.77		

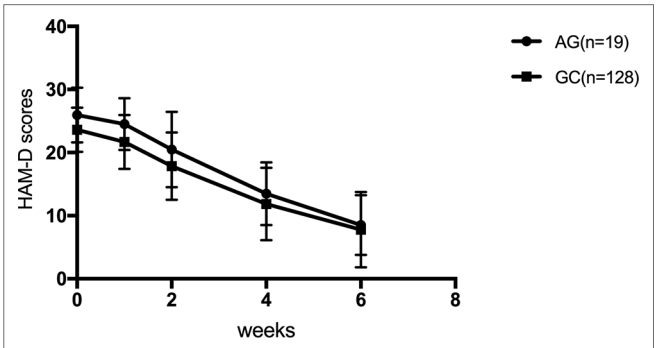

FIGURE 1 | Hamilton Rating Scale for Depression (HAM-D) scores at the first, second, fourth, and sixth week.

drugs that have been identified as substrates of P-gp (amitriptyline, paroxetine, venlafaxine, and escitalopram). However, Mihaljevic et al. (2008) found that MDR1 variants *G2677T* (rs2032582) and *C3435T* (rs1045642) are not associated with therapeutic response to paroxetine in patients with MDD (*n* = 127). Furthermore, Peters et al. (2008) did not find an association between *ABCB1C3435T*, *G2677T*, and *C1236T* polymorphisms and response and tolerance to citalopram in a large study sample (*n* = 831).

ABCB1 gene polymorphism loci mutation might cause the variation of P-gp, thereby increasing drug concentrations in the brain to improve therapeutic effects. The specific function of rs2032583 (intron 22) is not clear. Clinical research has found the association between rs2032583 and antidepressant effects. The wild-type allele of rs2032583 is T and the mutant allele is C.

TABLE 6 | Genotype, allelic distribution of all genotyped SNPs among the treatment responders and nonresponders for serotonin-norepinephrine reuptake inhibitors (SNRIs).

	Responders (*n* = 80) (%)	Nonresponders (*n* = 26) (%)	X^2	*p*	OR (95% CI)	Adjust OR (95% CI)
rs1045642						
CC	31 (38.8)	12 (46.2)			1	1
CT	37 (46.3)	12 (46.2)	1.059	0.589	1.194 (0.47–3.03)	1.898 (0.644–5.593)
TT	12 (15.0)	2 (7.7)			2.323 (0.451–11.96)	1.499 (0.263–8.537)
C allele	99 (61.9)	36 (69.2)			1	1
T allele	61 (38.1)	16 (30.8)	0.918	0.338	1.386 (0.71–2.709)	1.11 (0.208–5.932)
rS2032583						
TT	69 (86.3)	17 (65.4)			1	1
CT	11 (13.8)	9 (34.6)	5.581	0.018*	0.301* (0.108–0.842)	0.261* (0.085–0.807)
T allele	149 (93.1)	43 (82.7)				1
C allele	11 (6.9)	9 (17.3)	4.999	0.025*	0.353* (0.137–0.907)	0.261* (0.085–0.807)
rs2032582						
GG	25 (31.3)	11 (42.3)			1	1
GT	28 (35)	11 (42.3)	3.254	0.196	1.12 (0.414–3.028)	1.466 (0.473–4.541)
TT	27 (33.8)	4 (15.4)			2.97 (0.836–10.55)	2.502 (0.644–9.72)
G allele	78 (48.75)	33 (63.5)			1	1
T allele	82 (51.25)	19 (36.5)	3.405	0.065	1.826 (0.959–3.477)	2.07 (0.598–7.170)
rs2235040						
AG	12 (15)	8 (30.8)			1	1
GG	68 (85)	18 (69.2)	3.188	0.074	2.519 (0.895–7.086)	2.98 (0.96–9.245)
A allele	12 (7.5)	8 (15.4)			1	1
G allele	148 (92.5)	44 (84.6)	2.856	0.091	2.242 (0.862–5.832)	2.98 (0.96–9.245)
rs1128503						
CC	10 (12.5)	6 (23.1)			1	1
CT	40 (50.0)	13 (50.0)	2.083	0.353	1.846 (0.562–6.068)	1.838 (0.495–6.818)
TT	30 (37.5)	7 (26.9)			2.571 (0.698–9.476)	1.819 (0.422–7.839)
C allele	60 (37.5)	25 (48.1)			1	1
T allele	100 (62.5)	27 (51.9)	1.828	0.176	1.543 (0.821–2.901)	1.149 (0.385–3.43)
rs2235015						
GG	68 (85.0)	18 (69.2)			1	1
GT	12 (15.0)	8 (30.8)	3.188	0.074	0.397 (0.141–1.117)	0.983 (0.944–1.024)
G allele	148 (92.5)	44 (84.6)			1	1
T allele	12 (7.5)	8 (15.4)	2.856	0.091	0.446 (0.171–1.16)	0.446 (0.171–1.16)

**Statistically significant difference between the groups (p < 0.05).*

TABLE 7 | Rs2032583 and response to antidepressants.

		1 week	2 weeks	4 weeks	6 weeks	F	*p*
Decreased score	CT (*n* = 17)	1.40 ± 1.79	4.60 ± 4.11	10.3 ± 6.33	13.1 ± 6.51	5.949	0.016*
	TT (*n* = 130)	2.23 ± 2.67	7.33 ± 4.62	12.86 ± 5.28	16.36 ± 5.29		
Reducing score rate (%)	CT (*n* = 17)	5.49 ± 7.33	18.69 ± 17.19	40.50 ± 24.09	51.4 ± 24.0	9.241	0.003*
	TT (*n* = 130)	9.71 ± 11.76	31.29 ± 19.91	53.91 ± 20.80	68.8 ± 20.77		

**Statistically significant difference between the groups (p < 0.05).*

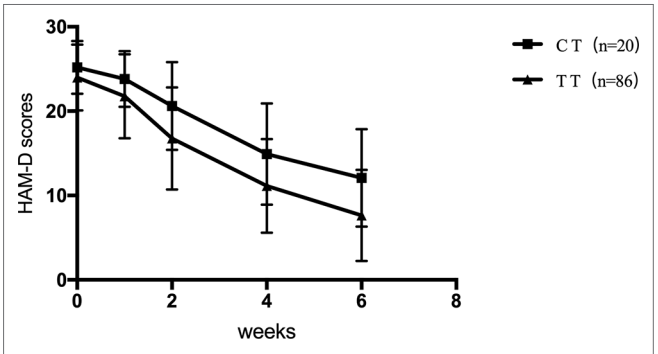

FIGURE 2 | HAM-D scores at the first, second, fourth, and sixth week (Rs2032583).

The study by Sarginson et al. (2010) showed that carriers of the C allele remitted faster than those with the TT genotype in the rs2032583 among paroxetine-treated patients and support the findings of Uhr et al. (2002) who found that rs2032583 genetic variants affected efficacy in patients of various ages treated with paroxetine and other *ABCB1* substrates (Uhr et al., 2008; Sarginson et al., 2010). By contrast, the two previous results are inconsistent with our present results. For rs2032583, we found that TT genotype has lower HAM-D17 scores than those of CT genotype and higher in decreased score and reducing score rate than those of CT genotype. This finding suggested that the TT genotype of rs2032583 is likely to be a predictive factor of better treatment response to SNRIs.

TABLE 8 | Rs2235040 and response to antidepressants.

		1 week	2 weeks	4 weeks	6 weeks	F	*p*
Decreased score	AG (*n* = 20)	1.45 ± 1.76	4.70 ± 4.07	10.75 ± 6.02	13.60 ± 6.06	4.288	0.041*
	GG (*n* = 86)	2.22 ± 2.68	7.30 ± 4.64	12.76 ± 5.41	16.24 ± 5.47		
Reducing score rate (%)	AG (*n* = 20)	5.74 ± 7.21	19.19 ± 17.07	42.75 ± 23.17	53.9 ± 22.57	6.64	0.011*
	GG (*n* = 86)	9.65 ± 11.80	31.18 ± 20.00	53.39 ± 21.33	68.22 ± 21.56		

**Statistically significant difference between the groups ($p < 0.05$).*

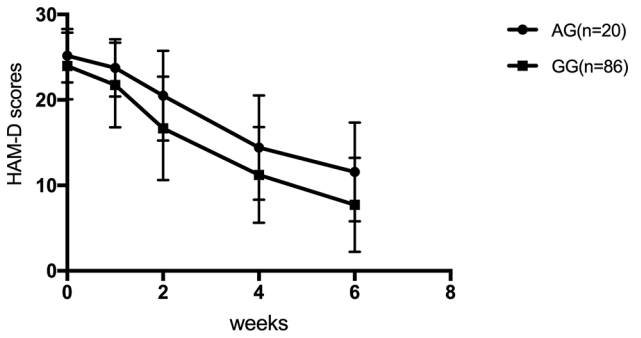

FIGURE 3 | HAM-D scores at the first, second, fourth, and sixth week (Rs2235040).

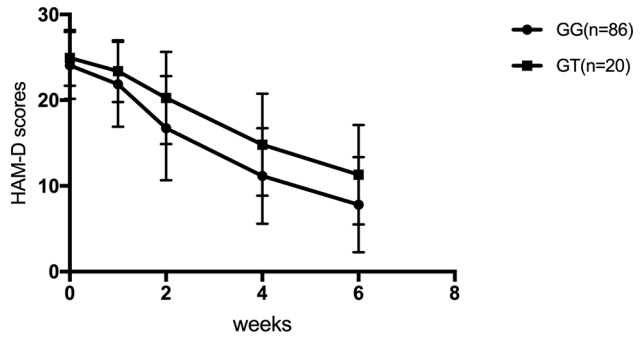

FIGURE 4 | HAM-D scores at the first, second, fourth, and sixth week (Rs2235015).

TABLE 9 | Rs2235015 and response to antidepressants.

		1 week	2 weeks	4 weeks	6 weeks	F	*p*
Decreased score	GG (*n* = 130)	2.20 ± 2.67	7.30 ± 4.64	12.90 ± 5.28	16.23 ± 5.42	4.93	0.029*
	GT (*n* = 17)	1.55 ± 1.85	4.70 ± 4.08	10.15 ± 6.25	13.65 ± 6.29		
Reducing score rate (%)	GG (*n* = 130)	9.53 ± 11.75	31.12 ± 20.0	53.96 ± 20.86	68.1 ± 21.32	7.151	0.009*
	GT (*n* = 17)	6.27 ± 7.82	19.44 ± 17.28	40.31 ± 23.73	54.4 ± 23.90		

**Statistically significant difference between the groups ($p < 0.05$).*

Whether the locus mutation manipulates the coding region of P-protein conformation remains to be further basic research. The rs2032583 locus mutation might change the dimensional conformation of P-gp by allowing entry of drugs and toxic substances into the brain simultaneously to exacerbate the symptoms. In addition, the locus mutation changes P-gp conformation and then stops the SNRIs into the brain but does not affect SSRI substrate. Furthermore, locus mutation may not change the conformation of P-gp. The positive results of SNRIs may be attributed to the small sample size, thereby causing false-positive results in the study. Foreign studies may have different results because of various factors such as race, region, environment, and diet.

Several limitations of the present study should be acknowledged. First, we did not distinguish the first and recurrence of depressive patients joining the patients' group. Regression analysis determines the total course of the disease and whether they accepted treatment; however, previous treatment had some influence on the overall response rate. Hence, the present study can only obtain a trend about differences. Second, the present study only selected the drugs that have been identified as substrates of P-gp. Future studies should include no-P-gp substrates such as mirtazapine. Third, genetic effect is slight because of the small sample size. A large sample size is needed to improve the power of the test. Fourth, many receptors are involved to determine the effect of antidepressant drugs; hence, a combination of gene should be considered. Larger and more homogenous samples will be included in our future research to improve the statistical power. Because there may be a delayed response to symptom relief, 6 weeks of treatment may not be sufficient to fully demonstrate the relationship between *ABCB1* gene and clinical response, and we consider extending the duration of efficacy observation in future studies.

ETHICS STATEMENT

The study protocol was approved by the Medical Ethics Committee of Second Xiangya Hospital, Central South University. Written informed consent was obtained from each patient after the study was explained.

AUTHOR CONTRIBUTIONS

X-XS and YQ contributed equally to this work, mainly responsible for essay writing and conducting the study. W-WX mainly participated in conducting the study. YY assisted the study. R-RW, H-SW and L-HL contributed to guide of conducting the study and essay writing.

FUNDING

This research was supported by National Natural Science Foundation of China (grant no. 81501163), National Natural Science Foundation of China (grant no. 81270019), National R&D Special Fund for Health Profession (grant no. 201002003), and National Science and Technology Major Projects for "Major New Drugs Innovation and Development" (2012ZX09303014-001).

REFERENCES

Ameyaw, M., Regateiro, F., Li, T., Liu, X., Tariq, M., Mobarek, A., et al. (2001). MDR1 pharmacogenetics: frequency of the C3435T mutation in exon 26 is significantly influenced by ethnicity. *Pharmacogenetics* 11 (3), 217–221. doi: 10.1097/00008571-200104000-00005

de Klerk, O. L., Nolte, I. M., Bet, P. M., Bosker, F. J., Snieder, H., Den Boer, J. A., et al. (2013). ABCB1 gene variants influence tolerance to selective serotonin reuptake inhibitors in a large sample of Dutch cases with major depressive disorder. *Pharmacogenomics J.* 13 (4), 349–353. doi: 10.1038/tpj.2012.16

Dong, C., Wong, M. L., and Licinio, J. (2009). Sequence variations of ABCB1, SLC6A2, SLC6A3, SLC6A4, CREB1, CRHR1 and NTRK2: association with major depression and antidepressant response in Mexican-Americans. *Mol. Psychiatry* 14 (12), 1105–1118. doi: 10.1038/mp.2009.92

Kato, M., Fukuda, T., Serretti, A., Wakeno, M., Okugawa, G., Ikenaga, Y., et al. (2008). ABCB1 (MDR1)gene polymorphisms are associated with the clinical response to paroxetine in patients with major depressive disorder. *Prog. Neuropsychopharmacol. Biol. Psychiatry* 15 (32), 398–404. doi: 10.1016/j.pnpbp.2007.09.003

Lin, K. M., Chiu, Y. F., Tsai, I. J., Chen, C. H., Shen, W. W., Liu, S. C., et al. (2011). ABCB1 gene polymorphisms are associated with the severity of major depressive disorder and its response to escitalopram treatment. *Pharmacogenet. Genomics* 21 (4), 163–170. doi: 10.1097/FPC.0b013e32833db216

Menu, P., Gressier, F., Verstuyft, C., Hardy, P., Becquemont, L., and Corruble, E. (2010). Antidepressants and ABCB1 gene C3435T functional polymorphism: a naturalistic study. *Neuropsychobiology* 62 (3), 193–197. doi: 10.1159/000319361

Mihaljevic Peles, A., Bozina, N., Saqud, M., and Roinic Kuzman, M. (2008). Lovric M. MDR1 gene polymorphism: therapeutic response to paroxetine among patients with major depression. *Prog. Neuropsychopharmacol. Biol. Psychiatry* 32 (6), 1439–1444. doi: 10.1016/j.pnpbp.2008.03.018

Nikisch, G., Eap, C. B., and Baumann, P. (2008). Citalopram enantiomers in plasma and cerebrospinal fluid of ABCB1 genotyped depressive patients and clinical response: A pilot study. *Pharmacol, Res.* 58 (5-6), 344–347. doi: 10.1016/j.phrs.2008.09.010

Peters, E. J., Slager, S. L., Kraft, J. B., Jenkins, G. D., Reinalda, M. S., McGrath, P. J., et al. (2008). Pharmacokinetic genes do not influence response or tolerance to citalopram in the STAR*D sample. *PLoS One* 3 (4), e1872. doi: 10.1371/journal.pone.0001872

Rosenhagen, M. C., and Uhr, M. (2011). The clinical impact of ABCB1 polymorphisms on the treatment of psychiatric diseases. *Curr. Pharm. Des.* 17 (26), 2843–2851. doi: 10.2174/138161211797440140

Sarginson, J. E., Lazzeroni, L. C., Ryan, H. S., Ershoff, B. D., Schatzberg, A. F., and Murphy, G. M., Jr. (2010). ABCB1 (MDR1) polymorphisms and antidepressant response in geriatric depression. *Pharmacogenet. Genomics* 20 (8), 467–775. doi: 10.1097/FPC.0b013e32833b593a

Singh, A. B., Bousman, C. A., Ng, C. H., Byron, K., and Berk, M. (2012). ABCB1 polymorphism predicts escitalopram dose needed for remission in major depression. *Transl. Psychiatry* 2, e198. doi: 10.1038/tp.2012.115

Uhr, M., Grauer, M. T., Yassouridis, A., and Ebinqer, M. (2007). Blood-brain barrier penetration and pharmacokinetics of amitriptyline and its metabolites in p-glycoprotein (abcb1ab) knock-out mice and controls. *J. Psychiatr. Res.* 41 (1–2), 179–188. doi: 10.1016/j.jpsychires.2005.10.005

Uhr, M., Grauer, M. T., and Holsboer, F. (2003). Differential enhancement of antidepressantpenetration into the brain in mice with abcb1ab (mdr1ab) P-glycoproteingene disruption. *Biol. Psychiatry* 54 (8), 840–846. doi: 10.1016/S0006-3223(03)00074-X

Uhr, M., Holsboer, F., and Müller, M. B. (2002). Penetration of endogenous steroid hormones corticosterone, cortisol, aldosterone and progesterone into the brain is enhanced in mice deficient for both mdr1a and mdr1b P-glycoproteins. *J. Neuroendocrinol.* 14, 753–759. doi: 10.1046/j.1365-2826.2002.00836.x

Uhr, M., Steckler, T., Yassouridis, A., and Holsboer, F. (2000). Penetration of amitriptyline, but not of fluoxetine, into brain is enhanced in mice with blood-brain barrier deficiency due to mdr1a P-glycoprotein gene disruption. *Neuropsychopharmacology* 22, 380–387. doi: 10.1016/S0893-133X(99)00095-0

Uhr, M., Tontsch, A., Namendorf, C., Ripke, S., Lucae, S., Ising, M., et al. (2008). Polymorphisms in the drug transporter gene ABCB1 predictantidepressant treatment response in depression. *Neuron* 57 (2), 203–209. doi: 10.1016/j.neuron.2007.11.017

Weizman, S., Gonda, X., Dome, P., and Faludi, G. (2012). Pharmacogenetics of antidepressive drugs: a way towards personalized treatment of major depressive disorder. *Neuropsychopharmacol. Hung.* 14 (2), 87–101. doi: 10.5706/nph201206002

Conflict of Interest Statement: The authors declare that the research was conducted in the absence of any commercial or financial relationships that could be construed as a potential conflict of interest.

frontiers in Neuroscience

ORIGINAL RESEARCH
published: 08 August 2019
doi: 10.3389/fnins.2019.00834

Revealing Antidepressant Mechanisms of Baicalin in Hypothalamus Through Systems Approaches in Corticosterone-Induced Depressed Mice

*Kuo Zhang, Meiyao He, Fan Wang, Haotian Zhang, Yuting Li, Jingyu Yang and Chunfu Wu**

Department of Pharmacology, Shenyang Pharmaceutical University, Shenyang, China

Baicalin, the main active flavonoid constituent of *Scutellaria baicalensis* Georgi, has been reported to exert antidepressant effects. Hypothalamic-pituitary-adrenal (HPA) axis plays important roles in depression. However, antidepressant effect and mechanism of baicalin on HPA axis in hypothalamus are still unknown. In present study, we find baicalin significantly attenuates the increase of immobility time in tail suspension and forced swimming, improves the decrease of spending time in open arms, and restores the aberrant negative feedback of HPA axis in chronic corticosterone (CORT)-induced depressed mice. Moreover, proteomics finds 370 differentially expressed proteins after baicalin treatment, including 114 up-regulation and 256 down-regulation in hypothalamus. Systems biology analysis indicates the functions of differentially expressed proteins focus on phosphoserine binding and phosphorylation, especially participate in GR signaling pathway. Finally, our findings demonstrate that baicalin normalizes hypothalamic GR nuclear translocation via reducing GR phosphorylation to remodel negative feedback of HPA axis in CORT-induced mice.

Keywords: baicalin, hypothalamus, proteomics, depression, glucocorticoid receptor

OPEN ACCESS

Edited by:
Pei Jiang,
Jining Medical University, China

Reviewed by:
Hui Wang,
Wuhan University, China
Neil M. Fournier,
Trent University, Canada

****Correspondence:***
Chunfu Wu
wucf@syphu.edu.cn;
zhangkuosyphu@163.com

Specialty section:
This article was submitted to Neuropharmacology, a section of the journal Frontiers in Neuroscience

Received: *09 May 2019*
Accepted: *26 July 2019*
Published: *08 August 2019*

Citation:
Zhang K, He M, Wang F, Zhang H, Li Y, Yang J and Wu C (2019) Revealing Antidepressant Mechanisms of Baicalin in Hypothalamus Through Systems Approaches in Corticosterone-Induced Depressed Mice. Front. Neurosci. 13:834. doi: 10.3389/fnins.2019.00834

INTRODUCTION

Depression is the kind of affective disorder, which seriously threatens human health and brings heavy social burdens (McEwen et al., 2015). Most antidepressant drugs are developed according to the phenomenon which deficient monoamine neurotransmitters are discovered in depressive patients (Boku et al., 2018). However, patients are usually unsatisfied with the therapeutic effects due to the delayed actions and side effects (Duman and Aghajanian, 2012). Many studies show that the abnormal HPA axis participates in depression (Anacker et al., 2011b). Especially, hypothalamus has important modulatory function in brain, which controls the activity of hypothalamic-pituitary-adrenal (HPA) axis and responds to the stress (Myers et al., 2014). However, the role of hypothalamus in abnormal HPA axis and the molecular mechanisms of antidepressant drug in hypothalamus have not been definitely illuminated. Proteomics is new-style development of biological systems, which possessed the powerful capacity to analyze proteins by high throughput

(Frantzi et al., 2019). Moreover, proteomics is also the powerful tool to explore the complex system of disease and the therapeutic target of new drug (Jiang et al., 2019).

Baicalin, the main active flavonoid constituent of *Scutellaria baicalensis* Georgi, which has reported to exert multiple pharmacological actions, including anti-inflammatory, anti-tumor, anti-ischemia (Li-Weber, 2009; Hou et al., 2012; Luan et al., 2019). Recent studies show baicalin has definite antidepressant-like activity which can improve olfactory functions by inhibiting APPL2-mediated glucocorticoid receptor (GR) hyperactivity (Gao et al., 2018). However, the effects of baicalin on HPA axis are still unknown. The definite molecular targets of baicalin on HPA axis in hypothalamus need to be further investigated.

In the present study, our results demonstrate that baicalin remarkably improves chronic corticosterone (CORT)-induced various depression-like behaviors and restores the negative feedback of HPA axis. Proteomics and systems biology indicate that the molecular mechanisms of baicalin on negative feedback of HPA axis involve normalizing GR nuclear translocation via regulating GR phosphorylation in hypothalamus. Our findings provide the new perspective on molecular targets of baicalin and will facilitate its application in clinic.

MATERIALS AND METHODS

Ethics Statement

Adult C57BL/6 male were supplied by the Experimental Animal Center of Shenyang Pharmaceutical University [License number: SYXK (Liao), 2014-0004]. This study was carried out in accordance with the principles of National Institutes of Health Guide for the Care and Use of Laboratory Animals (Publication No. 85-23). All efforts were made to minimize suffering. The protocol was approved by the local ethic committee of Shenyang Pharmaceutical University.

Animals, Drugs, and Biochemical Reagents

Adult 8 week old C57BL/6 male mice weighing 18–22 g are supplied by the Experimental Animal Centre of Shenyang Pharmaceutical University. Animals are fed in standardized environment of 12 h light and dark cycle, with room temperature at 22 ± 2°C. Mice are given free access to food and water, adapted for 7 days before experiment.

Baicalin (purity >99%) is purchased Nanjing Zelang Medical Technology Company Limited in China. The mouse anti-GR (ab2768), anti-phospho-GR (S203, ab195703), anti-phospho-GR (S226, ab195789) are purchased from Abcam. The anti-phospho-GR (S211, 4161) is purchased from CST. The anti-β-actin (sc-47778) is purchased from Santa Cruz. The rabbit anti-Lamin B1 (12987-1-AP) is purchased from Proteintech.

Group and Drug Treatment

A total of 90 mice are randomly assigned to six groups (n = 15/group), including control group, CORT group, baicalin (40, 80, and 160 mg/kg) group, and fluoxetine (18 mg/kg) group. Among them, eight mice randomly selected from each group are used in behavioral testing. Four mice randomly selected from each group are used in western blot analysis. Three mice randomly selected from each group are used in proteomic analysis. The mice of western blot analysis and proteomic analysis are not used in behavioral testing to avoid behavior influence. The doses of baicalin in this study according to our previous study (Zhang et al., 2016). The procedure of CORT administration is performed as previously described (Wu et al., 2013). In brief, mice are injected subcutaneously with CORT (40 mg/kg, Tokyo Chemical Industry) which is dissolved in saline (0.45% Hydroxypropyl-β-Cyclodextrin, Sigma) between 8:00 am and 10:00 am for 8 weeks. Pharmacological treatment started in the 4th week after the beginning of the CORT protocol. Baicalin and fluoxetine are administrated by gastric gavages 30 min prior to the corticosterone injection until the end of the experiment. Detailed experimental procedure is showed in **Figure 1**.

Tail Suspension Test

Tail suspension test is executed according to previous study (Steru et al., 1985). The mice are respectively, pasted on the suspension instrument at 1 cm from the tip of the tail with the medical adhesive strip. The behavior of mice is recorded by the high-definition camera for 6 min. In brief, the mice are firstly adaptively suspended for 2 min, and then accumulated the immobility time for remaining 4 min. The video is analyzed by video traceable system (Ethovision Vision-XT 8.0).

Forced Swimming Test

Forced swimming test is executed according to previous study (Porsolt et al., 1978). The mice are respectively, placed in a plexiglass cylinder (height 40 cm, diameter 12 cm) for 6 min, which is filled at the depth of 10 cm with 23 ± 2°C water. The behavior of mice is recorded and observed by the high-definition camera. In brief, the mice are firstly adapted for 2 min in the water, and then accumulated the immobility time for remaining 4 min. The video is analyzed by video traceable system (Ethovision Vision-XT 8.0).

Elevated Plus Maze

Elevated plus maze is executed according to previous study with some modifications (Nollet et al., 2012). The mice are placed in the center of the maze, and their heads are orientated to the open arm, and the accumulated time of the mice entered in the arms is recorded for 5 min. The behavior of mice is recorded and observed by the high-definition camera. The video is analyzed by video traceable system (Ethovision Vision-XT 8.0).

Dexamethasone Suppression Test

Eight mice randomly selected from each group are used in this test. In brief, mice are intraperitoneally injected with dexamethasone (0.1 mg/kg in 0.9% NaCl, n = 4) or saline (0.9% NaCl, n = 4). Then, mice are suffered by the stressor after 30 min under dexamethasone or saline treatment. Finally, mice are anesthetized and serum are collected for serum

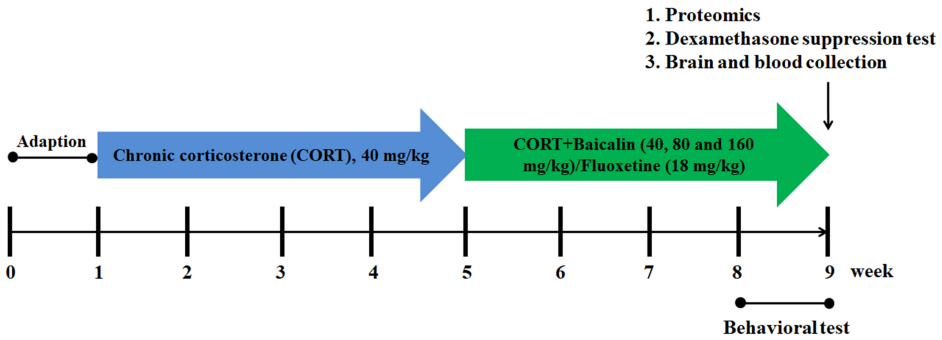

FIGURE 1 | Schematic representation of the experimental procedure.

corticosterone analyses after 120 min under dexamethasone or saline treatment. The rate of DEX-induced CORT suppression was calculated as a ratio of the amount of the level of corticosterone under dexamethasone treatment to the level of corticosterone under saline treatment: the rate of DEX-induced CORT suppression (%) = the level of corticosterone under dexamethasone treatment/the level of corticosterone under saline treatment.

Measurement of Serum Corticosterone

Blood samples are separated by refrigerated centrifuge (4000 rpm, 5 min). Serum corticosterone is measured by ELISA kits according to the operating guide.

Western Blot Analysis

Four mice randomly selected from each group are used in this test. The hypothalamus is homogenized in cold RIPA buffer containing 1 mM PMSF, 1 mM NaF and 1 mM Na_3VO_4 for 30 min. The samples are centrifuged at 12000 rpm for 20 min at 4°C. The concentration of protein is detected by bicinchoninic acid method. Then, denatured proteins (20–25 ug) are separated by 12% SDS-PAGE and transferred to PVDF membranes (Millipore). The membranes are steeped with 5% non-fat milk for 1 h, then incubated with primary antibody at 4°C overnight and appropriate secondary antibody at room temperature for 60 min. Finally, membranes are visualized and analyzed by Image J software.

Proteomics and Systems Biology Analysis

In present study, we tested three doses of baicalin (40, 80, and 160 mg/kg) in several behavioral testing and confirmed that 160 mg/kg was the best effective dose of baicalin on depression. As a consequence, we chose the best effective dose 160 mg/kg of baicalin to analyze quantitative proteomics by iTRAQ. Three mice randomly selected from each group are used in this test. At the end of experiment, 1 h after baicalin/CORT administration, mice were euthanized and sacrificed, then hypothalamus was quickly isolate. The samples are homogenized by lysis buffer and centrifuged. The supernatant is filtered and digested. iTRAQ reagent (AB SCIEX) is applied to label the peptide mixture. The peptide mixture is fractionated by SCX chromatography. LC-MS/MS analysis is operated by Q Exactive mass spectrometer. Detailed conditions are executed according to our previous study. Systems biology analysis contains gene ontology (GO) annotation and enrichment analysis, clustering analysis and protein-protein interaction analysis. In GO annotation, the functions of proteins are analyzed by cellular component, molecular function, and biological process. In clustering analysis, hierarchical clustering is carried out by euclidean distance algorithm and average linkage clustering algorithm. In protein-protein interaction analysis, the database of STRING is used. The importance of the node can be evaluated by degree of node in protein-protein interaction network.

Statistical Analyses

All data are analyzed by SPSS 22.0 and expressed as the mean ± SEM. Data are analyzed by one-way ANOVA followed by *post hoc* Fisher's LSD test. $P < 0.05$ is considered to be statistically significant.

RESULTS

Effects of Baicalin on Depression-Like Behaviors in CORT-Induced Mice

It had been demonstrated that chronic CORT could induce multiple anxiety/depression-like behaviors in mice. Therefore, we first verified the establish of CORT-induced depression model, and then assessed the protective effects of baicalin in CORT-induced mice. The results showed that the immobility time in tail suspension test and forced swimming test was increased by chronic CORT ($P = 0.024$, $P = 0.002$), while baicalin (tail suspension test, $P = 0.049$, $P = 0.003$ and $P = 0.0011$; forced swimming test, $P = 0.046$, $P = 0.006$, and $P = 0.002$) and fluoxetine treatment could recover this enhancement (**Figures 2A,B**). In elevated plus maze test (**Figure 2E**), the spending time of mice in open arms was decreased by chronic CORT ($P = 0.003$), but application of baicalin ($P = 0.037$, $P = 0.007$, and $P = 0.035$) and fluoxetine could recover this decline (**Figure 2C**). These data indicate that baicalin has definite antidepressant effect in CORT-induced mice.

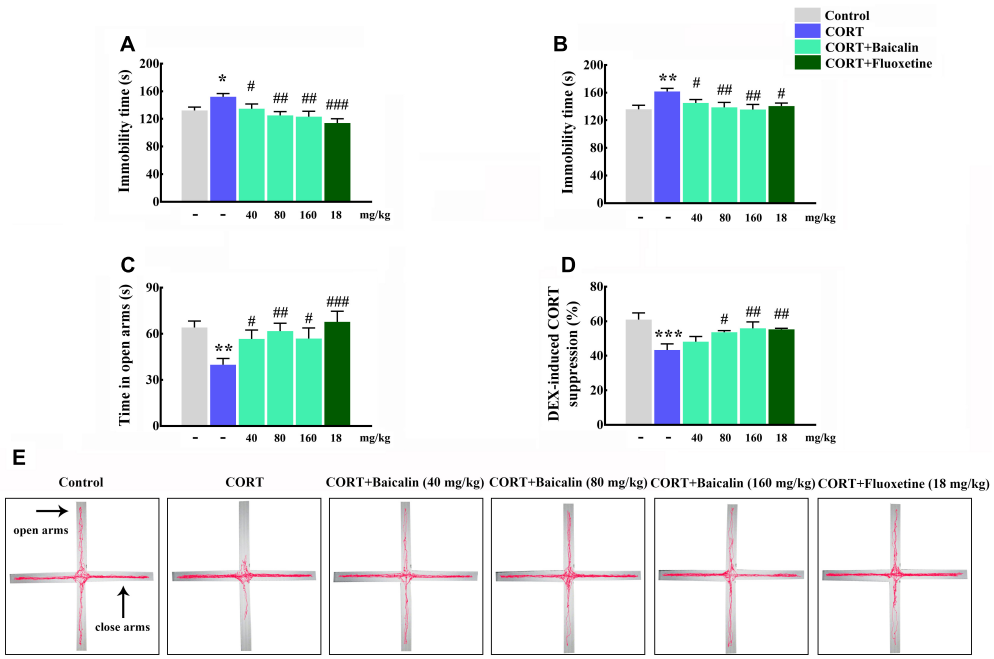

FIGURE 2 | Effects of baicalin on tail suspension test **(A)**, forced swimming test **(B)**, elevated plus maze **(C)**, and DEX-induced corticosterone suppression **(D)** in CORT-induced mice. Representative movement tracks in the elevated plus maze are showed in **(E)**. Data are expressed as means ± SEM (n = 8–12 mice/group). $^{*}P < 0.05$, $^{**}P < 0.01$, and $^{***}P < 0.001$ vs. control. $^{\#}P < 0.05$, $^{\#\#}P < 0.01$, and $^{\#\#\#}P < 0.001$ vs. CORT model.

Effects of Baicalin on Negative Feedback of HPA Axis in CORT-Induced Mice

Next, in order to explore potential mechanism of baicalin, the negative feedback of HPA axis was assessed by DEX suppression test. The results showed that the ratio of DEX-induced serum corticosterone suppression was decreased by chronic CORT (**Figure 2D**, P = 0.0004). On the contrary, the reducing of DEX-induced serum CORT suppression could be reversed by baicalin (P = 0.023, P = 0.007) and fluoxetine treatment (**Figure 2D**). These data suggest that baicalin has definite regulatory effect on the abnormal negative feedback of HPA axis.

Proteomics and Systems Biology Uncover Molecular Mechanisms of Baicalin in Hypothalamus in CORT-Induced Mice

In order to reveal the precise molecular mechanisms of baicalin on negative feedback of HPA axis, isobaric tags for relative and absolute quantification (iTRAQ) quantitative proteomics was used to assess the hypothalamic differentially expressed proteins after baicalin treatment in CORT-induced mice. A total of 4776 proteins were confirmed by high reliability at 1% false discovery rate (**Figure 3A**). Then, further analysis found 370 differentially expressed proteins after baicalin treatment, including 114 up-regulation and 256 down-regulation (**Figure 3B**). The detailed information of differentially expressed proteins was showed in **Supplementary Table S1**. Then, to verify the veracity of differentially expressed proteins, hierarchical clustering analysis was used. The result showed that differentially expressed proteins after baicalin and chronic CORT treatment were separated into two obvious distinguishing branches (**Figure 3C**). It is definitely indicated that these proteins have distinct expression between baicalin and chronic CORT group.

Moreover, to further uncover the function of differentially expressed proteins, differentially expressed proteins were assessed by GO functional annotations and enrichment analysis. In biological process, differentially expressed proteins mainly involved cellular process, single-organism process, and metabolic process (**Figure 4A**). In molecular function, differentially expressed proteins mainly involved binding and catalytic activity (**Figure 4A**). In cellular component, differentially expressed proteins mainly involved cell, organelle and membrane (**Figure 4A**). Then, GO enrichment showed that positive regulation of biological process, positive regulation of metabolic process, positive regulation of phosphorylation, and nuclear pore complex might be the chief functions of differentially expressed proteins (**Figure 4B**). Next, protein-protein interaction analysis was used to predict potential molecular targets of baicalin by STRING (**Figure 5**). According to the degree of nodes, the name, molecular function and biological process of high degree nodes were showed in **Supplementary Table S2**. Among them, a large number of molecular function and biological process indicated that GR signaling pathway, especially GR binding, phosphoserine binding and protein phosphorylation, and might be the molecular targets of baicalin on negative feedback of HPA axis in hypothalamus.

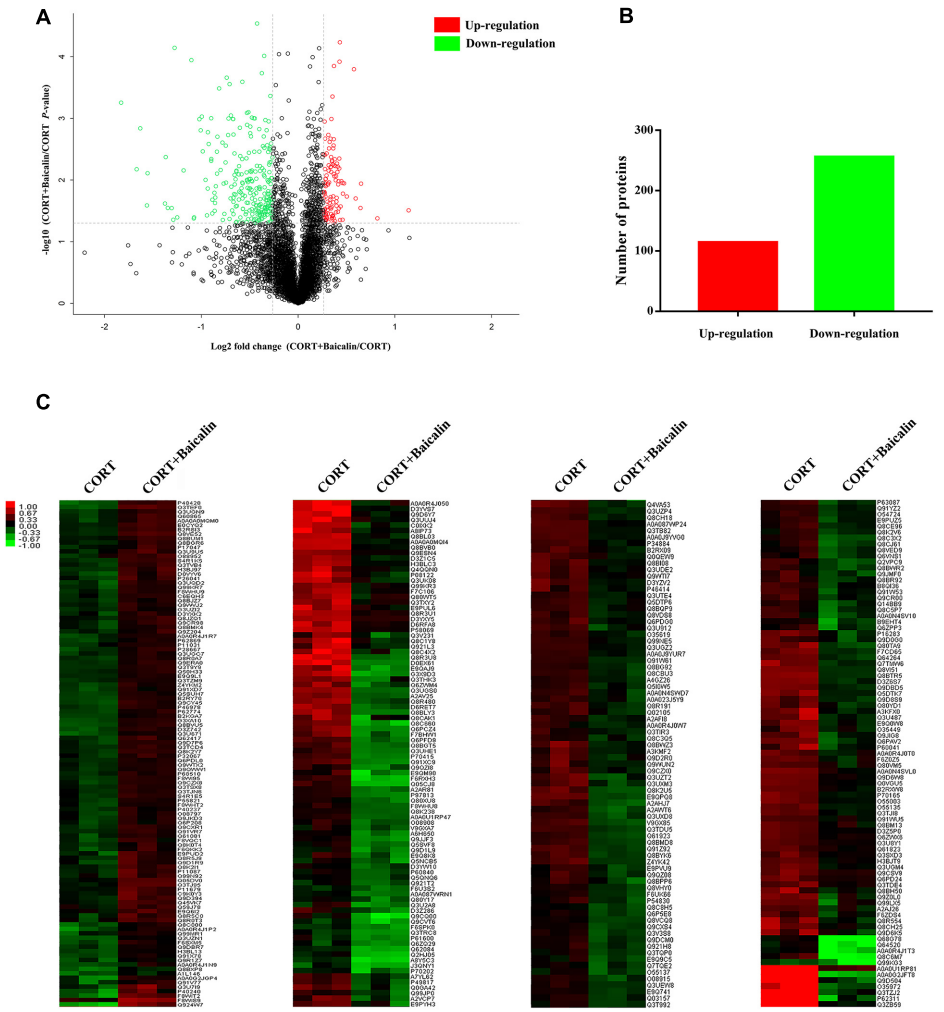

FIGURE 3 | Volcano plot **(A)**, quantitative analysis **(B)**, and hierarchical clustering **(C)** of differentially expressed proteins after baicalin treatment in CORT-induced mice. The log2-transformed value of cluster analysis was showed by red-green color scale **(C)**. Red meant high expression and green meant low expression.

Effects of Baicalin on Hypothalamic GR Nuclear Translocation and Phosphorylation in CORT-Induced Mice

According to the results of proteomics and systems biology, we focus on the level of GR, GR nuclear translocation and phosphorylation in hypothalamus (**Figure 6A**), which might be antidepressant molecular targets of baicalin. Our results showed that the level of total GR in hypothalamus had no change under chronic CORT, baicalin or fluoxetine treatment (**Figure 6B,** $P = 0.658$). It was noteworthy that the level of GR in cytoplasm was decreased ($P = 0.007$) and the level of GR in nucleus was increased by chronic CORT (**Figure 6C**, $P < 0.001$). The decline of GR in cytoplasm could be improved by baicalin ($P = 0.0101$, $P = 0.012$, and $P = 0.008$), but fluoxetine had no effect on this decline (**Figure 6C**). In addition, the enhancement of GR in nucleus could be decreased by both baicalin ($P = 0.002$, $P = 0.002$) and fluoxetine treatment (**Figure 6D**). Moreover, the phosphorylation status of the crucial serine residues was detected, which could play the important role in regulating GR nuclear translocation. The level of pSer203 and pSer211 in cytoplasm was increased by chronic CORT ($P = 0.0079$, $P = 0.0081$), and this enhancement could be decreased by baicalin (pSer203, $P = 0.011$, $P = 0.02$, and $P = 0.004$; pSer211, $P = 0.012$, $P = 0.039$, and $P = 0.004$) and fluoxetine treatment (**Figures 6E,F**). The pSer226 level in nucleus was decreased by chronic CORT ($P = 0.008$), but no effects were observed by baicalin and fluoxetine treatment (**Figure 6G**). Above data indicate that baicalin can recover abnormal GR nuclear translocation by regulating GR phosphorylation.

DISCUSSION

Depression is a common affective disorder, which people persistently feel loneliness and sadness. Although depression seriously threatens human health, the pathophysiological mechanism of depression is still unknown (Blier, 2016). Clinical studies find that

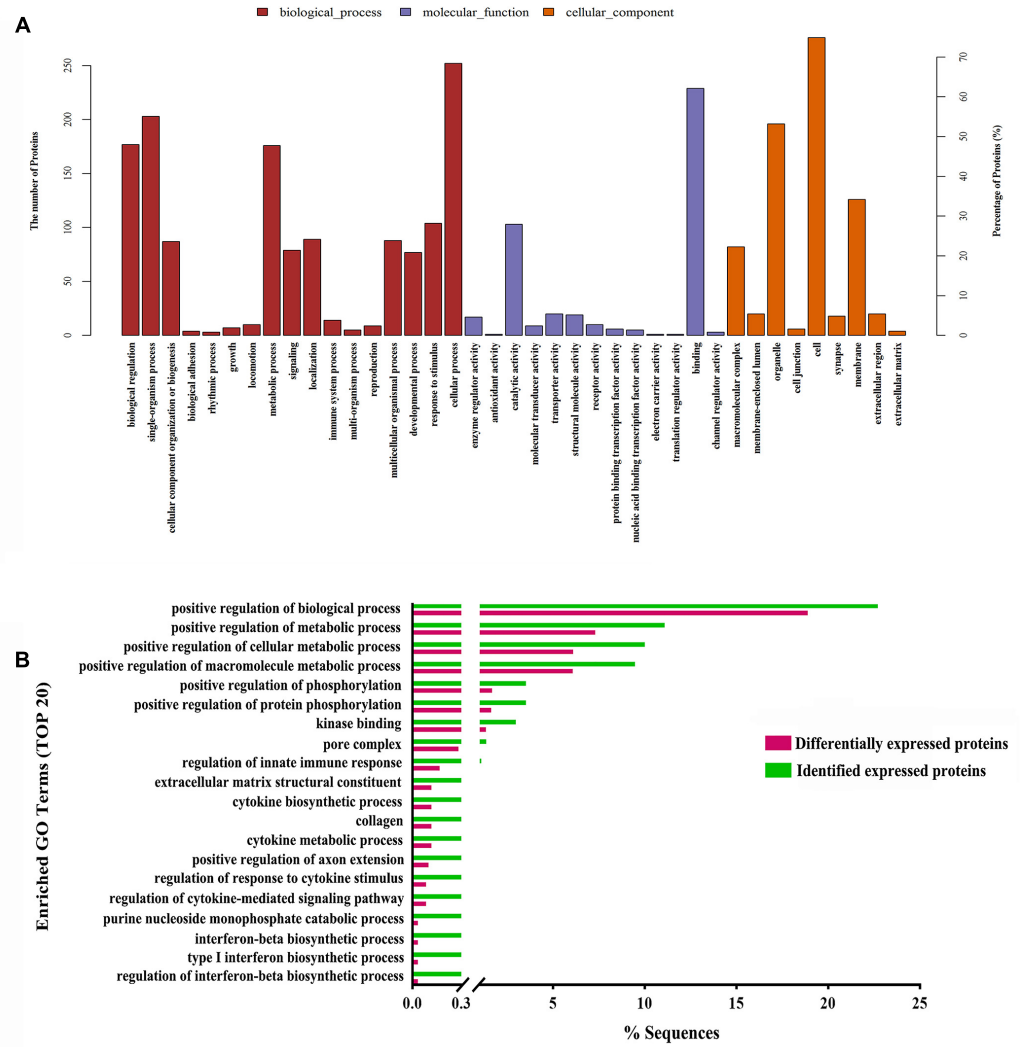

FIGURE 4 | GO functional annotations **(A)** and GO enrichment analysis **(B)** of differentially expressed proteins after baicalin treatment in CORT-induced mice.

major depression disorders usually exhibit high level of CORT in serum, whereas antidepressant drugs decrease CORT level, and improve depressive symptom (Pariante and Lightman, 2008). Moreover, previous studies also demonstrate that chronic CORT induces depression-like behaviors in mice (David et al., 2009; Wu et al., 2013). Baicalin, one of predominant flavonoid compounds in Radix Scutellariae, has showed definite antidepressant effects. For example, baicalin exerted antidepressant effects which improved olfactory functions by inhibiting APPL2-mediated GR hyperactivity in olfactory bulb (Gao et al., 2018). Our previous study showed that baicalin also promoted hippocampal neurogenesis via SGK1 and FKBP5-mediated GR phosphorylation in hippocampus (Zhang et al., 2016). However, the antidepressant effects and mechanisms of baicalin in hypothalamus are still unknown and need to be further investigated. Therefore, in present study, we establish the chronic CORT-induced mouse model of depression to assess the antidepressant effect and mechanism of baicalin. Tail suspension test and forced swimming test are two classic behavioral despair model, and the immobility time of mice will be decreased if drugs have definite antidepressant effect. On the other hand, elevated plus maze is a contradictory conflict test: the drive to new environment and the fear to enter high and dangling open arms, and anxiolytic drugs can increase the spending time in open arms. The same as previous study (David et al., 2009), our study finds that chronic CORT significantly increases the immobility time in tail suspension test and forced swimming test and decreases the spending time in open arms, which indicates that the model of depression has been successfully established and make sure chronic CORT indeed induces anxiety/depression-like behaviors. After baicalin treatment, above anxiety/depression-like behaviors are significantly improved. These data demonstrate that baicalin has definite antidepressant-like activity in CORT-induced mice.

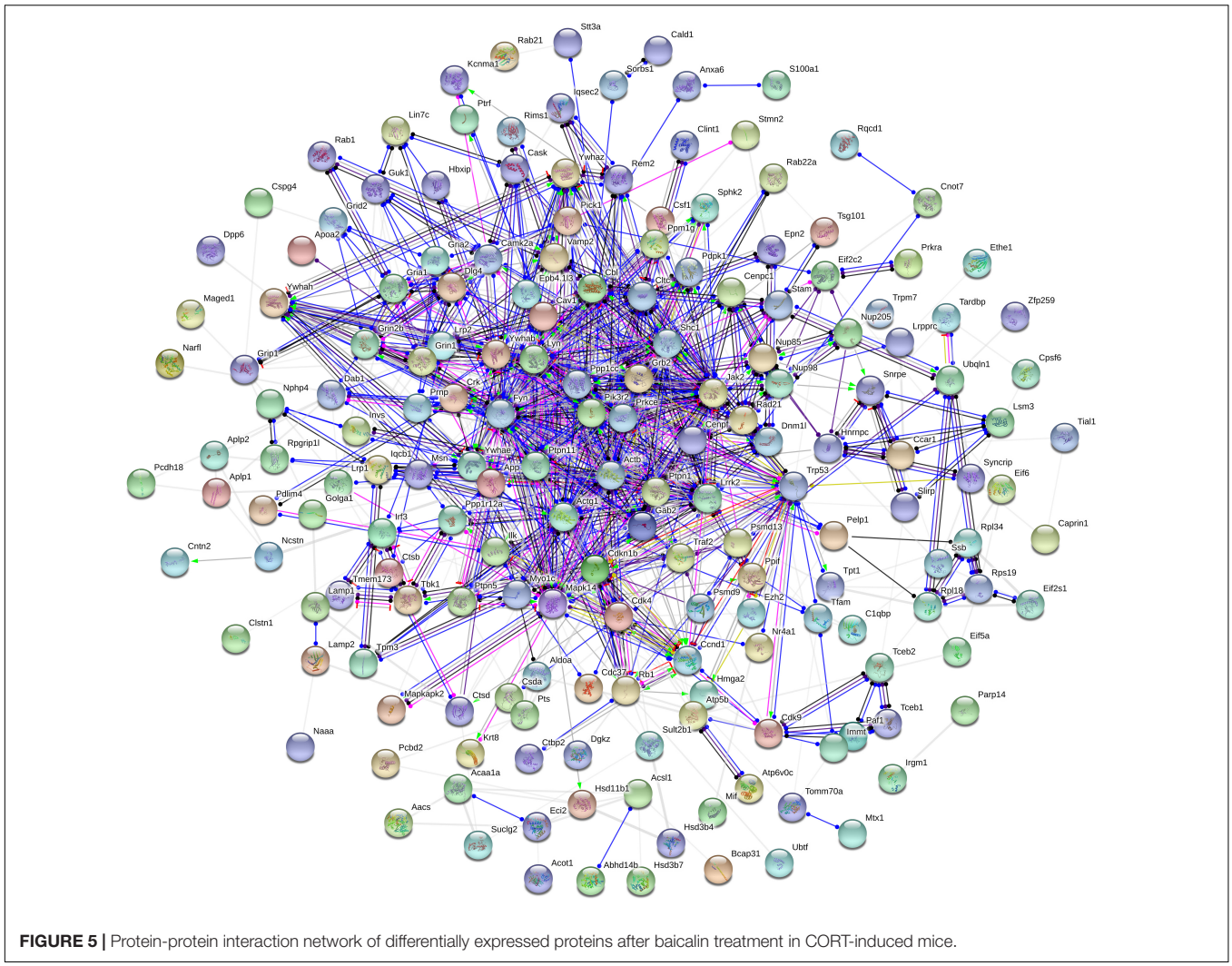

FIGURE 5 | Protein-protein interaction network of differentially expressed proteins after baicalin treatment in CORT-induced mice.

The HPA axis is important neuroendocrine system, which regulates stress response, emotion, digestion and immune system (Pariante and Lightman, 2008). Chronic stress persistently activates HPA axis and leads to long period high level of CORT. More importantly, hyperactivity of the HPA axis usually is found in major depression disorders (Tsigos and Chrousos, 2002). Above phenomenon indicates the negative feedback of HPA axis is damaged in depression. Moreover, some studies show unpredictable chronic mild stress destroys negative feedback of HPA axis, and antidepressant drugs improve this damage (Nollet et al., 2012). Based on the importance of HPA axis, we evaluate the effect of baicalin on negative feedback of HPA axis in CORT-induced mice by dexamethasone suppression test. Dexamethasone is an artificially synthesized powerful glucocorticoid, which can suppress the release of CORT (Anacker et al., 2011a). Then, the ratio of DEX-induced serum CORT suppression is significantly decreased by chronic CORT, which indicates that chronic CORT destroys negative feedback of HPA axis. The same as clinic treatment, fluoxetine can restore the negative feedback of HPA axis in CORT mice. Interestingly, baicalin normalizes DEX-induced serum CORT suppression rate. These data demonstrate that baicalin exerts antidepressant effect by restoring negative feedback of HPA axis, but accurate regulatory mechanisms and targets need to be illuminated.

Aim to dissect the regulatory mechanisms and targets of baicalin on negative feedback of HPA axis, proteomics and systems biology to are applied in this study. Proteomics is a scientific and systematic approach for clarifying the interrelation of proteins, which has been widely applied to search targets of drugs (Frantzi et al., 2019). In our study, 370 differentially expressed proteins (114 up-regulation and 256 down-regulation) in hypothalamus are found after baicalin treatment by iTRAQ quantitative proteomics. Among them, some differentially expressed proteins have been reported to involve in anxiety and depression-like behavior, such as Nrxn2 and 5-HT_{1A} (Born et al., 2015; Albert et al., 2019). Moreover, quantitative results are also verified by hierarchical clustering. Hierarchical clustering shows that 370 differentially expressed proteins are separated into two obvious distinguishing branches, which indicates that the quantitative results are distinct and

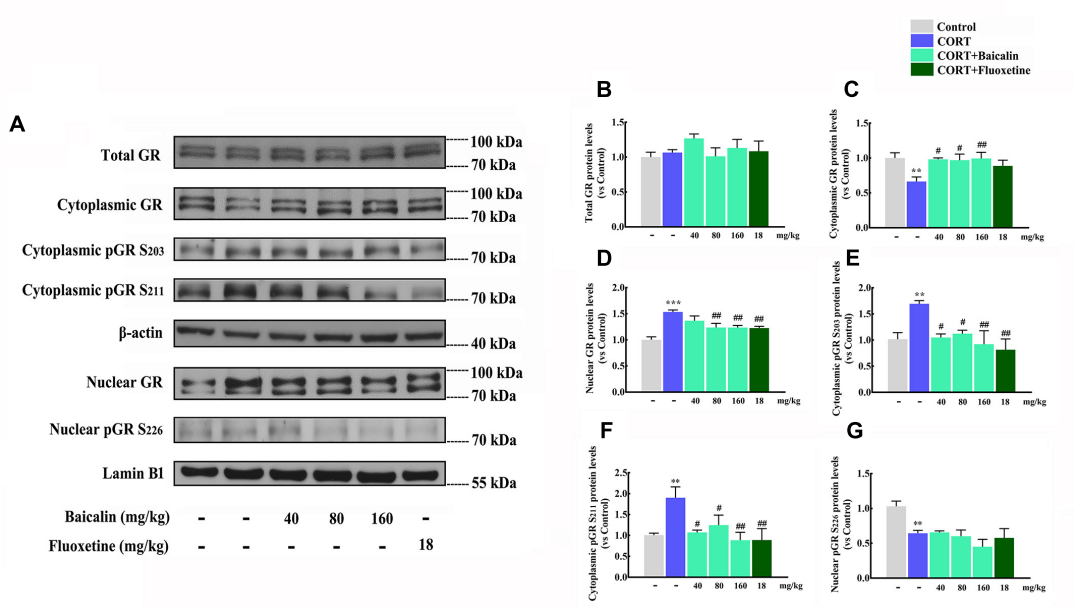

FIGURE 6 | Effects of baicalin on GR nuclear translocation and phosphorylation in CORT-induced mice. Representative western blots of GR and phosphorylated GR expression are showed **(A)**. Quantification analyze of total GR **(B)**, cytoplasmic GR **(C)**, nuclear GR **(D)**, cytoplasmic pGR S203 **(E)**, cytoplasmic pGR S211 **(F)**, and nuclear pGR S226 **(G)**. Data are expressed as means ± SEM (n = 3–5 mice/group). $^{**}P < 0.01$ and $^{***}P < 0.001$ vs. vehicle. $^{\#}P < 0.05$, $^{\#\#}P < 0.01$ vs. CORT model.

credible. Then, the function of differentially expressed proteins is analyzed by GO functional annotations and enrichment analysis. GO functional annotations find binding is the largest proportion of molecular function of differentially expressed proteins. GO enrichment analysis finds phosphorylation is the main biological process of differentially expressed proteins. These results indicate differentially expressed proteins which regulate phosphorylation by non-covalently binding may be the molecular targets of baicalin in hypothalamus. Next, protein-protein interaction analysis finds several high degree of nodes in neural network, such as 14-3-3 eta (Ywhah), 14-3-3 epsilon (Ywhae), 14-3-3 zeta (Ywhaz), NADPH-dependent 3-keto-steroid reductase Hsd3b4 (Hsd3b4), and nuclear pore complex protein Nup98-Nup96 (Nup98). High degree of nodes usually play a crucial part in protein-protein interaction network. In accordance with the results of GO, the function of above high degree nodes mainly focuses on GR signaling pathway by phosphoserine binding and phosphorylation. Previous studies show that GR is the crucial target of baicalin for antidepressant effects in olfactory bulb and hippocampus (Zhang et al., 2016; Gao et al., 2018), which indicates that GR is also the pivotal target of baicalin in hypothalamus for depression. Taken together, proteomics and systems biology data find that baicalin regulates some noteworthy proteins which are involved in GR signaling pathway, and indicate GR signaling pathway may be the regulatory mechanism of baicalin on negative feedback of HPA axis.

According to the results of proteomics and systems biology, we focus on the functions of GR in GR signaling pathway in hypothalamus. GR is one of the nuclear receptor subfamily members, which binds glucocorticoids and controls metabolism, development, and immune (Myers et al., 2014). More importantly, GR is also the control core for negative feedback of HPA axis in hypothalamus (Pariante and Lightman, 2008). Some studies show chronic stress decreases the expression of GR in hypothalamus (Cai et al., 2015). Therefore, we first assess the expression of total GR in hypothalamus. Whereas, the level of total GR is not affected by chronic CORT or baicalin. This result is in accordance with some studies, which chronic CORT do not change the expression of GR in hypothalamus (Wu et al., 2013). As we know, the function of GR is executed via GR transfers from the cytoplasm to the nucleus. So we next assess the level of GR in cytoplasm and nucleus. Interestingly, chronic CORT significantly decreases GR level in cytoplasm and increases GR level in nucleus, which indicates GR nuclear translocation is abnormality. This abnormal GR nuclear translocation may enhance the negative effects of GR and result in damaged negative feedback of HPA axis (Myers et al., 2014). After baicalin treatment, the distribution of GR in cytoplasm and nucleus are normalized. Noteworthy, fluoxetine normalizes the chronic CORT-induced increase in GR nuclear translocation and also does not affect total GR protein levels. Interestingly, this results are in line with the proteomics and systems biology analysis which baicalin can regulate differentially expressed proteins in GR signaling pathway. Moreover, many studies suggest that the phosphorylation status of the crucial serine residues on GR play the important role in regulating GR nuclear translocation (Guidotti et al., 2013). Proteomics and systems biology results also indicate that protein phosphorylation is the molecular targets of baicalin. Therefore, phosphorylation

status of the crucial serine residues on GR in hypothalamus are assessed. Many studies showed that that phosphorylation at sites Ser203 and Ser211 facilitate nuclear translocation and increase the transcriptional activities of the receptor, while conversely, phosphorylation at site Ser226 inhibits nuclear translocation and decreases GR transcriptional activities (Anacker et al., 2013). Our data find that pSer203 and pSer211 level are remarkably increased in cytoplasm under chronic CORT treatment, which can enhance GR nuclear translocation (Anacker et al., 2013). This result also explains the reason why GR level in nucleus is increased. Baicalin can reduce pSer203 and pSer211 level in GR, and then recover this abnormal GR nuclear translocation. In accordance with this result, our previous study also found that baicalin could promote hippocampal neurogenesis by mediating GR phosphorylation (Zhang et al., 2016). Moreover, some studies have proposed that cAMP/PKA signaling pathway is involved in GR function (Anacker et al., 2011b). GR could interact with TrkB to promotes BDNF-triggered PLC-γ signaling pathway (Numakawa et al., 2009). However, definite downstream signals which can be affected by GR are still vague. Taken together, our results reveal baicalin normalizes GR nuclear translocation via reducing GR phosphorylation in hypothalamus, and then restores negative feedback of HPA axis.

CONCLUSION

Our results demonstrate that baicalin remarkably improves chronic CORT-induced various depression-like behaviors and restores the negative feedback of HPA axis. Proteomics and systems biology indicate that the molecular mechanisms of baicalin involve normalizing GR nuclear translocation via regulating GR phosphorylation in hypothalamus. Our findings provide the new perspective on molecular targets of baicalin and will facilitate its clinical application.

DATA AVAILABILITY

The raw data supporting the conclusions of this manuscript will be made available by the authors, without undue reservation, to any qualified researcher.

ETHICS STATEMENT

This study was carried out in accordance with the principles of National Institutes of Health Guide for the Care and Use of Laboratory Animals (Publication No. 85-23). All efforts were made to minimize suffering.

AUTHOR CONTRIBUTIONS

KZ, JY, CW, YL, and HZ designed the study and drafted the manuscript. KZ, MH, and FW carried out the study. All authors read and approved the final manuscript.

FUNDING

This work was supported by the Project of National Natural Science Foundation of China (81803508), the Doctoral Scientific Research Foundation of Liaoning Province (20170520193), and the Young and Middle-Aged Teachers' Career Development Project of Shenyang Pharmaceutical University (ZQN2016022).

SUPPLEMENTARY MATERIAL

The Supplementary Material for this article can be found online at: https://www.frontiersin.org/articles/10.3389/fnins.2019.00834/full#supplementary-material

REFERENCES

Albert, P. R., Le Francois, B., and Vahid-Ansari, F. (2019). Genetic, epigenetic and posttranscriptional mechanisms for treatment of major depression: the 5-HT1A receptor gene as a paradigm. *J. Psychiatry Neurosci.* 44, 1–13. doi: 10.1503/jpn.180209

Anacker, C., Cattaneo, A., Musaelyan, K., Zunszain, P. A., Horowitz, M., Molteni, R., et al. (2013). Role for the kinase SGK1 in stress, depression, and glucocorticoid effects on hippocampal neurogenesis. *Proc. Natl. Acad. Sci. U.S.A.* 110, 8708–8713. doi: 10.1073/pnas.1300886110

Anacker, C., Zunszain, P. A., Carvalho, L. A., and Pariante, C. M. (2011a). The glucocorticoid receptor: pivot of depression and of antidepressant treatment? *Psychoneuroendocrinology* 36, 415–425. doi: 10.1016/j.psyneuen.2010.03.007

Anacker, C., Zunszain, P. A., Cattaneo, A., Carvalho, L. A., Garabedian, M. J., Thuret, S., et al. (2011b). Antidepressants increase human hippocampal neurogenesis by activating the glucocorticoid receptor. *Mol. Psychiatry* 16, 738–750. doi: 10.1038/mp.2011.26

Blier, P. (2016). Neurobiology of depression and mechanism of action of depression treatments. *J. Clin. Psychiatry* 77:e319. doi: 10.4088/JCP.13097tx3c

Boku, S., Nakagawa, S., Toda, H., and Hishimoto, A. (2018). Neural basis of major depressive disorder: beyond monoamine hypothesis. *Psychiatry Clin. Neurosci.* 72, 3–12. doi: 10.1111/pcn.12604

Born, G., Grayton, H. M., Langhorst, H., Dudanova, I., Rohlmann, A., Woodward, B. W., et al. (2015). Genetic targeting of NRXN2 in mice unveils role in excitatory cortical synapse function and social behaviors. *Front. Synaptic Neurosci.* 7:3. doi: 10.3389/fnsyn.2015.00003

Cai, L., Li, R., Tang, W. J., Meng, G., Hu, X. Y., and Wu, T. N. (2015). Antidepressant-like effect of geniposide on chronic unpredictable mild stress-induced depressive rats by regulating the hypothalamus-pituitary-adrenal axis. *Eur. Neuropsychopharmacol.* 25, 1332–1341. doi: 10.1016/j.euroneuro.2015.04.009

David, D. J., Samuels, B. A., Rainer, Q., Wang, J. W., Marsteller, D., Mendez, I., et al. (2009). Neurogenesis-dependent and -independent effects of fluoxetine in an animal model of anxiety/depression. *Neuron* 62, 479–493. doi: 10.1016/j.neuron.2009.04.017

Duman, R. S., and Aghajanian, G. K. (2012). Synaptic dysfunction in depression: potential therapeutic targets. *Science* 338, 68–72. doi: 10.1126/science.1222939

Frantzi, M., Latosinska, A., and Mischak, H. (2019). Proteomics in drug development: the dawn of a new era? *Proteomics Clin. Appl.* 13:e1800087. doi: 10.1002/prca.201800087

Gao, C., Du, Q., Li, W., Deng, R., Wang, Q., Xu, A., et al. (2018). Baicalin modulates APPL2/Glucocorticoid receptor signaling cascade, promotes neurogenesis, and attenuates emotional and olfactory dysfunctions in chronic corticosterone-induced depression. *Mol. Neurobiol.* 55, 9334–9348. doi: 10.1007/s12035-018-1042-8

Guidotti, G., Calabrese, F., Anacker, C., Racagni, G., Pariante, C. M., and Riva, M. A. (2013). Glucocorticoid receptor and FKBP5 expression is altered

following exposure to chronic stress: modulation by antidepressant treatment. *Neuropsychopharmacology* 38, 616–627. doi: 10.1038/npp.2012.225

Hou, J., Wang, J., Zhang, P., Li, D., Zhang, C., Zhao, H., et al. (2012). Baicalin attenuates proinflammatory cytokine production in oxygen-glucose deprived challenged rat microglial cells by inhibiting TLR4 signaling pathway. *Int. Immunopharmacol.* 14, 749–757. doi: 10.1016/j.intimp.2012.10.013

Jiang, Y., Sun, A., Zhao, Y., Ying, W., Sun, H., Yang, X., et al. (2019). Proteomics identifies new therapeutic targets of early-stage hepatocellular carcinoma. *Nature* 567, 257–261. doi: 10.1038/s41586-019-0987-8

Li-Weber, M. (2009). New therapeutic aspects of flavones: the anticancer properties of *Scutellaria* and its main active constituents Wogonin, Baicalein and Baicalin. *Cancer Treat. Rev.* 35, 57–68. doi: 10.1016/j.ctrv.2008.09.005

Luan, Y., Sun, C., Wang, J., Jiang, W., Xin, Q., Zhang, Z., et al. (2019). Baicalin attenuates myocardial ischemia-reperfusion injury through Akt/NF-kappaB pathway. *J. Cell Biochem.* 120, 3212–3219. doi: 10.1002/jcb.27587

McEwen, B. S., Bowles, N. P., Gray, J. D., Hill, M. N., Hunter, R. G., Karatsoreos, I. N., et al. (2015). Mechanisms of stress in the brain. *Nat. Neurosci.* 18, 1353–1363. doi: 10.1038/nn.4086

Myers, B., McKlveen, J. M., and Herman, J. P. (2014). Glucocorticoid actions on synapses, circuits, and behavior: implications for the energetics of stress. *Front. Neuroendocrinol.* 35, 180–196. doi: 10.1016/j.yfrne.2013.12.003

Nollet, M., Gaillard, P., Tanti, A., Girault, V., Belzung, C., and Leman, S. (2012). Neurogenesis-independent antidepressant-like effects on behavior and stress axis response of a dual orexin receptor antagonist in a rodent model of depression. *Neuropsychopharmacology* 37, 2210–2221. doi: 10.1038/npp.2012.70

Numakawa, T., Kumamaru, E., Adachi, N., Yagasaki, Y., Izumi, A., and Kunugi, H. (2009). Glucocorticoid receptor interaction with TrkB promotes BDNF-triggered PLC-gamma signaling for glutamate release via a glutamate transporter. *Proc. Natl. Acad. Sci. U.S.A.* 106, 647–652. doi: 10.1073/pnas.0800888106

Pariante, C. M., and Lightman, S. L. (2008). The HPA axis in major depression: classical theories and new developments. *Trends Neurosci.* 31, 464–468. doi: 10.1016/j.tins.2008.06.006

Porsolt, R. D., Anton, G., Blavet, N., and Jalfre, M. (1978). Behavioural despair in rats: a new model sensitive to antidepressant treatments. *Eur. J. Pharmacol.* 47, 379–391. doi: 10.1016/0014-2999(78)90118-8

Steru, L., Chermat, R., Thierry, B., and Simon, P. (1985). The tail suspension test: a new method for screening antidepressants in mice. *Psychopharmacology* 85, 367–370. doi: 10.1007/bf00428203

Tsigos, C., and Chrousos, G. P. (2002). Hypothalamic-pituitary-adrenal axis, neuroendocrine factors and stress. *J. Psychosom. Res.* 53, 865–871. doi: 10.1016/s0022-3999(02)00429-4

Wu, T. C., Chen, H. T., Chang, H. Y., Yang, C. Y., Hsiao, M. C., Cheng, M. L., et al. (2013). Mineralocorticoid receptor antagonist spironolactone prevents chronic corticosterone induced depression-like behavior. *Psychoneuroendocrinology* 38, 871–883. doi: 10.1016/j.psyneuen.2012.09.011

Zhang, K., Pan, X., Wang, F., Ma, J., Su, G., Dong, Y., et al. (2016). Baicalin promotes hippocampal neurogenesis via SGK1- and FKBP5-mediated glucocorticoid receptor phosphorylation in a neuroendocrine mouse model of anxiety/depression. *Sci. Rep.* 6:30951. doi: 10.1038/srep30951

Conflict of Interest Statement: The authors declare that the research was conducted in the absence of any commercial or financial relationships that could be construed as a potential conflict of interest.

frontiers in Neuroscience

ORIGINAL RESEARCH
published: 23 August 2019
doi: 10.3389/fnins.2019.00833

Unraveling the Serum Metabolomic Profile of Post-partum Depression

Zoe Papadopoulou[1], Angeliki-Maria Vlaikou[2], Daniela Theodoridou[1], Chrysoula Komini[2], Georgia Chalkiadaki[3], Marina Vafeiadi[3], Katerina Margetaki[3], Theoni Trangas[2], Chris W. Turck[4], Maria Syrrou[1†], Leda Chatzi[5†] and Michaela D. Filiou[2,6†]*

[1] Laboratory of Biology, Faculty of Medicine, School of Health Sciences, University of Ioannina, Ioannina, Greece, [2] Laboratory of Biochemistry, Department of Biological Applications and Technology, School of Health Sciences, University of Ioannina, Ioannina, Greece, [3] Department of Social Medicine, Faculty of Medicine, University of Crete, Heraklion, Greece, [4] Proteomics and Biomarkers, Department of Translational Research in Psychiatry, Max Planck Institute of Psychiatry, Munich, Germany, [5] Department of Preventive Medicine, University of Southern California, Los Angeles, CA, United States, [6] Department of Stress Neurobiology and Neurogenetics, Max Planck Institute of Psychiatry, Munich, Germany

Post-partum depression (PPD) is a severe psychiatric disorder affecting ∼15% of young mothers. Early life stressful conditions in periconceptual, fetal and early infant periods or exposure to maternal psychiatric disorders, have been linked to adverse childhood outcomes interfering with physiological, cognitive and emotional development. The molecular mechanisms of PPD are not yet fully understood. Unraveling the molecular underpinnings of PPD will allow timely detection and establishment of effective therapeutic approaches. To investigate the underlying molecular correlates of PPD in peripheral material, we compared the serum metabolomes of an in detail characterized group of mothers suffering from PPD and a control group of mothers, all from Heraklion, Crete in Greece. Serum samples were analyzed by a mass spectrometry platform for targeted metabolomics, based on selected reaction monitoring (SRM), which measures the levels of up to 300 metabolites. In the PPD group, we observed increased levels of glutathione-disulfide, adenylosuccinate, and ATP, which associate with oxidative stress, nucleotide biosynthesis and energy production pathways. We also followed up the metabolomic findings in a validation cohort of PPD mothers and controls. To the very best of our knowledge, this is the first metabolomic serum analysis in PPD. Our data show that molecular changes related to PPD are detectable in peripheral material, thus paving the way for additional studies in order to shed light on the molecular correlates of PPD.

Keywords: PPD, early life stress, pregnancy, psychiatric disorders, metabolomics, biomarkers, serum

OPEN ACCESS

Edited by:
HuaLin Cai,
Second Xiangya Hospital, Central South University, China

Reviewed by:
Chi Chen,
University of Minnesota Twin Cities, United States
Jean-Philippe Guilloux,
Université Paris-Sud, France

***Correspondence:**
Michaela D. Filiou
mfiliou@uoi.gr

† These authors have contributed equally to this work

Specialty section:
This article was submitted to Neuropharmacology, a section of the journal Frontiers in Neuroscience

Received: *01 March 2019*
Accepted: *25 July 2019*
Published: *23 August 2019*

Citation:
Papadopoulou Z, Vlaikou A-M, Theodoridou D, Komini C, Chalkiadaki G, Vafeiadi M, Margetaki K, Trangas T, Turck CW, Syrrou M, Chatzi L and Filiou MD (2019) Unraveling the Serum Metabolomic Profile of Post-partum Depression. Front. Neurosci. 13:833. doi: 10.3389/fnins.2019.00833

INTRODUCTION

Depression, the leading cause of disability worldwide (WHO, 2015), is more prevalent in women than men (Van de Velde et al., 2010; Rich et al., 2013). PPD is the most common psychiatric disorder in women after childbirth, with an increasing risk occurring during the first post-partum year (Gaillard et al., 2014). Although most women suffering from PPD show mild symptoms for

Abbreviations: EPDS, Edinburgh postnatal depression scale; FDR, false discovery rate; PLS-DA, partial least squares-discriminant analysis; PPD, post-partum depression; Prdx3, peroxiredoxin-3; SAM, significance analysis of microarray; SEM, standard error of the mean; SRM, selected reaction monitoring; TAC, total antioxidant capacity.

a short period of time that gradually disappear, a percentage of women experiences heavier depressive symptoms (even post-partum psychosis) and need pharmacological treatment and psychotherapy (Leigh and Milgrom, 2008). Lack of psychiatric/therapeutic care may have dramatic consequences for the mother and the whole family (Pollock and Percy, 1999; Evins et al., 2000; Kurki et al., 2000). PPD has been also demonstrated to affect the development of the newborn with lasting effects to adulthood (Reck et al., 2004). Psychological and socio-economic factors have been implicated in the onset of PPD during the postnatal period. Socio-demographic variables, such as social support and high maternal educational level, have been negatively correlated with PPD, whereas young maternal age and smoking positively correlated with PPD (deCastro et al., 2011; Katon et al., 2014). Moreover, history of depression, anxiety and adverse life events are PPD risk factors (Verreault et al., 2014).

At the molecular level, hormonal changes have been described in relation to PPD. At birth, progesterone and estrogen levels significantly increase compared to pregnancy (Kumar and Magon, 2012; O'Hara and Wisner, 2014). Progesterone and estrogen levels are reduced post-partum and their variation has been implicated in mood changes (Hendrick et al., 1998). Active forms of estrogens (estradiol and estriol) are produced by the placenta and increase during pregnancy. Cortisol, a glucocorticoid steroid hormone, is an important marker of the stress response and is implicated in depression and PPD (Seth et al., 2016). A correlation between cortisol and PPD is well-established (Ehlert et al., 1990; Okano and Nomura, 1992; Taylor et al., 1994). Women with depressive symptoms after birth show elevated cortisol levels compared to controls (Okano and Nomura, 1992), although other studies have reported a negative correlation between cortisol levels and PPD, 4–6 weeks and 12 months post-partum (Parry et al., 2003; Groer and Morgan, 2007). In addition, the association between PPD and high levels of cortisol in hair during pregnancy has been proposed as a predictive marker for PPD (Diego et al., 2004). Amino acid metabolism has a key role in pregnancy and in the development of PPD (Duan et al., 2018). Lower plasma tryptophan levels are reported in PPD (Ogawa et al., 2014) and a poor tryptophan diet may induce depressive symptoms (Ellenbogen et al., 1999). Polymorphisms in genes of the tryptophan-serotonin pathway could affect the sensitivity to stress during pregnancy and post-partum, having an impact on the development of depressive symptoms (Figueiredo et al., 2015; Duan et al., 2018). Furthermore, altered levels of neurosteroids and GABA in PPD women suggest that their interaction could play a key role in the development of depression during pregnancy and post-partum (Deligiannidis et al., 2016).

Besides these molecular changes, the implicated molecular mechanisms at a systemic level in PPD are incompletely understood. To identify molecular signatures of PPD in peripheral material, we performed a detailed metabolomic analysis in serum of women diagnosed with PPD compared to controls recruited from the same geographical region. This is one of the very few metabolomic studies available for PPD.

MATERIALS AND METHODS

Human Cohorts

This is a study within the Rhea pregnancy child cohort in Crete, Greece (Chatzi et al., 2017). The study and validation populations were Caucasian pregnant women who live in Heraklion, Crete. Women were contacted at the first and third trimester of pregnancy, at birth, and at 8 weeks post-partum. Face-to-face structured interviews, together with self-administered questionnaires and medical records, were used to obtain information on several psychosocial, dietary and environmental exposures during pregnancy and post-partum. The metabolomic study cohort included women diagnosed with PPD (EPDS score $\geq$ 13, n = 10) and women with no PPD (EPDS score $<$ 13, n = 10) (**Supplementary Table S1**). For further investigation of the metabolomic analysis results a validation cohort was studied, including eight women diagnosed with PPD (EPDS score $\geq$ 13) and seven women with no PPD (EPDS score $<$ 13) (**Supplementary Table S2**). All women were 20–35 years old, non-smokers, non-obese (BMI $<$ 35) and became pregnant between February 2007 and February 2008. Twin pregnancies, women under fertilization treatment, women with gestational diabetes, preeclampsia and women with psychological disorders before or during pregnancy were excluded from the study. The study was approved by the Ethical Committee of the University Hospital in Heraklion, Crete, Greece. Written informed consent was obtained from all participants.

Protocol for Assessing Depression

Maternal depressive symptoms were assessed (antenatally at 28–32 weeks of gestation and postnatally at 8 weeks post-partum) using the EPDS as previously described (Cox et al., 1987). The EPDS is a widely used 10-item, self-reported questionnaire providing an indication of the severity of mother's mood during the past 7 days. Items are rated on a 4-point Likert scale ranging from 0 (not at all) to 3 (most of the time) and refers to depressed mood, anhedonia, guilt, anxiety and suicidal ideation (possible range 0–30). A cut-off score of $\geq$ 13 on the EPDS has been found to identify probable clinical postnatal depression with a sensitivity of 86% and a specificity of 78% (Matthey et al., 2006). This cut-off is also consistent with previous work in our cohort (Vivilaki et al., 2009; Chatzi et al., 2011; Koutra et al., 2014, 2017, 2018). The EPDS has been translated and validated for the Greek population by two research groups (Leonardou et al., 2009; Vivilaki et al., 2009) and showed a very high overall internal consistency.

Serum Sample Collection

Blood samples were collected from pregnant women in Vacutainer SST Plastic Serum Tubes (BD 367958). Median gestational age at blood collection was the 14th week. To isolate serum, samples were centrifuged immediately after blood sampling collection for 10 min at 2500 rpm, room temperature. Serum samples were stored in 0.5 ml aliquots into cryovial sterile tubes at −80°C.

Serum Sample Preparation

Serum metabolites were extracted with a fourfold excess (v/v) of 100% cold methanol as previously described (Filiou et al., 2014). After vortexing for 2 min, samples were incubated on dry ice for 2 h and centrifuged (2053 *g*, 100 min, 4°C). Supernatants were filtered using 0.22 μm SpinX ultrafiltration tubes (Corning, NY, United States), the filtrates were lyophilized and stored at −80°C for metabolomic analysis.

Mass Spectrometry-Based Metabolomics

Serum metabolite extracts (100 μl per subject) were analyzed at the Metabolomics Core, Beth Israel Deaconess Medical Center (Harvard Medical School) by a SRM-based targeted metabolomics platform using a 5500 QTRAP triple quadrupole mass spectrometer coupled to a Prominence UFCL HPLC system, as previously described (Filiou et al., 2014). This platform quantifies the levels of up to 300 metabolites involved in major metabolic pathways (Yuan et al., 2012).

Western Blot

For assessing the levels of the antioxidant enzyme Prdx3 in the validation cohort, Western blot analysis was performed as previously described (Filiou et al., 2010) with slight modifications. Briefly, protein content was measured by Bradford Assay. From each serum sample, 25 μg were diluted in RIPA buffer (1:2, v/v), electrophorized and electrotransferred with a semi-dry, *trans*-blot turbo transfer system (Bio-Rad, Hercules, CA, United States). Membranes were incubated with an anti-Prdx3 primary antibody (Abcam ab16751, mouse monoclonal, 1:2000) and an anti-mouse secondary antibody (sc-Santa Cruz Biotechnology, Heidelberg, Germany). Signal intensity was measured using ImageJ. Equal total protein loading was ensured by Coomassie gel staining and signal intensity comparison.

Total Antioxidant Capacity

The determination of total antioxidant capacity (TAC) in serum samples of the validation cohort, was performed as previously described (Ciuti and Liguri, 2017). Briefly, serum samples and glutathione (used as calibrator) were mixed 1:5 (v/v) with a pre-heated chromogenic reagent as described (Ciuti and Liguri, 2017) in a multi-well plate. Absorbance at 630 nm was determined in a UT2100C microplate reader (MRC, Holon, Israel) and measurements were taken at 20 and 120 s after the last reagent dispensing. TAC quantification was performed as previously described (Ciuti and Liguri, 2017).

Statistical Analysis

Metabolomic Study and Validation Cohort Demographic Data Analysis

A descriptive analysis of the study population characteristics was conducted. Categorical variables are presented as *N*(%) while continuous variables are presented as mean ± SD. We then compared the characteristics between PPD and control women and between the metabolomic study and validation groups utilizing Fisher's exact test and Student's *t*-test ($p < 0.05$).

Metabolomic Data Analysis

Metabolomic data analysis was performed by Metaboanalyst[1] (v4.0) (Xia et al., 2009). Using the mass spectrometry-based metabolomics platform, 302 features were quantified. For metabolites measured both in positive and negative ion mode, only the measurement with the higher intensities across samples was included. In total, 285 metabolites were considered for analysis. Of those, metabolites with > 50% missing values were excluded. For the remaining metabolites, missing values were replaced by default small values in Metaboanalyst. Metabolite data were median-normalized, log-transformed and pareto-scaled. To evaluate the discriminative features between the PPD and control group we used the supervised PLS-DA feature in Metaboanalyst. To identify individual metabolite level changes between the PPD and control groups, we employed the SAM in Metaboanalyst using the siggenes R package. FDR was used to correct for multiple comparisons and the cut-off for the adjusted *p*-value (*q*-value) was set at 0.1.

Multivariable Analysis

For the quantified metabolites (normalized values) with altered levels in PPD compared to controls in the metabolomic study cohort, we performed linear regression analysis to further evaluate the observed associations adjusting for potential confounding factors. Using standard bivariate statistical tests (Fisher's exact test, Student's *t*-test, Pearson correlation coefficient) we identified variables associated with either the selected metabolites or with PPD at 10% level and we included those variables in the linear models. The selected covariates were age at blood sampling, working during pregnancy, educational status and pre pregnancy overweight (Model 1). In a second model, we included clinical characteristics, namely history of dyslipidemia and history thyroid disease (Model 2). Effect estimates are presented in terms of beta coefficients and 95% confidence intervals (95% CIs). Multivariable analyses were performed in Stata 13[2].

Western Blot and TAC Data Analysis

Western blot and TAC statistical analysis was performed by GraphPad Prism7 (GraphPad, San Diego, CA, United States) using the Mann–Whitney non-parametric statistical test ($p < 0.05$). Data are presented as mean ± SEM.

RESULTS

Metabolomic Study and Validation Cohorts

Detailed information on the demographic characteristics of the metabolomic study and validation cohorts is provided in **Supplementary Tables S1**, **S2**, respectively. Briefly, regarding the metabolomic study cohort, the mean (SD) age of the

[1]http://www.metaboanalyst.ca

[2]https://www.stata.com/support/updates/stata13.html

participating women was 29.1 (3.8) years and the mean (SD) BMI was 23.2 (3.5) kg/m^2 (**Supplementary Table S1**). Validation cohort characteristics were similar (**Supplementary Table S2**). To ensure that the metabolomic study and validation cohorts were not demographically different, a comparison between the two cohorts was performed showing no differences in demographic characteristics (all p-values > 0.05, **Supplementary Table S3**).

Altered Levels of Serum Metabolites in PPD

We performed a targeted metabolomic analysis in serum of pregnant women who developed PPD compared to unaffected women from the same geographical region. Quantification raw data for all 285 metabolites considered for the analysis are shown in **Supplementary Table S4**. The PLS-DA separation score plots of the two groups are shown in **Figure 1**. We identified three serum metabolites with altered levels in women with PPD compared to the control group. These included glutathione-disulfide, adenylosuccinate, and ATP. All three were found in elevated levels in PPD compared to the control group (**Figure 2**). These metabolites are associated with oxidative stress, nucleotide biosynthesis and energy production, respectively. We also found a positive association between normalized glutathione-disulfide levels with the continuous EPDS score (Pearson $r = 0.7449$, $p < 0.001$) (**Figure 3**). The results of the multivariable linear regression analysis are presented in **Table 1**. After adjustment for demographic characteristics, the observed associations remained significant. PPD was associated with higher levels of adenylosuccinate, glutathione-disulfide and ATP. The results remained similar after the adjustment for clinical characteristics with the exception of adenylosuccinate, where significance was lost.

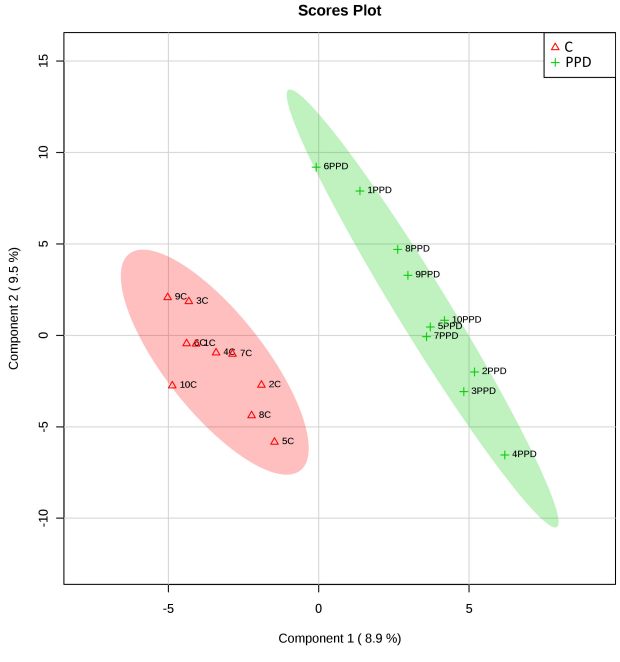

FIGURE 1 | Score plots of metabolomic profiles of women suffering from PPD compared to controls in the metabolomic study cohort. C: control.

Investigation of Oxidative Stress-Related Changes in a Validation Cohort

Given the positive correlation of glutathione-disulfide with the continuous EPDS score, we then went on to further investigate oxidative stress-related changes in serum of a validation cohort of women diagnosed with PPD vs. controls from the same geographical area (**Supplementary Table S2**). We assessed the levels of Prdx3, a member of the peroxiredoxin family of antioxidant enzymes, and found a trend for decreased Prdx3 expression in PPD samples (**Figure 4A** and **Supplementary Figure S1**). In the validation cohort, we also assessed the serum TAC and found no difference between the PPD and control samples (**Figure 4B**).

DISCUSSION

The aim of this work was to identify molecular signatures for PPD by comparing the serum metabolomic profiles of women with PPD vs. control subjects. Multi-omics approaches have the potential to shed light on molecular mechanisms of psychiatric disorders in a high-throughput and data-driven manner (Filiou, 2015). Metabolomic analyses provide valuable information for dissecting neuropsychiatric conditions, as the metabolome correlates directly with the phenotype and is very sensitive to environmental stressors and changes (Quinones and Kaddurah-Daouk, 2009; Turck and Filiou, 2015). Metabolomic approaches have been used to study depression both in patient cohorts and animal models (Pan et al., 2018; Zhang et al., 2018). To the best of our knowledge, this is the first metabolomics study in serum of PPD.

We report altered levels of three serum metabolites: glutathione-disulfide, adenylosuccinate, and ATP. Glutathione is a low molecular mass thiol and one of the most important endogenous antioxidant compounds (Freed et al., 2017). Under oxidative conditions, glutathione (reduced form) is converted into glutathione-disulfide (oxidized form). The glutathione/glutathione-disulfide ratio is considered as a prognostic factor for oxidative stress (Tietze, 1969; Freed et al., 2017). Both glutathione levels and the glutathione-disulfide/glutathione ratio of premature infants with idiopathic respiratory distress syndrome are increased compared to control newborns (Giustarini et al., 2016). Maternal prenatal distress was also shown to reduce placental glutathione/glutathione-disulfide ratios (Chang et al., 2016). Oxidative stress and pertinent markers are increased in patients with major depressive disorder (Dowlati et al., 2010; Black et al., 2015; Lindqvist et al., 2017). The correlation between oxidative stress and depression is not yet fully understood, however,

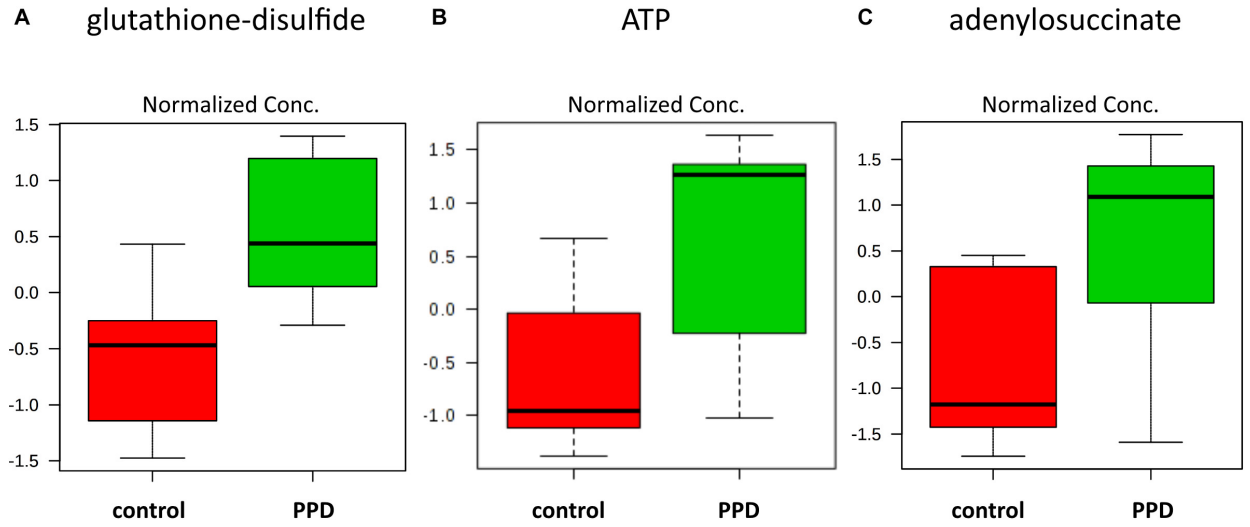

FIGURE 2 | Increased metabolite levels in PPD serum compared to controls in the metabolomic study cohort **(A)** glutathione-disulfide (d = 2.6504, SD = 0.2543, and q = 0.0567) **(B)** ATP (d = 2.3833, SD = 0.3788, and q = 0.0567) **(C)** adenylosuccinate (d = 2.2390, SD = 0.4445, and q = 0.0825).

the brain is reported to be particularly sensitive to oxidative damage due to elevated oxygen levels and free radicals (Ng et al., 2008). Free radicals may affect methylation patterns by hydroxylation of pyrimidines and 5-methylcytosine (Lewandowska and Bartoszek, 2011) and influence histone modifications through intracellular metabolites such as acetyl-CoA, ketoglutarate, NAD^+, and S-adenosylmethionine (Simpson et al., 2012). Adenylosuccinate is an intermediate in nucleotide biosynthesis, involved in the conversion of inosine monophosphate (IMP) to adenosine monophosphate (AMP) (Gooding et al., 2015). ATP is the main cellular energy currency. Astrocyte-derived ATP was shown to modulate depression-like behaviors and brain ATP levels were lower in mice susceptible to chronic social defeat (Cao et al., 2013).

To follow up on the glutathione-disulfide level changes that correlated with the depressive status of the patients, we further investigated oxidative stress-related alterations in a validation cohort of PPD patients and controls. We found a trend for decreased expression of the antioxidant enzyme Prdx3 and an overall unchanged total antioxidant status of the PPD patients compared to controls in the validation cohort. Decreased expression of Prdx3 in PPD is in line with decreased expression of glutathione, which may result from the increased levels of glutathione-disulfide. It should be, however, noted that the complex interplay of various antioxidants performing complementary antioxidant functions may result in an overall unchanged TAC. From a technical perspective, immunochemical and colorimetric biochemical methods show significantly lower sensitivity compared to mass spectrometry-based metabolomics. The ability to identify changes by metabolomics which are undetectable by conventional biochemical methodologies highlights the need to use metabolomic approaches for the identification of low fold metabolite level changes. This is of particular interest for multifactorial disorders such as PPD, which are characterized by mild changes in multiple factors. In addition, the high sensitivity of mass

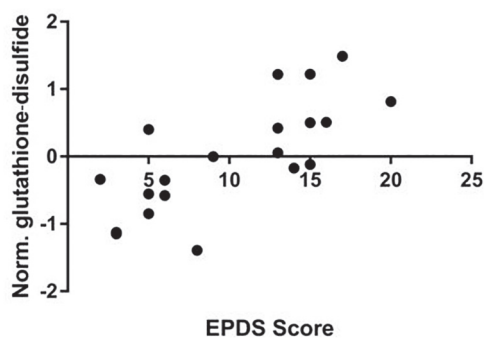

FIGURE 3 | Correlation of EPDS scores and normalized glutathione-disulfide levels in the metabolomic study cohort (Pearson r = 0.7449, $p < 0.001$).

TABLE 1 | Adjusted associations between selected metabolites and PPD.

	Model 1		Model 2	
	Beta (95% CI)	***p*-Value**	**Beta (95% CI)**	***p*-Value**
ATP	1.12 (0.44, 1.80)	0.004	1.78 (0.99, 2.56)	<0.001
Glutathione-disulfide	0.94 (0.31, 1.57)	0.006	0.94 (0.00, 1.88)	0.051
Adenylosuccinate	1.34 (0.01, 2.68)	0.049	0.59 (−1.27, 2.44)	0.501

Model 1: Adjusted for age at blood sampling, working and educational status and overweight pre pregnancy. Model 2: Model 1, additionally adjusted for history of dyslipidemia and history of thyroid disease.

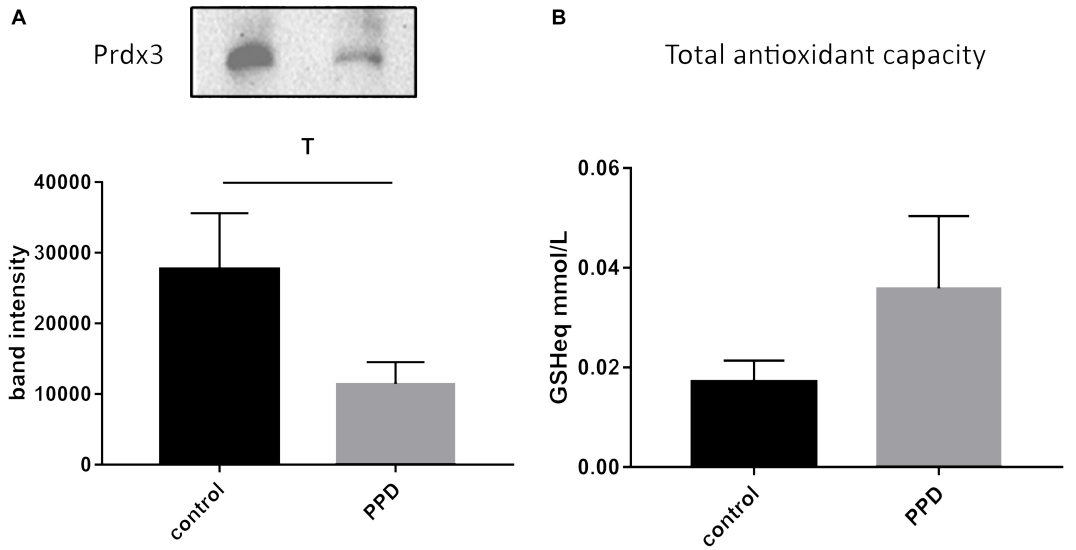

FIGURE 4 | (A) A trend toward decreased expression of Prdx3 (p = 0.0939) in PPD (11437 ± 3068) compared to controls (27685 ± 7926) serum in the validation cohort. **(B)** No changes in total antioxidant capacity (expressed in terms of mmol/L of reduced glutathione, GSHeq, p = 0.554) in the validation cohort between PPD (0.0359 ± 0.0145) and controls (0.0171 ± 0.0042).

spectrometry-based metabolomics is more appropriate for investigating peripheral material in brain disorders, where we do not expect to see dramatic fold changes, as brain-related pathophysiology alterations are attenuated in the periphery.

Metabolomic studies are indeed scarce in the context of PPD. A recent work compared urinary metabolites of PPD women, post-partum women with no PPD and healthy controls by gas-chromatography mass spectrometry-based metabolomics. In this study, 68 metabolites were identified and a panel of five metabolites was identified (formate, succinate, 1-methylhistidine, α-glucose, and dimethylamine), which was able to discriminate the PPD group. Interestingly, succinate is a precursor of adenylosuccinate, which was also found elevated in PPD in our study (Lin et al., 2017). A second study investigating the urine metabolome of PPD subjects compared to controls using untargeted mass spectrometry-based metabolomics indicated altered metabolomic profiles between the two groups (Zhang et al., 2019). A targeted steroid metabolome approach based on gas chromatography-mass spectrometry in maternal blood samples from PPD women revealed that an interplay of maternal derived testosterone and fetus derived estrogens may affect mood changes (Parizek et al., 2014).

Despite the small size of the population analyzed in this study, this is a well-characterized cohort with homogeneous demographic characteristics (women living in the same region and becoming pregnant at the same time). Future studies in larger sample sizes and other PPD cohorts are required to validate our results. The investigation of additional enzymes involved in antioxidant defense and biosynthetic processes will shed light on the role of these pathways in PPD pathogenesis. Combining metabolomic with genetic and epigenetic data might reveal risk markers of early stressful experiences. The acquired knowledge will be valuable for estimating the risk for future health disorders of the "stressed" newborns based on their individual genetic, epigenetic and metabolomic profiles.

Importantly, our data show that PPD-induced molecular changes are detectable in peripheral material. Identification of disease-related molecular correlates in peripheral material has been facing a series of challenges (Filiou and Turck, 2011), yet studies in the periphery are crucial for developing safe, non-invasive diagnostic and screening approaches for psychiatric disorders (Pinto et al., 2017). Intriguingly, a recent study in serum of post-partum women which had been exposed to different levels of childhood maltreatment, revealed a set of metabolites that could differ between varying levels of childhood trauma (Koenig et al., 2018). Our work may open up new perspectives for additional studies aiming at early detection and more accurate diagnosis using peripheral material for PPD and pave the way toward candidate biomarker identification.

DATA AVAILABILITY

All datasets generated for this study are included in the manuscript and/or the **Supplementary Files**.

ETHICS STATEMENT

The study was approved by the Ethical Committee of the University Hospital in Heraklion, Crete, Greece. Written informed consent was obtained from all participants.

AUTHOR CONTRIBUTIONS

ZP, A-MV, and CK performed the experiments. GC, MV, KM, and LC provided the clinical samples. TT, CT, MS, and MF designed and supervised the study. LC supervised the clinical sample and questionnaire collection. A-MV, DT, CK, KM, and MF analyzed the data. ZP, MS, and MF wrote the manuscript with input from all coauthors.

FUNDING

This work was funded by the Max Planck Society, and a grant from the Hellenic Foundation for Research and Innovation (HFRI) and the General Secretariat for Research and Technology (GSRT) to MF (Grant No: 660).

ACKNOWLEDGMENTS

We thank John Asara for metabolomic measurements.

SUPPLEMENTARY MATERIAL

The Supplementary Material for this article can be found online at: https://www.frontiersin.org/articles/10.3389/fnins.2019.00833/full#supplementary-material

FIGURE S1 | Western blot analysis of Prdx3 in the validation cohort.

TABLE S1 | Characteristics of the metabolomic study cohort subjects according to PPD status, Rhea mother-child cohort, Crete, Greece. For demographics with no numerical values, an index is provided below each question. NAV denotes no available answer from the corresponding subject. NAP denotes a not applicable question for the corresponding subject.

TABLE S2 | Characteristics of the validation cohort subjects according to PPD status, Rhea mother-child cohort, Crete, Greece. For demographics with no numerical values, an index is provided below each question. NAV denotes no available answer from the corresponding subject. NAP denotes a not applicable question for the corresponding subject.

TABLE S3 | Comparison of subject characteristics in the metabolomic study and validation cohorts.

TABLE S4 | Raw quantification data for measured metabolites (signal intensities). NA denotes non-quantified metabolites for the corresponding subject.

REFERENCES

Black, C. N., Bot, M., Scheffer, P. G., Cuijpers, P., and Penninx, B. W. (2015). Is depression associated with increased oxidative stress? A systematic review and meta-analysis. *Psychoneuroendocrinology* 51, 164–175. doi: 10.1016/j.psyneuen.2014.09.025

Cao, X., Li, L. P., Wang, Q., Wu, Q., Hu, H. H., Zhang, M., et al. (2013). Astrocyte-derived ATP modulates depressive-like behaviors. *Nat. Med.* 19, 773–777. doi: 10.1038/nm.3162

Chang, H. Y., Suh, D. I., Yang, S. I., Kang, M. J., Lee, S. Y., Lee, E., et al. (2016). Prenatal maternal distress affects atopic dermatitis in offspring mediated by oxidative stress. *J. Allergy Clin. Immunol.* 138, 468.e5–475.e5. doi: 10.1016/j.jaci.2016.01.020

Chatzi, L., Leventakou, V., Vafeiadi, M., Koutra, K., Roumeliotaki, T., Chalkiadaki, G., et al. (2017). cohort profile: the mother-child cohort in crete, greece (Rhea Study). *Int. J. Epidemiol.* 46, 1392k–1393k.

Chatzi, L., Melaki, V., Sarri, K., Apostolaki, I., Roumeliotaki, T., Georgiou, V., et al. (2011). Dietary patterns during pregnancy and the risk of postpartum depression: the mother-child 'Rhea' cohort in crete, greece. *Public Health Nutr.* 14, 1663–1670. doi: 10.1017/S1368980010003629

Ciuti, R., and Liguri, G. (2017). A novel assay for measuring total antioxidant capacity in whole blood and other biological samples. *J. Biomedical. Sci. Eng.* 10, 60–76. doi: 10.4236/jbise.2017.102007

Cox, J. L., Holden, J. M., and Sagovsky, R. (1987). Detection of postnatal depression. development of the 10-item edinburgh postnatal depression scale. *Br. J. Psychiatr.* 150, 782–786. doi: 10.1192/bjp.150.6.782

deCastro, F., Hinojosa-Ayala, N., and Hernandez-Prado, B. (2011). Risk and protective factors associated with postnatal depression in Mexican adolescents. *J. Psychosom. Obstet. Gynaecol.* 32, 210–217. doi: 10.3109/0167482X.2011.626543

Deligiannidis, K. M., Kroll-Desrosiers, A. R., Mo, S., Nguyen, H. P., Svenson, A., Jaitly, N., et al. (2016). Peripartum neuroactive steroid and gamma-aminobutyric acid profiles in women at-risk for postpartum depression. *Psychoneuroendocrinology* 70, 98–107. doi: 10.1016/j.psyneuen.2016.05.010

Diego, M. A., Field, T., Hernandez-Reif, M., Cullen, C., Schanberg, S., and Kuhn, C. (2004). Prepartum, postpartum, and chronic depression effects on newborns. *Psychiatry* 67, 63–80. doi: 10.1521/psyc.67.1.63.31251

Dowlati, Y., Herrmann, N., Swardfager, W., Liu, H., Sham, L., Reim, E. K., et al. (2010). A meta-analysis of cytokines in major depression. *Biol. Psychiatry* 67, 446–457. doi: 10.1016/j.biopsych.2009.09.033

Duan, K. M., Ma, J. H., Wang, S. Y., Huang, Z., Zhou, Y., and Yu, H. (2018). The role of tryptophan metabolism in postpartum depression. *Metab. Brain Dis.* 33, 647–660. doi: 10.1007/s11011-017-0178-y

Ehlert, U., Patalla, U., Kirschbaum, C., Piedmont, E., and Hellhammer, D. H. (1990). Postpartum blues: salivary cortisol and psychological factors. *J. Psychosom. Res.* 34, 319–325. doi: 10.1016/0022-3999(90)90088-l

Ellenbogen, M. A., Young, S. N., Dean, P., Palmour, R. M., and Benkelfat, C. (1999). Acute tryptophan depletion in healthy young women with a family history of major affective disorder. *Psychol. Med.* 29, 35–46. doi: 10.1017/s0033291798007685

Evins, G. G., Theofrastous, J. P., and Galvin, S. L. (2000). Postpartum depression: a comparison of screening and routine clinical evaluation. *Am. J. Obstet. Gynecol.* 182, 1080–1082. doi: 10.1067/mob.2000.105409

Figueiredo, F. P., Parada, A. P., De Araujo, L. F., Silva, W. A. Jr., and Del-Ben, C. M. (2015). The Influence of genetic factors on peripartum depression: a systematic review. *J. Affect. Disord.* 172, 265–273. doi: 10.1016/j.jad.2014.10.016

Filiou, M. D. (2015). Can proteomics-based diagnostics aid clinical psychiatry? *Proteomics Clin. Appl.* 9, 885–888. doi: 10.1002/prca.201400144

Filiou, M. D., Asara, J. M., Nussbaumer, M., Teplytska, L., Landgraf, R., and Turck, C. W. (2014). Behavioral extremes of trait anxiety in mice are characterized by distinct metabolic profiles. *J. Psychiatr. Res.* 58, 115–122. doi: 10.1016/j.jpsychires.2014.07.019

Filiou, M. D., Bisle, B., Reckow, S., Teplytska, L., Maccarrone, G., and Turck, C. W. (2010). Profiling of mouse proteome and phosphoproteome by IEF. *Electrophoresis* 31, 1294–1301. doi: 10.1002/elps.200900647

Filiou, M. D., and Turck, C. W. (2011). General overview: biomarkers in neuroscience research. *Int. Rev. Neurobiol.* 101, 1–17. doi: 10.1016/B978-0-12-387718-5.00001-8

Freed, R. D., Hollenhorst, C. N., Weiduschat, N., Mao, X., Kang, G., Shungu, D. C., et al. (2017). A pilot study of cortical glutathione in youth with depression. *Psychiatry Res. Neuroimaging* 270, 54–60. doi: 10.1016/j.pscychresns.2017.10.001

Gaillard, A., Le Strat, Y., Mandelbrot, L., Keita, H., and Dubertret, C. (2014). Predictors of postpartum depression: prospective study of 264 women followed during pregnancy and postpartum. *Psychiatry Res.* 215, 341–346. doi: 10.1016/j.psychres.2013.10.003

Giustarini, D., Tsikas, D., Colombo, G., Milzani, A., Dalle-Donne, I., Fanti, P., et al. (2016). Pitfalls in the analysis of the physiological antioxidant glutathione (GSH) and its disulfide (GSSG) in biological samples: an elephant in the room. *J. Chromatogr. B Analyt. Technol. Biomed. Life Sci.* 1019, 21–28. doi: 10.1016/j.jchromb.2016.02.015

Gooding, J. R., Jensen, M. V., Dai, X., Wenner, B. R., Lu, D., Arumugam, R., et al. (2015). Adenylosuccinate is an insulin secretagogue derived from glucose-induced purine metabolism. *Cell Rep.* 13, 157–167. doi: 10.1016/j.celrep.2015.08.072

Groer, M. W., and Morgan, K. (2007). Immune, health and endocrine characteristics of depressed postpartum mothers. *Psychoneuroendocrinology* 32, 133–139. doi: 10.1016/j.psyneuen.2006.11.007

Hendrick, V., Altshuler, L. L., and Suri, R. (1998). Hormonal changes in the postpartum and implications for postpartum depression. *Psychosomatics* 39, 93–101. doi: 10.1016/s0033-3182(98)71355-6

Katon, W., Russo, J., and Gavin, A. (2014). Predictors of postpartum depression. *J. Womens Health* 23, 753–759. doi: 10.1089/jwh.2014.4824

Koenig, A. M., Karabatsiakis, A., Stoll, T., Wilker, S., Hennessy, T., Hill, M. M., et al. (2018). Serum profile changes in postpartum women with a history of childhood maltreatment: a combined metabolite and lipid fingerprinting study. *Sci. Rep.* 8:3468. doi: 10.1038/s41598-018-21763-6

Koutra, K., Roumeliotaki, T., Kyriklaki, A., Kampouri, M., Sarri, K., Vassilaki, M., et al. (2017). Maternal depression and personality traits in association with child neuropsychological and behavioral development in preschool years: mother-child cohort (rhea study) in crete. *Greece. J. Affect. Disord.* 217, 89–98. doi: 10.1016/j.jad.2017.04.002

Koutra, K., Vassilaki, M., Georgiou, V., Koutis, A., Bitsios, P., Chatzi, L., et al. (2014). Antenatal maternal mental health as determinant of postpartum depression in a population based mother-child cohort (rhea study) in crete. *Greece. Soc. Psychiatry Psychiatr Epidemiol.* 49, 711–721. doi: 10.1007/s00127-013-0758-z

Koutra, K., Vassilaki, M., Georgiou, V., Koutis, A., Bitsios, P., Kogevinas, M., et al. (2018). Pregnancy, perinatal and postpartum complications as determinants of postpartum depression: the rhea mother-child cohort in crete. *Greece. Epidemiol. Psychiatr Sci.* 27, 244–255. doi: 10.1017/S2045796016001062

Kumar, P., and Magon, N. (2012). Hormones in pregnancy. *Niger. Med. J.* 53, 179–183. doi: 10.4103/0300-1652.107549

Kurki, T., Hiilesmaa, V., Raitasalo, R., Mattila, H., and Ylikorkala, O. (2000). Depression and anxiety in early pregnancy and risk for preeclampsia. *Obstet. Gynecol.* 95, 487–490. doi: 10.1016/s0029-7844(99)00602-x

Leigh, B., and Milgrom, J. (2008). Risk factors for antenatal depression, postnatal depression and parenting stress. *BMC Psychiatry* 8:24. doi: 10.1186/1471-244X-8-24

Leonardou, A. A., Zervas, Y. M., Papageorgiou, C. C., Marks, M. N., Tsartsara, E. C., Antsaklis, A., et al. (2009). Validation of the Edinburgh postnatal depression scale and prevalence of postnatal depression at two months postpartum in a sample of greek mothers. *J. Reprod. Infant Psychol.* 27, 28–39. doi: 10.1080/02646830802004909

Lewandowska, J., and Bartoszek, A. (2011). DNA methylation in cancer development, diagnosis and therapy–multiple opportunities for genotoxic agents to act as methylome disruptors or remediators. *Mutagenesis* 26, 475–487. doi: 10.1093/mutage/ger019

Lin, L., Chen, X. M., and Liu, R. H. (2017). Novel urinary metabolite signature for diagnosing postpartum depression. *Neuropsychiatr. Dis. Treat.* 13, 1263–1270. doi: 10.2147/NDT.S135190

Lindqvist, D., Dhabhar, F. S., James, S. J., Hough, C. M., Jain, F. A., Bersani, F. S., et al. (2017). Oxidative stress, inflammation and treatment response in major depression. *Psychoneuroendocrinology* 76, 197–205. doi: 10.1016/j.psyneuen.2016.11.031

Matthey, S., Henshaw, C., Elliott, S., and Barnett, B. (2006). Variability in use of cut-off scores and formats on the edinburgh postnatal depression scale: implications for clinical and research practice. *Arch. Womens Ment. Health* 9, 309–315. doi: 10.1007/s00737-006-0152-x

Ng, F., Berk, M., Dean, O., and Bush, A. I. (2008). Oxidative stress in psychiatric disorders: evidence base and therapeutic implications. *Int. J. Neuropsychopharmacol.* 11, 851–876. doi: 10.1017/S1461145707008401

Ogawa, S., Fujii, T., Koga, N., Hori, H., Teraishi, T., Hattori, K., et al. (2014). Plasma L-tryptophan concentration in major depressive disorder: new data and meta-analysis. *J. Clin. Psychiatry* 75, e906–e915. doi: 10.4088/JCP.13r08908

O'Hara, M. W., and Wisner, K. L. (2014). Perinatal mental illness: definition, description and aetiology. *Best Pract. Res. Clin. Obstet. Gynaecol.* 28, 3–12. doi: 10.1016/j.bpobgyn.2013.09.002

Okano, T., and Nomura, J. (1992). Endocrine study of the maternity blues. *Prog. Neuropsychopharmacol. Biol. Psychiatry* 16, 921–932. doi: 10.1016/0278-5846(92)90110-z

Pan, J. X., Xia, J. J., Deng, F. L., Liang, W. W., Wu, J., Yin, B. M., et al. (2018). Diagnosis of major depressive disorder based on changes in multiple plasma neurotransmitters: a targeted metabolomics study. *Transl. Psychiatry* 8:130. doi: 10.1038/s41398-018-0183-x

Parizek, A., Mikesova, M., Jirak, R., Hill, M., Koucky, M., Paskova, A., et al. (2014). Steroid hormones in the development of postpartum depression. *Physiol. Res.* 63(Suppl. 2), S277–S282.

Parry, B. L., Sorenson, D. L., Meliska, C. J., Basavaraj, N., Zirpoli, G. G., Gamst, A., et al. (2003). Hormonal basis of mood and postpartum disorders. *Curr. Womens Health Rep.* 3, 230–235.

Pinto, J. V., Moulin, T. C., and Amaral, O. B. (2017). On the transdiagnostic nature of peripheral biomarkers in major psychiatric disorders: a systematic review. *Neurosci. Biobehav. Rev.* 83, 97–108. doi: 10.1016/j.neubiorev.2017.10.001

Pollock, P. H., and Percy, A. (1999). Maternal antenatal attachment style and potential fetal abuse. *Child Abuse Negl.* 23, 1345–1357. doi: 10.1016/s0145-2134(99)00101-5

Quinones, M. P., and Kaddurah-Daouk, R. (2009). Metabolomics tools for identifying biomarkers for neuropsychiatric diseases. *Neurobiol. Dis.* 35, 165–176. doi: 10.1016/j.nbd.2009.02.019

Reck, C., Hunt, A., Fuchs, T., Weiss, R., Noon, A., Moehler, E., et al. (2004). Interactive regulation of affect in postpartum depressed mothers and their infants: an overview. *Psychopathology* 37, 272–280. doi: 10.1159/000081983

Rich, J. L., Byrne, J. M., Curryer, C., Byles, J. E., and Loxton, D. (2013). Prevalence and correlates of depression among Australian women: a systematic literature review. January 1999- January 2010. *BMC Res. Notes* 6:424. doi: 10.1186/1756-0500-6-424.

Seth, S., Lewis, A. J., and Galbally, M. (2016). Perinatal maternal depression and cortisol function in pregnancy and the postpartum period: a systematic literature review. *BMC Pregnancy Childbirth* 16:124. doi: 10.1186/s12884-016-0915-y

Simpson, N. E., Tryndyak, V. P., Pogribna, M., Beland, F. A., and Pogribny, I. P. (2012). Modifying metabolically sensitive histone marks by inhibiting glutamine metabolism affects gene expression and alters cancer cell phenotype. *Epigenetics* 7, 1413–1420. doi: 10.4161/epi.22713

Taylor, A., Littlewood, J., Adams, D., Dore, C., and Glover, V. (1994). Serum cortisol levels are related to moods of elation and dysphoria in new mothers. *Psychiatry Res.* 54, 241–247. doi: 10.1016/0165-1781(94)90018-3

Tietze, F. (1969). Enzymic method for quantitative determination of nanogram amounts of total and oxidized glutathione: applications to mammalian blood and other tissues. *Anal. Biochem.* 27, 502–522. doi: 10.1016/0003-2697(69)90064-5

Turck, C. W., and Filiou, M. D. (2015). What have mass spectrometry-based proteomics and metabolomics (not) taught us about psychiatric disorders? *Mol. Neuropsychiatry* 1, 69–75. doi: 10.1159/000381902

Van de Velde, S., Bracke, P., and Levecque, K. (2010). Gender differences in depression in 23 european countries. cross-national variation in the gender gap in depression. *Soc. Sci. Med.* 71, 305–313. doi: 10.1016/j.socscimed.2010.03.035

Verreault, N., Da Costa, D., Marchand, A., Ireland, K., Dritsa, M., and Khalife, S. (2014). Rates and risk factors associated with depressive symptoms during pregnancy and with postpartum onset. *J. Psychosom. Obstet. Gynaecol.* 35, 84–91. doi: 10.3109/0167482X.2014.947953

Vivilaki, V. G., Dafermos, V., Kogevinas, M., Bitsios, P., and Lionis, C. (2009). The Edinburgh Postnatal Depression Scale: translation and validation for a Greek sample. *BMC Public Health* 9:329. doi: 10.1186/1471-2458-9-329

WHO, (2015). *Fact sheet N*. Available at: https://www.who.int/en/news-room/fact-sheets/detail/depression (accessed October 2015).

Xia, J., Psychogios, N., Young, N., and Wishart, D. S. (2009). Metaboanalyst: a web server for metabolomic data analysis and interpretation. *Nucleic Acids Res.* 37, W652–W660. doi: 10.1093/nar/gkp356

Yuan, M., Breitkopf, S. B., Yang, X., and Asara, J. M. (2012). A positive/negative ion-switching, targeted mass spectrometry-based metabolomics platform for bodily fluids, cells, and fresh and fixed tissue. *Nat. Protoc.* 7, 872–881. doi: 10.1038/nprot.2012.024

Zhang, L., Zou, W., Huang, Y., Wen, X., Huang, J., Wang, Y., et al. (2019). A Preliminary study of uric metabolomic alteration for postpartum depression based on liquid chromatography coupled to quadrupole time-of-flight mass spectrometry. *Dis. Markers* 2019:4264803. doi: 10.1155/2019/4264803

Zhang, Y., Yuan, S., Pu, J., Yang, L., Zhou, X., Liu, L., et al. (2018). Integrated metabolomics and proteomics analysis of hippocampus in a rat model of depression. *Neuroscience* 371, 207–220. doi: 10.1016/j.neuroscience.2017.12.001

Conflict of Interest Statement: The authors declare that the research was conducted in the absence of any commercial or financial relationships that could be construed as a potential conflict of interest.

frontiers in Pharmacology

REVIEW
published: 04 February 2020
doi: 10.3389/fphar.2019.01669

Progress in Genetic Polymorphisms Related to Lipid Disturbances Induced by Atypical Antipsychotic Drugs

Nana Li[1,2], *Ting Cao*[1,2], *Xiangxin Wu*[1,2], *Mimi Tang*[3,4], *Daxiong Xiang*[1,2] *and Hualin Cai*[1,2]*

[1] Department of Pharmacy, The Second Xiangya Hospital of Central South University, Changsha, China, [2] Institute of Clinical Pharmacy, Central South University, Changsha, China, [3] Department of Pharmacy, Xiangya Hospital, Central South University, Changsha, China, [4] Institute of Hospital Pharmacy, Xiangya Hospital, Central South University, Changsha, China

Metabolic side effects such as weight gain and disturbed lipid metabolism are often observed in the treatment of atypical antipsychotic drugs (AAPDs), which contribute to an excessive prevalence of metabolic syndrome among schizophrenic patients. Great individual differences are observed but the underlying mechanisms are still uncertain. Research on pharmacogenomics indicates that gene polymorphisms involved in the pathways controlling food intake and lipid metabolism may play a significant role. In this review, relevant genes (*HTR2C*, *DRD2*, *LEP*, *NPY*, *MC4R*, *BDNF*, *MC4R*, *CNR1*, *INSIG2*, *ADRA2A*) and genetic polymorphisms related to metabolic side effects of AAPDs especially dyslipidemia were summarized. Apart from clinical studies, *in vitro* and *in vivo* evidence is also analyzed to support related theories. The association of central and peripheral mechanisms is emphasized, enabling the possibility of using peripheral gene expression to predict the central status. Novel methodological development of pharmacogenomics is in urgent need, so as to provide references for individualized medication and further to shed some light on the mechanisms underlying AAPD-induced lipid disturbances.

Keywords: atypical antipsychotic drugs, weight gain, metabolic syndrome, pharmacogenomics, single nucleotide polymorphisms, leptin, 5-HT_{2C} receptor

OPEN ACCESS

Edited by:
Fabiana Novellino, Institute of Molecular Bioimaging and Physiology (CNR), Italy

Reviewed by:
Maria Salsone, Italian National Research Council (CNR), Italy
Giulia Donzuso, University of Catania, Italy
Graziella Mangone, INSERM CIC1422 CIC Pitié Neurosciences, France

***Correspondence:**
Hualin Cai
hualincai@csu.edu.cn

Specialty section:
This article was submitted to Neuropharmacology, a section of the journal Frontiers in Pharmacology

Received: *27 December 2018*
Accepted: *20 December 2019*
Published: *04 February 2020*

Citation:
Li N, Cao T, Wu X, Tang M, Xiang D and Cai H (2020) Progress in Genetic Polymorphisms Related to Lipid Disturbances Induced by Atypical Antipsychotic Drugs. Front. Pharmacol. 10:1669. doi: 10.3389/fphar.2019.01669

INTRODUCTION

Schizophrenia is a severe mental disorder with a lifetime morbid risk of approximately 1% across the world (McGrath et al., 2008). Continuous treatment with sufficient dosage of antipsychotic drugs is essential in the therapy and management of schizophrenia (Emsley, 2018). Second-generation antipsychotics [also called atypical antipsychotic drugs (AAPDs)] are first-line

Abbreviations: AAPD, atypical antipsychotic drug; 5-HT, 5-hydroxytryptamine/serotonin; DRD2, dopamine receptor D2; LEP, leptin; NPY, neuropeptide Y; MC4R, the melanocortin 4 receptor; BDNF, the brain-derived neurotrophic factor; CNR1, the cannabinoid 1 receptor; *INSIG*, insulin-induced gene; ADRA2A, adrenergic α-2A receptors; SNP, single nucleotide polymorphism; BMI, body mass index; HDL, high-density lipoprotein; AgRP, agouti-related protein; CART, amphetamine-regulated transcript; POMC, pro-opiomelanocortin.

antipsychotics with greater improvement of negative symptoms and fewer extrapyramidal symptoms than first-generation antipsychotics. However, metabolic side effects (e.g., weight gain, dyslipidemia, hyperglycemia, etc.) induced by AAPDs raise the risk of cardiovascular diseases, which results in patient noncompliance, relapse, and increased mortality (Mottillo et al., 2010; Mitchell et al., 2013; Ringen et al., 2014). Several studies have reported that antipsychotic-induced weight gain is reversible among pediatric and adult patients who discontinued treatment of antipsychotics (de Kuijper et al., 2013; Upadhyay et al., 2019). It is usually uneasy to make an optimum choice since benefits of these drugs have to be weighed against risks.

Although there have been tremendous reports on the metabolic side effects of atypical antipsychotic drugs, the mechanisms remain elusive (Reynolds and McGowan, 2017). Available evidence has suggested that the clinical responses to antipsychotics and related side effects could vary from patient to patient. The large variability can be attributed to a variety of complex factors, in which genetic factors may play a dominant role. Numerous studies on pharmacogenomics have been conducted to elucidate gene variants related to antipsychotic-induced weight gain or metabolic disturbances (Lett et al., 2011; Zhang et al., 2016; Zai et al., 2018). A meta-analysis has revealed that the genes of pharmacodynamic targets of antipsychotics like *HTR2C*, *DRD2*, *ADRA2A* and genes implicated in obesity such as *MC4R*, *GNB3*, *FTO*, *LEP*, *LEPR*, *BDNF*, and *INSIG2* seem to be consistently relevant to antipsychotic-induced weight gain (Zhang et al., 2016). The current systematic review aims to provide an update on the gene polymorphisms related to lipid disturbances of AAPDs and to find the possible relations between central and peripheral pathways.

METHODS

Literature research was conducted on PubMed (last: 31 October 2019) with the combinations of the key words: antipsychotic* neuroleptic*, gene, pharmacogen*, polymorphism, weight gain, metabolic, and dyslipidemia. Inclusion criteria were: 1) patients with mental illness; 2) under the treatment of atypical antipsychotic drugs; 3) specific gene polymorphisms were studied; 4) outcomes involved in lipid metabolism such weight, BMI, and percentage of metabolic syndrome, etc. Exclusion criteria were: 1) a review or letter; 2) studies on animals; 3) studies of genes not examined in other studies. Totally, 43 studies were selected for this review (see **Figure 1** and **Table 1** for details).

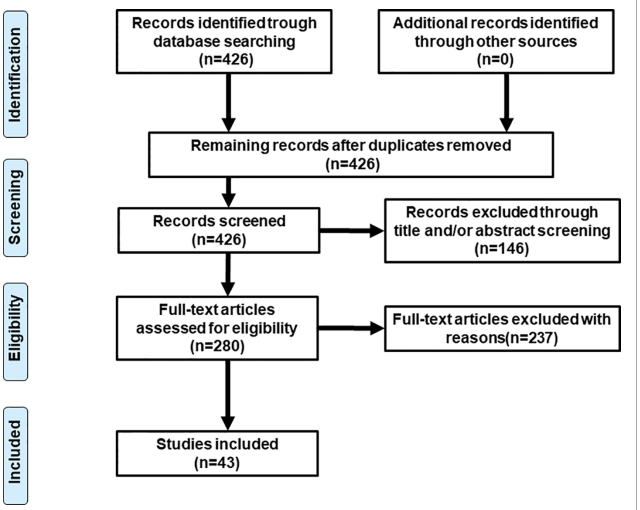

FIGURE 1 | Flowchart of study selection.

GENE POLYMORPHISMS RELATED TO CENTRAL NERVOUS SYSTEM

The Serotonin 5-HT_{2c} Receptor

Central serotonin system is associated with the modulation of feeding behavior (Lam et al., 2010). There are at least seven subtypes of 5-HT receptors, of which the 5-HT_2 subtype is divided into 5-HT_{2A}, 5-HT_{2B}, and 5-HT_{2C}. The serotonin 5-HT_{2C} receptor has shown the most consistent findings in studies on atypical antipsychotic drug-induced lipid disturbances. The serotonin 5-HT_{2C} receptor is present in hypothalamic nuclei such as the arcuate nucleus (ARC) and the ventral tegmental area (VTA) (Faton et al., 2018). Animal experiments have shown that 5-HT_{2C} receptor agonists reduce feeding (Clifton et al., 2000), and the antagonists increase feeding and lead to weight gain (Bonhaus et al., 1997). The serotonin 5-HT_{2C} receptor gene knockout mice ate more than the controls and became obesity (Tecott et al., 1995). Numerous studies have indicated that 5-HT_{2C} receptor mediates leptin-induced anorexia, but reports regarding serotonin-leptin interactions are discrepant (von Meyenburg et al., 2003; Voigt and Fink, 2015; Wierucka-Rybak et al., 2016). Cannabinoid receptor 1 (CB_1 receptor) stimulation could inhibit the secretion of cerebral serotonin in the mouse brain (Nakazi et al., 2000). Coupled with the inhibition of neuropeptide Y (NPY)/agouti-related protein (AgRP) neurons by 5-HT_{1B} receptor action, 5-HT_{2C} receptor mediates the activation of pro-opiomelanocortin (POMC) neurons as a downstream pathway of serotonin controlling food intake (Lam et al., 2010). Showing the highest antagonizing affinity to 5-HT_{2C} receptor among antipsychotic drugs, clozapine and olanzapine exert the most serious effects of weight gain in patients (Allison et al., 1999). It suggested that the antagonism against 5-HT_{2C} receptor by antipsychotic drugs may lead to increased food intake and eventually weight gain. This is supported by the observation that olanzapine exerts its metabolic side effects by targeting 5-HT_{2C} receptor in mouse model (Lord et al., 2017).

The promoter region of *HTR2C* gene is mainly influenced by -759C/T (rs3813929) and -697G/C (rs518147) polymorphisms. *HTR2C* -759C/T polymorphism was the first single nucleotide polymorphism (SNP) to be reported as an associated *HTR2C* polymorphism with antipsychotic drug-induced weight gain

TABLE 1 | Demographic, treatment, and lipid parameters of mentioned studies.

Reference	Genes (SNPs)	Functional SNPs	Risk allele	Period	APs (n)	% Caucasian	Sample size (M/F), %FEDN	Age	Diagnoses	Single/multi-center	Lipid parameters
Reynolds et al., 2002	*HTR2C* rs3813929 (-759C/T)	Yes	C	6, 10 wk	CP (69), RIS (46), CLO (4), FLU (3), SUL (1)	0 (100% Asian)	123 (61/62), 100%	26.6 ± 7.7	SCZ	Single	BMI change, >7% weight gain
Templeman et al., 2005	*HTR2C* rs3813929	–	C	6 wk, 3 mo, 9 mo	RIS (26), OLZ (19), HAL (10), QUE (11), ZIP (6), AMI (1)	100	73 (55/18), 100%	25.2 ± 0.78	Psychosis	Single	BMI change, >7% BMI increase
	LEP rs7799039 (-2548A/G)	Yes	G								
Ryu et al., 2007	*HTR2C* rs3813929	–	C	4 wk	RIS (53), OLZ (12), AMI (5), QUE (4), SGAs (10)	0 (100% Asian)	84 (39/45), 69%	30.1 ± 7.4	SCZ	Single	>5, >7% BMI increase
Mulder et al., 2007	*HTR2C* rs3813929	–	NS	Cross-sectional study	CLO, OLZ, RIS (> 80%); others	88	112 (74/38), 0%	36 ± 10	SCZ (63%), SZA (25%), others (12%)	Single	Presence of MS, HDL-C, TG, Waist, BP
	HTR2C rs518147 (-697G/C)	Yes	C								
Kuzman et al., 2008	*HTR2C* rs3813929	–	NS	4 mo	OLZ (61), RIS (47)	100	108 (0/108), 89%	30.6 ± 11.5	SCZ, SZA	Two sites	≥7% weight gain
Sicard et al., 2010	*HTR2C* rs3813929	–	NS	6 wk	CLO or OLZ (130), others	68	205 (141/64), N/A	35.9 ± 10.1	SCZ, SZA	Multiple	>7% weight gain, % weight change
	HTR2C rs518147	–	G								
	HTR2C rs6318 (Ser23Cys)	Yes	NS								
Kuzman et al., 2011	*HTR2C* rs3813929	–	T	3 mo	OLZ (61), RIS (40)	100	101 (0/101), 100%	33.47 ± 10.62	SCZ (76%), SZA (7%), delusional disorder (17%)	Single	FBG, TC, LDL, HDL, TG, BP, Waist, Hip; occurrence of MS
Hong et al., 2010	*DRD2* rs4436578	N/A	C	48.2 ± 27.8 mo	CLO (239), OLZ (70), RIS (170)	0 (100% Asian)	479 (292/187), 0%	47.2 ± 13.2	SCZ	Single	≥7% weight gain
Lencz et al., 2010	*DRD2* rs1799732 (-141C Ins/Del)	Yes	Del	6 wk	RIS (32), OLZ (26)	28 (40% African-American)	58 (44/14), 100%	23.5 ± 4.9	SCZ	Two sites	The log of the ratio of weight relative to baseline weight
Muller et al., 2012	*DRD2* rs6277 (-957C/T)	N/A	C	6, 14 wk	CLO or OLZ (132), others	62 (28% African American)	206 (141/65), N/A	35.69 ± 19.55	SCZ, SZA	Three sites	≥7% weight gain, % weight change
	DRD2 rs1079598	N/A	C								
	DRD2 rs1800497 (TaqIA)	N/A	A1 (T)								
Tybura et al., 2014	*DRD2* rs1799732	–	NS	12 wk	ZIP (59), OLZ (82), perazine (60)	100	191 (89/102), N/A	36.1 ± 12.4	SCZ	Two sites	Average weight change
	DRD2 rs1800497	–	NS								
Alladi et al., 2017	*DRD2* rs1799732	–	NS	4 wk	RIS	100% South Indian	289 (175/114), N/A	35.3 ± 10.0	SCZ	Single	>5% weight gain
	HTR2C rs3813929	–	NS								
de Leon et al., 2008	*NPY* rs1468271	N/A	G	Cross-sectional study	OLZ, QUE, or CP (165); others (192)	88	357 (229/128), 0%	37.6 ± 10.6	Severe mental illnesses	Three sites	Serum glucose, TC, HDL-C, TG
Tiwari et al., 2013	*NPY* rs10551063	N/A	NS	7.03 ± 3.4 wk	CLO (99), HAL (18), OLZ (37), RIS (40), others (32)	70 (25% African American)	226 (151/75), 58%	35.78 ± 10.6	SCZ, SZA	Three sites	≥7% weight gain, % weight change
	NPY rs16147	Yes	C								

(Continued)

TABLE 1 | Continued

Reference	Genes (SNPs)	Functional SNPs	Risk allele	Period	APs (n)	% Caucasian	Sample size (M/F), %FEDN	Age	Diagnoses	Single/multi-center	Lipid parameters
	NPY rs5573	Yes	A								
	NPY rs5574	Yes	T								
	NPY rs16475	Yes	NS								
Malhotra et al., 2012	*MC4R* rs489693	N/A	A	12 wk	RIS (84), QUE (25), ARI (30)	55.4 (23.0% African American)	139 (81/58), 100%	13.38 ± 3.75	Various diagnoses (5% SCZ)	Multiple	BMI change, weight change, fat mass, TG, TC, HDL-C, LDL-C, glucose, insulin, HOMA-IR index, leptin
				6 wk	CLO	70	73 (45/28), 0%	33.48 ± 8.33	SCZ		
				6 wk	RIS (20), QUE (5), ARI (15)	100	40 (22/18), 0%	35.20 ± 11.33	SCZ, SZA		
				12 wk	HAL (31), AMI (21), QUE (25), ZIP (15)	100	92 (53/39), 100%	26.02 ± 5.17	SCZ, SZA, SZP		
Czerwensky et al., 2013a	*MC4R* rs17782313	N/A	C	4 wk	OLZ (135), CLO, RIS, PAL, QUE, AMI	100	345 (138/207), 26%	40.1 ± 14.7	Various diagnoses	Single	% weight gain, % BMI increase
Czerwensky et al., 2013b	*MC4R* rs489693	–	A	4 wk	OLZ (135), CLO, RIS, PAL, QUE, AMI	100	341 (143/198), 25%	41.3 ± 15.0	Various diagnoses	Single	% weight gain, % BMI increase
Chowdhury et al., 2013	*MC4R* rs17782313	–	NS	6-14 wk	CLO (99), HAL (16), OLZ (36), RIS (40), others (33)	70 (25% African American)	224 (150/74), N/A	35.63 ± 10.50	SCZ, SZA	Three sites	% weight gain
	MC4R rs11872992	N/A	NS								
	MC4R rs8087522	N/A	A								
Zhang et al., 2019	*MC4R* rs489693	–	A	6 wk	ZIP (330), ARI (313), OLZ (341), QUE (332), RIS (344), HAL (166), perphenazine (165)	0 (100% Asian)	1991 (999/992), 28%	31.95 ± 7.93	SCZ	Multiple	>7% BMI gain, % change of BMI, Waist, glucose, TG, HDL, LDL
	MC4R rs17782313	–	NS								
Zhang et al., 2008	*BDNF* rs6265 (Val66Met)	Yes	Met	18 ± 6 y	CLO (98), RIS (36), FGAs (62)	0 (100% Asian)	196 (130/66) patients, 0% 50 (34/16) controls	N/A N/A	SCZ	Single	BMI gain
Tsai et al., 2011	*BDNF* rs6265	–	NS	49.2 ± 28.2 mo	CLO (266), OLZ (79), RIS (136)	0 (100% Asian)	481 (293/188), 0%	43.9 ± 8.9	SCZ	Single	% weight gain
	BDNF rs11030101	N/A	T								
	BDNF rs12291186	N/A	NS								
Zai et al., 2012	*BDNF* rs6265	–	NS	6 wk	CLO or OLZ (207); others	100	257 (188/69), 0%	31.8 ± 7.9	SCZ, SZA	Multiple	≥7% weight gain
	BDNF rs1519480	N/A	A								
Zhang et al., 2013	*BDNF* rs6265	–	Met	Cross-sectional study	CLO	0 (100% Asian)	199 (143/56), 0%	55.3 ± 6.9	SCZ	Single	Presence of MS, individual parameters
Fonseka et al., 2015	*BDNF* rs6265	–	Val	7.26 ± 3.5	CLO (87), OLZ (32), RIS (31), HAL (15), others	68 (27% African American)	188 (126/62), 0%	35.8 ± 10.0	SCZ, SZA	Three sites	≥7% weight gain, % weight change
Fang et al., 2016	*BDNF* rs6265	–	Met	Cross-sectional study	CLO (156), RIS (86), SGAs (66)	0 (100% Asian)	308 (205/103) patients, 0% 304 (180/124) controls	44.6 ± 10.3 44.5 ± 14.4	SCZ	Single	BMI
Tiwari et al., 2010a	*CNR1* rs806378	N/A	T	7.54 ± 3.55 wk	CLO (101), OLZ (34), HAL (12), RIS (36)	64 (30% African-American)	183 (124/59), 0%	36.12 ± 10.17	SCZ, SCA	Three sites	% weight gain

(Continued)

TABLE 1 | Continued

Reference	Genes (SNPs)	Functional SNPs	Risk allele	Period	APs (n)	% Caucasian	Sample size (M/F), %FEDN	Age	Diagnoses	Single/multi-center	Lipid parameters
Monteleone et al., 2010	*CNR1* rs1049353 (-1359G/A)	N/A	NS	24 wk	CLO (25), OLZ (22), RIS (14), QUE (6), ARI (6), HAL (10)	100	83 (50/33) patients, 0% 80 (40/40) controls	44.0 ± 10.5 49.4 ± 12.9	SCZ (86%)	Two sites	>7% weight gain
Park et al., 2011b	*CNR1* rs1049353	–	NS	Over 1 y	OLZ	0 (100% Asian)	78 (52/26), N/A	46.4 ± 11.6	SCZ	Three sites	≥7% weight gain
	CNR1 rs806368	–	NS								
	CNR1 rs4707436	N/A	NS								
Yu et al., 2013	*CNR1* rs6928499	N/A	G	Cross-sectional study	CLO or OLZ (197); others	95.1	407 (274/133), 0%	35.6 ± 11.0	SCZ (69.3%), SZA (20.1%), SZP (10.6%)	Single	Presence of MS, individual parameters
	CNR1 rs1535255	N/A	T								
	CNR1 rs2023239	N/A	T								
Kang et al., 2008	*LEP* rs7799039 (-2548A/G)	Yes	A	453 ± 289 d	OLZ	0 (100% Asian)	74 (50/24), N/A	47.2 ± 11.6	SCZ	Three sites	≥7% weight gain
Yevtushenko et al., 2008	*LEP* rs7799039	–	G	Cross-sectional study	CLO (21), OLZ (31), RIS (16)	100	134 (87/47), 0%	41.6 ± 11.8	SCZ, SZA	Two sites	Presence of MS, Waist, BMI, BMI ≥30 kg/m^2, presence of central obesity
	HTR2C rs3813929 (-759C/T)	–	NS								
Gregoor et al., 2010	*LEP* rs7799039	–	A	Cross-sectional study	OLZ (99), CLO (86), QUE (56), RIS (46), ARI (14)	100	353 (184/169), 0%	N/A	Psychotic disorder (50.7%)	Single	Serum TC/HDL
Gregoor et al., 2011	*LEP* rs7799039	–	NS	within 1 y	CLO (68), OLZ (54), QUE (31), ARI (23), RIS (30)	100	141 (82/59), 0%	N/A	Psychotic disorder (63.1%)	Single	BMI >30, BMI change, BMI change per week
Brandl et al., 2012	*LEP* rs7799039	–	NS	7.19 ± 3.47 wk	CLO (80), OLZ (28), RIS (32), HAL (16), others (24)	70.2 (23.8% African-American)	181 (118/63), N/A	35.93 ± 10.94	SCZ, SZA	Three sites	% weight change
	LEP rs10954173	N/A	NS								
	LEP rs3828942	N/A	NS								
Le Hellard et al., 2009	*INSIG2* rs17587100	N/A	N/A	12 ± 1.2 wk	CLO	100	160 (97/63), 0%	21.9 ± 8.9	Schizophrenia spectrum disorders	Single	BMI change
	INSIG2 rs10490624	N/A	N/A								
	INSIG2 rs17047764	N/A	N/A								
Opgen-Rhein et al., 2010	*INSIG2* rs17587100	–	NS	6 wk	CLO, OLZ, RIS, AMI, QUE, SGAs	100	128 (48/80), 17%	38.63 ± 11.96	SCZ, SZA	Three sites	≥7% weight gain, % weight change
	INSIG2 rs10490624	–	NS								
	INSIG2 rs17047764	–	NS								
Tiwari et al., 2010b	*INSIG2* rs17587100	–	NS	7.94 ± 3.74 wk	CLO (96), OLZ (34), RIS (12), HAL (12)	57.8 (35.1% African-American)	154 (110/44), 0%	35.78 ± 9.82	SCZ, SZA	Three sites	≥7% weight gain, % weight change
	INSIG2 rs10490624	–	NS								
	INSIG2 rs17047764	–	NS								
Liou et al., 2012	*INSIG2* rs11123469	N/A	C	Cross-sectional study	CLO (171), OLZ (91), RIS (194)	0 (100% Asian)	456 (369/157), 0%	N/A	SCZ	Single	Prevalence of MS
	INSIG2 rs10185316	N/A	NS								
	INSIG2 rs1559509	N/A	NS								
Wang et al., 2005	*ADRA2A* rs1800544 (-1291C/G)		G	14.0 ± 6.2 mo	CLO	0 (100% Asian)	93 (49/44), 0%	38.4 ± 8.1	SCZ	Single	Weight gain, >7% weight gain

(Continued)

TABLE 1 | Continued

Reference	Genes (SNPs)	Functional SNPs	Risk allele	Period	APs (n)	% Caucasian	Sample size (M/F), %FEDN	Age	Diagnoses	Single/multi-center	Lipid parameters
Park et al., 2006	*ADRA2A* rs1800544	–	G	Over 1 y	OLZ	0 (100% Asian)	62 (44/18), 0%	46.5 ± 11.1	SCZ	Two sites	>10% weight gain, % weight change
Sickert et al., 2009	*ADRA2A* rs1800544	–	C	8.4 ± 3.6 wk	CLO (85), OLZ (20), RIS (13), HAL (11)	50 (42% African-American)	129 (96/33), 0%	36.5 ± 9.0	SCZ, SZA	Multiple	weight gain, % weight change
Risselada et al., 2010	*ADRA2A* rs1800544	–	NS	Cross-sectional study	OLZ (106), RIS (103), CLO (102), ARI (21), QUE (12), SGAs (69)	94	470 (320/150), 0%	38 ± 10	SCZ (78%), SZA (17%)	Multiple	Presence of MS, HDL, TC, Waist, BP, glucose
De Luca et al., 2011	*ADRA2A* rs1800544	–	NS	8.3 ± 3.7 wk	CLO (91), OLZ (22), HAL (12), RIS (14)	51.8 (40.3% African-American	139 (101/38), N/A	36.2 ± 9.4	SCZ	Three sites	% weight change, weight gain >8%

SCZ, schizophrenia; SZA, schizoaffective disorder; SZP, schizophreniform disorder; FEDN, first-episode drug-naive patients; SNPs, single nucleotide polymorphisms; N/A, not available; NS, not significant; APs, antipsychotics; FGAs, first-generation antipsychotics; FLU, fluphenazine; HAL, haloperidol; CP, chlorpromazine; CLO, clozapine; OLZ, olanzapine; RIS, risperidone; ARI, aripiprazole; QUE, quetiapine; AMI, amisulpride; ZIP, ziprasidone; PAL, paliperidone; SUL, sulpiride; d, days; wk, weeks; mo, months; y, years; M, male; F, female; MS, metabolic syndrome; HDL, high-density lipoprotein; HDL-C, HDL cholesterol; LDL, low-density lipoprotein; LDL-C, LDL cholesterol; FBG, fasting blood glucose; BP, blood pressure; TG, triglycerides; TC, total cholesterol; HOMA-IR index, the homeostasis model assessment insulin resistance index; Waist, waist circumference; Hip, hip circumference.

(Reynolds et al., 2002). Besides, it is the most replicated gene polymorphism related to AAPD-induced weight gain (Zhang et al., 2016). Various clinical studies suggested that *HTR2C* -759C allele was a risk allele of a substantial weight gain (over 7% than baseline) in patients treated with typical or atypical antipsychotic drugs (Reynolds et al., 2002; Templeman et al., 2005; Ryu et al., 2007). A study in first episode drug-naive female patients with schizophrenia showed that -759T is associated with an increase in waist circumference, fasting blood glucose, and blood triglyceride levels (Kuzman et al., 2011). However, associations between *HTR2C* -759C/T polymorphism and weight gain or presence of metabolic syndrome were reported to be nonsignificant in other studies (Mulder et al., 2007; Kuzman et al., 2008; Sicard et al., 2010; Alladi et al., 2017). Despite the negative results, haplotype analyses suggested that *HTR2C* 759C-697G-Cys23 haplotype was associated with the most percentage weight gain induced by various antipsychotics (Sicard et al., 2010).

Dopamine Receptor D2

Dopamine receptor D2 (DRD2) is the main target of antipsychotic drugs. An animal study found that the availability of striatal D2 receptor in obese rats was lower than that in lean controls (Hamdi et al., 1992). In a human study, the striatal dopamine transporter availability was negatively correlated with body mass index (BMI) in a group of healthy volunteers (Chen et al., 2008). It is postulated that it could be a mechanism of overeating that the neuropeptides regulating homeostatic energy balance also modulate the activity of dopamine neurons and the rewarding circuits underlying food intake (Volkow et al., 2011). Therefore, Blum et al. hypothesized that as dopamine D2 receptor antagonists, antipsychotic drugs cause a hypodopaminergic reward circuitry, leading to excessive food intake and ultimately obesity (Blum et al., 2014). Functional magnetic resonance imaging (fMRI) showed that an increased activity in striatal regions of the reward system was positively correlated with weight gain after 6-week amisulpride treatment (Nielsen et al., 2016).

The role of *DRD2* rs4436578-C in weight gain induced by atypical antipsychotics is verified in 479 chronic schizophrenic patients under long-term treatment of clozapine, olanzapine, or risperidone (Hong et al., 2010). *DRD2* promoter region polymorphism -141C Ins/Del (rs1799732) was also reported to be associated with weight gain in 58 first episode patients treated with randomly-assigned olanzapine or risperidone for 6 weeks (Lencz et al., 2010), whereas nonsignificant associations were found in later studies of larger samples (Tybura et al., 2014; Alladi et al., 2017). A systematic analysis of genetic polymorphisms spanning the five dopamine receptor genes (*DRD1–DRD5*) found only *DRD2* rs6277 (C957T), rs1079598, and rs1800497 (TaqIA) to be significantly associated with antipsychotic-induced weight gain in chronic patients with schizophrenia or schizoaffective disorder (Muller et al., 2012). It was suggested that the C957T polymorphism would not change the amino acid sequence of the dopamine D2 receptor, but it was related to the stability of the striatum D2 receptor (Hirvonen et al., 2009) and the stability and half-life of the *DRD2*

messenger RNA (mRNA) (Duan et al., 2003). The TaqIA polymorphism is located in coding region of the adjacent *ANKK1* gene and overlaps with the 3' end region of the *DRD2* gene. So, it may be in linkage disequilibrium with a functional polymorphism of *DRD2*, or may affect the dopamine signaling through the *ANKK1* gene. Studies have shown that if the TaqIA site is A1, it may result in decreased expression of *DRD2* and decreased dopaminergic activity (Giegling et al., 2013).

Neuropeptide Y

NPY is a 36-amino-acid peptide expressed in the central and peripheral nervous system. In the ARC neurons, NPY colocalizes with AgRP, which can antagonize α-melanocyte-stimulating hormones (α-MSH) binding to melanocortin-3 receptor (MC3R) and melanocortin-4 receptor (MC4R). Another group of neurons co-express POMC and cocaine and amphetamine-regulated transcript (CART) and inhibit food intake (Arora and Anubhuti, 2006). Low leptin levels can upregulate neuropeptide Y and exert orexigenic effects. Leptin directly and differentially regulates NPY and POMC neurons, and then controls feeding behavior and energy homeostasis (Elias et al., 1999). Outside the hypothalamus, NPY mainly exists in the brainstem and the catecholaminergic neurons in the sympathetic nervous system. Results *in vitro* indicate that NPY may inhibit lipolysis in murine adipocytes (Bradley et al., 2005). Transgenic mice overexpressing NPY showed significant obesity and the lipogenic effects as well as inhibition of catecholaminergic tone of NPY were suggested (Vahatalo et al., 2015). NPY and leptin are recognized to interact in a homeostatic loop to regulate energy balance not only in the brain, but also directly at the adipocyte level (Martinez et al., 2000).

Chronic treatment of atypical antipsychotic drugs increased NPY immunoreactivity and mRNA expression in the rat hypothalamus (Kirk et al., 2006; Weston-Green et al., 2012). *NPY* rs1468271 was associated with hypercholesterolemia in patients taking olanzapine, quetiapine, or chlorpromazine (de Leon et al., 2008). Significant associations between the SNPs rs16147, rs5573, and rs5574 in *NPY* and weight gain in clozapine or olanzapine-treated patients of European ancestry were reported (Tiwari et al., 2013). Compared with carriers of TT genotype at rs16147, individuals with the C allele showed a higher risk of weight gain probably due to increased NPY levels. Besides, genetic interaction between rs16147 in *NPY* and rs806378 in cannabinoid receptor 1 gene further supports their biological interaction (Tiwari et al., 2013).

The Melanocortin 4 Receptor

The MC4R is a transmembrane G protein-coupled receptor expressed in the hypothalamus and peripheral tissues. The central melanocortin system potently regulates feeding and directly controls lipid metabolism in liver and adipocytes (Nogueiras et al., 2007). MC4R plays a key role in suppressing food intake. *MC4R* gene is the most common single-gene effect of human obesity (Beckers et al., 2011). Rodent experiments showed that *Mc4r* knockout mouse exhibited hyperinsulinemia, hyperglycemia, and adult obesity syndrome (Srisai et al., 2011). Multiple pathways are involved in the regulation of central melanocortin system in energy homeostasis (Shen et al., 2017). MC4R signaling regulates energy balance through stimulating brain-derived neurotrophic factor (BDNF) expression in the ventromedial hypothalamus (VMH) (Xu et al., 2003). Central melanocortin pathway through MC4R is an indispensable downstream mediator of the anorexigenic effect of serotonin (Lam et al., 2008). The expression of MC4R in the rat hypothalamus is increased under the long-term treatment of antipsychotics probably through a compensatory mechanism (Rojczyk et al., 2015). A genome-wide association study found that *MC4R* rs489693 demonstrated consistent effects on weight gain, as well as on levels of triglycerides, leptin, and insulin, HOMA-IR index (the homeostasis model assessment insulin resistance index), and total fat mass (Malhotra et al., 2012). Afterward, the association between *MC4R* rs489693 A-allele and greater weight gain was confirmed (Czerwensky et al., 2013b). They also reported carriers of *MC4R* rs17782313 C-allele at risk of greater percentage weight gain after taking atypical antipsychotics (Czerwensky et al., 2013a). However, Chowdhury et al. didn't replicate the significant association of rs17782313, but they reported that carriers of rs8087522-A gained significantly more weight than non-carriers in white Americans (Chowdhury et al., 2013). Located in the *MC4R* promoter region, rs8087522 A-allele may affect the gene expression of *MC4R* by binding to an unknown nuclear protein, while the G-allele has no effect. A large-scale pharmacogenetic study in Chinese schizophrenia patients reported the ubiquitous association between rs489693 and metabolic measures, while rs17782313 is less involved in antipsychotic-induced metabolic disturbances (Zhang et al., 2019).

Brain-Derived Neurotrophic Factor

The BDNF is a member of the neurotrophic factor family abundantly expressed in the hippocampus and hypothalamus. Beyond a fundamental role in the brain development and plasticity, BDNF is thought to play a major part in the regulation of food intake (Rosas-Vargas et al., 2011). It is reported that central infusion of BDNF can induce dose-dependent food restriction and weight loss, perhaps *via* its up-regulation of hypothalamic serotonin activity (Pelleymounter et al., 1995). BDNF was also observed to regulate food intake *via* its inhibitory effect on NPY and modulation of the dopamine system (Wang et al., 2007; Cordeira et al., 2010). Researchers have found reduced serum BDNF levels in first-episode drug naive psychosis patients and a trend of greater reductions in female patients (Jindal et al., 2010). Moreover, a significant increase in BDNF levels in prefrontal cortex and cerebrospinal fluid samples of postmortem schizophrenia patients was reported (Issa et al., 2010). Thus, alterations in BDNF may play a role in the pathophysiology of schizophrenia (Favalli et al., 2012). Both typical (haloperidol) and atypical antipsychotic drugs (clozapine, risperidone) decrease serum BDNF levels in schizophrenia patients (Xiu et al., 2009) and the expression of *Bdnf* mRNA in the hippocampus of rats (Angelucci et al., 2000; Lipska et al., 2001; Chlan-Fourney et al., 2002) although results are inconsistent in some studies (Bai et al., 2003; Park et al., 2011a). Further, reduced serum

BDNF levels may be related with weight gain in female but not in male patients with schizophrenia under long-term antipsychotic treatment (Zhang et al., 2007). The effect of BDNF on weight gain induced by antipsychotics seems to be gender-specific but the results are inconsistent.

Human *BDNF* gene is located on chromosome 11p14.1. The Val66Met variant (rs6265) in the *BDNF* promoter region is the most investigated SNP of the gene, showing an association of cognitive impairment (Bath and Lee, 2006) and obesity (Skledar et al., 2012). It markedly alters the intracellular trafficking and packaging of pro-BDNF and impacts the activity-dependent secretion of the mature peptide (Egan et al., 2003). The Met/Met genotype of the *BDNF* Val66Met polymorphism has a significant effect on BMI gain and metabolic syndrome in male but not female schizophrenic patients treated with long-term antipsychotic drugs (Zhang et al., 2008; Zhang et al., 2013; Fang et al., 2016). However, these results are incompatible with some studies that indicate Val/Val was associated with greater weight gain induced by antipsychotics (Fonseka et al., 2015). Tsai et al. failed to replicate the relationship between the Val66Met polymorphism and body weight gain after long-term antipsychotic treatment, but they found a visible difference in percentage weight change in patients with different copies of haplotype GTA (rs6265-rs11030101-rs12291186) (Tsai et al., 2011). Additionally, a two-marker haplotype rs6265-rs1519480 was also reported to be associated with antipsychotic-induced weight change in European ancestry (Zai et al., 2012).

The Cannabinoid 1 Receptor

The endocannabinoid system is involved in modulating energy homeostasis by controlling food intake *via* central and peripheral pathways, as well as stimulating lipogenesis and fat accumulation (Di Marzo and Matias, 2005; Bluher et al., 2006). It may be negatively regulated by leptin in the neural circuitry (Di Marzo et al., 2001). In the hypothalamus, the interaction between the endocannabinoid and NPY systems appears to be bidirectional, and peripheral endocannabinoid levels are increased in obese mice induced by neuropeptide Y overexpression (Vähätalo et al., 2015). Encoding by the gene *CNR1*, the CB_1 receptor mediates the effects of cannabinoid binding primarily in the brain and also presents in peripheral tissues, including adipocytes (Bensaid et al., 2003), hepatocytes (Osei-Hyiaman et al., 2005), pancreas (Nakata and Yada, 2008), muscle (Mendizabal-Zubiaga et al., 2016), and the gut (Coutts and Izzo, 2004). *Cnr1* knockout mice experienced food restriction compared with wild-type littermates (Di Marzo et al., 2001). Selective CB_1 receptor antagonist SR141716A (rimonabant) ameliorates diet-induced obesity of mice through enhancement of fatty acid oxidation and energy expenditure in white adipocytes (Jbilo et al., 2005), or modulating macrophage inflammatory mediators *via* gut microbiota alterations (Mehrpouya-Bahrami et al., 2017). Clinical trials proved that rimonabant decreased body weight and waist circumference in overweight or obese patients (Van Gaal et al., 2005; Pi-Sunyer et al., 2006). The 3813G allele at the exon 4 of *CNR1* is associated with obesity-related phenotypes like waist circumference and subscapular skinfold thickness in adult men (Russo et al., 2007).

Evidence from pre-clinical, clinical, genetic, postmortem, and neuroimaging studies have indicated an important role of the endocannabinoid system and cannabinoid receptors in the pathophysiology of schizophrenia (Fakhoury, 2017). The G allele frequency of the *CNR1* 1359G/A gene polymorphism potentially relates to therapeutic response to atypical antipsychotics (Hamdani et al., 2008). Alterations in CB_1 receptor-mediated G-protein signaling by antipsychotic treatment was different in a sex- and age-selective manner (Wiley et al., 2008). Chronic treatment with aripiprazole upregulated the gene expression of *Cnr1* in the frontal cortex of rats (Cheng et al., 2008). Risperidone increased CB_1 receptor binding in rat brain (Secher et al., 2010). Oral intake of haloperidol or olanzapine produces region-specific increase in cannabinoid receptor levels distinctly (Delis et al., 2017). Both CB_1 receptor antagonist NESS06SM and inverse agonist rimonabant reduced food intake and weight gain and restored all blood parameters in a rat model treated with olanzapine (Lazzari et al., 2017). However, the results of the relationship between *CNR1* polymorphisms and antipsychotic-induced lipid disturbances differ from various single nucleotide polymorphisms. A study of 20 tag SNPs found the rs806378 polymorphism to be associated with weight gain in European patients treated with clozapine or olanzapine (Tiwari et al., 2010a). *CNR1* polymorphisms -1359 G/A (rs1049353, rs806368, and rs4707436) were not associated with antipsychotic-induced weight gain (Monteleone et al., 2010; Park et al., 2011b). A cross-sectional study of a naturalistic cohort of 407 patients with schizophrenia showed the minor alleles of rs6928499, rs1535255, and rs2023239 were associated with lower levels of high-density lipoprotein cholesterol and fasting glucose (Yu et al., 2013).

GENE POLYMORPHISMS RELATED TO PERIPHERAL TISSUES

Leptin

Leptin is a peptide hormone predominantly secreted by adipocytes, targeting hypothalamic nerve network to suppress appetite. At peripheral level, leptin is involved in the regulation of lipid and glucose metabolism in adipose tissue, liver, and skeletal muscle, as well as gastrointestinal nutrient absorption (Sáinz et al., 2015). Leptin resistance primarily takes responsibility for obesity in some studies (Sáinz et al., 2015). Serum leptin levels were elevated significantly after treatment of olanzapine, clozapine, and quetiapine, whereas haloperidol and risperidone produced nonsignificant leptin changes (Potvin et al., 2015). The significant association between leptin increases and BMI changes was observed across studies. Two hypotheses about the role played by leptin in antipsychotic-induced weight gain were proposed: leptin as an epiphenomenon of weight gain, or antipsychotic-induced leptin resistance causing weight gain (Panariello et al., 2012).

Therefore, the correlation between leptin gene (*LEP*) and lipid disturbances induced by atypical antipsychotics has been a research hotspot. Among the polymorphisms, *LEP* rs7799039

(-2548A/G) was verified to be associated with weight gain in many studies (Templeman et al., 2005; Kang et al., 2008; Shen et al., 2014). A cross-sectional study showed that serum total cholesterol (TC)/high-density lipoprotein (HDL) ratio in *LEP* -2548G male carriers was lower than that of non-carriers after taking AAPDs for more than 3 months, but not significant in female patients (Gregoor et al., 2010). However, a longitudinal study conducted by the same group found *LEP* -2548G was not significantly associated with BMI change during treatment of atypical antipsychotics (Gregoor et al., 2011). A haplotype of *LEP* rs7799039G-rs10954173G-rs3828942G showed a significant association with weight gain despite results of all the SNPs were not significant (Brandl et al., 2012). A meta-analysis indicated that the *LEP* -2548A allele was associated with an increased risk of antipsychotic-induced weight gain in Asian patients, while it seemed to decrease the risk in European populations (Shen et al., 2014). Combined genotype analysis revealed that gene-gene interaction between the *LEP* and *HTR2C* polymorphisms was highly significant in their associations with occurrences of metabolic syndrome, BMI, and waist circumference (Yevtushenko et al., 2008).

Insulin-Induced Gene 2

In the endoplasmic reticulum (ER), insulin-induced gene (INSIG) proteins form complexes with sterol-regulatory element-binding proteins (SREBPs) and SREBP cleavage activating proteins (SCAP), regulating cholesterol and lipid fatty acid biosynthesis (McPherson and Gauthier, 2004). There are two isoforms of INSIG proteins, INSIG1 and INSIG2. INSIG2 is not a transcriptional target of SREBPs as INSIG1, but it can also cause the retention of the SCAP/SREBP complex in the ER in a sterol dependent way and thereby blocks cholesterol synthesis (Yabe et al., 2002). The INSIG2/SCAP/SREBP signaling may be altered by various antipsychotic drugs. Both clozapine and haloperidol can activate the gene expressions of the SREBP system in human glioma cells, which may be a mechanism of therapeutic efficacy (Ferno et al., 2005). But the upregulation of the lipogenesis in peripheral tissues can be a cause of the metabolic side effects induced by antipsychotics. Clozapine and risperidone significantly reduced INSIG2 and activated the expression of SCAP/SREBP in rat liver (Cai et al., 2015). It is reported that AAPD treatment induces early-stage lipid biosynthesis in adipose-derived stem cells (ASCs) and such abnormal lipogenesis can be reversed when INSIG2 expression was increased (Chen et al., 2017). Three markers (rs17587100, rs10490624, and rs17047764) localized within or near the *INSIG2* gene had a strong association with clozapine-induced BMI gain in German patients with schizophrenia (Le Hellard et al., 2009). However, significant associations of the three aforementioned SNPs weren't replicated in other European patients (Opgen-Rhein et al., 2010; Tiwari et al., 2010b). Liou et al. demonstrated that the C-C-C haplotype of *INSIG2* rs11123469-rs10185316-rs1559509 significantly elevated the risk of AAPD-induced metabolic syndrome (Liou et al., 2012). This association can be attributed to the action of *INSIG2* independently or the gene-gene interaction with *INSIG1*.

Adrenergic Alpha-2a Receptor

The sympathetic nervous system regulated by the hypothalamus plays an important role in energy expenditure and lipolysis. Adrenergic α-2 receptors are classified into three subtypes, α_{2A}, α_{2B}, and α_{2C}. Mice lacking α_{2A}-adrenoceptors (ADRA2A) showed increased energy expenditure, lipolysis, and hyperinsulinemia (Ruohonen et al., 2018). Atypical antipsychotics have affinities for adrenergic receptors, including subtypes of α_{2A}, α_{2B}, α_{2C}, α_{1A}, α_{1B} (Roth et al., 2004). The -1291 C/G promoter polymorphism (rs1800544) located in the regulatory promoter sequence of the *ADRA2A* gene may influence the transcription factor control. Association between *ADRA2A* rs1800544 polymorphism and schizophrenia was found in a study of Czech male patients with schizophrenia (Lochman et al., 2013). Carriers of *ADRA2A* 1291-GG gained more weight than the subjects with genotype 1291-CC in Asian patients after long-term treatment of clozapine or olanzapine (Wang et al., 2005; Park et al., 2006). But results of European-Americans showed the carriers of the *ADRA2A* -1291C allele gained more weight during treatment of 8.4 weeks on average (Sickert et al., 2009). The association between *ADRA2A* -1291C/G and the prevalence of metabolic syndrome wasn't significant among white patients using antipsychotics (Risselada et al., 2010). No significant association between *ADRA2A* -1291C/G and weight gain could be detected in another study among complex ethnic subjects treated with different antipsychotic drugs (De Luca et al., 2011). Conflicting results might be attributed to ethnic differences and diverse observation periods.

RELATIONS BETWEEN GENES IN CENTRAL NERVOUS SYSTEM AND PERIPHERAL TISSUES

Gene expression in central nervous system is not readily available, therefore, it is of great importance to find equivalent evidence from the peripheral blood. It was reported that gene expression in peripheral blood mononuclear cells could be used as a fingerprint of central nervous system disease (Achiron and Gurevich, 2006). Thus, we focus on the network connections between the regulatory mechanisms of central nervous system pathways and peripheral pathways. The connection of the overall related genes mentioned in this review is shown in **Figure 2**. It is obvious that antipsychotics might induce weight gain or metabolic syndrome through central and peripheral ways. In central nervous system, *HTR2C*, *DRD2*, *LEP*, *NPY*, *MC4R*, *BDNF*, *CNR1* polymorphisms play an important role in regulating food intake, and they can be affected by AAPDs. Besides, the lipid metabolism in peripheral tissues may be altered by the SNPs of *LEP*, *NPY*, *MC4R*, *CNR1*, *INSIG2*, and *ADRA2A*. As we can see in **Figure 2**, complex pathways are involved in the modulation of energy intake and energy expenditure, that is orexigenic and anorexigenic mechanisms. NPY/AgRP neurons and POMC neurons play a fundamental role in the downstream of the pathway of *LEP*, *CNR1*, and *HTR2C*. *NPY* is an orexigenic

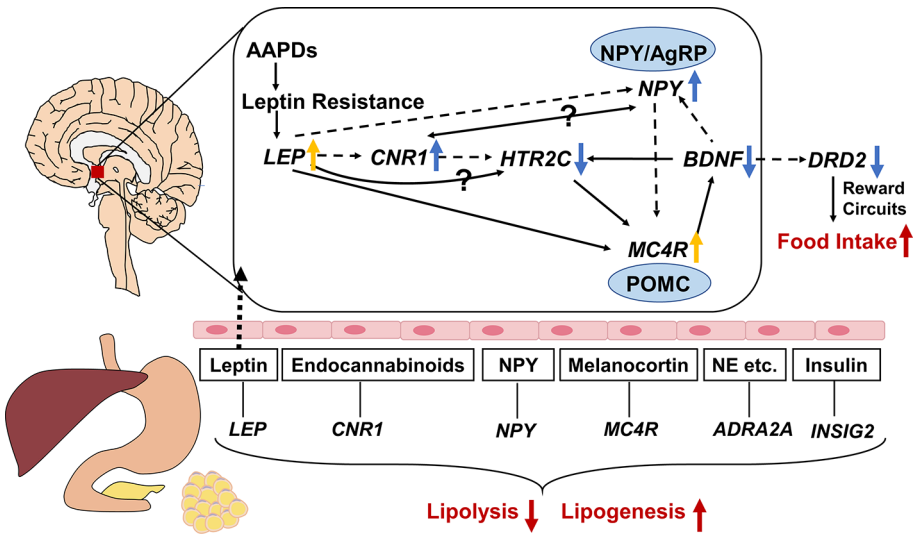

FIGURE 2 | Gene-gene interaction among genes associated with atypical antipsychotic-induced lipid disturbances. The central and peripheral pathways are separated by brain-blood barrier, with leptin through it. Neuropeptide Y (NPY)/agouti-related protein (AgRP) neurons and pro-opiomelanocortin (POMC) neurons play a fundamental role in the downstream of the pathway of *LEP*, *CNR1*, and *HTR2C*. NPY is an orexigenic mediator whereas melanocortin-4 receptor (MC4R) exert anorexigenic effects. *HTR2C* mediates the effects of multiple genes, such as *LEP*, *CNR1*, and *BDNF*. Dopamine regulate appetite mainly through brain reward circuits. As a bridge between the central and peripheral ways, leptin inhibits food intake by triggering multiple signaling cascades like *NPY*, *MC4R*, *CNR1*. In peripheral tissues, multiple hormones or peptides modulating lipid metabolism, such as leptin, neuropeptide Y, melanocortin, endocannabinoids, insulin, and norepinephrine etc. Inhibition of lipolysis and stimulation of lipogenesis lead to hyperlipemia and obesity. The solid and dotted lines indicate upregulation and downregulation respectively. ↑: activated by AAPDs; ↓: inhibited by AAPDs; yellow arrows indicate compensatory effects rather than direct effects; NE, norepinephrine.

mediator whereas *MC4R* exerts anorexigenic effects. *HTR2C* mediates the effects of multiple genes, such as *LEP*, *CNR1*, and *BDNF*. Dopamine regulates appetite mainly through brain reward circuits. Leptin is an upstream molecular bridging the peripheral tissue and central nervous system. Secreted from fat cells, leptin acts on the hypothalamus through the blood-brain barrier, and ultimately suppresses appetite by triggering multiple signaling cascades like *NPY*, *MC4R*, *CNR1*. In peripheral tissues, multiple hormones or peptides affect lipid metabolism, such as leptin, neuropeptide Y, melanocortin, endocannabinoids, insulin, and norepinephrine, etc. Inhibition of lipolysis and stimulation of lipogenesis lead to hyperlipemia and obesity.

CONCLUSION

Pharmacogenomics helps to find possible genetic polymorphisms related to lipid disturbances induced by atypical antipsychotic drugs and the variation among different patients. Nevertheless, inconsistency and limitations have impeded the progress in this field. As mentioned above, discrepancies often occur between different studies on the same SNP. Several reasons are to be noted. A small sample size may reduce the statistical power; and the representativeness of the sample can be weakened if the frequency of a certain base is low in a small sample. Ethnic, gender, and age differences should be taken into account. Evidence has shown worse lipid metabolic dysfunction in female schizophrenia patients due to antipsychotics (Castellani et al., 2019). Sex differences were also found in gene expression associated with antipsychotic induced weight gain (Sainz et al., 2019). Younger age has been reported to be a risk of greater antipsychotic-related weight gain (Maayan and Correll, 2010; Greil et al., 2013). The degree of the metabolic side effects varies from antipsychotics and doses. Evidence suggested a dose-dependent effect between serum levels and metabolic side effects of clozapine and olanzapine although the relationship between daily dose and metabolic disturbances is not clear. (Simon et al., 2009). First episode drug-naive patients are more sensitive to the AAPDs than chronic ones, which may cause the distinct exposure to the adverse drug reaction. Long-term treatment and short-term treatment might be different in the effects of weight gain or metabolic syndrome. To observe the alteration of BMI, a long enough study duration makes it easier to get a significant result. For instance, *LEP* -2548A/G polymorphism showed nonsignificant association with short-term (6-week and 3-month) weight change but was associated with 9-month antipsychotic-induced weight gain (Templeman et al., 2005). Meanwhile, although metabolic syndrome was verified to be related to weight gain for patients under the treatment of clozapine (Bai et al., 2011), different indicators (BMI or blood lipid levels, etc.) and diverse definitions can lead to inconsistency. Significant end points vary from body weight (or BMI) increase ≥7% of baseline to change of metabolic parameters or presence of metabolic syndrome. Hyperlipidemia (hypertriglyceridemia or hypercholesterolemia) may be the outcome of weight gain or a direct effect of antipsychotics. A rodent experiment found that

only olanzapine significantly induced weight increase in rats, but both olanzapine and clozapine elevated blood lipid levels after 9-week treatment at clinic equivalent doses (Liu et al., 2017). Therefore, different outcome variables of lipid disturbances may be analyzed separately. As for animal studies, we should pay more attention to the different regions (the striatum, the hypothalamus, etc.) and species differences when we compare the various conclusions from a bulk of published work. For example, anatomical studies and physiological experiments have suggested significant interspecies differences in the distribution of the cannabinoid 1 receptor both in central and peripheral nervous system (Howlett et al., 2002). Furthermore, since some genes participate in the metabolic side effects as well as the pharmaceutical effect, the functions of the AAPDs can be complex to analyze.

Genetic correlation study consists of single nucleotide polymorphisms, haplotype analysis, gene-gene interaction, genome wide association study (GWAS), etc. Several susceptibility gene loci have been reported but the exact mechanism hasn't been illuminated. Additionally, correlations do not imply causations. Hence, *in vitro* and *in vivo* studies are needed to explore the specific effects of AAPDs on these related genes and gene-gene interactions. Further functional analyses are also required to verify which are the functional polymorphisms and the specific functional consequences of these SNPs. Moreover, both obesity and schizophrenia are polygenic diseases, so we can speculate that the metabolic side effects of atypical antipsychotics cannot be monogenic. Research strategies of monogenic diseases are inapplicable to find out the complex causations currently. Given the limitations of such research, more efficient methods are in great need. The International Schizophrenia Consortium proposed a polygenic risk score (PRS) test for schizophrenia (International Schizophrenia C. et al., 2009). Now schizophrenia polygenic risk score has been reported to be a potential predictor of antipsychotic efficacy in patients with first-episode psychosis (Jian-Ping Zhang et al., 2018). In addition, the hypothesis of an omnigenic model proposed by Boyle et al. provide us with a new perspective to understand gene effects—core genes and peripheral genes. (Boyle et al., 2017).

FUTURE PERSPECTIVE

Although the pharmacological mechanisms and pharmacogenomics of atypical antipsychotic drugs seem to be hard to figure out, research on weight gain and dyslipidemia induced by atypical antipsychotics is of great significance. On one hand, combining genetic markers and relevant clinical indicators, a pharmacogenetic model can be built to predict the risk of lipid disturbances for an individual patient using atypical antipsychotics. Consequently, it will allow clinicians to select appropriate medication with less metabolic side effects and enough efficacy for every patient and promote individualized treatment. A multigene risk-model has showed promising results of predicting antipsychotic-induced weight gain (Tiwari et al., 2014). Moreover, the combinatorial model of genetic and clinical data could help to identify patients at high risk for early weight gain (Vandenberghe et al., 2016). On the other hand, the more we know about the mechanism of the metabolic side effects of atypical antipsychotics, the better we can tackle with this troublesome adverse drug reaction. More specifically, maybe we can develop novel molecules with high receptor selectivity or new drug targets. And toxicities could be designed out by counter-screening approaches combined with medicinal chemistry methods when discovering selectively non-selective drugs representing highly effective treatments (Roth et al., 2004). Besides, combination with lipid-lowering medication might help to attenuate weight gain or dyslipidemia. Metformin is a good try. In a double-blind and placebo-controlled study, metformin addition showed great efficacy, safety, and good adherence in preventing olanzapine-induced weight gain in drug-naive first-episode schizophrenia patients (Wu et al., 2008). In addition, recently a preclinical study indicates that the selective protein kinase Cβ (PKCβ) inhibitor, ruboxistaurin (LY-333531) prevent long-term clozapine-induced weight gain through the inhibition of the lipid droplet-selective autophagy process (Rimessi et al., 2017). In summary, further studies focusing on the prediction model and drug combination are needed. Decreasing the adverse drug reaction will help improve the compliance of patients, ensure the therapeutic effect, and promote the life quality of them.

AUTHOR CONTRIBUTIONS

NL wrote the manuscript and designed the figures and the table. TC and XW participated in the survey of the literatures and organization of the table. MT and DX contributed to manuscript reviewing and revisions. HC conceived the idea, supervised the whole work, and critically revised the paper.

FUNDING

This work was supported by the National Natural Science Foundation of China (81401113) and the Natural Science Foundation of Hunan Province (2017JJ3444).

REFERENCES

Achiron, A., and Gurevich, M. (2006). Peripheral blood gene expression signature mirrors central nervous system disease: the model of multiple sclerosis. *Autoimmun. Rev.* 5 (8), 517–522. doi: 10.1016/j.autrev.2006.02.009

Alladi, C. G., Mohan, A., Shewade, D. G., Rajkumar, R. P., Adithan, S., and Subramanian, K. (2017). Risperidone-Induced adverse drug reactions and role of DRD2 (-141 C Ins/Del) and 5HTR2C (-759 C > T) genetic polymorphisms in patients with schizophrenia. *J. Pharmacol. Pharmacother.* 8 (1), 28–32. doi: 10.4103/jpp.JPP_197_16

Allison, D. B., Mentore, J. L., Heo, M., Chandler, L. P., Cappelleri, J. C., Infante, M. C., et al. (1999). Antipsychotic-induced weight gain: a comprehensive research synthesis. *Am. J. Psychiatry* 156 (11), 1686–1696. doi: 10.1176/ajp.156.11.1686

Angelucci, F., Mathe, A. A., and Aloe, L. (2000). Brain-derived neurotrophic factor and tyrosine kinase receptor TrkB in rat brain are significantly altered after haloperidol and risperidone administration. *J. Neurosci. Res.* 60 (6), 783–794. doi: 10.1002/1097-4547(20000615)60:6<783::AID-JNR11>3.0.CO;2-M

Arora, S., and Anubhuti, (2006). Role of neuropeptides in appetite regulation and obesity–a review. *Neuropeptides* 40 (6), 375–401. doi: 10.1016/j.npep.2006.07.001

Bai, O., Chlan-Fourney, J., Bowen, R., Keegan, D., and Li, X. M. (2003). Expression of brain-derived neurotrophic factor mRNA in rat hippocampus after treatment with antipsychotic drugs. *J. Neurosci. Res.* 71 (1), 127–131. doi: 10.1002/jnr.10440

Bai, Y. M., Lin, C. C., Chen, J. Y., Chen, T. T., Su, T. P., and Chou, P. (2011). Association of weight gain and metabolic syndrome in patients taking clozapine: an 8-year cohort study. *J. Clin. Psychiatry* 72 (6), 751–756. doi: 10.4088/JCP.09m05402yel

Bath, K. G., and Lee, F. S. (2006). Variant BDNF (Val66Met) impact on brain structure and function. *Cogn. Affect. Behav. Neurosci.* 6 (1), 79–85. doi: 10.3758/CABN.6.1.79

Beckers, S., Zegers, D., de Freitas, F., Mertens, I. L., Van Gaal, L. F., and Van Hul, W. (2011). Association study of MC4R with complex obesity and replication of the rs17782313 association signal. *Mol. Genet. Metab.* 103 (1), 71–75. doi: 10.1016/j.ymgme.2011.01.007

Bensaid, M., Gary-Bobo, M., Esclangon, A., Maffrand, J. P., Le Fur, G., Oury-Donat, F., et al. (2003). The cannabinoid CB1 receptor antagonist SR141716 increases Acrp30 mRNA expression in adipose tissue of obese fa/fa rats and in cultured adipocyte cells. *Mol. Pharmacol.* 63 (4), 908–914. doi: 10.1097/00007890-199904150-00827

Bluher, M., Engeli, S., Kloting, N., Berndt, J., Fasshauer, M., Batkai, S., et al. (2006). Dysregulation of the peripheral and adipose tissue endocannabinoid system in human abdominal obesity. *Diabetes* 55 (11), 3053–3060. doi: 10.2337/db06-0812

Blum, K., Thanos, P. K., and Gold, M. S. (2014). Dopamine and glucose, obesity, and reward deficiency syndrome. *Front. Psychol.* 5, 919. doi: 10.3389/fpsyg.2014.00919

Bonhaus, D. W., Weinhardt, K. K., Taylor, M., DeSouza, A., McNeeley, P. M., Szczepanski, K., et al. (1997). RS-102221: a novel high affinity and selective, 5-HT2C receptor antagonist. *Neuropharmacology* 36 (4-5), 621–629. doi: 10.1016/S0028-3908(97)00049-X

Boyle, E. A., Li, Y. I., and Pritchard, J. K. (2017). An Expanded View of Complex Traits: From Polygenic to Omnigenic. *Cell* 169 (7), 1177–1186. doi: 10.1016/j.cell.2017.05.038

Bradley, R. L., Mansfield, J. P., and Maratos-Flier, E. (2005). Neuropeptides, including neuropeptide Y and melanocortins, mediate lipolysis in murine adipocytes. *Obes. Res.* 13 (4), 653–661. doi: 10.1038/oby.2005.73

Brandl, E. J., Frydrychowicz, C., Tiwari, A. K., Lett, T. A., Kitzrow, W., Buttner, S., et al. (2012). Association study of polymorphisms in leptin and leptin receptor genes with antipsychotic-induced body weight gain. *Prog. Neuropsychopharmacol. Biol. Psychiatry* 38 (2), 134–141. doi: 10.1016/j.pnpbp.2012.03.001

Cai, H. L., Tan, Q. Y., Jiang, P., Dang, R. L., Xue, Y., Tang, M. M., et al. (2015). A potential mechanism underlying atypical antipsychotics-induced lipid disturbances. *Translational Psychiatry* 5, e661. doi: 10.1038/tp.2015.161

Castellani, L. N., Costa-Dookhan, K. A., McIntyre, W. B., Wright, D. C., Flowers, S. A., Hahn, M. K., et al. (2019). Preclinical and clinical sex differences in antipsychotic-induced metabolic disturbances: a narrative review of adiposity and glucose metabolism. *J. Psychiatr. Brain Sci.* 4, e190013. doi: 10.20900/jpbs.20190013

Chen, P. S., Yang, Y. K., Yeh, T. L., Lee, I. H., Yao, W. J., Chiu, N. T., et al. (2008). Correlation between body mass index and striatal dopamine transporter availability in healthy volunteers–a SPECT study. *Neuroimage* 40 (1), 275–279. doi: 10.1016/j.neuroimage.2007.11.007

Chen, C. C., Hsu, L. W., Huang, K. T., Goto, S., Chen, C. L., and Nakano, T. (2017). Overexpression of Insig-2 inhibits atypical antipsychotic-induced adipogenic differentiation and lipid biosynthesis in adipose-derived stem cells. *Sci. Rep.* 7 (1), 10901. doi: 10.1038/s41598-017-11323-9

Cheng, M. C., Liao, D. L., Hsiung, C. A., Chen, C. Y., Liao, Y. C., and Chen, C. H. (2008). Chronic treatment with aripiprazole induces differential gene expression in the rat frontal cortex. *Int. J. Neuropsychopharmacol.* 11 (2), 207–216. doi: 10.1017/s1461145707008048

Chlan-Fourney, J., Ashe, P., Nylen, K., Juorio, A. V., and Li, X. M. (2002). Differential regulation of hippocampal BDNF mRNA by typical and atypical antipsychotic administration. *Brain Res.* 954 (1), 11–20. doi: 10.1016/S0006-8993(02)03215-8

Chowdhury, N. I., Tiwari, A. K., Souza, R. P., Zai, C. C., Shaikh, S. A., Chen, S., et al. (2013). Genetic association study between antipsychotic-induced weight gain and the melanocortin-4 receptor gene. *Pharmacogenomics J.* 13 (3), 272–279. doi: 10.1038/tpj.2011.66

Clifton, P. G., Lee, M. D., and Dourish, C. T. (2000). Similarities in the action of Ro 60-0175, a 5-HT2C receptor agonist and d-fenfluramine on feeding patterns in the rat. *Psychopharmacol. (Berl)* 152 (3), 256–267. doi: 10.1007/s002130000504

Cordeira, J. W., Frank, L., Sena-Esteves, M., Pothos, E. N., and Rios, M. (2010). Brain-derived neurotrophic factor regulates hedonic feeding by acting on the mesolimbic dopamine system. *J. Neurosci.* 30 (7), 2533–2541. doi: 10.1523/JNEUROSCI.5768-09.2010

Coutts, A. A., and Izzo, A. A. (2004). The gastrointestinal pharmacology of cannabinoids: an update. *Curr. Opin. Pharmacol.* 4 (6), 572–579. doi: 10.1016/j.coph.2004.05.007

Czerwensky, F., Leucht, S., and Steimer, W. (2013a). Association of the common MC4R rs17782313 polymorphism with antipsychotic-related weight gain. *J. Clin. Psychopharmacol.* 33 (1), 74–79. doi: 10.1097/JCP.0b013e31827772db

Czerwensky, F., Leucht, S., and Steimer, W. (2013b). MC4R rs489693: a clinical risk factor for second generation antipsychotic-related weight gain? *Int. J. Neuropsychopharmacol.* 16 (9), 2103–2109. doi: 10.1017/S1461145713000849

de Kuijper, G., Mulder, H., Evenhuis, H., Visser, F., and Hoekstra, P. J. (2013). Effects of controlled discontinuation of long-term used antipsychotics on weight and metabolic parameters in individuals with intellectual disability. *J. Clin. Psychopharmacol.* 33 (4), 520–524. doi: 10.1097/JCP.0b013e3182905d6a

de Leon, J., Correa, J. C., Ruaño, G., Windemuth, A., Arranz, M. J., and Diaz, F. J. (2008). Exploring genetic variations that may be associated with the direct effects of some antipsychotics on lipid levels. *Schizophrenia Res.* 98 (1), 40–46. doi: 10.1016/j.schres.2007.10.003

De Luca, V., Souza, R. P., Viggiano, E., Sickert, L., Teo, C., Zai, C., et al. (2011). Genetic interactions in the adrenergic system genes: analysis of antipsychotic-induced weight gain. *Hum. Psychopharmacol.* 26 (6), 386–391. doi: 10.1002/hup.1219

Delis, F., Rosko, L., Shroff, A., Leonard, K. E., and Thanos, P. K. (2017). Oral haloperidol or olanzapine intake produces distinct and region-specific increase in cannabinoid receptor levels that is prevented by high fat diet. *Prog. Neuropsychopharmacol. Biol. Psychiatry* 79 (Pt B), 268–280. doi: 10.1016/j.pnpbp.2017.06.005

Di Marzo, V., and Matias, I. (2005). Endocannabinoid control of food intake and energy balance. *Nat. Neurosci.* 8 (5), 585–589. doi: 10.1038/nn1457

Di Marzo, V., Goparaju, S. K., Wang, L., Liu, J., Batkai, S., Jarai, Z., et al. (2001). Leptin-regulated endocannabinoids are involved in maintaining food intake. *Nature* 410 (6830), 822–825. doi: 10.1038/35071088

Duan, J., Wainwright, M. S., Comeron, J. M., Saitou, N., Sanders, A. R., Gelernter, J., et al. (2003). Synonymous mutations in the human dopamine receptor D2 (DRD2) affect mRNA stability and synthesis of the receptor. *Hum. Mol. Genet.* 12 (3), 205–216. doi: 10.1093/hmg/ddg055

Egan, M. F., Kojima, M., Callicott, J. H., Goldberg, T. E., Kolachana, B. S., Bertolino, A., et al. (2003). The BDNF val66met polymorphism affects activity-dependent secretion of BDNF and human memory and hippocampal function. *Cell* 112 (2), 257–269. doi: 10.1016/S0092-8674(03)00035-7

Elias, C. F., Aschkenasi, C., Lee, C., Kelly, J., Ahima, R. S., Bjorbæk, C., et al. (1999). Leptin differentially regulates NPY and pomc neurons projecting to the lateral hypothalamic area. *Neuron* 23 (4), 775–786. doi: 10.1016/S0896-6273(01)80035-0

Emsley, R. (2018). Antipsychotic maintenance treatment in schizophrenia and the importance of preventing relapse. *World Psychiatry: Off. J. World Psychiatr. Association (WPA)* 17 (2), 168–169. doi: 10.1002/wps.20521

Fakhoury, M. (2017). Role of the endocannabinoid system in the pathophysiology of schizophrenia. *Mol. Neurobiol.* 54 (1), 768–778. doi: 10.1007/s12035-016-9697-5

Fang, H., Zhen, Y. F., Liu, X. Y., Xu, G., Soares, J. C., Zhao, J., et al. (2016). Association of the BDNF Val66Met polymorphism with BMI in chronic schizophrenic patients and healthy controls. *Int. Clin. Psychopharmacol.* 31 (6), 353–357. doi: 10.1097/YIC.0000000000000142

Faton, S., Tassin, J.-P., Duranton, F., Bagnol, D., and Lajoix, A.-D. (2018). 5-HT2C receptors in the ventral tegmental area, but not in the arcuate nucleus, mediate the hypophagic and hypolocomotor effects of the selective 5-HT2C receptor agonist AR231630 in rats. *Behav. Brain Res.* 347, 234–241. doi: 10.1016/j.bbr.2018.03.006

Favalli, G., Li, J., Belmonte-de-Abreu, P., Wong, A. H., and Daskalakis, Z. J. (2012). The role of BDNF in the pathophysiology and treatment of schizophrenia. *J. Psychiatr. Res.* 46 (1), 1–11. doi: 10.1016/j.jpsychires.2011.09.022

Ferno, J., Raeder, M. B., Vik-Mo, A. O., Skrede, S., Glambek, M., Tronstad, K. J., et al. (2005). Antipsychotic drugs activate SREBP-regulated expression of lipid biosynthetic genes in cultured human glioma cells: a novel mechanism of action? *Pharmacogenomics J.* 5 (5), 298–304. doi: 10.1038/sj.tpj.6500323

Fonseka, T. M., Tiwari, A. K., Goncalves, V. F., Lieberman, J. A., Meltzer, H. Y., Goldstein, B. I., et al. (2015). The role of genetic variation across IL-1beta, IL-2, IL-6, and BDNF in antipsychotic-induced weight gain. *World J. Biol. Psychiatry* 16 (1), 45–56. doi: 10.3109/15622975.2014.984631

Giegling, I., Balzarro, B., Porcelli, S., Schafer, M., Hartmann, A. M., Friedl, M., et al. (2013). Influence of ANKK1 and DRD2 polymorphisms in response to haloperidol. *Eur. Arch. Psychiatry Clin. Neurosci.* 263 (1), 65–74. doi: 10.1007/s00406-012-0348-1

Gregoor, J. G., van der Weide, J., Loovers, H. M., van Megen, H. J., Egberts, T. C., and Heerdink, E. R. (2010). Association between LEP and LEPR gene polymorphisms and dyslipidemia in patients using atypical antipsychotic medication. *Psychiatr. Genet.* 20 (6), 311–316. doi: 10.1097/YPG.0b013e32833b6378

Gregoor, J. G., van der Weide, J., Loovers, H. M., van Megen, H. J., Egberts, T. C., and Heerdink, E. R. (2011). Polymorphisms of the LEP, LEPR and HTR2C gene: obesity and BMI change in patients using antipsychotic medication in a naturalistic setting. *Pharmacogenomics* 12 (6), 919–923. doi: 10.2217/pgs.11.40

Greil, W., Haberle, A., Schuhmann, T., Grohmann, R., and Baumann, P. (2013). Age and adverse drug reactions from psychopharmacological treatment: data from the AMSP drug surveillance programme in Switzerland. *Swiss. Med. Wkly* 143, w13772. doi: 10.4414/smw.2013.13772

Hamdani, N., Tabeze, J. P., Ramoz, N., Ades, J., Hamon, M., Sarfati, Y., et al. (2008). The CNR1 gene as a pharmacogenetic factor for antipsychotics rather than a susceptibility gene for schizophrenia. *Eur. Neuropsychopharmacol.* 18 (1), 34–40. doi: 10.1016/j.euroneuro.2007.05.005

Hamdi, A., Porter, J., and Prasad, C. (1992). Decreased striatal D2 dopamine receptors in obese Zucker rats: changes during aging. *Brain Res.* 589 (2), 338–340. doi: 10.1016/0006-8993(92)91296-Q

Hirvonen, M. M., Laakso, A., Nagren, K., Rinne, J. O., Pohjalainen, T., and Hietala, J. (2009). C957T polymorphism of dopamine D2 receptor gene affects striatal DRD2 *in vivo* availability by changing the receptor affinity. *Synapse* 63 (10), 907–912. doi: 10.1002/syn.20672

Hong, C. J., Liou, Y. J., Bai, Y. M., Chen, T. T., Wang, Y. C., and Tsai, S. J. (2010). Dopamine receptor D2 gene is associated with weight gain in schizophrenic patients under long-term atypical antipsychotic treatment. *Pharmacogenet. Genomics* 20 (6), 359–366. doi: 10.1097/FPC.0b013e3283397d06

Howlett, A. C., Barth, F., Bonner, T. I., Cabral, G., Casellas, P., Devane, W. A., et al. (2002). International union of pharmacology. XXVII. classification of cannabinoid receptors. *Pharmacol. Rev.* 54 (2), 161–202. doi: 10.1124/pr.54.2.161

International Schizophrenia, C., Purcell, S. M., Wray, N. R., Stone, J. L., Visscher, P. M., O'Donovan, M. C., et al. (2009). Common polygenic variation contributes to risk of schizophrenia and bipolar disorder. *Nature* 460 (7256), 748–752. doi: 10.1038/nature08185

Issa, G., Wilson, C., Terry, A. V.Jr., and Pillai, A. (2010). An inverse relationship between cortisol and BDNF levels in schizophrenia: data from human postmortem and animal studies. *Neurobiol. Dis.* 39 (3), 327–333. doi: 10.1016/j.nbd.2010.04.017

Jbilo, O., Ravinet-Trillou, C., Arnone, M., Buisson, I., Bribes, E., Peleraux, A., et al. (2005). The CB1 receptor antagonist rimonabant reverses the diet-induced obesity phenotype through the regulation of lipolysis and energy balance. *FASEB J.* 19 (11), 1567–1569. doi: 10.1096/fj.04-3177fje

Jindal, R. D., Pillai, A. K., Mahadik, S. P., Eklund, K., Montrose, D. M., and Keshavan, M. S. (2010). Decreased BDNF in patients with antipsychotic naive first episode schizophrenia. *Schizophr. Res.* 119 (1-3), 47–51. doi: 10.1016/j.schres.2009.12.035

Kang, S. G., Lee, H. J., Park, Y. M., Choi, J. E., Han, C., Kim, Y. K., et al. (2008). Possible association between the -2548A/G polymorphism of the leptin gene and olanzapine-induced weight gain. *Prog. Neuropsychopharmacol. Biol. Psychiatry* 32 (1), 160–163. doi: 10.1016/j.pnpbp.2007.08.002

Kirk, S. L., Cahir, M., and Reynolds, G. P. (2006). Clozapine, but not haloperidol, increases neuropeptide Y neuronal expression in the rat hypothalamus. *J. Psychopharmacol.* 20 (4), 577–579. doi: 10.1177/0269881106061199

Kuzman, M. R., Medved, V., Bozina, N., Hotujac, L., Sain, I., and Bilusic, H. (2008). The influence of 5-HT(2C) and MDR1 genetic polymorphisms on antipsychotic-induced weight gain in female schizophrenic patients. *Psychiatry Res.* 160 (3), 308–315. doi: 10.1016/j.psychres.2007.06.006

Kuzman, M. R., Medved, V., Bozina, N., Grubisin, J., Jovanovic, N., and Sertic, J. (2011). Association study of MDR1 and 5-HT2C genetic polymorphisms and antipsychotic-induced metabolic disturbances in female patients with schizophrenia. *Pharmacogenomics J.* 11 (1), 35–44. doi: 10.1038/tpj.2010.7

Lam, D. D., Przydzial, M. J., Ridley, S. H., Yeo, G. S., Rochford, J. J., O'Rahilly, S., et al. (2008). Serotonin 5-HT2C receptor agonist promotes hypophagia *via* downstream activation of melanocortin 4 receptors. *Endocrinology* 149 (3), 1323–1328. doi: 10.1210/en.2007-1321

Lam, D. D., Garfield, A. S., Marston, O. J., Shaw, J., and Heisler, L. K. (2010). Brain serotonin system in the coordination of food intake and body weight. *Pharmacol. Biochem. Behav.* 97 (1), 84–91. doi: 10.1016/j.pbb.2010.09.003

Lazzari, P., Serra, V., Marcello, S., Pira, M., and Mastinu, A. (2017). Metabolic side effects induced by olanzapine treatment are neutralized by CB1 receptor antagonist compounds co-administration in female rats. *Eur. Neuropsychopharmacol.* 27 (7), 667–678. doi: 10.1016/j.euroneuro.2017.03.010

Le Hellard, S., Theisen, F. M., Haberhausen, M., Raeder, M. B., Ferno, J., Gebhardt, S., et al. (2009). Association between the insulin-induced gene 2 (INSIG2) and weight gain in a German sample of antipsychotic-treated schizophrenic patients: perturbation of SREBP-controlled lipogenesis in drug-related metabolic adverse effects? *Mol. Psychiatry* 14 (3), 308–317. doi: 10.1038/sj.mp.4002133

Lencz, T., Robinson, D. G., Napolitano, B., Sevy, S., Kane, J. M., Goldman, D., et al. (2010). DRD2 promoter region variation predicts antipsychotic-induced weight gain in first episode schizophrenia. *Pharmacogenet. Genomics* 20 (9), 569–572. doi: 10.1097/FPC.0b013e32833ca24b

Lett, T. A. P., Wallace, T. J. M., Chowdhury, N. I., Tiwari, A. K., Kennedy, J. L., and Müller, D. J. (2011). Pharmacogenetics of antipsychotic-induced weight gain: review and clinical implications. *Mol. Psychiatry* 17, 242. doi: 10.1038/mp.2011.109

Liou, Y. J., Bai, Y. M., Lin, E., Chen, J. Y., Chen, T. T., Hong, C. J., et al. (2012). Gene-gene interactions of the INSIG1 and INSIG2 in metabolic syndrome in schizophrenic patients treated with atypical antipsychotics. *Pharmacogenomics J.* 12 (1), 54–61. doi: 10.1038/tpj.2010.74

Lipska, B. K., Khaing, Z. Z., Weickert, C. S., and Weinberger, D. R. (2001). BDNF mRNA expression in rat hippocampus and prefrontal cortex: effects of neonatal ventral hippocampal damage and antipsychotic drugs. *Eur. J. Neurosci.* 14 (1), 135–144. doi: 10.1046/j.1460-9568.2001.01633.x

Liu, X., Wu, Z., Lian, J., Hu, C.-H., Huang, X.-F., and Deng, C. (2017). Time-dependent changes and potential mechanisms of glucose-lipid metabolic disorders associated with chronic clozapine or olanzapine treatment in rats. *Sci. Rep.* 7 (1), 2762. doi: 10.1038/s41598-017-02884-w

Lochman, J., Balcar, V. J., Stastny, F., and Sery, O. (2013). Preliminary evidence for association between schizophrenia and polymorphisms in the regulatory regions of the ADRA2A, DRD3 and SNAP-25 Genes. *Psychiatry Res.* 205 (1-2), 7–12. doi: 10.1016/j.psychres.2012.08.003

Lord, C. C., Wyler, S. C., Wan, R., Castorena, C. M., Ahmed, N., Mathew, D., et al. (2017). The atypical antipsychotic olanzapine causes weight gain by targeting serotonin receptor 2C. *J. Clin. Invest.* 127 (9), 3408–3412. doi: 10.1172/jci93362

Maayan, L., and Correll, C. U. (2010). Management of antipsychotic-related weight gain. *Expert Rev. Neurother.* 10 (7), 1175–1200. doi: 10.1586/ern.10.85

Malhotra, A. K., Correll, C. U., Chowdhury, N. I., Muller, D. J., Gregersen, P. K., Lee, A. T., et al. (2012). Association between common variants near the melanocortin 4 receptor gene and severe antipsychotic drug-induced weight gain. *Arch. Gen. Psychiatry* 69 (9), 904–912. doi: 10.1001/archgenpsychiatry.2012.191

Martinez, J. A., Aguado, M., and Fruhbeck, G. (2000). Interactions between leptin and NPY affecting lipid mobilization in adipose tissue. *J. Physiol. Biochem.* 56 (1), 1–8. doi: 10.1007/bf03179770

McGrath, J., Saha, S., Chant, D., and Welham, J. (2008). Schizophrenia: a concise overview of incidence, prevalence, and mortality. *Epidemiol. Rev.* 30, 67–76. doi: 10.1093/epirev/mxn001

McPherson, R., and Gauthier, A. (2004). Molecular regulation of SREBP function: the Insig-SCAP connection and isoform-specific modulation of lipid synthesis. *Biochem. Cell Biol.* 82 (1), 201–211. doi: 10.1139/o03-090

Mehrpouya-Bahrami, P., Chitrala, K. N., Ganewatta, M. S., Tang, C., Murphy, E. A., Enos, R. T., et al. (2017). Blockade of CB1 cannabinoid receptor alters gut microbiota and attenuates inflammation and diet-induced obesity. *Sci. Rep.* 7 (1), 15645. doi: 10.1038/s41598-017-15154-6

Mendizabal-Zubiaga, J., Melser, S., Benard, G., Ramos, A., Reguero, L., Arrabal, S., et al. (2016). Cannabinoid CB1 receptors are localized in striated muscle mitochondria and regulate mitochondrial respiration. *Front. Physiol.* 7, 476. doi: 10.3389/fphys.2016.00476

Mitchell, A. J., Vancampfort, D., Sweers, K., van Winkel, R., Yu, W., and De Hert, M. (2013). Prevalence of metabolic syndrome and metabolic abnormalities in schizophrenia and related disorders–a systematic review and meta-analysis. *Schizophr Bull* 39 (2), 306–318. doi: 10.1093/schbul/sbr148

Monteleone, P., Milano, W., Petrella, C., Canestrelli, B., and Maj, M. (2010). Endocannabinoid Pro129Thr FAAH functional polymorphism but not 1359G/A CNR1 polymorphism is associated with antipsychotic-induced weight gain. *J. Clin. Psychopharmacol.* 30 (4), 441–445. doi: 10.1097/JCP.0b013e3181e742c5

Mottillo, S., Filion, K. B., Genest, J., Joseph, L., Pilote, L., Poirier, P., et al. (2010). The metabolic syndrome and cardiovascular risk a systematic review and meta-analysis. *J. Am. Coll C.ardiol.* 56 (14), 1113–1132. doi: 10.1016/j.jacc.2010.05.034

Mulder, H., Franke, B., van der-Beek van der, A. A., Arends, J., Wilmink, F. W., Scheffer, H., et al. (2007). The association between HTR2C gene polymorphisms and the metabolic syndrome in patients with schizophrenia. *J. Clin. Psychopharmacol.* 27 (4), 338–343. doi: 10.1097/JCP.0b013e3180a76dc0

Muller, D. J., Zai, C. C., Sicard, M., Remington, E., Souza, R. P., Tiwari, A. K., et al. (2012). Systematic analysis of dopamine receptor genes (DRD1-DRD5) in antipsychotic-induced weight gain. *Pharmacogenomics J.* 12 (2), 156–164. doi: 10.1038/tpj.2010.65

Nakata, M., and Yada, T. (2008). Cannabinoids inhibit insulin secretion and cytosolic Ca2+ oscillation in islet beta-cells *via* CB1 receptors. *Regul Pept.* 145 (1-3), 49–53. doi: 10.1016/j.regpep.2007.08.009

Nakazi, M., Bauer, U., Nickel, T., Kathmann, M., and Schlicker, E. (2000). Inhibition of serotonin release in the mouse brain *via* presynaptic cannabinoid CB1 receptors. *Naunyn Schmiedebergs Arch. Pharmacol.* 361 (1), 19–24. doi: 10.1007/s002109900147

Nielsen, M. O., Rostrup, E., Wulff, S., Glenthoj, B., and Ebdrup, B. H. (2016). Striatal reward activity and antipsychotic-associated weight change in patients with schizophrenia undergoing initial treatment. *JAMA Psychiatry* 73 (2), 121–128. doi: 10.1001/jamapsychiatry.2015.2582

Nogueiras, R., Wiedmer, P., Perez-Tilve, D., Veyrat-Durebex, C., Keogh, J. M., Sutton, G. M., et al. (2007). The central melanocortin system directly controls peripheral lipid metabolism. *J. Clin. Invest.* 117 (11), 3475–3488. doi: 10.1172/jci31743

Opgen-Rhein, C., Brandl, E. J., Muller, D. J., Neuhaus, A. H., Tiwari, A. K., Sander, T., et al. (2010). Association of HTR2C, but not LEP or INSIG2, genes with antipsychotic-induced weight gain in a German sample. *Pharmacogenomics* 11 (6), 773–780. doi: 10.2217/pgs.10.50

Osei-Hyiaman, D., DePetrillo, M., Pacher, P., Liu, J., Radaeva, S., Batkai, S., et al. (2005). Endocannabinoid activation at hepatic CB1 receptors stimulates fatty acid synthesis and contributes to diet-induced obesity. *J. Clin. Invest.* 115 (5), 1298–1305. doi: 10.1172/JCI23057

Panariello, F., Polsinelli, G., Borlido, C., Monda, M., and De Luca, V. (2012). The role of leptin in antipsychotic-induced weight gain: genetic and non-genetic factors. *J. Obes.* 2012, 572848. doi: 10.1155/2012/572848

Park, Y. M., Chung, Y. C., Lee, S. H., Lee, K. J., Kim, H., Byun, Y. C., et al. (2006). Weight gain associated with the alpha2a-adrenergic receptor -1,291 C/G polymorphism and olanzapine treatment. *Am. J. Med. Genet. B. Neuropsychiatr. Genet.* 141B (4), 394–397. doi: 10.1002/ajmg.b.30311

Park, S. W., Phuong, V. T., Lee, C. H., Lee, J. G., Seo, M. K., Cho, H. Y., et al. (2011a). Effects of antipsychotic drugs on BDNF, GSK-3beta, and beta-catenin expression in rats subjected to immobilization stress. *Neurosci. Res.* 71 (4), 335–340. doi: 10.1016/j.neures.2011.08.010

Park, Y. M., Choi, J. E., Kang, S. G., Koo, S. H., Kim, L., Geum, D., et al. (2011b). Cannabinoid type 1 receptor gene polymorphisms are not associated with olanzapine-induced weight gain. *Hum. Psychopharmacol.* 26 (4-5), 332–337. doi: 10.1002/hup.1210

Pelleymounter, M. A., Cullen, M. J., and Wellman, C. L. (1995). Characteristics of BDNF-induced weight loss. *Exp. Neurol.* 131 (2), 229–238. doi: 10.1016/0014-4886(95)90045-4

Pi-Sunyer, F. X., Aronne, L. J., Heshmati, H. M., Devin, J., Rosenstock, J., and Group, R.I.-N.A.S. (2006). Effect of rimonabant, a cannabinoid-1 receptor blocker, on weight and cardiometabolic risk factors in overweight or obese patients: RIO-North America: a randomized controlled trial. *JAMA* 295 (7), 761–775. doi: 10.1001/jama.295.7.761

Potvin, S., Zhornitsky, S., and Stip, E. (2015). Antipsychotic-induced changes in blood levels of leptin in schizophrenia: a meta-analysis. *Can J. Psychiatry* 60 (3 Suppl 2), S26–S34.

Reynolds, G. P., and McGowan, O. O. (2017). Mechanisms underlying metabolic disturbances associated with psychosis and antipsychotic drug treatment. *J. Psychopharmacol.* 31 (11), 1430–1436. doi: 10.1177/0269881117722987

Reynolds, G. P., Zhang, Z. J., and Zhang, X. B. (2002). Association of antipsychotic drug-induced weight gain with a 5-HT2C receptor gene polymorphism. *Lancet* 359 (9323), 2086–2087. doi: 10.1016/S0140-6736(02)08913-4

Rimessi, A., Pavan, C., Ioannidi, E., Nigro, F., Morganti, C., Brugnoli, A., et al. (2017). Protein Kinase C β: a new target therapy to prevent the long-term atypical antipsychotic-induced weight gain. *Neuropsychopharmacology* 42, 1491. doi: 10.1038/npp.2017.20

Ringen, P. A., Engh, J. A., Birkenaes, A. B., Dieset, I., and Andreassen, O. A. (2014). Increased mortality in schizophrenia due to cardiovascular disease – a non-systematic review of epidemiology, possible causes, and interventions. *Front. Psychiatry* 5 (137). doi: 10.3389/fpsyt.2014.00137

Risselada, A. J., Vehof, J., Bruggeman, R., Wilffert, B., Cohen, D., Al Hadithy, A. F., et al. (2010). Association between the 1291-C/G polymorphism in the adrenergic alpha-2a receptor and the metabolic syndrome. *J. Clin. Psychopharmacol.* 30 (6), 667–671. doi: 10.1097/JCP.0b013e3181fbfac4

Rojczyk, E., Pałasz, A., and Wiaderkiewicz, R. (2015). Effect of short and long-term treatment with antipsychotics on orexigenic/anorexigenic neuropeptides expression in the rat hypothalamus. *Neuropeptides* 51, 31–42. doi: 10.1016/j.npep.2015.04.001

Rosas-Vargas, H., Martinez-Ezquerro, J. D., and Bienvenu, T. (2011). Brain-derived neurotrophic factor, food intake regulation, and obesity. *Arch. Med. Res.* 42 (6), 482–494. doi: 10.1016/j.arcmed.2011.09.005

Roth, B. L., Sheffler, D. J., and Kroeze, W. K. (2004). Magic shotguns versus magic bullets: selectively non-selective drugs for mood disorders and schizophrenia. *Nat. Rev. Drug Discov.* 3 (4), 353–359. doi: 10.1038/nrd1346

Ruohonen, S., Valve, L., Tuomainen, K., Ailanen, L., Roytta, M., Manz, G., et al. (2018). Increased energy expenditure, lipolysis, and hyperinsulinemia confer resistance to central obesity and type 2 diabetes in mice lacking alpha2A-adrenoceptors. *Neuroendocrinology* 107 (4), 324–339. doi: 10.1159/000492387

Russo, P., Strazzullo, P., Cappuccio, F. P., Tregouet, D. A., Lauria, F., Loguercio, M., et al. (2007). Genetic variations at the endocannabinoid type 1 receptor gene (CNR1) are associated with obesity phenotypes in men. *J. Clin. Endocrinol. Metab.* 92 (6), 2382–2386. doi: 10.1210/jc.2006-2523

Ryu, S., Cho, E. Y., Park, T., Oh, S., Jang, W.-S., Kim, S.-K., et al. (2007). –759 C/T polymorphism of 5-HT2C receptor gene and early phase weight gain associated with antipsychotic drug treatment. *Prog. Neuro-Psychopharmacol. Biol. Psychiatry* 31 (3), 673–677. doi: 10.1016/j.pnpbp.2006.12.021

Sáinz, N., Barrenetxe, J., Moreno-Aliaga, M. J., and Martínez, J. A. (2015). Leptin resistance and diet-induced obesity: central and peripheral actions of leptin. *Metabolism* 64 (1), 35–46. doi: 10.1016/j.metabol.2014.10.015

Sainz, J., Prieto, C., and Crespo-Facorro, B. (2019). Sex differences in gene expression related to antipsychotic induced weight gain. *PLoS One* 14 (4), e0215477. doi: 10.1371/journal.pone.0215477

Secher, A., Husum, H., Holst, B., Egerod, K. L., and Mellerup, E. (2010). Risperidone treatment increases CB1 receptor binding in rat brain. *Neuroendocrinology* 91 (2), 155–168. doi: 10.1159/000245220

Shen, J., Ge, W., Zhang, J., Zhu, H. J., and Fang, Y. (2014). Leptin -2548g/a gene polymorphism in association with antipsychotic-induced weight gain: a meta-analysis study. *Psychiatr. Danub* 26 (2), 145–151.

Shen, W. J., Yao, T., Kong, X., Williams, K. W., and Liu, T. (2017). Melanocortin neurons: Multiple routes to regulation of metabolism. *Biochim Biophys Acta Mol. Basis Dis.* 1863 (10 Pt A), 2477–2485. doi: 10.1016/j.bbadis.2017.05.007

Sicard, M. N., Zai, C. C., Tiwari, A. K., Souza, R. P., Meltzer, H. Y., Lieberman, J. A., et al. (2010). Polymorphisms of the HTR2C gene and antipsychotic-induced weight gain: an update and meta-analysis. *Pharmacogenomics* 11 (11), 1561–1571. doi: 10.2217/pgs.10.123

Sickert, L., Muller, D. J., Tiwari, A. K., Shaikh, S., Zai, C., De Souza, R., et al. (2009). Association of the alpha 2A adrenergic receptor -1291C/G polymorphism and antipsychotic-induced weight gain in European-Americans. *Pharmacogenomics* 10 (7), 1169–1176. doi: 10.2217/pgs.09.43

Simon, V., van Winkel, R., and De Hert, M. (2009). Are weight gain and metabolic side effects of atypical antipsychotics dose dependent? A literature review. *J. Clin. Psychiatry* 70 (7), 1041–1050. doi: 10.4088/jcp.08r04392

Skledar, M., Nikolac, M., Dodig-Curkovic, K., Curkovic, M., Borovecki, F., and Pivac, N. (2012). Association between brain-derived neurotrophic factor Val66Met and obesity in children and adolescents. *Prog. Neuropsychopharmacol. Biol. Psychiatry* 36 (1), 136–140. doi: 10.1016/j.pnpbp.2011.08.003

Srisai, D., Gillum, M. P., Panaro, B. L., Zhang, X. M., Kotchabhakdi, N., Shulman, G. I., et al. (2011). Characterization of the hyperphagic response to dietary fat in the MC4R knockout mouse. *Endocrinology* 152 (3), 890–902. doi: 10.1210/en.2010-0716

Tecott, L. H., Sun, L. M., Akana, S. F., Strack, A. M., Lowenstein, D. H., Dallman, M. F., et al. (1995). Eating disorder and epilepsy in mice lacking 5-HT2c serotonin receptors. *Nature* 374 (6522), 542–546. doi: 10.1038/374542a0

Templeman, L. A., Reynolds, G. P., Arranz, B., and San, L. (2005). Polymorphisms of the 5-HT2C receptor and leptin genes are associated with antipsychotic drug-induced weight gain in Caucasian subjects with a first-episode psychosis. *Pharmacogenet. Genomics* 15 (4), 195–200. doi: 10.1097/01213011-200504000-00002

Tiwari, A. K., Zai, C. C., Likhodi, O., Lisker, A., Singh, D., Souza, R. P., et al. (2010a). A common polymorphism in the cannabinoid receptor 1 (CNR1) gene is associated with antipsychotic-induced weight gain in Schizophrenia. *Neuropsychopharmacology* 35 (6), 1315–1324. doi: 10.1038/npp.2009.235

Tiwari, A. K., Zai, C. C., Meltzer, H. Y., Lieberman, J. A., Muller, D. J., and Kennedy, J. L. (2010b). Association study of polymorphisms in insulin induced gene 2 (INSIG2) with antipsychotic-induced weight gain in European and African-American schizophrenia patients. *Hum. Psychopharmacol.* 25 (3), 253–259. doi: 10.1002/hup.1111

Tiwari, A. K., Brandl, E. J., Weber, C., Likhodi, O., Zai, C. C., Hahn, M. K., et al. (2013). Association of a functional polymorphism in neuropeptide Y with antipsychotic-induced weight gain in schizophrenia patients. *J. Clin. Psychopharmacol.* 33 (1), 11–17. doi: 10.1097/JCP.0b013e31827d145a

Tiwari, A. K., Brandl, E. J., Chowdhury, N. I., Zai, C. C., Lieberman, J. A., Meltzer, H. Y., et al. (2014). A Genetic risk-model for antipsychotic induced weight gain. *Biol. Psychiatry* 75 (9), 73S–73S.

Tsai, A., Liou, Y. J., Hong, C. J., Wu, C. L., Tsai, S. J., and Bai, Y. M. (2011). Association study of brain-derived neurotrophic factor gene polymorphisms and body weight change in schizophrenic patients under long-term atypical antipsychotic treatment. *Neuromol. Med.* 13 (4), 328–333. doi: 10.1007/s12017-011-8159-5

Tybura, P., Trzesniowska-Drukala, B., Bienkowski, P., Beszlej, A., Frydecka, D., Mierzejewski, P., et al. (2014). Pharmacogenetics of adverse events in schizophrenia treatment: comparison study of ziprasidone, olanzapine and perazine. *Psychiatry Res.* 219 (2), 261–267. doi: 10.1016/j.psychres.2014.05.039

Upadhyay, N., Patel, A., Chan, W., Aparasu, R. R., Ochoa-Perez, M., Sherer, J. T., et al. (2019). Reversibility of psychotropic medication induced weight gain among children and adolescents with bipolar disorders. *Psychiatry Res.* 276, 151–159. doi: 10.1016/j.psychres.2019.05.005

Vähätalo, L. H., Ruohonen, S. T., Mäkelä, S., Ailanen, L., Penttinen, A. M., Stormi, T., et al. (2015). Role of the endocannabinoid system in obesity induced by neuropeptide Y overexpression in noradrenergic neurons. *Nutr. Diabetes* 5 (4), e151–e151. doi: 10.1038/nutd.2015.1

Vahatalo, L. H., Ruohonen, S. T., Makela, S., Kovalainen, M., Huotari, A., Makela, K. A., et al. (2015). Neuropeptide Y in the noradrenergic neurones induces obesity and inhibits sympathetic tone in mice. *Acta Physiol. (Oxf)* 213 (4), 902–919. doi: 10.1111/apha.12436

Van Gaal, L. F., Rissanen, A. M., Scheen, A. J., Ziegler, O., and Rössner, S. (2005). Effects of the cannabinoid-1 receptor blocker rimonabant on weight reduction and cardiovascular risk factors in overweight patients: 1-year experience from the RIO-Europe study. *Lancet* 365 (9468), 1389–1397. doi: 10.1016/S0140-6736(05)66374-X

Vandenberghe, F., Saigi-Morgui, N., Delacretaz, A., Quteineh, L., Crettol, S., Ansermot, N., et al. (2016). Prediction of early weight gain during psychotropic treatment using a combinatorial model with clinical and genetic markers. *Pharmacogenet. Genomics* 26 (12), 547–557. doi: 10.1097/FPC.0000000000000249

Voigt, J.-P., and Fink, H. (2015). Serotonin controlling feeding and satiety. *Behav. Brain Res.* 277, 14–31. doi: 10.1016/j.bbr.2014.08.065

Volkow, N. D., Wang, G.-J., and Baler, R. D. (2011). Reward, dopamine and the control of food intake: implications for obesity. *Trends Cogn. Sci.* 15 (1), 37–46. doi: 10.1016/j.tics.2010.11.001

von Meyenburg, C., Langhans, W., and Hrupka, B. J. (2003). Evidence for a role of the 5-HT2C receptor in central lipopolysaccharide-, interleukin-1 beta-, and leptin-induced anorexia. *Pharmacol. Biochem. Behav.* 74 (4), 1025–1031. doi: 10.1016/S0091-3057(03)00030-3

Wang, Y. C., Bai, Y. M., Chen, J. Y., Lin, C. C., Lai, I. C., and Liou, Y. J. (2005). Polymorphism of the adrenergic receptor alpha 2a -1291C > G genetic variation and clozapine-induced weight gain. *J. Neural Transm. (Vienna)* 112 (11), 1463–1468. doi: 10.1007/s00702-005-0291-7

Wang, C., Bomberg, E., Levine, A., Billington, C., and Kotz, C. M. (2007). Brain-derived neurotrophic factor in the ventromedial nucleus of the hypothalamus reduces energy intake. *Am. J. Physiol. Regul Integr. Comp. Physiol.* 293 (3), R1037–R1045. doi: 10.1152/ajpregu.00125.2007

Weston-Green, K., Huang, X. F., and Deng, C. (2012). Alterations to Melanocortinergic, GABAergic and Cannabinoid Neurotransmission Associated with Olanzapine-Induced Weight Gain. *Plos One* 7 (3), 12. doi: 10.1371/journal.pone.0033548

Wierucka-Rybak, M., Wolak, M., Juszczak, M., Drobnik, J., and Bojanowska, E. (2016). The inhibitory effect of combination treatment with leptin and cannabinoid Cb1 receptor agonist on food intake and body weight gain is mediated by serotonin 1b and 2c receptors. *J. Physiol. Pharmacol.* 67 (3), 457–463.

Wiley, J. L., Kendler, S. H., Burston, J. J., Howard, D. R., Selley, D. E., and Sim-Selley, L. J. (2008). Antipsychotic-induced alterations in CB1 receptor-mediated G-protein signaling and *in vivo* pharmacology in rats. *Neuropharmacology* 55 (7), 1183–1190. doi: 10.1016/j.neuropharm.2008.07.026

Wu, R. R., Zhao, J. P., Guo, X. F., He, Y. Q., Fang, M. S., Guo, W. B., et al. (2008). Metformin addition attenuates olanzapine-induced weight gain in drug-naive first-episode schizophrenia patients: a double-blind, placebo-controlled study. *Am. J. Psychiatry* 165 (3), 352–358. doi: 10.1176/appi.ajp.2007.07010079

Xiu, M. H., Hui, L., Dang, Y. F., Hou, T. D., Zhang, C. X., Zheng, Y. L., et al. (2009). Decreased serum BDNF levels in chronic institutionalized schizophrenia on long-term treatment with typical and atypical antipsychotics. *Prog. Neuropsychopharmacol. Biol. Psychiatry* 33 (8), 1508–1512. doi: 10.1016/j.pnpbp.2009.08.011

Xu, B., Goulding, E. H., Zang, K., Cepoi, D., Cone, R. D., Jones, K. R., et al. (2003). Brain-derived neurotrophic factor regulates energy balance downstream of melanocortin-4 receptor. *Nat. Neurosci.* 6 (7), 736–742. doi: 10.1038/nn1073

Yabe, D., Brown, M. S., and Goldstein, J. L. (2002). Insig-2, a second endoplasmic reticulum protein that binds SCAP and blocks export of sterol regulatory element-binding proteins. *Proc. Natl. Acad. Sci. U.S.A.* 99 (20), 12753–12758. doi: 10.1073/pnas.162488899

Yevtushenko, O. O., Cooper, S. J., O'Neill, R., Doherty, J. K., Woodside, J. V., and Reynolds, G. P. (2008). Influence of 5-HT2C receptor and leptin gene polymorphisms, smoking and drug treatment on metabolic disturbances in patients with schizophrenia. *Br. J. Psychiatry* 192 (6), 424–428. doi: 10.1192/bjp.bp.107.041723

Yu, W., De Hert, M., Moons, T., Claes, S. J., Correll, C. U., and van Winkel, R. (2013). CNR1 gene and risk of the metabolic syndrome in patients with schizophrenia. *J. Clin. Psychopharmacol.* 33 (2), 186–192. doi: 10.1097/JCP.0b013e318283925e

Zai, G. C., Zai, C. C., Chowdhury, N. I., Tiwari, A. K., Souza, R. P., Lieberman, J. A., et al. (2012). The role of brain-derived neurotrophic factor (BDNF) gene variants in antipsychotic response and antipsychotic-induced weight gain. *Prog. Neuropsychopharmacol. Biol. Psychiatry* 39 (1), 96–101. doi: 10.1016/j.pnpbp.2012.05.014

Zai, C. C., Tiwari, A. K., Zai, G. C., Maes, M. S., and Kennedy, J. L. (2018). New findings in pharmacogenetics of schizophrenia. *Curr. Opin. Psychiatry* 31 (3), 200–212. doi: 10.1097/YCO.0000000000000417

Zhang, X. Y., Tan, Y. L., Zhou, D. F., Cao, L. Y., Wu, G. Y., Xu, Q., et al. (2007). Serum BDNF levels and weight gain in schizophrenic patients on long-term treatment with antipsychotics. *J. Psychiatr. Res.* 41 (12), 997–1004. doi: 10.1016/j.jpsychires.2006.08.007

Zhang, X. Y., Zhou, D. F., Wu, G. Y., Cao, L. Y., Tan, Y. L., Haile, C. N., et al. (2008). BDNF levels and genotype are associated with antipsychotic-induced weight gain in patients with chronic schizophrenia. *Neuropsychopharmacology* 33 (9), 2200–2205. doi: 10.1038/sj.npp.1301619

Zhang, Y., Chen, M., Wu, Z., Chen, J., Yu, S., Fang, Y., et al. (2013). Association study of Val66Met polymorphism in brain-derived neurotrophic factor gene with clozapine-induced metabolic syndrome: preliminary results. *PLoS One* 8 (8), e72652. doi: 10.1371/journal.pone.0072652

Zhang, J. P., Lencz, T., Zhang, R. X., Nitta, M., Maayan, L., John, M., et al. (2016). Pharmacogenetic associations of antipsychotic drug-related weight gain: a systematic review and meta-analysis. *Schizophr. Bull* 42 (6), 1418–1437. doi: 10.1093/schbul/sbw058

Zhang, Jian-Ping, Robinson, Delbert, Yu, Jin, Gallego, Juan, Fleischhacker, W. Wolfgang, . Kahn, Rene S, et al. (2018). Schizophrenia polygenic risk score as a predictor of antipsychotic efficacy in first-episode psychosis. *Am. J. Psychiatry* 0 (0), appi.ajp.2018.17121363. doi: 10.1176/appi.ajp.2018.17121363

Zhang, Y., Ren, H., Wang, Q., Deng, W., Yue, W., Yan, H., et al. (2019). Testing the role of genetic variation of the MC4R gene in Chinese population in antipsychotic-induced metabolic disturbance. *Sci. Chin. Life Sci.* 62 (4), 535–543. doi: 10.1007/s11427-018-9489-x

Conflict of Interest: The authors declare that the research was conducted in the absence of any commercial or financial relationships that could be construed as a potential conflict of interest.

frontiers in Neuroscience

ORIGINAL RESEARCH
published: 29 July 2020
doi: 10.3389/fnins.2020.00784

Reduced Levels and Disrupted Biosynthesis Pathways of Plasma Free Fatty Acids in First-Episode Antipsychotic-Naïve Schizophrenia Patients

Xiang Zhou[1,2], Tao Long[1,2], Gretchen L. Haas[2,3], HuaLin Cai[4,5] and Jeffrey K. Yao[1,2,3]**

[1] Department of Pharmaceutical Sciences, University of Pittsburgh School of Pharmacy, Pittsburgh, PA, United States, [2] Medical Research Service and The VISN 4 Mental Illness Research, Education, and Clinical Center, VA Pittsburgh Healthcare System, Pittsburgh, PA, United States, [3] Department of Psychiatry, University of Pittsburgh School of Medicine, Pittsburgh, PA, United States, [4] The Department of Pharmacy, The second Xiangya Hospital of Central South University, Changsha, China, [5] Institute of Clinical Pharmacy, Central South University, Changsha, China

OPEN ACCESS

Edited by:
Adrian Preda,
University of California, Irvine,
United States

Reviewed by:
Błażej Misiak,
Wrocław Medical University, Poland
Raquel Romay-Tallon,
University of Illinois at Chicago,
United States

***Correspondence:**
HuaLin Cai
hualincai@csu.edu.cn
Jeffrey K. Yao
jkyao@pitt.edu

Specialty section:
This article was submitted to Neuropharmacology, a section of the journal Frontiers in Neuroscience

Received: 12 December 2018
Accepted: 03 July 2020
Published: 29 July 2020

Citation:
Zhou X, Long T, Haas GL, Cai H and Yao JK (2020) Reduced Levels and Disrupted Biosynthesis Pathways of Plasma Free Fatty Acids in First-Episode Antipsychotic-Naïve Schizophrenia Patients. Front. Neurosci. 14:784. doi: 10.3389/fnins.2020.00784

Membrane phospholipid deficits have been well-documented in schizophrenia (SZ) patients. Free fatty acids (FFAs) partially come from the hydrolysis of membrane phospholipids and serve as the circulating pool of body fatty acids. These FFAs are involved in many important biochemical reactions such as membrane regeneration, oxidation, and prostaglandin production which may have important implications in SZ pathology. Thus, we compared plasma FFA levels and profiles among healthy controls (HCs), affective psychosis (AP) patients, and first-episode antipsychotic-naïve schizophrenia (FEANS) patients. A significant reduction of total FFAs levels was observed in SZ patients. Specifically, significant reductions of 16:0, 18:2n6c, and 20:4n6 levels were detected in FEANS patients but not in APs when compared with levels in HCs. Also, disrupted metabolism of fatty acids especially in saturated and n-6 fatty acid families were observed by comparing correlations between precursor and product fatty acid levels within each fatty acid family. These findings may suggest an increased demand of membrane regeneration, a homeostatic imbalance of fatty acid biosynthesis pathway and a potential indication of increased beta oxidation. Collectively, these findings could help us better understand the lipid metabolism with regard to SZ pathophysiology.

Keywords: first-episode schizophrenia, free fatty acids, antipsychotic-naïve, fatty acid pathway, plasma

INTRODUCTION

Schizophrenia (SZ) is a devastating neuropsychiatric disorder that affects approximately 20 million people worldwide (GBD 2017 Disease and Injury Incidence and Prevalence Collaborators, 2018). It imposes a massive economic burden on individuals with SZ, their families and the society. Previous studies have linked SZ to widespread structural and functional brain alterations, including multiple neurotransmitter pathway disruptions (Walsh et al., 2008; Kerner, 2009; Karam et al., 2010; Brisch et al., 2014), white matter changes (Kubicki et al., 2005; Lener et al., 2014), and prefrontal-limbic

network dysfunctions (Weinberger et al., 1988, 1992). Despite plenty of theories proposed on the pathophysiology of SZ, none of them can fully explain its symptomatology and underlying etiology. Given the diverse biological findings reported in SZ, it is possible that the etiologic heterogeneity of SZ could result from a common pathogenic pathway (or a few pathways) that eventually leads to the clinical syndromes.

As far as we know, currently no literature data illustrating whether direct correlations between levels of plasma free fatty acids (FFAs) and the composition of membrane FAs has been reported. However, there is some evidence from two aspects which suggests indirect associations between them. Firstly, plasma FFAs have long been considered as a pivotal indicator of essential FAs status of humans, reflecting the amount of FA source that can be utilized in membrane phospholipid metabolism (Holman et al., 1979). In support, a study has reported about the FA composition of plasma and erythrocyte membranes in normal individuals (Manku et al., 1983). It shows that most ratios of FAs in plasma are like those in erythrocyte membranes except for 18:2n-6 and 22:4n-6, thought the phenomenon was not discussed. Secondly, *in vitro*, the cellular FA composition is likely to change due to the altered FA levels in serum used to grow established cell lines (Stoll and Spector, 1984). *In vivo*, supplementation of cod fish oil which is rich in omega-3 polyunsaturated fatty acids (PUFA), will result in increased eicosapentanoic and docosahexaenoic acid incorporations into the total phospholipids of plasma, platelets, and erythrocytes in a dose- and time-dependent manner (Von Schacky and Weber, 1985). Moreover, it is well-established that phospholipase A_2 (PLA_2) can recognize and cleave FAs from membrane phospholipids. It can bind to the sn-2 acyl bond of phospholipids and catalytically hydrolyze it, releasing arachidonic acid and lysophosphatidic acid into the blood stream (Dennis, 1994). These may suggest that plasma FA and membrane FA composition are dynamically linked.

As a major class of components of myelin, phospholipids play a crucial role in maintaining myelinated neuronal axons in the central nervous system (CNS) and peripheral nervous system (PNS). Studies show that at least 70% of the dry mass of both CNS and PNS myelin is formed by phospholipids (Baumann and Pham-Dinh, 2001; Chrast et al., 2010). Interestingly, previous findings (Gattaz et al., 1990; Horrobin et al., 1991; Pettegrew et al., 1991; Noponen et al., 1993) have indicated that in both CNS and peripheral tissues, SZ patients had an increased breakdown of membrane phospholipids due to PLA_2 activity. Recent studies have shown that calcium-independent PLA_2 plays a crucial role in the regulation of phospholipid metabolism and cell membranes functionality in the CNS (St-Gelais et al., 2004; Schaeffer et al., 2005). In addition, increased activities PLA_2 in SZ patients including drug-naïve patients, drug-free patients and patients with different stages of SZ have been observed (Smesny et al., 2005; Šakić et al., 2016). It is also reported that higher concentrations of PLA_2 in those patients are positively correlated with the illness duration and episode numbers (Šakić et al., 2016), while other studies suggest significant correlations between PLA_2 activity and positive symptoms (Gattaz et al., 1990; Ross et al., 1997). The resulting FFAs, which are not bound on cell membranes or proteins, are involved in many important biochemical reactions such as regeneration of membrane phospholipids (Rapoport, 2001; Yehuda et al., 2002), production of prostaglandins (Flower and Blackwell, 1976; Kuehl and Egan, 1980) and generation of adenosine triphosphates via beta-oxidation in the mitochondria. FFAs originate from lipolysis of membrane phospholipids and serve as dynamic lipid pools in the body. Therefore, changes of FFA levels may have significant implications in the SZ pathology. While lots of studies focused on membrane phospholipid abnormalities, no study has investigated the potential role of plasmatic FFAs in SZ pathology. The aim of the current study thus is to test whether levels and biosynthesis of plasma FFAs are altered in SZ patients at early stage of disease development. Levels of FFAs were measured and compared between the HC group and first-episode antipsychotic-naïve schizophrenia (FEANS) group. To test if those potential alterations of FFA profiles were unique features on SZ patients and could be served as potential biomarkers of SZ, the affective psychosis (AP) group including patients with bipolar disorder and major depression was further added to the comparisons of FFAs levels with the HC and FEANS groups. Furthermore, correlations between the levels of different types of fatty acids were explored in distinct groups of patients and controls.

MATERIALS AND METHODS

Clinical Design

Forty SZ antipsychotic-naïve patients were recruited during their first episode of psychosis after they provisionally met diagnostic and statistical manual of mental disorders (DSM-IV) criteria for schizophrenia or schizophreniform disorder based on the Structured Clinical Interview for DSM Disorders. In addition, 52 age-, race-, BMI-, and gender-matched healthy control (HC) subjects and 24 patients with other psychotic disorders (including psychotic bipolar disorder and major depression with psychotic features), herein referred to as AP subjects, were also recruited from the same community. Subjects in AP group were in drug-free status at the time of enrollment. Statistical Manual of Mental Disorders (DSM) version 4 was used to diagnose the patients. To be diagnosed with SZ, two of the following characteristic symptoms need to be met over at least 1 month: delusions, hallucinations, disorganized speech, grossly disorganized or catatonic behavior or negative symptoms (e.g., flattened affect, alogia, amotivation, and avolition). Also, the person should have social or occupational dysfunction or failure to achieve a level of functioning expected for their age and socioeconomic background. Lastly, continuous signs of the disturbance must persist for a minimum of 6 months. No somatic and psychiatric comorbidities were recorded on those SZ patients. None of subjects were taking alcohol or cigarettes for at least 14 days prior to the study or during the study. Also, none of the subjects were on anticoagulants or lipid lowering agents before or during the study. We confirmed that all participants did not have an unbalanced diet, restricted diet or abnormal eating habits. Eating habits between patients and HCs were basically similar. In addition, blood samples were collected after overnight fasting protocol to minimize the diet effect as well.

Collected fresh blood was immediately separated for plasma and transferred to the −70°C freezer. Clinical symptoms were evaluated prior to initiation of clinicians' choice of antipsychotic agents. Scale for the assessment of positive symptoms (SAPS) and scale for the assessment of negative symptoms (SANS) were used with the FEANS and AP group evaluation. The SAPS has 34 items (including four global items) that constitute four subscales measuring hallucinations, delusions, bizarre behavior, and positive formal thought disorder. The SANS has 25 items (including five global items) that constitutes five subscales measuring affective flattening or blunting, alogia, avolition-apathy, anhedonia-asociality, and attention. Each item was scored by clinicians from 0 (no symptom) to 5 (most severe) to evaluate the degree of each symptom. The demographic and clinical characteristics of subjects are shown in **Table 1**.

Clinical Ethics

The study was approved by the Institutional Review Boards of the University of Pittsburgh and the VA Pittsburgh Healthcare System. All patients and control subjects were recruited from UPMC Western Psychiatric Hospital in Pittsburgh. Diagnostic assessments and clinical symptom ratings were performed by experienced research clinicians, then reviewed and confirmed by senior diagnosticians during diagnostic conferences attended by research faculty experienced psychiatrists. All subjects including controls were provided written informed consent prior to participation in the research procedures.

Fatty Acid Methylation and Gas Chromatography Analysis

Plasma FFAs were quantitatively determined by capillary gas chromatography (GC) according to the procedure described by Lepage and Roy (1988). In brief, FFAs were extracted from 50 μl of plasma containing internal standard (Tridecanoic acid) and then converted to methyl esters by acetyl chloride-methanol reagent. After the preparation, 1 μl of the resulting fatty acid methyl esters was injected into GC for analysis. The procedure used for GC analysis has been previously described (Yao et al., 2002; Reddy et al., 2004). Briefly, prepared samples including internal standard were injected into the capillary column, with programmed control of oven temperatures. Each sample was run under a splitless injection mode with helium as the carrier gas (3 mL/minute) and with an inlet pressure of 6.5 psi. All major peaks were eluted within 16 min. Typical chromatography from a HC subject is shown in **Supplementary Figure 2**. These peaks were then identified and determined by comparing the retention times with those of standard mixtures (Supelco, Inc.). Linear standard curve range of this assay is from 0.25 nmol/mL to 1250 nmol/mL. The Lower Limit of Quantification is 0.05 nmol/mL. Concentrations of each FFA were then calculated by Agilent ChemStation. Each sample was tested in duplicates and quality control samples made from the plasma pool were used to check the differences between batches. Intra-assay percentage of CV was below 5.0% and inter-assay percentage of CV was below 6.5%.

Data Analysis Packages and Procedures

All tests were done using STATA (v 15.0) software packed. Two-tailed *p*-values were applied to test the fatty acid levels between groups. First, All data were checked for skewness by quantile–quantile plots. Second, for FFA levels comparisons, analysis of variance (ANOVA) with Bonferroni corrections on *post hoc* comparisons were conducted across the HC, AP, and FEANS groups. Third, Pearson correlation coefficients were used to test associations between precursor FAs and product FAs within certain fatty acid pathways. Fourth, Pearson correlation coefficients were used to test associations between FAs and clinical scales.

As there were significant differences between groups in terms of sex and race (**Table 1**), these variables were used as covariates in the statistical analysis. ANOVA analysis with Bonferroni corrections on *post hoc* comparisons were conducted to test differences between FFA levels across the HC, AP, and FEANS groups. The Bonferroni correction was applied when testing multiple null hypothesis in one data set. Therefore, the critical *p*-value was adjusted to the number of comparisons in a specific ANOVA *post hoc* test. Since FFAs levels among three groups (three comparisons) were compared, the critical *p*-value was set to: 0.05/3 = 0.0167. Pearson correlation coefficients were used to test associations between precursor FAs and product FAs within certain fatty acid pathways. These precursor/product FFAs correlation analyses were run with sex and race as covariates. These correlations were utilized to reflect connections between the precursor and product FFAs. We hypothesize that in SZ patients, a disturbance of FFAs pathways will lead to the loss of tight connections between precursor and product FFAs in comparison to those in control groups. Also, correlations between precursor and product FAs can indirectly implicated the activity of the elongase and desaturase as indicated in **Supplementary Figure 1**. Therefore, Correlation analysis were conducted among major FAs within each FA family (n-6, n-7, n-9, n-3, and saturated fatty acids) pathway. Specifically, 18:2n6, 18:3n6, 20:3n6, 20:4n6, and 22:4n6 were included in n-6 correlation analyses; 16:1n7t, 16:1n7c, and 18:1n7 were included in n-7 correlation analyses; 18:1n9t and 18:1n9c were included in n-9 correlation analyses; 22:5n3 and 22:6n3 were included in n-3 correlation analyses; 14:0, 15:0, 16:0, 17:0, 18:0, 21:0, 22:0, and 17:1 were included in saturated correlation analyses. Bonferroni corrections were applied to the number of comparisons in the correlation analyses. Precursor/product pairs that were analyzed: 18:2n6/18:3n6, 18:3n6/20:3n6, 20:3n6/20:4n6, 20:4n6/22:4n6, 18:2n6/20:3n6, 18:2n6/20:4n6, 18:2n6/22:4n6, 18:3n6/20:4n6, 20:3n6/22:4n6, and 20:3n6/22:4n6 for the n-6 family (Bonferroni corrected α level = 0.05/10 = 0.005); 16:1n7t/16:1n7c, 16:1n7t/18:1n7, and 16:1n7c/18:1n7 for the n-7 family (Bonferroni corrected α level = 0.05/3 = 0.0167); 18:1n9t/18:1n9c for the n-9 family (α level = 0.05); 22:5n3/22:6n3 for the n-3 family (α level = 0.05); 14:0/16:0, 16:0/18:0, 18:0/22:0, 14:0/18:0, 14:0/22:0, 16:0/22:0, 15:0/17:0, and 17:0/17:1 for the saturated fatty acids (Bonferroni corrected α level = 0.05/8 = 0.0063). For the significant correlations that found between n-3 FFAs

TABLE 1 | Demographic data of recruited subjects.

	HC	AP	FEANS	Comparisons		
				HC vs. AP	HC vs. FEANS	AP vs. FEANS
Numbers	52	24	40	NA	NA	NA
Sex[a]	31/20	13/11	26/14	<0.001	<0.001	<0.001
Age[1]	26.3 ± 7.4	26.9 ± 9.9	22.7 ± 8.1	ns	ns	ns
BMI[2]	25.2 ± 4.4	25.2 ± 6.9	23.3 ± 5.3	ns	ns	ns
Race[b]	34/10/3/4	17/5/1/1	20/16/2/2	<0.001	<0.001	<0.001
SAPS[3]	NA	18.2 ± 14.9	26.0 ± 12.2	NA	NA	0.0265
SANS[4]	NA	37.6 ± 9.5	44.1 ± 11.1	NA	NA	0.0202

[a]Male/Female. Significant differences were observed in Sex ratios as tested by Pearson Chi-square test. [b]Caucasian/African American/Pacific Asian/Others. Significant differences were observed in race ratios by comparing ratios of major race (Caucasian) numbers vs. other races numbers in total, as tested by Pearson Chi-square test. [1,2]No significant difference was found in age, BMI, and SANS values as tested by analysis of variance among three groups. [3,4]Significant differences were observed in SAPS and SANS between AP and FEANS group as tested by two sample t-test. HC, healthy controls; AP, affective psychosis; FEANS, first-episode antipsychotic-naïve schizophrenia patients; NA, Not Applicable; ns, no significant difference; BMI, body mass index; SAPS, scale for the assessment of positive symptoms; SANS, scale for the assessment of negative symptoms. Note: Age, BMI, and clinical scores are expressed as mean ± standard deviation. In HC group, one subject is missing the information of sex and race. Three subjects in FEANS group and one subject in AP group are missing BMI data due to missing height/weight values.

levels and clinical scales, the corrected Bonferroni corrected α level = 0.05/4 = 0.0125 (SAPS/22:5n3, SAPS /22:6n3, SANS/22:5n3, and SANS/22:6n3).

RESULTS

Comparisons of Plasma Fatty Acids Levels Among All Groups

Significantly lower total levels of plasma FFAs were detected in FEANS subjects than in HC and AP subjects (**Table 2**). Specifically, the reductions of plasma FFAs were mostly noted in saturated and n-6 fatty acid families (**Table 2**). Among saturated fatty acids, the 16:0 levels were significantly decreased in the FEANS group as compared with those in the HC and AP groups (**Table 2**). Among the n-6 family of fatty acids, the 18:2n6c and 20:4n6 levels were significantly lower in the FEANS group as compared with the HC and AP groups (**Table 2**). On the other hand, no significant differences were observed in each of these FFA levels between HC and AP groups. Among the n-3 family of fatty acids, significantly lower total levels of n-3 FFAs were observed in the FEANS group as compared with the HC group. However, no significant differences in n-3 FFA levels were detected between the FEANS group and the AP group compared to the n-3 FFAs.

Correlations Within Fatty Acid Families in HC, AP, and FEANS Groups

There was no significant correlation between any covariate (sex/age) and any FFA index. In the present study, correlations between fatty acids within each fatty acid family were also examined with sex and age as covariates. As expected, there were significant correlations between product and precursor within certain fatty acid families, among the HC, AP, and FEANS groups. Specifically, significant correlations were detected mainly in saturated fatty acids, between 16:0 and 18:0, 16:0 and 22:0, and between 18:0 and 22:0 (**Figure 1**). For the other families of fatty acids, however, significant correlations were only observed in one or two of the three groups.

In contrast with the findings mentioned above, significant correlations between 18:3n6 and 20:4n6, as well as between 16:1n7c and 18:1n7, were identified only in the HC group, but not in FEANS or AP groups (**Figure 2**). Interestingly, significant correlations between 17:0 and 17:1, as well as between 18:3n6 and 20:3n6, were observed both in HC and AP groups, but not in the FEANS group (**Figure 3**).

Correlations Between Free Fatty Acid Levels and Clinical Scales in FEANS and AP Groups

In FEANS and AP groups, no significant correlation was found between SANS scores and total or any single FFA levels. However, we observed a significant reversed correlation between levels of 22:6n3 and SAPS scores in the FEANS group when comparing with that in the AP group (**Figure 4**).

DISCUSSION

In this study, levels of plasma FFAs were determined in SZ patients experiencing their first episode of schizophrenia, patients with a first episode of other (non-schizophrenia) psychotic disorders and HC subjects. Understanding FFA profiles will help us to better comprehend the altered lipid metabolism in SZ. A recent meta-analysis study has revealed that several polyunsaturated FAs levels were decreased in erythrocyte membranes of SZ patients (Van der Kemp et al., 2012). It has also been well-documented that the increased breakdown of membrane phospholipids is mainly due to elevated PLA_2 activities in SZ patients (Smesny et al., 2005), both in peripheral tissues (Gattaz et al., 1990; Noponen et al., 1993) and CNS (Horrobin et al., 1991; Pettegrew et al., 1991). It has been well-documented that there is an increased breakdown of membrane phospholipids due to elevated PLA_2 activity in SZ patients, both in peripheral tissues (Gattaz et al., 1990; Noponen et al.,

TABLE 2 | Fatty acid concentrations in healthy controls (HCs, *n* = 52), affective psychosis (AP, *n* = 24), and first-episode antipsychotic-naïve schizophrenia patients (FEANS, *n* = 40).

Fatty acid[a]	HC	AP	FEANS	Comparisons			
				F[b]	HC vs. AP	HC vs. FEANS	AP vs. FENAS
Saturates							
14:0	35 ± 16	29 ± 12	34 ± 20	1.065	ns	ns	ns
15:0	4.5 ± 1.8	5.9 ± 1.6	3.9 ± 1.9	**9.313**	0.002	ns	<0.0001
16:0	357 ± 95	356 ± 82	295 ± 74	**6.889**	ns	0.0007	0.007
17:0	6.6 ± 4.5	6.6 ± 2.7	4.9 ± 1.8	3.001	ns	ns	ns
18:0	109 ± 30	125 ± 28	98 ± 21	**7.917**	ns	ns	0.0004
21:0	5.1 ± 3.6	6.5 ± 2.5	4.5 ± 3.6	2.615	ns	ns	ns
22:0	11.2 ± 4.7	12.6 ± 4.5	9.0 ± 3.2	**6.160**	ns	ns	0.001
Monoenes							
16:1n7t	5.8 ± 2.4	6.9 ± 2.3	4.5 ± 1.6	**9.963**	ns	ns	<0.0001
16:1n7c	22.6 ± 10.7	26.7 ± 11.2	17.1 ± 7.8	**7.577**	ns	ns	0.0003
17:1	9.2 ± 7.0	12.2 ± 4.1	7.8 ± 5.3	**4.053**	ns	ns	0.014
18:1n9t	25 ± 14	27 ± 11	21 ± 12	1.864	ns	ns	ns
18:1n9c	227 ± 73	213 ± 54	181 ± 46	**6.549**	ns	0.001	ns
18:1n7	25 ± 10	28 ± 8	22 ± 8	**4.304**	ns	ns	0.006
Dienes							
18:2n6c	314 ± 75	322 ± 65	255 ± 62	**10.511**	ns	<0.0001	<0.0001
20:2n6	5.1 ± 3.6	5.1 ± 2.3	3.6 ± 2.4	**3.594**	ns	0.013	ns
Trienes							
18:3n6	5.6 ± 2.7	5.3 ± 1.9	4.6 ± 2.1	2.445	ns	ns	ns
20:3n6	5.3 ± 2.9	5.3 ± 2.3	4.3 ± 2.8	1.605	ns	ns	ns
Tetraenes							
20:4n6	70 ± 17	75 ± 10	60 ± 16	**7.748**	ns	0.004	0.0004
22:4n6	13.4 ± 4.6	15.4 ± 4.1	12.9 ± 4.5	2.527	ns	ns	ns
Pentanenes							
22:5n3	5.0 ± 2.6	5.7 ± 2.2	3.9 ± 2.7	**3.869**	ns	ns	0.009
Hexananes							
22:6n3	26 ± 9	25 ± 7	22 ± 3	**4.584**	ns	0.004	ns
Totals							
Saturates	529 ± 129	542 ± 118	450 ± 91	**7.012**	ns	0.001	0.002
n-3 fatty acids	31 ± 10	31 ± 8	26 ± 5	**5.756**	ns	0.006	ns
n-6 fatty acids	413 ± 90	428 ± 65	340 ± 74	**12.509**	ns	<0.0001	<0.0001
Grand totals	1288 ± 297	1315 ± 213	1069 ± 205	**10.738**	ns	<0.0001	0.0003

[a]All concentration values are expressed as mean ± standard deviation. Units: nmol/mL. [b]F-value with significant p in the analysis of variance (ANOVA) analysis has been shown in bold. Critical p-values after Bonferroni Correction: 0.0167.

1993) and CNS (Horrobin et al., 1991; Pettegrew et al., 1991). Gattaz and Brunner (1996) proposed that increased PLA_2 activity in the prefrontal cortex could contribute to membrane phospholipid deficits and eventually lead to hypofrontality in schizophrenia. Several later studies supported this theory which linked membrane phospholipid deficits to myelin dysfunctions (Schmitt et al., 2004; Peters et al., 2012) and prefrontal cortex abnormality (Taha et al., 2013). It is hypothesized that increased lipolysis of membrane lipids would also be associated with the dyslipidemia in SZ patients. Both increased levels of serum triglycerides and decreased levels of serum high density lipoproteins were found in antipsychotic-naïve SZ patients, suggesting the disturbance of lipid profiles could occur during the early course of the disease (Misiak et al., 2017). The FFAs released from membrane phospholipids after hydrolysis by PLA enter into the circulating system. Therefore, an increased breakdown of membrane phospholipids through PLA could potentially lead to higher levels of FFAs as we originally hypothesized. However, instead of observing increased FFAs resulting from increased breakdown of membrane phospholipids, we observed significantly lower levels of plasma FFAs and disrupted linkages in FFA biosynthesis pathways among FEANS patients. More importantly, we did not observe significantly reduced FFAs levels in AP group subjects, suggesting such reductions may be trait features of SZ. Since many important biochemical reactions were involved in those FFAs such as regeneration of membrane phospholipids (Rapoport, 2001; Yehuda et al., 2002), production of prostaglandins (Flower and Blackwell, 1976; Kuehl and Egan, 1980) and generation of adenosine triphosphates via beta-oxidation in the mitochondria, significantly lower

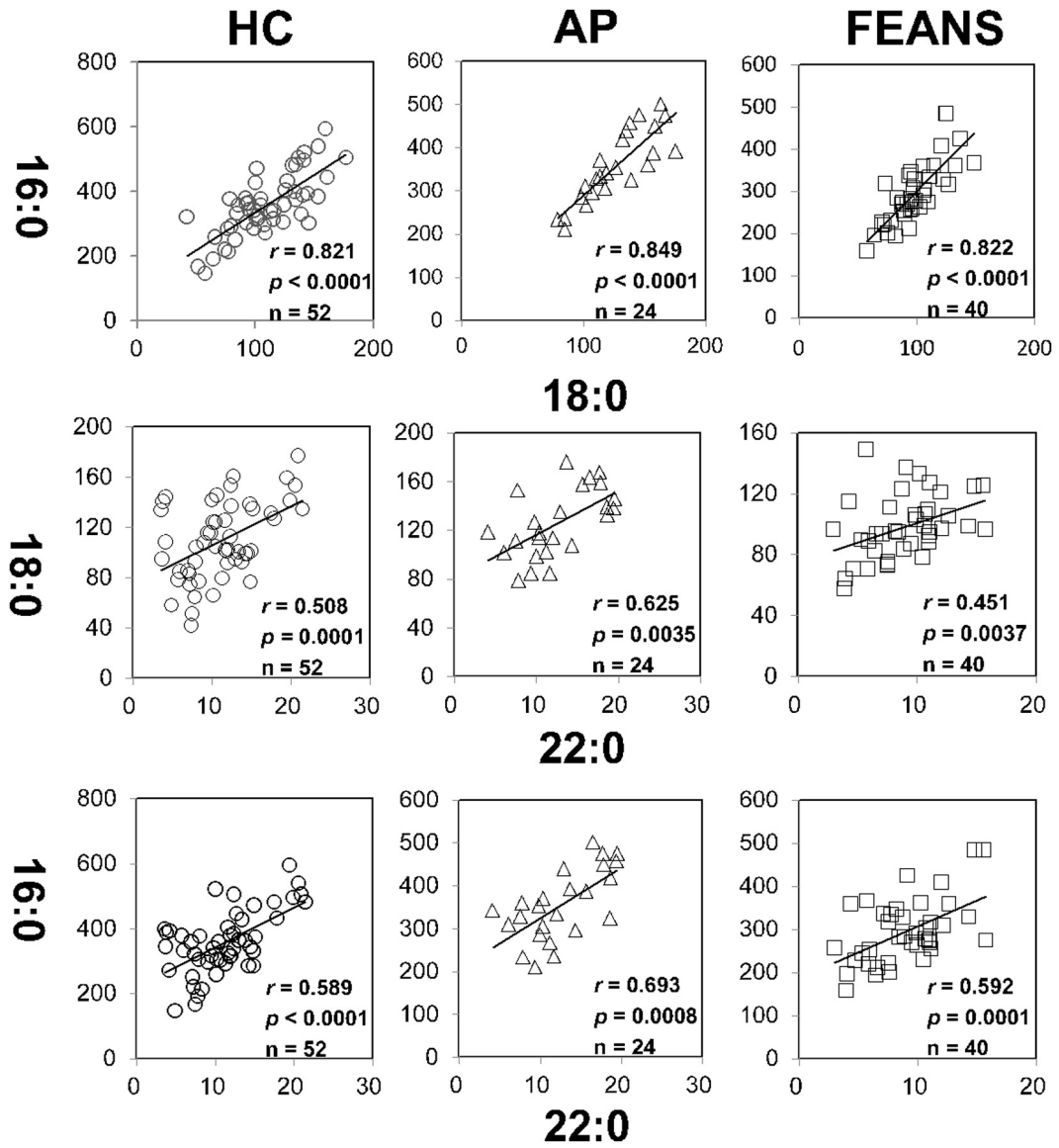

FIGURE 1 | Tight correlations of fatty acids among healthy control (HC) subjects, affective psychosis (AP) patients, and first-episode antipsychotic-naïve schizophrenia patients (FEANS). Critical *p*-value after Bonferroni correction: 0.0063.

levels of plasma FFAs and breakdown of correlations between precursor/product FAs may serve as biomarkers of SZ, which lead to three important implications with regard to SZ's pathophysiology.

First, reduced total FFA levels may imply an increased regeneration of cell membranes and possible alterations in beta-oxidations of fatty acid metabolism at the early course of SZ. While plenty of studies have focused on the PUFA levels in SZ (Van der Kemp et al., 2012), few have discussed other FAs and the total FA levels in SZ (McEvoy et al., 2013; Yang et al., 2017). Recently, a decreased total plasma FFA levels was detected in FEANS patients with limited sample sizes (Zhou et al., 2017, 2018). Unfortunately, the portion of plasma FFAs after the hydrolysis by PLA_2 from those membrane phospholipids has not yet been explored. In our working hypothesis, reduced levels of plasma FFAs may reflect a depleted pool of those fatty acids resulting from an increased demand of cell membrane regeneration during the early course of SZ development. It is speculated that such demand was due to the membrane phospholipid deficits. As suggested by previous literature, oxidative stress could lead to such deficits through membrane lipid peroxidation in SZ patients (Dietrich-Muszalska and Kontek, 2010; Bitanihirwe and Woo, 2011; Boskovic et al., 2011). Notably, while there is a general trend of decrease among all families of FFAs, we found that n-6 and saturated family FFA levels in FEANS group are significantly lower than those in HC and AP groups. This finding implies that these two fatty acid families are most vulnerable to oxidative stress at

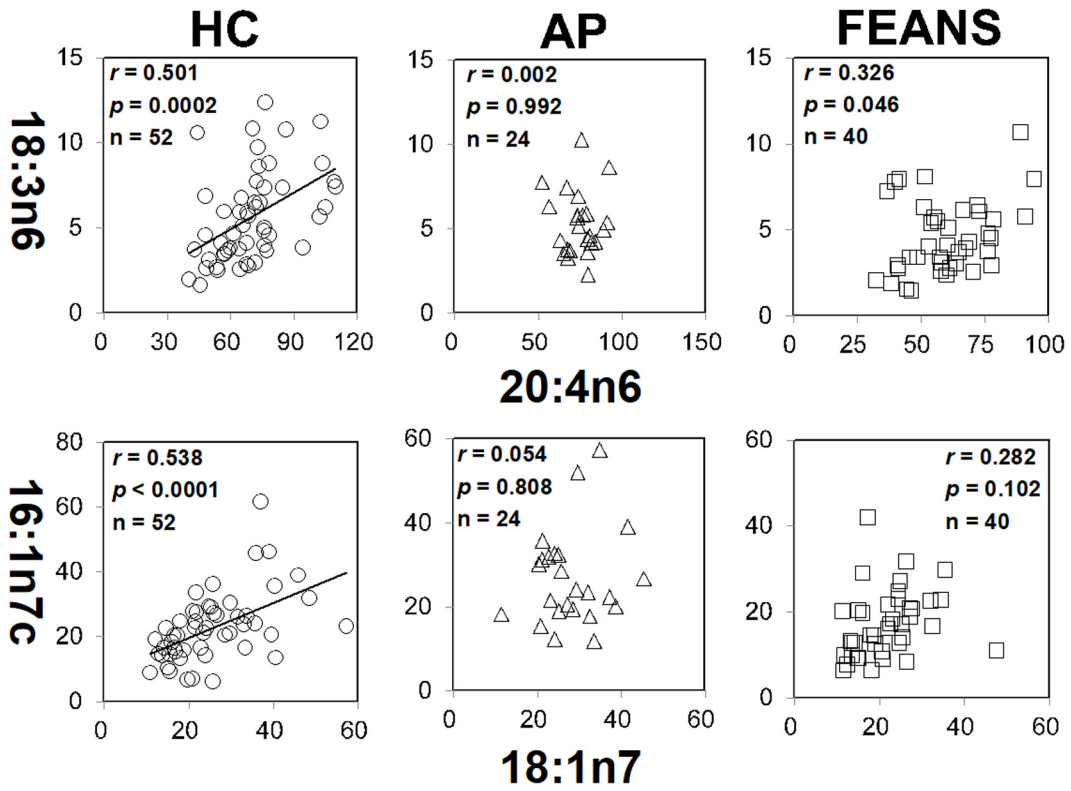

FIGURE 2 | Disrupted correlations of fatty acids both shown in affective psychosis (AP) patients and first-episode antipsychotic-naïve patients (FEANS). Critical *p*-value after Bonferroni correction: for 18:3n6/20:4n6, critical $p = 0.005$; for 16:1n7c/18:1n7, critical $p = 0.0167$.

the early stage of SZ. As the body cannot synthesize n-6 fatty acids by itself, it might be interesting to discuss the potential dietary effects on these fatty acids here. When the fats get absorbed through digestion system, they will breakdown and then converted to triglycerides and lipoproteins, incorporated into membrane phospholipids and further be broken down into FFAs. Our previous study showed that when comparing membrane-bound fatty acid levels in red blood cell samples, no significant difference in either saturated or monounsaturated fatty acids was observed between FEANS and control groups (Yao et al., 2002). This finding suggested that dietary effects might not have a significant impact on membrane phospholipid levels. In the present study, there was no evidence of metabolic dysfunction observed in these FEANS patients. At the meantime, FEANS subjects' BMI data were comparable with those in controls (**Table 1**). Therefore, it's not likely that the dietary effects played a significant role here. Furthermore, previous studies showed that several fatty acid beta-oxidation enzymes were significantly increased in the brains of SZ patients, which implied enhanced beta-oxidation in FEANS patients (Prabakaran et al., 2004). Up-regulated beta-oxidation in peripheral tissues of SZ patient has also been suggested by comparing product-to-precursor ratios of serum FFAs (Yang et al., 2017). The decreased FFAs levels thus may result from a depleted source in membrane phospholipids as lipids metabolism was shifted toward beta-oxidation in the cytosol. Oxidative stress might play a role in promoting lipid beta-oxidation here, although the impact on FFA metabolism by oxidative stress is still unclear and the mechanism by which it caused the up-regulation of the beta-oxidation remains to be determined. In summary, it is speculated that the reduction of plasma FFA levels may be due to the increased regeneration of membrane phospholipids and hyperactivity of beta-oxidation in SZ pathology. A postulated model is proposed below to explain the reductions of FFA levels (**Figure 5**) in SZ patients. In brief, the extent of oxidative stress was accumulated in SZ patients due to environmental or genetic factors. The increased oxidative stress levels led to membrane phospholipid deficits, and thus, more FFAs were taken up for regenerating cell membranes in SZ patients. Also, increased oxidative stress levels resulted in an increased activity of beta-oxidation on FFAs, and thus more FFAs were metabolized through this reaction in SZ patients. As a result, reduced levels of total plasma FFAs were observed in the FEANS group when compared with the HC and the AP groups.

Second, our findings reflect a homeostatic imbalance of fatty acid biosynthesis at the early stage of SZ. Most FFAs can be synthesized by elongases and desaturases, and then go through beta-oxidation to generate energy (**Supplementary Figure 2**). Although some of precursor to product correlations persisted across disease and normal status, some appeared to be lost in the FEANS group. Our results suggest that the potential for steady formation of fatty acids is altered early in the course of illness. While alterations were also observed in the saturated

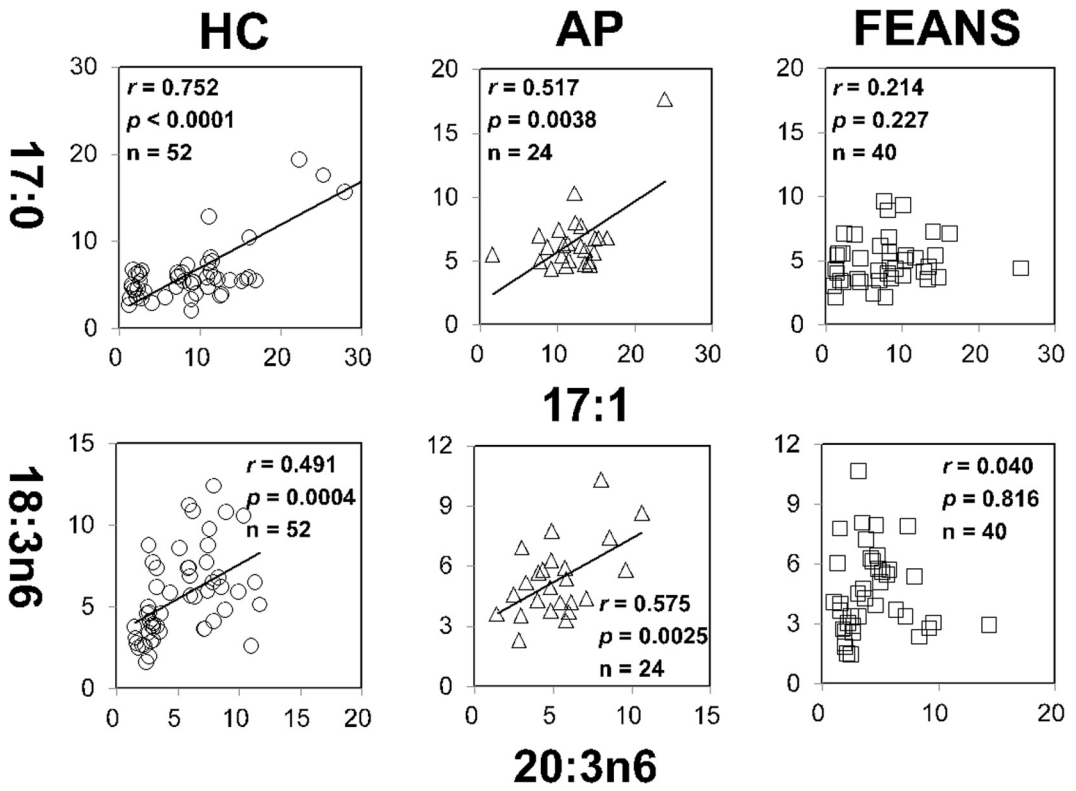

FIGURE 3 | Disrupted correlations of fatty acids only present in first-episode antipsychotic-naïve patients (FEANS). Critical *p*-value after Bonferroni correction: for 17:0/17:1, critical $p = 0.0063$; for 18:3n6/20:4n6, critical $p = 0.005$.

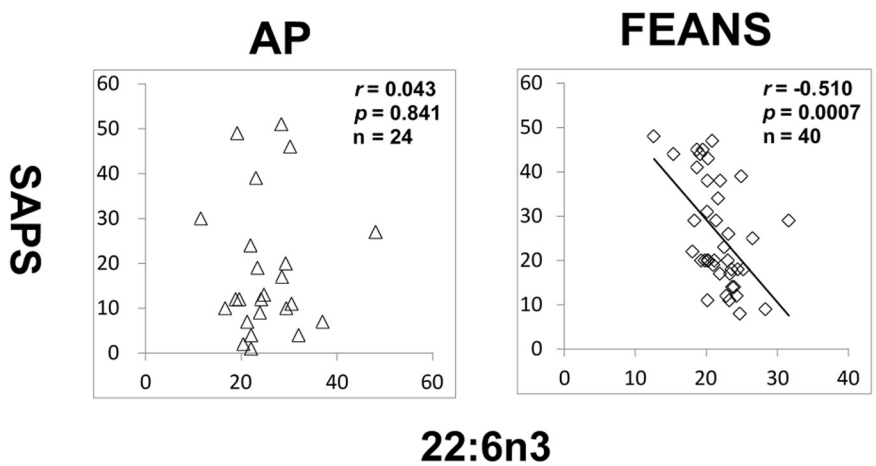

FIGURE 4 | Significant reversed correlations between 22:6n3 and assessment of positive symptoms (SAPS) in first-episode antipsychotic-naïve patients (FEANS). Critical *p*-value after Bonferroni correction: $p = 0.125$.

fatty acid family, it appears that the n-6 fatty acid family is the one that was most altered in FEANS subjects but not in the AP subjects. This may suggest that the n-6 fatty acid biosynthesis is more disrupted than other fatty acid families at the early course of the SZ while not in the other psychiatric disorders. Although there was no difference of 22:6n3 between FEANS and AP groups (**Table 2**), 22:6n3 levels were negatively associated with SAPS scores only in FEANS and this very correlation is absent in AP group (**Figure 4**). N-6 PUFA (especially arachidonic acid and palmitic acid) can be viewed as proinflammatory molecules, whereas n-3 PUFA (especially eicosapentaenoic acid and docosahexaenoic acid) can be viewed as anti-inflammatory

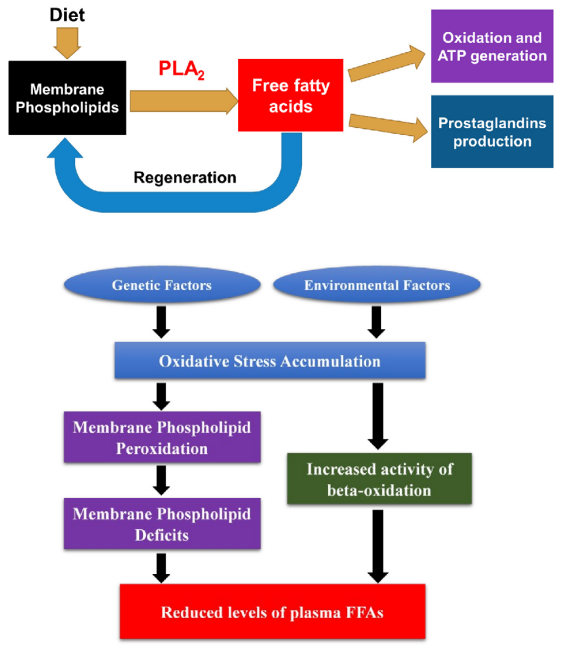

FIGURE 5 | Free fatty acids (FFAs) in lipid metabolism and postulated model of reduced plasma FFA levels and its underlying mechanism in schizophrenia pathophysiology. FFAs come from the lipolysis of membrane phospholipids and serve as an active circulating pool in body. They are involved in many important biochemical reactions including regeneration of membrane phospholipids, beta-oxidation, and production of prostaglandins. In schizophrenia, oxidative stress level was accumulated due to environmental or genetic factors. Consequently, oxidative stress led to membrane phospholipid deficits and increased activity of beta-oxidation of FFAs. Since more FFAs were utilized to regenerate cell membranes and were metabolized through beta-oxidation, levels of plasma FFAs were reduced in SZ patients. PLA_2, phospholipase A_2.

molecules (Sears and Perry, 2015). More disrupted n-6 fatty acid biosynthesis may be considered as a trait-like marker reflecting a severer inflammatory status of SZ patients. However, n-3 PUFA such as 22:6n3 levels could preferably serve as a state-like marker in SZ, which is linked to the symptomatology. However, the exact mechanisms of such alteration on n-6 family FFAs are still unknown. In summary, our findings suggest a disrupted biosynthesis of fatty acids, especially on n-6 fatty acids in the early stage of SZ.

Third, a significantly reduced n-6 FAs may be attributed to the blunted niacin-induced skin flushing in a subgroup of SZ patients, which might be clinically useful in the diagnosis of schizophrenia (Morrow et al., 1989, 1992; Ward et al., 1998; Puri et al., 2001; Benyó et al., 2005; Maciejewski-Lenoir et al., 2006; Tang et al., 2006; Lai et al., 2007; Messamore and Yao, 2016). While the cause of such blunted skin flushing in SZ is still unclear, our findings of a significant decreased arachidonic acid (20:4n6) as well as its precursors in FEANS patients may offer a possible explanation to the underlying mechanism that caused the blunted niacin-induced response in SZ. It is speculated that reduced levels of 18:2n6 and 20:4n6 may reflect a decreased pool for subsequent production of prostaglandin vasodilators (PGD_2 and PGF_2), which could lead to the blunted niacin-induced flushing response in those SZ patients (Messamore et al., 2010).

LIMITATIONS

The present study of FFAs was mainly focused on FEANS patients, while antipsychotic treatment effects on those FFAs might also be an interesting research target. This is due to the high prevalence of metabolic syndrome among antipsychotic-treated SZ patients, especially among those treated by second-generation antipsychotics (Casey et al., 2004; Wu et al., 2006). Although promising clinical data showed the metabolic improvement of SZ patient by n-3 FAs supplementation in a randomized placebo-controlled trial (Xu et al., 2019), no literature had reported the possible impact of antipsychotics on FFA profiles in terms of metabolic syndrome. A previous preliminary study was conducted by our group to demonstrate a significant increase of total levels of FFAs after risperidone (a second-generation antipsychotic) treatment when compared to baseline FEANS patients (Zhou et al., 2017, 2018). Future in-depth study will be conducted to investigate the effect of antipsychotics on lipid profiles among SZ patients.

Based on our findings, significantly decreased levels of FFAs within n-6 family were observed in the FEANS group, which may imply a possible link to the blunted niacin-induced skin flushing in a subgroup of SZ patients. However, niacin response data in this clinical group was not available to validate the potential relationship between n-6 FFAs and niacin-induced skin flushing responses. Further studies are required to correlate plasma n-6 FFAs, especially arachidonic acid, with niacin response data. Also, since only a subgroup of SZ patients are presenting such blunted skin flushing, it would be interesting to see if there is a significant difference between a positive-flushing group and a minimal/non-flushing group in terms of arachidonic acid levels.

Most FFAs are synthesized by elongases and desaturases from substrate FFAs, and then go through beta-oxidation to generate energy. However, this study did not measure the activity of elongase and desaturase in those clinical subjects. Instead, comparisons of correlations between precursor and product FFAs among FEANS and control subjects were used to indirectly reflect a possible disruption within metabolic pathways.

Last of all, subjects in the AP group were in drug-free status at the time of enrollment. Patients in this group were recruited after the relapse without at least 30 days of treatment. Therefore, we cannot completely tease out the medication effect on the AP groups in terms of FFA levels. Moreover, low sample size and a lack of information regarding smoking status also became the limitations of the study.

CONCLUSION

Significantly reduced plasma FFAs levels were observed for FEANS patients, especially in 16:0, 18:2n6c, 20:4n6, and total FFA levels, when compared with those levels in the (AP and HC) control groups. Also, disrupted correlations of fatty acids within saturated and n-6 fatty acid families were observed.

These findings suggested an increased demand of membrane regeneration, a homeostatic imbalance of the fatty acid biosynthesis pathway, and a potential increase in beta oxidations.

DATA AVAILABILITY STATEMENT

The raw data supporting the conclusions of this article will be made available by the authors, without undue reservation, to any qualified researcher.

ETHICS STATEMENT

All participants provided written informed consent prior to participation in any research procedures. The study was approved by the Institutional Review Boards of the University of Pittsburgh and the VA Pittsburgh Healthcare System.

AUTHOR CONTRIBUTIONS

XZ and JY designed the research. XZ and TL performed the research. XZ, TL, GH, and HC wrote the manuscript. All authors contributed to the article and approved the submitted version.

FUNDING

This project was supported in part by the Merit Reviews 1I01CX000110 (JY) and Senior Research Career Scientist Award (JY) from the United States (U.S.) Department of Veterans Affairs Biomedical Laboratory Research and Development Service (JY), infrastructure supported from the Veterans Affairs VISN 4 Mental Illness Research, Education, and Clinical Center, and supported from the National Institutes of Health [MH58141, R21 MH102565, and R03 MH070434 (JY); MH64023 and K02 MH01180 (Matcheri Keishavan, MD); MH45156 (David Lewis, MD, Director); and NIH/NCRR/GCRC M01 RR00056 (Arthur Levine, MD)], Hunan Provincial Natural Science Foundation of China [2017JJ3444 (HC)], National Natural Science Foundation of China [NSFC81401113 (HC)], Wu Jieping Medical Foundation Funded Special Clinical Research Project [320.6750.2020-04-2 (HC)], and the Fundamental Research Funds for the Central Universities of Central South University [2019zzts1049 and 2020zzts884 (HC)].

ACKNOWLEDGMENTS

We would like to thank Dr. Debra Montrose, Dr. Ravinder Reddy, and Dr. Matcheri Keshavan for the recruitment of patients and leadership in the collection of clinical data for this study. The views expressed in this article are those of the authors and do not necessarily represent the position or policy of the Department of Veterans Affairs or the United States Government.

SUPPLEMENTARY MATERIAL

The Supplementary Material for this article can be found online at: https://www.frontiersin.org/articles/10.3389/fnins.2020.00784/full#supplementary-material

REFERENCES

Baumann, N., and Pham-Dinh, D. (2001). Biology of oligodendrocyte and myelin in the mammalian central nervous system. *Physiol. Rev.* 81, 871–927. doi: 10.1152/physrev.2001.81.2.871

Benyó, Z., Gille, A., Kero, J., Csiky, M., Suchánková, M. C., Nüsing, R. M., et al. (2005). GPR109A (PUMA-G/HM74A) mediates nicotinic acid–induced flushing. *J. Clin. Invest.* 115, 3634–3640. doi: 10.1172/JCI23626

Bitanihirwe, B. K., and Woo, T. U. W. (2011). Oxidative stress in schizophrenia: an integrated approach. *Neurosci. Biobehav. Rev.* 35, 878–893. doi: 10.1016/j.neubiorev.2010.10.008

Boskovic, M., Vovk, T., Kores Plesnicar, B., and Grabnar, I. (2011). Oxidative stress in schizophrenia. *Curr. Neuropharmacol.* 9, 301–312. doi: 10.2174/157015911795596595

Brisch, R., Saniotis, A., Wolf, R., Bielau, H., Bernstein, H.-G., Steiner, J., et al. (2014). The Role of dopamine in schizophrenia from a neurobiological and evolutionary perspective: old fashioned, but still in vogue. *Front. Psychiatry* 5:47. doi: 10.3389/fpsyt.2014.00047

Casey, D. E., Haupt, D. W., Newcomer, J. W., Henderson, D. C., Sernyak, M. J., Davidson, M., et al. (2004). Antipsychotic-induced weight gain and metabolic abnormalities: implications for increased mortality in patients with schizophrenia. *J. Clin. Psychiatry* 65, 4–18.

Chrast, R., Saher, G., Nave, K. A., and Verheijen, M. H. (2010). Lipid metabolism in myelinating glial cells: lessons from human inherited disorders and mouse models. *J. Lipid Res.* 52, 419–434. doi: 10.1194/jlr.R009761

Dennis, E. A. (1994). Diversity of group types, regulation, and function of phospholipase A2. *J. Biol. Chem.* 269, 13057–13060.

Dietrich-Muszalska, A., and Kontek, B. (2010). Lipid peroxidation in patients with schizophrenia. *Psychiatry Clin. Neurosci.* 64, 469–475. doi: 10.1111/j.1440-1819.2010.02132.x

Flower, R. J., and Blackwell, G. J. (1976). The importance of phospholipase-A2 in prostaglandin biosynthesis. *Biochem. Pharmacol.* 25, 285–291. doi: 10.1016/0006-2952(76)90216-1

Gattaz, W. F., and Brunner, J. (1996). Phospholipase A2 and the hypofrontality hypothesis of schizophrenia. *Prostaglandins Leukotrienes Essential Fatty Acids* 55, 109–113. doi: 10.1016/S0952-3278(96)90154-4

Gattaz, W. F., Hübner, C. V., Nevalainen, T. J., Thuren, T., and Kinnunen, P. K. (1990). Increased serum phospholipase A2 activity in schizophrenia: a replication study. *Biol. Psychiatry* 28, 495–501.

GBD 2017 Disease and Injury Incidence and Prevalence Collaborators, (2018). Global, regional, and national incidence, prevalence, and years lived with disability for 354 diseases and injuries for 195 countries and territories, 1990–2017: a systematic analysis for the Global Burden of Disease Study 2017. *Lancet* 392, 1789–1858. doi: 10.1016/S0140-6736(18)32279-7

Holman, R. T., Smythe, L., and Johnson, S. (1979). Effect of sex and age on fatty acid composition of human serum lipids. *Am. J. Clin. Nutr.* 32, 2390–2039. doi: 10.1093/ajcn/32.12.2390

Horrobin, D. F., Manku, M. S., Hillman, H., Iain, A., and Glen, M. (1991). Fatty acid levels in the brains of schizophrenics and normal controls. *Biol. Psychiatry* 30, 795–805. doi: 10.1016/0006-3223(91)90235-e

Karam, C. S., Ballon, J. S., Bivens, N. M., Freyberg, Z., Girgis, R. R., Lizardi-Ortiz, J. E., et al. (2010). Signaling Pathways in Schizophrenia: emerging targets and therapeutic strategies. *Trends Pharmacol. Sci.* 31, 381–390. doi: 10.1016/j.tips.2010.05.004

Kerner, B. (2009). Glutamate Neurotransmission in Psychotic Disorders and Substance Abuse. *Open Psychiatry J.* 3, 1–8. doi: 10.2174/1874354400903010001

Kubicki, M., McCarley, R. W., and Shenton, M. E. (2005). Evidence for white matter abnormalities in schizophrenia. *Curr. Opin. Psychiatry* 18, 121–134. doi: 10.1097/00001504-200503000-00004

Kuehl, F. A., and Egan, R. W. (1980). Prostaglandins, arachidonic acid, and inflammation. *Science* 210, 978–984. doi: 10.1126/science.6254151

Lai, E., De Lepeleire, I., Crumley, T. A., Liu, F., Wenning, L. A., Michiels, N., et al. (2007). Suppression of niacin-induced vasodilation with an antagonist to prostaglandin D2 receptor subtype 1. *Clin. Pharmacol. Therapeut.* 81, 849–857. doi: 10.1038/sj.clpt.6100180

Lener, M. S., Wong, E., Tang, C. Y., Byne, W., Goldstein, K. E., Blair, N. J., et al. (2014). White matter abnormalities in schizophrenia and schizotypal personality disorder. *Schizophrenia Bull.* 41, 300–310. doi: 10.1093/schbul/sbu093

Lepage, G., and Roy, C. C. (1988). Specific methylation of plasma nonesterified fatty acids in a one-step reaction. *J. Lipid Res.* 29, 227–235.

Maciejewski-Lenoir, D., Richman, J. G., Hakak, Y., Gaidarov, I., Behan, D. P., and Connolly, D. T. (2006). Langerhans cells release prostaglandin D2 in response to nicotinic acid. *J. Invest. Dermatol.* 126, 2637–2646. doi: 10.1038/sj.jid.5700586

Manku, M. S., Horrobin, D. F., Huang, Y. S., and Morse, N. (1983). Fatty acids in plasma and red cell membranes in normal humans. *Lipids* 18, 906–908. doi: 10.1007/BF02534572

McEvoy, J., Baillie, R. A., Zhu, H., Buckley, P., Keshavan, M. S., Nasrallah, H. A., et al. (2013). Lipidomics reveals early metabolic changes in subjects with schizophrenia: effects of atypical antipsychotics. *PLoS One* 8:e68717. doi: 10.1371/journal.pone.0068717

Messamore, E., Hoffman, W. F., and Yao, J. K. (2010). Niacin sensitivity and the arachidonic acid pathway in schizophrenia. *Schizophr. Res.* 122, 248–256. doi: 10.1016/j.schres.2010.03.025

Messamore, E., and Yao, J. K. (2016). Phospholipid, arachidonate and eicosanoid signaling in schizophrenia. *OCL* 23:D112. doi: 10.1051/ocl/2015054

Misiak, B., Stanczykiewicz, B., Laczmanski, L., and Frydecka, D. (2017). Lipid profile disturbances in antipsychotic-naive patients with first-episode non-affective psychosis: a systematic review and meta-analysis. *Schizophr. Res.* 190, 18–27. doi: 10.1016/j.schres.2017.03.031

Morrow, J. D., Awad, J. A., Oates, J. A., and Roberts, L. J. II (1992). Identification of skin as a major site on prostaglandin D2 release following oral administration of niacin in humans. *J. Invest. Dermatol.* 98, 812–815. doi: 10.1111/1523-1747.ep12499963

Morrow, J. D., Parsons, W. G. III, and Roberts, L. J. II (1989). Release of markedly increased quantities of prostaglandin D2 in vivo in humans following the administration of nicotinic acid. *Prostaglandins* 38, 263–274. doi: 10.1016/0090-6980(89)90088-9

Noponen, M., Sanfilipo, M., Samanich, K., Ryer, H., Ko, G., Angrist, B., et al. (1993). Elevated PLA2 activity in schizophrenics and other psychiatric patients. *Biol. Psychiatry* 34, 641–649. doi: 10.1016/0006-3223(93)90157-9

Peters, B. D., Machielsen, M. W., Hoen, W. P., Caan, M. W., Malhotra, A. K., Szeszko, P. R., et al. (2012). Polyunsaturated fatty acid concentration predicts myelin integrity in early-phase psychosis. *Schizophr. Bull.* 39, 830–838. doi: 10.1093/schbul/sbs089

Pettegrew, J. W., Keshavan, M. S., Panchalingam, K., Strychor, S., Kaplan, D. B., Tretta, M. G., et al. (1991). Alterations in brain high-energy phosphate and membrane phospholipid metabolism in first-episode, drug-naive schizophrenics: a pilot study of the dorsal prefrontal cortex by in vivo phosphorus 31 nuclear magnetic resonance spectroscopy. *Arch. Gen. Psychiatry* 48, 563–568.

Prabakaran, S., Swatton, J. E., Ryan, M. M., Huffaker, S. J., Huang, J. J., Griffin, J. L., et al. (2004). Mitochondrial dysfunction in schizophrenia: evidence for compromised brain metabolism and oxidative stress. *Mol. Psychiatry* 9:684.

Puri, B. K., Easton, T., Das, I., Kidane, L., and Richardson, A. J. (2001). The niacin skin flush test in schizophrenia: a replication study. *Int. J. Clin. Pract.* 55, 368–370.

Rapoport, S. I. (2001). In vivo fatty acid incorporation into brain phosholipids in relation to plasma availability, signal transduction and membrane remodeling. *J. Mol. Neurosci.* 16, 243–261. doi: 10.1385/JMN:16:2-3:243

Reddy, R. D., Keshavan, M. S., and Yao, J. K. (2004). Reduced red blood cell membrane essential polyunsaturated fatty acids in first episode schizophrenia at neuroleptic-naive baseline. *Schizophr. Bull.* 30, 901–911. doi: 10.1093/oxfordjournals.schbul.a007140

Ross, B. M., Hudson, C., Erlich, J., Warsh, J. J., and Kish, S. J. (1997). Increased phospholipid breakdown in schizophrenia: evidence for the involvement of a calcium-independent phospholipase A2. *Arch. Gen. Psychiatry* 54, 487–494. doi: 10.1001/archpsyc.1997.01830170113015

Šakić, M., Karlović, D., Vidrih, B., Peitl, V., Crnković, D., and Vrkić, N. (2016). Increased calcium-independent lipoprotein phospholipase A2 but not protein S100 in patients with schizophrenia. *Psychiatr. Danubina* 28, 0–50.

Schaeffer, E. L., Bassi, F., and Gattaz, W. F. (2005). Inhibition of phospholipase A2 activity reduces membrane fluidity in rat hippocampus. *J. Neural. Transm.* 112, 641–647. doi: 10.1007/s00702-005-0301-9

Schmitt, A., Wilczek, K., Blennow, K., Maras, A., Jatzko, A., Petroianu, G., et al. (2004). Altered thalamic membrane phospholipids in schizophrenia: a postmortem study. *Biol. Psychiatry* 56, 41–45. doi: 10.1016/j.biopsych.2004.03.019

Sears, B., and Perry, M. (2015). The role of fatty acids in insulin resistance. *Lipids Health Dis.* 14:121. doi: 10.1186/s12944-015-0123-121

Smesny, S., Kinder, D., Willhardt, I., Rosburg, T., Lasch, J., Berger, G., et al. (2005). Increased calcium-independent phospholipase A2 activity in first but not in multiepisode chronic schizophrenia. *Biol. Psychiatry* 57, 399–405. doi: 10.1016/j.biopsych.2004.11.018

St-Gelais, F., Ménard, C., Congar, P., Trudeau, L. E., and Massicotte, G. (2004). Postsynaptic injection of calcium-independent phospholipase A2 inhibitors selectively increases AMPA receptor-mediated synaptic transmission. *Hippocampus* 14, 319–325. doi: 10.1002/hipo.10176

Stoll, L. L., and Spector, A. A. (1984). Changes in serum influence the fatty acid composition of established cell lines. *In Vitro* 20, 732–738. doi: 10.1007/BF02618879

Taha, A. Y., Cheon, Y., Ma, K., Rapoport, S. I., and Rao, J. S. (2013). Altered fatty acid concentrations in prefrontal cortex of schizophrenic patients. *J. Psychiatr. Res.* 47, 636–643. doi: 10.1016/j.jpsychires.2013.01.016

Tang, Y., Zhou, L., Gunnet, J. W., Wines, P. G., Cryan, E. V., and Demarest, K. T. (2006). Enhancement of arachidonic acid signaling pathway by nicotinic acid receptor HM74A. *Biochem. Biophys. Res. Commun.* 345, 29–37. doi: 10.1016/j.bbrc.2006.04.051

Van der Kemp, W. J. M., Klomp, D. W. J., Kahn, R. S., Luijten, P. R., and Pol, H. H. (2012). A meta-analysis of the polyunsaturated fatty acid composition of erythrocyte membranes in schizophrenia. *Schizophr. Res.* 141, 153–161. doi: 10.1016/j.schres.2012.08.014

Von Schacky, C., and Weber, P. C. (1985). Metabolism and effects on platelet function of the purified eicosapentaenoic and docosahexaenoic acids in humans. *J. Clin. Invest.* 76, 2446–2450. doi: 10.1172/JCI112261

Walsh, T., McClellan, J. M., McCarthy, S. E., Addington, A. M., Pierce, S. B., Cooper, G. M., et al. (2008). Rare structural variants disrupt multiple genes in neurodevelopmental pathways in schizophrenia. *Science* 320, 539–543. doi: 10.1126/science.1155174

Ward, P. E., Sutherland, J., Glen, E. M. T., and Glen, A. I. M. (1998). Niacin skin flush in schizophrenia: a preliminary report. *Schizophr. Res.* 29, 269–274. doi: 10.1016/s0920-9964(97)00100-x

Weinberger, D. R., Berman, K. F., and Illowsky, B. P. (1988). Physiological dysfunction of dorsolateral prefrontal cortex in schizophrenia: III. A new cohort and evidence for a monoaminergic mechanism. *Arch. Gen. Psychiatry* 45, 609–615.

Weinberger, D. R., Berman, K. F., Suddath, R., and Torrey, E. F. (1992). Evidence of dysfunction of a prefrontal-limbic network in schizophrenia: a magnetic resonance imaging and regional cerebral blood flow study of discordant monozygotic twins. *Am. J. Psychiatry* 149, 890–897. doi: 10.1176/ajp.149.7.890

Wu, R. R., Zhao, J. P., Liu, Z. N., Zhai, J. G., Guo, X. F., Guo, W. B., et al. (2006). Effects of typical and atypical antipsychotics on glucose–insulin homeostasis and lipid metabolism in first-episode schizophrenia. *Psychopharmacology* 186, 572–578. doi: 10.1007/s00213-006-0384-5

Xu, F., Fan, W., Wang, W., Tang, W., Yang, F., Zhang, Y., et al. (2019). Effects of omega-3 fatty acids on metabolic syndrome in patients with schizophrenia: a 12-week randomized placebo-controlled trial. *Psychopharmacology* 236, 1273–1279. doi: 10.1007/s00213-018-5136-9

Yang, X., Sun, L., Zhao, A., Hu, X., Qing, Y., Jiang, J., et al. (2017). Serum fatty acid patterns in patients with schizophrenia: a targeted

metabonomics study. *Transl. Psychiatry* 7:e1176. doi: 10.1038/tp.2017.152

Yao, J. K., Stanley, J. A., Reddy, R. D., Keshavan, M. S., and Pettegrew, J. W. (2002). Correlations between peripheral polyunsaturated fatty acid content and in vivo membrane phospholipid metabolites. *Biol. Psychiatry* 52, 823–830. doi: 10.1016/S0006-3223(02)01397-5

Yehuda, S., Rabinovitz, S., Carasso, R. L., and Mostofsky, D. I. (2002). The role of polyunsaturated fatty acids in restoring the aging neuronal membrane. *Neurobiol. Aging* 23, 843–853. doi: 10.1016/S0197-4580(02)00074-X

Zhou, X., Reddy, R., Montrose, D., Haas, G., Keshavan, M., and Yao, J. (2018). S218. A Potential Therapeutic Target of Plasma Free Fatty Acids in First-Episode Antipsychotic-Naïve Patients With Schizophrenia. *Biol. Psychiatry* 83:S432. doi: 10.1016/j.biopsych.2018.02.1110

Zhou, X., Reddy, R., Montrose, D., Haas, G., Keshavan, M. S., and Yao, J. (2017). A potential role of plasma free fatty acids in schizophrenia pathology. *Schizophr. Bull.* 43:S12. doi: 10.1093/schbul/sbx021.033

Conflict of Interest: The authors declare that the research was conducted in the absence of any commercial or financial relationships that could be construed as a potential conflict of interest.

frontiers in Psychiatry

ORIGINAL RESEARCH
published: 12 August 2020
doi: 10.3389/fpsyt.2020.00760

Altered Expression of Glucocorticoid Receptor and Neuron-Specific Enolase mRNA in Peripheral Blood in First-Episode Schizophrenia and Chronic Schizophrenia

*Yong Liu[1], Yamei Tang[2], Cunyan Li[3], Huai Tao[4], Xiudeng Yang[5], Xianghui Zhang[1] and Xuyi Wang[1]**

[1] National Clinical Research Center for Mental Disorders, and Department of Psychaitry, The Second Xiangya Hospital of Central South University, Changsha, China, [2] Department of Laboratory Medicine, The Second Xiangya Hospital, Central South University, Changsha, China, [3] Department of Laboratory Medicine, Hunan Provincial People's Hospital, The First Affiliated Hospital of Hunan Normal University, Changsha, China, [4] Department of Biochemistry and Molecular Biology, Hunan University of Chinese Medicine, Changsha, China, [5] Department of Laboratory Medicine, The First Affiliated Hospital of Shaoyang University, Shaoyang, China

OPEN ACCESS

Edited by:
Pei Jiang,
Jining First People's Hospital, China

Reviewed by:
Junichi Iga,
Ehime University, Japan
Robert C. Smith,
New York University, United States

***Correspondence:**
Xuyi Wang
wangxuyi.@csu.edu.cn

Specialty section:
This article was submitted to Behavioral and Psychiatric Genetics, a section of the journal Frontiers in Psychiatry

Received: *09 April 2019*
Accepted: *17 July 2020*
Published: *12 August 2020*

Citation:
Liu Y, Tang Y, Li C, Tao H, Yang X, Zhang X and Wang X (2020) Altered Expression of Glucocorticoid Receptor and Neuron-Specific Enolase mRNA in Peripheral Blood in First-Episode Schizophrenia and Chronic Schizophrenia. Front. Psychiatry 11:760. doi: 10.3389/fpsyt.2020.00760

Introduction: It is well-known that altered hypothalamus–pituitary–adrenal (HPA) axis process has an important role in the neurodegenerative process in schizophrenia (SZ). However, this neurodegenerative mechanism has not been clarified in SZ. Therefore, the main purpose of this study was to determine HPA axis damage in the first-episode, unmedicated schizophrenia (FES) patients and chronic schizophrenia (CSZ) patients in comparison with healthy controls (HC) by means of quantitative analysis of the peripheral blood mRNA expression of glucocorticoid receptor (GR), GR transcripts containing exons 1B (GR-1B), and neuron specific enolase (NSE) genes and serum cortisol and NSE, a specific serum marker for neuronal damage.

Methods: In the present study, 43 FES patients, 39 CSZ, and 47 HC were included. The peripheral blood mRNA expressions for GR, GR-1B, and NSE genes were determined by real-time quantitative polymerase chain reaction (RT-qPCR). Serum cortisol and NSE were analyzed by electrochemiluminescence immunoassay technique.

Results: Levels of GR mRNA were significantly lower in FES and CSZ than that in HC. The expression of GR-1B mRNA was significantly decreased in CSZ when compared with that in FES. Levels of NSE mRNA were significantly lower in CSZ than that in FES patients or HC patients. CSZ patients showed significantly lower cortisol concentrations than FES and HC patients. FES patients showed significantly higher NSE concentrations than CSZ and HC.

Conclusion: Our findings support that there is disrupted HPA axis system in the SZ and suggest that CSZ patients suffer a greater HPA axis damage than FES patients. Our

research implicated underlying GR mRNA dysregulation in SZ and the potential importance of the functional GR-1B transcription in CSZ.

Keywords: first-episode unmedicated schizophrenia (FES), chronic schizophrenia, glucocorticoid receptor, GR transcripts containing exons 1B (GR-1B), cortisol, neuron-specific enolase, mRNA

INTRODUCTION

Schizophrenia (SZ) is a chronic severe neuropsychiatric disorder affecting almost 1% of the population worldwide (1). The neural diathesis stress model suggests that inappropriate and prolonged psychosocial stress can trigger or worsen the schizophrenic symptoms *via* the hypothalamus–pituitary–adrenal (HPA) axis (2, 3), which is a neuroendocrine system that mediates the stress response by secreting cortisol and maintains homeostasis in various physiological systems (4).

The glucocorticoid receptor (GR) is an important mediator of the maladaptive stress response by binding cortisol (5). Many researches showed decreased expression of total GR mRNA in the temporal cortex, in the dorsolateral prefrontal cortex (DLPFC), hippocampus, and amygdala in SZ and bipolar disorder (6–8). The human GR gene is a region of more than 80 kb within chromosome 5q31–q32, consisting of eight coding exons (exons 2–9) and nine 5′ non-coding first exons (exons A, B, C, D, E, F, H, I, J) (9, 10). Rodents and human GR levels are almost completely mediated at transcriptional level, and each non-coding exon variant is regulated by its own promoter, which is conducive to the tissue specificity of GR expression (10–13).

Indeed, an analysis suggested decreased GR transcripts containing exons 1B (GR-1B) mRNA expression in the DLPFC in SZ cases, and GR-1B mRNA levels accounted for 48% of variance in GR mRNA levels in the DLPFC (5). It is not known whether GR mRNA and protein abnormalities occurring in the orbitofrontal cortex (OFC), in the DLPFC, and/or in other brain regions in psychotic illness may also be found in the peripheral blood and to what extent GR expression patterns are found there.

Neuron-specific enolase (NSE) is an intracytoplasmic protein primarily localized in neurons and neuroendocrine tissue and is not actively secreted (14). Increased NSE in cerebrospinal fluid or blood indicates neuronal destruction or brain damage. NSE has been extensively regarded as a marker for neuronal damage in several mental disorders, such as meningeal hemorrhage, Guillain–Barre syndrome, the Creutzfeldt–Jakob disease, thrombosis (15–17). NSE is also used for auxiliary diagnosis of central nervous system (CNS) tumors and for damage evaluation after traumatic brain injury and cerebral ischemia (17, 18). Other studies found significant rising of NSE in sensory and temporal cortex of schizophrenics and rising of serum NSE concentrations in treatment refractory schizophrenics compared to healthy controls (HC) (19). Egan et al. (20) found first-episode, unmedicated schizophrenia (FES) patients had decreased concentration of NSE in the cerebrospinal fluid (CSF) when compared with those in chronic schizophrenia (CSZ) subjects.

Although altered HPA axis process is related to the pathogenesis of SZ, only limited studies have been focused on the systemic changes of mRNA and protein in FES and CSZ patients and the change of serum concentrations that is easily available in psychiatric patients. Moreover, several studies have produced conflicting results (14, 21–24).

Based on the above referred publications, the purpose of the present study was to determine whether CSZ patients suffer greater HPA axis abnormalities than FES patients. In order to address this aim, the expressions of GR mRNA and GR-1B mRNA in the peripheral blood and the serum concentrations of cortisol and NSE were quantified in FES, CSZ, and HC. We sought to: 1) determine whether expression levels of GR and GR-1B mRNA are altered in FES and/or CSZ cases compared to controls; 2) quantify the expression of serum concentrations of cortisol and NSE in FES and/or CSZ cases relative to controls, and 3) determine if selected GR and GR-1B mRNA are related to protein expression.

MATERIALS AND METHODS

Subjects

43 FES patients, 39 CSZ patients, and 47 HC were recruited from the Department of Psychiatry in the Second Xiangya Hospital, Central South University. All the patients were diagnosed formally with SZ by two senior psychiatrists according to the *Diagnostic and Statistical Manual of Mental Disorders, Fifth Edition* (DSM-V) and evaluated using Positive and Negative Symptom Scale (PANSS) by a senior psychiatrist. There is no history of antipsychotics for CSZ patients for at least one month prior to study enrollment. All of the patients signed an informed consent before participating in this study. Patients were excluded from the study if they met one or more of the following criteria: comorbid mental disorders, other blood disease, a history of traumatic brain injury or intellectual disability, or cardiac–cerebral vascular disease.

Analysis of Cortisol and NSE

Blood samples of participants were collected between 7.00 a.m. and 8.00 a.m. before food consumption. Serum cortisol and NSE were determined using an electrochemiluminescence immunoassay technique on a Cobas600 (Roche Diagnostics, IN, USA).

RT-qPCR

10 ml peripheral venous blood samples were drawn from fasting FES, CSZ patients, and HC in the morning into EDTA tube.

Abbreviations: SZ, schizophrenia; CSZ, chronic schizophrenia; HC, healthy controls; HPA axis, hypothalamus–pituitary–adrenal axis; FES, the first-episode, unmedicated schizophrenia; GR, glucocorticoid receptor; GR-1B, GR transcripts containing exons 1B; NSE, neuron specific enolase; RT-qPCR, real-time quantitative polymerase chain reaction.

Peripheral blood mononuclear cells (PBMCs) were isolated and stored at −80°C until the RNA extraction.

The RNA was extracted from PBMCs in MagNA Pure LC2.0 Automatic extractor with MagNA Pure LC Total Nucleic Acid Isolation Kit–High Performance: automatic RNA extraction using magnetic beads (Roche Diagnostics, IN, USA). Complementary DNA (cDNA) was synthesized using Transcriptor First Strand cDNA Synthesis Kit (Roche Applied Science). Primers sequences were shown in **Table 1**. Each reaction contained 10 μl 2× SYBR Green Mastermix (Roche Applied Science), 1 μl of each primer pair (5 μM), and 5 μl of template cDNA in a 20 μl reaction volume. All reactions were performed with the Roche LightCycler 480 (Roche) using the LightCycler 480 SYBR Green I Master (Roche). The reaction mix was incubated at 95°C (10 min), followed by 40 cycles of 95°C (10 s), 60°C (10 s), and 72°C (20 s). A single fluorescence read was taken at the end of each 72°C step. Melting curve analysis controlled the specificity of the amplification. Reactions were performed in triplicate for each sample. The average value of the replicates for each sample was calculated and expressed as a cycle threshold (Ct). The housekeeper gene, β-actin and GAPDH were used as the internal control. The relative mRNA amounts of target genes were calculated by the $2^{-\Delta\Delta Ct}$ method.

Statistical Analysis

Data were shown as mean ± SD for normal distribution variables (normality determined by Kolmogorov–Smirnov test). SPSS 18.0 software (version 18.0; Chicago, IL, USA) was used for statistical analysis. Categorical data were analyzed using the χ^2 test. Data were analyzed by one-way ANOVA followed by Bonferroni *post hoc* corrected significance levels for comparison between each of the three groups. Spearman correlation coefficients were calculated for associations among variables. $P < 0.05$ was considered statistically significant.

RESULTS

Demographic Characteristics

The demographic data of FES, CSZ patients, and HC were shown in **Table 2**. There were no significant differences in the mean age, gender among three groups ($P > 0.05$). FES and CSZ groups showed no significant between-group differences in PANSS ($P > 0.05$).

TABLE 1 | Primer sequences of the target genes and reference gene.

Gene	Primer sequences	Amplicon length (bp)
GR	F-CAGCTCCTCAACAGCAACAACA	139
	R-GTGCTGTCCTTCCACTGCTC	
GR-1B	F-CCGGGCCCAAATTGATATTCACT	205
	R-GTCTTCGCTGCTTGGAGTCTG	
NSE	F-GAACAGTGAAGCCTTGGAGCT	218
	R-TGGAGACCACAGATAGTCCC	
β-actin	F-TCCCTGGAGAAGAGCTACGA	136
	R-TGAAGGTAGTTTCGTGGATGC	
GAPDH	F-CGAGATCCCTCCAAAATCAA	170
	R-TTCACACCCATGACGAACAT	

TABLE 2 | Demographic data for FES, CSZ patients and HC.

	FES	CSZ	HC	F or χ^2	P
Sex	**N (%)**	**N (%)**	**N (%)**		
Male	27(62.8)	24(61.5%)	29(61.7)		
Female	16(37.2)	15(38.5%)	18(38.3)		
Total	43	39	47	0.017	0.992
Smoking				0.171	0.918
Yes	22	19	25		
No	21	20	22		
Age(Mean ± SD)	22.26 ± 4.49	24.10 ± 4.60	23.32 ± 2.68	2.971	0.055
Male	21.70 ± 3.24	23.34 ± 4.34	22.79 ± 2.73		
Female	23.19 ± 5.73	25.43 ± 3.98	24.11 ± 2.47		
PANSS					
Total	72.57 ± 20.50	72.20 ± 18.70	/	0.156	0.877
Positive	19.79 ± 4.97	18.1 ± 6.01	/	0.311	0.757
Negative	19.33 ± 6.85	21.08 ± 7.10	/	0.823	0.413
General	33.45 ± 9.77	32.90 ± 9.35	/	0.248	0.804

Whole Blood Glucocorticoid Receptor mRNA Expression Levels

The semiquantitative evaluation of mRNA expression of GR genes was performed using real-time PCR, and β-actin was used as the internal control in peripheral blood. ANOVA analysis revealed significant difference among these three groups, for GR (F = 5.152, df = 128, $P = 0.007$). **Figure 1** showed that levels of GR mRNA were significantly lower ($P = 0.008$ and $P = 0.005$,

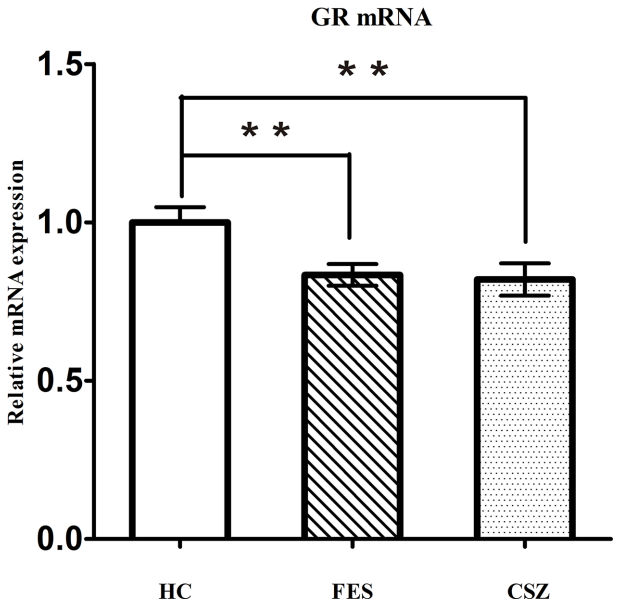

FIGURE 1 | Representative of the relative mRNA expression of GR gene. ** means $P < 0.01$. Error bars denote mean and SD. FES, first-episode schizophrenia; CSZ, chronic schizophrenia; HC, healthy controls; GR, glucocorticoid receptor.

respectively) in FES patients (0.834 ± 0.226) and CSZ patients (0.820 ± 0.318) than that in HC (1.000 ± 0.316).

Human GR-1B mRNA Expression Levels

ANOVA analysis revealed significant difference among these three groups, for GR-1B (F = 3.527, df = 128, $P = 0.032$). **Figure 2** showed that the expression of GR-1B mRNA was significantly decreased ($P = 0.009$) in CSZ patients (0.886 ± 0.319) when compared with that in FES (1.000 ± 0.381).

Human NSE mRNA Expression Levels

ANOVA analysis revealed significant difference among these three groups, for NSE (F = 3.491, df = 128, $P = 0.034$). **Figure 3** showed that levels of NSE mRNA were significantly higher ($P = 0.021$ and $P = 0.024$, respectively) in FES patients (1.005 ± 0.414) and HC patients (1.000 ± 0.381) than that in CSZ (0.806 ± 0.362).

Human Cortisol Expression Levels

ANOVA analysis revealed significant effects among these three groups for cortisol (F = 4.177, df = 128, $P = 0.018$). The serum level of cortisol in the CSZ group (430.51 ± 117.49 nmol/L) was significantly lower than that in the FES group (494.51 ± 95.22 nmol/L) ($P = 0.007$) or in the HC group (482.66 ± 105.69 nmol/L) ($P = 0.025$), while no significant difference was found in serum levels of cortisol between the FES group and HC group ($P = 0.598$) (**Figure 4**).

Human NSE Expression Levels

ANOVA analysis revealed significant effects among these three groups for NSE (F = 5.644, df = 128, $P = 0.004$).

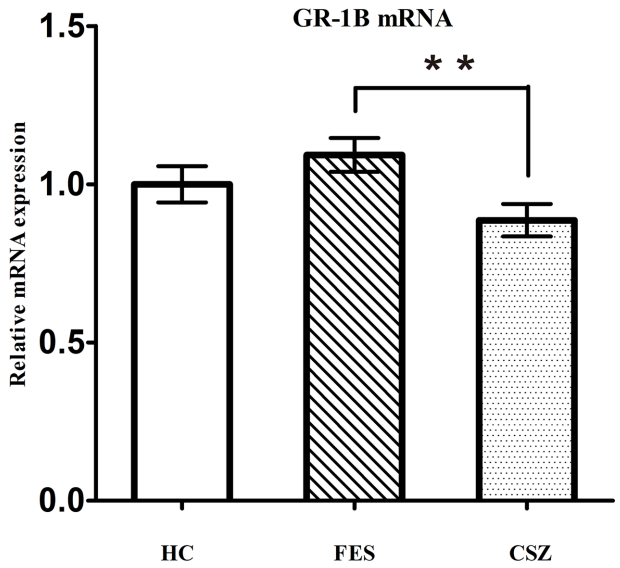

FIGURE 2 | Representative of the relative mRNA expression of GR 1B gene. ** means $P < 0.01$. Error bars denote mean and SD. FES, first-episode schizophrenia; CSZ, chronic schizophrenia; HC, healthy controls; GR 1B, GR transcripts containing exons 1B.

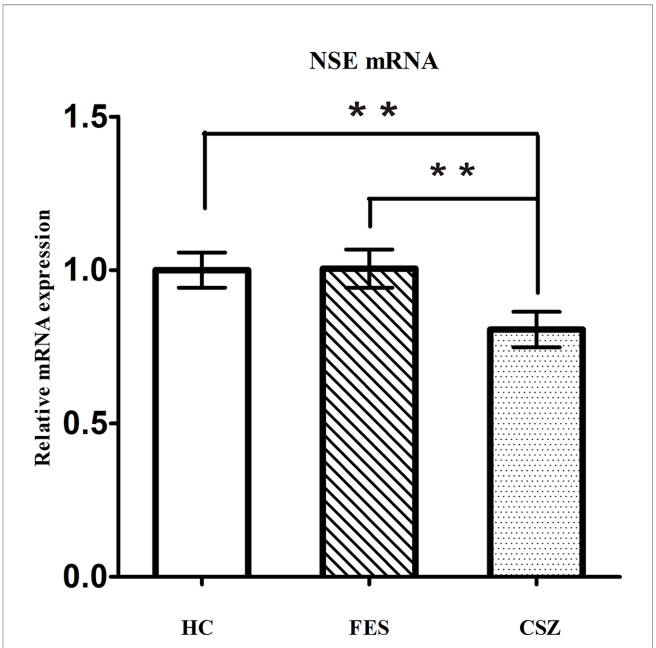

FIGURE 3 | Representative of the relative mRNA expression of NSE gene. ** means $P < 0.01$. Error bars denote mean and SD. FES, first-episode schizophrenia; CSZ, chronic schizophrenia; HC, healthy controls; NSE, neuron-specific enolase.

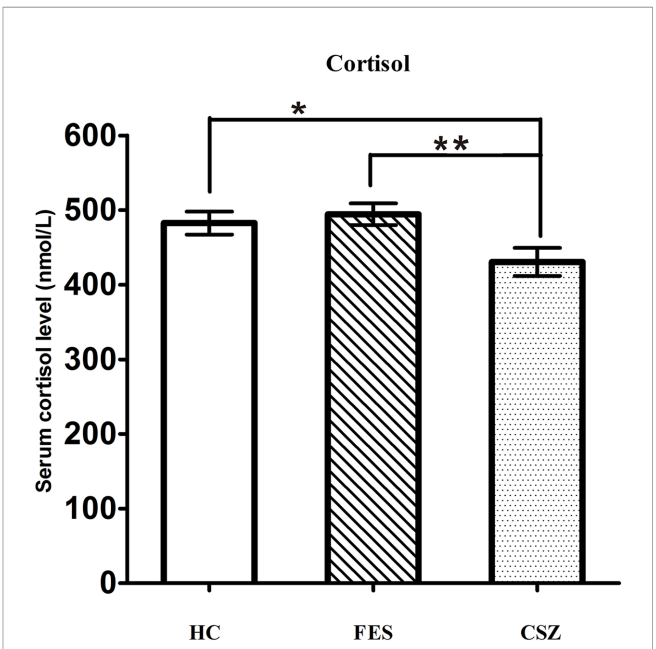

FIGURE 4 | Representative of serum level of cortisol. * means $P < 0.05$, ** means $P < 0.01$. Error bars denote mean and SD. FES, first-episode schizophrenia; CSZ, chronic schizophrenia; HC, healthy controls.

Bonferroni *post hoc* test showed that the serum protein level of NSE in the FES group (13.18 ± 2.76 ng/ml) was significantly increased when compared with the HC group (11.54 + 2.20 ng/ml) ($P = 0.003$) or the CSZ group (11.63 ± 2.73 ng/ml)

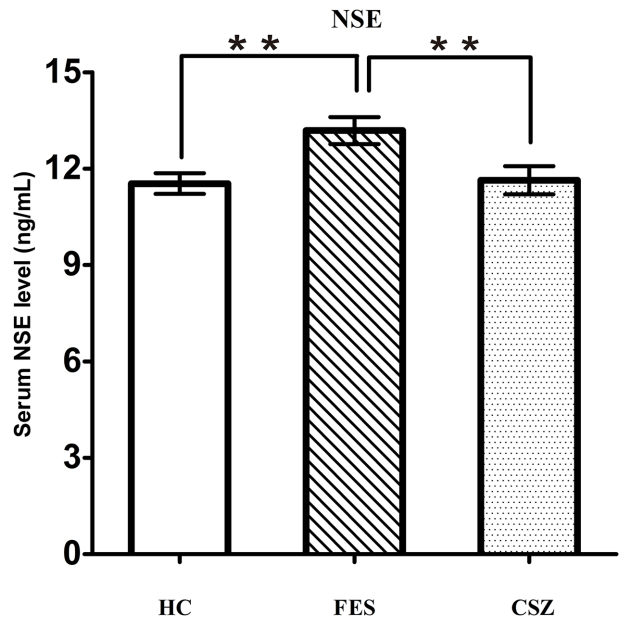

FIGURE 5 | Representative of serum level of NSE. ** means $P < 0.01$. Error bars denote mean and SD. FES, first-episode schizophrenia; CSZ, chronic schizophrenia; HC, healthy controls; NSE, neuron-specific enolase.

($P = 0.007$), while no significant difference was found in serum levels of NSE between the CSZ group and HC group ($P = 0.855$) (**Figure 5**).

The Relationships Between GR and GR-1B mRNA Transcription With NSE mRNA Levels and Serum Cortisol Level Related to Serum NSE Levels

We also assessed the relationships between GR and GR-1B mRNA transcription with NSE mRNA levels and serum cortisol level related to serum NSE levels using Spearman correlations. However, there were no statistically significant correlations of GR and GR-1B mRNA transcripts with NSE mRNA levels or serum cortisol level and serum NSE levels ($P > 0.05$).

DISCUSSION

In this study, we identified abnormal serum levels of cortisol in CSZ patients and NSE protein levels in FES patients. We provide further evidence of altered NSE mRNA in CSZ, GR mRNA in FES and CSZ and decreased GR-1B mRNA in CSZ compared to FES. These abnormalities particularly implicated the HPA axis disorder in SZ and down-regulated GR mRNA in SZ, decreased GR-1B mRNA transcriptional variant in CSZ. Our results also suggest that dysregulation of GR mRNA and protein expression arises in a different SZ stage.

Our results indicated the serum level of cortisol in CSZ patients was significantly lower than that in the FES group or in the HC group ($P < 0.05$). This concurs with other researches (22, 25–28). Rui Peng, et al. (22) reported that atypical antipsychotics could suppress the HPA axis activity by lowering cortisol levels in serum based on the measured levels between before and after treatment. However, another study showed that atypical antipsychotic treatment could contribute to increase serum levels of the cortisol (29). In addition, our findings also showed no significant difference in serum cortisol levels between the FES and HC groups ($P > 0.05$), which is consistent with previous researches (24, 30, 31), while some findings showed that CSZ patients had higher cortisol concentration (22, 29) or no elevated diurnal cortisol level in antipsychotic-naive, putatively at-risk children who present multiple antecedents of SZ or a family history of illness (23). Furthermore, dysfunctional HPA axis activities with reduced cortisol decline have been associated with poorer cognitive performance and memory deficits (25), poorer chronic response to daily stressors (failure to dampen during the day) (26), activation of dysfunctional dopamine pathways, and greater symptom severity (27, 28) in SZ patients. Taken together, these findings imply CSZ patients have more serious HPA axis dysfunctions than FES patients.

In accordance with most reported studies in the dorsolateral prefrontal cortex (DLPFC) (6, 23, 25–28, 32), we found that decreased GR mRNA expression in the peripheral blood was common to FES and CSZ, while decreased GR-1B mRNA expression was present only in CSZ. This may occur because other GR mRNA transcriptions including GR-1C (make up about 66% of total GR mRNA) may dilute the diagnostic effect (5). These results indicate that there is a significant imbalance in the expression of GR mRNA in different schizophrenic cohorts (7) and suggest GR-1B mRNA may be involved in the transcriptional regulatory mechanisms in CSZ governing GR-1B mRNA expression in CSZ. GR-1B mRNA transcript expression can be regulated by tissue-specific transcription factors (33, 34), GR promoter methylation (35), sequence variation in the GR gene promoter region in the human DLPFC (34). However, further research should be taken to verify and clarify the role of GR-1B expression in SZ.

However, our results showed that although GR mRNA was significantly reduced in both FES and CSZ, there were normal serum levels of cortisol in FES but reduced cortisol in CSZ. We hypothesize that feedback-regulated compensatory changes the activity of the *HPA axis* may cause an increased cortisol output in early stages of SZ, but this feedback compensation does not persist as schizophrenia continues over time in CSZ subjects (36). This may occur if GR-1B mRNA has an important role in regulating the expression of cortisol since this was decreased in CSZ and not FES.

In our present study, we only found increased serum NSE level in FES and no differences between CSZ patients and control subjects, while decreased NSE mRNA was found in CSZ patients. These results are in agreement with the study reporting increased serum levels of NSE in FES and normal

serum levels of NSE in SZ (21). We speculate that CSZ patients have more serious neuronal destruction, which contributes to decrease of NSE mRNA in CSZ. The significant increase of serum NSE level in FES may owe to a greater neuronal disorder, which does not necessarily response to an active neurodegenerative process but to the failure of the neuronal energy mechanism that destroys membrane integrity and thus impacts its permeability (16). In addition, we observe neither correlation of NSE mRNA transcriptions with GR and GR-1B mRNA levels nor serum NSE level related to serum cortisol levels, suggesting that the change of NSE concentration has no direct correlation with HPA axis disorder, which may be regulated by other mechanisms.

LIMITATIONS

There are certain limitations in the study. The first limitation is caused by the fact that we did not examine the impact of other possible risk factors on cortisol, such as rhythmic time, the potential role of antipsychotics and alcohol. In addition, the concentrations of these proteins and mRNA transcription before *versus* after antipsychotics treatment were not monitored. Last, this was a pilot study, the sample size in this study might not be large.

CONCLUSION

Our findings of altered mRNA and protein expressions associated with HPA axis are consistent with many previous findings that SZ patients suffer HPA axis abnormalities. Our research also shows that some GR mRNA abnormalities found in the brains of patients with SZ can also be found in the mononuclear cells of living patients and may help specify that a decrease in GR-1B transcript subtype may be particularly important in the later stages of the disease characterized as chronic schizophrenia.

DATA AVAILABILITY STATEMENT

All relevant data is contained within the article. The original contributions presented in the study are included in the article/supplementary material, further inquiries can be directed to the corresponding author/s.

ETHICS STATEMENT

This study was approved by the Ethics Committee of Second Xiangya Hospital, Central South University and was performed in accordance with the Declaration of Helsinki.

AUTHOR CONTRIBUTIONS

XW and YL designed the study. YT and XZ acquired the data, which XY and HT analyzed. CL wrote the article, which all authors reviewed. All authors contributed to the article and approved the submitted version.

FUNDING

This work was supported by the National Natural Science Foundation of China (No. 81571307, 81771448, 81503276); the Hunan Provincial Natural Science Foundation of China (No. 2015JJ4069, 2018JJ2580, 2018JJ3387); the Hunan Provincial Science and Technology Bureau Foundation of China (No. 2017SK50509).

ACKNOWLEDGMENTS

We thank all of the participants for their commitment to this study.

REFERENCES

1. Murray CJ, Lopez AD. Alternative projections of mortality and disability by cause 1990-2020: Global Burden of Disease Study. *Lancet* (1997) 349:1498–504. doi: 10.1016/S0140-6736(96)07492-2
2. Walker E, Kestler L, Bollini A, Hochman KM. Schizophrenia: etiology and course. *Annu Rev Psychol* (2004) 55:401–30. doi: 10.1146/annurev.psych.55.090902.141950
3. Walker EF, Diforio D. Schizophrenia: a neural diathesis-stress model. *Psychol Rev* (1997) 104:667–85. doi: 10.1037/0033-295X.104.4.667
4. Gunnar M, Quevedo K. The neurobiology of stress and development. *Annu Rev Psychol* (2007) 58:145–73. doi: 10.1146/annurev.psych.58.110405.085605
5. Sinclair D, Fullerton JM, Webster MJ, Shannon Weickert C. Glucocorticoid receptor 1B and 1C mRNA transcript alterations in schizophrenia and bipolar disorder, and their possible regulation by GR gene variants. *PLoS One* (2012) 7:e31720. doi: 10.1371/journal.pone.0031720
6. Webster MJ, Knable MB, O'Grady J, Orthmann J, Weickert CS. Regional specificity of brain glucocorticoid receptor mRNA alterations in subjects with schizophrenia and mood disorders. *Mol Psychiatry* (2002) 7:985–94. doi: 10.1038/sj.mp.4001139
7. Sinclair D, Tsai SY, Woon HG, Weickert CS. Abnormal glucocorticoid receptor mRNA and protein isoform expression in the prefrontal cortex in psychiatric illness. *Neuropsychopharmacology* (2011) 36:2698–709. doi: 10.1038/npp.2011.160
8. Perlman WR, Webster MJ, Kleinman JE, Weickert CS. Reduced glucocorticoid and estrogen receptor alpha messenger ribonucleic acid levels in the amygdala of patients with major mental illness. *Biol Psychiatry* (2004) 56:844–52. doi: 10.1016/j.biopsych.2004.09.006
9. Breslin MB, Geng CD, Vedeckis WV. Multiple promoters exist in the human GR gene, one of which is activated by glucocorticoids. *Mol Endocrinol* (2001) 15:1381–95. doi: 10.1210/mend.15.8.0696
10. Turner JD, Muller CP. Structure of the glucocorticoid receptor (NR3C1) gene 5' untranslated region: identification, and tissue distribution of multiple new human exon 1. *J Mol Endocrinol* (2005) 35:283–92. doi: 10.1677/jme.1.01822
11. Pedersen KB, Geng CD, Vedeckis WV. Three mechanisms are involved in glucocorticoid receptor autoregulation in a human T-lymphoblast cell line. *Biochemistry* (2004) 43:10851–8. doi: 10.1021/bi049458u

12. Nunez BS, Vedeckis WV. Characterization of promoter 1B in the human glucocorticoid receptor gene. *Mol Cell Endocrinol* (2002) 189:191–9. doi: 10.1016/S0303-7207(01)00676-1
13. Geng CD, Vedeckis WV. Steroid-responsive sequences in the human glucocorticoid receptor gene 1A promoter. *Mol Endocrinol* (2004) 18:912–24. doi: 10.1210/me.2003-0157
14. Steiner J, Bielau H, Bernstein HG, Bogerts B, Wunderlich MT. Increased cerebrospinal fluid and serum levels of S100B in first-onset schizophrenia are not related to a degenerative release of glial fibrillar acidic protein, myelin basic protein and neurone-specific enolase from glia or neurones. *J Neurol Neurosurg Psychiatry* (2006) 77:1284–7. doi: 10.1136/jnnp.2006.093427
15. Parma AM, Marangos PJ, Goodwin FK. A more sensitive radioimmunoassay for neuron-specific enolase suitable for cerebrospinal fluid determinations. *J Neurochem* (1981) 36:1093–6. doi: 10.1111/j.1471-4159.1981.tb01704.x
16. Marangos PJ, Schmechel DE. Neuron specific enolase, a clinically useful marker for neurons and neuroendocrine cells. *Annu Rev Neurosci* (1987) 10:269–95. doi: 10.1146/annurev.ne.10.030187.001413
17. Vermuyten K, Lowenthal A, Karcher D. Detection of neuron specific enolase concentrations in cerebrospinal fluid from patients with neurological disorders by means of a sensitive enzyme immunoassay. *Clin Chim Acta* (1990) 187:69–78. doi: 10.1016/0009-8981(90)90332-M
18. Isgro MA, Bottoni P, Scatena R. Neuron-Specific Enolase as a Biomarker: Biochemical and Clinical Aspects. *Adv Exp Med Biol* (2015) 867:125–43. doi: 10.1007/978-94-017-7215-0_9
19. Medina-Hernandez V, Ramos-Loyo J, Luquin S, Sanchez LF, Garcia-Estrada J, Navarro-Ruiz A. Increased lipid peroxidation and neuron specific enolase in treatment refractory schizophrenics. *J Psychiatr Res* (2007) 41:652–58. doi: 10.1016/j.jpsychires.2006.02.010
20. Egan MF, el-Mallakh RS, Suddath RL, Lohr JB, Bracha HS, Wyatt RJ. Cerebrospinal fluid and serum levels of neuron-specific enolase in patients with schizophrenia. *Psychiatry Res* (1992) 43:187–95. doi: 10.1016/0165-1781(92)90133-N
21. Schroeter ML, Abdul-Khaliq H, Krebs M, Diefenbacher A, Blasig IE. Neuron-specific enolase is unaltered whereas S100B is elevated in serum of patients with schizophrenia–original research and meta-analysis. *Psychiatry Res* (2009) 167:66–72. doi: 10.1016/j.psychres.2008.01.002
22. Peng R, Li Y. Association among serum cortisol, dehydroepiandrosterone-sulfate levels and psychiatric symptoms in men with chronic schizophrenia. *Compr Psychiatry* (2017) 76:113–8. doi: 10.1016/j.comppsych.2017.03.011
23. Cullen AE, Day FL, Roberts RE, Pariante CM, Laurens KR. Pituitary gland volume and psychosocial stress among children at elevated risk for schizophrenia. *Psychol Med* (2015) 45:3281–92. doi: 10.1017/S0033291715001282
24. Simsek S, Gencoglan S, Yuksel T, Aktas H. Cortisol and ACTH levels in drug-naive adolescents with first-episode early onset schizophrenia. *Asia Pac Psychiatry* (2017) 9:1–3. doi: 10.1111/appy.12264
25. Cullen AE, Zunszain PA, Dickson H, Roberts RE, Fisher HL, Pariante CM, et al. Cortisol awakening response and diurnal cortisol among children at elevated risk for schizophrenia: relationship to psychosocial stress and cognition. *Psychoneuroendocrinology* (2014) 46:1–13. doi: 10.1016/j.psyneuen.2014.03.010
26. Ho RT, Fong TC, Wan AH, Au-Yeung FS, Chen EY, Spiegel D. Associations between diurnal cortisol patterns and lifestyle factors, psychotic symptoms, and neurological deficits: A longitudinal study on patients with chronic schizophrenia. *J Psychiatr Res* (2016) 81:16–22. doi: 10.1016/j.jpsychires.2016.06.014
27. Walder DJ, Walker EF, Lewine RJ. Cognitive functioning, cortisol release, and symptom severity in patients with schizophrenia. *Biol Psychiatry* (2000) 48:1121–32. doi: 10.1016/S0006-3223(00)01052-0
28. Ko YH, Jung SW, Joe SH, Lee CH, Jung HG, Jung IK, et al. Association between serum testosterone levels and the severity of negative symptoms in male patients with chronic schizophrenia. *Psychoneuroendocrinology* (2007) 32:385–91. doi: 10.1016/j.psyneuen.2007.02.002
29. Pandya CD, Crider A, Pillai A. Glucocorticoid regulates parkin expression in mouse frontal cortex: implications in schizophrenia. *Curr Neuropharmacol* (2014) 12:100–7. doi: 10.2174/1570159X11666131120224950
30. Petrikis P, Tigas S, Tzallas AT, Archimandriti DT, Skapinakis P, Mavreas V. Prolactin levels in drug-naive patients with schizophrenia and other psychotic disorders. *Int J Psychiatry Clin Pract* (2016) 20:165–9. doi: 10.1080/13651501.2016.1197274
31. Petrikis P, Tigas S, Tzallas AT, Papadopoulos I, Skapinakis P, Mavreas V. Parameters of glucose and lipid metabolism at the fasted state in drug-naive first-episode patients with psychosis: Evidence for insulin resistance. *Psychiatry Res* (2015) 229:901–4. doi: 10.1016/j.psychres.2015.07.041
32. Yilmaz N, Herken H, Cicek HK, Celik A, Yurekli M, Akyol O. Increased levels of nitric oxide, cortisol and adrenomedullin in patients with chronic schizophrenia. *Med Princ Pract* (2007) 16:137–41. doi: 10.1159/000098367
33. Cao-Lei L, Leija SC, Kumsta R, Wust S, Meyer J, Turner JD, et al. Transcriptional control of the human glucocorticoid receptor: identification and analysis of alternative promoter regions. *Hum Genet* (2011) 129:533–43. doi: 10.1007/s00439-011-0949-1
34. Turner JD, Schote AB, Macedo JA, Pelascini LP, Muller CP. Tissue specific glucocorticoid receptor expression, a role for alternative first exon usage? *Biochem Pharmacol* (2006) 72:1529–37. doi: 10.1016/j.bcp.2006.07.005
35. Labonte B, Yerko V, Gross J, Mechawar N, Meaney MJ, Szyf M, et al. Differential glucocorticoid receptor exon 1(B), 1(C), and 1(H) expression and methylation in suicide completers with a history of childhood abuse. *Biol Psychiatry* (2012) 72:41–8. doi: 10.1016/j.biopsych.2012.01.034
36. Walker E, Mittal V, Tessner K. Stress and the hypothalamic pituitary adrenal axis in the developmental course of schizophrenia. *Annu Rev Clin Psychol* (2008) 4:189–216. doi: 10.1146/annurev.clinpsy.4.022007.141248

Conflict of Interest: The authors declare that the research was conducted in the absence of any commercial or financial relationships that could be construed as a potential conflict of interest.

frontiers in Pharmacology

ORIGINAL RESEARCH
published: 08 March 2021
doi: 10.3389/fphar.2021.612083

A Potential Mechanism Underlying the Therapeutic Effects of Progesterone and Allopregnanolone on Ketamine-Induced Cognitive Deficits

*Ting Cao[1,2†], MiMi Tang[3,4†], Pei Jiang[5], BiKui Zhang[1,2], XiangXin Wu[1,2], Qian Chen[1,2], CuiRong Zeng[1,2], NaNa Li[1,2], ShuangYang Zhang[1,2] and HuaLin Cai[1,2]**

[1]Department of Pharmacy, Second Xiangya Hospital, Central South University, Changsha, China, [2]Institute of Clinical Pharmacy, Second Xiangya Hospital, Central South University, Changsha, China, [3]Department of Pharmacy, Xiangya Hospital of Central South University, Changsha, China, [4]Institute of Hospital Pharmacy, Xiangya Hospital, Central South University, Changsha, China, [5]Institute of Clinical Pharmacology, Jining First People's Hospital, Jining Medical University, Jining, China

OPEN ACCESS

Edited by:
Damiana Leo,
University of Mons, Belgium

Reviewed by:
Ilya Sukhanov,
Pavlov First Saint Petersburg State Medical University, Russia
Dr. Vinod Tiwari,
Indian Institute of Technology (BHU), India

***Correspondence:**
HuaLin Cai
hualincai@csu.edu.cn

†These authors have contributed equally to this work

Specialty section:
This article was submitted to Neuropharmacology, a section of the journal Frontiers in Pharmacology

Received: 30 September 2020
Accepted: 29 January 2021
Published: 08 March 2021

Citation:
Cao T, Tang M, Jiang P, Zhang B, Wu X, Chen Q, Zeng C, Li N, Zhang S and Cai H (2021) A Potential Mechanism Underlying the Therapeutic Effects of Progesterone and Allopregnanolone on Ketamine-Induced Cognitive Deficits. Front. Pharmacol. 12:612083. doi: 10.3389/fphar.2021.612083

Ketamine exposure can model cognitive deficits associated with schizophrenia. Progesterone (PROG) and its active metabolite allopregnanolone (ALLO) have neuroprotective effects and the pathway involving progesterone receptor membrane component 1 (PGRMC1), epidermal growth factor receptor (EGFR), glucagon-like peptide-1 receptor (GLP-1R), phosphatidylinositol 3 kinase (PI3K), and protein kinase B (Akt) appears to play a key role in their neuroprotection. The present study aimed to investigate the effects of PROG (8,16 mg kg^{-1}) and ALLO (8,16 mg kg^{-1}) on the reversal of cognitive deficits induced by ketamine (30 mg kg^{-1}) via the PGRMC1 pathway in rat brains, including hippocampus and prefrontal cortex (PFC). Cognitive performance was evaluated by Morris water maze (MWM) test. Western blot and real-time quantitative polymerase chain reaction were utilized to assess the expression changes of protein and mRNA. Additionally, concentrations of PROG and ALLO in plasma, hippocampus and PFC were measured by a liquid chromatography-tandem mass spectrometry method. We demonstrated that PROG or ALLO could reverse the impaired spatial learning and memory abilities induced by ketamine, accompanied with the upregulation of PGRMC1/EGFR/GLP-1R/PI3K/Akt pathway. Additionally, the coadministration of AG205 abolished their neuroprotective effects and induced cognitive deficits similar with ketamine. More importantly, PROG concentrations were markedly elevated in PROG-treated groups in hippocampus, PFC and plasma, so as for ALLO concentrations in ALLO-treated groups. Interestingly, ALLO (16 mg kg^{-1}) significantly increased the levels of PROG. These findings suggest that PROG can exert its neuroprotective effects via activating the PGRMC1/EGFR/GLP-1R/PI3K/Akt pathway in the brain, whereas ALLO also restores cognitive deficits partially via increasing the level of PROG in the brain to activate the PGRMC1 pathway.

Keywords: cognitive deficits, neuroprotection, PGRMC1 signaling, progesterone, allopregnanolone, ketamine

INTRODUCTION

Cognitive deficits have been recognized as a core feature of first-episode and drug-naive schizophrenia patients (Aas et al., 2014; Chu et al., 2019). Evidence indicates that cognitive symptoms in schizophrenia involve alterations of the function of hippocampus (Driesen et al., 2008) and prefrontal cortex (PFC) (Blot et al., 2015), particularly during working memory tasks (Song et al., 2018). Cognitive deficits can strongly predict long-term functional disability in schizophrenia patients, but current antipsychotic treatments lack efficacy for improving cognition in patients (Hill et al., 2010). New adjunctive procognitive drugs are urgently needed and are pivotal for achieving robust cognitive and functional improvement in schizophrenia. Evidence supports that antagonists of NMDA receptors such as PCP, ketamine or MK801 can produce cognitive deficits manifested as relevant to schizophrenia along with certain pathological disturbances seen in the illness (Neill et al., 2010).

Increasing evidence suggests that neurosteroids have neuroprotective properties on the central nervous system (Rajagopal et al., 2018). Previous studies have shown that lack of steroid hormones has an important role in the development of neurological diseases including schizophrenia (Moore et al., 2013), Parkinson's disease (Nezhadi et al., 2016). It has been demonstrated that the neurosteroids progesterone (PROG) and allopregnanolone (ALLO) exert several functional effects in the brain, such as neuroprotection against some nervous system diseases, including traumatic brain injury (TBI) (Si et al., 2013) and spinal cord injury (Cooke et al., 2013) and schizophrenia-related cognitive dysfunction (Cai et al., 2018a). The underlying mechanisms and the targets of their neuroprotective effects have not been elucidated. As the major active metabolite of PROG, ALLO has been shown to have neuroprotective properties both *in vitro* (Frank and Sagratella, 2000) and *in vivo* (Morali et al., 2011). The prevailing view holds that PROG exerts its neuroprotective effects through multiple receptors: classical progesterone receptors (Pgr), PGRMC1, membrane progesterone receptors (mPR), and $GABA_A$ receptors after conversion to ALLO (Cooke et al., 2013; Guennoun et al., 2015).

Progesterone receptor membrane component 1 (PGRMC1), also called 25-Dx, is a multiprotein complex highly expressed in the brain, especially in the hippocampus (Rohe et al., 2009). One of the appealing features of PGRMC1 is its high affinity for PROG and other steroids, which can promote cell survival and damage resistance (Losel et al., 2008). Accumulating evidence supports that PGRMC1 has unique effects in mediating the effects of PROG in preventing apoptosis and promoting cell proliferation and survival (Liu et al., 2009; Peluso et al., 2009). Specifically, it has been demonstrated that increased proliferation induced by PROG in neuroprogenitor cells from the adult rat hippocampus is mediated through PGRMC1 since these cells lack Pgr and that proliferation is inhibited after treatment with PGRMC1 siRNA (Liu et al., 2009). Likewise, treatment with PROG after spinal cord injury can upregulate PGRMC1 without affecting Pgr expression, and this neuroprotective role of PROG through PGRMC1 can also occur in the brain following TBI (Guennoun et al., 2008).

The PI3K/Akt signaling pathway is known to be pivotal for cell survival and the maintenance of several neuronal functions, such as memory formation and potentiation (Zhou et al., 2014). Under certain conditions, the PI3K/Akt pathway can be activated to exert its neuroprotective function by phosphorylating a battery of protein substrates, including Nuclear factor erythroid-2-related factor 2 (Nrf2), caspase-3/9, cAMP response element-binding protein (CREB) and brain-derived neurotrophic factor (BDNF). It is notable that PGRMC1 is able to activate intracellular Akt signaling in cancer (Hand and Craven, 2003) through the epidermal growth factor receptor (EGFR) tyrosine kinase (Aizen and Thomas, 2015), the typical trafficking target for PGRMC1. Moreover, increased PGRMC1-to-Akt activation could increase survival signaling in ER (Estrogen receptor)-negative tumors (Craven, 2008). A recent study reported that the knockdown of PGRMC1 and AG205 treatment both potentiated insulin-mediated phosphorylation of the IR signaling mediator Akt (Hampton et al., 2018).

Cogent evidence has revealed that the PI3K/Akt pathway is a putative downstream signaling pathway regulated by EGFR (MacDonald et al., 2003) and GLP-1R to elicit multiple biological responses, especially cognitive function (Zhu et al., 2016; Xie et al., 2018). Intriguingly, PGRMC1 co-precipitates and co-localizes with EGFR in cytoplasmic vesicles in cells (Ahmed et al., 2010) and also serves as a novel component of the liganded GLP-1R complex (Zhang et al., 2014). Therefore, it was likely that PGRMC1 dually regulates the PI3K/Akt signaling pathway by combining with GLP-1R and EGFR.

Taken together, the present study aimed to figure out 1) whether the PGRMC1/EGFR/GLP-1R/PI3K/Akt pathway underlies the mechanism of the neuroprotective effect of PROG against ketamine-induced cognitive dysfunction and 2) how ALLO exerts its neuroprotective function in the ketamine-induced model. The mechanisms of the potential effects were validated via AG205, a specific inhibitor of PGRMC1.

MATERIALS AND METHODS

Animals

To avoid possible influence of cyclic, systemic PROG fluctuation caused by estrous cycle (Grassi et al., 2011; Di Mauro et al., 2015), only male Sprague–Dawley rats were used in our study. Rats weighting between 150 and 200 g (approximately 5 weeks old) were purchased from Hunan Slack Jingda Experimental Animal Co., Ltd. (Changsha, Hunan). In experiment 1 and 2, 18 rats (n = 3/group) were used to assess the effect of PROG and ALLO on PGRMC1 expression in basal conditions. In experiment 3, 12 rats (n = 6/group) were used for the validation of the inhibitory effects of AG205 on PGRMC1. In experiment 4, a total of 49 rats were used for exploring the potential mechanism underneath the therapeutic effects of PROG and ALLO against ketamine-induced cognitive deficits.

All rats were housed with free access to food and water, under the conditions of a light-dark cycle (12 h/12 h), humidity at 45–50%, and room temperature (24–25°C). The animal housing conditions were set as follows: home cage size at

470 mm × 312 mm × 260 mm (length×width×height), three rats per cage, poplar sawdust bedding. The water bottle was fulfilled with purified water daily. The beddings were changed and cages were cleaned and disinfected every 2 days. All rats were acclimatized for 1 week before experimentation. The animal research protocol was approved by the local Ethics Committee of the Second Xiangya Hospital of Central South University (Approval No. 2020008). All efforts were made to reduce animal suffering and the number of animals used.

Chemicals and Reagents

2-Hydroxypropyl β–cyclodextrin was purchased from Sigma-Aldrich Inc. (St. Louis, MO, United States). HPLC grade acetonitrile (ACN), methanol and methyl tert-butyl ether (MTBE) were supplied by Merck KGaA (Darmstadt, Germany), and 2-propanol (IPA) was provided by Anaqua Chemical Supply Inc. (Wilmington, DE, United States). PROG and ALLO standards were purchased from Sigma-Aldrich (Shanghai, China) and Steraloids Inc. (Wilton, NH, United States), respectively. AG205 (purity ≥ 97.5%) was synthesized by Jining Drug Research and Development Center. PROG (purity ≥ 99.5%) and ALLO (purity ≥ 99.0%) were obtained from Wuhan Chemduro Pharm Co., Ltd. Injectable ketamine was acquired from the Second Xiangya Hospital of Central South University. Based on most preclinical studies (Kumon et al., 2000; Wali et al., 2014; Andrabi et al., 2017), PROG or ALLO at 8 mg kg^{-1} or 16 mg kg^{-1} was mostly adopted and further proved to exert neuroprotective effects in rats with brain injury. The dose used for the PROG and ALLO treatments was based on previous results suggesting that 8 and 16 mg kg^{-1} of PROG and ALLO were optimal for facilitating recovery of cognitive outcome in CNS impairment (Goss et al., 2003; Djebaili et al., 2004; Morali et al., 2011). Moreover, we chose five-day regime with one injection per day based on the two considerations: 1) good cognitive and sensory recovery could be obtained when 5 days of post-injury neurosteroid injections are provided (Goss et al., 2003; Djebaili et al., 2004) and 2) five-day administration was employed in building the animal model of ketamine-induced cognitive deficits and the treatment with neurosteroids should be conducted accordingly.

Enzyme activity assay kits for superoxide dismutase (SOD), catalase (CAT) and glutathione peroxidase (GSH-Px) were purchased from Nanjing Jiancheng Bioengineering Institute. The Pentobarbital sodium solutions used for surgical procedures were purchased as commercial preparations for veterinary use.

Preparation of Drug Solution

Five ampoules of ketamine injection (0.1 g/2 ml) were diluted with an additional volume of 100 ml of 0.9% saline water to achieve a final concentration of 4.5 mg ml^{-1}. PROG (8 mg ml^{-1}), ALLO (8 mg ml^{-1}) and AG205 (7.3 mg ml^{-1}) were initially dissolved in 5% (v/v) ethanol and then further diluted in 0.9% saline water containing 22.5% 2-hydroxypropyl β–cyclodextrin to obtain the final concentration. All the solutions were injected intraperitoneally. Due to lack of evidence in application of AG205 in animal models, we calculated the AG205 dose converted from PROG according to their molecular docking score binding to PGRMC1 (Detailed information of the calculation process is illustrated in **Supplementary Tables S1–S3**).

Experimental Schedule

In experiment 1 (**Supplementary Figure S1i**) and 2 (**Supplementary Figure S1ii**), rats were randomly assigned to vehicle- and PROG- or ALLO-treated groups. The vehicle-treated animals received 0.9% saline water containing 22.5% 2-hydroxypropyl β–cyclodextrin and the PROG- or ALLO-treated groups received PROG (8 or 16 mg kg^{-1}) or ALLO (8 or 16 mg kg^{-1}) daily for five consecutive days. In experiment 3 (**Supplementary Figure S1iii**), animals were randomly assigned to vehicle and AG205-treated groups. Intraperitoneal injection of AG205 (7.3 mg kg^{-1}) was conducted daily for five consecutive days. Before sacrificing, a five-day MWM task was carried out to evaluate the learning ability and spatial memory of rats, including a four-day hidden platform trial and probe trial on the fifth day. In experiment 4 (**Figure 1A**), the whole cohort was divided in two main groups, referred to normal control (NC) group (n = 7) and ketamine-exposed rats (Ket, n = 42). Firstly, in order to mimic schizophrenia-like cognitive deficits in rats, ketamine was given intraperitoneally daily at a dose of 30 mg kg^{-1} for five consecutive days (Day 1–Day 5). Subsequently, MWM task (Day 5–Day 11) was utilized to test spatial memory and learning ability to further evaluated the effects of ketamine on cognitive function. Ketamine-exposed rats were randomly assigned to six groups (n = 7, each group) with different treatments: 1) vehicle; 2) PROG (8 mg kg^{-1}); 3) PROG (16 mg kg^{-1}); 4) ALLO (8 mg kg^{-1}); 5) ALLO (16 mg kg^{-1}); and 6) PROG (8 mg kg^{-1})+AG205. They were administered intraperitoneal injection of vehicle (0.9% saline containing 22.5% 2-hydroxypropyl β–cyclodextrin), PROG (8 mg kg^{-1}), PROG (16 mg kg^{-1}), ALLO (8 mg kg^{-1} per day), ALLO (16 mg kg^{-1}), PROG (8 mg kg^{-1})+AG205 (7.3 mg kg^{-1}) daily for five consecutive days (Day 11–Day 16). Before sacrificing, the MWM task were carried out from day 16 to day 20. All rats were fasted for 12 h before sacrifice. The rats were anesthetized with 2% pentobarbital sodium solution (0.2 ml/100 g), and tissue samples from the PFC and hippocampus were collected and frozen immediately in liquid nitrogen. Blood was collected from the truncal vessel in EDTA anticoagulation vacuum tubes. The plasma was centrifuged at 4°C, 3,000 rpm for 15 min stored at −80°C before analysis.

Morris Water Maze

In order to evaluate the cognitive performance including learning and spatial memory, we performed the MWM task experiments. The water maze (Gene&I instruments, Beijing, China, model number: CSI-MZ-WM-H) consisted of a circular pool, 1.8 m in diameter, 60 cm in height, and 4.7 mm in thickness surrounded by curtains. There were four different geometric shapes positioned on the four walls as spatial cues. The pool was filled with tap water at a depth of approximately 50 cm, and the water temperature was maintained at 24–25°C. Meanwhile, a sufficient amount of edible black pigment was added to obscure the water. An escape platform was fixed in the center of the target quadrant 1.0 cm underneath the surface of the water. Each rat was

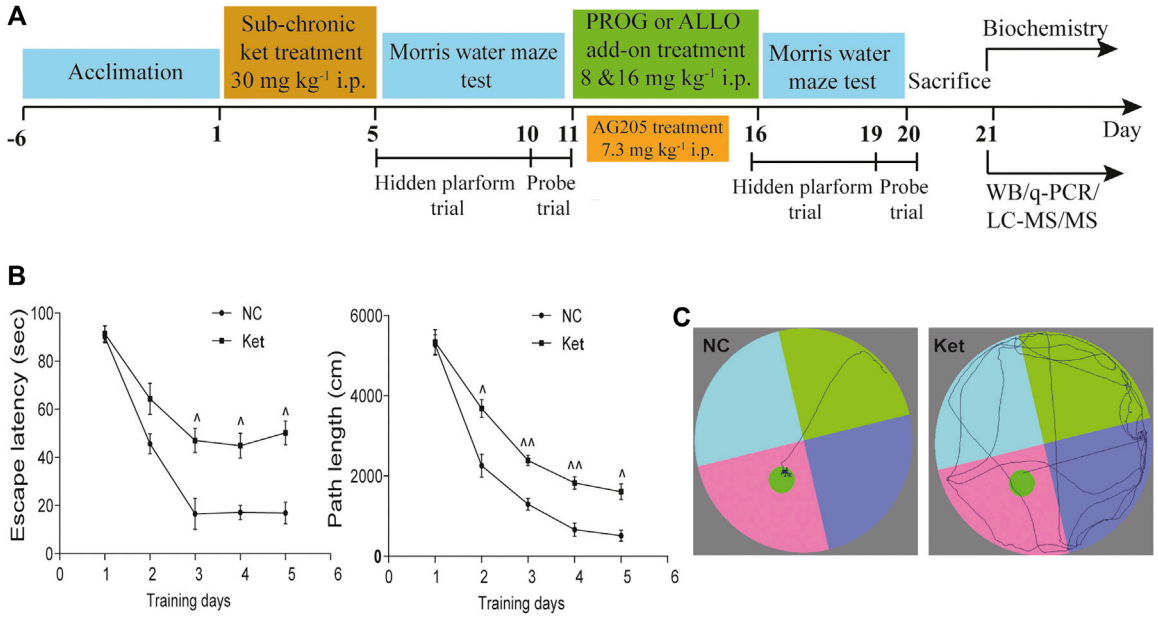

FIGURE 1 | Cognitive performance in the hidden platform trials of MWM test after ketamine exposure. **(A)** A diagram of the time course illustrating when the procedures took place. **(B)** Learning ability manifested as escape latency and path length of ketamine-exposed rats ($n = 42$) vs. NC ($n = 7$). **(C)** The swimming traces of the rats are illustrated (NC vs. Ket). $\hat{p} < 0.05$, $\hat{p} < 0.01$, and $\hat{p} < 0.001$ for Ket vs. NC.

released along the wall into the center of one of three randomly chosen quadrants of the maze. Trials were recorded and captured using a video tracking system (Topscan system 3.0, CleverSys Inc.) connected to a computer.

As described in previous studies (Moosavi et al., 2007; Moosavi et al., 2012; Wang et al., 2014), in the hidden platform trial, the rats were allowed to swim in the maze for no more than 90 s until it located the hidden platform. If a rat did not reach the platform within 90 s, the experimenter would guide it to the platform, where it was kept for 20 s. There was a 30-s interval before the next trial. A total of three training trials were carried out in one day. In the probe trial phase, the platform was removed from the pool. Each rat was placed in the center of the farthest quadrant from the target quadrant, and each rat performed only one trial. The tracking system recorded the swimming path of each rat within 120 s. After the training trials were finished, the rats were dried with towels before being returned to their cages.

Western Blot

Proteins were extracted from the collected hippocampus and PFC tissues and concentrations were measured as described previously (Cai et al., 2015). Approximately 20 μg of protein was loaded onto a 10% or 12% sodium dodecyl sulfate-polyacrylamide gel, transblotted onto PVDF membranes, blocked with 5% nonfat milk in TBST (0.1 M Tris–HCl, pH 8.5, 1.5 M NaCl, 0.5% Tween-20) or 5% BSA at room temperature for an hour and incubated overnight at 4°C with a primary antibody diluted to the appropriate concentration. Primary antibodies, including rabbit anti-PGRMC1 polyclonal antibody (12990-1-AP; 1:1,000), rabbit anti-EGFR polyclonal antibody (18986-1-AP; 1:1,000), rabbit anti-GLP-1R polyclonal antibody (26196-1-AP; 1:1,000), mouse anti-PI3K monoclonal antibody (60225-1-lg; 1:5,000), rabbit anti-Akt polyclonal antibody (10176-2-AP; 1:2,000), rabbit anti-CREB polyclonal antibody (12208-1-AP; 1:1,000), mouse anti-Caspase 9 monoclonal antibody (66169-1-Ig; 1:500) were purchased from Proteintech Group (Wuhan, China). Mouse anti-p-EGFR monoclonal antibody (#2236; 1:1,000), rabbit anti-p-PI3K monoclonal antibody (#4228S; 1:1,000), rabbit anti-p-Akt monoclonal antibody (#4060; 1:1,000) and rabbit anti-Caspase 3 monoclonal antibody (#9662; 1:1,000) were purchased from Cell Signaling Technology, Inc. (Boston, United States). Rabbit anti-BDNF monoclonal antibody (ab108319; 1:1,000) was ordered from Abcam (United Kingdom). After washing with TBST, the membranes were incubated with horseradish peroxidase–conjugated goat anti-rabbit IgG (BA1054; 1:5,000; Boster, Wuhan, China) or goat anti-mouse IgG (BA1050; 1:5,000; Boster, Wuhan, China) for 1 h at room temperature. The film signal was digitally scanned and then quantified using ImageJ software (National Institutes of Health, Bethesda, MD, United States). The ratio to β-actin was calculated, and the mean value of the NC group was set at 1.

Real-Time qPCR and Biochemical Assays

Total RNA from the hippocampus and PFC was isolated with Trizol reagent and then converted to cDNA via the cDNA Synthesis Kit (Life Technologies) according to the manufacturer's protocol. After the quantification of mRNAs, amplification was performed with the following gene-specific primers: Nfr2, forward: 5′-AGTGCAAGGCGGAGGTGA-3′

and reverse: 5′-AGCCCGTTGGTGAACATAG-3'; β-actin, forward: 5′- CATCCTGCGTCTGGACCTGG-3′ and reverse: 5′-TAATGTCACGCACGATTTCC-3'. The amplification reaction consisted of an initial activation at 95°C for 15 min and 40 cycles of denaturation at 95°C followed by a 30-s extension at 60°C. The results are presented as the ratio to β-actin and were normalized to the NC group.

The activity of antioxidant enzymes (CAT, SOD, GSH-Px) was measured using commercial enzyme activity assay kits according to the attached protocols.

Determination of Concentrations of PROG and ALLO

Aliquots of 0.1 g of PFC/hippocampal tissue were homogenized with 1 ml of prechilled methanol using a Bioprep-24 Homogenizer System (speed: 3,500 rpm, time: 30 s, cycles: 3, interval: 30 s). Then, an aliquot of 300 μl of the tissue homogenate or plasma was transferred and mixed with 1,500 μl of methyl tert-butyl ether/methanol (1:1, v/v) extraction solvent, vortexed for 3 min and centrifuged at 20627 *g* for 10 min at 4°C. A volume of 1,500 μl of the resulting supernatant was evaporated to dryness using a centrifugal vacuum concentrator at 4°C. The residue was further resuspended with 100 μl of 2-propanol/acetonitrile/water (21:9:70, v/v/v) solvent mixture. Finally, the concentrations of PROG and ALLO in the tissues and plasma were determined by an LC–MS/MS method as reported elsewhere (Cai et al., 2019). Both lower limit of quantifications (LLOQs) of PROG and ALLO were 0.05 ng/ml for plasma, and were 0.15 ng/g for brain tissue, respectively. For intra-assay, the coefficient of variance (CV) in PROG ranged from 2.4 to 9.6%, whereas CV in ALLO ranged from 3.9 to 5.7%. For inter-assay, the CV in PROG varied between 3.9 and 7.1%, whereas CV in ALLO varied between 4.5 and 8.3%.

Statistical Analysis

The data are presented as the mean ± SD and were analyzed using GraphPad Prism 8.0 (GraphPad Software, San Diego, CA, United States). After ketamine exposure, performance in the hidden platform trials in the MWM was analyzed using repeated measures analysis of variance (RM-ANOVA), with treatment and time as two independent variables, followed by Dunnett's *t*-test for post hoc test. For parameters in the first probe trial, Mann-Whitney *U* test was used to evaluate ketamine induced behavioral changes when building the animal model of cognitive deficits. Differences in the behavioral tests, mRNA expression, protein expression and the enzyme activities in hippocampus across groups were determined using Kruskal-Wallis one-way analysis of variance followed by post hoc Dunn's multiple comparisons test. Statistical significance was considered at $p < 0.05$.

RESULTS

The Effects of PROG, ALLO and AG205 on PGRMC1 Expression in Basal Conditions

As illustrated in **Supplementary Figure S1**, compared with NC group, sub-chronic PROG (16 mg kg^{-1}) treatment markedly downregulated the PGRMC1 expression both in hippocampus ($H = 5.956$, $p = 0.0250$; post hoc $p = 0.0341$) and PFC ($H = 6.252$, $p = 0.0143$; post hoc $p = 0.0270$). However, the inhibitory effects of PROG (8 mg kg^{-1}) and ALLO on PGRMC1 did not approach significance (all $p > 0.05$). As depicted in **Supplementary Figure S1D**, compared with NC group, AG205-treated rats exhibited significantly longer escape latency on the 2nd, third, fourth and fifth day respectively. For escape latency, an effect of treatment [$F(1, 25) = 92.76$, $p < 0.0001$] and an effect of time [$F(4, 25) = 297.4$, $p < 0.0001$], but no interaction [$F(4, 25) = 0.9234$, $p = 0.2632$]. while in the probe trial, AG205 treatment reduced the number of target crossings ($U = 0$, $p = 0.0022$), the permanence time (PT) ($U = 0$, $p = 0.0022$) and PT% in the target quadrant [$U = 0$, $p = 0.0022$]. Western blot experiment was utilized to measure the level of PGRMC1 in rat brain including hippocampus and PFC. As shown in **Supplementary Figure S1C**, AG205 markedly downregulated the expression of PGRMC1 in hippocampus ($U = 0$, $p = 0.0022$) and PFC ($U = 0$, $p = 0.0022$) compared with normal rats, which provided support for the role of AG205 in co-administration with PROG.

Ketamine Exposure Impaired Memory Performance in the MWM Test

First, we explored whether rats exposed to 30 mg kg^{-1} ketamine sub-chronically for 5 days show memory impairment in the MWM test. In the hidden platform phase, compared with NC group, ketamine-exposed rats exhibited significantly prolonged escape latency and path lengths on the third, fourth and fifth day respectively (**Figure 1B**). For escape latency, an effect of treatment [$F(1, 250) = 14.40$, $p = 0.0002$] and an effect of time [$F(4, 250) = 15.22$, $p < 0.0001$] were observed without interaction [$F(4, 250) = 0.9594$, $p = 0.4304$]. Similarly, for path lengths there were an effect of treatment [$F(1, 770) = 16.00$, $p < 0.0001$] and an effect of time [$F(4, 770) = 41.40$, $p < 0.0001$], but no interaction [$F(4, 770) = 0.9234$, $p = 0.4497$] existed. However, in the probe trial, the ketamine-exposed rats showed significantly less target quadrant crosses ($U = 9.00$, $p < 0.0001$, Cohen's $d = 1.363$) and PT in the target area ($U = 61.50$, $p = 0.0080$, Cohen's $d = 0.745$) and a reduced PT% in the target area ($U = 67.50$, $p = 0.0136$, Cohen's $d = 0.686$) (**Table 1**).

In order to avoid the influences of the performance during the first MWM learning in ketamine-treated animals on the results of the second MWM. As shown in **Table 2**, it indicated that there are no differences in escape latency ($H = 0.6189$, $p = 0.9871$, Cohen's $d = 0.744$) and path length ($H = 0.8866$, $p = 0.9712$, Cohen's $d = 0.718$) on the third day among the groups randomly distributed with the animals during first MWM test.

TABLE 1 | Parameters of the probe trial in MWM test (mean ± SD).

Experiments	Groups	Parameters		
		Number of the target crossings[a]	PT in the target quadrant (sec)[b]	Percentage (%) of PT in the target quadrant[c]
[A]Ketamine exposure	NC (n = 7)	8.57 ± 3.11	24.21 ± 5.02	35.68 ± 11.23
	Ket (n = 42)	2.22 ± 1.55$^{\hat{}}$	16.83 ± 6.50$^{\hat{}}$	24.85 ± 8.43
[B]Add-on treatments (n = 7/group)	NC	5.14 ± 1.57	41.70 ± 5.09	35.74 ± 6.73
	Ket	1.71 ± 0.95$^{\hat{}}$	22.46 ± 7.47$^{\hat{}}$	21.02 ± 3.81$^{\hat{}}$
	PROG (8 mg kg^{-1})	4.43 ± 0.79**	36.51 ± 8.57*	35.24 ± 4.77*
	PROG (16 mg kg^{-1})	2.29 ± 0.95	26.70 ± 6.07	27.78 ± 4.17
	ALLO (8 mg kg^{-1})	4.00 ± 0.82*	37.13 ± 8.71*	39.79 ± 8.59**
	ALLO (16 mg kg^{-1})	3.71 ± 1.11*	33.17 ± 9.71*	34.00 ± 9.41*
	PROG (8 mg kg^{1}) +AG205	2.57 ± 0.97$^{\#}$	22.63 ± 8.38$^{\#}$	17.71 ± 8.43$^{\#\#}$

A *Before add-on treatments, ketamine strongly decreased the number of target crossings [*U = 9.00, p < 0.0001, Cohen's d = 1.363*] along with permanence time [*U = 61.50, p = 0.0080, Cohen's d = 0.745*] in the target area and reduced percentage of permanence time in target area [*U = 67.50, p = 0.0136, Cohen's d = 0.686*] in rats, as revealed by Mann-Whitney U test.*
B *The effects of add-on treatments on MWM performance. Kruskal-Wallis test was used for analysis followed by Dunn's multiple comparisons test for post hoc test. Data are expressed as mean ± SD, n = 7 for each group.* $^{\hat{}}$*p < 0.05,* $^{\hat{}}$*p < 0.01, and* $^{\hat{}}$*p < 0.0001 for Ket vs. NC.* **p < 0.05,* ***p < 0.01 and* ****p < 0.0001 for add-on of PROG and ALLO vs. Ket.* $^{\#}$*p < 0.05,* $^{\#\#}$*p < 0.01 and* $^{\#\#\#}$*p < 0.0001 for PROG (8 mg kg^{-1})+AG205 vs. PROG (8 mg kg^{-1}).*
[a]*Number of the target crossings [*H = 29.62, p < 0.0001, Cohen's d = 2.267*].*
[b]*PT in the target quadrant [*H = 22.79, p = 0.0009, Cohen's d = 1.632*].*
[c]*Percentage (%) of PT in the target quadrant [*H = 28.85, p < 0.0001, Cohen's d = 2.185*].*

TABLE 2 | Performance of ketamine-treated rats randomly assigned to each group before add-on treatments (mean ± SD).

[A] Ketamine exposure	Groups	Parameters on the 3rd day during the first MWM learning trial	
		Escape latency (sec)[a]	Path length (cm)[b]
Ket-exposed rats (n = 7/group)	Ket	51.00 ± 13.56	1699.0 ± 283.7
	PROG (8 mg kg^{-1})	49.14 ± 17.68	1574.0 ± 361.6
	PROG (16 mg kg^{-1})	50.00 ± 24.15	1714.0 ± 347.6
	ALLO (8 mg kg^{-1})	50.14 ± 26.44	1570.0 ± 331.1
	ALLO (16 mg kg^{-1})	51.43 ± 22.43	1652.0 ± 398.3
	PROG (8 mg kg^{-1})+AG205	49.86 ± 16.89	1646.0 ± 394.1

Kruskal-Wallis test was used for analysis followed by Dunn's multiple comparisons test for post hoc test. Data are expressed as mean ± SD, n = 7 for each experimental group.
[a]*There are no differences in escape latency [*H = 0.6189, p = 0.9871, Cohen's d = 0.744*].*
[b]*There are no differences in path length [*H = 0.8866, p = 0.9712, Cohen's d = 0.718*] on the third day among the ketamine-treated groups during first MWM test before add-on treatments.*

Neuroprotective Effects of PROG and ALLO on MWM Performance

Cognitive performance was evaluated by MWM task after add-on PROG and ALLO treatments. In the hidden platform trial, path length and escape latency were robustly shortened after PROG and ALLO treatments (**Figures 2A,B**). For path length, an effect of treatment [F (6, 420) = 169.7, p < 0.0001], an effect of time [F (2, 420) = 664.3, p < 0.0001], and an interaction between factors [F (12, 420) = 30.07, p < 0.0001]. For escape latency, an effect of treatment [F (6, 420) = 343.2, p = 0.0002], an effect of time [F (2, 420) = 857.7, p < 0.0001] and an interaction between factors [F (12, 420) = 50.30, p < 0.0001]. Not all parameters related to cognitive function were significantly affected in a dose-dependent manner. In the probe trial, as compared with ketamine group, treatments with PROG (8 mg kg^{-1}) or ALLO (8/16 mg kg^{-1}) led to a significant increase in the number of target crossings (H = 29.62, p < 0.0001, Cohen's d = 2.267), less PT in the target area (H = 22.79, p = 0.0009, Cohen's d = 1.632) and a reduced PT% in the target area (H = 28.85, p < 0.0001, Cohen's d = 2.185) (**Table 1**). In order to reflect the variances between ketamine and NC groups more directly, **Figures 2C,D** indicated that escape latency on the third day (H = 42.49, p < 0.0001, Cohen's d = 5.147) and path lengths on the third day (H = 45.40, p < 0.0001, Cohen's d = 7.786) were shortened by treatments of PROG or ALLO in comparison with ketamine treatment.

Suppression of the PGRMC1 Signaling Pathway by Ketamine and the Reversal Effects of PROG and ALLO

To explore the potential modulatory effects of ketamine, PROG and ALLO add-on treatments on the PGRMC1/EGFR/GLP-1R/PI3K/Akt signaling pathway, the protein expression of the five key factors (PGRMC1, EGFR, GLP-1R, PI3K, Akt) and their phosphorylated forms (p-EGFR, p-PI3K, p-Akt) in the hippocampus and PFC was compared among groups.

In the hippocampus, sub-chronic ketamine treatment significantly downregulated the protein expression of the five

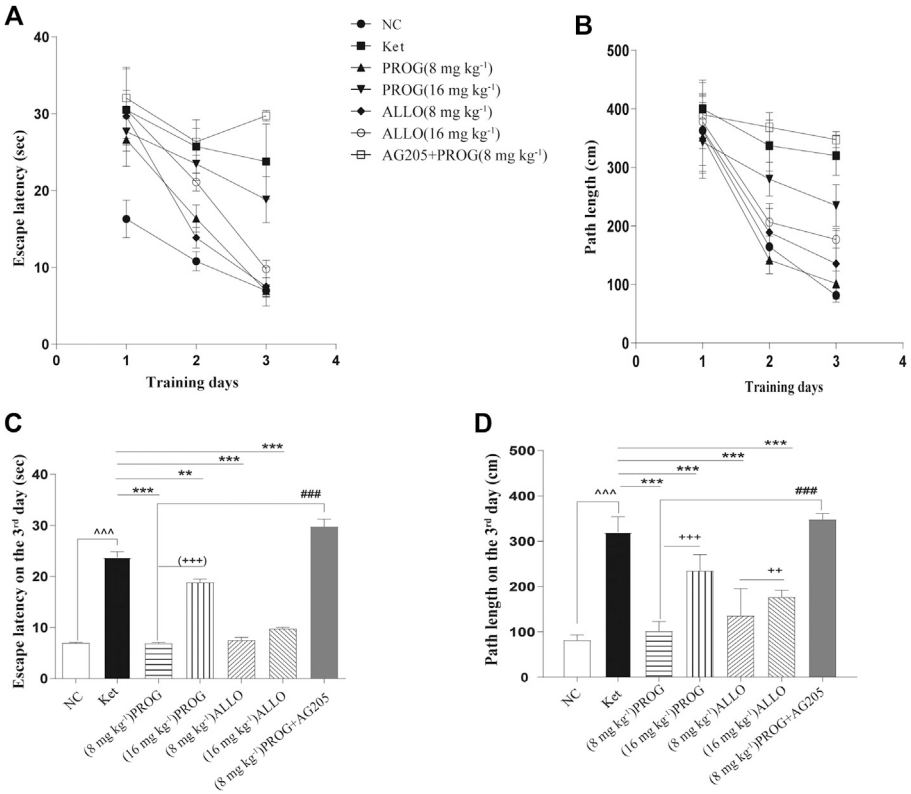

FIGURE 2 | Cognitive performance in the hidden platform trials of MWM test after add-on PROG and ALLO treatments. **(A)** Escape latency **(B)** Path length **(C)** Escape latency on the third day and **(D)** path lengths on the third day were shortened by PROG (all $p < 0.01$) or ALLO treatment (all $p < 0.0001$) in comparison with ketamine treatment. Data are expressed as mean ± SD, $n = 7$ for each experimental group. $^{*}p < 0.05$, $^{**}p < 0.01$ and $^{***}p < 0.001$ for add-on of PROG and ALLO vs. Ket. $^{\#}p < 0.05$, $^{\#\#}p < 0.01$ and $^{\#\#\#}p < 0.001$ for PROG (8 mg kg^{-1})+AG205 vs. PROG (8 mg kg^{-1}). $^{+}p < 0.05$, $^{++}p < 0.01$ and $^{+++}p < 0.001$ for PROG (16 mg kg^{-1}) vs. PROG (8 mg kg^{-1}) and ALLO (16 mg kg^{-1}) vs. ALLO (8 mg kg^{-1}).

key factors (PGRMC1: $H = 38.01$, $p = 0.0002$; post hoc $p = 0.0001$; GLP-1R: $H = 31.91$, $p = 0.0002$; post hoc $p = 0.0003$; EGFR: $H = 26.80$, $p = 0.0002$; post hoc $p = 0.0014$; PI3K: $H = 30.78$, $p < 0.0001$; post hoc $p = 0.0005$; p-EGFR: $H = 32.44$, $p < 0.0001$; post hoc $p = 0.0014$; p-PI3K: $H = 33.76$, $p < 0.0001$, post hoc $p < 0.0001$; p-Akt: $H = 39.09$, $p < 0.0001$; post hoc $p < 0.0001$) without affecting Akt ($p > 0.9999$) compared to NC group (**Figure 3**). Intriguingly, PROG administration did not activate the PGRMC1 signaling pathway in a dose-dependent manner. Only low dose of PROG significantly upregulated the protein expression of PGRMC1 pathway (PGRMC1, $p = 0.0004$; GLP-1R, $p = 0.0214$; EGFR, $p = 0.0046$; PI3K, $p = 0.0298$; *p*-EGFR, $p = 0.0399$; p-PI3K, $p = 0.0159$; p-Akt, $p = 0.0373$) without affecting Akt ($p > 0.9999$) compared to Ket group (**Figure 3**). In contrast, both doses of ALLO administration increased the protein expression of PGRMC1 ($p = 0.0130$, $p = 0.0030$), GLP-1R ($p = 0.0169$, $p = 0.0039$), PI3K ($p = 0.0329$, $p = 0.0237$), p-Akt ($p = 0.0015$, $p = 0.0005$). There was a significant difference in PGRMC1 expression between the low dose and high dose of PROG (PGRMC1, $p = 0.0144$), so as the case for ALLO (PGRMC1, $p = 0.0176$) (**Figure 3A**). Similar with the hippocampus, the synchronous expression of proteins involved in the PGRMC1 signaling pathway also occurred in the PFC, and the results are shown in **Supplementary Figure S2**.

Add-on PROG and ALLO Treatments Alleviated the Modulatory Effects of Ketamine on Downstream Molecules.

To gain insights into the PGRMC1-regulated signaling pathway, the protein expression of downstream cognitive function-related molecules regulated by the PGRMC1 signaling pathway (including CREB, caspase-3/9, their cleaved forms, and BDNF) were assessed by Western blot experiments in the rat hippocampus and PFC after add-on treatments. As shown in **Figures 4A–F**, the hippocampal protein expression of CREB ($H = 39.75$, $p < 0.0001$; post hoc $p = 0.0008$) and truncated BDNF ($H = 44.92$, $p < 0.0001$; post hoc $p < 0.0001$) was significantly reduced and the protein levels of mature BDNF ($H = 42.13$, $p < 0.0001$; post hoc $p = 0.0001$) and the ratio of cleaved caspase-3/9 (including cleaved caspase-3 (17 kDa)/caspase-3 [$H = 44.76$, $p < 0.0001$; post hoc $p < 0.0001$], cleaved caspase-3 (19 kDa)/caspase-3 ($H = 44.80$, $p < 0.0001$; post hoc $p < 0.0001$), and cleaved caspase-9/caspase-9 ($H =$

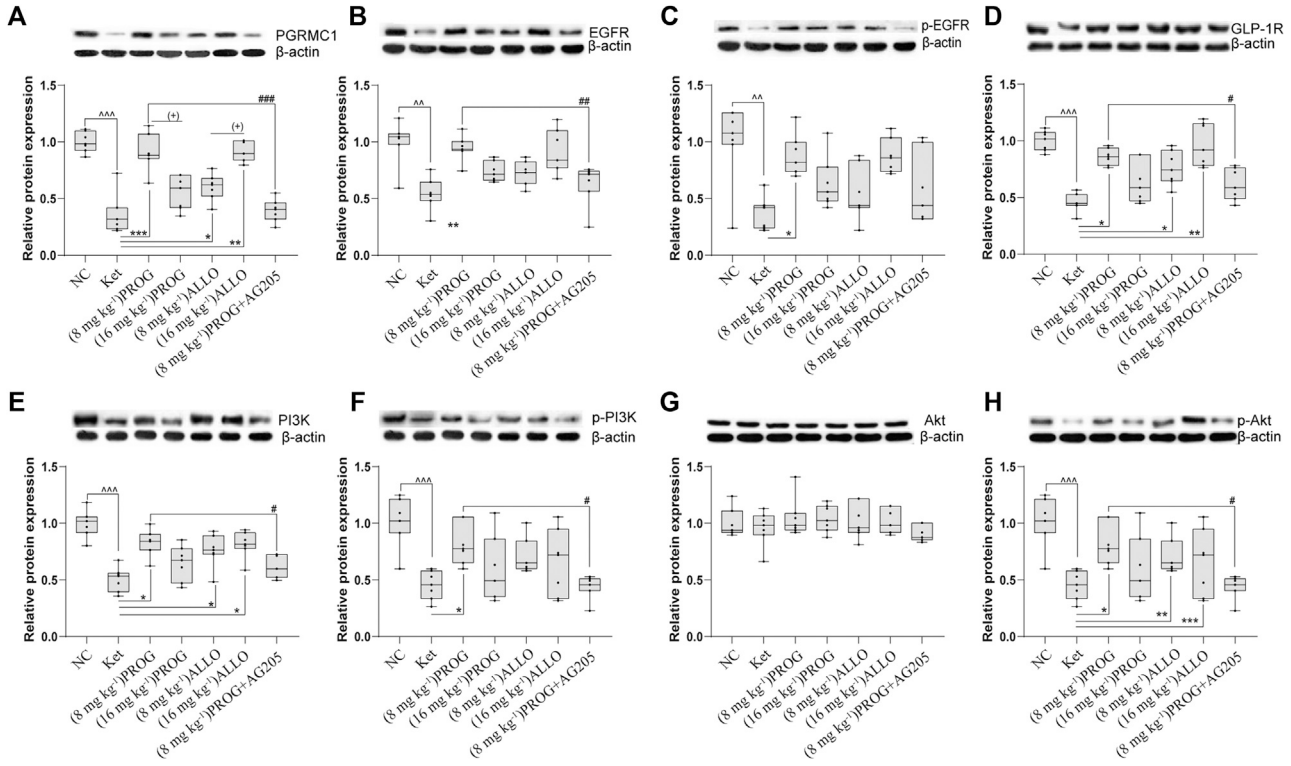

FIGURE 3 | Basal protein expression profile of the PGRMC1/EGFR/GLP-1R/PI3K/Akt pathway in the hippocampus. **(A)** PGRMC1, **(B)** EGFR, **(C)** *p*-EGFR, **(D)** GLP-1R, **(E)** PI3K, **(F)** p-PI3K, **(G)** Akt, **(H)** p-Akt. Data are expressed as mean ± SD, $n = 7$ for each experimental group. $^{\wedge}p < 0.05$, $^{\wedge\wedge}p < 0.01$, and $^{\wedge\wedge\wedge}p < 0.001$ for Ket vs. NC. $^{*}p < 0.05$, $^{**}p < 0.01$ and $^{***}p < 0.001$ for add-on of PROG and ALLO vs. Ket. $^{\#}p < 0.05$, $^{\#\#}p < 0.01$ and $^{\#\#\#}p < 0.001$ for PROG (8 mg kg^{-1})+AG205 vs. PROG (8 mg kg^{-1}). $^{+}p < 0.05$, $^{++}p < 0.01$ and $^{+++}p < 0.001$ for PROG (16 mg kg^{-1}) vs. PROG (8 mg kg^{-1}) and ALLO (16 mg kg^{-1}) vs. ALLO (8 mg kg^{-1}). The relative expression data are presented as the ratio to the β-actin protein level. **Note:** In our study, the prototype protein and its phosphorylated form were separated in one gel simultaneously. Therefore, the loading control images of β-actin are re-used for illustrative purposes in **B** and **C**, **E** and **F**, **G** and **H**.

45.91, $p < 0.0001$; post hoc $p < 0.0001$) were upregulated by ketamine exposure.

PROG and ALLO may regulate hippocampal protein expression in a dose-dependent manner but in a contradictory way. Add-on treatment with PROG at 8 mg kg^{-1} or ALLO at 16 mg kg^{-1} markedly mitigated the increased level of mature BDNF (PROG, $p = 0.0171$; ALLO, $p = 0.0216$) and the ratios of cleaved caspase-3 (PROG, $p = 0.0008$; ALLO, $p = 0.0310$) and cleaved caspase-9 (PROG, $p = 0.0255$; ALLO, $p < 0.0001$) induced by ketamine. Meanwhile, PROG (8 mg kg^{-1}) or ALLO (16 mg kg^{-1}) also ameliorated the decreases in CREB ($p = 0.0176$; $p = 0.0003$) and truncated BDNF ($p = 0.0001$; $p = 0.0144$).

Furthermore, we examined the mRNA expression of Nrf2 and the activity of antioxidant enzymes in the hippocampus and PFC. The quantification of antioxidant enzymes acts as an indirect measure of oxidative stress. As illustrated in **Figures 5A–D**, compared with NC group, ketamine markedly reduced the mRNA expression of Nrf2 ($H = 29.06$, $p < 0.0001$; post hoc $p = 0.0238$), the activity of CAT ($H = 42.91$, $p < 0.0001$; post hoc $p < 0.0001$), GSH-Px ($H = 41.75$, $p < 0.0001$; post hoc $p = 0.0060$) and SOD ($H = 38.71$, $p < 0.0001$; post hoc $p = 0.0425$) in the hippocampus. Only PROG at 8 mg kg^{-1} ameliorated ketamine-induced decreases in Nrf2 mRNA expression ($p = 0.0453$) and CAT ($p < 0.0001$), GSH-Px ($p < 0.0001$), SOD ($p = 0.0006$) activity. Synchronous changes in the PGRMC1 signaling pathway also occurred in the PFC, and the results are shown in **Supplementary Figure S3**.

Involvement of PGRMC1 in the Reversal Effects of PROG on Ketamine-Induced Cognitive Impairment

To confirm the regulation of PROG-mediated neuroprotection by PGRMC1, PROG-treated rats were co-administrated with AG205, which significantly weakened the protective effects of PROG against ketamine-induced cognitive impairment. On one hand, rats treated with the coadministration of AG205 and PROG (8 mg kg^{-1}) exhibited poorer cognitive performance manifested as prolonged escape latencies (an effect of treatment [$F(6, 420) = 343.2$, $p = 0.0002$], an effect of time [$F(2, 420) = 857.7$, $p < 0.0001$] and an interaction between factors [$F(12, 420) = 50.30$, $p < 0.0001$] in the MWM test compared with those of the PROG monotherapy group (**Figure 2**). On the other hand, the addition of AG205 abolished the neuroprotective effect of 8 mg kg^{-1} PROG against the ketamine-induced downregulated expression of the PGRMC1 signaling pathway as well as the changes in

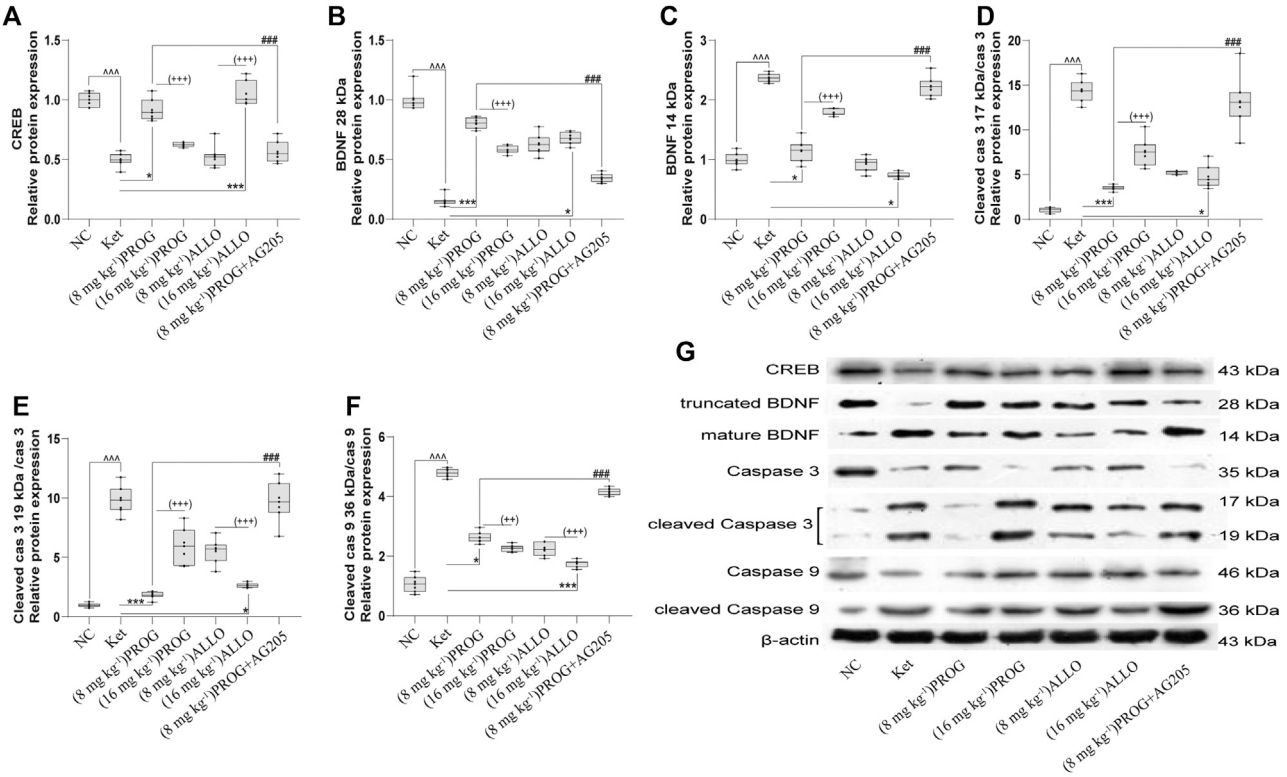

FIGURE 4 | Basal CREB/BDNF/caspase-3/9 protein expression in the hippocampus. **(A)** CREB, **(B)** truncated BDNF, **(C)** mature BDNF, **(D)** cleaved caspase-3 (17 kDa)/caspase-3, **(E)** cleaved caspase-3 (19 kDa)/caspase-3, **(F)** cleaved caspase-9/caspase-9. A representative blot is shown in **(G)**. Data are expressed as mean ± SD, $n = 7$ for each experimental group. $\hat{p} < 0.05$, $\hat{p} < 0.01$, and $\hat{p} < 0.001$ for Ket vs. NC. $^{*}p < 0.05$, $^{**}p < 0.01$ and $^{***}p < 0.001$ for add-on of PROG and ALLO vs. Ket. $^{\#}p < 0.05$, $^{\#\#}p < 0.01$ and $^{\#\#\#}p < 0.001$ for PROG (8 mg kg^{-1})+AG205 vs. PROG (8 mg kg^{-1}). $^{+}p < 0.05$, $^{++}p < 0.01$ and $^{+++}p < 0.001$ for PROG (16 mg kg^{-1}) vs. PROG (8 mg kg^{-1}) and ALLO (16 mg kg^{-1}) vs. ALLO (8 mg kg^{-1}). The relative expression data are presented as the ratio to the β-actin protein level.

downstream molecules [AG205+PROG (8 mg kg^{-1}) *vs* PROG (8 mg kg^{-1}), all $p < 0.05$, **Figures 3–5**].

Concentrations of PROG and ALLO in the Plasma, Hippocampus and PFC after Different Treatments

To investigate the relationship between the doses and therapeutic effects of PROG and ALLO, we analyzed the concentrations of PROG and ALLO in these tissues as depicted in **Figure 5**. Compared with NC group, ketamine-treated rats did not exhibit higher concentrations of PROG and ALLO in hippocampus, PFC and plasma. When compared to ketamine group, add-on treatments of PROG at 8 and16 mg kg^{-1} significantly increased the levels of PROG without affecting the levels of ALLO in hippocampus [$H = 41.34$, $p < 0.0001$; post hoc $p = 0.0310$ (PROG at 8 mg kg^{-1}), $p = 0.0007$ (PROG at 16 mg kg^{-1})], PFC [$H = 43.18$, $p < 0.0001$; post hoc $p = 0.0482$ (PROG at 8 mg kg^{-1}), $p = 0.0017$ (PROG at 16 mg kg^{-1})] and plasma [$H = 39.53$, $p < 0.0001$; post hoc $p = 0.0375$ (PROG at 8 mg kg^{-1}), $p = 0.0023$ (PROG at 16 mg kg^{-1})]. As expected, ALLO concentrations in these tissues were markedly elevated in both ALLO treated groups at 8 mg kg^{-1} (all $p < 0.001$) and 16 mg kg^{-1} (all $p < 0.001$) vs. ketamine group. Interestingly, ALLO treatment at 16 mg kg^{-1} also significantly increased the levels of PROG in hippocampus ($p = 0.0100$), PFC ($p = 0.0113$) and plasma ($p = 0.0453$) as compared with ketamine group.

DISCUSSION

Several key findings emerged in the present study. First, in basal conditions, both PROG and AG205 administration showed inhibitory effect on PGRMC1 expression in hippocampus and PFC as well as impaired MWM performance in AG205-treated rats. Second, ketamine significantly impaired hippocampal-dependent memory performance of the rats in the MWM test and downregulated the PGRMC1 pathway. Third, the cognitive impairment induced by ketamine was reversed by PROG and ALLO add-on treatments, and the PGRMC1/EGFR/GLP-1R/PI3K/Akt pathway was upregulated. Fourth, the coadministration of AG205 abolished the efficacy of PROG in the MWM test and offset the regulatory effect of PROG on the abovementioned PGRMC1 signaling pathway. Finally, high dose of ALLO administration led to increased concentrations of PROG in the plasma and brain, and this may be able to explain some of its neuroprotective efficacy.

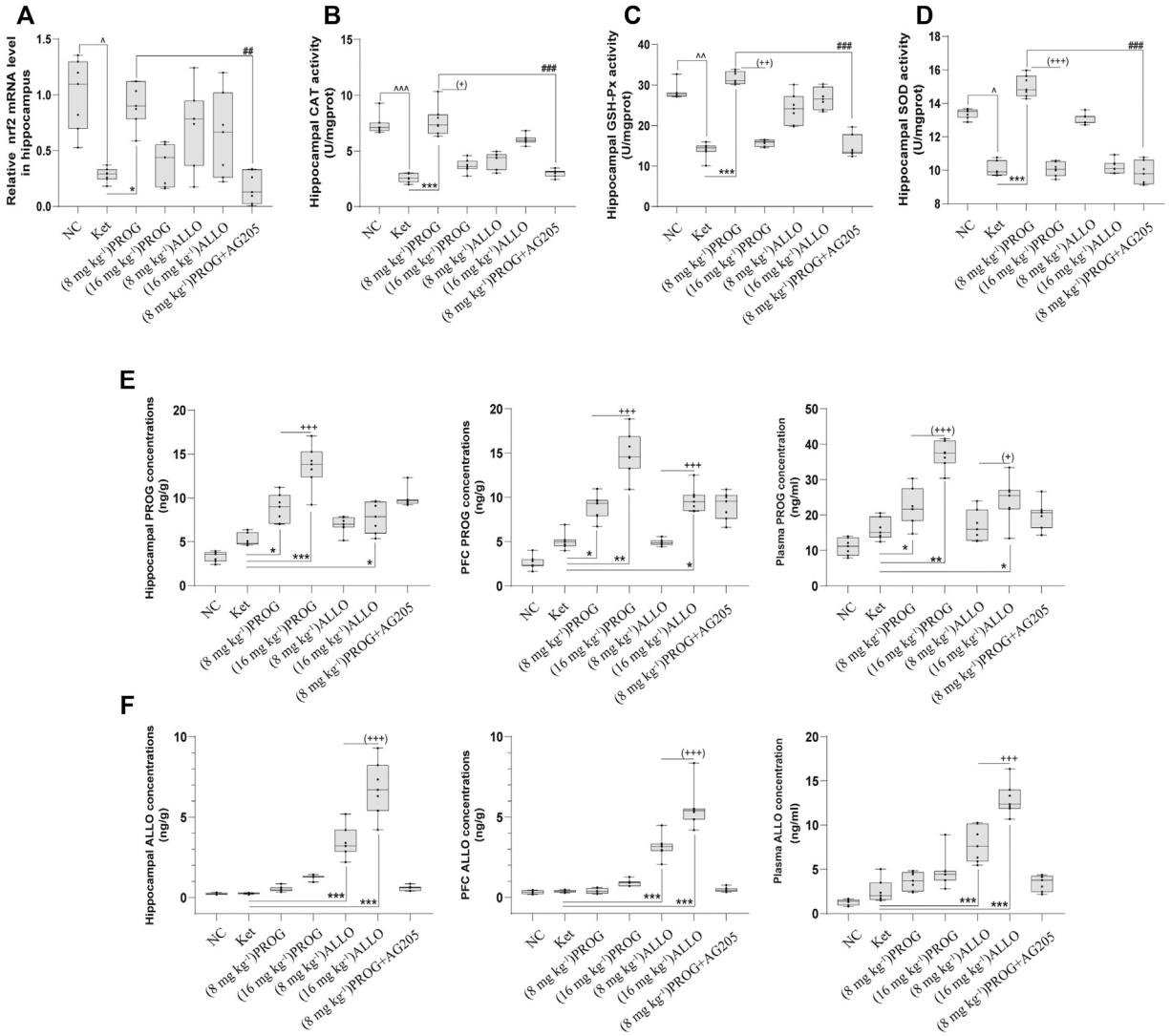

FIGURE 5 | Hippocampal Nrf2 mRNA expression and the enzyme activity of CAT, SOD, GSH-Px and the concentrations of PROG and ALLO in hippocampus, PFC and plasma. **(A)** Nrf2, **(B)** CAT, **(C)** GSH-Px, **(D)** SOD, **(E)** PROG concentrations, **(F)** ALLO concentrations. $^{*}p < 0.05$, $^{**}p < 0.01$ and $^{***}p < 0.001$ for add-on of PROG and ALLO vs. Ket. $^{+}p < 0.05$, $^{++}p < 0.01$ and $^{+++}p < 0.001$ for PROG (16 mg kg^{-1}) *vs* PROG (8 mg kg^{-1}) and ALLO (16 mg kg^{-1}) vs. ALLO (8 mg kg^{-1}).

Effects of PROG, ALLO and AG205 on PGRMC1 Expression in Basal Conditions

In healthy status, overload of exogenous PROG/ALLO administration does appear to impair non-social learning and memory tasks in normal rodents (Johansson et al., 2002; Bychowski and Auger, 2012), which is in accordance with the previous observation that administration of PROG represses PGRMC1 transcription in rats *in vivo*. (Losel et al., 2008; Zhang et al., 2014). However, when ketamine-induced neurotoxicity and resulting suppression of PGRMC1 happen, add-on PROG may switch its role and exert the neuroprotective function via upregulation of PGRMC1 at an appropriate dose. So far, the therapeutic effect of RPOG has not been reported in ketamine-induced neurotoxicity, apart from the combination of estrogen and PROG in ketamine-induced disrupted PPI in rats (Van den Buuse et al., 2015). The discrepancy of PROG actions was possibly due to different basal conditions (healthy vs. injured) before PROG treatment, which warrants further exploration in future studies. More interest has been aroused to explore whether the neuroprotective effect of PROG can be observed when an injury or deficiency is present, as in the case of sub-chronic ketamine administration.

Effects of PROG and ALLO on Cognitive Deficits Induced by Ketamine

Ketamine impairs cognition in both humans and animals (Moosavi et al., 2012; Parwani et al., 2005), which can model

cognitive deficits associated with schizophrenia. It has been reported that cognitive impairment induced by sub-chronic ketamine exposure (30 mg kg^{-1} per day for five consecutive days) remains stable for 21 days (Rushforth et al., 2011). The MWM task was selected based on the extensive literatures (Zheng et al., 2015; Sun et al., 2016) indicating that NMDA receptor antagonists produce impairments in the MWM test.

Consistent with the emerging evidence, the data in our study showed that rats exposed to sub-chronic ketamine for five consecutive days exhibited impaired cognitive performance. It has been previously reported that PROG exerts neuroprotective effects in glutamate toxicity models (Van den Buuse et al., 2015) and improves spatial learning performance in the MWM test after traumatic brain injury (Djebaili et al., 2004; Jones et al., 2005). In the present experiment, we observed that PROG and ALLO were both able to attenuate ketamine-induced cognitive impairment in the MWM test.

PROG and ALLO Reversed the Inhibitory Effects of Ketamine on the PI3K/Akt Pathway and Its Downstream Molecules

It has been reported that decreased activity of the PI3K/Akt pathway can, at least in part, explain the cognitive deficits in schizophrenia (Zheng et al., 2012; Zuo et al., 2016). Based on the fact that the level of Akt is significantly decreased in schizophrenia (Zheng et al., 2012), our present study also revealed the downregulation of the PI3K/Akt pathway in sub-chronic ketamine-exposed rats with cognitive impairment. Preclinical evidence has also revealed that the phosphorylation of Akt, which is crucial for PI3K-mediated memory enhancement via boosting cell survival and protein synthesis, can be elicited by PROG (Singh, 2001; Labombarda et al., 2003). Therefore, it is inferred that an increase in PI3K/Akt may be a contributing mechanism to improvements in spatial learning by PROG. Interestingly, our data showed that both PROG and its active metabolite ALLO increased the expression of the PI3K/Akt signaling pathway.

CREB, as a key transcriptional regulator, participates in multiple critical functions of the brain, including learning and cell survival (Peltier et al., 2007). Akt is capable of activating CREB, which then improves the expression of BDNF in pro-survival signaling (Aguiar et al., 2011). BDNF is thought to be a key regulator of learning and memory, which is involved in the pathogenesis of schizophrenia and is especially related to cognitive deficits (Nieto et al., 2013). Previous studies have suggested that ketamine impairs the learning and memory ability of rats and simultaneously markedly reduces the protein expression of p-Akt, p-CREB and BDNF (28 kDa, also called truncated BDNF) (Zuo et al., 2016). In addition, activated CREB and BDNF can further modulate the transcription process in the cell survival mechanism to ameliorate the neurotoxicity induced by ketamine (Zuo et al., 2016). In accordance with our study, cogent evidence has revealed that PROG (Singh and Su, 2013) and its active metabolite ALLO (Nin et al., 2011) can strengthen cognitive function by upregulating the expression of BDNF. Unlike truncated BDNF, another form of BDNF (14 kDa, called mature BDNF) was markedly downregulated by PROG and ALLO and upregulated by ketamine. Consistently, data (Carlino et al., 2011) has revealed an increase in the level of mature BDNF and a reduction in truncated BDNF in patients with schizophrenia with cognitive deficits. Evidence has suggested (Carlino et al., 2011) that truncated BDNF has similar properties as those of pro-BDNF (the precursor of BDNF) and can serve as an alternative of the inactive form of pro-BDNF, leading to an increase in pro-BDNF. Furthermore, cognitive impairment can mostly induce a compensatory increase in the processing of pro-BDNF to generate mature BDNF. This may provide an explanation for the reduction in truncated BDNF and the upregulation of mature BDNF in the ketamine group.

Caspase-3 and -9 belong to a family of cysteinyl-aspartate-specific proteases involved in apoptotic cell death. Previous studies have shown that prolonged ketamine exposure significantly increases cleaved caspase-3 and -9 levels, hence providing direct evidence for the activation of the intrinsic apoptotic pathway (Zou et al., 2009; Liu et al., 2013). In addition, another study (Djebaili et al., 2004) showed that, compared with vehicle alone, ALLO (16 mg kg^{-1}) and PROG (8 mg kg^{-1}) are able to decrease cleaved caspase-3 compared in injured rats.

Nrf2, a crucial regulator of oxidative stress, is activated by PI3K/Akt signaling (Lee et al., 2014). Reduced activity of Nrf2 and related antioxidant enzymes, including SOD, CAT and GSH-Px, have been observed in ketamine-exposed rats (Zugno et al., 2014). PROG reportedly protects neuronal cells from oxidative stress by upregulating antioxidative enzymes (Sharma et al., 2011).

Consistent with the evidence above, we confirmed that ketamine produced a significant increase in cleaved caspase-3 and caspase-9 and a decrease in CREB, BDNF and Nfr2, whereas coadministration with PROG or ALLO ameliorated these changes (**Figure 3**). Therefore, it is suggested that the therapeutic effects of PROG and ALLO are associated with their ability to influence CREB, BDNF, caspase-3/9 and Nrf2 expression to protect against ketamine-induced neurotoxicity.

Add-On PROG and ALLO Treatments Reversed the Suppression of EGFR and GLP-1R Induced by Ketamine

EGFR and GLP-1R are both positive regulators of the PI3K/Akt pathway. Studies have shown that exendin-4 (an agonist of GLP-1R) inhibits neuronal apoptosis by upregulating the GLP-1R/PI3K/Akt signaling pathway (Xie et al., 2018). Preclinical evidence has also suggested that GLP-1R in the brain represents a promising new target for both cognitive-enhancing and neuroprotective agents (During et al., 2003). Similarly, it has also been reported that an adenosine A_1 receptor agonist can activate the EGFR/PI3K/Akt pathway to mediate neuroprotection in cortical neurons (Xie et al., 2009). It is also known that EGFR can mediate Nrf2 signaling activation by several other stimuli in the process of neuroprotection (Gu et al., 2015). Although few studies have investigated the effect of ketamine on EGFR and GLP-1R, it has been demonstrated that neuroprotection mediated by EGFR and GLP-1R can be abolished by using selective kinase inhibitors (Xie et al., 2009). In support of the evidence above, our data also provides evidence that PROG and ALLO exert their neuroprotective effects against

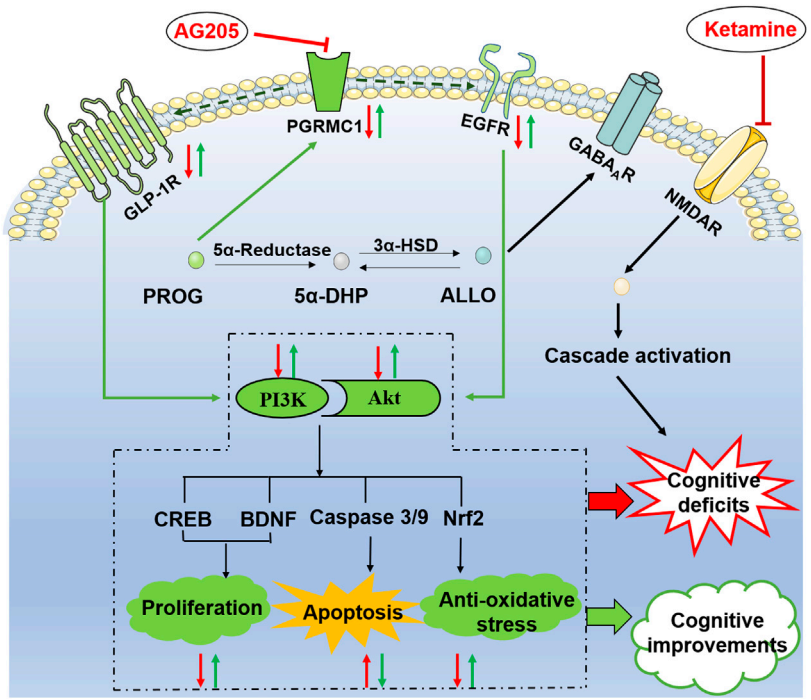

FIGURE 6 | Illustrative model of the mechanism underlying the neuroprotective effects of PROG and ALLO against ketamine-induced cognitive deficits. Under certain conditions, the PI3K/Akt pathway can be activated to exert its neuroprotective function by phosphorylating a battery of protein substrates, including Nuclear factor erythroid-2-related factor 2 (Nrf2), caspase-3/9, cAMP response element-binding protein (CREB) and brain-derived neurotrophic factor (BDNF). Furthermore, the PI3K/Akt pathway is a putative downstream signaling pathway regulated by EGFR and GLP-1R to elicit multiple biological responses, especially cognitive function. Intriguingly, PGRMC1 co-precipitates and co-localizes with EGFR in cytoplasmic vesicles in cells and also serves as a novel component of the liganded GLP-1R complex. In the present study, the therapeutic effect of PROG or ALLO at least in part rely on the activation of PGRMC1/EGFR/GLP-1R/PI3K/Akt pathway in the brain. Moreover, the PRGMC1-specific inhibitor AG205 significantly antagonized the therapeutic effects of PROG in the MWM task and downregulated the PGRMC1/EGFR/GLP-1R pathway, which supports a role for PGRMC1 in the functional regulation of EGFR and GLP-1R, as well as their relation to neuroprotective effects.

ketamine by upregulating EGFR and GLP-1R signaling and downstream molecules.

Role of PGRMC1 in the PROG-Mediated Therapeutic Effects

As illustrated in **Figure 6**, PGRMC1 has the ability to interact with EGFR and GLP-1R (Zhang et al., 2014). In the present study, the PRGMC1-specific inhibitor AG205 significantly antagonized the therapeutic effects of PROG in the MWM task and downregulated the PGRMC1/EGFR/GLP-1R pathway, which supports a role for PGRMC1 in the functional regulation of EGFR and GLP-1R (Zhang et al., 2014).

Consistent with our results, previous findings have also revealed that PGRMC1 protein levels are upregulated by PROG in the brain after TBI (Meffre et al., 2005). Although classic Pgr has multiple physiological functions, there is a lack of evidence suggesting that the neuroprotection of PROG is mediated by classic Pgr. Interestingly, our data demonstrate that cotreatment with AG205, a specific inhibitor of PGRMC1, reversed the neuroprotective effect of PROG. Given that PROG possesses a high affinity for PGRMC1, the data suggest that the neuroprotective effects of PROG against ketamine's neurotoxicity are mediated by PGRMC1. Studies on the potential role of PGRMC1 as a participant in the antiapoptotic process of PROG in rats have been performed (Qin et al., 2015). Additionally, data (Su et al., 2012) have revealed that PROG can elicit the release of BDNF in glia via a PGRMC1-mediated signaling mechanism. Taken together, the evidence above suggests that the upregulation of PGRMC1 expression after an increase in brain PROG levels is associated with its neuroprotective mechanism.

Neuroprotective Role of PGRMC1 Depends on the Conversion between PROG and ALLO

On one hand, ALLO is biosynthesized from PROG in the brain through 5α-reductase- and 3α-hydroxysteroid dehydrogenase-mediated reactions, which are irreversible and rate-limited by the 5α-reductase step (Dong et al., 2001). Due to its lipophilicity, peripheral ALLO can readily cross into brain (Paul and Purdy, 1992). In ALLO-treated groups, the concentrations of PROG are both endogenous and at the same baseline level before add-on ALLO treatments. Exogenous-administration of ALLO can interfere the normal conversion process from PROG to ALLO. In our study, high dose of ALLO provided higher exogenous concentration of ALLO, which could exert a much stronger

interfering effect in the conversion process than the ALLO (8 mg kg^{-1}) group, finally resulting in significantly elevated PROG levels in the ALLO (16 mg kg^{-1}) group. This fully explains the higher level of PROG observed in the ALLO (16 mg kg^{-1}) group than in the ALLO (8 mg kg^{-1}) group (**Figure 5**).

Consistently, ALLO (16 mg kg^{-1}) also exhibited a stronger therapeutic effect in regulating the PGRMC1 pathway. On the other hand, ALLO does not bind to classical intracellular PROG receptors and exerts its neuroprotective actions via the modulation of membrane-associated $GABA_A$ receptor sites (Ishihara et al., 2013). Additionally, a clinical finding (Cai et al., 2018b) suggested that low levels of ALLO may lead to weaker neuroprotection or that excessive levels of ALLO are involved in neuroprotection against excitotoxic damage in patients with schizophrenia. This evidence suggests the possibility of a dual action of ALLO in the present study, i.e. directly via $GABA_A$ receptors at a lower ALLO and via attenuating the conversion process simultaneously at high level of ALLO resulting in an increased level of PROG in the brain to directly activate PGRMC1. Intriguingly, a low dose of PROG did not alter ALLO levels in these tissues and exhibited stronger therapeutic effects than a low dose of ALLO, which suggests that the neuroprotective effect of PROG is mostly mediated by PROG itself, not via its metabolite ALLO.

Reports (Goss et al., 2003) have indicated that low and moderate doses of PROG (8, 16 mg kg^{-1}) are beneficial for facilitating behavioral recovery, while a high dose (32 mg kg^{-1}) is either ineffective or potentially harmful in the MWM test in rats. In accordance with this finding, our data also support that either 8 or 16 mg kg^{-1} PROG possesses therapeutic effects. However, the fact that 8 mg kg^{-1} PROG displayed better therapeutic efficiency than 16 mg kg^{-1} PROG cannot be ignored and greatly aroused our interest. First, previous studies on PROG dose-response were conducted in a model of TBI, while our study mimicked the ketamine-induced schizophrenia; this difference probably led to complexities and differences in PROG dose-response. Second, the accumulation of PROG was reported to possibly mediate its suppressive effect on PGRMC1 expression (Losel et al., 2008), which may result in reduced neuroprotection and even further lead to neurotoxicity under some circumstances. In agreement with our hypothesis, previous studies have reported that subcutaneous injection of PROG at a lower dose acutely or sub-chronically impairs social recognition memory of normal rats both in a social discrimination task and in a spatial task (Sun et al., 2010; Bychowski and Auger, 2012). Nevertheless, the therapeutic differences in the doses of PROG remain unclear at this stage and require further elucidation.

Limitation

Although prepulse inhibition (PPI) is used to analyze early attentional gating mechanisms in animal models of schizophrenia, the reasons why our study selected MWM test are as follows:

1. PPI deficits have been observed not only in schizophrenia but also in other neuropsychiatric disorders, in which an increased dopamine functioning is involved not in NMDA system (Geyer, 2006; Schellekens et al., 2010).
2. Animal models (Vargas et al., 2016) and clinical data (Dawson et al., 2000) both indicated that PPI deficits not only correlate with cognitive impairment such as working memory or alternation behavior, locomotion activity, but also some negative symptoms described in schizophrenia.

In view of lacking specificity, the PPI deficits is not suitable for evaluating the cognitive impairment modeled by ketamine. Nowadays, there is still controversy about the use of ketamine and other NMDAR inhibitors in well-establishment of schizophrenia models in animals. However, it is well-recognized that sub-chronic ketamine administration induced neurotoxicity in rodents manifested as cognitive impairments in the MWM test, as well as its relevance to schizophrenia-like cognitive deficits (Moosavi et al., 2012; Sabbagh et al., 2012). So far, a larger amount of preclinical researches (Sun et al., 2016; Lu et al., 2017; Li et al., 2019) have supported the application of MWM maze for the evaluation of cognitive deficits induced by ketamine. Take these factors into consideration, the MWM maze test is an appropriate choice for our experiment.

Future Remarks

Evidence (Roof and Hall, 2000) suggests that the greater neuroprotection afforded to females is likely due to the effects of circulating estrogens and progestins. The neuroprotection provided by exogenous administration of these hormones extends to males as well. However, it is evident (Chen et al., 2018) that the efficacy of neurosteorids for cognitive function may differ between the genders. Moreover, neurosteroids may be involved in the gender differences found in the susceptibility to schizophrenia (Huang et al., 2017). In future clinical practice, it is recommended to measure the concentrations of PROG to optimize the therapeutic regimen based on gender differences.

CONCLUSION

In conclusion, our study demonstrated that treatments with PROG or ALLO significantly ameliorate the cognitive impairment due to ketamine's neurotoxicity. The therapeutic effects at least in part rely on the activation of PGRMC1/EGFR/GLP-1R/PI3K/Akt pathway in the brain. Co-administration with AG205, the specific inhibitor of PGRMC1, abolished

the therapeutic effect of PROG on ketamine-induced neurotoxicity, verifying the key role of PGRMC1. Therefore, PROG or ALLO supplementation might be a potential therapeutic strategy to restore cognitive function in clinical practice. Specifically, the present study may shed light on future possibilities for neurosteroid treatments to enhance cognitive performance in neuropsychiatric diseases and for the development of pharmacological solutions to improve cognitive function by targeting on PGRMC1 signaling.

DATA AVAILABILITY STATEMENT

The raw data supporting the conclusions of this article will be made available by the authors, without undue reservation.

ETHICS STATEMENT

The animal study was reviewed and approved by the local Ethics Committee of the Second Xiangya Hospital of Central South University.

AUTHOR CONTRIBUTIONS

All authors contributed to and have approved the final manuscript. HC: Conceptualization, Methodology, Writing-Reviewing and Editing; TC: Data curation, Writing- Original draft preparation; MT: Methodology, Validation, Software; PJ: Writing- Reviewing and Editing; NL, QC, CZ, SZ, BZ, and XW: Visualization, Investigation, Validation.

FUNDING

This work was supported in part by the grants from the Nature Science Foundation of China (NSFC81401113 (HC)), Hunan Provincial Natural Science Foundation of China (2017JJ3444 (HC)) Hunan Provincial Health Commission Research Project (202113010595 (HC)) Wu Jieping Medical Foundation Funded Special Clinical Research Project (320.6750.2020-04-2 (HC)), Changsha Municipal Natural Science Foundation (kq2007045 (HC)) and the Fundamental Research Funds for the Central Universities of Central South University (2019zzts1049 (TC), 2020zzts884 (NL)).

ACKNOWLEDGMENTS

We are deeply grateful for the support by Mental Health Research Center of the Second Xiangya Hospital, Central South University. We thank Mimi Tang (Central South University) for her superb technical assistance.

SUPPLEMENTARY MATERIAL

The Supplementary Material for this article can be found online at: https://www.frontiersin.org/articles/10.3389/fphar.2021.612083/full#supplementary-material.

REFERENCES

Aas, M., Dazzan, P., Mondelli, V., Melle, I., Murray, R. M., and Pariante, C. M. (2014). A systematic review of cognitive function in first-episode psychosis, including a discussion on childhood trauma, stress, and inflammation. *Front. Psychiatry* 4, 182. doi:10.3389/fpsyt.2013.00182

Aguiar, A. S., Castro, A. A., Moreira, E. L., Glaser, V., Santos, A. R. S., Tasca, C. I., et al. (2011). Short bouts of mild-intensity physical exercise improve spatial learning and memory in aging rats: involvement of hippocampal plasticity via AKT, CREB and BDNF signaling. *Mech. Ageing Dev.* 132 (11–12), 560–567. doi:10.1016/j.mad.2011.09.005

Ahmed, I. S., Rohe, H. J., Twist, K. E., and Craven, R. J. (2010). Pgrmc1 (progesterone receptor membrane component 1) associates with epidermal growth factor receptor and regulates erlotinib sensitivity. *J. Biol. Chem.* 285 (32), 24775–24782. doi:10.1074/jbc.M110.134585

Aizen, J., and Thomas, P. (2015). Role of Pgrmc1 in estrogen maintenance of meiotic arrest in zebrafish oocytes through Gper/Egfr. *J. Endocrinol.* 225 (1), 59–68. doi:10.1530/joe-14-0576

Andrabi, S. S., Parvez, S., and Tabassum, H. (2017). Progesterone induces neuroprotection following reperfusion-promoted mitochondrial dysfunction after focal cerebral ischemia in rats. *Dis. Model. Mech.* 10 (6), 787–796. doi:10.1242/dmm.025692

Blot, K., Kimura, S., Bai, J., Kemp, A., Manahan-Vaughan, D., Giros, B., et al. (2015). Modulation of hippocampus-prefrontal cortex synaptic transmission and disruption of executive cognitive functions by MK-801, *Cereb. Cortex* 25 (5), 1348–1361. doi:10.1093/cercor/bht329

Bychowski, M. E., and Auger, C. J. (2012). Progesterone impairs social recognition in male rats. *Horm. Behav.* 61 (4), 598–604. doi:10.1016/j.yhbeh.2012.02.009

Cai, H. L., Cao, T., Li, N., Fang, P., Xu, P., Wu, X., et al. (2019). Quantitative monitoring of a panel of stress-induced biomarkers in human plasma by liquid chromatography-tandem mass spectrometry: an application in a comparative study between depressive patients and healthy subjects. *Anal. Bioanal. Chem.* 411 (22), 5765–5777. doi:10.1007/s00216-019-01956-2

Cai, H. L., Cao, T., Zhou, X., and Yao, J. K. (2018a). Neurosteroids in schizophrenia: pathogenic and therapeutic implications. *Front. Psychiatry* 9, 73. doi:10.3389/fpsyt.2018.00073

Cai, H. L., Tan, Q. Y., Jiang, P., Dang, R. L., Xue, Y., Tang, M. M., et al. (2015). A potential mechanism underlying atypical antipsychotics-induced lipid disturbances. *Transl. Psychiatry* 5, e661. doi:10.1038/tp.2015.161

Cai, H. L., Zhou, X., Dougherty, G. G., Reddy, R. D., Haas, G. L., Montrose, D. M., et al. (2018b). Pregnenolone-progesterone-allopregnanolone pathway as a potential therapeutic target in first-episode antipsychotic-naive patients with schizophrenia. *Psychoneuroendocrino* 90, 43–51. doi:10.1016/j.psyneuen.2018.02.004

Carlino, D., Leone, E., Di Cola, F., Baj, G., Marin, R., Dinelli, G., et al. (2011). Low serum truncated-BDNF isoform correlates with higher cognitive impairment in schizophrenia. *J. Psychiatr. Res.* 45 (2), 273–279. doi:10.1016/j.jpsychires.2010.06.012

Chen, C. Y., Wu, C. C., Huang, Y. C., Hung, C. F., and Wang, L. J. (2018). Gender differences in the relationships among neurosteroid serum levels, cognitive function, and quality of life. *Neuropsychiatr. Dis. Treat.* 14, 2389–2399. doi:10.2147/ndt.s176047

Chu, A. O. K., Chang, W. C., Chan, S. K. W., Lee, E. H. M., Hui, C. L. M., and Chen, E. Y. H. (2019). Comparison of cognitive functions between first-episode schizophrenia patients, their unaffected siblings and individuals at clinical high-risk for psychosis. *Psychol. Med.* 49, 1929–1936. doi:10.1017/s0033291718002726

Cooke, P. S., Nanjappa, M. K., Yang, Z., and Wang, K. K. (2013). Therapeutic effects of progesterone and its metabolites in traumatic brain injury may involve non-classical signaling mechanisms. *Front. Neurosci.* 7, 108. doi:10.3389/fnins.2013.00108

Craven, R. J. (2008). PGRMC1: a new biomarker for the estrogen receptor in breast cancer. *Breast Cancer Res.* 10 (6), 113. doi:10.1186/bcr2191

Dawson, M. E., Schell, A. M., Hazlett, E. A., Nuechterlein, K. H., and Filion, D. L. (2000). On the clinical and cognitive meaning of impaired sensorimotor gating in schizophrenia. *Psychiatry Res.* 96 (3), 187–197. doi:10.1016/s0165-1781(00)00208-0

Di Mauro, M., Tozzi, A., Calabresi, P., Pettorossi, V. E., and Grassi, S. (2015). Neosynthesis of estrogenic or androgenic neurosteroids determine whether long-term potentiation or depression is induced in hippocampus of male rat. *Front. Cell. Neurosci.* 9, 376. doi:10.3389/fncel.2015.00376

Djebaili, M., Hoffman, S. W., and Stein, D. G. (2004). Allopregnanolone and progesterone decrease cell death and cognitive deficits after a contusion of the rat pre-frontal cortex. *Neuroscience* 123 (2), 349–359. doi:10.1016/j.neuroscience.2003.09.023

Dong, E., Matsumoto, K., Uzunova, V., Sugaya, I., Takahata, H., Nomura, H., et al. (2001). Brain 5alpha-dihydroprogesterone and allopregnanolone synthesis in a mouse model of protracted social isolation. *Proc. Natl. Acad. Sci. U.S.A.* 98 (5), 2849–2854. doi:10.1073/pnas.051628598

Driesen, N. R., Leung, H. C., Calhoun, V. D., Constable, R. T., Gueorguieva, R., Hoffman, R., et al. (2008). Impairment of working memory maintenance and response in schizophrenia: functional magnetic resonance imaging evidence. *Biol. Psychiatry* 64 (12), 1026–1034. doi:10.1016/j.biopsych.2008.07.029

During, M. J., Cao, L., Zuzga, D. S., Francis, J. S., Fitzsimons, H. L., Jiao, X., et al. (2003). Glucagon-like peptide-1 receptor is involved in learning and neuroprotection. *Nat. Med.* 9 (9), 1173–1179. doi:10.1038/nm919

Frank, C., and Sagratella, S. (2000). Neuroprotective effects of allopregnenolone on hippocampal irreversible neurotoxicity *in vitro*. *Prog. Neuropsychopharmacol. Biol. Psychiatry* 24 (7), 1117–1126. doi:10.1016/S0278-5846(00)00124-X

Geyer, M. A. (2006). The family of sensorimotor gating disorders: comorbidities or diagnostic overlaps? *Neurotox. Res.* 10 (3–4), 211–220. doi:10.1007/bf03033358

Goss, C. W., Hoffman, S. W., and Stein, D. G. (2003). Behavioral effects and anatomic correlates after brain injury: a progesterone dose-response study. *Pharmacol. Biochem. Behav.* 76 (2), 231–242. doi:10.1016/j.pbb.2003.07.003

Grassi, S., Tozzi, A., Costa, C., Tantucci, M., Colcelli, E., Scarduzio, M., et al. (2011). Neural 17β-estradiol facilitates long-term potentiation in the hippocampal CA1 region. *Neuroscience* 192, 67–73. doi:10.1016/j.neuroscience.2011.06.078

Gu, D.-M., Lu, P.-H., Zhang, K., Wang, X., Sun, M., Chen, G.-Q., et al. (2015). EGFR mediates astragaloside IV-induced Nrf2 activation to protect cortical neurons against *in vitro* ischemia/reperfusion damages. *Biochem. Biophys. Res. Commun.* 457 (3), 391–397. doi:10.1016/j.bbrc.2015.01.002

Guennoun, R., Labombarda, F., Gonzalez Deniselle, M. C., Liere, P., De Nicola, A. F., and Schumacher, M. (2015). Progesterone and allopregnanolone in the central nervous system: response to injury and implication for neuroprotection. *J. Steroid Biochem. Mol. Biol.* 146, 48–61. doi:10.1016/j.jsbmb.2014.09.001

Guennoun, R., Meffre, D., Labombarda, F., Gonzalez, S. L., Gonzalez Deniselle, M. C., Stein, D. G., et al. (2008). The membrane-associated progesterone-binding protein 25-Dx: expression, cellular localization and up-regulation after brain and spinal cord injuries. *Brain Res. Rev.* 57 (2), 493–505. doi:10.1016/j.brainresrev.2007.05.009

Hampton, K. K., Anderson, K., Frazier, H., Thibault, O., and Craven, R. J. (2018). Insulin receptor plasma membrane levels increased by the progesterone receptor membrane component 1. *Mol. Pharmacol.* 94 (1), 665–673. doi:10.1124/mol.117.110510

Hand, R. A., and Craven, R. J. (2003). Hpr6.6 protein mediates cell death from oxidative damage in MCF-7 human breast cancer cells. *J. Cell. Biochem.* 90 (3), 534–547. doi:10.1002/jcb.10648

Hill, S. K., Bishop, J. R., Palumbo, D., and Sweeney, J. A. (2010). Effect of second-generation antipsychotics on cognition: current issues and future challenges. *Expert Rev. Neurother* 10 (1), 43–57. doi:10.1586/ern.09.143

Huang, Y. C., Hung, C. F., Lin, P. Y., Lee, Y., Wu, C. C., Hsu, S. T., et al. (2017). Gender differences in susceptibility to schizophrenia: potential implication of neurosteroids. *Psychoneuroendocrinology* 84, 87–93. doi:10.1016/j.psyneuen.2017.06.017

Ishihara, Y., Kawami, T., Ishida, A., and Yamazaki, T. (2013). Allopregnanolone-mediated protective effects of progesterone on tributyltin-induced neuronal injury in rat hippocampal slices. *J. Steroid Biochem. Mol. Biol.* 135, 1–6. doi:10.1016/j.jsbmb.2012.12.013

Johansson, I. M., Birzniece, V., Lindblad, C., Olsson, T., and Bäckström, T. (2002). Allopregnanolone inhibits learning in the Morris water maze. *Brain Res.* 934 (2), 125–131. doi:10.1016/s0006-8993(02)02414-9

Jones, N. C., Constantin, D., Prior, M. J., Morris, P. G., Marsden, C. A., and Murphy, S. (2005). The neuroprotective effect of progesterone after traumatic brain injury in male mice is independent of both the inflammatory response and growth factor expression. *Eur. J. Neurosci.* 21 (6), 1547–1554. doi:10.1111/j.1460-9568.2005.03995.x

Kumon, Y., Kim, S. C., Tompkins, P., Stevens, A., Sakaki, S., and Loftus, C. M. (2000). Neuroprotective effect of postischemic administration of progesterone in spontaneously hypertensive rats with focal cerebral ischemia. *J. Neurosurg.* 92 (5), 848–852. doi:10.3171/jns.2000.92.5.0848

Labombarda, F., Gonzalez, S. L., Gonzalez Deniselle, M. C., Vinson, G. P., Schumacher, M., De Nicola, A. F., et al. (2003). Effects of injury and progesterone treatment on progesterone receptor and progesterone binding protein 25-Dx expression in the rat spinal cord. *J. Neurochem.* 87 (4), 902–913. doi:10.1046/j.1471-4159.2003.02055.x

Lee, T.-M., Lin, S.-Z., and Chang, N.-C. (2014). Antiarrhythmic effect of lithium in rats after myocardial infarction by activation of Nrf2/HO-1 signaling. *Free Radic. Biol. Med.* 77, 71–81. doi:10.1016/j.freeradbiomed.2014.08.022

Li, Q., Wu, H. R., Fan, S. J., Liu, D. X., Jiang, H., Zhang, Q., et al. (2019). The effects of sub-anesthetic ketamine plus ethanol on behaviors and apoptosis in the prefrontal cortex and hippocampus of adolescent rats. *Pharmacol. Biochem. Behav.* 184, 172742. doi:10.1016/j.pbb.2019.172742

Liu, J. R., Baek, C., Han, X. H., Shoureshi, P., and Soriano, S. G. (2013). Role of glycogen synthase kinase-3β in ketamine-induced developmental neuroapoptosis in rats. *Br. J. Anaesth.* 110 (Suppl. 1), i3–i9. doi:10.1093/bja/aet057

Liu, L. F., Wang, J. M., Zhao, L. Q., Nilsen, J., McClure, K., Wong, K., et al. (2009). Progesterone increases rat neural progenitor cell cycle gene expression and proliferation via extracellularly regulated kinase and progesterone receptor membrane components 1 and 2. *Endocrinology* 150 (7), 3186–3196. doi:10.1210/en.2008-1447

Losel, R. M., Besong, D., Peluso, J. J., and Wehling, M. (2008). Progesterone receptor membrane component 1–many tasks for a versatile protein. *Steroids* 73 (9–10), 929–934. doi:10.1016/j.steroids.2007.12.017

Lu, Y., Giri, P. K., Lei, S., Zheng, J., Li, W. S., Wang, N., et al. (2017). Pretreatment with minocycline restores neurogenesis in the subventricular zone and subgranular zone of the hippocampus after ketamine exposure in neonatal rats. *Neuroscience* 352, 144–154. doi:10.1016/j.neuroscience.2017.03.057

MacDonald, P. E., Wang, X., Xia, F., El-kholy, W., Targonsky, E. D., Tsushima, R. G., et al. (2003). Antagonism of rat beta-cell voltage-dependent K+ currents by exendin 4 requires dual activation of the cAMP/protein kinase A and phosphatidylinositol 3-kinase signaling pathways. *J. Biol. Chem.* 278 (52), 52446–52453. doi:10.1074/jbc.M307612200

Meffre, D., Delespierre, B., Gouezou, M., Leclerc, P., Vinson, G. P., Schumacher, M., et al. (2005). The membrane-associated progesterone-binding protein 25-Dx is expressed in brain regions involved in water homeostasis and is up-regulated after traumatic brain injury. *J. Neurochem.* 93 (5), 1314–1326. doi:10.1111/j.1471-4159.2005.03127.x

Moore, L., Kyaw, M., Vercammen, A., Lenroot, R., Kulkarni, J., Curtis, J., et al. (2013). Serum testosterone levels are related to cognitive function in men with schizophrenia. *Psychoneuroendocrinology* 38 (9), 1717–1728. doi:10.1016/j.psyneuen.2013.02.007

Moosavi, M., Naghdi, N., Maghsoudi, N., and Zahedi Asl, S. (2007). Insulin protects against stress-induced impairments in water maze performance. *Behav. Brain Res.* 176 (2), 230–236. doi:10.1016/j.bbr.2006.10.011

Moosavi, M., Yadollahi Khales, G., Rastegar, K., and Zarifkar, A. (2012). The effect of sub-anesthetic and anesthetic ketamine on water maze memory acquisition, consolidation and retrieval. *Eur. J. Pharmacol.* 677 (1–3), 107–110. doi:10.1016/j.ejphar.2011.12.021

Morali, G., Montes, P., Hernandez-Morales, L., Monfil, T., Espinosa-Garcia, C., and Cervantes, M. (2011). Neuroprotective effects of progesterone and allopregnanolone on long-term cognitive outcome after global cerebral ischemia. *Restor Neurol. Neurosci.* 29 (1), 1–15. doi:10.3233/rnn-2011-0571

Neill, J. C., Barnes, S., Cook, S., Grayson, B., Idris, N. F., McLean, S. L., et al. (2010). Animal models of cognitive dysfunction and negative symptoms of schizophrenia: focus on NMDA receptor antagonism. *Pharmacol. Ther.* 128 (3), 419–432. doi:10.1016/j.pharmthera.2010.07.004

Nezhadi, A., Sheibani, V., Esmaeilpour, K., Shabani, M., and Esmaeili-Mahani, S. (2016). Neurosteroid allopregnanolone attenuates cognitive dysfunctions in 6-OHDA-induced rat model of Parkinson's disease. *Behav. Brain Res.* 305, 258–264. doi:10.1016/j.bbr.2016.03.019

Nieto, R., Kukuljan, M., and Silva, H. (2013). BDNF and schizophrenia: from neurodevelopment to neuronal plasticity, learning, and memory. *Front. Psychiatry* 4, 45. doi:10.3389/fpsyt.2013.00045

Nin, M. S., Martinez, L. A., Pibiri, F., Nelson, M., and Pinna, G. (2011). Neurosteroids reduce social isolation-induced behavioral deficits: a proposed link with neurosteroid-mediated upregulation of BDNF expression. *Front. Endocrinol. (Lausanne)* 2, 73. doi:10.3389/fendo.2011.00073

Parwani, A., Weiler, M. A., Blaxton, T. A., Warfel, D., Hardin, M., Frey, K., et al. (2005). The effects of a subanesthetic dose of ketamine on verbal memory in normal volunteers. *Psychopharmacology (Berl)* 183 (3), 265–274. doi:10.1007/s00213-005-0177-2

Paul, S. M., and Purdy, R. H. (1992). Neuroactive steroids. *FASEB J.* 6 (6), 2311–2322.

Peltier, J., O'Neill, A., and Schaffer, D. V. (2007). PI3K/Akt and CREB regulate adult neural hippocampal progenitor proliferation and differentiation. *Dev. Neurobiol.* 67 (10), 1348–1361. doi:10.1002/dneu.20506

Peluso, J. J., Liu, X., Gawkowska, A., and Johnston-MacAnanny, E. (2009). Progesterone activates a progesterone receptor membrane component 1-dependent mechanism that promotes human granulosa/luteal cell survival but not progesterone secretion. *J. Clin. Endocrinol. Metab.* 94 (7), 2644–2649. doi:10.1210/jc.2009-0147

Qin, Y. B., Chen, Z. S., Han, X. L., Wu, H. H., Yu, Y., Wu, J., et al. (2015). Progesterone attenuates Aβ(25-35)-induced neuronal toxicity via JNK inactivation and progesterone receptor membrane component 1-dependent inhibition of mitochondrial apoptotic pathway. *J. Steroid Biochem. Mol. Biol.* 154, 302–311. doi:10.1016/j.jsbmb.2015.01.002

Rajagopal, L., Soni, D., and Meltzer, H. Y. (2018). Neurosteroid pregnenolone sulfate, alone, and as augmentation of lurasidone or tandospirone, rescues phencyclidine-induced deficits in cognitive function and social interaction. *Behav. Brain Res.* 350, 31–43. doi:10.1016/j.bbr.2018.05.005

Rohe, H. J., Ahmed, I. S., Twist, K. E., and Craven, R. J. (2009). PGRMC1 (progesterone receptor membrane component 1): a targetable protein with multiple functions in steroid signaling, P450 activation and drug binding. *Pharmacol. Ther.* 121 (1), 14–19. doi:10.1016/j.pharmthera.2008.09.006

Roof, R. L., and Hall, E. D. (2000). Gender differences in acute CNS trauma and stroke: neuroprotective effects of estrogen and progesterone. *J. Neurotrauma* 17 (5), 367–388. doi:10.1089/neu.2000.17.367

Rushforth, S. L., Steckler, T., and Shoaib, M. (2011). Nicotine improves working memory span capacity in rats following sub-chronic ketamine exposure. *Neuropsychopharmacology* 36 (13), 2774–2781. doi:10.1038/npp.2011.224

Sabbagh, J. J., Heaney, C. F., Bolton, M. M., Murtishaw, A. S., and Kinney, J. W. (2012). Examination of ketamine-induced deficits in sensorimotor gating and spatial learning. *Physiol. Behav.* 107 (3), 355–363. doi:10.1016/j.physbeh.2012.08.007

Schellekens, A. F. A., Grootens, K. P., Neef, C., Movig, K. L. L., Buitelaar, J. K., Ellenbroek, B., et al. (2010). Effect of apomorphine on cognitive performance and sensorimotor gating in humans. *Psychopharmacology (Berl)* 207 (4), 559–569. doi:10.1007/s00213-009-1686-1

Sharma, A. K., Bhattacharya, S. K., Khanna, N., Tripathi, A. K., Arora, T., Mehta, A. K., et al. (2011). Effect of progesterone on phosphamidon-induced impairment of memory and oxidative stress in rats. *Hum. Exp. Toxicol.* 30 (10), 1626–1634. doi:10.1177/0960327110396522

Si, D., Wang, H., Wang, Q., Zhang, C., Sun, J., Wang, Z., et al. (2013). Progesterone treatment improves cognitive outcome following experimental traumatic brain injury in rats. *Neurosci. Lett.* 553, 18–23. doi:10.1016/j.neulet.2013.07.052

Singh, M. (2001). Ovarian hormones elicit phosphorylation of Akt and extracellular-signal regulated kinase in explants of the cerebral cortex. *Endocrine* 14 (3), 407–415. doi:10.1385/endo:14:3:407

Singh, M., and Su, C. (2013). Progesterone, brain-derived neurotrophic factor and neuroprotection. *Neuroscience* 239, 84–91. doi:10.1016/j.neuroscience.2012.09.056

Song, D., Yang, Q., Lang, Y., Wen, Z., Xie, Z., Zheng, D., et al. (2018). Manipulation of hippocampal CA3 firing via luminopsins modulates spatial and episodic short-term memory, especially working memory, but not long-term memory. *Neurobiol. Learn. Mem.* 155, 435–445. doi:10.1016/j.nlm.2018.09.009

Su, C., Cunningham, R. L., Rybalchenko, N., and Singh, M. (2012). Progesterone increases the release of brain-derived neurotrophic factor from glia via progesterone receptor membrane component 1 (Pgrmc1)-dependent ERK5 signaling. *Endocrinology* 153 (9), 4389–4400. doi:10.1210/en.2011-2177

Sun, W. L., Luine, V. N., Zhou, L., Wu, H. B., Weierstall, K. M., Jenab, S., et al. (2010). Acute progesterone treatment impairs spatial working memory in intact male and female rats. *Ethn. Dis.* 20 (1 Suppl. 1), S1–S83. doi:10.1017/S0950268810000622.7

Sun, Y. T., Hou, M., Zou, T., Liu, Y., Li, J., and Wang, Y. L. (2016). Effect of ketamine anesthesia on cognitive function and immune function in young rats. *Cell. Mol. Biol. (Noisy-le-grand)* 62 (4), 63–66. doi:10.14715/cmb/2016.62.4.12

Van den Buuse, M., Mingon, R. L., and Gogos, A. (2015). Chronic estrogen and progesterone treatment inhibits ketamine-induced disruption of prepulse inhibition in rats. *Neurosci. Lett.* 607, 72–76. doi:10.1016/j.neulet.2015.09.019

Vargas, J. P., Diaz, E., Portavella, M., and Lopez, J. C. (2016). Animal models of maladaptive traits: disorders in sensorimotor gating and attentional quantifiable responses as possible endophenotypes. *Front. Psychol.* 7, 206. doi:10.3389/fpsyg.2016.00206

Wali, B., Ishrat, T., Won, S., Stein, D. G., and Sayeed, I. (2014). Progesterone in experimental permanent stroke: a dose-response and therapeutic time-window study. *Brain* 137 (Pt 2), 486–502. doi:10.1093/brain/awt319

Wang, J., Zhou, M., Wang, X. B., Yang, X. L., Wang, M. H., Zhang, C. X., et al. (2014). Impact of ketamine on learning and memory function, neuronal apoptosis and its potential association with miR-214 and PTEN in adolescent rats. *Plos One* 9 (6), e99855. doi:10.1371/journal.pone.0099855

Xie, K.-Q., Zhang, L.-M., Cao, Y., Zhu, J., and Feng, L.-Y. (2009). Adenosine A(1) receptor-mediated transactivation of the EGF receptor produces a neuroprotective effect on cortical neurons *in vitro*. *Acta Pharmacol. Sin* 30 (7), 889–898. doi:10.1038/aps.2009.80

Xie, Z., Enkhjargal, B., Wu, L., Zhou, K., Sun, C., Hu, X., et al. (2018). Exendin-4 attenuates neuronal death via GLP-1R/PI3K/Akt pathway in early brain injury after subarachnoid hemorrhage in rats. *Neuropharmacology* 128, 142–151. doi:10.1016/j.neuropharm.2017.09.040

Zhang, M., Robitaille, M., Showalter, A. D., Huang, X. Y., Liu, Y., Bhattacharjee, A., et al. (2014). Progesterone receptor membrane component 1 is a functional part of the glucagon-like peptide-1 (GLP-1) receptor complex in pancreatic β cells. *Mol. Cell. Proteomics* 13 (11), 3049–3062. doi:10.1074/mcp.M114.040196

Zheng, W., Wang, H., Zeng, Z., Lin, J., Little, P. J., Srivastava, L. K., et al. (2012). The possible role of the Akt signaling pathway in schizophrenia. *Brain Res.* 1470, 145–158. doi:10.1016/j.brainres.2012.06.032

Zheng, X. Z., Zhou, J. L., and Xia, Y. F. (2015). The role of TNF-α in regulating ketamine-induced hippocampal neurotoxicity. *Arch. Med. Sci.* 11 (6), 1296–1302. doi:10.5114/aoms.2015.56355

Zhou, J., Ping, F. F., Lv, W. T., Feng, J. Y., and Shang, J. (2014). Interleukin-18 directly protects cortical neurons by activating PI3K/AKT/NF-κB/CREB pathways. *Cytokine* 69 (1), 29–38. doi:10.1016/j.cyto.2014.05.003

Zhu, H., Zhang, Y., Shi, Z., Lu, D., Li, T., Ding, Y., et al. (2016). The neuroprotection of liraglutide against ischaemia-induced apoptosis through the activation of the PI3K/AKT and MAPK pathways. *Sci. Rep.* 6, 26859. doi:10.1038/srep26859

Zou, X., Patterson, T. A., Divine, R. L., Sadovova, N., Zhang, X., Hanig, J. P., et al. (2009). Prolonged exposure to ketamine increases neurodegeneration in the developing monkey brain. *Int. J. Dev. Neurosci.* 27 (7), 727–731. doi:10.1016/j.ijdevneu.2009.06.010

Zugno, A. I., Chipindo, H. L., Volpato, A. M., Budni, J., Steckert, A. V., De Oliveira, M. B., et al. (2014). Omega-3 prevents behavior response and brain oxidative damage in the ketamine model of schizophrenia. *Neuroscience* 259, 223–231. doi:10.1016/j.neuroscience.2013.11.049

Zuo, D., Lin, L., Liu, Y., Wang, C., Xu, J., Sun, F., et al. (2016). Baicalin attenuates ketamine-induced neurotoxicity in the developing rats: involvement of PI3K/Akt and CREB/BDNF/Bcl-2 pathways. *Neurotox. Res.* 30 (2), 159–172. doi:10.1007/s12640-016-9611-y

Conflict of Interest: The authors declare that the research was conducted in the absence of any commercial or financial relationships that could be construed as a potential conflict of interest.

Advantages of publishing in Frontiers

OPEN ACCESS
Articles are free to read for greatest visibility and readership

FAST PUBLICATION
Around 90 days from submission to decision

HIGH QUALITY PEER-REVIEW
Rigorous, collaborative, and constructive peer-review

TRANSPARENT PEER-REVIEW
Editors and reviewers acknowledged by name on published articles

Frontiers
Avenue du Tribunal-Fédéral 34
1005 Lausanne | Switzerland

Visit us: www.frontiersin.org
Contact us: frontiersin.org/about/contact

REPRODUCIBILITY OF RESEARCH
Support open data and methods to enhance research reproducibility

DIGITAL PUBLISHING
Articles designed for optimal readership across devices

FOLLOW US
@frontiersin

IMPACT METRICS
Advanced article metrics track visibility across digital media

EXTENSIVE PROMOTION
Marketing and promotion of impactful research

LOOP RESEARCH NETWORK
Our network increases your article's readership